ISSN 0031 - 9465

PHYTOPATHOLOGIA MEDITERRANEA

Plant health and food safety

Volume 60 • No. 3 • December 2021

The international journal of the
Mediterranean Phytopathological Union

FIRENZE UNIVERSITY PRESS

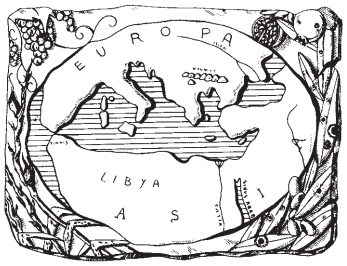

PHYTOPATHOLOGIA MEDITERRANEA

Plant health and food safety

The international journal edited by the Mediterranean Phytopathological Union
founded by A. Ciccarone and G. Goidànich

Phytopathologia Mediterranea is an international journal edited by the Mediterranean Phytopathological Union The journal's mission is the promotion of plant health for Mediterranean crops, climate and regions, safe food production, and the transfer of knowledge on diseases and their sustainable management.
The journal deals with all areas of plant pathology, including epidemiology, disease control, biochemical and physiological aspects, and utilization of molecular technologies. All types of plant pathogens are covered, including fungi, nematodes, protozoa, bacteria, phytoplasmas, viruses, and viroids. Papers on mycotoxins, biological and integrated management of plant diseases, and the use of natural substances in disease and weed control are also strongly encouraged. The journal focuses on pathology of Mediterranean crops grown throughout the world.
The journal includes three issues each year, publishing Reviews, Original research papers, Short notes, New or unusual disease reports, News and opinion, Current topics, Commentaries, and Letters to the Editor.

PHYTOPATHOLOGIA MEDITERRANEA

The international journal of the Mediterranean Phytopathological Union

Volume 60, December, 2021

Firenze University Press

***Phytopathologia Mediterranea*. The international journal of the Mediterranean Phytopathological Union**
Published by
Firenze University Press – University of Florence, Italy
Via Cittadella, 7–50144 Florence–Italy
http://www.fupress.com/pm
Direttore Responsabile: **Giuseppe Surico**, University of Florence, Italy

Phytopathologia Mediterranea
The international journal of the
Mediterranean Phytopathological Union

Firenze University Press
www.fupress.com/pm

Review

Allexivirus: review and perspectives

Faten MANSOURI*, Pavel RYŠÁNEK

Department of Crop Protection, Faculty of Agrobiology, Food and Natural Resources, Czech University of Life Sciences Prague, Kamýcká 129, 165 00, Praha-Suchdol, Czech Republic
*Corresponding author. E-mail: feten.mansouri@live.fr

OPEN ACCESS

Citation: F. Mansouri, P. Ryšánek (2021) *Allexivirus*: review and perspectives. *Phytopathologia Mediterranea* 60(3): 389-402. doi: 10.36253/phyto-12043

Accepted: August 11, 2021

Published: November 15, 2021

Data Availability Statement: All relevant data are within the paper and its Supporting Information files.

Competing Interests: The Author(s) declare(s) no conflict of interest.

Editor: Arnaud G Blouin, New Zealand Institute for Plant and Food Research, Auckland, New Zealand.

Summary. *Allexivirus* (*Alphaflexiviridae*) was first described in 1970 by Razvjazkina. Since then, *Allexivirus* species have been detected in many countries. Although this genus primarily infects plants in the *Amaryllidaceae*, other hosts include plants in the *Fabaceae*, *Rosaceae* and *Orchidaceae*. Thirteen *Allexivirus* species have been assigned. Eight of these infect *Allium* hosts, and these include: shallot virus X (ShVX), garlic virus A (GarV-A), garlic virus B (GarV-B), garlic virus C (GarV-C), garlic virus D (GarV-D), garlic virus E (GarV-E), garlic virus X (GarV-X), and garlic-mite filamentous virus (GarMbFV). Five have been described from non-*Allium* hosts, including blackberry virus E (BVE), vanilla latent virus (VLV), alfalfa virus S (AVS), Arachis pintoi virus (ApV), and Senna severe yellow mosaic virus (SSYMV). This review analyzes the taxonomic positions of the thirteen recognized species and four unassigned species (Allexivirus DS-2013/CZE isolate, shallot mite-borne latent virus (SMbLV), cassia mild mosaic virus (CaMMV), and papaya virus A (PaVA)). Based on the inspection of data, we have concluded that PaVA is an *Allexivirus*, DS-2013/CZE is an isolate of GarV-D, and SMbLV is an isolate of ShVX. Current knowledge of the host ranges, symptoms, genome structure and modes of transmission of these viruses is also summarized, and control measures employed against them are outlined.

Keywords. Taxonomy, genome organization, hosts, transmission, disease management.

INTRODUCTION

Plant viruses cause major problems for agriculture, affecting crop quality and yields (Van der Vlugt, 2006). Several studies have been carried out to understand the emergence, taxonomy, and evolution of different viruses. *Allexivirus* includes thirteen species recognized by the International Committee on Taxonomy of Viruses (ICTV). Allexiviruses are considered as threats to several economically important hosts, due to their occurrence as mixed infections. To date, eight species have been described, primarily infecting alliums, and their major vector has been shown to be the eriophyid mite *Aceria tulipae* (Van Dijk *et al*., 1991). Five other *Allexivirus* species have been described from blackberry, vanilla, forage peanut alfalfa plant, and *Senna rizzinii* (syn. *Cassia chrysocarpa* var. *psilocarpa* Benth.), without their insect vectors being identified.

Allium-infecting allexiviruses were initially found infecting garlic and onion crops (Razvjazkina, 1970). Later, these viruses were described more thoroughly by Van Dijk *et al*. (1991). They were first referred to as onion mite-borne latent virus (OMbLV), shallot mite-borne latent virus (SMbLV) and garlic strain of onion mite-borne latent virus (OMbLV-G) (Van Dijk *et al*., 1991). Kanyuka *et al*. (1992) and Vishnichenko *et al*. (1993) reported the presence of a virus in shallot and named it shallot virus X (ShVX), and this virus was later considered synonymous to OMbLV and SMbLV (Van Dijk and Van der Vlugt, 1994). Allexiviruses were first assigned to *Rymovirus* (*Potyviridae*), based on their transmission by mites and the morphology of the virus particles (Barg *et al*., 1994). Subsequently, they were classified to "*Allexivirus*" within *Alphaflexiviridae*, for which ShVX is the type (Pringle, 1999).

Considerable progress has been made to characterize the genomes and expression of allexiviruses. Determining their biology and epidemiology is important, to be able to apply appropriate disease management strategies. This paper reviews the taxonomic status of *Allexivirus* through phylogenetic analyses and describes their biological properties and the impacts and management of the disease they cause. Perspectives for future research are also provided.

BIOLOGICAL PROPERTIES OF ALLEXIVIRUSES

Current taxonomy

Allexivirus has been assigned to *Alphaflexiviridae* in *Tymovirales* (Kreuze *et al*., 2020). The genus currently comprises thirteen species recognized by the ICTV, distinguished by their coat protein (CP) and replicase coding regions. According to the species demarcation criteria, members of *Allexivirus* share less than 72% nucleotide sequence identity (or 80% amino acid sequence identity) between their CP and replicase, and react differently with antisera (King *et al*., 2012).

The eight allexiviruses that have been detected in *Allium* species are ShVX, garlic virus A (GarV-A), garlic virus B (GarV-B), garlic virus C (GarV-C), garlic virus D (GarV-D), garlic virus E (GarV-E), garlic virus X (GarV-X) and garlic mite-borne filamentous virus (GarMbFV) (King *et al*., 2012). Five additional viruses were assigned to *Allexivirus* based on their genome organization and sequence identities between replicases and/or CP sequences. These viruses are blackberry virus E (BVE), vanilla latent virus (VLV), alfalfa virus S (AVS), Arachis pintoi virus (ApV), and Senna severe yellow mosaic virus (SSYMV) (Sabanadzovic *et al*., 2011; Gutiérrez Sánchez *et al*., 2016; Grisoni *et al*., 2017; Nemchinov *et al*., 2017; Alves *et al*., 2020).

In addition, new virus accessions have been shown to be related to *Allexivirus* but remain unassigned until an assessment by ICTV members. Based on sequence analyses, the unassigned viruses share a high degree of nucleotide (nt) and amino acid (aa) sequence similarity with the existing members of *Allexivirus*. The unassigned viruses comprised four species: SMbLV that was identified as ShVX isolate (GeneBank accession EU835196.1), Allexivirus DS-2013/CZE isolate (JX682826.1), and cassia mild mosaic virus (CaMMV) isolate (partial sequence GU481094.1) (Beserra *et al*. 2011). The *Senna macranthera* isolate was given the name cassia mild mosaic virus based on particle morphology and host range (J.E.A Beserra, personal communication). However, since there was no available information about the nucleotide sequence of the virus, the authors referred to the newly identified allexivirus as Senna virus X (SVX) (Beserra *et al*., 2011).

Phylogenetic analyses and taxonomic impact

Given the global distribution of allexiviruses, insights from phylogenetic analyses provides understanding of the origins and the relatedness between members of the genus. Sequence alignments were performed with MUSCLE (Edgar, 2004) and trees were constructed with nucleotide sequences of the complete genome and CP from selected allexiviruses and closely related unassigned member sequences available in NCBI (https://www.ncbi.nlm.nih.gov/). Phylogenetic trees were constructed using the neighbour-joining (NJ) method with a bootstrap value of 1000 using MEGA X (http://www.megasoftware.net/mega.php) (Kumar *et al*., 2018; Stecher *et al*., 2020) (Figure 1). Only partial sequences of GarMbFV were available in GenBank, so this virus was only included in the analysis of the CP. For the unassigned species CaMMV, only the replicase sequence was available so this species was not included in the analysis. New viruses have been deposited in GenBank as tentative *Allexivirus* species and these include: papaya virus A (PaVA; MN418120.1) (Read *et al*., 2020), garlic virus F (GarV-F; MN059330.1), garlic virus H (GarV-H; MN059332.1), garlic virus G (GarV-G; MN059331.1), garlic virus I (GarV-I; MN059334.1), and garlic yellow virus (GYV; MN059396.1). The viruses PaVA, GarV-F, -H, -G, and -I have been included in the analysis. However, GYV lacks the 42 KDa protein and is more related to *Carlavirus* (>76% nt and aa sequence identity of the CP to *Garlic latent virus*), so GYV was not considered in this review. Potato virus M (PVM, *Carlavirus*) was used

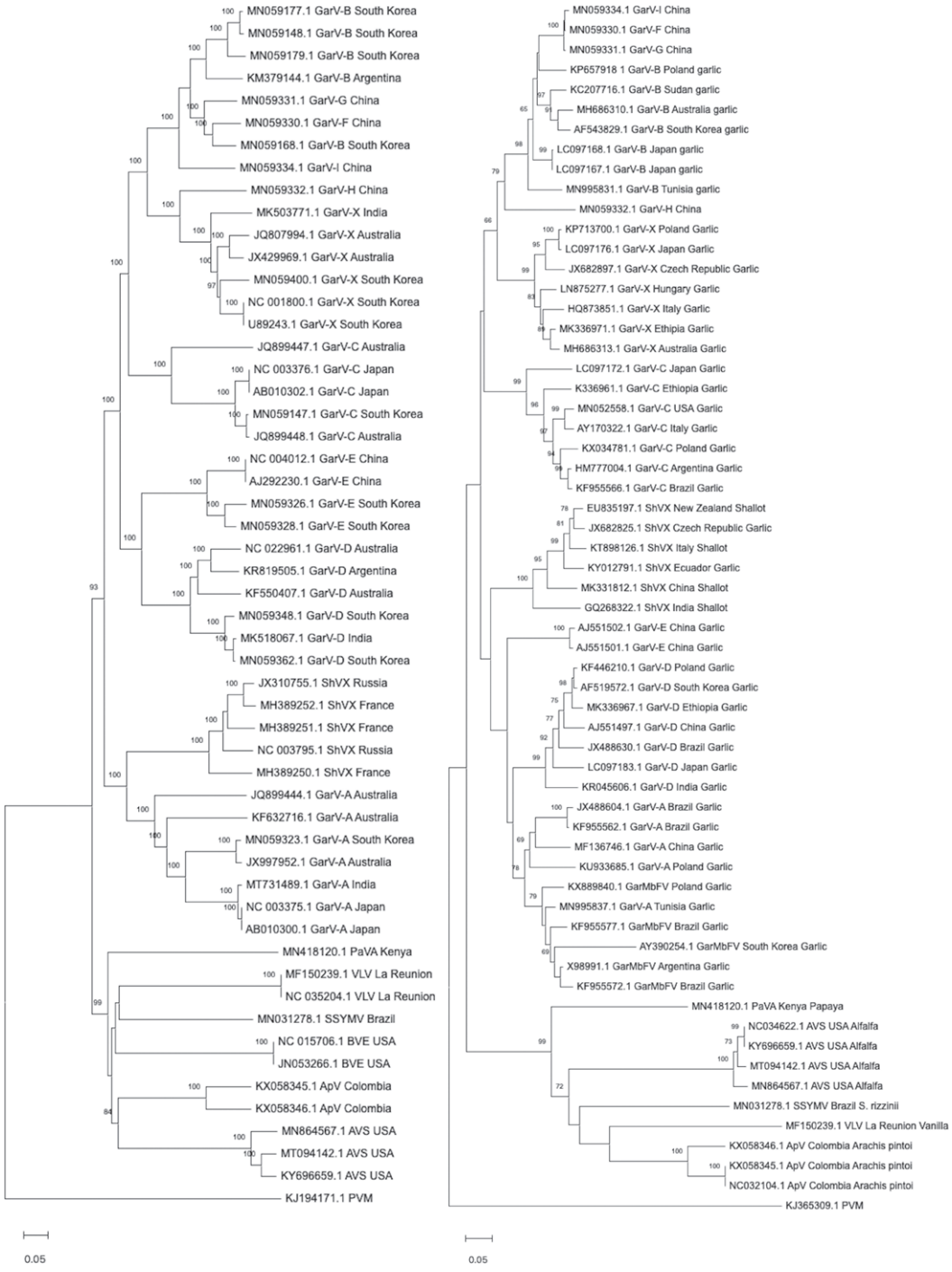

Figure 1. Phylogenetic analysis among *Allexivirus* isolates (ShVX, GarV-A, -B, -C, -D, -E, -X, -F, -G, -H, -I, GarMbFV, AVS, BVE, ApV, VLV, SSYMV, and unclassified PaVA) based on alignment of nucleotide sequences of complete genomes (**A**) and of coat proteins (**B**). Potato virus M (PVM; *Carlavirus*, *Betaflexiviridae*) was used as the outgroup. For the generation of the tree, nucleotide sequences were aligned using MUSCLE (Edgar, 2004), and the tree was constructed using MEGA x (Kumar *et al.*, 2018). The neighbour-joining method was used for the construction of the tree, and the reliability of the branches was inferred from a bootstrap analysis of 1000 replicates. Abbreviations indicated are: shallot virus X (ShVX), garlic virus A (GarV-A), garlic virus B (GarV-B), garlic virus C (GarV-C), garlic virus D (GarV-D), garlic virus E (GarV-E), garlic virus X (GarV-X), garlic mite-borne filamentous virus (GarMbFV), blackberry virus E (BVE), vanilla latent virus (VLV), alfalfa virus S (AVS) and Arachis pintoi virus (ApV), Severe yellow mosaic virus (SSYMV), garlic virus F (GarV-F), garlic virus H (GarV-H), garlic virus I (GarV-I), garlic virus G (GarV-G), and papaya virus A (PaVA). The countries of origin and the accession numbers of the selected *Allexivirus* sequences retrieved from GenBank are shown next to the virus acronyms.

as an outgroup. Sequence similarity and identity analyses were performed in BioEdit (Hall, 1999).

Whole genome phylogenetic analysis divided the allexiviruses into the *Allium* and non-*Allium*-infecting viruses (Figure 1A). Two clades were observed within the *Allium*-infecting group, separating ShVX and GarV-A from the remaining *Allium*-infecting allexiviruses. The unassigned PaVA together with the non-*Allium* allexiviruses BVE, VLV, ApV, AVS, and SSYMV, formed a monophyletic group of distant accessions. Similarly, the CP-based phylogenetic analysis showed the same two clades of the *Allium*-infecting allexivirus group and the non-*Allium* group (Figure 1B). Within the *Allium*-infecting allexivirus clade, two groups were observed: the first comprised GarV-X, -B, -I, -H, -F, -G, and -C isolates. The second group included GarV-D and -E, GarV-A and GarMbFV isolates, and grouped together with ShVX isolates. The second clade included the four non-*Allium* allexiviruses AVS, BVE, VLV, ApV, and SSYMV, while PaVA formed a very distant monophyletic isolate. In view of the high homology in the CP, and based on the phylogenetic tree, the species PaVA could be considered as new species of allexivirus.

Coat protein sequence analysis showed that the SMbLV sequence shared 90.5–97.1% nt sequence identity (97.0–98.0% aa sequence identity) to ShVX isolates (GeneBank: MH389253.1, MH389252.1, KY012791.1). Similarly, DS-2013/CZE isolate (GeneBank: JX682826.1) shared 84.2% nt sequence identity (95.0% aa sequence identity) to GarV-D isolates (GeneBank: JX682863.1, AJ551490.1). Therefore, SMbLV should be considered as an isolate of ShVX, and ShVX should be retained as an ICTV recognized species, and DS-2013/CZE isolate should be considered an isolate of GarV-D. In addition, identity pairwise comparisons of the CP gene of GarV-I, GarV-F and GarV-G showed high degrees of sequence similarity (99.1-99.6% nt sequence identity; 97.9-98.9% aa sequence identity), while GarV-H shared, respectively, 73.0%, 72.6%, and 72.5% nt sequence identity (66.1%, 65.7%, and 65.9% aa sequence identity) with, respectively, GarV-I, -G, and -F. The CP gene of GarV-I shared 85.4 to 99.5% nt sequence identity (72.7–98.9% aa sequence identity) with GarV-B isolates, but the replicase gene analysis of GarV-I identified high identity values with GarV-D isolates (92.1–95.3% nt sequence identity, 96.1-99.7% aa sequence identity). CP sequence analysis also showed that GarV-F, GarV-G, and GarV-H shared high similarity to GarV-B isolates (68.6–99.8% nt identity, 75.6–98.9% aa identity). These values suggest that GarV-F, -G, and -H are different isolates of GarV-B. Based on our analyses, these new accessions retrieved from GenBank as allexiviruses have similar structure, and they are closely related to *Allexivirus*, with evidence of recombination between the species. However, since information about these new accessions is limited, additional information is required to give accurate taxonomic assignation.

The CP and replicase genes have been used to classify species within the genus. Although this criterion has been widely used, there is growing evidence of high similarities existing between some of the *Allexivirus* species (Celli *et al*., 2018; Geering and McTaggart, 2019). For example, when available GarMbFV CP sequences were compared with GarV-A CP sequences, the identity values for CP among the isolates were 79.5 to 81.1% for nt sequences (76.6–81.8% aa sequence identity), all values of which are above the taxonomic classification criteria. Based on the phylogenetic analyses, both species formed a separate well-supported monophyletic cluster (Figure 1B), with the exception of GarV-A Tunisian isolate (GenBank: MN995837.1) that groups with GarMbFV isolates (Figure 1B). The Tunisian GarV-A shared 91.5 to 93.6% nt sequence identity (97.1–98.5% aa sequence identity) with GarMbFV isolates. Our data analysis therefore indicated that the two species are very similar and may be different isolates of the same species. The high similarity observed between the species has been clearly demonstrated by Geering and McTaggart (2019), clarifying the taxonomic position of GarMbFV and GarV-A. These authors concluded that the two species are conspecific. Additionally, since the replicase region used in taxonomic classification is absent, the risk of errors occurring in classification increases, especially in cases when only partial sequences have been determined. In view of these high proportions of sequence identity and as previously proposed (Geering and McTaggart, 2019), we suggest that GarMbFV should be considered as a strain of GarV-A species. Isolation of GarMbFV complete genome sequence is required to confirm the relationship of GarMbFV with GarV-A.

During the CP and replicase gene analysis, high similarity was observed between GarV-B and GarV-X isolates. GarV-B and GarV-X isolates shared 75.4 to 78.1% nt sequences identity (84.4–89.6% aa sequence identity) between the CP sequences, and 73.4 to 74.1% nt sequences identity (81.6–82.9% aa sequence identity) between the replicase sequences, both values of which are greater than demarcation criteria of *Allexivirus* (King *et al*., 2012). Although the different accessions of both isolates are well separated in the phylogenetic analysis, GarV-B and GarV-X have enough homology to be considered as different strains of the same species. Our data analysis confirms previous results of Celli *et al*. (2018), that also indicated possible recombination events within the complete genome of *Allium*-infecting allexiviruses.

Based on the data analysis, we suggest that SMbLV is an isolate of ShVX, DS-2013/CZE is an isolate of GarV-D, while GarMbFV and GarV-A are conspecific, and GarV-B and GarV-X are also conspecific. More data are required to assess the taxonomic status of the sequences of GarV-F, -G, -H, and -I.

The genetic diversity of allexivirus populations has been reported when comparing the CP and the replicase sequences, indicating population differentiation (Chen *et al*., 2001; Melo-Filho *et al*., 2004; Mohammed *et al*., 2013). Our data indicates that phylogenetic clustering among allexivirus isolates was independent of geographical area (Figure 1B). This means that the overall variability is largely due to global trade between countries, and evolutionary forces such as virus occurrence in mixed infections and interactions between different genotypes of the same species (Melo-Filho *et al*., 2004; Mohammed *et al*., 2013). More analysis of the of allexivirus population genetics is required to allow precise understanding of their evolution and genomic diversity within virus populations.

Genome organization and virion properties

Members of *Allexivirus* are single-stranded positive-sense RNA viruses with genome sizes of approx. 9 kb (Chen *et al*., 2004). Virions are flexuous and filamentous, approx. 800 nm in length and 12 nm in diameter (Figure 2). These viruses induce granular inclusion bodies and small bundles of flexible particles in the cytoplasm of the epidermis cells of infected plants (Kang *et al*., 2007). The RNA of allexiviruses is capped at the 5' untranslated region (UTR) terminus with a 7-methylguanosine cap (m_7G) and has a polyadenylated tail at the 3' UTR terminus.

The genome organization of *Allexivirus* members is outlined in Table 1. The number of open reading frames (ORFs) varies among species. The genomes of seven *Allium*-infecting allexiviruses (GarV-A, -B, -C, -D, -E, -X, and ShVX) contains seven ORFs, whereas those of AVS, VLV, ApV and SSYMV contains six ORFs, and that of BVE contains five ORFs (Table 1), and there is no published complete genome sequence of GarMbFV. The first ORF in all *Allexivirus* species is the largest gene, which encodes a putative replicase protein with three conserved motifs: methyl transferase (MET), NTPase/helicase (HEL) and RNA-dependent RNA polymerase (RdRp) (Song *et al*., 1998). The replicase protein of ShVX and AVS contains an oxidative demethylase domain (AlkB) located between the MET and HEL domains that is present in some members of the *Alphaflexiviridae* (Van den Born *et al*., 2008; Nemchinov *et al*., 2017).

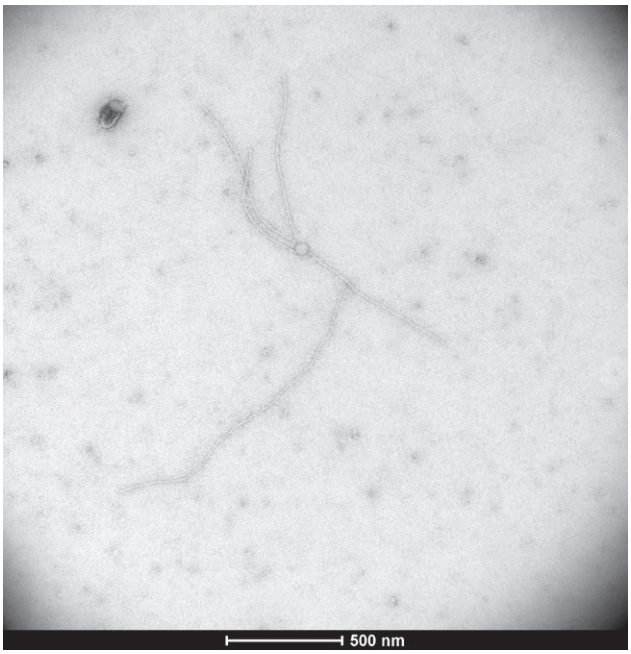

Figure 2. Transmission electron microscopy showing particles of *Garlic virus D* from garlic plants (negative staining with 1 % uranyl acetate). Particle sizes are approx. 800 nm length and 12 nm diameter. Bars represent 500 nm.

Allexiviruses also contains triple gene blocks (TGBs); TGB1 encodes helicase and TGB2 encodes virus movement domains. The two TGBs were shown to be required for viral cell-to-cell movement through plasmodesmata and systemic transport via host phloem tissues (Lezzhov *et al*., 2015). The TGB3 protein was found in all the *Allium*-infecting allexiviruses and in BVE and ApV but lacked the initiation codon. TGB3 synthesis requires a leaky ribosome scanning initiated by a TGB3 CUG initiator codon, rather than internal ribosome entry (Lezzhov *et al*., 2015). This mechanism is commonly used by RNA viruses to translate functionally multicistronic messages (Firth and Brierley, 2012). The TGB3 of the VLV, AVS, SSYMV and the unclassified virus PaVA had the initiation AUG start codon (Grisoni *et al*., 2017; Nemchinov *et al*., 2017; Read *et al*., 2020; Alves *et al*., 2020). Presumably, the TGB3 may have an accessory function alongside the TGB1 and TGB2 in cell-to-cell movement of the viruses (Morozov and Solovyev, 2003).

Another large ORF, downstream of the TGB, encoding a protein of approx. 42 KDa, is found in all allexiviruses, and this has no homology to any known protein of other genera (King *et al*., 2012). The 42 KDa protein contains a serine and threonine-rich protein and has been shown to be involved in virion assembly and act as

Table 1. Genome size, number and molecular weight of proteins encoded by the genes of each *Allexivirus*.

Virus species	GenBank accession	Genome size (nt)[1]	Number of ORF	Molecular weight (KDa)							Reference
				Replicase	TGB1	TGB2	TGB3	42K protein	CP	NABP	
GarV-A	AB010300	8660	7	183	28	11	7*	39	28	15	Sumi *et al*., 1999
GarV-B	KM379144	8327	7	168	27	12	7*	39	27	14	Celli *et al*., 2018
GarV-C	AB010302	8405	7	175	27	11	7*	41	28	15	Sumi *et al*., 1999
GarV-D	KF555653	8424	7	177	26	11	7*	40	27	15	Wylie *et al*., 2014
GarV-E	AJ292230	8451	7	176	27	11	7*	40	35	15	Chen and Chen, 2002
GarV-X	U89243	8458	7	174	26	12	7*	32	36	15	Song *et al*., 1998
ShVX	M97264	8890	7	195	26	11	7*	42	28	15	Kanyuka *et al*., 1992
BVE	JN053266	7718	5	169	27	12	11*	40	25	-**	Sabanadzovic *et al*., 2011
AVS	KY696659	8349	6	188	26	11	10	38	32	-**	Nemchinov *et al*., 2017
ApV	KX058345	7599	6	158	26	12	8	41	26	-**	Gutiérrez Sánchez *et al*., 2016
VLV	MF150239	7462	6	161	26	11	8	41	25	-**	Grisoni *et al*., 2017
SSYMV	MN031278	7829	6	164	26	11	9	37	28	-**	Alves *et al*., 2020

[1] nt= nucleotides, ORF= open reading frame, TGB = triple gene block, 42K protein = protein of unknown function, CP = Coat protein, NABP = nucleic acid binding protein, GarV-A = *Garlic virus A*, GarV-B = *Garlic virus B*, GarV-C = *Garlic virus C*, GarV-D = *Garlic virus D*, GarV-E = *Garlic virus E*, GarV-X = *Garlic virus X*, ShVX = *Shallot virus X*, BVE = *Blackberry virus E*, VLV = *Vanilla latent virus*, AVS = *Alfalfa virus S*, ApV = *Arachis pintoi virus*.

* Untranslated TGB-like gene that lacks the initiator AUG codon and partially overlapping with the TGB2 genes.

** No sequence was identified.

a co-factor to facilitate the interaction of the capsid protein with genomic RNA during assembly (Vishnichenko *et al*., 2002).

The coat protein (25-36 KDa) shares the conserved structural core and evolutionary origin of some families of filamentous plant viruses and shows high similarity to carla- and potex-viruses (Kanyuka *et al*., 1992; Martelli *et al*., 2007). Only the eight viruses infecting *Allium* (ShVX, GarV-A, -B, -C, -D, -E, -X, and GarMbFV) have an additional ORF, that contains a nucleic acid binding domain (NABP). This ORF contains a small cysteine-rich protein (CRP), a basic arginine-rich domain and a zinc-finger motif at the 3'-terminal region (Song *et al*., 1998; Kanyuka *et al*., 1992). Although CRPs of many plant viruses were shown to act as RNA silencing suppressors (Senshu *et al*., 2011; Fujita *et al*., 2018), Arkhipov *et al*. (2013) did not observe this activity in ShVX. The allexivirus CPR is likely to be necessary for the regulation of virus RNA replication, together with pathogenicity determinants during allexivirus evolution and control interactions of the viruses with their plant hosts (Lukhovitskaya *et al*., 2014, Yoshida *et al*., 2018).

Various nucleotide insertions between CP and CRP genes have been observed in GarV-B, GarV-C and GarV-X. These insertions are complementary to garlic 18S ribosomal RNA (rRNA) and are probably involved in the termination-reinitiation translation mechanism (Yoshida *et al*., 2018). It is possible that GarV-B, -C, and -X utilize this mechanism to regulate the expression of virus protein, to enable adaptations to specific hosts and vectors (Gramstat *et al*., 1994).

Virus proteins are often multifunctional, and each function is essential for virus survival and can be dependent on virus species, host and/or vector. Further research is required to clarify the entire allexiviruses infection process. How these viruses avoid host defense mechanisms and what are the functional features of the virus genomes, are essential questions to allow full understanding of the expression of allexiviruses and their interactions with their hosts plants.

PATHOLOGY AND MANAGEMENT OF ALLEXIVIRUSES

Distribution, host range, and transmission

To date, *Allium*-infecting allexiviruses have been recorded in all *Allium* producing regions (Table 2), while the non-*Allium*-infecting allexiviruses have only been reported in countries where they were first described (Sabanadzovic *et al*., 2011; Gutiérrez Sánchez *et al*., 2016; Grisoni *et al*., 2017; Nemchinov *et al*., 2017; Alves *et al*., 2020). However, it is most likely that these viruses are more broadly distributed than currently is known, especially where their host plants are cultivated.

The natural host range of allexiviruses has been reported to be restricted to several cultivated, ornamen-

Table 2. Geographical distribution of allexiviruses.

Location	Detected viruses[1]	References
China	GarV-A, -D, -E, -X, ShVX, GarV-B (GarV-F, GarV-I, GarV-G, and GarV-H)[2]	Chen *et al*., 2001, 2004
Japan	GarV-A, -B, -C, -D, GarMbFV	Sumi *et al*., 1993; Yamashita *et al*., 1996
South Korea	GarV-A, -B, -C, -D, -E, -X	Kang *et al*., 2007; lee *et al*., 2007
India	GarV-A, -C, -D, -X, GarMbFV, ShVX	Mandal *et al*., 2017
Iran	GarV-A, -B, -C, -D, ShVX	Shahraeen *et al*., 2008
Russia	ShVX	Kanyuka *et al*., 1992; Vishnichenko *et al*., 1993
Turkey	GarV-B, -D, -X, GarMbFV	Fidan, 2010; Fidan *et al*., 2013
Italy	GarV-B, -D, -X, ShVX	Taglienti *et al*., 2017
Poland	GarV-A, -B, -D, -X, GarMbFV, ShVX	Bereda *et al*., 2017
France	ShVX	Marais *et al*., 2019
Greece	GarV-C, -D, GarMbFV	Dovas *et al*., 2001
Czech Republic	GarV-A, -B, -C, -D, -E, -X, GarMbFV, ShVX	Klukáčková *et al*., 2007
Slovenia	GarV-A, -B, -C, -D, -E, -X, GarMbFV, ShVX	Mavrič and Ravnikar, 2005
Spain	GarV-B, -D, -X	Tabanelli *et al*., 2004
United Kingdom	ShVX	Ryabov *et al*., 1996
Netherlands	OMBLV, SMbLV[3]	Van Dijk *et al*., 1991
Argentina	GarV-A, -B, -C	Cafrune *et al*., 2006a
Mexico	GarV-D	Rocha and Esmeralda, 2019
Brazil	GarV-A, -B, -D, -X, GarMbFV, SSYMV	Oliveira *et al*., 2014; Alves *et al*., 2020
Colombia	ApV	Gutiérrez Sánchez *et al*., 2016
Ecuador	ShVX	Granda *et al*., 2017
USA	GarV-B, -C,-D, -E, ShVX, AVS, BVE	Gieck *et al*., 2009; Sabanadzovic *et al*., 2011; Nemchinov *et al*., 2017; Wijayasekara *et al*., 2019
Sudan	GarV-A, -B, -X, ShVX	Mohammed *et al*., 2013; Hamed *et al*., 2012
La reunion	VLV	Grisoni *et al*., 2017
Ethiopia	GarV-B, -C, -D, -X	Jemal *et al*., 2015; Abraham *et al*., 2019
DR Congo	GarV-D	Majumder *et al*., 2019
New Zealand	GarV-A, -B, -D, ShVX	Ward *et al*., 2009
Australia	GarV-A, -B, -C, -D, -E, -X	Wylie *et al*., 2014; Nurulita *et al*., 2020

[1] GarV-A = *Garlic virus A*, GarV-B = *Garlic virus B*, GarV-C = *Garlic virus C*, GarV-D = *Garlic virus D*, GarV-E = *Garlic virus E*, GarV-X = *Garlic virus X*, GarV-F = *Garlic virus F* (GenBank accession MN059330.1), GarV-H = *Garlic virus H* (MN059332.1), GarV-G = *Garlic virus G* (MN059331.1), GarV-I = *Garlic virus I* (MN059334.1), GarMbFV = *Garlic-mite borne filamentous virus*, ShVX = *Shallot virus X*, BVE = *Blackberry virus E*, VLV = *Vanilla latent virus*, AVS = *Alfalfa virus S*, ApV = *Arachis pintoi virus*.
[2] Based on phylogenetic and sequence analysis, GarV-F, -H, -G, and -I are conspecific of GarV-B.
[3] Onion mite-borne latent virus (OMbLV) and shallot mite-borne latent virus (SMbLV) were the first name species given for *Allium*-infecting allexiviruses, later identified as shallot virus X (ShVX).

tal, and wild *Allium* species (Table 3). *Allium*-infecting allexiviruses, have been shown to only infect monocotyledon plants in the *Asparagales* (Van Dijk *et al*., 1991; Fidan *et al*., 2013). The only exception was detection of GarV-D on *Drimia maritima* (L.) (*Asparagaceae*), which is, to date, the only reported natural occurrence of *Allium*-infecting allexiviruses in a non-*Alliaceae* host (Fidan *et al*., 2013). The presence of *Allium*-infecting allexiviruses in *D. maritima* suggests that either the virus is expanding its host range (new host adaptation), or that it has always been present unnoticed in other host families.

ApV, AVS, BE, VLV, and SSYMV have been reported to naturally infect dicotyledonous plants in the *Rosaceae, Fabaceae, Orchidaceae* and *Caricaceae* (Table 3). The unclassified allexivirus PaVA was detected in *Carica papaya* L. (Read *et al*., 2020) and CaMMV was detected in *S. macranthera* (Beserra *et al*., 2011).

Most members of *Allexivirus* are transmissible from natural to experimental hosts by mechanical inoculation. *Allium*-infecting allexiviruses can be transmitted to several diagnostic hosts, including *Chenopodium quinoa*, *C. murale*, *C. amaranthicolor, Gomphrena globosa,*

Table 3. Natural hosts and experimental host range when mechanically inoculated with one of allexiviruses.

Virus species[1]	Natural hosts	References	Experimental hosts (References)
GarV-A	*Allium ampeloprasum, A. angulosum, A. ascalonicum, A. anisopodium, A. caesium, A. chinense, A. bucharicum, A. carinatum, A. cyathophorum, A. cernuum, A. flavum, A. hybridum, A. ledebourianum, A. microdictyon, A. moly, A. narcissiflorum, A. neapolitanum, A. nutans, A. oleraceum, A. ramosum, A. runyonii, A. roseum, A. rotundum, A. sativum, A. senescens, A. scabriscapum, A. schoenoprasum, A. scorodoprasum, A. sphaerocephalon, A. stipitatum, A. suaveolens, A. tuberosum, A. thunbergii, A. ursinum, A. victorialis* var. *platyphyllum*, *A. vineale*	Yamashita *et al*., 1996; Ward *et al*., 2009; Park *et al*., 2011; Mansouri *et al*., 2021a	*Chenopodium murale*, *Gomphrena globosa*, *C. amaranticolor*, *C. quinoa, Atriplex hortensis, C. foliosum, C. opulifolium*, *A.cepa*, *A. ampeloprasum, Nicotiana benthamiana* (Van Dijk *et al*., 1991, Yamashita *et al*., 1996; Melo-Filho *et al*., 2004; Cafrune *et al*., 2006a; Dąbrowska *et al*., 2020)
GarV-B	*A. anisopodium, A. chinense, A. caeruleum, A. caesium, A. sphaerocephalum, A. cyathophorum, A. cernuum, A. flavum, A. ledebourianum, A. hybridum, A. narcissiflorum, A. neapolitanum, A. nutans, A. oleraceum, A. oreophilum, A. sativum, A. schoenoprasum, A. scorodoprasum, A. senescens, A. stipitatum, A. suaveolens, A. tuberosum, A. ursinum*	Ward *et al*., 2009; Bampi *et al*., 2015; Paduch-Cichal and Bereda, 2017; Mansouri *et al*., 2021a	
GarV-C	*A. ampeloprasum, A. caeruleum, A. angulosum, A. bulgaricum, A. carinatum, A. caesium, A. cepa L., A. cyathophorum, A. cernuum, A. flavum, A. microdictyon, A. moly, A. narcissiflorum, A. neapolitanum, A. nutans, A. oleraceum, A. oreophilum, A. ramosum, A. roseum, A. rotundum, A. sativum, A. sphaerocephalum, A. schoenoprasum, A. scorodoprasum, A. senescens, A. suaveolens, A. tuberosum, A. ursinum, A. vineale*	Shahraeen *et al*., 2008; Ward *et al*., 2009; Bampi *et al*., 2015 ; Mansouri *et al*., 2021a	
GarV-D	*A. atropurpureum, A. sativum, A. cepa L., A. caesium, Drimia maritima, A. ascalonicum, A. fistulosum, A. caeruleum, A. sphaerocephalum, A. angulosum, A. flavum, A. hybridum, A. karataviense, A. macrostemon, A. moly, A. oreophilum, A. scabriscapum, A. senescens, A. thunbergii*	Ward *et al*., 2009; Fidan *et al*., 2013; Bampi *et al*., 2015; Paduch-Cichal and Bereda, 2017; Mansouri *et al*., 2021a	
GarV-E	*A. caeruleum, A. cernuum, A. flavum, A. sativum, A sphaerocephalum, A. scorodoprasum*	Chen and Chen, 2002; Bampi *et al*., 2015; Mansouri *et al*., 2021a	
GarV-X	*A. caesium, A. hybridum, A. karataviense, A. sativum, A. schubertii*	Song *et al*., 1998; Mansouri *et al*., 2021a	
GarMbFV	*A. caesium, A. cepa L., A. cernuum, A. flavum, A. hybridum, A. karataviense, A. moly, A. oreophilum, A. sativum, A. schubertii*	Dovas *et al*., 2001; Mansouri *et al*., 2021a	
ShVX	*A. angulosum, A. altaicum, A. ascalonicum, A. anisopodium, A. bucharicum, A. caeruleum, A. caesium, A. sativum, A. cepa L.* var. *aggregatumA. ledebourianum, A. hybridum, A. sphaerocephalum, A. flavum, A. bulgaricum, A. cyathophorum, A. cernuum, A. microdictyon, A. moly, A. narcissiflorum, A. neapolitanum, A. nutans, A. oleraceum, A. oreophilum, A. przewalskianum, A. ramosum, A. rotundum, A. scabriscapum, A. scorodoprasum, A. stipitatum, A. suaveolens, A. tuberosum, A. ursinum, A. vineale*	Ward *et al*., 2009; Hamed *et al*., 2012; Bampi *et al*., 2015; Taglienti *et al*., 2017; Paduch-Cichal and Bereda, 2017; Mansouri *et al*., 2021a	
BVE	*Rubus* L.	Sabanadzovic *et al*., 2011	
VLV	*Vanilla planifolia, V. pompona, V. humblotii*	Grisoni *et al*., 2017	*V. planifolia*
ApV	*Arachis pintoi*	Gutiérrez Sánchez *et al*., 2016	
AVS	*Medicago sativa*	Nemchinov *et al*., 2017	
SSYMV	*Senna rizzini*	Alves *et al*., 2020	*C. amaranticolor*, *C. quinoa*, *G. globosa*, *S. rizzinii*, *S. occidentalis*

[1] GarV-A = *Garlic virus A*, GarV-B = *Garlic virus B*, GarV-C = *Garlic virus C*, GarV-D = *Garlic virus D*, GarV-E = *Garlic virus E*, GarV-X = *Garlic virus X*, GarMbFV = *Garlic-mite borne filamentous virus*, ShVX = *Shallot virus X*, BVE = *Blackberry virus E*, VLV = *Vanilla latent virus*, AVS = *Alfalfa virus S*, ApV = *Arachis pintoi virus*.

Nicotiana occidentalis and *Atriplex hortensis* (Van Dijk *et al*., 1991; Yamashita *et al*., 1996). VLV is mechanically transmitted to its natural vanilla host (*Vanilla planifolia*) (Grisoni *et al*., 2017). SSYMV is mechanically transmitted to *S. rizzinii*, *S. occidentalis, C. amaranticolor*, *G. globosa*, and the unassigned CaMMV is transmitted mechanically to *S. macranthera, Phaseolus vulgaris*, and *G. globosa* (Beserra *et al*., 2011; Alves *et al*., 2020).

Allium-infecting allexiviruses are transmitted by their major vector, the eriophyid mite *Aceria tulipae* Keifer (Van Dijk *et al*., 1991). The *Allium*-infecting allexiviruses have been successfully transmitted to leek plants (*Allium ampeloprasum*) by *A. tulipae* (Dąbrowska *et al*., 2020; Mansouri *et al*., 2021b). The transmission characteristics of these viruses, including acquisition time, inoculation time, persistence in the vector, and effectiveness of the transmission, have been recently described as semipersistent (Mansouri *et al*., 2021b). Studies on other mite-transmitted viruses indicated a similar mode of transmission (Gispert *et al*., 1998; Kulkarni *et al*., 2002).

Potential vectors of the non-*Allium* allexiviruses have not yet been identified and are different to the those of other allexiviruses, because *A. tulipae* was shown to be restricted to alliums (Kiedrowicz *et al*., 2017). Dissemination of these viruses probably takes place through the distribution of infected propagative materials, which is a major mode for the long-distance dissemination of allexiviruses (King *et al*., 2012). In addition, detailed studies on the transmission of the non-*Allium* allexiviruses are required to understand and prevent their dissemination.

Economic impacts and disease management

The *Allium*-infecting allexiviruses are responsible for important economic impacts, although they only cause mild host symptoms (mild mosaic, yellow stripes, stunted growth) in natural infections (Kang *et al*., 2007). These viruses have been reported to cause yield losses and reduce quality of several *Allium* crops (Cafrune *et al*., 2006b). Single infection with either GarV-C or GarV-A resulted in decreased garlic bulb weight (approx. 15% reduction) and diameter (approx. 5%) (Cafrune *et al*., 2006a; Perotto *et al*., 2010). Single infection with GarV-D caused a 12% reduction in garlic bulb weight and 7% of bulb quality (Celli *et al*., 2016). Although infections of garlic crops by one of the *Allium*-infecting allexiviruses alone could result in diseases, yield losses were considerably more severe when allexiviruses occurred in mixed infections, especially in the presence of *Potyvirus* and *Carlavirus* species (Conci *et al*., 2003). Little research has been reported on the non-*Allium* allexiviruses since their discovery, suggesting that they have low prevalence on their host crops. Although BVE and ApV cause mild host symptoms (e.g., chlorosis and vein yellowing), it is possible that these symptoms are exhibited due to mixed virus infections (Sabanadzovic *et al*., 2011; Martin and Tzanetakis, 2015; Gutiérrez Sánchez *et al*., 2016).

Allexiviruses present distinct challenges for control and management of their spread and emergence in several crops. These viruses are not seedborne, but they have been introduced in different countries via infected plant material. Disease control methods, including diagnosis, sanitation, sanitary certification, host resistance and vector management, are all likely to be key factors for the effective management of these diseases. Other approaches, such as conventional host breeding, transgenic methods, and gene silencing strategies, have been used to control RNA viruses (Chaudhary, 2018). It is therefore important that the biology of viruses is fully understood so that these methods can be utilized to limit the spread of viruses.

The use of healthy planting material is one of the most effective methods for controlling viruses and maintaining good crop yields (Torres *et al*., 2000; Salomon, 2002). *In vitro* tissue culture techniques, such as micropropagation, meristem culture, thermotherapy, chemotherapy, cryotherapy, and somatic embryogenesis, have been used for production of virus-free garlic plants (Ghaemizadeh *et al*., 2014; Manjunathagowda *et al*., 2017). Although these techniques have been used successfully in the elimination of allexiviruses in alliums, these viruses remain major problems because these crops are easily re-infected once they are planted in fields. Re-infections occur from vector transmission from nearby infected crops, such as garlic and onion (Taglienti *et al*., 2017). Regular crop inspection for vectors and strict pest control management are essential throughout crop growth.

There have been no reports of *in vitro* sanitation and control management for BVE, ApV, AVS, VLV and the newly unassigned viruses. However, the use of virus-free planting material can effectively control these viruses. Development of transgenic berry crops and legumes has been reported to limit damaging viruses in different families (Hill *et al*., 1991; Divakaran *et al*., 2008; Martin and Tzanetakis, 2015). Therefore, the use of host resistance and transgenic varieties may be worthwhile strategies for management of allexiviruses. Although limited effectiveness has been reported, further research is required on the modes of transmission of the non-allium allexiviruses.

PERSPECTIVES

Plant viruses are major problems in many vegetable and ornamental crops, causing economic losses as high as 50 billion euros per year (Zhao *et al*., 2017), especially in crops for which no virus-resistant varieties are available. Allexiviruses continue to be threats to *Allium* production. Key areas for future research are: i) the understanding of basic allexivirus biology, including how their genomes contribute to infection processes; and ii) the underlying mechanisms governing their interactions with host plants, and their vectors.

The trade of infected plant material locally, regionally, and globally has been the most important factor in dissemination of allexiviruses, causing high yield losses. Improved techniques for rapid detection and diagnosis, including the use of molecular and serological tools such as enzyme-linked immunosorbent assay (ELISA), reverse transcription polymerase chain reaction (RT-PCR), and RT quantitative PCR (RT-qPCR), are essential to assist effective disease management decisions. In addition to the use of traditional cultural practices, especially control of nearby infected crops and vector hosts, management tactics must also account for climate change. Use of high phytosanitary standards for exchanged plant material, grower, and public education about these viruses their management, are all important to avoid crop yield losses.

Climate change poses a new challenge that may affect the distribution and survival of plant viruses and their vectors, and is likely to aggravate virus epidemics (Jones, 2014; 2018). Climate change can also affect virulence and pathogenicity of plant viruses including allexiviruses, by increasing disease and insect pest outbreaks (Trebicki, 2020). Outbreaks of severe epidemics, coupled with increased long-distance pathogen and vector dispersal through the exchange of infected plant material, will lead to yield losses. Therefore, understanding of *Allexivirus* epidemiology is required to anticipate challenges ahead, and to develop effective strategies to secure global food production for the future (Trebicki, 2020).

The use of sensitive methods, such as transcriptomic analysis and RNA sequencing (RNAseq), may provide valuable insights into host factors that differentially interact with viruses (Kamenetsky *et al*., 2015; Khandagale *et al*., 2020). These methods can enhance understanding of host-virus interaction mechanisms and can lead to the discovery of genes involved in plant defense responses. One recent addition to genetic engineering is the development of the characteristic clustered regularly interspaced short palindromic repeats-associated 9 (CRISPR/Cas9) protein, that has emerged as a potent genome-editing tool to confer resistance against viruses (Khan *et al*., 2018). Implementation of CRISPR/Cas9 to modify host plants and introduce effective resistance against allexiviruses and their vectors could be worthwhile (Khandagale *et al*., 2020). These host modification techniques will complement traditional resistance breeding strategies to achieve improve levels of virus resistance.

ACKNOWLEDGEMENTS

Dr Katja Richert-Pöggeler and her staff (Institute for Epidemiology and Pathogen Diagnostics, Julius Kühn Institute) are thanked for assistance with transmission electron microscopy. Professor Marek Szndel (Warsaw University of Life Sciences, Poland) and Dr. Khushwant Singh (Crop Research Institute, Czech Republic) critically reviewed the manuscript of this paper, and anonymous referees who also improved and clarified the manuscript. This review was supported by CIGA grant (CIGA 20182014), Czech University of Life Sciences Prague in the Czech Republic.

LITERATURE CITED

Abraham A.D., Kidanemariam D.B., Holton T.A., 2019. Molecular identification, incidence and phylogenetic analysis of seven viruses infecting garlic in Ethiopia. *European Journal of Plant Pathology* 155:181–191.

Alves T.M., Silva de Novaes Q., de Paula A., Camelo-García V. M., Nagata T., … Kitajima E.W., 2020. Near-complete genome sequence and biological properties of an *Allexivirus* found in *Senna Rizzinii* in Brazil. *Archives of Virology* 165: 1463–1467.

Arkhipov A.V., Solovyev A.G., Vishnichenko V.K., 2013. Reproduction of *Shallot virus X* in absence of its own active suppressor protein of RNA silencing. *Russian Agricultural Sciences* 39: 218–221.

Bampi D., Reinsel M.D., Hammond J., 2015. Viruses present in ornamental *Allium* in the United States. In: *Proceedings of the APS Annual Meeting 1st-5th August, Pasadena, California,* USA, 513.

Barg E., Lesemann D.E., Vettren H.J., Green S.K., 1994. Identification, partial characterization and distribution of viruses infecting *Allium* crops in South and Southeast Asia. *Acta Horticulturae* 358: 251–258.

Bereda M., Paduch-Cichal E., Dąbrowska E., 2017. Occurrence and phylogenetic analysis of allexiviruses identified on garlic from China, Spain and Poland commercially available on the Polish retail market. *European Journal of Plant Pathology* 149: 227–237.

Beserra J.E.A., de Carvalho M.G., Barguil B.M., Murilo Zerbini F., 2011. Partial genome sequence of a Potyvirus and of a virus in the order Tymovirales found in *Senna macranthera* in Brazil. *Tropical Plant Pathology* 36: 116–120.

Cafrune E.E., Perotto M.C., Conci V.C., 2006a. Effect of two *Allexivirus* isolates on garlic yield. *Plant Disease* 90: 898–904.

Cafrune E.E., Balzarini M., Conci V.C., 2006b. Changes in the concentration of an *Allexivirus* during the crop cycle of two garlic cultivars. *Plant Disease* 90: 1293–1296.

Celli M.G., Perotto M.C., Buraschi D., Conci V.C., 2016. Biological and molecular characterization of *Garlic virus D* and its effects on yields of garlic. *Acta Horticulturae* 1143: 193–200.

Celli M.G., Perotto M.C., Luciani C.E., Pozzi E.A., Conci V.C., 2018. Molecular characterization of the *Garlic virus B* genome and evidence of *Allexivirus* recombination. *European Journal of Plant Pathology* 153: 307–316.

Chaudhary K., 2018. CRISPR/Cas13a targeting of RNA virus in plants. *Plant Cell Reports* 37: 1707–1712.

Chen J., Chen J., 2002. Genome organization and phylogenetic tree analysis of *Garlic virus E*, a new member of genus *Allexivirus*. *Chinese Science Bulletin* 47: 33–37.

Chen J., Chen J., Adams M.J., 2001. Molecular characterization of a complex mixture of viruses in garlic with mosaic symptoms in China. *Archives of Virology* 146: 1841–1853.

Chen J., Zheng H.Y., Antoniw J.F., … Lin, L., 2004. Detection and classification of allexiviruses from garlic in China. *Archives of Virology*, 149: 435–44.

Conci V. C., Canavelli, A., Lunello, P., Di Rienzo, J., Nome, S. F., Zumelzu, G., Italia, R., 2003. Yield losses associated with virus-infected garlic plants during five successive years. *Plant Disease* 87: 1411–1415.

Dąbrowska E., Lewandowski M., Koczkodaj S., Paduch-Cichal E., 2020. Transmission of Garlic virus B, Garlic virus C, Garlic virus D and Garlic virus X by *Aceria tulipae* (Keifer) in leek. *European Journal of Plant Pathology* 157: 215–222.

Divakaran M., Pillai G.S., Babu K.N., Peter, K.V., 2008. Isolation and fusion of protoplasts in Vanilla species. *Current Science* 94:115–120.

Dovas C.I., Hatziloukas E., Salomon R., Barg E., Shiboleth Y., Katis N.I., 2001. Incidence of viruses infecting *Allium* spp. in Greece. *Journal of Phytopathology* 149: 1–7.

Edgar R.C., 2004. MUSCLE: multiple sequence alignment with high accuracy and high throughput. *Nucleic Acids Research* 32: 1792–1797.

Fidan H., 2010. *Detection of Main Virus Diseases on Garlic, Onion and Leek Plants and Determination of Reaction of Taşköprü 56 Garlic Types Against to Common Virus Diseases in Turkey*. (Doctoral dissertation, Çukurova University)

Fidan H., Çaglar B.K., Baloglu S., Yilmaz M.A., 2013. *Urginea maritima (L.)* is a new host of *Allexivirus* group on onion and garlic plants in Turkey. *Acta Horticulturae* 1002: 309–312.

Firth A.E., Brierley I., 2012. Non-Canonical Translation in RNA Viruses. *Journal of General Virology* 93: 1385–1409.

Fujita N., Komatsu K., Ayukawa Y., Matsuo Y., Hashimoto M., … Arie T., 2018. N-terminal region of cysteine-rich protein (CRP) in carlaviruses is involved in the determination of symptom types. *Molecular Plant Pathology* 19: 180–90.

Geering A.D.W., Mctaggart A.R., 2019. Questions surrounding the taxonomic validity of the species Garlic miteborne filamentous virus (genus *Allexivirus*). *Archives of Virology* 164: 2367–2370.

Ghaemizadeh F., Dashti F., Khodakaramian G., Sarikhani H., 2014. Combination of stem-disc dome culture and thermotherapy to eliminate Allexiviruses and *Onion yellow dwarf virus* from garlic (*Allium sativum* cv. Hamedan). *Archives of Phytopathology and Plant Protection* 47: 499–507.

Gieck S.L., Hamm P.B., David N.L., Pappu H.R., 2009. First report of *Garlic virus B* and *Garlic virus D* in garlic in the Pacific Northwest. *Plant Disease* 93: 431.

Gispert C., Oldfield, G.N., Perring, T.M., Creamer, R., 1998. Biology of the transmission of peach mosaic virus by *Eriophyes insidiosus* (Acari: Eriophyidae). *Plant Disease* 82: 1371–1374.

Gramstat A., Prüfer D., Rohde, W., 1994. The nucleic acid-binding zinc finger protein of potato virus M is translated by internal initiation as well as by ribosomal frameshifting involving a shifty stop codon and a novel mechanism of P-site slippage. *Nucleic Acids Research* 22: 3911–3917.

Granda R., Landázuri G., Arkhipov A.V., 2017. First Report of *Shallot virus X* in Garlic in Ecuador. *Plant Disease* 101: 1066.

Grisoni M., Marais A., Filloux D., Saison A., Faure C., … Candresse T., 2017. Two novel *Alphaflexiviridae* members revealed by deep sequencing of the Vanilla (*Orchidaceae*) virome. *Archives of Virology* 162: 3855–3861.

Gutiérrez Sánchez P.A., Jaramillo Mesa H., Marin Montoya M., 2016. Next generation sequence analysis of the forage peanut (*Arachis pintoi*) virome. *Revista Facultad Nacional de Agronomía* 69: 7881–7891.

Hall T.A., 1999. BioEdit: a user-friendly biological sequence alignment editor and analysis program for windows 95/98/ NT. *Nucleic Acids Symposium Series* 41: 95–98.

Hamed K., Menzel W., Mohamed M. E., Dafallah G., Gadelseed A.M.A., Winter S., 2012. First Report of *Shallot virus X* in Onion in Sudan. *Plant Disease* 96: 1075–1075.

Hill K., Jarvis-Eagan N., Halk E., Krahn K.J., Liao L.W., … Loesch-Fries L.S., 1991. The Development of Virus-Resistant Alfalfa, Medicago sativa L. *Biotechnology* 9: 373–377.

Jemal K., Abraham A., Feyissa T., 2015. The Occurrence and Distribution of Four Viruses on Garlic (Allium sativum L.) in Ethiopia. *International Journal of Basic and Applied Sciences* 4: 5–11.

Jones R.A.C., 2014. Plant virus ecology and epidemiology: Historical perspectives, recent progress and future prospects. *Annals of Applied Biology* 164: 320–347.

Jones R.A.C., 2018. Future Scenarios for Plant Virus Pathogens as Climate Change Progresses. *Advances in Virus Research* 95: 87–147.

Kamenetsky R., Faigenboim A., Mayer E.S., Michael T.B., Gershberg C., … Sherman A., 2015. Integrated transcriptome catalogue and organ-specific profiling of gene expression in fertile garlic (*Allium sativum* L.). *BMC Genomics* 16: 12.

Kang S.G., Bong J.K., Eun T.L., Moo U.C., 2007. *Allexivirus* transmitted by eriophyoid mites in garlic plants. *Journal of Microbiology and Biotechnology* 17: 1833–1840.

Kanyuka K.V., Vishichenko V.K., Levy K.E., Zavriev S.K., 1992. Nucleotide sequence of *shallot virus X* RNA reveals a 5'-proximal cistron closely related to those of potexviruses and a unique arrangement of the 3'-proximal cistrons. *Journal of General Virology* 73: 2553.

Khan M.Z., Amin I., Hameed A., Mansoor S., 2018. CRISPR–Cas13a: Prospects for Plant Virus Resistance. *Trends in Biotechnology* 36: 1207–1210.

Khandagale K., Krishna R., Roylawar P., Ade1 A.B., Benke A., … Rai A., 2020. Omics approaches in Allium research: Progress and way ahead. *PeerJ* 8: 1–34.

Kiedrowicz A., Szydło W., Skoracka A., 2017. Population growth rate of dry bulb mite, Aceria tulipae (Acariformes: Eriophyidae), on agriculturally important plants and implications for its taxonomic status. *Experimental Applied Acarology* 73: 1–10.

King A.M.Q., Adams M.J., Carsten E.B., Lefkowitz E.J., 2012. Virus Taxonomy: Classification and Nomenclature of Viruses. Ninth Report of the International Committee on Taxonomy of Viruses. Elsevier Inc.

Klukáčková J., Navratil M., Duchoslav M., 2007. Natural infection of garlic (*Allium sativum* L.*)* by viruses in the Czech Republic. *Journal of Plant Diseases* 114: 97–100.

Kreuze, J.F., Vaira, A.M., Menzel, W., Candresse, T., Zavriev, S K., Hammond, J., Ryu, K.H., 2020. ICTV virus taxonomy profile: *Alphaflexiviridae*. *Journal of General Virology* 101: 699–700.

Kulkarni N.K., Kumar, P.L., Muniyappa, V., Jones, A.T., Reddy, D.V.R., 2002. Transmission of Pigeon pea sterility mosaic virus by the Eriophyid Mite, *Aceria cajani* (Acari: Arthropoda). *Plant Disease* 86: 1297–1302.

Kumar S., Stecher G., Li M., Knyaz C., Tamura K., 2018. MEGA X: Molecular Evolutionary Genetics Analysis across computing platforms. *Molecular Biology and Evolution* 35: 1547–1549.

Lee E.T., Koo B.J., Jung J.H., Chang M.U., Kang S.G., 2007. Detection of allexiviruses in the garlic plants in Korea. *Journal of Plant Pathology* 23: 266–271.

Lezzhov A.A., Gushchin V.A., Lazareva E.A., Vishnichenko V.K., Morozov S.Y., Solovyev A.G., 2015. Translation of the *Shallot virus X* TGB3 gene depends on non-AUG initiation and leaky scanning. *Journal of General Virology* 96: 3159–3164.

Lukhovitskaya N.I., Vetukuri R.R., Sama I., Thaduri S., Solovyev A.G., Savenkov E.I., 2014. A viral transcription factor exhibits antiviral RNA silencing suppression activity independent of its nuclear localization. *Journal of General Virology* 95: 2831–2837.

Majumder S., Mbay, K., Singh, J., 2018. First report of garlic virus D in garlic from D.R. Congo. *Journal of Plant Pathology* 100: 143.

Mandal B., Rao G.P., Baranwal V.K., Jain R.K., 2017. *A Century of Plant Virology in India*. Springer Nature Singapore Pte Ltd.

Manjunathagowda D.C., Gopal J., Archana R., Asiya K.R., 2017. Virus Free Seed Production of Garlic (*Allium sativum* L.*). Status and Prospects* 6: 2446–2456.

Mansouri F., Krahulec F., Duchoslav M., Ryšánek P., 2021a. Newly identified host range of viruses infecting species of the genus *Allium* L. and their distribution in six habitats in the Czech Republic. *Plant Pathology* 70: 1496–1507.

Mansouri F., Richert-Pöggeler K.R., Lewandowski M., Ryšánek, P., 2021b. Transmission characteristics of allexiviruses by the eriophyid mite, *Aceria tulipae* (Keifer) (Acari: Eriophyidae) from naturally mixed infected garlic (*Allium sativum* L.). *European Journal of Plant Pathology* 160(4): 789–796.

Marais A., Faure C., Theil S., Candresse, T., 2019. Characterization of the virome of shallots affected by the

shallot mild yellow stripe disease in France. *PLoS ONE* 14: 1–15.

Martelli G.P., Adams M.J., Kreuze J.F., Dolja V.V., 2007. Family *Flexiviridae*: A Case Study in Virion and Genome Plasticity. *Annual Review of Phytopathology* 45: 73–100.

Martin R.R., Tzanetakis I.E., 2015. Control of Virus Diseases of Berry Crops. *Advances in Virus Research* 91: 271–309.

Mavrič I., Ravnikar M., 2005. A carlavirus serologically closely related to Carnation latent virus in Slovenian garlic. *Acta Agriculturae Slovenica* 85: 343–349.

Melo-Filho P., Nagata T., Dusi A.N., Buso J.A., Torres A.C., Eiras M., Resende R.O., 2004. Detection of three *Allexivirus* species infecting garlic in Brazil. *Pesquisa Agropecuaria Brasileira* 39: 735–740.

Mohammed S.H., Zicca S., Manglli A., Mohamed M.E., El Siddig M.A.R., … Tomassoli L., 2013. Occurrence and phylogenetic analysis of potyviruses, carlaviruses and allexiviruses in garlic in Sudan. *Journal of Phytopatology* 161: 642–650.

Morozov S.Y., Solovyev A.G., 2003. Triple gene block: Modular design of a multifunctional machine for plant virus movement. *Journal of General Virology* 84: 1351–1366.

Nemchinov L.G., Grinstead S.C., Mollov D.S., 2017. *Alfalfa virus S*, a new species in the family *Alphaflexiviridae*. *PLoS ONE* 12: e0178222.

Nurulita S., Geering A.D.W., Crew K.S., Harper S., Thomas J.E., 2020. First report of garlic virus E in Australia. *Australasian Plant Disease Notes* 15: 1–3.

Oliveira M.L., De Marchi B.R., Mituti T., Pavan M.A., Krause-Sakate R., 2014. Identification and sequence analysis of five allexiviruses species infecting garlic crops in Brazil. *Tropical Plant Pathology* 39: 483–489.

Paduch-Cichal E., Bereda M., 2017. Viruses infecting ornamental *Allium* species in Poland. *Journal of Plant Pathology* 99: 509–512.

Park S.J., Nam M., Kim J.S., Lee Y.H., Lee J.B., … Lee S.H., 2011. First Report of the Virus Diseases in Victory Onion (*Allium victorialis* var. *platyphyllum*). *Research in Plant Disease* 17: 66–74.

Perotto M.C., Cafrune E.E., Conci V.C., 2010. The effect of additional viral infections on garlic plants initially infected with Allexiviruses. *European Journal of Plant Pathology* 126: 489–495.

Pringle, C.R., 1999. Virus Taxonomy at the XIth International Congress of Virology in Sydney, Australia. *Archives of Virology* 144: 421–429.

Razvjazkina G.M., 1970. Das Zwiebelmosaikvirus und seine Verbreitung im Freiland. *Tagungs-Berichte der Deutschen Akademie der Landwirtschaftswissenschaften* 115: 69–76.

Read D.A., Muoma J., Thompson G.D., 2020. Metaviromic analysis reveals coinfection of papaya in western Kenya with a unique strain of Moroccan watermelon mosaic virus and a novel member of the family *Alphaflexiviridae*. *Archives of Virology* 165: 1231–1234.

Rocha A., Esmeralda A., 2019. *Identificación e Incidencia de Virus Patógenos en el Cultivo de Ajo (Allium sativum L.) en Aramberri, Nuevo León*. Maestría thesis, Universidad Autónoma de Nuevo León. (Doctoral dissertation, Universidad Autónoma de Nuevo León)

Ryabov E.V., Generozov E.V., Vetten H.J., Zavriev S.K., 1996. Analysis of the 30-region of the mite borne filamentous virus genome testifies its relation to the shallot virus X group. *Molecular Biology* 30: 103–110.

Sabanadzovic S., Ghanem-Sabanadzovic N.A., Tzanetakis I.E., 2011. *Blackberry virus E*: An unusual *Flexivirus*. *Archives of Virology* 156: 1665–1669.

Salomon R., 2002. Virus diseases in garlic and propagation of virus free plants. In: *Allium Crop Sciences (*H.D. Rabinowitch, L. Currah, Ed), CAB Internacional, Wallingford, United Kingdom, 311–328.

Senshu H., Yamaji Y., Minato N., Shiraishi T., Maejima K., … Namba S., 2011. A Dual Strategy for the Suppression of Host Antiviral Silencing: Two Distinct Suppressors for Viral Replication and Viral Movement Encoded by Potato Virus M. *Journal of Virology* 85: 10269–10278.

Shahraeen N., Lesemann D.E., Ghotbi T., 2008. Survey for viruses infecting onion, garlic and leek crops in Iran. *EPPO Bulletin* 38: 131–135.

Song S.I., Song J.T., Kim C.H., Lee J.S., Choi Y.D., 1998. Molecular characterization of the *garlic virus X* genome. *Journal of General Virology* 79: 155–159.

Stecher G., Tamura K., Kumar S., 2020. Molecular Evolutionary Genetics Analysis (MEGA) for macOS. *Molecular Biology and Evolution* 37: 1237–1239.

Sumi S., Matsumi, T., Tsuneyoshi, T., 1999. Complete nucleotide sequences of garlic viruses A and C , members of the newly ratified genus Allexivirus. *Archives of Virology* 144: 1819–1826.

Tabanelli D., Bertaccini A., Bellardi M.G., 2004. Molecular detection of filamentous viruses infecting garlic from different geographic origins. *Journal of Plant Pathology* 86: 335–335.

Taglienti A., Tiberini, A., Manglli, A., Rea, R., Paoletti, S., Taviani, P., Tomassoli, L., 2017. Molecular identification of allexiviruses in a complex mixture of garlic viruses in Latium (Central Italy). *European Journal of Plant Pathology* 150: 797–801.

Torres A.C., Fajardo T.V., Dusi A.N., 2000. Shoot tip culture and thermotherapy for recovering virus-free plants of garlic. *Horticulture* 18: 192–195.

Trebicki P., 2020. Climate change and plant virus epidemiology. *Virus Research* 286.

Van den Born E., Omelchenko M.V., Bekkelund A., Leihne V., Koonin V.E. … Falnes P., 2008. Viral AlkB proteins repair RNA damage by oxidative demethylation. *Nucleic Acids Research* 36: 5451–5461.

Van der Vlugt R.A.A., 2006. Plant viruses in European agriculture: current problems and future aspects. In: *Virus Diseases and Crop Biosecurity,* NATO Security through Science Series, Springer, Dordrecht, 33–44.

Van Dijk P., and Van der Vlugt R.A.A., 1994. New mite-borne virus isolates from rakkyo, shallot and wild leek species. *European Journal of Plant Pathology* 100: 269–277.

Van Dijk P., Verbeek M., Bos L., 1991. Mite-borne virus isolates from cultivated *Allium* species, and their classification into two new rymoviruses in the family *Potyviridae*. *European Journal of Plant Pathology* 97: 381–399.

Vishnichenko V.K., Konareva T.N., Zavriev S.K., 1993. A new filamentous virus in shallot. *Plant Pathology* 42: 121–126.

Vishnichenko V.K., Stel'mashchuk V.Y., Zavriev S.K., 2002. The 42K protein of *shallot virus X* participates in formation of virus particles. *Molecular Biology* 36: 879–882.

Ward L.I., Perez-Egusquiza Z., Fletcher J.D., Clover G.R.G., 2009. A survey of viral diseases of *Allium* crops in New Zealand. *Australasian Plant Pathology* 38: 533–539.

Wijayasekara D., Ferguson C., Ali A., 2019. First Report of Garlic virus C, Occurring on Garlic Plants (*Allium sativum*) with Various Mosaic-Like Symptoms, in the United States. *Plant Disease* 103: 12.

Wylie S.J., Li H., Saqib M., Jones M.G.K., 2014. The global trade in fresh produce and the vagility of plant viruses: A case study in garlic. *PLoS ONE* 9: e105044.

Yamashita K., Sakai J., Hanada K., 1996. Characterization of a new virus from garlic (*Allium sativum L.*), *garlic mite-borne mosaic virus*. *Annual Phytopathology Society* 62: 483–489.

Yoshida N., Shimura H., Masuta C., 2018. Allexiviruses may have acquired inserted sequences between the CP and CRP genes to change the translation reinitiation strategy of CRP. *Archives of Virology* 163: 1419–1427.

Zhao L., Feng C., Wu K., Chen W., Chen Y., Hao X., Wu, Y., 2017. Advances and prospects in biogenic substances against plant virus: A review. *Pesticide Biochemistry and Physiology* 135: 15–26.

Phytopathologia Mediterranea
The international journal of the
Mediterranean Phytopathological Union

Firenze University Press
www.fupress.com/pm

Short Notes

Sternbergia lutea, a new host of *Narcissus late season yellows virus*

János ÁGOSTON[1,2], Asztéria ALMÁSI[3], Katalin SALÁNKI[3], László PALKOVICS[1,4,*]

[1] *Hungarian University of Agriculture and Life Sciences, Institute of Plant Protection, Department of Plant Pathology, Ménesi Road 44., H-1118 Budapest, Hungary*
[2] *Department of Agriculture, Faculty of Horticulture and Rural Development, John Von Neumann University, Mészöly Gyula Square 1-3., H-6000 Kecskemét, Hungary*
[3] *Eötvös Lóránd Research Network, Centre for Agricultural Research, Plant Protection Institute, Herman Ottó Street 15., H-1022 Budapest, Hungary*
[4] *Széchenyi István University, Faculty of Agriculture and Food Sciences, Department of Plant Sciences, Vár square 2., H-9200 Mosonmagyaróvár, Hungary*
*Corresponding author. E-mail: palkovics.laszlo.amand@sze.hu

Summary. In autumn 2017, autumn daffodil plants with yellow-green stripes on the leaves were observed at a botanical garden in Budapest, Hungary. Indicator plants were inoculated, but symptoms did not develop. RT-PCR tests of the indicator plants were also negative for the viruses. *Potyvirus* specific ACP-ELISA and RT-PCR were carried out on the symptomatic *S. lutea* leaf samples. RT-PCR with universal potyvirus primers resulted in one, approx. 1700 base pair PCR product. Phylogenetic analysis of the nucleotide sequence of the coat protein demonstrated 98.78-99.51% identity with three Japanese isolates of *Narcissus late season yellows virus*. While unidentified potyvirus infection of autumn daffodil has been previously reported, sequence data have not been published. Therefore, this is the first report of *Sternbergia lutea* as a host of *Narcissus late season yellows virus*.

Keywords. *Potyvirus*, Hungary, daffodil.

Citation: J. Ágoston, A. Almási, K. Salánki, L. Palkovics (2021) *Sternbergia lutea*, a new host of *Narcissus late season yellows virus*. *Phytopathologia Mediterranea* 60(3): 403-407. doi: 10.36253/phyto-12709

Accepted: July 13, 2021

Published: November 15, 2021

Data Availability Statement: All relevant data are within the paper and its Supporting Information files.

Competing Interests: The Author(s) declare(s) no conflict of interest.

Editor: Assunta Bertaccini, Alma Mater Studiorum, University of Bologna, Italy.

INTRODUCTION

Sternbergia lutea (autumn daffodil, *Amaryllidaceae*) is an ornamental plant in the family (Bryan, 2002, 2005), which is grown for golden yellow flowers it produces in autumn, when other flowers are scarce. Leaves also appear in autumn (Bryan, 2002, 2005) and remain till the end of the following, unless damaged by hard frosts. Dry summers and full sun are necessary for flowering (Bryan, 2002, 2005).

In the autumn of 2017, bulbous plants in the botanical garden of the Hungarian University of Agriculture and Life Sciences, Buda Campus (Budapest, Hungary) were surveyed for possible virus infections. Several *Sternbergia lutea* plants showed heavy, 2–5 mm wide, yellow to yellow-green stripe

Figure 1. Symptoms of possible virus infection on leaves of *Sternbergia lutea.*

mosaic symptoms parallel to the veins on the entire length of leaves, that were indicative of possible virus infection (Figure 1).

Flowering of these plants has not been observed since the first year of planting in 2006, probably because the plants were planted below shadowing trees, but virus infections may have had also prevented flowering. There has been only one report of presumed potyvirus infection of autumn daffodil (Pleše, 1993) but the virus species was not identified, nor were sequence data published.

MATERIALS AND METHODS

Plant samples

A symptomatic clump of *S. lutea* plants were dug up in the autumn of 2017 from the Buda Campus botanical garden. Plants were potted and kept in an insect-free greenhouse in the first growing cycle, and were later planted in open-field conditions.

ELISA tests

In January of 2018 leaf samples were collected from the potted plants. ACP-ELISA tests were carried out by Agdia, based on the MAb PTY1 antibody (RRID:AB_2819158) (Jordan and Hammond, 1991). All tests were carried out in duplicate, according to the manufacturer's protocol. For each sample, 200 mg of leaf tissue was ground in 20 mL (1: 100 m:v) of indirect sample extraction buffer. Aliquots of 100 µL of the diluted sample were added to each test plate well, and then incubated at room temperature for 1 h. The wells were then emptied and washed seven times with phosphate buffered saline Tween (PBST). The monoclonal detection antibody, in mouse against potyvirus coat protein (Clone PTY1), was diluted 1: 100 (v:v) in conjugate buffer (ECI buffer), and 100 µL was added and incubated overnight at 4°C. Plates were then washed eight times with PBST. The enzyme conjugate polyclonal rabbit antibody against mouse IgG was diluted with ECI buffer to 1: 100 (v:v), and 100 µL was added to each plate well and incubated at room temperature. The plates were then washed eight times with PBST. Paranitrophenyl phosphate (pNPP) was added to PNP buffer at 1 mg mL^{-1}, and 100 µL was added to each plate well. Absorbance values were measured at 405 nm wavelength 30 min after addition of pNPP, using a Labsystem Multiskan MS ELISA reader. Positive controls were provided by the manufacturer, and negative controls were prepared from *Chenopodium amaranticolor* seedlings grown in an insect-free greenhouse. A sample was considered positive if the sample absorbance was at least three times greater than that of the negative control.

Herbaceous indexing

Chenopodium foetidum, *Nicotiana benthamiana* and *N. tabacum* 'Xanthi' plants were inoculated mechanically (0,02 M Sörensen's phosphate buffer, celite) with the sap of the same leaf used for ACP-ELISA testing. Plants were grown in an insect-free greenhouse, and symptom development was assessed during a 5-week post inoculation period.

RNA extraction, RT-PCR, and cloning

Total RNA was extracted from the same symptomatic leaf of *Sternbergia lutea* collected for ELISA and

inoculation tests, and from leaves of the inoculated herbaceous indexing plants, 5 weeks post inoculation. The protocol of White and Kaper (1989) was used. RT-PCR was carried out with universal potyvirus primers poty7941 and poly T_2 (Salamon and Palkovics, 2005). The primers amplified the C terminal part of the RNA-dependent RNA polymerase (RdRp, NIb) including the highly conserved GNNSGQP motif, the complete coat protein (CP) sequence, and the complete 3' untranslated region (UTR) to the first few bases of the polyA tail. PCR products were separated in 1% (w/v) agarose gel electrophoresis in 1× Tris-Borate-EDTA (TBE) buffer. The gel was stained with ethidium bromide and the products were visualized and photographed under UV light. Amplicons of the expected size (approx. 1700 nt) were purified using the High Pure PCR Product Purification Kit (Roche). The PCR product was cloned into pGEM®-T Easy vector (Promega), following manufacturer's instructions. *Pst*I digestion of the purified PCR product was carried out to verify its ability to be digested for further cloning.

Additionally, RT-PCR was carried out for *Cucumber mosaic virus* (CMV), using the protocol described by Nemes and Salánki (2020). CMV is known to have a wide host range and also infects monocotyledonous bulbous ornamental plants (van Rijn *et al*., 1995; de Best *et al*., 2000). The sample was also tested for *Narcissus latent virus* (NLV) and *Narcissus mosaic virus* (NMV), using multiplex RT-PCR (He *et al*., 2019), as these viruses have been reported to infect daffodils in Hungary (Ágoston *et al*., 2020).

Koch's postulates

To fulfill Koch's postulates, an asymptomatic *S. lutea* plant was mechanically inoculated with sap from the symptomatic *S. lutea* plant in April 2019, as described above. Molecular identification for virus from the inoculated plant was performed as described above.

Sequencing, and sequence analyses

The cloned fragment was sequenced in both directions using M13 forward and reverse primers in an ABI Prism automatic sequencer (BaseClear B.V.). Nucleotide sequence identities were determined by BLAST analyses. Further phylogenetic analyses were carried out with the MEGA-X program (Kumar *et al*., 2018). ClustalW (Larkin *et al*., 2007) multiple sequence alignment was carried out (gap opening penalty 15.00, gap extension penalty 6.66 for pairwise and multiple alignment, transition weight 0.5, ClustalW weight matrix, no negative matrix was used) on the complete coat protein (CP) sequences.

A Maximum Likelihood phylogenetic tree (Felsenstein, 1981) was constructed with the Hasegawa-Kishino-Yano model (Hasegawa *et al*., 1985) with gamma distribution and invariant sites. This substitution model had the lowest Bayesian Information Criterion (5682.807). To test the phylogeny the tree was bootstrapped 1,000 times (Felsenstein, 1985).

RESULTS AND DISCUSSION

Mechanical inoculation of herbaceous test plants *C. foetidum*, *N. benthamiana* and *N. tabacum* 'Xanthi' with plant sap of symptomatic *Sternbergia* leaf resulted in plants remaining symptomless throughout the 5 week observation period. RT-PCR tests were also negative. Most potyviruses with monocotyledonous hosts do not infect dicotyledonous plants (Mowat *et al*., 1988). In the ACP-ELISA tests, the absorbances were 0.947 and 0.953, while respective negative controls were 0.034 and 0.047, indicating the presence of *Potyvirus* infections. Universal potyvirus group specific RT-PCR resulted in an approx. 1700 nt product. RT-PCR tests for CMV, NLV and NMV were negative.

The mechanically inoculated *S. lutea* plant showed the same symptoms as the original infected plant (Figure 1), but the symptoms appeared only in the next growing season, in October of 2019, approx. 7 months after inoculation. Flowering of the inoculated *S. lutea* was not observed, possibly because the bulb was not of flowering size. RT-PCR of the inoculated plant also resulted in the expected PCR products size of approx. 1700 nt.

The nucleotide sequence of the cloned PCR product from the original symptomatic *S. lutea* plant, coding the complete coat protein region, included a unique *Pst*I recognition site (GenBank accession No. MK783944). *Pst*I digestion of the original PCR product and from the inoculated plant resulted the two predicted fragments. This indicated identification of a single *Potyvirus* in the infected leaf tissues and in the inoculated plant, confirming the virus as the agent causing the observed disease (fulfilment of Koch's postulates). BLAST analysis of the CP nucleotide sequence revealed greatest identity with Hungarian (MK132194 – 98.64%, MK132193 – 98.34%), Australian (MH886515 – 96.47%), and Japanese (LC158450 – 99.51%, LC158451 – 99.39%, LC158467 – 98.78%) isolates of *Narcissus late season yellows virus* (NLSYV) deposited in GenBank.

Further phylogenetic analyses were carried out with the following NLSYV GenBank sequences:

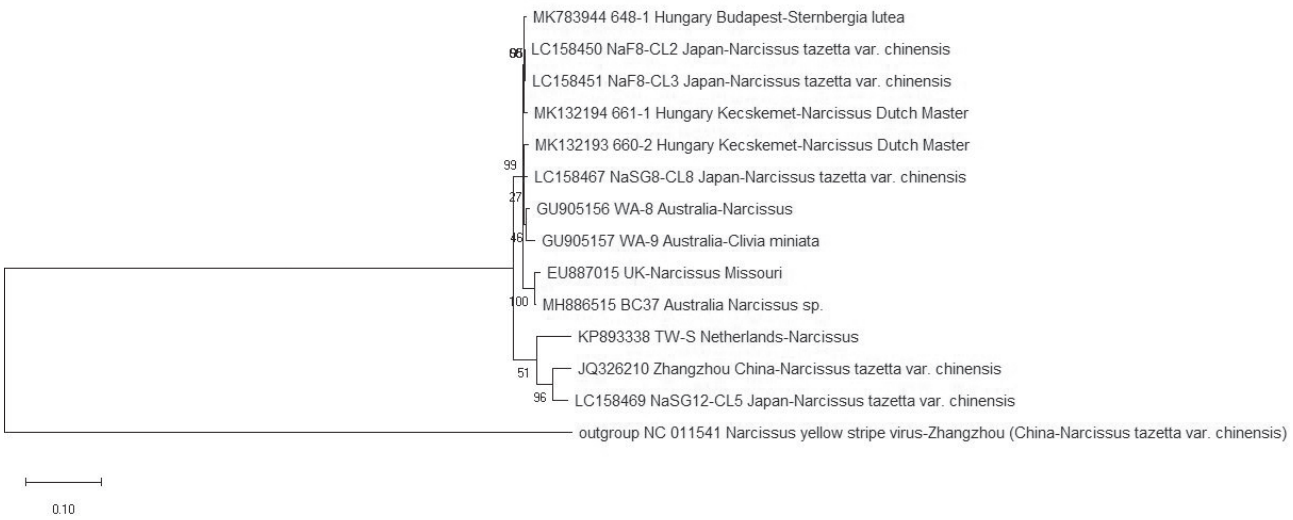

Figure 2. Phylogenetic tree of *Narcissus late season yellows virus* nucleotide sequences of the complete coat protein regions.

EU887015, GU905156, GU905157, JQ326210, KP893338, LC158450, LC158451, LC158467, LC158469, MH886515, MK132193, MK132194, MK783944, and for the outgroup sequence of *Narcissus yellow stripe virus* (GenBak accession number NC_011541) was used. After production of the first ClustalW alignment (Larkin *et al.*, 2007) on the complete CP sequence tested, DNA evolutionary models were applied, and a Maximum Likelihood phylogenetic tree (Felsenstein, 1981) was constructed (Figure 2).

The phylogenetic tree divided the virus isolates in two clades. One clade consisted of three NLSYV strains from *Narcissus* sp. from the Netherlands, China and Japan, while the other was composed of ten strains, eight collected from *Narcissus* and two isolated from different plant species, i.e., *Clivia miniata* from Australia and the Hungarian strain from *S. lutea*. With the exception of the GenBank accession GU905157 from *C. miniata* from Australia, the other NLSYV strains present in the analysis derived from *Narcissus* varieties. This is because daffodil is the main host of NLSYV, although not all the cultivars were reported to be susceptible to this virus (Mowat *et al.*, 1988).

Only one presumable *Potyvirus* infection has been previously reported from *S. lutea*, where electron microscopy of the leaf tissue showed cylindrical inclusions and filamentous particles in the cytoplasm (Pleše, 1993), but the virus was not identified to species level. The present report confirms the presence of a potyvirus in *S. lutea*, which has been identified as *Narcissus late season yellows virus*.

ACKNOWLEDGEMENTS

This research was supported by the project EFOP-3.6.1-16-2016-00006 "The development and enhancement of the research potential at John von Neumann University". The study was funded by the Hungarian Government and co-financed by the European Social Fund, and by the Ministry for Innovation and Technology within the framework of the Thematic Excellence Programme 2020- Institutional Excellence Subprogram (TKP2020-IKA-12) for research on plant breeding and plant protection.

LITERATURE CITED

Ágoston J., Almási A., Nemes K., Salánki K., Palkovics L., 2020. First report of hippeastrum mosaic virus, narcissus late season yellows virus, narcissus latent virus and narcissus mosaic virus in daffodils from Hungary. *Journal of Plant Pathology* 102: 1275–1276. DOI: 10.1007/s42161-020-00556-9.

Bryan J.E., 2002. *Bulbs*. Portland, Or, Timber Press, 524 pp.

Bryan J.E., 2005. *Timber Press Pocket Guide to Bulbs*. Portland, Or, Timber Press, 227 pp.

de Best A.L.I.C., Zwart M.J., van Aartrijk J., van den Ende J.E., Peeters J.M.M., 2000. *Ziekten en afwijkingen bij bolgewassen:* Liliaceae. Lisse, Laboratorium voor Bloembollenonderzoek.

Felsenstein J., 1981. Evolutionary trees from DNA sequences: A maximum likelihood approach. *Journal*

of Molecular Evolution 17: 368–376. DOI: 10.1007/BF01734359.

Felsenstein J., 1985. Confidence limits on phylogenies: an approach using the bootstrap. *Evolution* 39: 783–791. DOI: 10.1111/j.1558-5646.1985.tb00420.x.

Hasegawa M., Kishino H., Yano T., 1985. Dating of the human-ape splitting by a molecular clock of mitochondrial DNA. *Journal of Molecular Evolution* 22: 160–174. DOI: 10.1007/BF02101694.

He Y., Gao F., Shen J., Liao F., Chen X., … Chen S., 2019. A multiplex RT-PCR method for the simultaneous detection of *Narcissus yellow stripe virus, Narcissus latent virus* and *Narcissus mosaic virus*. *Canadian Journal of Plant Pathology* 41: 115–123. DOI: 10.1080/07060661.2018.1513074.

Jordan R., Hammond J., 1991. Comparison and differentiation of potyvirus isolates and identification of strain-, virus-, subgroup-specific and potyvirus group-common epitopes using monoclonal antibodies. *Journal of General Virology* 72: 25–36. DOI: 10.1099/0022-1317-72-1-25.

Kumar S., Stecher G., Li M., Knyaz C., Tamura K., 2018. MEGA X: Molecular Evolutionary Genetics Analysis across computing platforms. *Molecular Biology and Evolution* (F.U. Battistuzzi, ed.) 35: 1547–1549. DOI: 10.1093/molbev/msy096.

Larkin M.A., Blackshields G., Brown N.P., Chenna R., McGettigan P.A., … Higgins D.G., 2007. ClustalW and ClustalX version 2.0. *Bioinformatics* 23: 2947–2948. DOI: 10.1093/bioinformatics/btm404.

Mowat W.P., Duncan G.H., Dawson S., 1988. Narcissus late season yellows potyvirus - symptoms, properties and serological detection. *Annals of Applied Biology* 113: 531–544. DOI: 10.1111/j.1744-7348.1988.tb03330.x.

Nemes K., Salánki K., 2020. A multiplex RT-PCR assay for the simultaneous detection of prevalent viruses infecting pepper (*Capsicum annuum* L.). *Journal of Virological Methods* 278: 113838. DOI: 10.1016/j.jviromet.2020.113838.

Pleše N., 1993. A presumable potyvirus infection of *Sternbergia lutea* (L.) Ker-G. (*Amaryllidaceae*). *Acta Botanica Croatica* 52: 5–7.

Salamon P., Palkovics L., 2005. Occurrence of Colombian datura virus in *Brugmansia* hybrids, *Physalis peruviana* L. and *Solanum muricatum* Ait. in Hungary. *Acta Virologica* 49: 117–122.

van Rijn J.F.A.T., Pfaff H.G.M., van Aartrijk J., van Nes C.R., Peters J.M.M., … de Rooy M., 1995. *Ziekten en afwijkingen bij bolgewassen:* Amaryllidaceae, Araceae, Begoniaceae, Compositae, Iridaceae, Oxalidaceae, Ranunculaceae. Lisse, Laboratorium voor Bloembollenonderzoek, 190 pp.

White J.L., Kaper J.M., 1989. A simple method for detection of viral satellite RNAs in small plant tissue samples. *Journal of Virological Methods* 23: 83–93. DOI: 10.1016/0166-0934(89)90122-5.

Phytopathologia Mediterranea
The international journal of the
Mediterranean Phytopathological Union

Firenze University Press
www.fupress.com/pm

Research Papers

Nightshade (*Solanum nigrum*), an intermediate host between tomato and cucurbits of *Tomato leaf curl New Delhi virus*

Mohammad ANSAR[1,*], Aniruddha Kumar AGNIHOTRI[2], Tushar RANJAN[3], Monika KARN[4], Srinivasaraghavan A[1], Ravi Ranjan KUMAR[3], Arun Prasad BHAGAT[1]

[1] *Department of Plant Pathology, Bihar Agricultural University, Sabour-813 210, Bhagalpur, Bihar, India*
[2] *Division of Crop Protection, Indian Institute of Pulses Research, Kanpur-208 024, U.P., India*
[3] *Department of Molecular Biology and Genetic Engineering, Bihar Agricultural University, Sabour-813 210 Bhagalpur, Bihar, India*
[4] *Department of Plant Pathology, Dr. Y S Parmar University of Horticulture and Forestry, Nauni Solan-173 230, Himanchal Pradesh, India*
*Corresponding author. E-mail: ansar.pantversity@gmail.com

Summary. Geminiviruses infect many crop plants, and are limiting factors for vegetable crop production. Begomoviruses (*Geminiviridae*) cause typical symptoms of leaf curling and puckering in nightshade (*Solanum nigrum*), a seasonal weed in Bihar, India. To investigate if nightshade was an intermediate host for begomovirus, virus DNA was extracted and characterized. The DNA-A of the virus yielded 2737 nt and DNA-B yielded 2706 nt. The intergenic region (IR) showed a conserved nonanucleotide sequence that potentially forms a stem-loop structure. The genomic sequence of DNA-A shared 94% identity with that of *Tomato leaf curl New Delhi virus* (ToLCNDV)-ivy gourd isolate. However, the sequence of DNA-B showed 95% identity with a bitter gourd isolate. PCR-based detection revealed the presence ToLCNDV in bottle gourd, pumpkin, sponge gourd, and bitter gourd. The IR sequences of the viruses isolated from these cucurbits and tomato were 100% identical. Whitefly-mediated transmission of the virus to cucurbits and tomato from nightshade was also demonstrated. These results indicate that nightshade may act as reservoir of ToLCNDV, and is involved in developing epidemics in cucurbit species. The strain of ToLCNDV has probably adapted from solanaceous to cucurbitaceous hosts. This is the first report of ToLCNDV infecting nightshade in India, highlighting this virus as a possible cause of disease epidemics in economically important cucurbits.

Keywords. *Begomovirus*, genetic diversity, leaf curl.

OPEN ACCESS

Citation: M. Ansar, A.K. Agnihotri, T. Ranjan, M. Karn, Srinivasaraghavan A, R.R. Kumar, A.P. Bhagat (2021) Nightshade (*Solanum nigrum*), an intermediate host between tomato and cucurbits of *Tomato leaf curl New Delhi virus*. *Phytopathologia Mediterranea* 60(3): 409-419. doi: 10.36253/phyto-12745

Accepted: July 13, 2021

Published: November 15, 2021

Data Availability Statement: All relevant data are within the paper and its Supporting Information files.

Competing Interests: The Author(s) declare(s) no conflict of interest.

Editor: Assunta Bertaccini, Alma Mater Studiorum, University of Bologna, Italy.

INTRODUCTION

Weed plants possess ecological adaptability, and are found throughout the world. They are sources and reservoirs of viruses infecting many economically

important crops. Weeds are also alternative hosts, where economically important pathogens can survive between crop cycles (Mubin *et al*., 2010; Papayiannis *et al*., 2011; Wyant *et al*., 2011; Jyothsna *et al*., 2013). For example, whitefly-transmitted geminiviruses (*Begomovirus*; *Geminiviridae*) are known to infect economically important crops as well as weed hosts (Seal *et al*., 2006; Mubin *et al*., 2009; Ansar *et al*., 2019; Agnihotri *et al*., 2019). *Tomato leaf curl New Delhi virus* (ToLCNDV) is an important bipartite geminivirus in *Begomovirus*, which infects approx. 43 different plant species in the Indian subcontinent, West Asia, and Europe (Moriones *et al*., 2017). The virus affects plant species in the *Cucurbitaceae*, *Fabaceae*, *Malvaceae*, *Euphorbiaceae*, and *Solanaceae* (Hussain *et al*., 2004; Ito *et al*., 2008; Naimuddin *et al*., 2016). ToLCNDV is an emerging virus in the Mediterranean basin. Alternative hosts of ToLCNDV were include *Ecballium elaterium*, *Datura stramonium*, *Sonchus oleraceus*, and *Solanum nigrum* (Miguel *et al*., 2019).

ToLCNDV is a bipartite virus that has two genomic DNAs, DNA-A and DNA-B. There are six open reading frames (ORFs) in DNA-A encoding six proteins that assist in replication, transcription, pathogenesis, and encapsidation. The DNA-B has two ORFs with products that play a major role during the movement of the virus through host plasmodesmata. Both DNA segments share a common region involved in the replication of DNA-B by a DNA-A-encoded replication initiator protein (Padidam *et al*., 1995; Hanley-Bowdoin *et al*., 2013).

In India, a great variety of vegetable crops are grown throughout each year to meet food demands. Tomato is mainly grown during the Rabi season (winter) in northern India, and several cucurbits, including bottle gourd (*Lagenaria siceraria*), pumpkin (*Cucurbita maxima*), sponge gourd (*Luffa cylindrica*), and bitter gourd (*Momordica charantia*), are commonly grown in this region. These crops can be infected by several monopartite and bipartite begomoviruses that induce typical curling and mosaic symptoms. More than 25 weed species grow in crops of the two main vegetables (tomato and cucurbits). Nightshade (*Solanum nigrum* L.), a seasonal weed, grows abundantly associated with tomato and remains in fields up to the peak of the cucurbit season. Nightshade plants have puckered leaves, a symptom previously and commonly attributed to insect feeding. Leaf puckering and mild leaf curling observed in nightshade at the Vegetable Research Farm, Bihar Agricultural University, Sabour, India, suggested an alternate host of ToLCNDV, possibly acting as a green bridge for the virus.

The present study investigated the causal virus of nightshade leaf distortions, and explored the possibility of host shift between two major families of vegetable crops.

MATERIALS AND METHODS

Collection of plant samples, DNA extraction, and PCR for virus detection

Symptomatic leaves of nightshade plants (n = 23) that showed leaf puckering and curling were collected along with symptomless leaves from the experimental vegetable field, at Bihar Agricultural University, Sabour, India, during 2016 to 2018. Total genomic DNA was extracted using a GeneJet DNA isolation kit (ThermoFisher). DNA was also extracted from curled and mosaic leaves of bitter gourd, mosaic leaves of sponge gourd and pumpkin, and mottled leaves of bottle gourd and tomato. PCR was carried out on the DNA samples using the whitefly-transmitted geminivirus-specific primer Deng541F/540R (Deng *et al*., 1994) to detect virus DNA. The PCR program was executed in Surecycler-8800 (Agilent) with the following steps: preheating at 94°C (3 min); 30 cycles of denaturation at 94°C (30 sec), annealing at 53°C (30 sec), extension at 72°C (1 min); and final extension at 72°C (10 min). This PCR was carried out with Dream Taq Green Master Mix (2×) (ThermoFisher) in total 25 µl reaction, which consisted of 2 µl template DNA (25 ng μL^{-1}), 1 µL each primer (20 pmol), 12.5 µL 2× master mix, and 8.5 µL nuclease-free water. Similarly, PCR was also carried out for DNA-B using the specific primer pair PVL1v2040/PCRc1 (Rojas *et al*., 1993). Amplified products were visualized using 1% agarose gel electrophoresis with 1× TAE buffer containing 0.1% ethidium bromide. The gel was examined under a documentation system (UV Tech). Five PCR-amplified products (each 15 µL) of nightshade were directly sequenced using Deng541F/540R primer (10 µL) at Xcelris Lab Ltd, Ahmedabad, India.

Rolling circle amplification and cloning

The DNA extracted from three symptomatic nightshade leaves was subjected to full genome amplification using the rolling circle (RCA) method and the REPLI-g Mini Kit (QIAGEN GmbH). The RCA products were digested with the five restriction enzymes *Sac*I, *Bgl*I, *Pst*I, *Eco31*I, and *Hind*III (ThermoFisher), to obtain a linearized fragment. The digested products were visualized on 1% agarose gel to select the ≈2.7 kb fragments. These were purified using a gel extraction kit (ThermoFisher), cloned into pJET/1.2 blunt cloning vector using the CloneJET cloning kit (ThermoFisher), and were then sequenced at Eurofins Genomics, Bengaluru, India.

Analysis of full genome sequences

The obtained sequences were assembled and analyzed using Bioedit (version 7.2) software. Multiple sequence alignments and phylogenetic trees were made using MEGA X. Both the sequences of ToLCNDV were submitted to GenBank under the acc. No.s MH465599 and MH465600 for, respectively, the genomes of the DNA-A and DNA-B. All ORFs were determined and compared with the representative sequences listed in Table 1, using available software at NCBI (http://www.ncbi.nlm.nih.gov/gorf/gorf.html). The sequences that showed maximum identity with the viral DNA sequences isolated from nightshade were selected for pairwise percent nucleotide identity using ClustalW (http://www.genome.jp/tools/clustalw/).

Amplification of the intergenic region and its sequence analysis

For the intergenic region (IR) amplification, PCR was carried out on the extracted DNAs reported above. The PCR steps were as follows: initial denaturation at 94°C (3 min); 35 cycles of denaturation at 94°C (30 sec), annealing at 54°C (30 sec), extension at 72°C (1 min); final extension at 72°C (10 min). The reaction mixture (25 µL) was prepared with Taq Mix (2×) (Sisco Research Laboratories), which consisted of 2 µL template DNA (25 ng μL^{-1}), 1 µL each of forward and reverse primer (20 pmol), 12.5 µL 2× mix, and 8.5 µL nuclease-free water. A specific primer pair of ToLCNDV-IR F 5'TGCCTTCGAACTGGATGAG3' and ToLCNDV-IR R 5'CCTACGCGATGTGTGAGT3' was designed from the 2.7 kb whole genome of ToLCNDV-nightshade (IR-F 2386-2404, IR-R 579-596). The primer pair was targeted to amplify the IR. From each amplified sample, two PCR products were directly sequenced. The sequences obtained were trimmed and aligned in MEGA X along with the full genome sequence of the nightshade ToLCNDV isolate. Multiple sequence alignments of the viral sequences obtained in the present study and other related viruses was carried out with Genomatix Software Suite v3.10 (http://www.genomatix.de) using default settings.

Table 1. Percentages of nucleotide and amino acid sequence identities between ToLCNDV-nightshade and isolates of other related viruses.

Virus: Host: Location	NCBI GenBank Acc. No.	% identity of whole genome (DNA-A)	% identity in different ORFs						
			AV1	AV2	AC1	AC2	AC3	AC4	AC5
ToLCNDV-Nightshade: India	MH465599	[X]100/2737	[Y]100/771 [Z]100/256	100/329 100/109	100/1086 100/361	100/420 100/139	100/411 100/136	100/294 100/97	100/486 100/161
ToLCNDV-Ivy gourd: India	KY780201	94/2737	93/771 94/256	97/330 100/109	94/1086 93/361	97/420 95/139	99/411 98/136	97/296 95/97	94/363 87/161
BGVMV-Bitter gourd: Bangladesh	KJ862841	93/2737	93/771 95/256	93/339 99/112	94/1086 93/361	97/420 97/139	96/411 96/136	97/296 96/97	-
ToLCNDV-Bitter gourd: India	KY780207	93/2737	92/771 94/256	95/339 100/112	92/1086 91/361	97/420 97/139	98/411 97/136	95/296 90/97	93/486 85/161
BGVMV-Lentil: India	KM190927	93/2740	92/774 95/256	93/342 100/113	93/1086 92/361	96/420 98/139	97/411 95/136	97/296 92/97	93/363 84/120
ToLCNDV-Bottle gourd: India	FN645905	93/2737	94/771 95/256	94/339 97/112	93/1086 91/361	96/420 96/139	95/411 94/136	96/296 92/97	96/225 91/74
BGVMV-Bitter gourd: Pakistan	AM491590	93/2732	92/771 94/256	94/339 98/112	93/1086 82/361	97/420 96/139	97/411 95/136	98/126 41/41	--
ToLCNDV-Poppy: India	KC513822	91/2739	95/771 98/256	94/339 96/112	86/1086 88/361	95/420 93/139	93/411 88/136	79/177 67/58	--
ToLCNDV-Chili: India	KU196750	90/2739	95/771 95/256	94/339 96/112	86/1086 87/361	94/420 92/139	93/411 88/136	79/177 67/58	--
ToLCNDV-Ridge gourd: India	HM989845	90/2739	95/771 96/256	93/339 94/112	86/1086 88/361	95/420 92/139	94/411 88/136	79/177 67/58	96/486 92/160
ToLCNDV-Pumpkin: Pakistan	KT948072	90/2739	92/771 96/256	93/339 95/112	86/1086 87/361	95/420 92/139	12/411 88/136	79/177 67/58	--

[X] % nucleotide identity/total nucleotides in DNA-A
[Y] % nucleotide identity/total nucleotides in the ORF
[Z] % amino acid identity/total amino acids in the ORF

Genetic recombination and phylogenetic relationships

The DNA-A and DNA-B sequences of the nightshade ToLCNDV isolate were used to determine the recombination events with the Recombination Detection Program (RDP4 v.4.36), using default settings (Martin *et al*., 2010). To make the phylogenetic tree, MEGA X software was used, with a bootstrap value of 1000 replicates, and all missing data and gaps were removed (Tamura *et al*., 2013). Thirty sequences of DNA-A and DNA-B of begomoviruses were selected to construct the tree.

Whitefly-mediated transmission in different host plants

Whitefly-mediated transmission of ToLCNDV was tested from nightshade to tomato and four cucurbit plant species. Non-viruliferous colonies of whiteflies (*Bemisia tabaci*) were raised on caged eggplant seedlings, as described by Muniyappa *et al*. (2000). The status of the virus-free colony was verified using PCR on randomly collected whiteflies. Total DNA was extracted using the DNeasy DNA kit (Qiagen) following the manufacturer's protocol. PCR was carried out using Deng541F/540R and ToLCNDV-AF 5'TACGATCTTGTCCGAGATCTCA3', ToLCNDV-AR 5'ACCCAGGTCCTTAAGTACCT3' (DNA-A) primers. A 25 µL reaction mixture, containing 12.5 µL of Dream Taq Green Master Mix (2×), 1 µL of each primer, 2 µL DNA, and 8.5 µL of nuclease-free water, was used for both sets of primers (Deng541F/540R and ToLCNDV-AF/ToLCNDV-AR). The reactions were run in an Eppendorf Nexus thermocycler, with the cycling parameters described above for the Deng541F/540R primer pair, except that the annealing temperature for the ToLCNDV-AF/ToLCNDV-AR primer pair was set at 54°C. Healthy seedlings of nightshade, tomato, bottle gourd, pumpkin, sponge gourd, and bitter gourd were grown separately in insect-proof cages. Eighteen plants of each species were grown in separate trays and replicated in five trays. The transmission assessment was carried out in three different sets of experiments. Non-viruliferous whiteflies (25 ± 2) were released on caged infected nightshade plants for 16 h of acquisition feeding. After that, ten whiteflies were collected and held for 6 h of fasting. They were then released on caged healthy plants. Whitefly-infested nightshade seedlings served as experimental control plants. The whiteflies were then allowed 48 h of inoculation feeding and were killed by spraying with 0.5% Thiamethoxam 25 WG (Syngenta). Inoculated plants with whiteflies were inspected for up to 30 d for symptom appearance.

Field and PCR monitoring for ToLCNDV in nightshade and cucurbits

For field-grown tomato plants, disease incidence (DI) was monitored from the first fortnight of February to July 2016–2018 (12 observations). Plants of nightshade and the cucurbits bottle gourd, pumpkin, sponge gourd, and bitter gourd were also observed for DI. For the cucurbits, 120 plants of each species were marked and monitored every 15 d. The percentage of symptomatic nightshade plants was assessed using 1 m^2 quadrat in each cucurbit plot. Plants that had curled and mosaic leaf symptoms were counted and tagged to record DI. During each observation, 18-26 leaves were collected from different plants of each species and processed for DNA extractions and PCR. Two sets of primers ToLCNDV-AF/ToLCNDV-AR and ToLCNDV-BF 5'ATTATGTATGGTTAAGCGATG3' and ToLCNDV-BR 5'GCGGCCAATATGTCAA3' (DNA-B) were used to confirm the presence of, respectively, DNA-A and DNA-B of ToLCNDV. The reaction (25 µL) was prepared with Taq Mix (2×) (Sisco Research Laboratories), with the PCR program set as described above. The annealing temperature for ToLCNDV-BF/ToLCNDV-BR was set at 48°C.

RESULTS

Presence of ToLCNDV in symptomatic nightshade leaves

The PCR amplification using the whitefly-transmitted geminivirus specific primer Deng541F/540R to detect the presence of virus DNA provided an amplified fragment of ≈530 bp in 16 out of 23 nightshade DNA samples. Of these, five PCR products were sequenced directly, and the NCBI database was searched for the best match of these sequences using BLAST (https://blast.ncbi.nlm.nih.gov). The BLAST results showed that these sequences matched with the sequences of ToLCNDV isolates (data now shown). Subsequently, presence of the virus was further confirmed in all five samples by performing a PCR using DNA-B-specific primers PVL1v2040/PCRc1, which produced a fragment of the expected size, i.e., ≈600 bp.

Genome organization of ToLCNDV

The linearized viral genome produced by *Sac*I digestion was 2737 nt, and its sequence was submitted to the NCBI database under the acc. No. MH465599. Analysis using BLASTn and ORF finder showed that the isolated virus genome had organization typical of geminiviruses,

and consisted of seven ORFs. Of these, two ORFs (AV1 and AV2) were in virion sense, and five (AC1, AC2, AC3, AC4 and AC5) were in the complementary sense separated by IR and a putative stem-loop structure within a conserved nonanucleotide sequence. The DNA fragment obtained by *Pst*I digestion was 2706 nt and had the two ORFs BV1 and BC1 (NCBI database acc. No. MH465600).

DNA-A sequence comparison of the nightshade ToLCNDV isolate with other viruses

The virus isolated from nightshade leaves was named as ToLCNDV-Ns (nightshade), as its genomic organization was identical with that of a ToLCNDV isolate. The DNA-A sequence of ToLCNDV-Ns was compared with that of other ToLCNDV isolates to determine the sequence identity (Table 1). In pairwise alignment, the DNA-A of ToLCNDV showed 94% identical with that of ToLCNDV-Ivy gourd isolate (NCBI database acc. No. KY780201) and 93% identical with that of five other isolates (NCBI database acc. No.s KJ862841, KY780207, KM190927, FN645905, and AM491590). In a general comparison of ORF, the AV1 gene was 771 nt encoding 256 aa as the other viruses used under this study. ToLCNDV-Ns showed a maximum nucleotide identity of 95% with three isolates of ToLCNDV (NCBI database acc. No.s KC513822, KU196750, HM989845). Of these, it showed 98% aa identity only with NCBI database acc. No. KC513822. The AV2 gene was 329 nt and encoded a 109 aa protein. This gene also showed maximum identity (97%) with the corresponding gene of NCBI database acc. No. KY780201. Although nucleotide identity differed across different isolates, 100% identity was found at amino acid sequence level with an ivy gourd isolate (NCBI database acc. No. KY780201), a bitter gourd isolate (NCBI database acc. No. KY780207), and a BGVMV lentil isolate (NCBI database acc. No. KM190927). The AC1, AC2, and AC3 genes with, respectively, 1086 nt/361 aa, 420 nt/139 aa, and 411 nt/136 aa, showed similarity with the corresponding genes of all the isolates used in this study. In ToLCNDV-Ns, the AC4 gene is 294 nt, whereas it is 296 nt in five isolates NCBI database acc. No.s KY780201, KJ862841, KY780207, KM190927, and FN645905. Furthermore, it is 177 nt in NCBI database acc. No.s KC513822, KU196750, HM989845, and KT948072. The AC5 gene (291 nt) was present in only five of the leaf curl viruses used in this comparison study, and its maximum identity was 96% with two isolates (NCBI database acc. No.s FN645905, HM989845), and 94% with NCBI database acc. No. KY780201.

IR sequence analysis

The IR sequence of ToLCNDV-Ns was identified from the 2.7 kb genome, and was aligned with the IR sequences of viruses infecting bottle gourd, pumpkin, sponge gourd, bitter gourd, and tomato. The conserved nonanucleotide sequence in the hairpin-loop (TAATATTAC) was examined, which is distinctive in *Begomovirus* of the family *Geminiviridae* (Fontes *et al*., 1994). The TATA box was recognized in the IR sequences of all isolates (Figure 1). The IR sequence of ToLCNDV-Ns was 100% identical with that of isolates from four cucurbits and tomato. However, it showed 86% to 89% identity with the IR sequences of ToLCNDV isolates from pumpkin (NCBI database acc. No. KT948072), ridge gourd (NCBI database acc. No. HM989845), chili (NCBI database acc. No. KU196750), and poppy (NCBI database acc. No. KC513822). The IR was 272 nt in three isolates, and 274 nt in four isolates.

Genetic recombination and phylogenetic relationships

The DNA-A of ToLCNDV-Ns (NCBI database acc. No. MH465599) was examined for recombination events. Two events in the DNA-A sequence were detected. ToLCNDV bottle gourd (NCBI database acc. No. FN645905) and bitter gourd (NCBI database acc. No. KJ862841) isolates were identified as major parents, with the first recombination breakpoint at residues 435–1035 nt. A second breakpoint was detected at 1368-1968 nt, with major isolate parents being the NCBI database acc. No.s KY780201 (ivy gourd), KJ862841, KY780207 (bitter gourd), and FN645905 (bottle gourd) isolates (Table 2). The minor parents in both recombination events were unknown. These recombination events were detected in the AV1, AV2, AC1, AC2, AC3, and AC5 genes. A putative recombination event detected in DNA-B of ToLCNDV (NCBI database acc. No. MH465600) was in the IR, with breakpoints at residues 128-168 nt. For this event, ToLCNDV NCBI database acc. No. KC545813 (cucumber) was recognized as major parent, and FN435312 (tomato) was recognized as the minor parent.

The DNA-A sequences of ToLCNDV and other begomoviruses were subjected to phylogenetic analysis. This showed that DNA-A sequences of begomoviruses and ToLCNDV-Ns (NCBI database acc. No. MH465599) were grouped with those of ToLCNDV isolates that mainly infect cucurbit hosts (clade G). There were two subclades with parallel evolution. The sequence of ToLCNDV probably evolved earlier, whereas that of the other four isolates (NCBI database acc. No.s KJ862841, AM491590, KY780201, and KY780207) probably evolved at a later stage. The DNA-B of ToLCNDV-Ns was like-

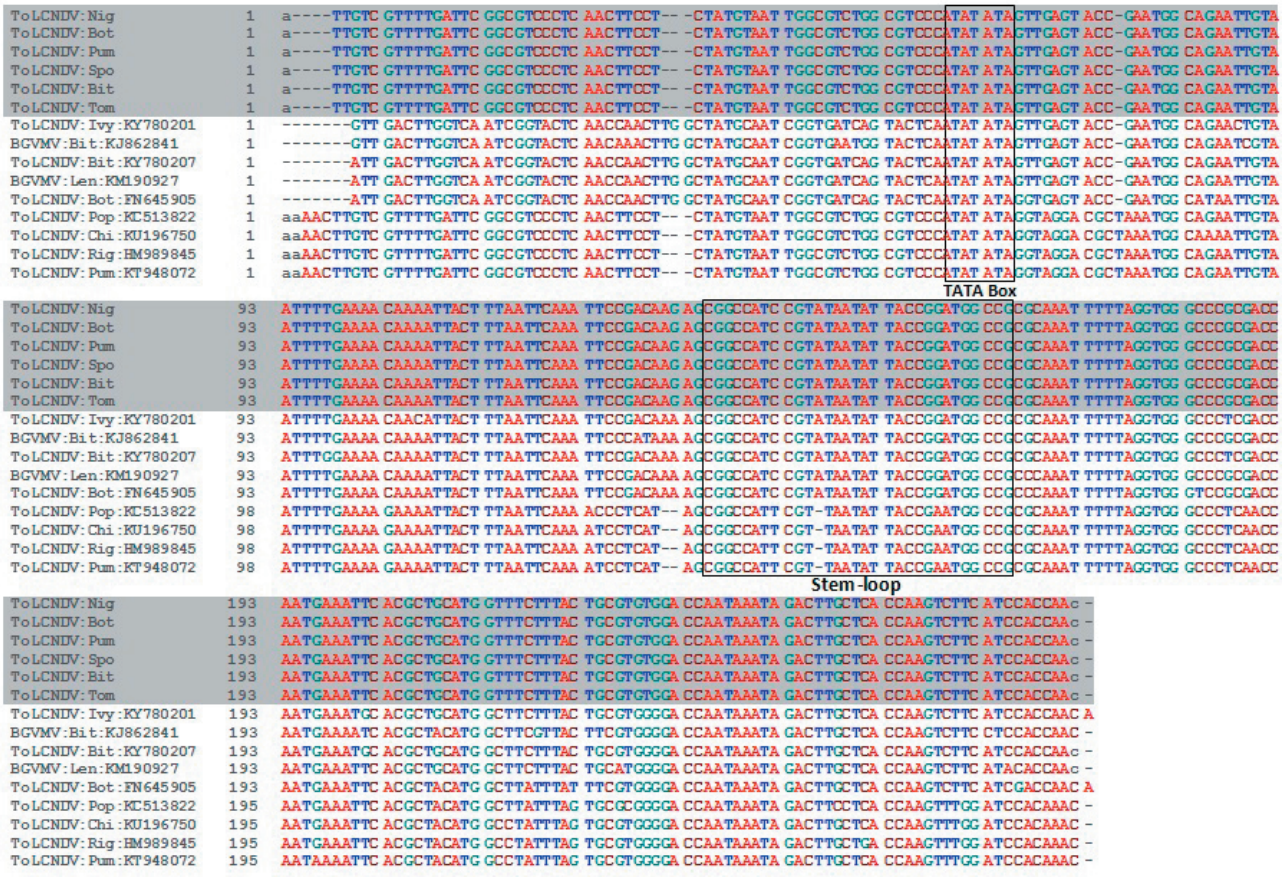

Figure 1. Multiple sequence alignment of IR sequences of ToLCNDV infecting nightshade, and other host plants (Nig = -nightshade, Bot = -bottle gourd, Pum = -pumpkin, Spo = -sponge gourd, Bit = -bitter gourd, Rig = ridge gourd, Ivy = -ivy gourd, Len = -lentil, Pop = -poppy, Tom = tomato, and Chi = -chili).

Table 2. Breakpoint analyses of DNA-A and DNA-B components and the putative parental sequences of ToLCNDV (nightshade), with respective *P*-values

Break points (begin-end	Minor parental sequence(s)	Major parental sequence(s)	RDP	GENECONV	Bootscan	Maxchi	Chimaera	SiSscan
DNA-A								
435-1035	Unknown (HM98984)	FN645905 KJ862841	3.75×10^{-10}	-	5.82×10^{-08}	1.46×10^{-03}	1.88×10^{-06}	5.42×10^{-04}
1368-1968	Unknown (HM989845) Unknown (KC513822) Unknown (KU196750) Unknown (HM007113) Unknown (KT948072)	KY780201 KJ862841 KY780207 FN645905	4.44×10^{-11}	3.59×10^{-06}	3.14×10^{-04}	8.45×10^{-06}	2.72×10^{-05}	2.80×10^{-40}
DNA-B								
128-168	FN435312	KC545813	1.435×10^{-03}	-	-	-	-	-

ly to be ancestral, and the corresponding sequences of other viruses probably diverged later. Other bipartite begomoviruses clustered into species-specific clades; for example, *Mungbean yellow mosaic India virus* (clade A), *Horsegram yellow mosaic virus* (clade B), *Rhyncosia yellow mosaic virus* (clade C), *Dolichos yellow mosaic virus*

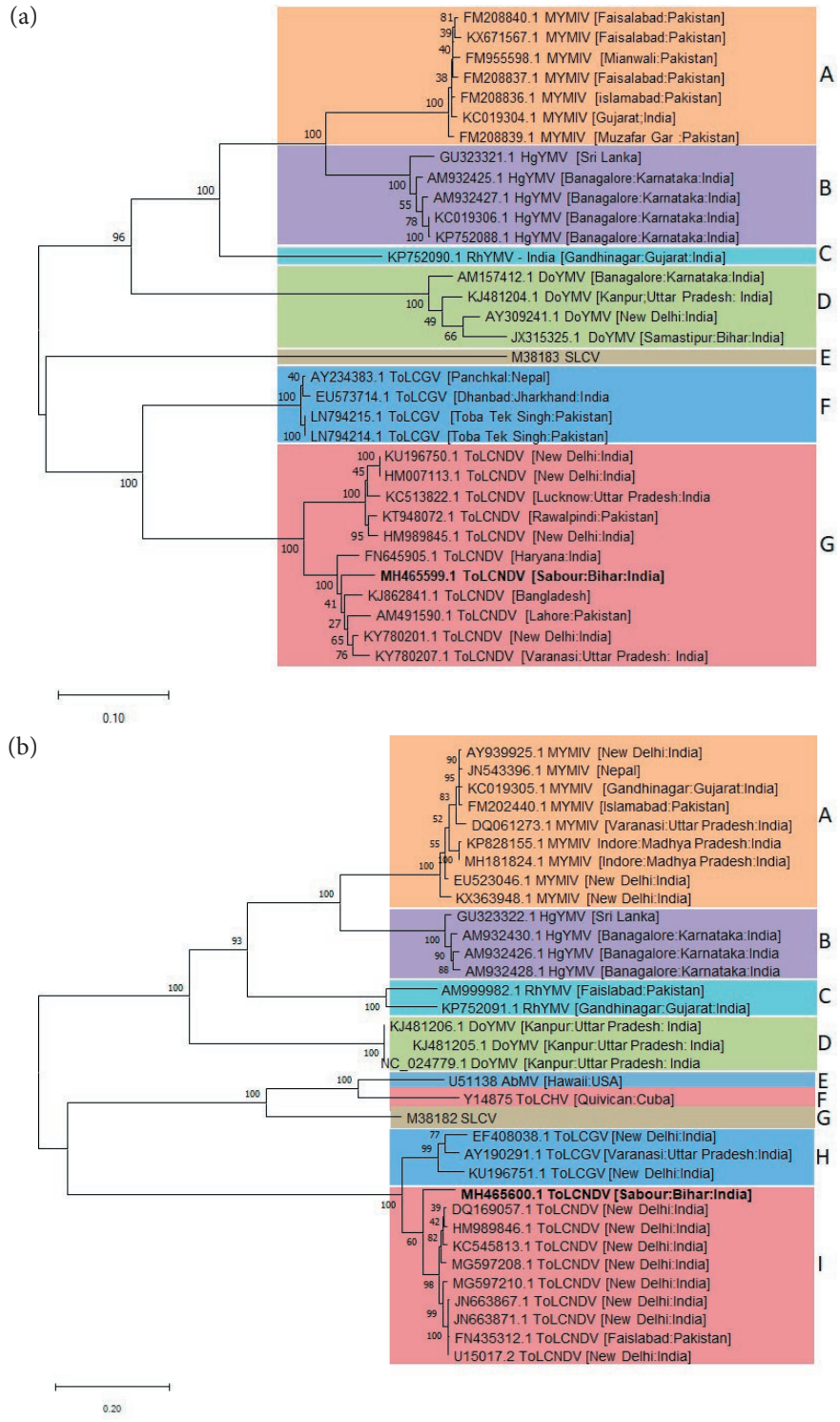

Figure 2. (a) Phylogenetic analysis of *Tomato leaf curl New Delhi virus* (ToLCNDV) DNA-A (present study, nightshade) with other leaf curl and mosaic begomoviruses, using the Maximum-likelihood method in MEGA X with bootstrap (1000 replicates). Clades A: *Mungbean yellow mosaic India virus* (MYMIV), B: *Horsegram yellow mosaic virus* (HgYMV), C: *Rhyncosia yellow mosaic virus* (RhYMV), D: *Dolichos yellow mosaic virus* (DoYMV), E: *Squash leaf curl virus* (SLCV), F: *Tomato leaf curl Gujarat virus* (ToLCGV), and G: ToLCNDV **(b)** Phylogenetic analysis of DNA-B of ToLCNDV (present study, - nightshade) with other reported begomoviruses using the Maximum-likelihood method in MEGA X with bootstrap (1000 replicates). Clades A: MYMIV, B: HgYMV, C: RhYMV, D: DoYMV, E: Abutilon mosaic virus (AbMV), F: Tomato leaf curl Hainan virus (ToLCHV), G: SLCV, H: ToLCGV, and I: ToLCNDV.

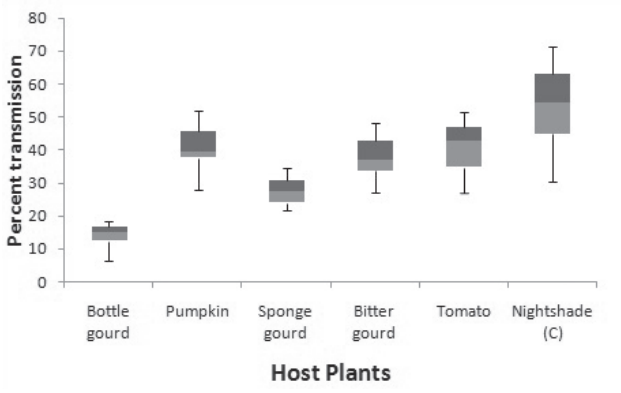

Figure 3. Box plots of mean percent whitefly-mediated transmission of ToLCNDV from nightshade to nightshade (experimental control, C) and different cucurbit hosts.

(clade D), and *Tomato leaf curl Gujarat virus* (clade F), were grouped into clades distinct from that of ToLCNDV (Figure 2a). In the analysis of DNA-B sequences, the present study isolate (MH465600) was also grouped with other ToLCNDV isolates (clade I), which were different from other bipartite begomoviruses (Figure 2b).

ToLCNDV whitefly transmissibility

The transmission experiments showed that ToLCNDV was acquired by whiteflies from infected nightshade plants, and was transmitted to bottle gourd, pumpkin, sponge gourd, and bitter gourd, tomato, and to nightshade (experimental controls). Virus transmission to pumpkin and bitter gourd was as efficient as that to tomato ($P < 0.05$). Lower rates of transmission were observed in bottle gourd (mean = 14.3%) and sponge gourd (28.2%); Figure 3). The symptoms appeared 18 to 25 d after inoculation, and were leaf curl, leaf puckering, and mosaic. Each typical symptom was confirmed by PCR using the primers ToLCNDV-AF/ToLCNDV-AR. Amplification was observed from each symptomatic plant (data not shown).

Field and PCR monitoring for ToLCNDV in nightshade and cucurbits

Symptom appearance in field-grown nightshade plants was noticed in mid February 2016-2018, with a progressive increase until June, and the overall average DI was 16.2%. DI was noticed in the first fortnight of April (except for bottle gourd), with mild leaf mottle and curling. In subsequent observations, symptoms of yellow mosaic, mottling, and curled leaves were increasingly expressed. Bottle gourd remained in the field until July with severe mottling symptoms. More than 77% of the symptomatic plants were infected with ToLCNDV. Pumpkin and bitter gourd developed mild to severe mosaic symptoms by June. Sponge gourd exhibited typical yel-

Host plants	February		March		April		May		June		July	
	Obs-1	Obs-2	Obs-3	Obs-4	Obs-5	Obs-6	Obs-7	Obs-8	Obs-9	Obs-10	Obs-11	Obs-12
Nightshade	+	+	+	++	++	+++	++	+++	+++	+++		
Bottle gourd						+	+	++	++	+++	++++	+++++
Pumpkin					+	+	++	+++	++++	++++		
Sponge gourd					+	++	+++	+++	++++	++++	+++++	
Bitter gourd					++	++	++	+++	++++	+++++		

Obs: Observation

Suspected virus disease incidence (symptomatic appearance)

Tomato leaf curl New Delhi virus PCR positive samples: + 10-15%, ++ >15-25%, +++ >25-35%, ++++>35-45%, +++++ >45%

DI <5% | DI 5-15% | DI 15-25% | DI 25-40%

Figure 4. Appearance and incidence of leaf curl symptoms in nightshade weeds and different cucurbit hosts during months of 2016-2018.

low spots, with 38% DI in the first fortnight of July (Figure 4). In earlier observations (first fortnight of March), 10%–15% of the nightshade samples were positive for ToLCNDV. In subsequent observations, the percentage of infected samples increased. In the late maturity phase, means of 58.3% the bitter gourd samples and 64.0% of sponge gourd were positive for ToLCNDV (Figure 4).

DISCUSSION

Begomoviruses widely affect economically important crops that include more than 300 species (Zerbini *et al*., 2017). These viruses are vectored by whiteflies, and they incite severe symptoms in dicot plants in tropical and subtropical regions (Kumari *et al*., 2010; Singh *et al*., 2012; Inoue-Nagata *et al*., 2016, Agnihotri *et al*., 2018). In the Indian subcontinent, leaf curl diseases are widely distributed in various crops, and cause severe crop and economic losses (Khan *et al*., 2006; Senanayake *et al*., 2007; Zehra *et al*., 2017). ToLCNDV is an important bipartite *Begomovirus*, which affects a diverse range of crops. This virus has expanded its host range, and has spread to new geographical regions including West Asia and the western Mediterranean basin (Fortes *et al*., 2016; Yazdani-Khameneh *et al*., 2016). How begomoviruses adapted to new hosts has become an important area of research.

In the present study, a strain of ToLCNDV is reported to be associated with leaf curl disease in nightshade in the north-eastern part of the Indo-Gangetic plains. Based on PCR detection approx. 70% symptomatic nightshade samples were shown to be infected with begomoviruses, and later confirmed to be infected with ToLCNDV. This virus also infected cucurbit crop plants growing in association with the nightshade weeds. Infections in nightshade probably resulted from infections in previously grown tomato crops, which were severely infected with ToLCNDV. Cucurbits are commonly grown during the summer season (April-July) after harvesting tomato crops (October-March). Between these two important crops, nightshade is a potential reservoir host for the virus.

The strain of the virus studied here was shown to transmit from tomato to cucurbits through nightshade. The IRs of the virus strains from nightshade, tomato, and four cucurbits were identical, and the sequences of these isolates showed high identity with those from some isolates from pumpkin and ridge gourd available in the GenBank database. The recombination analysis indicated that the major parents of these virus isolates were strains that commonly infect cucurbits, particularly bottle gourd and bitter gourd. The whitefly-mediated transmission of these viruses from nightshade to tomato and four cucurbits was also demonstrated, indicating the probable leaf curl disease cycle in this region. In previous studies, ToLCNDV was shown to infect cucumber, melon, and zucchini squash (Mnari-Hattab *et al*., 2015; Panno *et al*., 2016). Nightshade was has also been reported to be infected by *Tomato leaf curl Joydebpur virus* (ToLCJV) along with betasatellite, which provides the link between tomato and chili crops (Ansar *et al*., 2018).

The confirmed presence of ToLCNDV and ToLCJV in nightshade indicates the probable role of this weed as reservoir for viruses that affect different economically important crops. However, a comprehensive detection program is required to determine presence of other viruses in the studied host species, which may cause economic losses. A reservoir host eradication programme with an integrated control approach may be beneficial for related economically important vegetable crops.

ACKNOWLEDGEMENTS

This research was supported by the Science and Engineering Research Board, Department of Science and Technology, Government of India, Young Scientist Scheme-YSS/2015/000923. The paper was developed under BAU communication number 895/201029. The assistance provided by Dr Vihang Ghalsasi for manuscript revision is greatly appreciated.

LITERATURE CITED

Agnihotri A.K., Mishra S.P., Tripathi R.C., Ansar M., Srivastava A., Tripathi I.P., 2018. First natural co-occurrence of tomato leaf curl New Delhi virus DNA-A and chili leaf curl betasatellite on tomato plants (*Solanum lycopersicum L.*) in India. *Journal of General Plant Pathology* 84: 414–417.

Agnihotri A.K., Mishra S.P., Ansar M., Tripathi R.C., Singh R., Akram M., 2019 Molecular Characterization of Mungbean yellow mosaic India virus infecting tomato (*Solanum lycopersicum* L.). *Australasian Plant Pathology* 48: 159-165.

Ansar M., Akram M., Agnihotri A.K., Srinivasaraghavan A., Saha T., Naimuddin., 2018. Characterization of leaf curl virus in chili and overwintering role of nightshade in linkage between chili and tomato. *Journal of Plant Pathology* 101: 307-314.

Ansar M., Agnihotri A.K., Akram M., Bhagat A.P., 2019. First report of Tomato leaf curl Joydebpur virus

infecting French bean (*Phaseolus vulgaris* L.). *Journal of General Plant Pathology* 85: 444-448.

Deng A., Mcgrath P.F., Robinson D.J., Harrison B.D., 1994. Detection and differentiation of whitefly transmitted geminiviruses in plants and vector insects by the polymerase chain reaction with degenerate primers. *Annals of Applied Biology* 125: 327–336.

Fontes E.P., Gladfelter H.J., Schaffer R.L., Petty I.T., Hanley-Bowdoin L. 1994. Geminivirus replication origins have a modular organization. *Plant Cell* 6: 405–416.

Fortes I.M., Sánchez-Campos S., Fiallo-Olivé E., Díaz-Pendón A.J., Navas-Castillo J., Moriones E., 2016. A novel strain of tomato leaf curl New Delhi virus has spread to the mediterranean basin. *Viruses* 8: 307.

Hanley-Bowdoin L., Bejarano E.R., Robertson D., Mansoor S., 2013. Geminiviruses: Masters at redirecting and reprogramming plant processes. *Nature Review Microbiology* 11: 777–788.

Hussain M., Mansoor S., Iram S., Zafar Y., Briddon R.W., 2004. First report of tomato leaf curl New Delhi virus affecting chili pepper in Pakistan. *Plant Pathology* 53: 794.

Ito T., Sharma P., Kittipakorn K., Ikegami M., 2008. Complete nucleotide sequence of a new isolate of tomato leaf curl New Delhi virus infecting cucumber, bottle gourd and muskmelon in Thailand. *Archives of Virology* 153: 611–613.

Inoue-Nagata A.K., Lima M.F., Gilbertson R.L. 2016. A review of geminivirus diseases in vegetables and other crops in Brazil: current status and approaches for management. *Horticultura Brasileira* 34: 008-018.

Jyothsna P., Haq Q.M.I., Singh P., Sumiya K.V., Praveen S.,… Malathi V.G., 2013. Infection of tomato leaf curl New Delhi virus (ToLCNDV), a bipartite *begomovirus* with beta satellites, results in enhanced level of helper virus components and antagonistic interaction between DNA B and beta satellites. *Applied Microbiology and Biotechnology* 97: 5457–5471.

Khan M.S., Raj S.K., Singh R., 2006. First report of tomato leaf curl New Delhi virus infecting chili in India. *Plant Pathology* 55: 289.

Kumari P., Singh A.K., Chattopadhyay B., Chakraborty S., 2010. Molecular characterization of a new species of Begomovirus and betasatellite causing leaf curl disease of tomato in India. *Virus Research* 152: 19–29.

Martin D.P., Lemey P., Lott M., Moulton V., Posada D., Lefeuvre P., 2010. RDP3: a flexible and fast computer program for analyzing recombination. *Bioinformatics* 26: 2462–2463.

Miguel J., Pilar R.M., Díaz M.L., Monia T., Ana G.P., Pedro G., 2019. Natural Hosts and Genetic Diversity of the Emerging Tomato Leaf Curl New Delhi Virus in Spain. *Frontiers in Microbiology* 10: 140.

Mnari-Hattab M., Zammouri S., Belkadhi M., Doña D.B., Ben Nahia E., Hajlaoui M., 2015. First report of tomato leaf curl New Delhi virus infecting cucurbits in Tunisia. *New Disease Report* 31: 21.

Moriones E., Praveen S., Chakraborty S., 2017. Tomato Leaf Curl New Delhi Virus: An emerging virus complex threatening vegetable and fibre crops. *Viruses* 9: 264.

Mubin M., Briddon R.W., Mansoor S., 2009. Diverse and recombinant DNA beta satellites are associated with a begomovirus disease complex of *Digera arvensis*, a weed host. *Virus Research* 142: 208-212.

Mubin M., Shahid M. S., Tahir M. N., Briddon R. W., Mansoor S., 2010. Characterization of begomovirus components from a weed suggests that begomoviruses may associate with multiple distinct DNA satellites. *Virus Genes* 40: 452-457.

Muniyappa V., Venkatesh H.M., Ramappa H.K., Kulkarni R.S., Zeidan M.,… Czosnek H., 2000. Tomato leaf curl virus from Bangalore (ToLCV-Ban4): sequence comparison with Indian ToLCV isolates, detection in plants and insects, and vector relationships. *Archives of Virology* 145: 1583–1598.

Naimuddin K., Akram M., Aniruddha A.K., 2016. Molecular characterization of a first begomovirus associated with lentil (*Lens culinaris*) from India. *Acta Virologica* 60 (3): 217-223.

Padidam M., Beachy R.N., Fauquet C.M., 1995. Tomato leaf curl geminivirus from India has a bipartite genome and coat protein is not essential for infectivity. *Journal of General Virology* 76: 25–35.

Panno S., Iacono G., Davino M., Marchione S., Zappardo V., … Davino S., 2016. First report of tomato leaf curl New Delhi virus affecting zucchini squash in an important horticultural area of southern Italy. *New Disease Report* 33: 6.

Papayiannis L.C., Katis N.I., Idris A.M., Brown J.K., 2011. Identification of weed hosts of Tomato yellow leaf curl virus in Cyprus. *Plant Disease* 95: 120-125.

Rojas M R., Gilbertson R.L., Russell D.R., Maxwell D.P., 1993. Use of degenerate primers in the polymerase chain reaction to detect whitefly transmitted geminiviruses. *Plant Disease* 77: 340-347.

Seal S.E., Jeger M.J., Vanden B.F., 2006. Begomovirus evolution and disease management. *Advances in Virus Research* 67: 297–316.

Senanayake D.M.J.B., Mandal B., Lodha S., Varma A., 2007. First report of Chili leaf curl virus affecting chili in India. *Plant Pathology* 56: 343.

Singh A.K., Chattopadhyay B., Chakraborty S., 2012. Biology and interactions of two distinct monopar-

tite begomoviruses and beta satellites associated with radish leaf curl disease in India. *Virology Journal* 9: 43.

Tamura K., Strecher G., Peterson D., Filipski A., Kumar S., 2013. MEGA6: Molecular Evolutionary Genetics Analysis version 6.0. *Molecular Biology and Evolution* 30: 2725–2739.

Wyant P.S., Gotthardt D., Schafer B., Krenz B., Jeske H., 2011. The genomes of four novel begomoviruses and a new Sidamicrantha mosaic virus strain from Bolivian weeds. *Arch of Virology* 156: 347-352.

Yazdani-Khameneh S., Aboutorabi S., Shoori M., Aghazadeh A., Jahanshahi P.,… Maleki M., 2016. Natural occurrence of tomato leaf curl New Delhi virus in Iranian cucurbit crops. *Plant Pathology Journal* 32: 201–208.

Zehra S.B., Ahmad A., Sharma A., Sofi S., Lateef A., … Rathore J.P., 2017. Chilli leaf curl virus an emerging threat to chili in India. *International Journal of Pure Applied Biosciences* 5 (5): 404–414.

Zerbini F.M., Briddon R.W., Idris A., Martin D.P., Moriones E., … Varsani A., 2017. ICTV Virus taxonomy profile: Geminiviridae. *Journal of General Virology* 98: 131–133.

Phytopathologia Mediterranea
The international journal of the
Mediterranean Phytopathological Union

Firenze University Press
www.fupress.com/pm

Short Notes

High-density 'Spadona' pear orchard shows reduced tree sensitivity to fire blight damage due to decreased tree vigour

Mery DAFNY-YELIN[1,*], Jehudith Clara MOY[1], Raphael A. STERN[1,2], Israel DORON[1], Miriam SILBERSTEIN[1], Daphna MICHAELI[3]

[1] *Northern Agriculture Research & Development, MIGAL – Galilee Research Institute, P.O.B. 831, Kiryat Shmona 11016, Israel*
[2] *Department of Biotechnology, Faculty of Life Sciences, Tel-Hai College, Upper Galilee 12210, Israel*
[3] *Tel Hai Rodman College, Kiryat Shmona 12208, Israel*
*Corresponding author. E-mail: merydy@gmail.com

Summary. Fire blight, caused by *Erwinia amylovora*, is a severe disease of pear (*Pyrus communis*). Highly vigorous trees are more sensitive to *E. amylovora* damage after summer pruning. Trees grown in high-density orchards have lower vigour than those in low-density orchards, reducing required inputs for pruning and tying, and increasing per hectare yields orchard profitability. Tree damage due to fire blight was assessed in high-density pear orchards *vs.* the common Israeli low-density orchards. Pear trees were planted at high densities using the spindle system (2500 trees ha^{-1} for 'Spadona' and 1250 trees ha^{-1} for 'Coscia'), or at low density (1000 trees ha^{-1}) using palmeta ('Spadona') or open vase ('Coscia') systems. Four years after planting, both orchards were similarly infected with fire blight (11–50 infected blossoms per tree), but 1 year after infection, trees in the high density orchard had fewer infections in the main limbs or trunk bases compared to the low-density orchard. At 3 years after initial infection, no trees had died in the high density orchard, whereas in the low density 'Spadona' orchard, 10% of the trees were wilted. For the more tolerant 'Coscia', infection did not progress at either orchard density. These results indicate that in fire blight-susceptible pear cultivars, a high density planting system, associated with reduced tree vigour, presents a decreased risk of fire blight damage.

Keywords. *Erwinia amylovora*, fire blight, high-density orchard, *Pyrus communis*.

OPEN ACCESS

Citation: M. Dafny-Yelin, J.C. Moy, R.A. Stern, I. Doron, M. Silberstein, D. Michaeli (2021) High-density 'Spadona' pear orchard shows reduced tree sensitivity to fire blight damage due to decreased tree vigour. *Phytopathologia Mediterranea* 60(3): 421-426. doi: 10.36253/phyto-12847

Accepted: July 16, 2021

Published: November 15, 2021

Data Availability Statement: All relevant data are within the paper and its Supporting Information files.

Competing Interests: The Author(s) declare(s) no conflict of interest.

Editor: Jesus Murillo, Public University of Navarre, Spain.

INTRODUCTION

Fire blight caused by *Erwinia amylovora* is the most severe disease of pear (*Pyrus communis*) trees and apple and other deciduous trees in the Rosacea. The bacteria enter host trees through flower nectarthodes (natural openings through which the nectar is secreted) or through wounds in young shoots caused by hail (Johnson, 2000; Bubán and Orosz-Kovács, 2003).

Erwinia amylovora can infect host leaves, blossoms, fruit, shoots and trunks (van der Zwet, and Beer 1995). Infections in the main limbs or trunk

bases can ultimately lead to tree death in subsequent years (Vanneste and Eden-Green, 2000).

The most common pear varieties in Israeli pear orchards are cvs 'Spadona' and 'Coscia'. Since the introduction of fire blight in Israel in 1985, some studies have concentrated on the sensitive 'Spadona'. Shtienberg *et al.* (2003) showed that summer pruning of 'Spadona' trees encouraged growth of vegetative tissues while also ridding the trees of infected branches. However, this procedure can lead to rapid movement of the bacteria in the infected trees, potentially reaching the main limbs and endangering tree life. Shtienberg *et al.* (2003) also showed that trees with high vigour are more sensitive to *E. amylovora* than low vigour trees following pruning.

Irrespective of sensitivity to fire blight, the number of fruit trees planted per hectare has increased in the past 50 years worldwide, Israel included. Trees in high density orchards are considered to have lower vigour relative to those in low density orchards, thus reducing the manpower required for pruning and tying. Despite lower yields per tree, total yields per hectare are enhanced, significantly increasing orchard profitability (Robinson *et al.*, 2004a and b). An increase in number of trees per unit area can be achieved using new dwarf rootstocks and novel crop design methods (Ferree and Warrington, 2003). In Israel, most of the old pear orchards are planted in the "Spanish method", which makes use of stronger rootstocks and generous applications of fertilizers, thereby improving yield per hectare but also potentially encouraging *E. amylovora's* movement in the tree branches.

The present study tested whether high density pear orchards planted using the spindle system had reduced fire blight damage in infected trees compared to a low density planting system.

MATERIALS AND METHODS

Pear tree experiment design

Pear plots were planted in 2013 specifically for this experiment, in the Hula valley orchard research station (coordinates: 33.1522059, 35.6242158). 'Spadona' plants were grafted on BA-29 10 rootstock, and Coscia plants were on Betulifolia rootstocks (Table 1). The maximum height of all trees was restricted to 2.5 m. Rows were planted for each of the cultivars in (i) a high density row system using the spindle tree design, or (ii) a low density system using palmeta (in 'spadona') or open vase design (in 'Coscia', see Table 1 and Figure 1).Rows were planted 4 m apart. Each row contained only one cultivar and one tree design.

For each cultivar, the same rootstock, nutrition, and growth hormone regulators were equally applied to low and high density trees. This aimed to eliminate any effect of rootstock or other treatments on the progression of fire blight in the trees, leaving only the effects of orchard density and individual tree design.

Tree vigour was estimated by measuring the main bark circumference. This measurement was performed in November 2017, 2018 and 2019 on six healthy trees for each design system, per cultivar, as described by Stern and Doron (2009) and Stern *et al.* (2013). The same trees were measured each year, 10 cm above their grafting sutures.

Disease assessments

Erwinia amylovora infections were estimated in spring 2017 in 4-year-old orchards, as numbers of infected blossoms per tree grouped into: 0, one to five, six to ten or 11–50 infected blossoms per tree. All trees in each treatment were evaluated (Table 1).

Fire blight progression was estimated in August/September each year for disease infection progress for 1 year prior, and estimates were classified into four groups: (i) no sign of disease progress (healthy tree); (ii) infected tree where infection was clearly identified in either the main limb or (iii) the trunk base; (iv) dead tree. All trees in each treatment (Table 1) were evaluated.

Statistical analyses

Statistical analyses were applied using JMP 13 software. T-tests were performed to compare tree circumferences between treatments. Chi-square tests (likelihood

Table 1. Experimental plot design (see also Figure 1).

Cultivar	Rootstock	Density	Tree Design	Distance between trees (m)	Number of trees per treatment	Number of trees ha^{-1}
Spadona	BA-29 10	High	Spindle	1.0	99	2500
		Low	Palmeta	2.5	40	1000
Coscia	Betulifolia	High	Spindle	1.0	93	2500
		Low	Open vase	2.0	50	1250

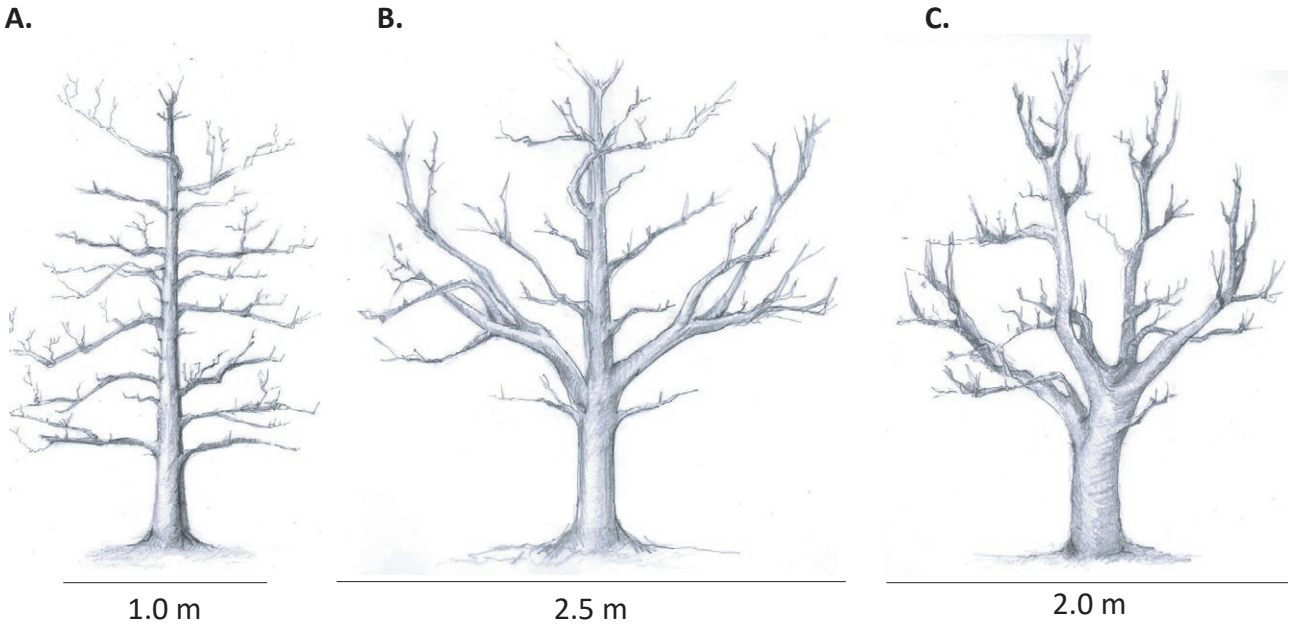

Figure 1. The tree design systems tested in this study. Schematic drawings of 7-year-old trees are shown. (A) 'Spadona' and 'Coscia' high-density system, spindle design; (B) 'Spadona' low-density system, palmeta design; (C) 'Coscia' low-density system, open vase design. Illustration: Reut Yelin-Alush.

ratio in contingency analysis) were used to compare infected trees within different categories, calculated as percentage of trees either without or with (i) infection in the main limb, (ii) infection in the trunk base, or (iii) dead trees. Tree was the experimental unit.

RESULTS

Trunk circumference for each rootstock–cultivar combination reflects tree vigour, where a large circumference reflects greater vegetative growth than a small circumference (Stern and Doron, 2009; Stern *et al*., 2013). In 'Spadona' grown in the palmeta tree design, trunk circumference was greatest (Figure 2A, B and C), with annual sequential differences accumulating to 23.2% in the sixth year (t = 4.90, *P* = 0.0008; Figure 2C), compared with 'Spadona' grown in the spindle design. In 'Coscia', the differences between trunk circumference in the spindle vs. open vase designs were smaller, with only up to 12.6% cumulative difference in the sixth year (t = -3.18, *P* = 0.0098; Figure 2C).

Disease assessments

Natural fire blight infections occurred in spring 2017 when the trees were 4 years old, with more than 97.4% of the trees infected at 11–50 blossoms per tree, in both 'Spadona' and 'Coscia'. In 'Spadona', the disease progressed to 41.0% infected trees in the palmeta tree design, but only 13.1% infected trees in the spindle design. The differences between the design infection levels were statistically significant (χ^2 = 12.105, *P* = 0.0005; Figure 3A). Infections continued to progress in the 5-year-old trees, to 75.0% of the palmeta trees and 50.5% of the spindle trees (χ^2 = 7.25, P = 0.0069; Figure 3A). Infections in the trunk bases, threatening tree life, was detected in 56.4% of the palmeta trees and 26.3% of the spindle trees (χ^2 = 10.893, P < 0.001; Figure 3B). Dead trees were only found for 'Spadona' grown in the palmeta design, with 5.0% of the 6-year-old trees dying (χ^2 = 5.055, P = 0.0246) and 10.0% of the 7-year-old trees dying (χ^2 = 10.263, P = 0.0014; Figure 3C).

In cv. Coscia, in the summer of 2017, a few months after the initial *E. amylovora* infections, the proportions of trees with apparent infection in the trunk base or in the main limb was significantly higher for the open vase vs. spindle design in Ca 2.5-fold. These differences may have been random, but in the following spring of 2018, all lesions recovered and the infections did not progress (Figure 3D and E). In the spring of the fifth year (2018), trees grown in the spindle design had infection scars on the trunk bases (1.1% of the trees) or the main limbs (7.5% of the trees). However, these

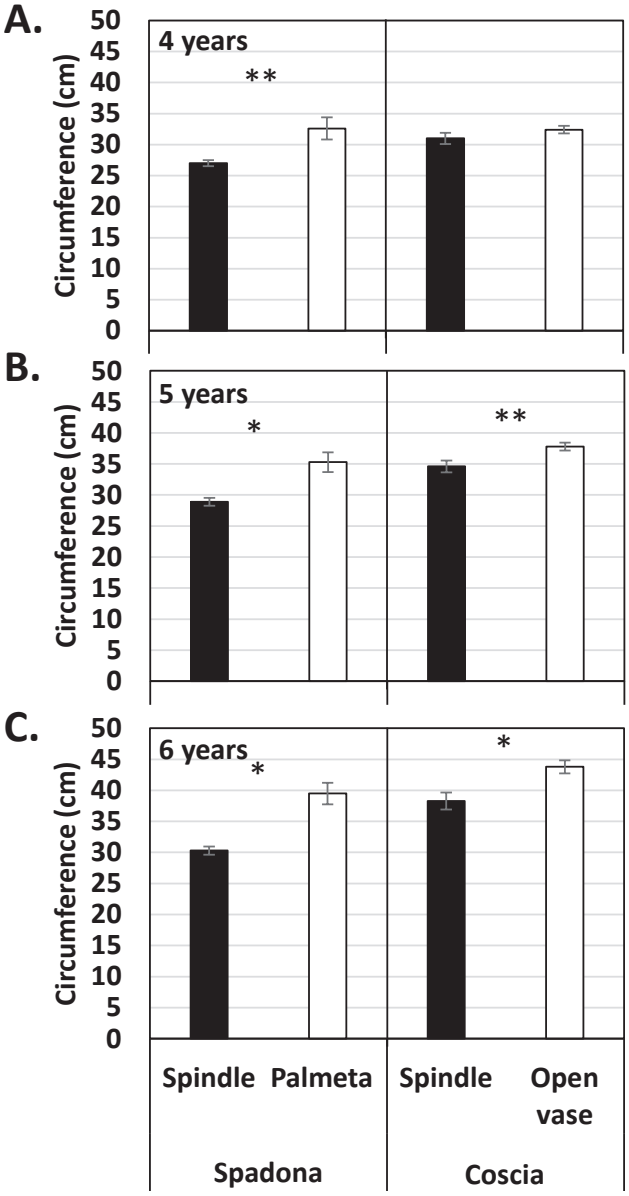

Figure 2. Mean trunk circumferences (cm) of 4-year-old (A), 5-year-old (B), or 6-year-old (C) pear trees. Trees were measured in November 2017 (A), 2018 (B), and 2019 (C), grown in a spindle design (low vigour, high density system for 'Spadona') , or Palmeta and open vase design (high vigour, low density system for 'Coscia'). Results are presented as averages ± SE. * indicates $P \leq 0.01$, and **$P \leq 0.05$, as shown by t-tests.

lesions were probably not active, because no disease progress was recorded in the following year (summer of 2018, Figure 3D and E). No 'Coscia' trees died from fire blight infections during the study.

DISCUSSION

High density pear orchards have many economic benefits over low density orchards, including greater yields, quicker returns on investment, more efficient utilization of pesticides and labour inputs, and improved fruit quality (Norelli *et al*., 2003; Majid *et al*., 2018). High density orchards can be profitable within the first 5 to 10 years from planting, which is less than for low density orchards (Robinson *et al*., 2004b). Although each low density tree gives less yield, there are significant positive effects on cumulative fruit yields per hectare. In the present study, tree population densities were varied using two different tree design systems, either spindle (in 'Coscia' and Spadona), palmeta (in 'Spadona') or open vase designs (in 'Coscia').

In 4- and 5-year-old 'Spadona' experimental plots, the spindle-shaped, low vigour trees had more restricted vegetative growth, measured as trunk circumference, than the palmeta trees. In the spindle-shaped trees, damage from fire blight infections was less in both the main limbs and the trunk bases, and no trees died after 7 years of growth and 4 years after severe infection. In contrast, in the palmeta, high vigour design system, in 10% of the trees the infection progress to the point of complete wilt. These results were not surprising, as Shtienberg *et al*. (2003) showed increased sensitivity of high vigour trees to fire blight progression in branches of 30 cm or longer. Similar results have also been obtained in apple. Norelli *et al*. (2000) reported that pruned and infected trees lost 10 times more yield than infected, unpruned trees, since pruning increased vegetative growth as well as the levels of primary metabolites and bacterial movement in the tree phloem.

In contrast to the present study results, however, Norelli *et al*. (2003) showed that high density orchards of apples grafted on a dwarf rootstock were very sensitive to fire blight. This sensitivity could have been due to the intensive summer pruning applied to the trees, as is common with this orchard design practice. Furthermore, summer pruning is used to improve fruit quantity and quality, and may also remove dead tissues and pathogen inoculum, and through reduced humidity, improve bactericide penetration into orchard canopies (Cooley *et al*., 2007). On the other hand, summer pruning can increase disease rates, if pruning is applied when disease risk is high (Cooley and Autio, 2011).

In Israel, 'Spadona' is the main cultivated pear variety, with 70 to 80% of sales, and 'Coscia' makes up the other 20 to 30% (http://agro.mashovgroup.net). 'Spadona' is considered to be more sensitive to fire blight damage than 'Coscia', so most fire blight studies in Israel have been

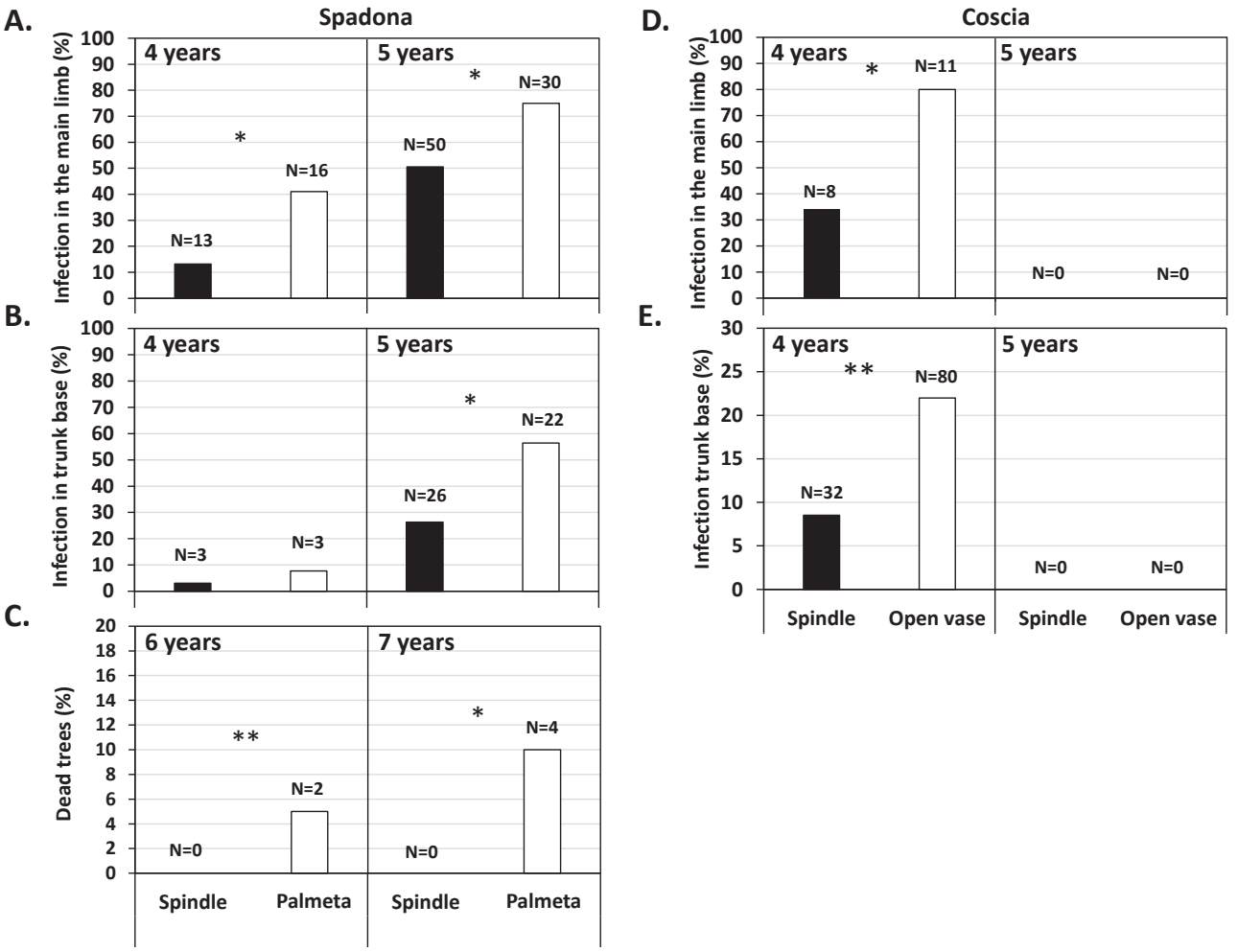

Figure 3. Mean proportions of pear trees infected with *Erwinia amylovora* out of all trees of different growth designs. A to C, 'Spadona' grown in spindle design (low vigour, high density) or palmeta design (high vigour, low density). D and E, 'Coscia' grown in spindle or open vase designs (high vigour, low density). A and D, Percent of trees with infections that reached the main limbs. B and E, percent of trees with infections that reached the trunk bases. C, percent of dead trees. Note that only 'Spadona' trees growing in the palmeta design (high vigour, low-density system) died due to fire blight. N = number of infected or dead trees. $*P < 0.01$, $**P < 0.05$ as indicated from contingency Chi-square analyses.

performed on 'Spadona' pear trees. The present study is the first to assess sensitivity of both of these cultivars under the same level of disease pressure, and to track disease severity over time. The 'Coscia' trees were naturally infected with fire blight at a level that was as severe as for 'Spadona', but the disease did not spread to the trunk bases or tree limbs in the subsequent year, and no fire blight symptoms appeared in the following 2 years. This was probably due to the more restricted innate vigour of 'Coscia'. Therefore, 'Coscia' tree design did not significantly affect *E. amylovora* progress in the trees.

In conclusions, 'Spadona' pear trees in high density (low vigour) plantings were less sensitive to fire blight damage than their low density, high vigour trees. Further agrotechnical methods to restrict tree vigour could be investigated for limiting infection in pear trees. In cv. Coscia, on the other hand, due to naturally low vigour, tree design had little impact on resistance to fire blight. Taken together, low-vigour, high-density orchard systems can be recommended for their increased profitability, and for their enhanced disease resistanceto fire blight.

ACKNOWLEDGMENTS

This research was funded by the Israeli Plant Production and Marketing Board. We thank Prof. Dani Shtienberg for help and advice relating to this study.

LITERATURE CITED

Bubán T., Orosz-Kovács Z., 2003. The nectary as the primary site of infection by *Erwinia amylovora* (Burr.) Winslow et al.: a mini review. *Plant Systematics and Evolution* 238(1): 183–194. https://doi.org/10.1007/s00606-002-0266-1

Cooley D.R., Autio W.R., 2011. Summer pruning of apple: impacts on disease management. *Advances in Horticultural Science* 25: 199–204. https://www.jstor.org/stable/42882838

Cooley D.R., Gamble J.W., Autio W.R., 2007. Summer pruning as a method for reducing fly speck disease on apple fruit. *Plant Disease* 81: 1123–1126. https://apsjournals.apsnet.org/doi/10.1094/PDIS.1997.81.10.1123

Ferree D.C., Warrington I.J., 2003. *Apples: Botany, Production and Uses*. CABI. https://www.cabi.org/ISC/ebook/20033083468

Johnson K.B., 2000. Fire blight of apple and pear. *The Plant Health Instructor.* https://doi.org/10.1094/PHI-I-2000-0726-01

Majid I., Khalil A., Nazir N., Majid I., 2018. Economic analysis of high density orchards. *International Journal of Advance Research in Science and Engineering* 7: 821–829. https://www.researchgate.net/profile/Insha_Majid/publication/343097407

Norelli J., Aldwinckle H., Momol T., Johnson B., DeMarree A., Reddy M.V.B., 2000. Fire blight of apple rootstocks. *New York Fruit Quarterly* 8: 5–8. https://nyshs.org/wp-content/uploads/2016/10/Fire-Blight-of-Apple-Rootstocks.pdf

Norelli J.L., Holleran H.T., Johnson W.C., Robinson T.L., Aldwinckle H.S., 2003. Resistance of Geneva and other apple rootstocks to *Erwinia amylovora*. *Plant Disease* 87: 26–32. https://doi.org/10.1094/PDIS.2003.87.1.26

Robinson T.L., 2004a. Effects of tree density and tree shape on apple orchard performance. In *VIII International Symposium on Canopy, Rootstocks and Environmental Physiology in Orchard Systems. Acta Horticulturae* 732: 405–414. https://www.actahort.org/books/732/732_61.htm.

Robinson T.L., 2004b. High density pear production: an opportunity for NY growers. *New York Fruit Quarterly* 18. https://fruit.webhosting.cals.wisc.edu/wp-content/uploads/sites/36/2016/03/1.High-Density-Pear-Production-An-Opportunity-for-NY-Growers.pdf

Robinson T.L., DeMarree A.M., Hoying S.A., 2004. An economic comparison of five high density apple planting systems. In *VIII International Symposium on Canopy, Rootstocks and Environmental Physiology in Orchard Systems. Acta Horticulturae* 732: 481–489. https://www.actahort.org/books/732/732_73.htm

Shtienberg D., Zilberstaine M., Oppenheim D., Levi S., Shwartz H., Kritzman G., 2003. New considerations for pruning in management of fire blight in pears. *Plant Disease* 87: 1083–1088. https://doi.org/10.1094/PDIS.2003.87.9.1083

Stern R.A., Doron I., 2009. Performance of 'Coscia' pear (*Pyrus communis*) on nine rootstocks in the north of Israel. *Scientia Horticulturae* 119: 252–256. https://doi.org/10.1016/j.scienta.2008.08.002

Stern R.A., Doron I., Rede G., Raz A., Goldway M., Holland D., 2013. Lavi 1—a new *Pyrus betulifolia* rootstock for 'Coscia' pear (*Pyrus communis*) in the hot climate of Israel. *Scientia Horticulturae* 161: 293–299. https://doi.org/10.1016/j.scienta.2013.04.040

van der Zwet T., Beer S.V., 1995. Fire blight – its nature, prevention, and control: a practical guide to integrated disease management. *US Department of Agriculture: Information Bullettin* No. 631. https://doi.org/10.5962/bhl.title.134796

Vanneste J.L., Eden-Green S., 2000. Migration of *Erwinia amylovora* in host plant tissues. In: *Fire Blight: the Disease and Its Causative Agent*, Erwinia amylovora. CABI, pp. 73–83.

Phytopathologia Mediterranea
The international journal of the
Mediterranean Phytopathological Union

Firenze University Press
www.fupress.com/pm

Research Papers

Fungal pathogens associated with harvested table grapes in Lebanon, and characterization of the mycotoxigenic genera

Wassim HABIB[1], Jack KHALIL[2,§], Annamaria MINCUZZI[3,§], Carine SAAB[1], Elvis GERGES[1], Hala Chahine TSOUVALAKIS[4], Antonio IPPOLITO[3], Simona Marianna SANZANI[2,*]

[1] *Laboratory of Mycology, Department of Plant Protection, Lebanese Agricultural Research Institute, Fanar, Lebanon*
[2] *CIHEAM Bari, Via Ceglie 9, 70010 Valenzano (Bari), Italy*
[3] *Department of Soil, Plant and Food Sciences, University of Bari Aldo Moro, Via Amendola 165/A, 70126 Bari, Italy*
[4] *Department of Plant Production, Faculty of Agricultural and Veterinary Sciences, Lebanese University, Dekwaneh, Lebanon*
§ Authors equally contributed to the research
* Corresponding author. E-mail: sanzani@iamb.it

Summary. Table grapes are exposed to fungal infections before and after harvest. In particular, *Aspergillus*, *Penicillium*, and *Alternaria* can cause decays and contamination by mycotoxins. The main fungi affecting Lebanese table grapes after harvest were assessed as epiphytic populations, latent infections, and rots. Effects of storage with and without SO_2 generating pads were also evaluated. Representative isolates of toxigenic genera were characterised, and their genetic potential to produce ochratoxin A, fumonisins, and patulin was established. The epiphytic populations mainly included wound pathogens (*Aspergillus* spp. and *Penicillium* spp.), while latent infections and rots were mostly caused by *Botrytis* spp. The use of SO_2 generating pads reduced the epiphytic populations and rots, but was less effective against latent infections. Characterization of *Aspergillus*, *Penicillium,* and *Alternaria* isolates showed that *A. tubingensis*, *P. glabrum,* and *A. alternata* were the most common species. Strains of *A. welwitschiae* and *P. expansum* were also found to be genetically able to produce, respectively, ochratoxin A plus fumonisins and patulin. These data demonstrate the need for effective measures to prevent postharvest losses caused by toxigenic fungi.

Keywords. Postharvest, *Aspergillus*, *Penicillium*, *Alternaria*, mycotoxins, sulphur dioxide.

OPEN ACCESS

Citation: W. Habib, J. Khalil, A. Mincuzzi, C. Saab, E. Gerges, H.C. Tsouvalakis, A. Ippolito, S.M. Sanzani (2021) Fungal pathogens associated with harvested table grapes in Lebanon, and characterization of the mycotoxigenic genera. *Phytopathologia Mediterranea* 60(3): 427-439. doi: 10.36253/phyto-12946

Accepted: September 8, 2021

Published: November 15, 2021

Data Availability Statement: All relevant data are within the paper and its Supporting Information files.

Competing Interests: The Author(s) declare(s) no conflict of interest.

Editor: Antonio Moretti, National Research Council, (CNR), Bari, Italy.

INTRODUCTION

Table grapes are among the most important fruit crops in Lebanon due to the favourable Mediterranean climatic conditions and long cultivation tradition. Table grapes are grown on 7,030 ha, with annual production of 62,014 t (FAOSTAT, 2019). Plantations for commercial production have long been made with the local cultivars Tfeifihi, Beitamouni, Maghdouchi, and Obeidi.

Recently, however, commercial cultivars have been introduced from Europe and the United States (Chalak *et al*., 2016). Thirty-eight packinghouses and storage facilities exist in Lebanon, of which 22 process table grapes (Lebanese Chamber of Commerce, 2019). Most of these facilities are in the Bekaa region in Eastern Lebanon, where most table grape production occurs. The most common pre-cooling method, present in almost all these facilities, is the room cooling, where pre-cooling and storage are carried out in the same room at appropriate temperatures.

Grapes are susceptible to many fungal diseases in the field and during storage. Postharvest diseases, in favourable conditions and particularly in developing countries, can cause losses in total production of up to 55% (Sanzani *et al*., 2016a). The most destructive postharvest disease of table grapes is grey mould caused by *Botrytis* spp. Infections often take place in the field, and the fungi remain latent until ripening (Sanzani *et al*., 2012). Other diseases can occur during storage, including blue mould caused by *Penicillium* spp., some of which can grow even in refrigerated conditions (Sanzani *et al*., 2013). The predominant *Penicillium* species isolated from grapes differ between vineyards and years, but the most common ones are *P. brevicompactum*, *P. citrinum*, *P. glabrum,* and *P. expansum* (Rousseaux *et al*., 2014). Other diseases are more recurrent in presence of warm temperatures (*e.g*., during transportation and marketing). These include rots caused by *Aspergillus* spp. (Droby and Lichter, 2007); the section *Nigri* is the most common on grapes, including the species *A. carbonarius*, *A. niger*, *A. tubingensis,* and *A. welwitschiae* (Perrone *et al*., 2007). *Alternaria* spp. have also been reported as responsible for pre- and postharvest losses of agricultural commodities, including grapes (Lorenzini and Zapparoli, 2014; Garganese *et al*., 2016), with *A. alternata* as most recurrent species (Stocco *et al*., 2019).

These fungi have additional important detrimental roles, being able to produce mycotoxins. Mycotoxin production is highly influenced by climatic conditions (*e.g*., temperature and humidity), berry characteristics (*e.g*., pH and available water), fungicide applications, and harvesting and storage conditions (Covarelli *et al*., 2012). The main mycotoxin produced by *Aspergillus* spp. on grapes and consequently grape-derived products is ochratoxin A (OTA), which is primarily produced by *A. carbonarius*, although *A. niger* and *A. welwitschiae* also contribute to contamination (de Souza Ferranti *et al*., 2018). *Aspergillus* spp., including *A. niger* and *A. welwitschiae*, are also able to produce fumonisins (mostly FB_2) (Samson *et al*., 2007; Hong *et al*., 2013). OTA is immunotoxic, nephrotoxic and possibly carcinogenic (IARC, 1993), so that the European Commission set its maximum limits in foodstuffs deriving from grapes (EC, 2006). Fumonisins, although reported to be possibly carcinogenic (IARC, 1993), are regulated in the EU only on cereals and derived products (EC, 2007). The main mycotoxin produced by *Penicillium* spp. (particularly *P. expansum*) on fruits is patulin, which has been mainly reported on pome fruits, but is associated with several other crops including grapes (Sanzani *et al*., 2013, 2016b). Patulin content is regulated in apple-derived products in the EU (EC, 2006); however, no official regulatory limits exist for grapes and derived products. Not less important is contamination by *Alternaria* and its related toxins, which have been reported on several commodities, including grapes, both in the field and during storage (Sanzani *et al*., 2016a). The most relevant of these mycotoxins are tenuazonic acid (TeA), alternariol (AOH) and alternariol monomethyl ether (AME) (Wenderoth *et al*., 2019). Although *Alternaria* toxins can cause adverse effects in human and animal systems (Schuchardt *et al*., 2014), no regulatory limits exist for these compounds. Nevertheless, EFSA (2011) published a scientific opinion on the risks for animal and public health related to the presence of *Alternaria* toxins in feed and food.

Among the different practices for the control of postharvest rots during storage, given the lack or limited use of conventional fungicides, SO_2 generating pads in packages remain an important tool due to their practicality, efficiency, low cost, and low health risks compared to fungicides (Franck *et al*., 2005).

The table grape production chain in Lebanon encounters many of these phytosanitary problems. Most important are postharvest rots, which result from poor practices in the field, at harvesting, and during storage. The aims of the present study were: i) to assess the fungal populations associated with table grapes in Lebanese packinghouses; ii) to determine the effects of storage conditions on the fungal populations; iii) to characterize at the species level the populations of the most represented mycotoxigenic genera; and iv) to molecularly characterize the putative ability of fungi to produce relevant mycotoxins.

MATERIALS AND METHODS

Assessments of the fungal population on table grape bunches by the end of storage

Sampling

Table grapes samples were collected from five packinghouses located in Central Bekaa district (Bekaa

region, Lebanon), which apply room cooling systems, during February 2020. The grapes had been stored for three months at 1±2°C, 95% relative humidity (RH), and with SO_2 generating pads. In each facility, the two most abundant cultivars were selected for sampling. For each cultivar, a sample of 15 bunches was randomly taken from at least five boxes, the bunches were transported in refrigerated containers to the laboratory, and were processed within a maximum of 12 h.

Assessment of epiphytic populations

From each sample, three replicates of 20 berries each were randomly taken and placed separately in a sterile plastic bag containing 200 mL of 0.05% Tween 20 (Sigma Aldrich). Replicates were shaken for 30 min on an orbital shaker at 150 rpm. For each replicate, aliquots of 200 µL were then plated on three Petri plates (90 mm diam.) containing Dichloran Glycerol 18% Agar (DG18, Deben Diagnostics Ltd), and these were incubated for 3-5 d in the dark at 24±1°C (Aşkun *et al*., 2007). Fungal colonies were then counted, and the associated epiphytic population was expressed as Colony Forming Units per gram of fresh berry weight (CFU g^{-1} fbw).

Assessment of latent infections by fungal pathogens

For each sample, three replicates of 20 berries each were surface decontaminated by soaking in 2% NaOCl solution for 2 min, rinsed with sterile distilled water for 2 min, and then dried under a laminar flow hood. Each replicate was aseptically placed in a sterile plastic bag and kept at -20±1°C for 2 h to facilitate the collapse of the berry tissues (Sanzani *et al*., 2012). The bags were then placed in an incubator at 24±1°C in the dark for a maximum of 7 d. Berries showing signs of fungal infections were counted and the incidence of latent infections expressed as percentage (%) of symptomatic berries. The recovered fungal colonies were identified based on the morphological characteristics (Barnett and Hunter, 1999), and the frequency of each genus was calculated as percentage of the total recovered colonies.

Assessment of rots

In each packinghouse and for each cultivar, five boxes were inspected at the end of storage. Each bunch was visually checked for the presence of rot symptoms. Disease severity was assessed using an empirical scale of eight classes: 0 = sound cluster; 1 = one-two infected berries; 2 = three-five infected berries; 3 = six-ten infected berries; 4 = less than 25% infected cluster; 5 = 26–50% infected cluster; 6 = 51–75% infected cluster; and 7 = more than 76% infected cluster. The average severity scale was then calculated and the disease severity index (DSI) was determined using the following equation: DSI (%) = [sum (class frequency × score of rating class)] [(total number of clusters) × (maximal disease index)]$^{-1}$ × 100 (Chiang *et al*., 2017).

Effects of storage conditions on the fungal populations

To study the effects of storage conditions on the fungal populations, particularly the use of SO_2 generating pads, samples of 15 bunches of 'Red Globe' and 'Crimson' grapes were collected from one packinghouse in Ferzoul (Packinghouse 2) after packing and just before pre-cooling (T_0) and at the end of the storage period (T_f). Sampling was made from packages in which an SO_2 pad was present ($+SO_2$) and from packages that underwent the same storage conditions but without SO_2 pads ($-SO_2$). Epiphytic fungal populations, latent infections, and rots were evaluated as described above.

Characterization of toxigenic fungal pathogens

From each trial, a representative number of fungal isolates, belonging to the toxigenic genera *Aspergillus*, *Penicillium,* and *Alternaria,* was collected for subsequent characterization at species level, according to, respectively, Samson *et al*. (2014), Visagie *et al*. (2014), and Woudenberg *et al*. (2013; 2015). Monoconidial isolates were obtained by spreading conidium suspensions on 2.5% water agar and collecting single germinated spores using stereomicroscope observation. Isolates were stored at 4±1°C on slants of Potato Dextrose Agar (PDA, Himedia).

DNA extraction

For each fungal isolate, five mycelium plugs were collected from 7-d-old PDA colonies, and used to inoculate Malt Extract Agar (MEA, Fluka) in Petri plates with the agar surfaces overlapped by sterilized cellophane disks. After incubation at 24±1°C for 2–3 d, the layers of fresh hyphae were removed using a scraper, and were placed in 2 mL capacity microcentrifuge tubes and stored at -20±1°C. DNA extraction was carried out according to Murray and Thompson (1980) as modified by Rogers and Bendich (1989) with further slight

modifications. Briefly, two iron balls (5 mm diam.) were added to 100 mg of mycelium followed by liquid nitrogen. Once nitrogen evaporated, the tubes were placed in a tissue lyser (Qiagen) at maximum frequency (30 osc s^{-1}) for 45 s. For each isolate, 600 µL of CTAB buffer (100 mM Tris-HCl pH 8.0, 1.4 M NaCl, 20 mM EDTA, 0.2% β-mercaptoethanol, 2% CTAB) (previously kept at 75±1°C for 30 min) were added to the sample and mixed gently. The samples were then frozen and defrozen three times, using liquid nitrogen and a water bath at 75±1°C. The samples were then kept in the water bath for 60 min at 75±1°C (inverted every 10 min). The tubes were then cooled, and 600 µL of chloroform were added to samples and vortexed. The tubes were then centrifuged at 14,000 rpm for 15 min, the liquid phase was transferred into new microcentrifuge tubes each containing 2 volumes of isopropanol, and the tubes were each inverted gently. The samples were maintained at -80±1°C for 30 min, and then centrifuged at 14,000 rpm and 4±1°C for 20 min. Each resulting pellet was washed with 200 µL 70% ethanol and centrifuged for 5 min in the same conditions. The pellets were then air-dried and re-suspended in 200 µL TE buffer (pH 8.0). The extracted DNA was quantified by a Nanodrop (Shimadzu) and diluted to 25 ng μL^{-1}.

High Resolution Melting assays to screen *Penicillium* and *Aspergillus* isolates

To screen the isolates belonging to *Penicillium* and *Aspergillus*, genus-specific primer pairs (Table 1), synthesized by Macrogen, were used in High Resolution Melting (HRM) reactions, run in a CFX96 Touch Real-time PCR Detection System (Bio-Rad) and analysed using CFX-Manager Software v1.6 (Bio-Rad), as reported by Mincuzzi *et al.* (2020). A cut-off genotype confidence percentage (GCP) ≥95% was set for assigning isolates to genotypes.

Molecular identification of fungi

All *Alternaria* (n = eight) isolates, and representative isolates of *Penicillium* (n = six) and *Aspergillus* (n = ten) selected based on the clusters obtained with HRM assays (at least one isolate per cluster) were sub-

Table 1. Primers for HRM screening, sequencing, and mycotoxin gene detection of *Penicillium*, *Aspergillus* and *Alternaria* isolates from grape samples.

Genus	Gene/ Region	Primer name	Sequence (5'- 3')	Amplicon size (bp)	Source
Penicillium	β-tubulin	Bt2a	GGTAACCAAATCGGTGCTGCTTTC	330	Glass and Donaldson, 1995
		Bt2b	ACCCTCAGTGTAGTGACCCTTGGC		
		PPF1	GAGCGYATGAACGTCTACTT	130	Mincuzzi *et al.*, 2020
		PPR1	ACVAGGACGGCACGGGGAAC		
	msas	Pe 11F	CACTTATTGTGACCCGCAGA	288	Sanzani *et al.*, 2009
		Pe 12R	CTCGAAGAGGATCCATGAGG		
Aspergillus	calmodulin	CMD5	CCGAGTACAAGGARGCCTTC	520	Hong *et al.*, 2005
		CMD6	CCGATRGAGGTCATRACGTGG		
		HRM-CMDF	ATAGGACAAGGATGGCGATG	205	Mincuzzi *et al.*, 2020
		HRM-CMDR	AGACTCGGAGGGGTTCTGGC		
	fum8	FUM8F	TTCGTTTGAGTGGTGGCA	651	Susca *et al.*, 2014
		FUM8R	CAACTCCATASTTCWWGRRAGCCT		
	fum15	FUM15F	CGATTGGTAGCCCGAGGAA	701	
		FUM15R	CTTGATATTGCGGAGTGGTCC		
	ota1	OTA1F	CAATGCCGTCCAACCGTATG	776	Susca *et al.*, 2016
		OTA1R	CCTTCGCCTCGCCCGTAG		
	ota3	OTA3F	TTAGACAAACTGCGCGAGGA	613	
		OTA3R	GCGTCGCTATGCCCAGATA		
Alternaria	OPA1-3	OPA1-3L	CAGGCCCTTCCAATCCAT	900	Peever *et al.*, 2004
		OPA1-3R	AGGCCCTTCAAGCTCTCTTC		
	pksI	pksI-F	CCTCTCTATCCCAAACTCCACAC	249	Sanzani *et al.*, 2021
		pksI-R	CACAGATTATGGCAAGGTTC		

Table 2. Reference strains used in phylogenetic analyses and their GenBank accession numbers.

Genus	Species	Strain	Accession No.
Alternaria	*A. alternata*	CBS 112249	MG063725
		CBS 116329	MF070417
		A214	MK204937
	A. arborescens	A43	KU933224
	A. solani	ASOL	KY561993
Aspergillus	*A. flavus*	CBS117733	EF202059
	A. nidulans	CBS 100522	KX423636
	A. porosus	CBS 375.75	LT671137
	A. tubingensis	AS5	MK919489
		AS18	MK919490
		DTO 178-B5	KP330146
	A. uvarum	AS13	MK919493
	A. welwitschiae	AS23	MK919491
		AS28	MK919492
		CBS 139.54	KC480196
		942	MH614648
Penicillium	*P. brevicompactum*	CMV006A8	MK451072
		G14	MK895703
	P. chrysogenum	CBS 109613	KJ866978
	P. expansum	CBS 48184	AY674399
	P. glabrum	DTO 057-A5	KM08875
	P. olsonii	CBS 38175	AY674444

jected to sequencing of portions of barcoding genes, using the primer pairs detailed in Table 1. PCR reactions were each carried out using 1× Ready Master Mix (Qiagen), 1.5 mM $MgCl_2$, 0.2 µM of each primer, and 25 ng of DNA template in a final volume of 25 µL. The amplifications were carried out in a T100 MyCycler thermal cycler (Bio-Rad) using the following conditions: 2 min at 95°C, followed by 40 cycles of 30 s at 95°C, 30 s at 55-58°C, 50 s at 72°C, and 5 min at 72°C. After this, 10 µL of each PCR product were loaded on a 1.5% agarose gel in 1× TAE buffer and visualized by the imager system Gel Doc 1000 (Bio-Rad). Purification of PCR products was then carried out using the QIAquick Gel Extraction Kit (Qiagen) following manufacturer's instructions. Purified PCR products were sequenced in both directions by the Medical Genetics Unit at Saint Joseph University (Beirut, Lebanon). For species identification, all sequences were aligned through Chromas software (https://chromas.software.informer.com/download/) and compared with the available sequences in NCBI BLAST database. Subsequently, using MEGA-X software (https://www.megasoftware.net/dload_win_gui), phylogenetic trees were constructed using the Maximum Likelihood method (Kumar *et al*., 2018), according to the Tamura-Nei model (1993) with 1000 bootstrap replications. Reference and CBS strains were included (Table 2).

Molecular characterization of putative ability to produce mycotoxins

According to genus and species, the strains were tested for the presence of genes involved in biosynthetic pathways of the most relevant mycotoxins. The assayed genes were: *pksI* for AOH/ AME biosynthesis, assayed for *Alternaria* strains; *ota1/ota3* for OTA and *fum8/ fum15* for fumonisin biosynthesis, assayed for *Aspergillus* strains; and *msas* for patulin biosynthesis, assayed for *Penicillium* strains. Primers, reported in Table 1, were synthesized by Eurofins Genomics. PCR mixtures were each of 25 µL, containing 25 ng of DNA, 0.2 µM of each primer, and 1× Dream Taq Hot Start Green PCR Master Mix (Thermo Fischer Scientific); reactions were carried out according to authors' conditions (Table 1). The presence/absence of these genes was estimated by running an amplicon aliquot on 1.5% agarose gel and UV visualization.

Statistical analyses

Statistical analyses were carried out using IBM SPSS software (version 23). One-way Analysis of Variance (ANOVA) was performed to verify the significance of differences between means, and means were separated using Duncan's Multiple Range test (DMRT).

RESULTS

Epiphytic fungal populations, latent infections, and severity of grape berry decay

Table grapes from five table grape packinghouses in different Lebanese areas were assessed for epiphytic populations of filamentous fungi, latent infections, and rots at the end of storage. Two cultivars from each packinghouse were inspected. Assessment of the epiphytic populations (Table 3) showed low CFU g^{-1} fbw values. Particularly, from 'Autumn King' and 'Superior' samples from Packinghouse 1 (Zahlé area) and 'Crimson' from Packinghouse 4 (Chtaura area), no fungal colonies were recovered. In the other cases, the total fungal counts varied from 1 to 64 CFU g^{-1} fbw. Significant differences ($P \leq 0.05$) were determined between the cultivars in the different packinghouses.

Table 3. Mean epiphytic fungal populations, latent infections and disease severities on table grapes from different packinghouses in Bekaa region (Lebanon) at the end of storage.

Packinghouse	Locality	Cultivar	Epiphytic population (CFU g^{-1} fbw)*	Latent infections (%)*	Disease severity	
					Scale*	DSI** (%)
1	Zahlé	Autumn King	0 c	10.0 ± 8.2 a	1.7 ± 0.3 a	24.8
		Superior	0 c	11.7 ± 2.7 a	0.6 ± 0.2 bc	8.6
2	Ferzoul	Crimson	24 ± 9 a	10.0 ± 0.0 a	0.8 ± 0.2 bc	11.4
		Red Globe	4 ± 4 bc	10.0 ± 4.7 a	0.2 ± 0.1 c	2.9
3	Zahlé	Black Pearl	34 ± 24 a	6.7 ± 1.4 a	0.3 ± 0.1 c	4.8
		Red Globe	19 ± 16 ab	8.3 ± 6.9 a	1.2 ± 0.2 ab	17.1
4	Chtaura	Autumn King	64 ± 35 a	15.0 ± 7.1 a	0.8 ± 0.2 bc	11.4
		Crimson	0 c	6.7 ± 1.4 a	1.1 ± 0.3 ab	16.2
5	Zahlé	Chile	3 ± 3 bc	0 b	0.1 ± 0.1 c	1.0
		Crimson	1 ± 1 c	0 b	0.3 ± 0.1 c	3.8

* Means ±standard errors. In each column, values accompanied by different letters are significantly different ($P \leq 0.05$).
** DSI = Disease severity index.

For example, samples of 'Autumn King' from two different packinghouses showed the opposite extreme values. Occurrence of latent infections at the end of the storage was evaluated (Table 3). Four packinghouses and related cultivars showed latent infection incidence varying from 6.7% on 'Black pearl' (Packinghouse 3) and 'Crimson' (Packinghouse 4) to 15% on 'Autumn King' (Packinghouse 4). The most frequent fungal genera causing latent infections were *Penicillium* (47.1%), followed by *Botrytis* (29.4%), *Alternaria* (7.8%), *Aspergillus* (5.9%), *Stemphylium* (4.0%), *Cladosporium* (3.9%), and other fungi (2.0%). Disease severity on bunches was measured at the end of storage in all packinghouses (Table 3). Significant differences were observed between the mean disease severities. The greatest severity (mean = 1.7, range 0-7) was recorded on 'Autumn King' samples from Packinghouse 1 (mean DSI = 24.8%), whereas the least severity (mean = 0.1) was detected on 'Chile' from Packinghouse 5 (mean DSI = 1%). In general, *Botrytis* was the predominant genus observed on stored bunches.

Effects of storage conditions on the fungal populations

Effects of the use of SO_2 generating pads were evaluated in Packinghouse 2, on 'Red Globe' and 'Crimson'. Large reductions in the epiphytic fungal populations on 'Red Globe' (97.9%) and 'Crimson' (99.3%) was detected between T_0 (beginning of storage) and T_f (end of storage) in presence of SO_2 pads (Figure 1). *Penicillium* growth was reduced by up to 99%. For *Aspergillus,* which was less than *Penicillium* at T_0, growth was completely prevented at T_f (Figure 1 a and b). However, the effect of SO_2 during storage on latent infections was variable, being effective on 'Red Globe' but not on 'Crimson'. Although SO_2 completely prevented *Botrytis* infections on both cultivars, it did not influence *Aspergillus* and *Penicillium* infections on 'Crimson' berries (Figure 1 c and d).

As confirmation, the effects of SO_2 were evaluated after three months of storage in the same packinghouse on boxes stored with or without SO_2 pads (Figures 2 and 3). Results confirmed the potential of the pads for reducing total latent infections (Figure 2). In the absence of pads, mean incidence of total latent infections at the end of storage was 31.7% on 'Red Globe' and 37.5% on 'Crimson', whereas in boxes stored with SO_2 pads, mean incidence was 10% on both cultivars. SO_2 generating pads completely prevented latent infections caused by *Botrytis* and *Alternaria*, whereas latent infections by *Penicillium* were observed in both types of packages, with mean incidence varying between 10 and 16.7%. Similarly, decay severity assessed after 3 months of storage on both cultivars was greater ($P \leq 0.05$) in boxes stored without SO_2 pads than in boxes containing the pads (Figure 3).

Characterization of fungal strains and their putative abilities to produce mycotoxins

During the assessments of epiphytic fungal populations, latent infections, and rots, three genera among mycotoxigenic fungi were identified: *Alternaria*, *Aspergillus*, and *Penicillium*. A total of 44 isolates were col-

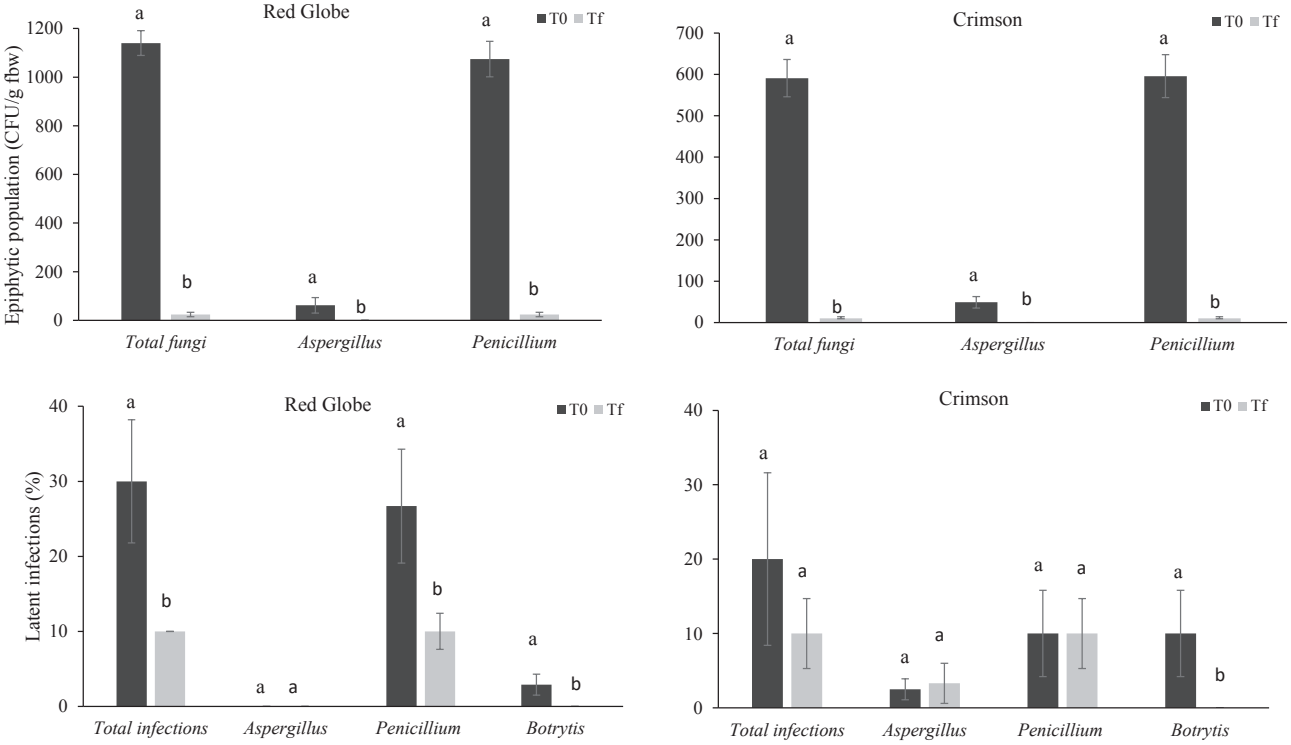

Figure 1. Mean populations of epihytic fungi, and proportions (%) of latent fungal infections, on 'Red Globe' and 'Crimson' table grapes, stored with SO_2 generating pads. For each variable, mean values at T_0 (black histogram, beginning of storage) and T_f (end of storage) accompanied by different letters are significantly different ($P \leq 0.05$). Bars represent standard errors of means, each from three replicates.

lected according to morphology and frequency of isolations. Twenty-four isolates were *Aspergillus*, 12 were *Penicillium*, and eight were *Alternaria*. All the isolates were assigned to a species according to morphological features on specific media and sequencing of barcoding genes/regions. *Aspergillus* and *Penicillium* isolates were the most abundant so these were initially screened by HRM to identify genetic clusters. For at least one isolate per cluster of *Aspergillus,* a portion of the calmodulin gene was sequenced, whereas for *Penicillium*, a portion of the β-tubulin gene was sequenced. Sequences were run against those in the GenBank database, and they showed 99-100% identity with relevant reference sequences. As further confirmation, a phylogenetic analysis was conducted including CBS and reference strains (Figures 4, 5 and 6).

For *Aspergillus*, all strains belonged to section *Nigri* and were divided into ten clusters (Table 4, Figure 4). Most of isolates belonged to series *Nigri*, being *A. tubingensis* (67%) and *A. welwitschiae* (12%), and the remaining were in series *Japonici*, as *A. uvarum* (21%). For *A. welwitschiae* strains (AS20, AS27, and AS31), the presence of key biosynthetic genes for OTA (*ota1* and *ota3*) and fumonisins (*fum8* and *fum15*) was assessed. Strains A27 and AS31, belonging to the same HRM cluster (9), possessed *ota3* and *fum15* genes, so were potential producers of OTA and fumonisins, while strain AS20 (HRM cluster 7) did not possess these genes (Table 4).

For *Penicillium* (Table 5, Figure 5), five HRM clusters were identified corresponding to three sections. The most abundant was sect. *Aspergilloides* with 50% of the strains identified as *P. glabrum*, followed by sect. *Brevicompacta* with *P. brevicompactum* (25%) and *P. olsonii* (17%), and sect. *Penicillium* with *P. expansum* (8%). *P expansum* strain P18 possessed *msas*, the key gene for patulin biosynthesis (Table 5).

For *Alternaria*, *A. alternata* and the *A. arborescens* species complex were identified (Table 6). Isolate identity was supported by a phylogenetic analysis, including CBS and references strains (Figure 6). Eighty-eight percent of the strains were *A. alternata* morphotype *alternata*, and 12% were in the *A. arborescens* species complex. Strains were tested for the presence of the *pksI* gene for alternariol biosynthesis and all were potential AOH/AME producers (Table 6).

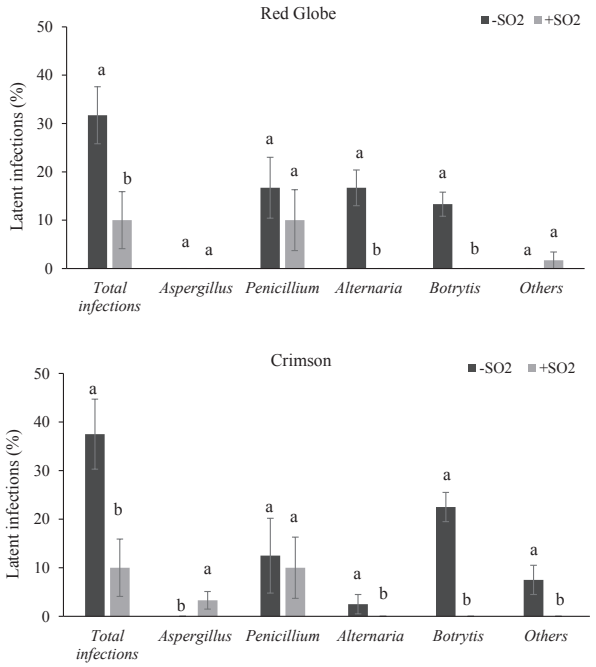

Figure 2. Mean proportions (%) of latent fungal infections on 'Red Globe' and 'Crimson' table grapes, stored either with (+SO_2) or without (black histograms, -SO_2) SO_2 pads, after three month of storage. For each variable, columns accompanied by different letters are significantly different ($P \leq 0.05$). Bars represent standard errors of mean, each from three replicates.

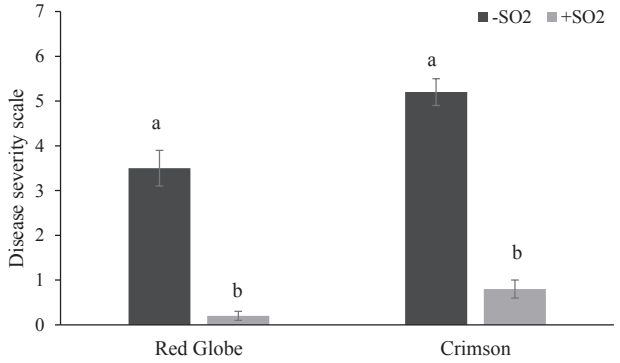

Figure 3. Disease severity (scale 0-7) on 'Red Globe' and 'Crimson' table grapes, stored either with (+SO_2) or without (black histograms, -SO_2) SO_2 pads, after three month of storage. Columns accompanied by different letters are significantly different ($P \leq 0.05$). Bars represent standard errors of means, each from three replicates.

DISCUSSION

Crops of table grapes are of increasing importance in Lebanon. However, there is little information available on the main fungal pathogens affecting table grape storability. The present study was conducted to collect information on the main threats to harvested table grapes, with particular attention on mycotoxigenic fungi. Five packinghouses were inspected in different areas of Lebanon for epiphytic fungal populations, latent infections, and rots. The study showed that *Botrytis*, *Penicillium*, *Aspergillus*, and *Alternaria* were the most abundant genera. These results are in line with other studies. Ding *et al.* (2019) reported epiphytic populations on grapes in subtropical China, and indicated that *Cladosporium, Penicillium, Aspergillus,* and *Alternaria* were among the most abundant fungi. Similarly, Oliveira *et al.* (2017) showed that these genera were the most frequently isolated from grape berries in Portugal. They also stressed the influence of atmospheric conditions on the composition of the fungal community detected. Abdelfattah *et al.* (2019) reported exchanges between grape plants and the surrounding environment, so that grape plants could be major sources of recruitment for the atmospheric microbiome.

Aspergillus and *Penicillium* species are considered to be the most important wound pathogens. They commonly enter host plants through wounds and natural openings. Wounds can be created at pre- and postharvest stages, especially if the products are subjected to improper handling either at harvesting or during packing and storage operations (Mincuzzi *et al.*, 2020). In the present study, different packinghouses were assessed, each with two grape cultivars. Although the epiphytic fungal populations were generally low, some differences were observed. For example, despite the same storage procedures, including air cooling and the use of SO_2 generating pads in the two different packinghouses, the grapes of 'Autumn King' and 'Crimson' had different amounts of contamination. This could be due to different field inoculum loads and composition. The present study showed different susceptibilities to SO_2 among fungi, with *Botrytis* more susceptible to SO_2 than *Penicillium*. Furthermore, the different responses among cultivars could be related to features such as berry epidermis thickness or compaction, cell wall thickness, and/or epidermis microstructure (Fernández-Trujillo *et al.*, 2012). Influences of vineyard management on epiphytic microbial composition could also be involved (Abdelfattah *et al.*, 2019).

Latent fungal infections were present on most of the cultivars. These results are not surprising since *Botrytis* is well known for its ability to infect grapevine from the flowering stage, and can remain latent/dormant until reactivation following suitable conditions (*i.e.*, ripening and favourable environmental conditions; Sanzani *et al.*, 2012). During packinghouse operations, berries may seem healthy, but eventually become rotted during

Table 4. *Aspergillus* HRM clusters, species, strains, GenBank accession numbers for the calmodulin gene, and presence of ochratoxin A (*ota1* and *ota3*) and fumonisins (*fum8* and *fum15*) biosynthetic genes.

HRM Cluster	Species	Strain	Accession no.*	Detection of biosynthetic genes**			
				ota1	ota3	fum8	fum15
1	*A. tubingensis*	AS17	n.a.	n.a.	n.a.	n.a.	n.a.
		AS21	MZ241120	n.a.	n.a.	n.a.	n.a.
		AS24	n.a.	n.a.	n.a.	n.a.	n.a.
2	*A. tubingensis*	AS15	MZ241118	n.a.	n.a.	n.a.	n.a.
		AS18	n.a.	n.a.	n.a.	n.a.	n.a.
		AS22	n.a.	n.a.	n.a.	n.a.	n.a.
3	*A. tubingensis*	AS2	MZ241114	n.a.	n.a.	n.a.	n.a.
		AS19	n.a.	n.a.	n.a.	n.a.	n.a.
		AS25	n.a.	n.a.	n.a.	n.a.	n.a.
4	*A. tubingensis*	AS14	MZ241117	n.a.	n.a.	n.a.	n.a.
		AS16	MZ241119	n.a.	n.a.	n.a.	n.a.
		AS23	n.a.	n.a.	n.a.	n.a.	n.a.
5	*A. tubingensis*	AS9	n.a.	n.a.	n.a.	n.a.	n.a.
		AS29	MZ241121	n.a.	n.a.	n.a.	n.a.
6	*A. uvarum*	AS1	n.a.	n.a.	n.a.	n.a.	n.a.
		AS10	MZ241125	n.a.	n.a.	n.a.	n.a.
		AS11	MZ241126	n.a.	n.a.	n.a.	n.a.
		AS26	MZ241127	n.a.	n.a.	n.a.	n.a.
		AS28	MZ241128	n.a.	n.a.	n.a.	n.a.
7	*A. welwitschiae*	AS20	MZ241122	-	-	-	-
8	*A. tubingensis*	AS13	MZ241116	n.a.	n.a.	n.a.	n.a.
9	*A. welwitschiae*	AS27	MZ241123	+	-	+	-
		AS31	MZ241124	+	-	+	-
10	*A. tubingensis*	AS12	MZ241115	n.a.	n.a.	n.a.	n.a.

* n.a. = not analyzed.
** The presence of OTA and fumonisin biosynthetic genes was checked in *A. welwitschiae* strains. + = Present; - = Absent.

storage. Being situated within berry grape tissues, *Botrytis* rots might not be prevented by surface treatments such as the SO_2 generated by the preservation pads. SO_2 does not penetrate deeply into berry tissues/skins (Smilanick *et al.,* 1990), especially the skins are particularly impenetrable. Thus, in the present study, rots, mostly caused by *B. cinerea*, were significantly reduced by SO_2 pads, although not prevented. The reduced sensitivity of 'Crimson' to SO_2 compared to 'Red Globe' may be a cultivar effect, or due to the extent or composition of pathogen contamination (*i.e.*, presence of *Penicillium* and *Aspergillus*). However, Youssef *et al.* (2020) found that SO_2 generating pads, even at different concentrations and release rates, could completely inhibit grape decay caused by *B. cinerea*, if combined with a field control strategy to reduce infections rate during grapevine growth. These field treatments should be scheduled from flowering, to reduce rots during cold storage of harvested grapes. Alternative treatments with little to no potential harmful environmental effects have raised public interest. For example, protein hydrolysates (*e.g.*, from soybean or casein) were tested with good results (Lachhab *et al.,* 2016).

The toxigenic fungi contaminating harvested Lebanese table grapes included *Aspergilli* of section *Nigri*. *A. tubingensis* is known as a non-producer of OTA (Storari *et al*., 2012); *A. uvarum* is a relatively newly discovered species, mostly occurring on grapes and is not toxigenic (Somma *et al*., 2012); and *A. welwitschiae* produces OTA and fumonisins (Perrone and Gallo, 2016), as observed for 2 of the 3 strains in the present study. For *Penicillium*, strains of *P. glabrum* and *P. brevicompactum* were found, which, despite being reported to possess genes for patulin biosynthesis (Bokhari and Aly, 2009; Diaz *et al.,* 2011), have recently been questioned for their ability to produce patulin (Frisvad, 2018). *P. olsonii*, quite common in confined environments but reported as a non-producer of patulin (Frisvad, 2018), was also present. In the pre-

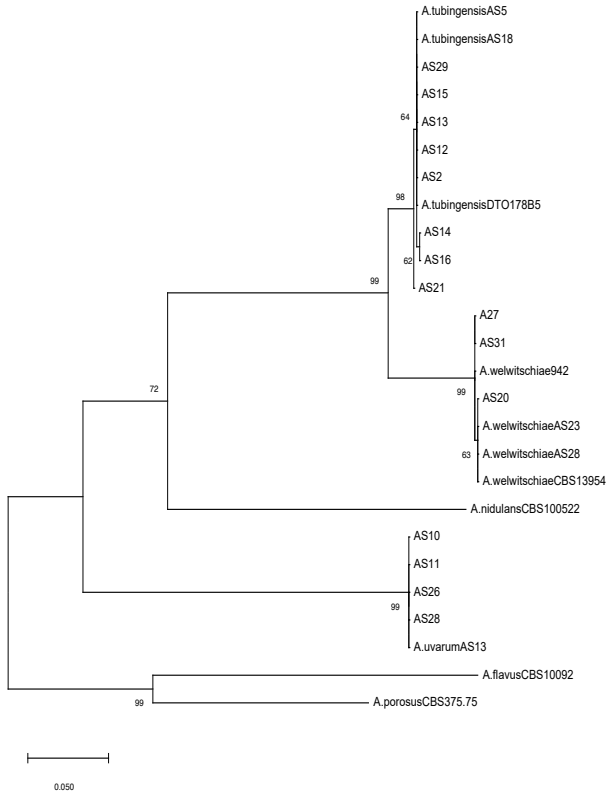

Figure 4. Phylogenetic tree for *Aspergillus* strains based on a portion of the calmodulin gene. Numbers on nodes represent the Maximum Likelihood bootstrap percentages. Branch lengths are proportional to the numbers of nucleotide substitutions and can be measured using the bar scale (0.05).

Table 5. *Penicillium* HRM clusters, species, strains, GenBank accession numbers for the β-tubulin gene, and presence of a patulin biosynthetic gene (*msas*).

HRM cluster	Species	Strain	Accession No.*	Detection of *msas***
1	*P. glabrum*	P6	n.a.	n.a.
		P7	MZ241137	n.a.
		P8	n.a.	n.a.
		P9	MZ241138	n.a.
		P10	n.a.	n.a.
		P11	n.a.	n.a.
2	*P. brevicompactum*	P14	MZ241140	n.a.
		P17	n.a.	n.a.
3	*P. brevicompactum*	P13	MZ241139	n.a.
4	*P. olsonii*	P12	n.a.	n.a.
		P16	MZ241141	n.a.
5	*P. expansum*	P18	MZ241142	+

* n.a.= not analyzed.
** The presence of patulin biosynthetic genes was checked in *P. expansum* strains. + = Present; - = Absent.

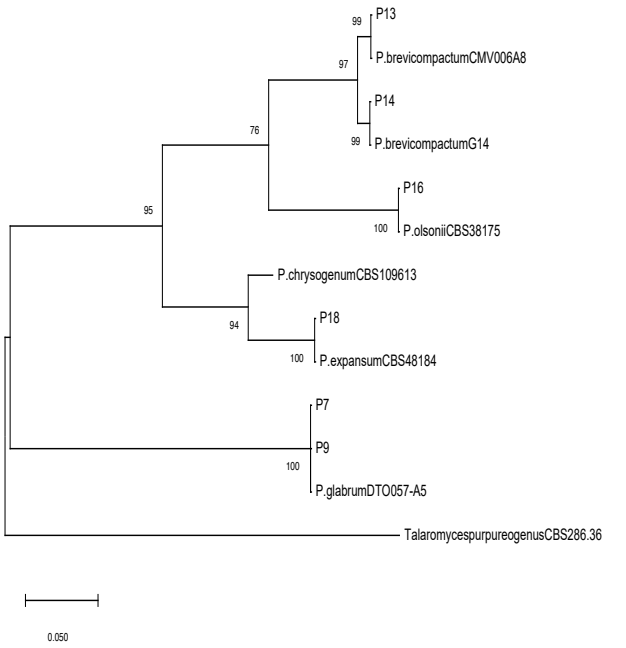

Figure 5. Phylogenetic tree for *Penicillium* strains based on a portion of the β-tubulin gene. Numbers on nodes represent the Maximum Likelihood bootstrap percentages. Branch lengths are proportional to the numbers of nucleotide substitutions and can be measured using the bar scale (0.05).

Table 6. *Alternaria* species/species complexes, morphotypes, strains, GenBank accession numbers for the OPA1-3 region, and presence of an alternariol biosynthetic gene (*pksI*).

Species	Morphotype	Strain	Accession No.	Detection of *pksI**
A. arborescens		Al1	MZ241129	+
A. alternata	*alternata*	Al2	MZ241130	+
		Al4	MZ241131	+
		Al5	MZ241132	+
		Al7	MZ241133	+
		Al11	MZ241134	+
		Al12	MZ241135	+
		Al16	MZ241136	+

* + = Present; - = Absent.

sent study, a single strain of *P. expansum* able to produce patulin was detected, belonging to the species known as the most potent patulin producer on fruit crops (Sanzani *et al.,* 2013). For *Alternaria*, *A. alternata* and the *A. arborescens* species complex were detected, and the strains proved to be AOH/AME producers. Similar results were found for grape bunch rot during withering (Lorenzini and Zapparoli, 2014). In general, the presence of fun-

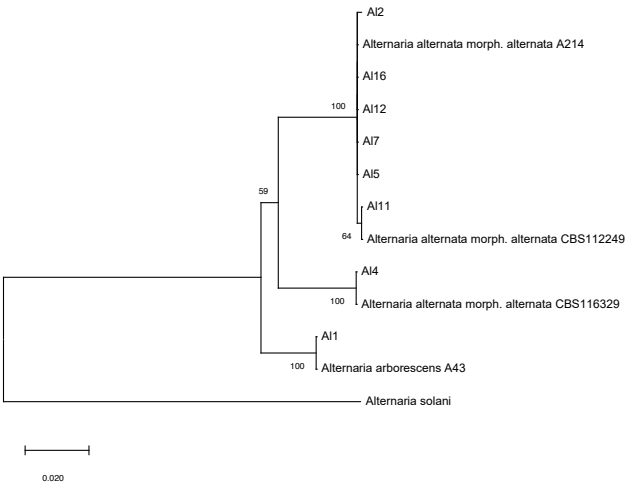

Figure 6. Phylogenetic tree for *Alternaria* strains based on a portion of the SCAR Marker OPA1-3. Numbers on nodes represent the Maximum Likelihood bootstrap percentages. Branch lengths are proportional to the numbers of nucleotide substitutions and can be measured using the bar scale (0.02).

gal pathogens was in line with other studies (Diaz *et al*., 2011; Oliveira *et al.,* 2017; Ding *et al*., 2019).

Fungi, including *Aspergillus, Penicillium,* and *Alternaria*, can switch lifestyle between saprophytic and plant pathogenic forms. Mycotoxin production by these fungi may even affect their positions in ecological niches and their interactions with plants, animals, and the environment (Pfliegler *et al*., 2019), causing major effects on the severity of the diseases caused (Sanzani *et al*., 2012; Zaccaria *et al*., 2015; Wenderoth *et al*., 2019).

Harvested Lebanese table grapes were shown to harbour relevant fungal pathogens from spoilage and food safety perspectives, both as epiphytic agents and latent infections. *Alternaria*, *Aspergillus*, *Penicillium,* and *Botrytis* were the most commonly identified fungi. Furthermore, SO_2 generating pads were found to be more effective for reducing epiphytic fungal populations during grape storage than for reducing latent infections, confirming the need of an effective field control of these infections. The mycotoxin producing genera *Aspergillus*, *Penicillium,* and *Alternaria* were characterized at species level. Strains of *A. welwitschiae* and *P. expansum* were also found, which are reported in grapes to be important producers of mycotoxins, the contents of which in food commodities is regulated by international legislation. As such, pre- and postharvest management should consider to control grape spoilage and to prevent mycotoxin production. Particularly, studies are recommended to assess conditions that favour fungal secretion of toxic secondary metabolites, and their fates during storage of table grapes.

ACKNOWLEDGEMENT

Jack Khalil was supported by a scholarship funded by CURE-XF, an EU-funded project coordinated by CIHEAM Bari (H2020-Marie Sklodowska-Curie Actions – Research and Innovation Staff Exchange. Reference number: 634353).

LITERATURE CITED

Abdelfattah A., Sanzani S.M., Wisniewski M., Berg G., Cacciola S.O., Schena L., 2019. Revealing cues for fungal interplay in the plant–air interface in vineyards. *Frontiers in Plant Science* 10: 922.

Aşkun T., Eltem R., Taşkın E., 2007. Comparison of Rose-Bengal chloramphenicol agar and Dichloran Glycerol Agar (DG18) for enumeration and isolation of moulds from raisins. *Journal of Applied Biological Science* 1(2): 71–75.

Barnett H.L., Hunter B.B., 1999. *Illustrated Genera of Imperfect Fungi*. 4th Edition, APS Press, St. Paul, MN, United States of America, 218 p.

Bokhari F., Aly M.M., 2009. Patulin production of *Penicillium glabrum* isolated from *Coffea Arabica* L. and the activities of some natural antifungal and antimycotoxin plants. *Egyptian Journal of Microbiology* 44: 47–59.

Chalak L., Touma S., Rahme S., Azzi R., Guiberteau F., Touma J.A., 2016. Assessment of the Lebanese grapevine germplasm reveals a substantial diversity and a high potential for selection. *BIO Web of Conferences* 7: 01020.

Chiang K.S., Liu H.I., Bock C.H., 2017. A discussion on disease severity index values. Part I: warning on inherent errors and suggestions to maximise accuracy. *Annals of Applied Biology* 171(2): 139–154.

Covarelli L., Beccari G., Marini A., Tosi L., 2012. A review on the occurrence and control of ochratoxigenic fungal species and Ochratoxin A in dehydrated grapes, non-fortified dessert wines and dried vine fruit in the Mediterranean area. *Food Control* 26(2): 347–356.

de Souza Ferranti L., Fungaro M.H.P., Massi F.P., da Silva J.J., Penha R.E.S., …, Iamanaka B.T., 2018. Diversity of *Aspergillus* section *Nigri* on the surface of *Vitis labrusca* and its hybrid grapes. *International Journal of Food Microbiology* 268: 53–60.

Díaz G.A., Yañez L., Latorre B.A., 2011. Low occurrence of patulin-producing strains of *Penicillium* in grapes and patulin degradation during winemaking in Chile. *American Journal of Ecology and Viticulture* 62: 542–546.

Ding S., Li N., Cao M., Huang Q., Chen G., …, Li W., 2019. Diversity of epiphytic fungi on the surface of Kyoho grape berries during ripening process in summer and winter at Nanning region, Guangxi, China. *Fungal Biology* 123(4): 283–289.

Droby S., Lichter A., 2007. Post-Harvest Botrytis Infection: Etiology, Development and Management. In: *Botrytis: Biology, Pathology and Control.* (Y. Elad, B. Williamson, P. Tudzynski, N. Delen, eds.), Springer, Dordrecht, Germany, 349–367.

EC, 2006. Commission Regulation (EC) No 1881/2006 setting maximum levels for certain contaminants in foodstuffs. *Official Journal of European Union* 364: 5–24.

EC, 2007. Commission regulation (EC) N° 1126/2007. 28 September 2007. Amending regulation (EC) N° 1881/2006 setting maximum levels for certain contaminants in foodstuffs as regards toxins in maize and maize products. *Official Journal of European Union* L 255: 14–17.

EFSA, 2011. Scientific opinion on the risks for animal and public health related to the presence of *Alternaria* toxins in feed and food. *EFSA Journal* 9(10): 2407.

FAOSTAT, 2019. Commodities by country. Available at http://www.fao.org/faostat/en/#rankings/commoditiesbycountry. Accessed April 25, 2020.

Fernandez-Trujillo J.P., Obando-Ulloa J.M., Baró R., Martinez J.A., 2012. Quality of two table grape guard cultivars treated with single or dual-phase release SO_2 generators. *Journal of Applied Botany and Food Quality* 82(1): 1-8.

Franck J., Latorre B.A., Torres R., Zoffoli J.P., 2005. The effect of preharvest fungicide and postharvest sulphur dioxide use on postharvest decay of table grapes caused by *Penicillium expansum*. *Postharvest Biology and Technology* 37(1): 20–30.

Frisvad J.C., 2018. A critical review of producers of small lactone mycotoxins: patulin, penicillic acid and moniliformin. *World Mycotoxin Journal* 11(1): 73–100.

Garganese F., Schena L., Siciliano I., Prigigallo M.I., Spadaro D., … Sanzani S.M., 2016. Characterization of citrus-associated *Alternaria* species in Mediterranean areas. *Plos One* 11(9): e0163255.

Glass L.N., Donaldson G.C., 1995. Development of primer sets designed for use with the PCR to amplify conserved genes from filamentous ascomycetes. *Applied Environmental Microbiology* 61(4): 1323–1330.

Hong S.-B., Go S.-J., Shin H.D., Frisvad J.C., Samson R.A., 2005. Polyphasic taxonomy of *Aspergillus fumigatus* and related species. *Mycologia* 97(6): 1316–1329.

Hong S.B., Lee M., Kim D.H., Varga J., Frisvad J.C., …, Samson R.A., 2013. *Aspergillus luchuensis*, an industrially important black *Aspergillus* in East Asia. *PLoS One* 8(5): e63769.

IARC, 1993. Some naturally occurring substances: food items and constituents, heterocyclic aromatic amines and mycotoxins. IARC Monographs on the Evaluation of the Carcinogenic Risk of Chemicals to Humans, 56. World Health Organization, Geneva, Switzerland, 599 p.

Kumar S., Stecher G., Li M., Knyaz C., Tamura K., 2018. MEGA X: molecular evolutionary genetics analysis across computing platforms. *Molecular Biology and Evolution* 35(6): 1547–1549.

Lachhab N., Sanzani S.M., Bahouaoui M.A., Boselli M., Ippolito A., 2016. Effect of some protein hydrolysates against gray mould of table and wine grapes. *European Journal of Plant Pathology* 144: 821–830.

Lebanese Chamber of Commerce, 2019. Agvisor (version 1.1) [mobile application software].

Lorenzini M., Zapparoli G., 2014. Characterization and pathogenicity of *Alternaria* spp. strains associated with grape bunch rot during post-harvest withering. *International Journal of Food Microbiology* 186: 1–5.

Mincuzzi A., Ippolito A., Montemurro C., Sanzani S.M., 2020. Characterization of *Penicillium* s.s. and *Aspergillus* sect. *nigri* causing postharvest rots of pomegranate fruit in Southern Italy. *International Journal of Food Microbiology* 314: 108389.

Murray M.G., Thompson W.F., 1980. Rapid isolation of high molecular weight plant DNA. *Nucleic Acids Research* 8(19): 4321–4326.

Oliveira M., Arenas M., Lage O., Cunha M., Amorim M.I., 2017. Epiphytic fungal community in *Vitis vinifera* of the Portuguese wine region. *Letters in Applied Microbiology* 66(1): 93–102.

Peever T.L., Su G., Carpenter-Boggs L., Timmer L.W., 2004. Molecular systematics of citrus-associated *Alternaria* species. *Mycologia* 96(1): 119–134.

Perrone G., Susca A., Cozzi G., Ehrlich K., Varga J., …, Samson R.A., 2007. Biodiversity of *Aspergillus* species in some important agricultural products. *Studies in Mycology* 59: 53–66.

Perrone G., Gallo A., 2016. *Aspergillus* Species and Their Associated Mycotoxins. *Methods in Molecular Biology* 1542: 33–49.

Pfliegler W.P., Pócsi I., Győri Z., Pusztahelyi T., 2019. The Aspergilli and their mycotoxins: metabolic interactions with plants and the soil biota. *Frontiers in Microbiology* 10: 2921.

Rogers S.O., Bendich A.J., 1989. Extraction of DNA from plant tissues. In: *Plant Molecular Biology Manual.*

(S.B. Gelvin, R.A. Schilperoort, D.P.S. Verma, eds.). Springer, Dordrecht, Germany, 73–83.

Rousseaux S., Diguta C.F., Radoï-Matei F., Alexandre H., Guilloux-Bénatier M., 2014. Non-Botrytis grape-rotting fungi responsible for earthy and moldy off-flavors and mycotoxins. *Food Microbiology* 38: 104–121.

Samson R.A., Noonim P., Meijer M., Houbraken J., Frisvad J.C., Varga J., 2007. Diagnostic tools to identify black Aspergilli. *Studies in Mycology* 59: 129–145.

Samson R.A., Visagie C.M., Houbraken J., Hong S.B., Hubka, V., …, Frisvad J.C., 2014. Phylogeny, identification and nomenclature of the genus *Aspergillus*. *Studies in Mycology* 78: 141–173.

Sanzani S.M., Schena L., Nigro F., De Girolamo A., Ippolito A., 2009. Effect of quercetin and umbelliferone on the transcript level of *Penicillium expansum* genes involved in patulin biosynthesis. *European Journal of Plant Pathology* 125(2): 223–233.

Sanzani S.M., Schena L., De Cicco V., Ippolito A., 2012. Early detection of *Botrytis cinerea* latent infections as a tool to improve postharvest quality of table grapes. *Postharvest Biology and Technology* 68: 64–71.

Sanzani S.M., Montemurro C., Di Rienzo V., Solfrizzo M., Ippolito A., 2013. Genetic structure and natural variation associated with host of origin in *Penicillium expansum* strains causing blue mould. *International Journal of Food Microbiology* 165(2): 111–120.

Sanzani S.M., Reverberi M., Geisen R., 2016a. Mycotoxins in harvested fruits and vegetables: Insights in producing fungi, biological role, conducive conditions, and tools to manage postharvest contamination. *Postharvest Biology and Technology* 122: 95–105.

Sanzani S.M., Miazzi M.M., Di Rienzo V., Fanelli V., Gambacorta G., …, Montemurro C., 2016b. A rapid assay to detect toxigenic *Penicillium* spp. contamination in wine and musts. *Toxins* 8(8): 235.

Sanzani S.M., Djenane F., Incerti O., Admane N., Mincuzzi A., Ippolito A., 2021. Mycotoxigenic fungi contaminating greenhouse-grown tomato fruit and their alternative control. *European Journal of Plant Pathology* 160: 287–300.

Schuchardt S., Ziemann C., Hansen T., 2014. Combined toxicokinetic and *in vivo* genotoxicity study on *Alternaria* toxins. *EFSA supporting publication* 2014: EN-679.

Simmons E.G., 2007. *Alternaria*. An identification manual. CBS biodiversity series 6. CBS Fungal Biodiversity Center, Utrecht, The Netherlands, 775 p.

Smilanick J.L, Harstell P.I., Henson D., Fouse D.C., Assemi M., Harris C.M., 1990. Inhibitory activity of Sulphur dioxide on the germination of spores of *Botrytis cinerea*. *Phytopathology* 80: 217–220.

Somma S., Perrone G., Logrieco A.F., 2012. Diversity of black Aspergilli and mycotoxin risks in grape, wine and dried vine fruits. *Phytopathologia Mediterranea* 51: 131–147.

Stocco A.F., Diaz M.E., Rodríguez Romera M.C., Mercado L.A., Rivero M.L., Ponsone M.L., 2019. Biocontrol of postharvest *Alternaria* decay in table grapes from Mendoza province. *Biological Control* 134: 114–122.

Storari M., Bigler, L., Gessler, C., Broggini, G.A.L., 2012. Assessment of the Ochratoxin A production ability of *Aspergillus tubingensis*. *Food Additive and Contaminants: Part A* 29(9): 1450–1454.

Susca A., Proctor R.H., Butchko R.A., Haidukowski M., Stea G., …, Moretti A., 2014. Variation in the fumonisin biosynthetic gene cluster in fumonisin-producing and nonproducing black aspergilli. *Fungal Genetics and Biology* 73: 39–52.

Susca A., Proctor R.H., Morelli M., Haidukowski M., Gallo A., …, Moretti A., 2016. Variation in fumonisin and ochratoxin production associated with differences in biosynthetic gene content in *Aspergillus niger* and *A. welwitschiae* isolates from multiple crop and geographic origins. *Frontiers in Microbiology* 7: 1412.

Tamura K., Nei M., 1993. Estimation of the number of nucleotide substitutions in the control region of mitochondrial DNA in humans and chimpanzees. *Molecular Biology and Evolution* 10(3): 512–526.

Visagie C.M., Houbraken J., Frisvad J.C., Hong S.B., Klaassen C.H.W., …, Samson R.A., 2014. Identification and nomenclature of the genus *Penicillium*. *Studies in Mycology* 78: 343–371.

Wenderoth M., Garganese F., Schmidt-Heydt M., Soukup S.T., Ippolito A., …, Fischer R., 2019. Alternariol as virulence and colonization factor of *Alternaria alternata* during plant infection. *Molecular Microbiology* 112(1): 131–146.

Woudenberg J.H.C., Groenewald J.Z., Binder M., Crous P.W., 2013. *Alternaria* redefined. *Studies in Mycology* 75(1): 171–212.

Woudenberg J.H.C., Seidl M.F., Groenewald J.Z., De Vries M., Stielow J.B., …, Crous P.W., 2015. *Alternaria* section Alternaria: Species, formae speciales or pathotypes? *Studies in Mycology* 82: 1-21.

Youssef K., Junior O.J.C., Mühlbeier D.T., Roberto S.R., 2020. Sulphur dioxide pads can reduce gray mold while maintaining the quality of Clamshell-packaged 'BRS Nubia' seeded table grapes grown under protected cultivation. *Horticulturae* 6(20): 2-9.

Zaccaria M., Ludovici M., Sanzani S.M., Ippolito A., Cigliano R.A., …, Reverberi M., 2015. Menadione-induced oxidative stress re-shapes the oxylipin profile of *Aspergillus flavus* and its lifestyle. *Toxins* 7(10): 4315–4329.

Phytopathologia Mediterranea
The international journal of the
Mediterranean Phytopathological Union

Firenze University Press
www.fupress.com/pm

Research Papers

Histopathological aspects of resistance in wheat to *Puccinia triticina*, induced by *Pseudomonas protegens* CHA0 and β-aminobutyric acid

Fares BELLAMECHE[1], Mohammed Abbas JASIM[1,§], Brigitte MAUCH-MANI[1], Fabio MASCHER[2,*]

[1] *University of Neuchâtel, Laboratory of Molecular and Cell Biology, rue Emile-Argand 11, 2000 Neuchâtel, Switzerland*
[2] *Agroscope, Crop Plant Breeding and Genetic Resources, Route de Duillier 50, 1260 Nyon, Switzerland*
[§] *Present address: University of Anbar, Biology department, Al Ramadi 31001, Iraq*
*Corresponding author. E-mail: fabio.mascher@agroscope.admin.ch

Summary. After perception of specific biotic or abiotic stimuli, such as root colonization by rhizobacteria or selected chemicals, plants can enhance their basal resistance against pathogens. Due to its likely sustainability, this induced resistance will be valuable for disease management in agriculture. This study examined resistance against wheat leaf rust (*Puccinia triticina*) induced by *Pseudomonas protegens* CHA0 (CHA0) and β-aminobutyric acid (BABA). Seed dressing with CHA0 reduced the number of sporulating pustules on leaves, and expression of resistance was visible as necrotic or chlorotic leaf flecks. Beneficial effect of CHA0 on wheat seedlings growth was observed in when they were challenged or not with leaf rust. BABA was tested at 10, 15 or 20 mM, and a dose-dependent reduction of leaf rust infections was observed with greatest protection at 20 mM. However, BABA treatment repressed plant growth at 20 mM. Balancing the BABA impact on plant growth and its protective capacity, 15 mM of the compound was selected as suitable to protect wheat seedlings against leaf rust, with the least impact on vegetative host growth. Histological aspects of the pathogen infection process was studied to understand mechanisms of behind the observed resistance. The pre-entry process was not affected by the two resistance inducers, but both treatments reduced fungus penetration and haustorium formation. Timing and amplitude of the resistance reactions were different after bacterial or chemical induction, leading to different levels of resistance. During fungal colonization of host tissues, high deposition of callose and accumulation of H_2O_2 in both CHA0- and BABA-treated plants indicated important contributions to resistance.

Keywords. Leaf rust, callose deposition, hydrogen peroxide (H_2O_2), plant resistance inducers.

OPEN ACCESS

Citation: F. Bellameche, M.A. Jasim, B. Mauch-Mani, F. Mascher (2021) Histopathological aspects of resistance in wheat to *Puccinia triticina*, induced by *Pseudomonas protegens* CHA0 and β-aminobutyric acid. *Phytopathologia Mediterranea* 60(3): 441-453. doi: 10.36253/phyto-13123

Accepted: September 29, 2021

Published: November 15, 2021

Data Availability Statement: All relevant data are within the paper and its Supporting Information files.

Competing Interests: The Author(s) declare(s) no conflict of interest.

Editor: Diego Rubiales, Institute for Sustainable Agriculture, CSIC, Cordoba, Spain.

INTRODUCTION

Plants use several layers of defense mechanisms to prevent pathogen attack. The first layer includes preformed physical and chemical barriers that

impede pathogen penetration to initiate infections (Ferreira *et al.*, 2006). Once pathogen presence has been detected, host plants activate further chemical and physical barriers that delay or block the attack (second layer; Jones and Dangl (2006)). Defense success depends on host readiness to detect the pathogen. For the interaction between wheat and the leaf rust pathogen (*Puccinia triticina*), the plant can detect specific fungal avirulence factors (effectors) with leaf rust resistance (*Lr*) genes. This gene-for-gene interaction is a very rapid recognition-reaction event leading to elevated resistance against the disease. However, the avirulence patterns can change and the pathogen may become undetectable by the plant. This wheat resistance breakdown has been reported for yellow rust (Hovmøller *et al.*, 2010) and stem rust (Singh *et al.*, 2011).

In non-specific pathogen recognition, plants can still contain pathogen development, but with reduced and variable degrees of infection severity (Jones and Dangl, 2006). The degree of this quantitative resistance is linked to the readiness of plant defenses and depends on a series of genetic and environmental factors. Beside the pathogen, biological and abiotic stimuli, and some chemicals, can enhance plant resistance (Mauch-Mani *et al.*, 2017). Induced resistance can be limited to the site of the inducing treatment, but it can also be systemic and thereby effective in parts of the plant distant from the site of induction (Van Loon, 1997). For example, some root-associated bacteria (*e.g* the biocontrol strain *Pseudomonas protegens* CHA0, formerly *P. fluorescens* CHA0) induce systemic resistance against virus and fungus diseases in various dicot (Maurhofer *et al.*, 1994; Haas and Keel, 2003; Iavicoli *et al.*, 2003) and monocot hosts (Sari *et al.*, 2008; Henkes *et al.*, 2011). Particular chemical compounds can also induce disease resistance in plants, including the non-protein amino-acid β-amino-n-butyric acid (BABA). Root colonizing bacteria and BABA root treatments reduce severity of infection by the oomycete *Hyaloperonospora arabidopsis* on *Arabidopsis thaliana*, and the induced state is regulated by different defense signalling pathways, depending on the inducing agent and the challenging pathogen (Van der Ent *et al.*, 2009).

The aim of the present study was to examine mechanisms underlying resistance induced by CHA0 and BABA in wheat against *P. triticina*. Sharifi-Tehrani *et al.* (2009) showed that root colonization by *Pseudomonas protegens* strain CHA0 reduced the number of leaf rust uredia on susceptible wheat seedlings. The enhanced resistance was possibly due to a resistance priming event by induction of systemic resistance (ISR). This priming enables hosts to cope with pathogens at early stages of infection. The present study followed the interaction between *P. triticina* and wheat at the microscopic level (De Vleesschauwer *et al.*, 2008).

The leaf rust infection process is well known (Bolton *et al.*, 2008). After adhesion of each urediniospore on the leaf surface, germination, directed germ tube growth on the plant surface towards a stoma, and recognition of host guard cell lips take place. A small appressorium is formed over the stomatal opening, and a penetration hypha then enters through the stomatal pore. Following penetration, a substomatal vesicle and haustorium develop (Bolton *et al.*, 2008).

Primed plants recognize the pathogen, and then produce reactive oxygen species (ROS) and deposit callose at the infection sites (Balmer *et al.*, 2015). This rapid local oxidative burst generates, among others, hydrogen peroxide (H_2O_2) during pre-haustorial resistance against wheat leaf rust caused by *P. triticina* (Wesp-Guterres *et al.*, 2013; Serfling *et al.*, 2016). Callose is an effective barrier that sometimes is induced at the sites of pathogen attack during the early stages invasion (Luna *et al.*, 2011). Strong deposition of callose has been reported for the wheat near-isogenic line Thatcher, which carries the leaf rust resistance gene *Lr9* (Wang *et al.*, 2013).

Few studies have investigated rhizobacteria- and BABA-induced resistance against wheat leaf rust. In the present study, mechanisms involved in CHA0-ISR and BABA-IR were compared during interaction between the pathogen and host. Development of fungal structures were examined microscopically, along with occurrence of callose deposition, and hydrogen peroxide accumulation in leaf tissues.

MATERIALS AND METHODS

Induced resistance assay

Plant material and growth conditions

Experiments were carried out with the leaf rust-susceptible bread wheat cultivar Arina (Agroscope/DSP). Surface sterilized seeds were used in all experiments. Seeds were rinsed in 70% ethanol, incubated for 5 min in 5% sodium hypochlorite solution (Fisher Chemical), and then washed three times in sterile distilled water. The sterilized seeds were germinated on moist filter paper (Filterkrepp Papier braun, E. Weber & Cie AG) in plastic bags maintained in the dark at room temperature. Three to 4 d later, resulting seedlings at similar growth states and morphology were selected and planted in 120 mL capacity polypropylene tubes (Semadeni) filled with a standard seedling growth medium

(peat/sand, 3:1, vol:vol). The tubes were then placed in a growth chamber set at 16 h light (300 mmol m^{-2} s^{-1}), 22°C, and 8 h dark, 18°C. The plants were watered regularly keeping the growth medium moist but avoiding saturation.

Bacterium inoculum

The bacterium inoculum was the biocontrol agent *P. protegens* strain CHA0-Rif (Natsch *et al.*, 1994) (hereafter referred to as CHA0), which is a spontaneous rifampicin resistant strain of *P. protegens* CHA0 (Stutz *et al.*, 1986; Ramette *et al.*, 2011). Both strains have similar growth rates, production of antimicrobial compounds (Natsch *et al.*, 1994) and capacities to induce resistance in wheat (Sharifi-Tehrani *et al.*, 2009). Routinely, strain CHA0-Rif was grown at 25°C in the dark for 3 d on solid King's medium B (Pseudomonas agar F, Merck KGaA) supplemented with 50 µg mL^{-1} rifampicin. For long-term storage, 1 mL of a freshly grown bacterial suspension in King's liquid medium B (30 g proteose-peptone, 1.5 g K_2HPO_4, 2.46 g $MgSO_4$, 1.5 g glycerol in 1 L distilled water) was mixed with 1 mL glycerol (87%) and stored at -80°C. For inoculum production, a single colony from a freshly grown culture was transferred to a 300 mL capacity Erlenmeyer flask containing 100 mL of King's liquid medium B supplemented with 50 µg mL^{-1} rifampicin. After 12 h incubation at 28°C with continuous shaking at 150 rpm, the resulting culture was centrifuged at 3700 rpm and washed twice with sterile 10 mM $MgSO_4$ solution. The cell pellet was re-suspended in 20 mL of sterile distilled water and adjusted to an OD_{600} of 0.1 corresponding to approx. 10^6 CFU mL^{-1}, and was then used for seed inoculation. For this, surface sterilized wheat seeds were immersed in the bacterial suspension for 6 h with shaking at 35–40 rpm at room temperature. Inoculated seeds were then pre-germinated (as above). Control seeds were soaked in distilled water for 6 h before pre-germination.

Treatments with β-aminobutyric acid

The resistance inducer BABA was obtained from Sigma-Aldrich (Buchs SG, Switzerland). Dilutions of 10, 15 and 20 mM of BABA in distilled water were used as soil drenches. For each of these, 10 mL of BABA solution were added to the soil containing wheat seedlings at the two leaf stage, 48 hours before inoculation with *P. triticina*. Control plants were treated with the same amount of distilled water.

Effects of CHA0 and BABA on plant development

In a first step, the effects of CHA0 and BABA treatments on wheat plants were assessed. To measure root colonization by CHA0, 0.1 g each of inoculated or control roots were each shaken in 10 mL of sterilized distilled water for 1 min on a benchtop vortex mixer, followed by 1 min of sonication. The resulting root extract was serially diluted and plated on solid King's medium B supplemented with 100 µg mL^{-1} of rifampicin. The plates were then incubated at 28°C in the dark, and the numbers of CFUs were determined after 24 to 36 h.

To investigate possible effects of CHA0 and BABA treatments on plant growth, the dry mass of the shoots of pre-treated seedlings was measured at 12 d after inoculation with *P. triticina*. Shoot length was defined as the upper part of each cut at the residue of the seed. Shoot fresh weights were measured, and they were then each placed on coffee filter paper and dried in an oven at 65°C until sample weight remained constant (shoot dry weight).

Inoculation with Puccinia triticina

Inoculations of wheat seedlings with *P. triticina* were carried out at the two -leaf stage (BBCH 12; Meier, 1997), using freshly harvested urediniospores of *P. triticina* isolate Pr2271 (Agroscope, Changins, Switzerland). In a differential test, this isolate showed the following avirulence/virulence properties; *Lr1, Lr2a, Lr2b, Lr2c, Lr3, Lr3bg, Lr9, Lr10, Lr14a, Lr26*/Lr3ka, Lr11, Lr12, Lr14b, Lr18, Lr25 (unpublished results). In a preliminary test, the isolate showed high aggressiveness towards the wheat cultivar Arina. Urediniospores were produced on leaves of cv. Arina. For inoculations, fresh urediniospores were mixed with talcum powder in a 1:9 w/w ratio, and were then rubbed gently on seedling leaf surfaces. Inoculated plants were placed in a dew box in the dark at 18 to 22°C for 24 h to promote infection. The plants were then placed in the growth chamber as described above. After 12 d or when symptoms were sufficiently developed on control plants, the leaf rust infection types were assessed using the 0 to 4 scale (Table S1) described by Stakman *et al.* (1962).

Histochemical assessments of leaf rust infections in presence of CHA0 and BABA

Assessments of fungal growth and development

Leaf rust growth was observed on 2 cm leaf segments from the centres of the second seedling leaves at

0, 6, 12, 24, 48, 72 and 96 h after inoculation (hai). Leaf segments were immersed in 96% ethanol for 2-3 d to remove chlorophyll. The leaf segments were then washed in an ethanol/water (1:2 v/v) solution, and then incubated in 0.5M sodium hydroxide for 15 min with slight shaking. The leaf segments were incubated for 15 min in distilled water and then immersed 2 h in 0.1 M Tris–HCl buffer (pH 8.5). Fungal structures were then stained with a 0.2% Calcofluor White solution in water (Sigma-Aldrich) for 5 min. After four washings in distilled water, the samples were stored in 50 % (v/v) glycerol for microscopic observation.

The preparations were examined with an epifluorescence microscope (Model E800; Nikon Instruments) using excitation at 365 nm in combination with a 450 nm barrier filter and a dichroic mirror at 400 nm. This lighting set-up allowed determination of positions and number of all fungal structures on and in the leaves, including germinated and non-germinated urediniospores, appressoria, sub-stomatal vesicles and haustoria.

Identification and quantification of callose deposition

Assessments of callose deposition were carried out for on segments from the centres of the second leaves of seedlings at 0, 24, 48 and 72 hai with *P. triticina*, using the methods of Scalschi *et al.* (2015). Leaf tissues were decoloured for 48 h in 96% ethanol until transparent. Leaf tissues were then rehydrated in 0.07 M phosphate buffer (pH = 9) for 30 min, and then incubated for 15 min 0.05% aniline blue (Sigma) prepared in 0.07 M phosphate buffer, and finally stained overnight in 0.5% aniline blue. Microscopic observations were carried out with the epifluorescence microscope using a UV filter, as described above.

The presence and quantity of deposited callose was determined from digital photographs (supplementary Figure 1S) by counting the white pixels (representing callose deposits) in 20 infection sites for each experimental replicate, using the GNU Image Manipulation Program (GIMP 2.10.10) software. Contrast settings of the photographs were adjusted to obtain an optimal separation of the callose signals from the background signals. Callose was automatically identified using the "Color Range" tool and callose-corresponding pixels were recorded as the area covered by the total number of selected pixels (Scalschi *et al.* 2015).

Accumulation of H_2O_2 at the infection sites

Detections of H_2O_2 were carried out using 3,3-diaminobenzidine (DAB; Sigma-Aldrich) staining, as described by Thordal-Christensen *et al.* (1997). The second fully expanded seedling leaves were cut at 0, 24, 48 and 72 hai and immediately immersed in a solution containing 1 mg mL^{-1} DAB dissolved in HCl acidified distilled water (pH = 3.8). Leaves were then incubated in the dark for 8 h to allow DAB uptake and reaction with H_2O_2. Subsequently, leaves were cleared in saturated chloral hydrate and scanned at 1.200 dpi (Epson perfection, V370 PHOTO).

In presence of H_2O_2, DAB is reduced to a dark brown deposit that can be easily visualized in leaves. The H_2O_2 content of the seedling leaves was quantified by counting the number of dark-brown DAB pixels using GIMP 2.10.10 software, and the proportions of DAB stain were calculated in relation to total leaf area (Luna *et al.* 2011). The dark brown DAB pixels were selected using "Color selection" and the total areas of leaves were determined using the "Free Selection" tool in the image analysis software.

Experimental set up and statistical analyses

All experiments were carried out, then repeated twice. The induced resistance assay consisted of seven biological replicates. The fungal growth and the callose deposition assessments were carried out with three independent replicates, and the H_2O_2 quantification was measured for ten biological replicates.

Fungal development structures were identified and counted at 50 sites in each replicate. The proportion parameters were calculated as follows: percentage of germinated spores = (germinated spores/observed spores) × 100; percentage of stomatal appressoria = (stomatal appressoria/germinated spores) × 100; percentage of sub-stomatal vesicles = (sub-stomatal vesicles/stomatal appressoria) × 100; and percentage of haustoria = (haustoria/sub-stomatal vesicles × 100).

Data were collected and stored in spreadsheets (Microsoft® Excel 2010). All statistical analyses were carried out with R (R Core Team, 2017).

In most experiments, statistically significant differences in responses to CHA0 and BABA treatments compared to controls were tested with Student's T-test. The exception was in the experiment testing effects of CHA0 and BABA on plant development, where data were analyzed by two-way ANOVA with the factors; treatment (CHA0 and BABA) and rust inoculation (infected or not). The Tukey Honest Significant Differences (HSD) test was used for multiple comparisons. Significant differences were considered at $P < 0.05$.

RESULTS

Plant growth and biomass in presence of CHA0, BABA and following inoculation with Puccinia triticina

Twelve days after planting of the seedlings, an average of 5×10^5 CFU g^{-1} of CHA0 were recovered on the fresh roots, demonstrating the capacity of the bacterium to successfully colonize the roots. In a preliminary experiment, the initial concentration of bacteria (either 10^4, 10^6 or 10^8 CFU mL^{-1}) used for seed inoculation did not affect the number of bacteria on the roots.

The effects of CHA0 and BABA on plant length and biomass are illustrated presented in Figure 1. The results indicated that seedlings treated with CHA0 were longer and had more biomass than untreated seedlings. These parameters were not influenced by the presence of the pathogen (Figure 1A and B). In contrast, plants treated with BABA at 20 mM were shorter and lighter than the untreated seedlings. The seedlings treated with 10 or 15 mM of BABA were not different to the untreated controls. Infections with *P. triticina* did not affect plant growth or biomass, except for the treatment with BABA at 20 mM (Figure 1C and D).

Phenotypic reaction to leaf rust of wheat seedlings pre-treated with CHA0 or BABA

Twelve days after inoculation with *P. triticina*, uninoculated control plants were healthy (Figure 2a) while the inoculated plants were chlorotic and covered with uredia corresponding to infection type score 3 (high infection type (HI) (Stakman *et al.*, 1962)) (Figure 2b). In plants treated with CHA0 (Figure 2c), the leaves showed overall less uredia compared to the inoculated controls. The symptoms were heterogeneous, including chlorotic flecks (score ";", low infection type (LI)), but also uredia without sporulation (score "2", LI) and with sporulation and chlorotic halos (score "3", HI).

The BABA treatments also resulted in a mix of chlorotic flecks (score ";") and small to medium pustules with and without low sporulation, scored as "1" and "2". Generally, all the BABA treatments gave low infection type symptoms. The scores were dose-dependent, since the greater the BABA concentration, the lower were the scores (Figure 2d, e and f).

Fungal infection structures

Calcofluor white staining was used to visualize the pathogen structures during the first 96 h after *P. triticina*

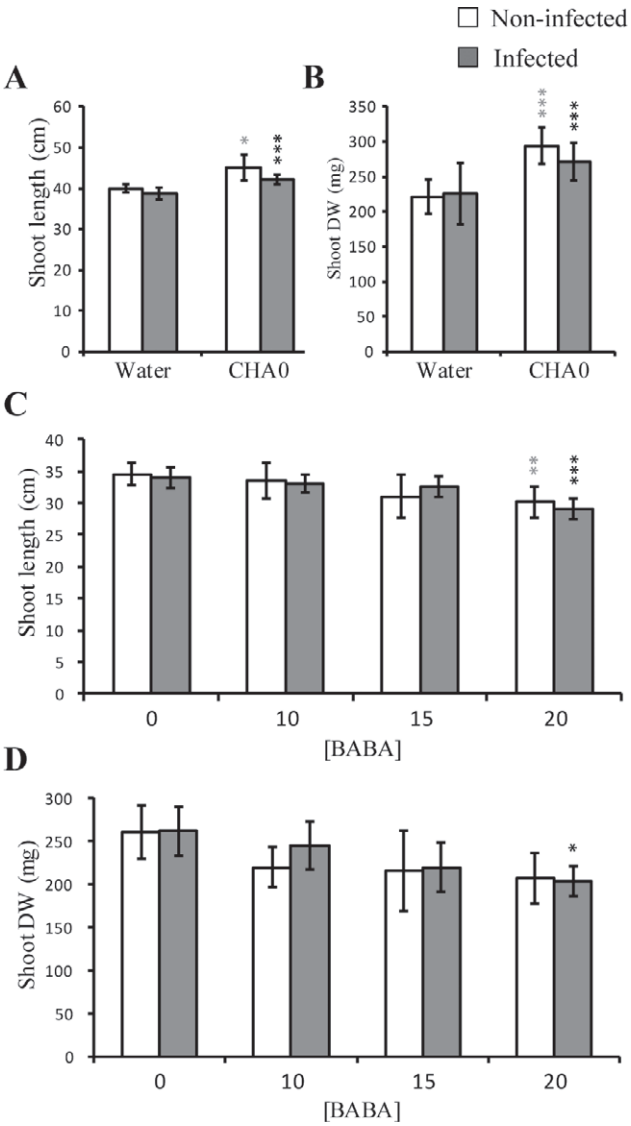

Figure 1. Mean lengths and shoot dry weights of wheat seedlings treated with CHA0 (**A** and **B**) and BABA (10, 15 or 20 mM) (**C** and **D**) at 12 dpi with *Puccinia triticina.* Shoot length was measured from each seed to the top of the longest leaf. Shoot dry weights were assessed after drying samples at 65°C until the weight remained constant. Error bars indicate the standard errors for the average values of seven replicates. Grey and dark stars indicate statistically significant differences compared to, respectively, non-infected and infected controls (Tukey's test; $*P < 0.05$; $**P < 0.01$; $***P < 0.001$).

infection (hai) in non-treated controls and on the plants pre-treated with CHA0 and BABA at 15mM. Within 6 hai, germ tubes started to elongate (Figure 3A, 1). Independent of the pre-treatments, about 90% of urediniospores had germinated within 6 hai, in all treatments (Figure 3B, 1). In the other treatments, the proportions of germinated spores remained constant.

Once germinated, the fungus forms appressoria at the

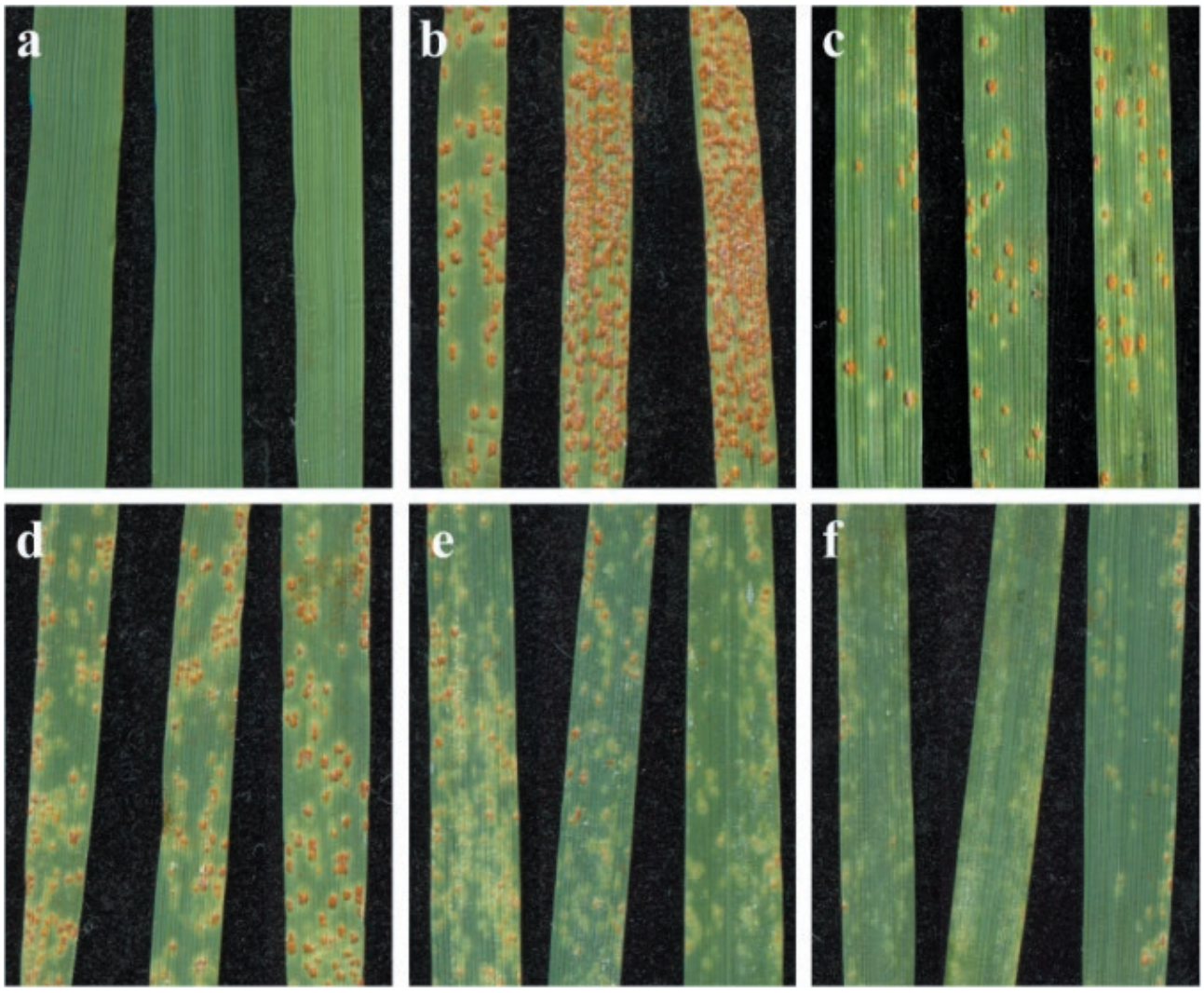

Figure 2. Leaf rust infections on seedling leaves of wheat cultivar Arina at 12 dpi. **a,** control plants non-infected; **b**, infected plants non-treated; **c**, infected plants pre-treated with CHA0; **d**, **e**, and **f**, infected plants treated with, respectively, 10, 15 or 20 mM of BABA. Images were obtained by scanning at 1,200 dpi a segment of 3 to 4 cm from the centre of the second leaf of each seedling.

stomatal regions (Figure 3A, 2). The formation of appressoria started at 6 hai (data not shown). At 24 hai, 85–88% of the germinated spores had formed appressoria (Figure 3B, 2). This proportion varied only slightly between the controls and the bacterial and BABA treatments.

Through appressoria, the fungus penetrated into the cavities below leaf stomata, forming infection vesicles in the substomatal cavities (Figure 3A, 3). Formation of vesicles were observed at 12 hai (data not shown). On leaves of non-treated control plants, approx. 37% of appressoria had formed vesicles after 24 hai, with the proportions increasing to 50% after 48 hai. In plants inoculated with CHA0, approx. 29% of the appressoria had formed vesicles. At 48 hai, the mean proportion of vesicles decreased slightly to approx. 23% but this decrease was not statistically significant compared to the proportion of vesicles at 24 hai. In BABA (15 mM) treated plants, the proportions of formed vesicles was 10%, and these increased to 30% at 48 hai (Figure 3B, 3).

At 48 h, formation of haustoria out of vesicles was observed (Figure 3A, 4). At 72 hai, more than 80% of the sub-stomatal vesicles had formed haustoria in the untreated control plants, and this mean proportion did not change at 96 hai. In the CHA0 treated plants, the proportions of formed haustoria were not different to the control plants, at both time points (72 and 96 hai). However, the absolute number of haustoria was significantly less in the CHA0-treated plants compared to the

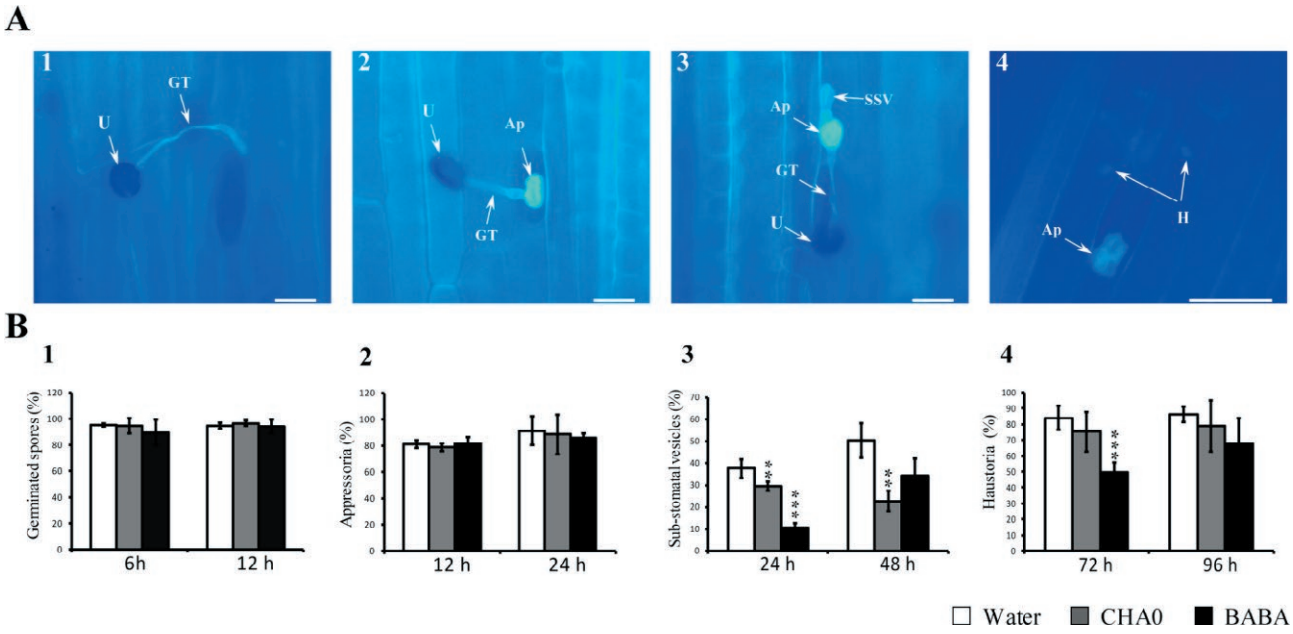

Figure 3. Microscopic observations and quantification of fungal structures *Puccinia triticina* in wheat seedlings. **A**, fungal structures stained with calcofluor white and visualized under the epifluorescence microscope. Bars = 20 µm. **B**, Mean percentages of fungal infection structures during infection of wheat by *P. triticina*: (1) spore germination, (2) appressoria, (3) sub-stomatal vesicles, and (4) haustoria. Treatments: **CHA0**, plants obtained from seeds inoculated with CHA0 (10^6 CFU mL^{-1}); **BABA**, plants soil-drenched with BABA (15 mM) 48 h before *P. triticina* inoculation; **Water**, plants treated with sterile distilled water. Fungal structures: **U**, urediniospore; **GT**, germ tube; **Ap**, appressorium; **H**, Haustoria. Error bars indicate standard errors of the average values of three replicates at 50 infection sites for each replicate. Asterisks indicate statistically significant differences in response to CHA0 or BABA treatments (Student's t-test; *P < 0.05; ** P < 0.01; *** P < 0.001).

controls. With BABA treatment, only about 50% of the vesicles formed haustoria, significantly less than haustorium formation in the controls. At 96 hai, haustorium formation increased in the BABA treatment to 70% and there was no significant difference from the other treatments. Also from the BABA treatment, the absolute number of haustoria was less compared to the control plants (Figure 3B, 4).

Callose deposition after Puccinia triticina *inoculation*

Callose deposition was quantified at 24, 48 and 72 hai after inoculations with *P. triticina* in the control, CHA0 and BABA 15mM treatments, using the aniline blue method (Supplementary Figure 1S). Callose deposition occurred in all treatments within the first 24 hai (Figure 4). However, in plants pre-treated with CHA0 and BABA, greater quantities of callose were detected compared to the controls. With CHA0, callose accumulated at the leaf guard cells and was greatest at 72 hai. In plants treated with BABA, greatest callose deposition was measured at 48 hai. Callose was observed in the guard cells of stomata) and eventually in leaf mesophyll cells, at 72 hai.

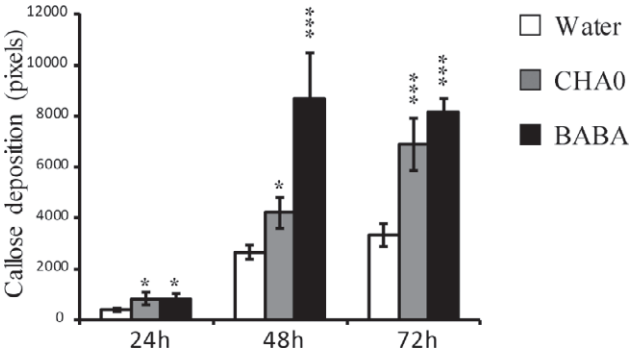

Figure 4. Callose deposition in wheat leaves in response to *Puccinia triticina* infection in treated and control plants at 24, 48 and 72 hai. Treatments: **CHA0**, plants obtained from seeds inoculated with CHA0 (10^6 CFU mL^{-1}); **BABA**, plants soil-drenched with BABA (15 mM) 48 h before inoculation; **Water**, plants treated with sterile distilled water. Bars indicate standard errors of the average values for 20 infection sites for each of three replicates. Asterisks indicate statistically significant differences in response to CHA0 or BABA treatments (Student's t-test; *P < 0.05; ** P < 0.01; *** P < 0.001).

Accumulation of H_2O_2 after Puccinia triticina *inoculation*

Hydrogen peroxide released by plant tissue was measured between 0 and 72 hai with *P. triticina* in the control,

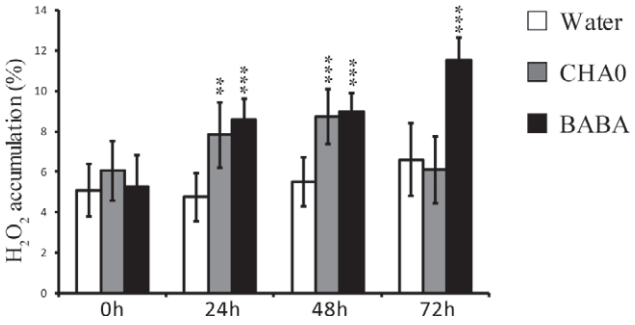

Figure 5. Mean proportions of hydrogen peroxide (H_2O_2) accumulation in wheat leaves in response to *Puccinia triticina* inoculations. Generation of H_2O_2 was visible as dark-brown dots after DAB staining. Treatments: **CHA0**, plants obtained from seeds inoculated with CHA0 (10^6 CFU mL^{-1}); **BABA**, plants soil-drenched with BABA (15 mM) 48 h before P. triticina inoculation; **Water**, plants treated with sterile distilled water. Bars indicate standard errors for average values of ten replicates. Asterisks indicate statistically significant differences in responses to CHA0 or BABA treatments (Student's t-test; *P <0.05; ** P < 0.01; *** P < 0.001).

CHA0 and BABA 15mM treatments. Hydrogen peroxide was monitored with the DAB staining that produces dark-brownish dots (Supplementary Figure 2S). Figure 5 shows the accumulation of H_2O_2 in leaves after the treatments. At 24 hai, H_2O_2 concentrations were greater in the CHA0 and the BABA treated plants than in the controls. Similarly, at 48 hai, in CHA0 and BABA treatments, the concentrations of released H_2O_2 were greater than in the controls. At 72 hai, accumulation of H_2O_2 in the CHA0 treatment decreased to the level of the controls, while the BABA treatment increased at this time.

DISCUSSION

Induced resistance has been demonstrated as a potential complementary control strategy for protecting wheat plants from foliar diseases (Görlach *et al.*, 1996; Sharifi-Tehrani *et al.*, 2009). The present study has confirmed the efficacy of beneficial bacteria CHA0 and BABA for induction of resistance in wheat to the leaf rust pathogen.

Effects of both resistance inducers were assessed on wheat growth. Efficient root colonization by a plant growth promoting bacterium is a prerequisite for successful biocontrol effects on host plants, either directly (*e.g.* disease suppression) or indirectly (*e.g.* ISR) (Lugtenberg and Kamilova, 2009; Beneduzi *et al.*, 2012). In the present study, after seed inoculation, CHA0 was colonized wheat roots, and more than 10^5 CFU g^{-1} root fresh weight were recovered. Preliminary results showed that the initial concentrations used for seed inoculum (10^4, 10^6 or 10^8 CFU mL^{-1}) did not affect final root colonization. The bacterial titre in wheat roots was great enough for effective plant protection, as has been shown for soils suppressive to take-all of wheat and barley caused by *Gaeumannomyces graminis* var. *tritici* (Weller *et al.* 2007), Fusarium wilt of pea caused by *Fusarium oxysporum* f. sp. *pisi* (Landa *et al.*, 2002), and black root rot of tobacco (Stutz *et al.*, 1986). Additionally, the growth promotion capacity of CHA0 was apparent with or without presence of *P. triticina* infections. In field experiments, positive effects of beneficial soil organism applications, including CHA0, on performance of wheat crops have been observed, especially when plants were under biotic stress (Imperiali *et al.*, 2017). The observed plant growth promotion of CHA0 could be from production of phytohormones and increased nutrient availability to plants, particularly phosphate. CHA0 can solubilize mineral phosphate and improve plant growth in phosphate-limiting conditions (de Werra *et al.*, 2009).

Thevenet *et al.* (2017) showed that BABA is a natural product in plants including wheat, but applications of BABA can reduce growth of some plants (Cohen *et al.*, 2016). At the concentration of 20 mM, BABA induced resistance to *P. triticina* but reduced growth of wheat plants. The costs of induced resistance have also previously been linked to reductions in plant growth (van Hulten *et al.*, 2006; Heil, 2007). Nevertheless, soil drenching with low concentrations of BABA (15 mM) did not affect plant growth and reduced infection types in wheat seedlings infected with leaf rust. This indicates the possibility to optimize the BABA dose rate for effective wheat protection against *P. triticina* with little impact on plant growth. Similarly, Luna *et al.* (2016) identified feasible BABA application methods by decreasing the concentration, which induced resistance in tomato against *Botrytis cinerea* without impacts on plant growth.

BABA is a well-recognized inducer of resistance against a broad spectrum of pathogens, including fungi, bacteria, viruses and nematodes (Baccelli and Mauch-Mani, 2016; Cohen *et al.*, 2016). This compound has often been applied as soil drenches (Hodge *et al.*, 2005; Luna *et al.*, 2016). Several studies demonstrate that BABA was effective when applied 1-3 d post-infection against a spectrum of pathogens (Justyna and Ewa, 2013). In the present study, BABA was applied as a soil drench 2 d before inoculation with *P. triticina*. This treatment reduced leaf rust in wheat similarly to results obtained with other rust diseases on wheat (Amzalek and Cohen, 2007; Barilli *et al.*, 2012). Inoculation with *P. protegens* strain CHA0 led to a specific reaction to infection with *P. triticina*: while plants without CHA0 inocu-

lation displayed many sporulating uredia (high infection type), plants with the bacterial treatment on the seeds had developed different severities of sporulating uredia and chlorotic and necrotic flecks. This indicated that *P. protegens* strain CHA0 partially reduced infections of *P. triticina* in the wheat seedlings.

Histopathological studies after induction of resistance were performed to identify the events that occurred during pathogenesis, and ultimately lead to increased understanding of the resistance mechanism. The infection process of *P. triticina* in wheat plants has been well described (Bolton *et al.*, 2008). During this process, growth of the fungus can be interrupted at different phases. In principle, each of these phases could be affected by the action of resistance inducers. The present results regarding infection events indicated that the pre-entry processes did not differ between plants treated with the two resistance inducers or the control plants. Other reports have also shown that the first steps of wheat rust infection (spore germination and appressorium formation) were not affected during the host-mediated resistance (Wang *et al.*, 2007; Orczyk *et al.*, 2010). However, after penetration, distinct differences in fungal spread and host responses between CHA0- and BABA-treated plants were observed. In BABA-treated plants, fungal penetration was strongly reduced at 24 hai, visible as a reduced proportions of substomatal vesicles. The percentage of haustoria formed in BABA-treated plant was also reduced at 72 hai. This has also been observed in durable resistance to leaf rust in the Brazilian wheat variety 'Toropi' (Wesp-Guterres *et al.*, 2013), where numbers of haustoria formed was reduced. Resistance against leaf rust can be pre- and post-haustorial. Pre-haustorial resistance matches with horizontal, quantitative resistance mechanisms, similar to that observed in 'Toropi'. This type of resistance is non-specific and durable. Resistance inducers, particularly BABA, enhances the non-specific responses against leaf rust, at pre-and post-haustorial infection phases.

In CHA0-treated plants, small to medium uredia with no or little sporulation were observed on wheat leaf surfaces, and the numbers of rust pustules were reduced compared to the inoculated controls. This infection type could be from partial effectiveness of the CHA0 treatment before haustorium formation, and reduced fungal penetration observed at 24 and 48 hai. The successful penetrations generated a fewer haustoria, later giving small uredia.

To investigate the observed effects on fungal spread exerted by BABA and CHA0 treatments, assessments were carried out of callose deposition and hydrogen peroxide (H_2O_2). During fungal infection, callose can be deposited at infection sites, which provides physical barriers preventing the pathogen penetration (Voigt, 2016). The present results showed that callose depositions were mainly detected in host guard cells. In support of these observations, Wang *et al.* (2015) demonstrated that the resistance response to *Puccinia graminis* f. sp. *tritici* was associated with callose deposition in the wheat guard cells. The increase of callose in BABA- and CHA0-treated plants could restrict penetration and development of *P. triticina*, correlating with the increase of resistance in wheat seedlings against the pathogen. This host defense mechanism is enhanced at the post-challenge primed stage after perception of a stimulus from beneficial bacteria and BABA (Mauch-Mani *et al.*, 2017). In addition to guard cells, callose was observed in leaf mesophyll cells of BABA-treated plants. This could also explain the high resistance observed compared to plants inoculated with bacteria. A similar pattern was observed in defence mechanisms induced by *P. fluorescens* WCS417r and BABA against *Hyaloperonospora arabidopsis*. Both WCS417r and BABA prime for enhanced deposition of callose, although more callose accumulated in BABA- than WCS417r-treated plants (Van der Ent *et al.*, 2009).

Reactive oxygen species (ROS), and especially H_2O_2, constitute a further important plant defense mechanism in interactions between plants and pathogens. H_2O_2 accumulation was investigated after infection with leaf rust in plants treated with BABA and CHA0. H_2O_2 accumulation was mostly detected in host guard cells. At these penetration sites, appressoria develop over the stomatal openings. During recognition or formation of appressoria, generation of H_2O_2 in guard cells is probably induced, possibly following secretion of rust effectors. Mechanical forces during adhesion of appressoria over stomata may also elicit H_2O_2 generation in guard cells. In *Arabidopsis*, it was reported that H_2O_2 accumulation in guard cells was involved in signal transduction during ABA-mediated stomatal closing (Sun *et al.*, 2017). This could explain how the present study results showing accumulation of H_2O_2 in guard cells following recognition of leaf rust structures may be involved in stomatal closure (data no presented). This is supported by the measurements of increased accumulation of ABA in plants infected with leaf rust.. It has been reported that appressorium formation of *P. triticina* also caused stoma closure in wheat leaves (Bolton *et al.*, 2008). Other studies have shown correlations between H_2O_2 generation and hypersensitive reaction (HR) in resistance against wheat rust species (Wang *et al.*, 2007; Orczyk *et al.*, 2010; Serfling *et al.*, 2016). In the present study, accumulation of H_2O_2 caused by resistance inducers was observed 24 hai, which corresponds to the begin-

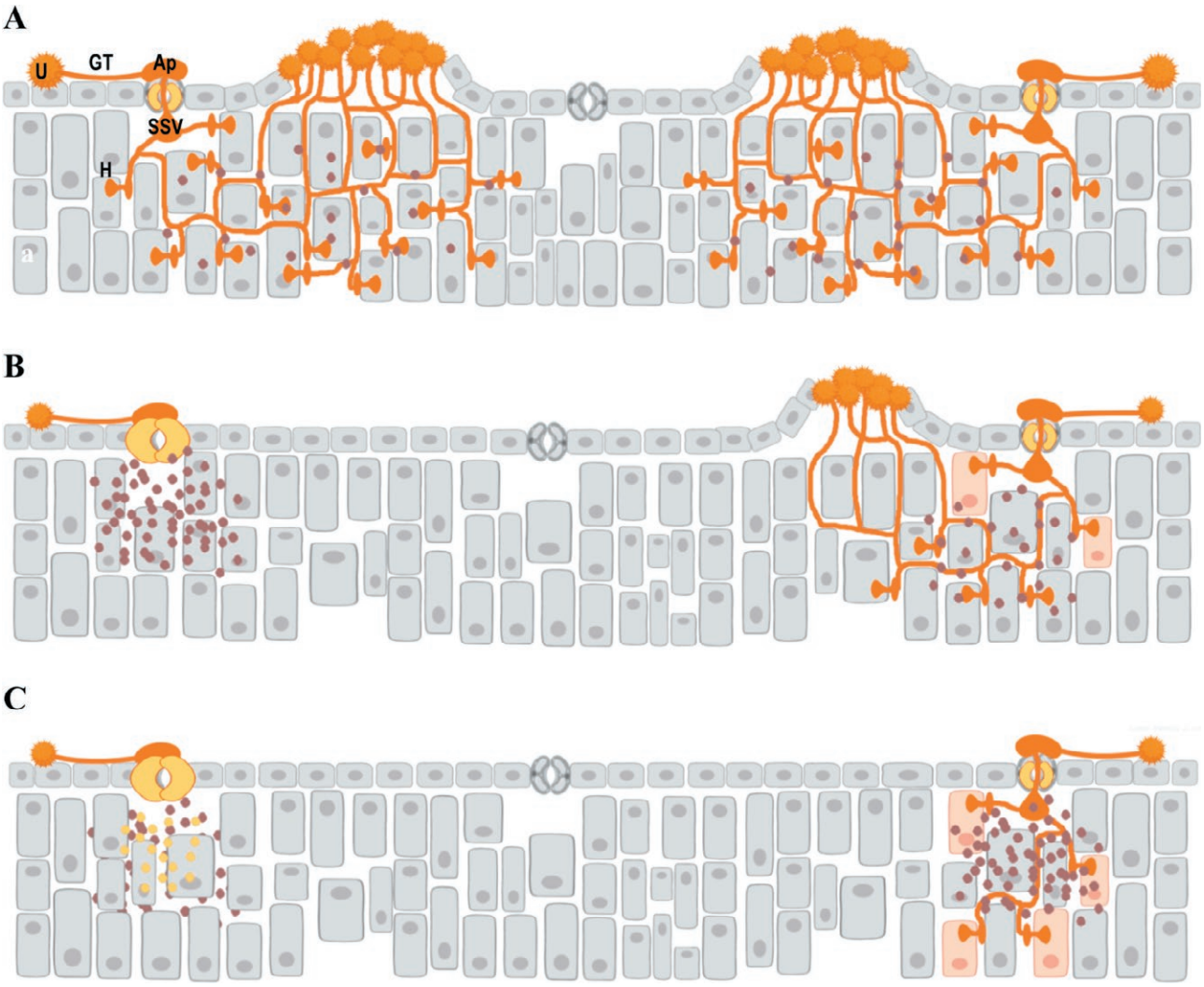

Figure 6. Diagrams illustrating an overview of fungal development and determined defense reactions of wheat to *Puccinia triticina* infection as affected by resistance inducers. **A**, compatible interaction between host and pathogen. In the untreated plant, *P. triticina* overcomes the resistance mechanisms, and is able to complete the infection cycle producing urediniospores (left and right). **B**, enhanced defense reactions in plants treated with CHA0: left, fungus penetration is aborted after callose deposition in leaf guard cells; right, the fungus spreads partially but is stopped after H_2O_2 accumulation and activation of HR in some haustorium penetration sites. Formation of small uredia without or with low spore production. **C**, enhanced defense reactions in BABA-treated plants: left, fungus penetration is aborted after callose deposition in leaf guard and mesophyll cells; right, fungus growth is totally blocked after accumulation of elevated amounts of H_2O_2, and HR activation occurs in cells penetrated by rust haustoria. Fungal structures: **U**, urediniospore; **GT**, germ tube; **SSV**, substomatal vesicle; **Ap**, appressorium; **H**, Haustorium. Yellow dots represent callose depositions. Brown spots indicate H_2O_2 generation.

ning of haustorium generation. This suggests that H_2O_2 initiated and HR defense mechanism. These results are similar to the observation of Serfling *et al.* (2016), where HR was observed in mesophyll cells that were in contact with fungal haustorium mother cells at 24 hai, and the observed pre-haustorial resistance in the resistant accession PI272560 was due to an early HR of the first infected mesophyll cells. Hypersensitive responses accompanied by H_2O_2 accumulation also occur in other interactions of plants with fungal parasites, and these caused non-host resistance to wheat stripe rust in broad bean (Cheng *et al.*, 2012).

Plant-pathogen interactions can be modulated after induced resistance. We present a model for the wheat-*P. triticina* interaction (Figure 6), where infection of a host plant and growth of fungal structures have been interrupted at different phases in response to BABA- or rhizobacteria-induced resistance. In experimental condi-

tions, urediniospores accomplish infection giving uredia of normal size (Figure 6A). In this case, callose accumulation in guard cells is not sufficient to prevent fungus penetration. Low generation of H_2O_2 is not able to initiate required mechanisms to prevent infection. In BABA- and CHA0-treated plants, pathogen spread is differently affected (Figure 6), with exception of the pre-entry process where spores germinate normally and appressoria are formed over stomatal openings in both cases. In CHA0-treated plants, callose deposition in guard cells is highly elevated leading to abortion of fungal penetration (Figure 6B, left). However, when the fungus overcomes the first barrier, callose deposition is no longer effective. Here, H_2O_2 accumulation can be accompanied by the activation of HR at some haustorium penetration sites which could partially stop fungal spread leading to formation of small uredia (Figure 6B, right). With BABA, in addition to what was observed after CHA0 treatment, an accumulation of callose occurs in leaf mesophyll cells. This could explain the high resistance observed after BABA treatment (Figure 6C, left). High accumulation of H_2O_2 initiates HR in cells penetrated by haustoria, and fungal spread is arrested without uredium formation (Figure 6B, right).

The present study has provided new insights into the histological basis of BABA- and rhizobacteria-induced resistance in wheat against leaf rust, showing the key roles of callose deposition and H_2O_2 generation in prevention of penetration and spread of leaf rust. Future studies will focus on expression analysis of some defense-related genes during the infection process, to underline differences and similarities in defense mechanisms induced by CHA0 and BABA.

ACKNOWLEDGEMENTS

Stefan Kellenberger, Agroscope Changins, Nyon, provided technical support advice for manipulating the leaf rust pathogen. FB gratefully acknowledges financial support from the Swiss Federal Commission for Scholarships for Foreign Students, and BMM acknowledges the financial support of the Swiss National Science Foundation, Grant No. 312 310030_160162.

LITERATURE CITED

Amzalek E., Cohen Y., 2007. Comparative efficacy of systemic acquired resistance-inducing compounds against rust infection in sunflower plants. *Phytopathology* 97, 179–186.

Baccelli I., Mauch-Mani B., 2016. Beta-aminobutyric acid priming of plant defense: the role of ABA and other hormones. *Plant Molecular Biology* 91, 703–711.

Balmer A., Pastor V., Gamir J., Flors V., Mauch-Mani B., 2015. The 'prime-ome': towards a holistic approach to priming. *Trends in Plant Science* 20, 443–452.

Barilli E., Rubiales D., Castillejo M.Á., 2012. Comparative proteomic analysis of BTH and BABA-induced resistance in pea (*Pisum sativum*) toward infection with pea rust (*Uromyces pisi*). *Journal of Proteomics* 75, 5189–5205.

Beneduzi A., Ambrosini A., Passaglia L.M., 2012. Plant growth-promoting rhizobacteria (PGPR): their potential as antagonists and biocontrol agents. *Genetics and Molecular Biology* 35, 1044–1051.

Bolton M.D., Kolmer J.A., Garvin D.F., 2008. Wheat leaf rust caused by *Puccinia triticina*. *Molecular Plant Pathology* 9, 563–575.

Cheng Y., Zhang H., Yao J., Wang X., Xu J., … Kang Z., 2012. Characterization of non-host resistance in broad bean to the wheat stripe rust pathogen. *BMC Plant Biology* 12, 96.

Cohen Y., Vaknin M., Mauch-Mani B., 2016. BABA-induced resistance: milestones along a 55-year journey. *Phytoparasitica* 44, 513–538.

de Werra P., Péchy-Tarr M., Keel C., Maurhofer M., 2009. Role of gluconic acid production in the regulation of biocontrol traits of *Pseudomonas fluorescens* CHA0. *Applied and Environmental Microbiology.* 75, 4162–4174.

De Vleesschauwer D., Djavaheri M., Bakker P.A.H.M., Höfte M., 2008. *Pseudomonas fluorescens* WCS374r-induced systemic resistance in rice against *Magnaporthe oryzae* is based on pseudobactin-mediated priming for a salicylic acid-repressible multifaceted defense response. *Plant Physiology* 148, 1996–2012.

Ferreira R.B., Monteiro S., Freitas R., Santos C.N., Chen Z., … Teixeira A.R., 2006. Fungal pathogens: the battle for plant infection. *Critical Reviews in Plant Sciences* 25, 505–524.

Görlach J., Volrath S., Knauf-Beiter G., Hengy G., Beckhove U., … Kessmann H., 1996. Benzothiadiazole, a novel class of inducers of systemic acquired resistance, activates gene expression and disease resistance in wheat. *The Plant Cell* 8, 629–643.

Haas D., Keel C., 2003. Regulation of antibiotic production in root-colonizing *Pseudomonas spp*. and relevance for biological control of plant disease. *Annual Review of Phytopathology* 41, 117–153.

Heil M., 2007. Trade-offs associated with induced resistance. In: *Induced Resistance for Plant Defence: a Sustainable Approch to Crop Protection* (D. Walters, A.

Newton, G Lyon, ed.). Blackwell Publishing, Oxford, UK, 157–177.

Henkes G.J., Jousset A., Bonkowski M., Thorpe M.R., Scheu S., … Röse U.S., 2011. *Pseudomonas fluorescens CHA0* maintains carbon delivery to *Fusarium graminearum*-infected roots and prevents reduction in biomass of barley shoots through systemic interactions. *Journal of Experimental Botany* 62, 4337–4344.

Hodge S., Thompson G., Powell G., 2005. Application of DL-β-aminobutyric acid (BABA) as a root drench to legumes inhibits the growth and reproduction of the pea aphid *Acyrthosiphon pisum* (Hemiptera: Aphididae). *Bulletin of Entomological Research* 95, 449–455.

Hovmøller M.S., Walter S., Justesen A.F., 2010. Escalating threat of wheat rusts. *Science*, 329, 369.

Iavicoli A., Boutet E., Buchala A., Métraux J.-P., 2003. Induced systemic resistance in *Arabidopsis thaliana* in response to root inoculation with *Pseudomonas fluorescens* CHA0. *Molecular Plant-Microbe Interactions* 16, 851–858.

Imperiali N., Chiriboga X., Schlaeppi K., Fesselet M., Villacrés D., … Van Der Heijden M.G., 2017. Combined field inoculations of *Pseudomonas* bacteria, arbuscular mycorrhizal fungi, and entomopathogenic nematodes and their effects on wheat performance. *Frontiers in Plant Science* 8, 1809.

Jones J.D., Dangl J.L., 2006. The plant immune system. *Nature* 444, 323–329.

Justyna P.-G., Ewa K., 2013. Induction of resistance against pathogens by β-aminobutyric acid. *Acta Physiologiae Plantarum* 35, 1735–1748.

Landa B.B., Mavrodi O.V., Raaijmakers J.M., Gardener B.B.M., Thomashow L.S., Weller D.M., 2002. Differential ability of genotypes of 2, 4-diacetylphloroglucinol-producing *Pseudomonas fluorescens* strains to colonize the roots of pea plants. *Applied and Environmental Microbiology.* 68, 3226–3237.

Lugtenberg B., Kamilova F., 2009. Plant-Growth-Promoting Rhizobacteria. *Annual Review of Microbiology* 63, 541–556.

Luna E., Beardon E., Ravnskov S., Scholes J., Ton J., 2016. Optimizing chemically induced resistance in tomato against *Botrytis cinerea*. *Plant disease* 100, 704–710.

Luna E., Pastor V., Robert J., Flors V., Mauch-Mani B., Ton J., 2011. Callose deposition: a multifaceted plant defense response. *Molecular Plant-Microbe Interactions* 24, 183–193.

Mauch-Mani B., Baccelli I., Luna E., Flors V., 2017. Defense priming: an adaptive part of induced resistance. *Annual Review of Plant Biology* 68, 485–512.

Maurhofer M., Hase C., Meuwly P., Metraux J.-P., Defago G., 1994. Induction of systemic resistance of tobacco to tobacco necrosis virus by the root-colonizing *Pseudomonas fluorescens* strain CHA0: influence of the gacA gene and of pyoverdine production. *Phytopathology (USA)*.

Meier U., 1997. *Growth Stages of Mono-and Dicotyledonous Plants*. BBCH Monograph, 2nd ed. Federal Biological Research Centre for Agriculture and Forestry, Bonn, Germany, 21 pp.

Natsch A., Keel C., Pfirter H.A., Haas D., Défago G., 1994. Contribution of the global regulator gene gacA to persistence and dissemination of *Pseudomonas fluorescens* biocontrol strain CHA0 introduced into soil microcosms. *Applied and Environmental Microbiology* 60, 2553–2560.

Orczyk W., Dmochowska-Boguta M., Czembor H., Nadolska-Orczyk A., 2010. Spatiotemporal patterns of oxidative burst and micronecrosis in resistance of wheat to brown rust infection. *Plant Pathology* 59, 567–575.

Ramette A., Frapolli M., Fischer-Le Saux M., Gruffaz C., Meyer J.-M., … Moënne-Loccoz Y., 2011. *Pseudomonas protegens* sp. nov., widespread plant-protecting bacteria producing the biocontrol compounds 2, 4-diacetylphloroglucinol and pyoluteorin. *Systematic and Applied Microbiology* 34, 180–188.

Sari E., Etebarian H.R., Aminian H., 2008. Effects of *Pseudomonas fluorescens* CHA0 on the resistance of wheat seedling roots to the take-all fungus *Gaeumannomyces graminis* var. *tritici*. *Plant Production Science* 11, 298–306.

Scalschi L., Llorens E., Camañes G., Pastor V., Fernández-Crespo E., … Vicedo B., 2015. Quantification of Callose Deposition in Plant Leaves. *Bio-protocol* 5, e1610.

Serfling A., Templer S.E., Winter P., Ordon F., 2016. Microscopic and molecular characterization of the prehaustorial resistance against wheat leaf rust (*Puccinia triticina*) in Einkorn (*Triticum monococcum*). *Frontiers in Plant Science* 7, 1668.

Sharifi-Tehrani A., Kellenberger S., Farzaneh M., Pechy-Tarr M., Keel C., Mascher F., 2009. Genotype-level interactions determine the degree of reduction of leaf rust on wheat by seed application of beneficial *pseudomonads ssp. IOBC/WPRS Bulletin* 43, 321–325.

Singh R.P., Hodson D.P., Huerta-Espino J., Jin Y., Bhavani S., … Govindan V., 2011. The emergence of Ug99 races of the stem rust fungus is a threat to world wheat production. *Annual Review of Phytopathology* 49, 465–481.

Stakman E.C., Stewart D.M., Loegering W.Q., 1962. Identification of physiologic races of *Puccinia graminis* var. *tritici*. Agricultural Research Service E617. (Unit-

ed States Department of Agriculture: Washington DC).

Stutz E., Défago G., Kern H., 1986. Naturally occurring fluorescent pseudomonads involved in suppression of black root rot of tobacco. *Phytopathology* 76, 181–185.

Sun L., Li Y., Miao W., Piao T., Hao Y., Hao F.-S., 2017. NADK2 positively modulates abscisic acid-induced stomatal closure by affecting accumulation of H2O2, Ca2+ and nitric oxide in Arabidopsis guard cells. *Plant Science* 262, 81–90.

Thevenet D., Pastor V., Baccelli I., Balmer A., Vallat A., … Mauch-Mani B., 2017. The priming molecule β-aminobutyric acid is naturally present in plants and is induced by stress. *New Phytologist* 213, 552–559.

Thordal-Christensen H., Zhang Z., Whang Z., Wei Y., Wei Y., Collinge D.B., 1997. Subcellular localization of H_2O_2 in plants. H_2O_2 accumulation in papillae and hypersensitive response during the barley-powdery mildew interaction. *The Plant Journal* 11, 1187–1194.

Van der Ent S., Van Hulten M., Pozo M.J., Czechowski T., Udvardi M.K., Pieterse C.M., Ton J., 2009. Priming of plant innate immunity by rhizobacteria and β-aminobutyric acid: differences and similarities in regulation. *New Phytologist* 183, 419–431.

van Hulten M., Pelser M., Van Loon L., Pieterse C.M., Ton J., 2006. Costs and benefits of priming for defense in Arabidopsis. *Proceedings of the National Academy of Sciences* 103, 5602–5607.

Van Loon L., 1997. Induced resistance in plants and the role of pathogenesis-related proteins. *European Journal of Plant Pathology* 103, 753–765.

Voigt C.A., 2016. Cellulose/callose glucan networks: the key to powdery mildew resistance in plants? *New Phytologist* 212, 303–305.

Wang C.F., Huang L.L., Buchenauer H., Han Q.M., Zhang H.C., Kang Z.S., 2007. Histochemical studies on the accumulation of reactive oxygen species (O_2 and H_2O_2) in the incompatible and compatible interaction of wheat-*Puccinia striiformis* f. sp. *tritici*. *Physiological and Molecular Plant Pathology* 71, 230–239.

Wang X., McCallum B., Fetch T., Bakkeren G., Marais G., Saville B., 2013. Comparative microscopic and molecular analysis of Thatcher near-isogenic lines with wheat leaf rust resistance genes *Lr2a*, *Lr3*, *LrB* or *Lr9* upon challenge with different *Puccinia triticina* races. *Plant Pathology* 62, 698–707.

Wang X., McCallum B., Fetch T., Bakkeren G., Saville B., 2015. *Sr36*-and Sr5-mediated resistance response to *Puccinia graminis* f. sp. *tritici* is associated with callose deposition in wheat guard cells. *Phytopathology* 105, 728–737.

Weller D.M., Landa B., Mavrodi O., Schroeder K., De La Fuente L., … Thomashow L., 2007. Role of 2, 4-diacetylphloroglucinol-producing fluorescent *Pseudomonas spp*. in the defense of plant roots. *Plant Biology* 9, 4-20.

Wesp-Guterres C., Martinelli J.A., Graichen F.A.S., Chaves M.S., 2013. Histopathology of durable adult plant resistance to leaf rust in the Brazilian wheat variety Toropi. *European Journal of Plant Pathology* 137, 181–196.

Phytopathologia Mediterranea
The international journal of the
Mediterranean Phytopathological Union

Firenze University Press
www.fupress.com/pm

Research Papers

Assessment of weed root extracts for allelopathic activity against *Orobanche* and *Phelipanche* species

Mónica FERNÁNDEZ-APARICIO[1,*], Alessio CIMMINO[2], Gabriele SORIANO[2], Marco MASI[2], Susana VILARIÑO[3], Antonio EVIDENTE[2,*]

[1] *Institute for Sustainable Agriculture-CSIC, Avda. Menéndez Pidal sn, 14004 Córdoba, Spain*
[2] *Department of Chemical Sciences, University of Naples Federico II, Complesso Universitario Monte S. Angelo, Via Cintia, 80126 Naples, Italy*
[3] *ALGOSUR S.A., Ctra Lebrija-Trebujena km 5.5, Lebrija – Sevilla, Spain*
*Corresponding author. E-mail: monica.fernandez@ias.csic.es; evidente@unina.it

Summary. Broomrapes (*Orobanche* and *Phelipanche* species) are holoparasitic weeds that infect roots of crop hosts from Asteraceae, Brassicaceae, Apiaceae, Fabaceae, and Solanaceae. The parasitic weeds are difficult to control selectively without crop damage once attached to their roots. Identification of natural compounds with herbicidal activity against pre-attached broomrape stages can provide control alternatives. With the aim to identify plant species with efficacy for broomrape control, organic and residual aqueous phase extracts from roots of seventeen weed species common in south Spanish broomrape-infested fields were assessed as potential inducers of suicidal broomrape germination and as inhibitors of broomrape radicle growth. Assessments were carried out *in vitro* using seeds and seedlings of four noxious broomrape species, *Orobanche crenata* Forsk., *Orobanche cumana* Wallr., *Orobanche minor* Sm. and *Phelipanche ramosa* (L.) Pomel. While root extracts from all the weed species did not induce suicidal germination on *O. crenata* seeds, most of the extracts induced germination of *P. ramosa* except for those obtained from *Amaranthus albus* L., *Amaranthus retroflexus* L. and *Convolvulus arvensis* L. Moderate levels of germination activity were induced in *O. cumana* and *O. minor* seeds by some of the root extracts tested, with strongest induction obtained from *Heliotropium europaeum* L. on *O. cumana* seeds, and from *Silybum marianum* (L.) Gaertn. on *O. minor* seeds. For root extract inhibition of broomrape radicles, the extract from *C. arvensis* roots strongly inhibited radicles of all the broomrape species. While extracts from the other weed species induced low or negligible inhibition of *O. cumana* and *O. crenata* radicle growth, many inhibited *P. ramosa* and *O. minor* radicles. Exceptions were root extracts from *Datura stramonium* L., *Heliotropium europaeum* L., *Malva sylvestris* L., *Solanum nigrum* L. and *Urtica dioica* L., which did not inhibit *P. ramosa* radicles, and those from *A. retroflexus*, *Datura stramonium* L., *Malva sylvestris* L., *Portulaca oleracea* L. and *S. nigrum*, which did not inhibit *O. minor* radicles. Among the active organic extracts assessed, those showing promising chemical profiles were selected for future studies to characterize natural compounds with potential herbicidal activity on early stages of broomrape growth.

Keywords. Allelopathy, broomrape weeds, parasitic weed management, sustainable crop protection.

OPEN ACCESS

Citation: M. Fernández-Aparicio, A. Cimmino, G. Soriano, M. Masi, S. Vilariño, A. Evidente (2021) Assessment of weed root extracts for allelopathic activity against *Orobanche* and *Phelipanche* species. *Phytopathologia Mediterranea* 60(3): 455-466. doi: 10.36253/phyto-12917

Accepted: October 6, 2021

Published: December 30, 2021

Data Availability Statement: All relevant data are within the paper and its Supporting Information files.

Competing Interests: The Author(s) declare(s) no conflict of interest.

Editor: Maurizio Vurro, National Research Council, (CNR), Bari, Italy.

INTRODUCTION

Among all pests, weeds have the largest economic impact in agriculture (Pimentel *et al.,* 2005), and among weeds, the holoparasitic broomrapes (*Orobanche* and *Phelipanche* species) are particularly noxious, since they compete with crops for nutrients by invading their roots for nutrient extraction. Broomrapes have expanded in importance, becoming threats to food security (Parker, 2009).

For successful crop plant infections, broomrape germination is inhibited until detection of host roots through root-derived germination stimulants (Lechat *et al.,* 2012; Fernández-Aparicio *et al.,* 2009). From each germinated broomrape seed a short radicle emerges that grows towards the host root and then develops a multicellular haustorium. This attaches and penetrates the host root, and forms connections with the host vascular system to withdraw water and nutrients (Riopel and Timko 1995; Joel, 2013). Nutrient withdrawal through haustorial connections results in severe reductions of crop yields (Fernández-Aparicio *et al.,* 2016). Because of synchronization of host-parasite life cycles and the intimate haustorial attachments, application of methods that kill the parasitic weeds without damaging host crop are not easy, so parasitic weeds are amongst the most difficult weeds to control (Fernández-Aparicio *et al.,* 2020).

The most used broomrape control methods are based on systemic herbicides commonly employed for the management other weeds, including inhibitors of aromatic synthesis (glyphosate) or branched-chain amino acid synthesis (imidazolinones and sulfonylureas) (Eizenberg et al., 2013). However, sustainability of herbicide control methods is threatened by the high capacity of weeds to develop resistance coupled with decline in authorized herbicides and lack of discovery of new herbicide mechanisms of action (Duke, 2012; Westwood *et al.,* 2018; Heap, 2021). The mechanisms that broomrapes use to infect crops, i.e. host-induced germination and radicle growth towards host roots for haustorium attachment, can be targeted by natural products which stimulate suicidal broomrape germination in the absence of host plants (Zwanenburg *et al.*, 2016), or which inhibit broomrape radicle growth towards host roots (Cimmino *et al.,* 2014). Development of control of parasitic plants based on natural substances could increase sustainability and efficacy of weed management, and potentially reduce environmental impacts and human health effects.

Allelochemicals are biologically active compounds released from donor plants with allelopathic potential against target plants. The International Allelopathy Society defined allelopathy as any process involving secondary metabolites produced by plants, algae, bacteria or fungi that influence the growth and development of agricultural and biological systems (International Allelopathy Society, 1996). Many natural compounds have potential as novel agrochemicals (Dayan and Duke, 2014), but only a few microbial or plant metabolites have been screened for their herbicidal activity (Westwood *et al.,* 2018). From screening of microbial or plant toxins, allelochemicals with activity against parasitic weeds have been discovered, which act on seed germination and radicle development (Evidente *et al.,* 2009; Vurro *et al.,* 2009; Evidente *et al.,* 2010; 2011; Cimmino *et al.,* 2014; Cimmino *et al.,* 2015).

The Lithica poem (circa 400 B.C.) noted that "All the pests that out of earth arise, the earth itself the antidote supplies" (Ibn *et al.,* 1781). This inspired the present study to consider the use of root extracts from autotrophic weeds as sources of metabolites in crop rhizosphere to control parasitic weeds. This paper reports the allelopathic activity of root extracts from 17 dicotyledonous weed species that usually thrive on broomrape-infested fields in the south of Spain. Extract activity was assessed for effects on germination and radicle growth of *Orobanche crenata* Forsk., *Orobanche cumana* Wallr., *Orobanche minor* Sm., and *Phelipanche ramosa* (L.) Pomel, which are four of the most noxious broomrape weeds affecting crops in many parts of the world (Parker, 2013).

MATERIALS AND METHODS

Plant material and growth conditions

Seeds of seventeen weed species (Table 1) were collected during the season of 2016–2017 from a buckwheat field at the Institute for Sustainable Agriculture (IAS-CSIC), Alameda del Obispo Research Center (Córdoba, southern Spain, coordinates 37.856 N, 4.806 W, datum WGS84). The weed species collected frequently occur in southern Spain agricultural fields where *O. crenata* and *O. cumana* also thrive in. In spring 2020, the collected weed seeds were surface sterilized by immersion in 0.5% (w/v) NaOCl and 0.02% (v/v) Tween 20 for 5 min, rinsed thoroughly with sterile distilled water, and dried in a laminar airflow cabinet. The seeds were then sown into pots each containing 1 L of 1:1 sand and peat, which were maintained in a greenhouse for 40 d with day/night regime of 23/20°C, 16/8 h light/dark.

Because broomrapes infect host crop roots and mostly develop underground, extracts from weed roots were used, aiming to identify potential allelopathic signals acting in plant rhizospheres. For collection of roots,

Table 1. Weed species investigated for root allelopathic activity against four broomrape species, and mean yields of organic extracts from the CH_2Cl_2 extractions from dry roots.

Plant family	Plant species	EPPO Code *	Weight in mg of CH_2Cl_2 organic extract. (% of root dry weight)
Weed species donor of the allelopathic activity			
Amaranthaceae	*Amaranthus albus*	EPPO:AMAAL	14.40 (0.23)
Amaranthaceae	*Amaranthus retroflexus*	EPPO:AMARE	19.93 (0.32)
Asteraceae	*Conyza bonariensis*	EPPO:ERIBO	23.60 (0.39)
Asteraceae	*Silybum marianum*	EPPO:SLYMA	16.67 (0.28)
Boraginaceae	*Heliotropium europaeum*	EPPO:HEOEU	21.24 (0.34)
Brassicaceae	*Capsella bursa-pastoris*	EPPO:CAPBP	22.13 (0.78)
Brassicaceae	*Diplotaxis erucoides*	EPPO:DIPER	29.62 (0.49)
Brassicaceae	*Diplotaxis virgata*	EPPO:DIPVG	41.93 (0.70)
Convolvulaceae	*Convolvulus arvensis*	EPPO:CONAR	77.42 (1.28)
Malvaceae	*Malva sylvestris*	EPPO:MALSI	36.24 (0.74)
Papaveraceae	*Fumaria officinalis*	EPPO:FUMOF	39.02 (1.85)
Polygonaceae	*Polygonum aviculare*	EPPO:POLAV	29.77 (0.49)
Portulacaceae	*Portulaca oleracea*	EPPO:POROL	25.53 (0.36))
Solanaceae	*Datura stramonium*	EPPO:DATST	18.64 (0.31)
Solanaceae	*Solanum nigrum*	EPPO:SOLNI	30.19 (0.49)
Urticaceae	*Urtica dioica*	EPPO:URTDI	19.35 (0.32)
Zygophyllales	*Tribulus terrestris*	EPPO:TRBTE	27.52 (0.46)
Parasitic weed species target of the allelopathic activity			
Orobanchaceae	*Orobanche crenata*	ORACR	
Orobanchaceae	*Orobanche cumana*	ORACE	
Orobanchaceae	*Orobanche minor*	ORAMI	
Orobanchaceae	*Phelipanche ramosa*	ORARA	

*EPPO Code. European and Mediterranean Plant Protection Organization. https://gd.eppo.int.

weed plants at vegetative stages were removed from the pots, their roots were carefully washed in distilled water, quickly dried with filter paper, and immediately frozen and maintained at -80°C until lyophilization.

Broomrape seeds were collected using a 0.6 mm mesh-size sieve (Filtra) from dry inflorescences of *O. crenata* infecting faba bean plants in Spain, *O. cumana* infecting sunflower plants in Turkey, *O. minor* infecting red clover in France and *P. ramosa* infecting oilseed rape in France, and these seeds were stored dry in the dark at 4°C until used.

Extraction of dried roots of weed plants

A general method was used to make extractions from the weed roots. Approximately 6 g of dried root tissue of each weed plant was milled in a Waring blender, and the resulting powder was extracted overnight in MeOH-H_2O (200 mL, 1:1, v:v) under stirring at room temperature in the dark. The resulting suspension was then centrifuged for 1 h at 7000 r.p.m. at 4°C. The supernatant was then extracted with CH_2Cl_2 (three × 200 mL). The organic extracts were combined, dried (Na_2SO_4), filtered and evaporated under reduced pressure.

Germination and radicle growth bioassays

Allelopathic effects of the organic and the aqueous phase extracts from weed roots (Table 1) were assessed for broomrape germination and radicle growth in independent bioassays that were conducted according to previously described protocols (Fernández-Aparicio *et al.,* 2013; Cimmino *et al.,* 2014). Broomrape seed germination is achieved through a two-step process, including warm stratification conditioning followed by chemical stimulation (Lechat *et al.*, 2012). For detection of stimulatory activity of germination, root extracts were dissolved in water, and water without root extracts was used as control. For the discov-

ery of inhibitory activity of radicle growth, the root extracts were mixed with GR24 and, GR24 without root extracts was used as a control.

Seeds of the four broomrape species were surface sterilized by immersion for 5 min in 0.5% (w/v) NaOCl and 0.02% (v/v) Tween 20, and were then rinsed thoroughly with sterile distilled water, and dried in a laminar air flow cabinet. Approximately 100 seeds of each broomrape species were placed separately on 9 mm diameter glass fiber filter paper disks (GFFP) (Whatman International Ltd.) each moistened with 50 µL of sterile distilled water and then placed in incubators at 23°C for 10 d inside Parafilm-sealed Petri dishes, to allow seed conditioning. The GFFP disks containing conditioned broomrape seeds were then each transferred onto a sterile sheet of filter paper to remove the excess of water and transferred to a new 10 cm diameter sterile Petri dish.

For germination induction assays, stock solutions of each root organic extract or root aqueous phase dissolved, respectively, in methanol or sterile distilled water, were mixed with sterile distilled water to equivalent concentrations of 0 (control), 10 or 100 µg dry extract per mL of distilled water. For radicle growth assays, the stock solutions of each root organic extract or root aqueous phase were each mixed with GR24 to concentrations of 0 (control), 10 or 100 µg extract per mL of 10^{-6} M GR24. Triplicate aliquots of 50 µL of each sample of each sample were applied to GFFP discs. Treated seeds were incubated in the dark at 23°C for 7 d and percent germination and radicle growth were determined for each GFFP disc as described by Cimmino *et al.* (2014) and Fernández-Aparicio *et al.* (2013), using a stereoscopic microscope (Leica S9i, Leica Microsystems GmbH). Broomrape seed germination was determined by counting the number of germinated seeds from 100 seeds for each GFFP disc (Fernández-Aparicio *et al.*, 2013). For assessing characteristics of radicle growth, the average of ten randomly selected radicles were examined (Westwood and Foy, 1999). The percentage germination induction from each treatment was then calculated relative to the average germination of control seeds (seeds treated with water), and the percentage of radicle growth inhibition for each treatment was calculated relative to the average radicle growth of control treatments (radicles treated with GR24).

TLC and HPLC analysis

Analytical and preparative Thin Layer Chromatography (TLC) of plant extracts were carried out on silica gel plates (Kieselgel 60 or F_{254}, respectively 0.25 and 0.5 mm), and on reverse phase plates (Kieselgel 60 RP-18, F_{254}, 0.20 mm) (Merck). Eluents used were: $CHCl_3$-iso-PrOH 9:1 v/v for direct-phase TLC and MeCN-H_2O 6:4 v/v for reverse-phase TLC analysis. Spots were visualized by exposure to UV light (254 nm), or by first spraying with 10% H_2SO_4 in methanol and then with 5% phosphomolybdic acid in ethanol, followed by heating at 110°C for 10 min. The High Performance Liquid Chromatography (HPLC) system used for the analyses of the plant root extracts was from Hitachi, and consisted of a pump (model 5160) and a spectrophotometric UV detector (model 5410) fixed at 254 nm. Metabolites separation was performed using a Phenomenex Luna C_{18} reversed-phase column (15 × 4.6 mm; 5 µm particle size), which was eluted at a flow rate of 0.5 mL min^{-1}. Two HPLC conditions were used. In the first, the gradient commenced from 50% MeCN – 50% 0.1% HCOOH for 20 min, and then linearly increased from 50% to 90% MeCN in 20 min, and remained at these conditions for 10 min. The phase was then followed by a re-equilibrium to the initial gradient composition in 10 min. In the second, the gradient commenced from 60% MeCN – 40% 0.1% HCOOH for 30 min, and then linearly increased from 60% to 90% MeCN in 20 min, and remained at these conditions for 10 min. The phase was then followed by a re-equilibrium to the initial gradient composition for 10 min.

Statistical analyses

Percentage data were approximated to normal distributions and stabilize variances using angular transformations (180/π × arcsine (sqrt[%/100]). Significance of the weed species donor of activity, the targeted broomrape species and their interactions on induction of suicidal broomrape germination and inhibition of radicle growth was assessed using two-way ANOVA (SPSS version 21.0; SPSS Inc.). For each broomrape species, the significance of mean differences among donor weed species was evaluated by the least significant difference (LSD) ($P < 0.05$). Null hypotheses were rejected at the level of 0.05.

RESULTS AND DISCUSSION

The weed root extractions yielded percentages of organic extract relative to the lyophilized root weight that ranged from 0.23% for *Amaranthus albus* L. to a maximum of 1.85% for *Fumaria officinalis* L. (Table 1). Firstly, the potential was assessed for the weed root extracts to induce broomrape suicidal germination. Germination of broomrape seeds in the absence of host roots is termed "suicidal" because the subsequent

broomrape growth cannot reach host plants which are the sole nutritive sources for the parasitic weeds (Zwanenburg *et al.*, 2016). All of the weed roots extracts were studied at two concentrations (10 or 100 µg of root extract per mL of distilled water) for effects on seeds of the four broomrape species. In all cases, no germination was observed (data not shown) when seeds of the different broomrape species were treated with the negative controls (0 µg of root extract per mL of distilled water). The null germination values induced by the negative controls was expected because broomrape seed germination remains inhibited in absence of germination stimulants (Lechat et al., 2012). The synthetic strigolactone GR24 used as a positive control induced the greatest proportions of mean germination of *O. crenata* seeds, 71.3 ± 3.1%, *O. cumana*, 70.8 ± 2.5%, *O. minor*, 72.8 ± 2.0%, and of *P. ramosa*, 94.6 ± 1.1%.

Different protocols have been previously used for isolation of germination stimulants in plant roots. Boutet-Mercey *et al.* (2018) extracted germination stimulants from pea roots, using a method which included 2 h shaking at 4°C of ground frozen roots, and after centrifugation, the supernatant was dissolved in heptane/EtOAc followed by solid phase extraction. Yoneyama *et al.* (2016) used a different method, which macerated sorghum root pieces in ethanol for up to 3 d. The efficiency of maceration and extraction methods from plant tissues depend on the cellular localization and polarity of the targeted compounds (Halouzka *et al.*, 2020). In the present study, weed root extracts were shown to induce broomrape seed germination (Figure 1). This indicates that extraction method used here was appropriate for identification of broomrape germination stimulants in root tissues.

Germination-inducing activity of weed root extracts was studied for two host-specialist broomrape species *O. crenata* and *O. cumana* and two host-generalist broomrape species *O. minor* and *P. ramosa*. Germination of *O. crenata* seeds was not induced (data not shown) by root extracts from any of the weed species tested at the assessed concentrations (10 or 100 µg dry extract per mL of distilled water). These results indicate that none of the weed root extracts have potential as sources of suicidal germination inducers for *O. crenata*-infested fields. Broomrape seed sensitivity to differing germination stimulants exuded by different crops is used a proxy of host specialization (Fernández-Aparicio *et al.*,

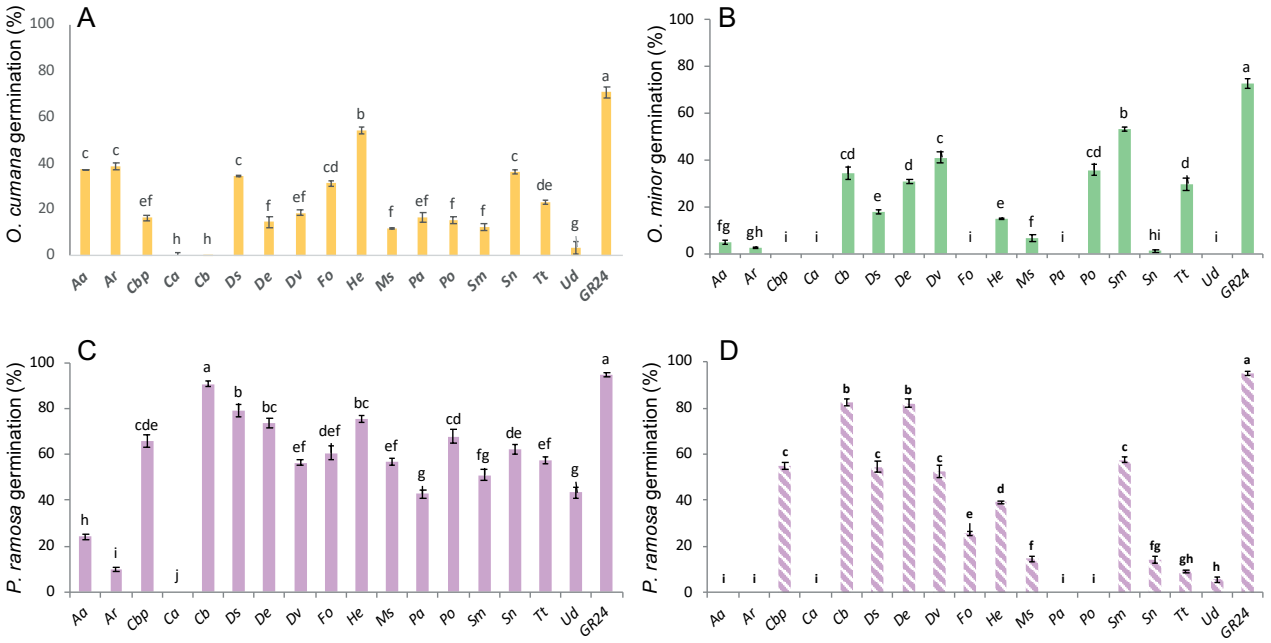

Figure 1. Mean seed germination proportions (%) of three broomrape species induced by organic extracts from roots of seventeen weed species, including *Amaranthus albus* L. (Aa); *Amaranthus retroflexus* L. (Ar); Cbp, *Capsella bursa-pastoris* (L.) Medik.; Ca, *Convolvulus arvensis* L.; Cb, *Conyza bonariensis* L.; Ds, *Datura stramonium* L.; De, *Diplotaxis erucoides* (L.) DC.; Dv, *Diplotaxis virgate* (Cav.) DC.; Fo, *Fumaria officinalis* L., He, *Heliotropium europaeum* L.; Ms, *Malva sylvestris* L.; Pa, *Polygonum aviculare* L.; Po, *Portulaca oleracea* L.; Sm, *Silybum marianum* (L.) Gaertn., *Solanum nigrum* L.; Tt, *Tribulus terrestris* Boiss.; Ud, *Urtica dioica* L.. Root extracts were applied at 100 µg (A-C) or 10 µg (D) of root organic extract per mL distilled water to seeds of *Orobanche cumana* Wallr. (A), *Orobanche minor* Sm. (B) or *Phelipanche ramosa* (L.) Pomel. (C and D). For each broomrape species, means accompanied by different letters are significantly different according to the LSD test ($P < 0.05$). Error bars represent the standard error of the mean.

2009; Fernández-Aparicio *et al.,* 2011; Huet *et al.,* 2020). *Orobanche crenata* has a narrow host range mainly specialized to Fabaceae and Apiaceae (Parker, 2013), and consistently with host range, its germination is induced by a narrow range of plant species and molecules when compared with other broomrape species (Fernández-Aparicio *et al.,* 2009).

When weed root extracts were applied to the other three broomrape species at 100 µg dry extract per mL distilled water (Figure 1A, B and C), significant effects were detected in the induction of suicidal germination for broomrape species target of allelopathic activity (ANOVA, $P < 0.001$) and weed species donor of allelopathic activity (ANOVA, $P < 0.001$). The host generalist *P. ramosa* attacks a wide range of crops in Solanaceae, Brassicaceae, Cannabaceae, Fabaceae, Apiaceae, and Asteraceae (Parker, 2013), and its parasitic life cycle is initiated by germination stimulants exuded by roots of many plant species (Fernández-Aparicio *et al.,* 2009). Germination of *P. ramosa* was strongly induced by root extracts of most of the weed species assessed. Exceptions were *A. albus* and *Amaranthus retroflexus* L. which induced low statistically significant germination, and *Convolvulus arvensis* L. that did not induce germination. Consistent with the present results, root exudates of *C. arvensis* were also shown to be inactive inducers of *P. ramosa* seed germination in investigations conducted by Gibot-Leclerc *et al.* (2013). Despite the usual correlations observed in broomrape species between broad host range and high germination sensitivity to different root exudates and germination stimulants released by diverse crop species, these correlations were not observed in the present study for *O. cumana* and *O. minor* against stimulation of different weed root extracts. While the germination of the sunflower specialist *O. cumana* was induced by root extracts of all the plant species assessed except *C. arvensis* and *Conyza bonariensis* L., germination of the host generalist *O. minor* was induced by few weeds species, mainly *C. bonariensis*, *Diplotaxis* spp., *Portulaca oleracea* L., *Silybum marianum (*L.) Gaertn and *Tribulus terrestris* Boiss.

A significant interaction was detected between effects of targeted broomrape species and weed species root extracts (ANOVA, $P < 0.001$). For example, the extracts from *Heliotropium europaeum* L. or *Solanum nigrum* L. gave high activity against seed germination of *O. cumana* and *P. ramosa* but not of *O. minor* or *O. crenata*. In contrast, *C. bonariensis* (Asteraceae) gave high germination induction for *P. ramosa* and *O. minor* but was not active for *O. crenata* or the sunflower specialist *O. cumana*. Root extracts of both species of *Amaranthus* induced high germination of *O. cumana* seeds but gave little or null activity for seeds of *O. crenata, O. minor* and *P. ramosa*. The root extract of *C. arvensis* did not induce germination for any of the broomrape species assessed. Different classes of broomrape germination stimulants have been detected in crops, and each crop species exudes a characteristic germination stimulant profile active in specific broomrape species. Specificity in recognition of different classes of germination stimulants by broomrape species has been reported (Fernández-Aparicio *et al.,* 2008; Fernández-Aparicio *et al.,* 2009; Xie *et al.,* 2010; Fernández-Aparicio *et al.,* 2014).

When weed root extracts from most of the assessed weed species were applied to seeds of *O. cumana* and *O. minor* at 10 µg per mL, activity on broomrape germination was reduced to negligible levels (data not shown). The exceptions were the extracts from *S. marianum* on germination of *O. cumana* (mean = 27.9 ± 0.4%) and *O. minor* (31.7 ± 0.9%), and for germination of *O. cumana* seeds which was induced by extracts from *Diplotaxis virgata* (Cav.) DC. (19.9 ± 0.8%), *F. officinalis* L. (14.9 ± 1.7%), *H. europaeum* (17.2 ± 1.0%), and *Polygonum aviculare* L. (9.4 ± 0.3%). Seeds of *P. ramosa* were more sensitive to the application of 10 µg per mL extracts (Figure 1D), with the most active extracts were those obtained from *C. bonariensis* (82.4 ± 1.7%) and *Diplotaxis erucoides* (L.) DC. (82.0 ± 1.7%). The main classes of identified broomrape germination stimulants are strigolactones (Xie *et al.,* 2010) biosynthetically derived from carotenoids (Matusova *et al.,* 2005). More than 25 strigolactones have been identified in crops (Aliche *et al.,* 2020) and their different structural conformations have species-specific activity for broomrape germination (Fernández-Aparicio *et al.,* 2011). Strigolactones are active on parasitic weed germination at very low concentrations when tested in pure solutions (Xie, 2016; Huet *et al.,* 2020). Other different natural substances (e.g. polyphenols, isothiocyanates, benzonitrils, saponins, and sesquiterpenes) isolated from plants species show broomrape germination stimulantion when tested at high concentrations (Cimmino *et al.,* 2018). The unknown metabolites contained in weed root extracts responsible for the suicidal germination activity recorded in the present study gave activity in the complex mixtures of metabolites present in root extracts of each weed investigated. This could indicate significant activity strength, so these compounds will be isolated and characterized in future studies.

The germination inducing activity of aqueous phase root extracts of each weed species was also studied for seeds of *O. crenata*, *O. cumana*, *O. minor*, and *P. ramosa* at 100 or 10 µg of root extract per mL distilled water. In most cases, no germination was observed. The exceptions were when seeds of *P. ramosa* were treated with the aqueous extracts from roots of *D. erucoides* or *D.*

virgata. At 100 µg of *D. erucoides* root extract per mL distilled water, mean germination of *P. ramosa* was 90.2 ± 0.7%, and for this concentration of extract from *D. virgata* was 56.8 ± 2.3%. At 10 µg per mL distilled water, extract from *D. erucoides* gave 63.6 ± 0.3% germination of *P. ramosa*, and extract from *D. virgata* gave 54.6 ± 2.3% germination of *P. ramosa*. Future characterization of a highly water-soluble molecule with broomrape germination activity could provide a tool for field applications to manage parasitic weeds.

In addition to the identification of potential root extracts as suicidal germination inducers, the organic and aqueous phase extracts from roots of seventeen weed species (Table 1) were also studied for their potential inhibitory activities towards broomrape radicle growth (Figures 2 and 3). All the root extracts were assessed at two concentrations (100 or 10 µg of root extract /mL GR24). No inhibitory activity of radicle growth was observed in any of the aqueous phases regardless the concentration tested nor in the organic extracts applied at the lowest concentration of 10 µg of root extract /mL GR24 (data not shown). At 100 µg, significant effects on radicle growth were detected for broomrape species target of allelopathic activity (ANOVA, $P < 0.001$) and weed species donors of allelopathic activity (ANOVA, $P < 0.001$) and their interactions (ANOVA, $P < 0.001$). Roots of *C. arvensis* consistently inhibited radicle growth of all the broomrape species studied (Figure 2, Figure 3A and D) in comparison with experimental controls (Figure 3C and F). The mean radicle growth inhibition induced by *C. arvensis* was 56.9 ± 4.7% for *O. crenata* radicles, 45.3 ± 3.2% for *O. cumana* radicles, 57.7 ± 1.1% for *O. minor* radicles, and 82.5 ± 1.2% for *P. ramosa* radicles. Besides inhibition of radicle growth, *C. arvensis* root extract induced staining of *O. crenata* radicles as intense yellow with swollen root tips (Figure 3A). The yellow stain was not observed in radicles of any other broomrape species treated with root extract of *C. arvensis* or any other weed. *Orobanche crenata* radicles were not inhibited by root extracts of any other weed species. In contrast, growth of *P. ramosa* radicles was inhibited by most weed extracts, except

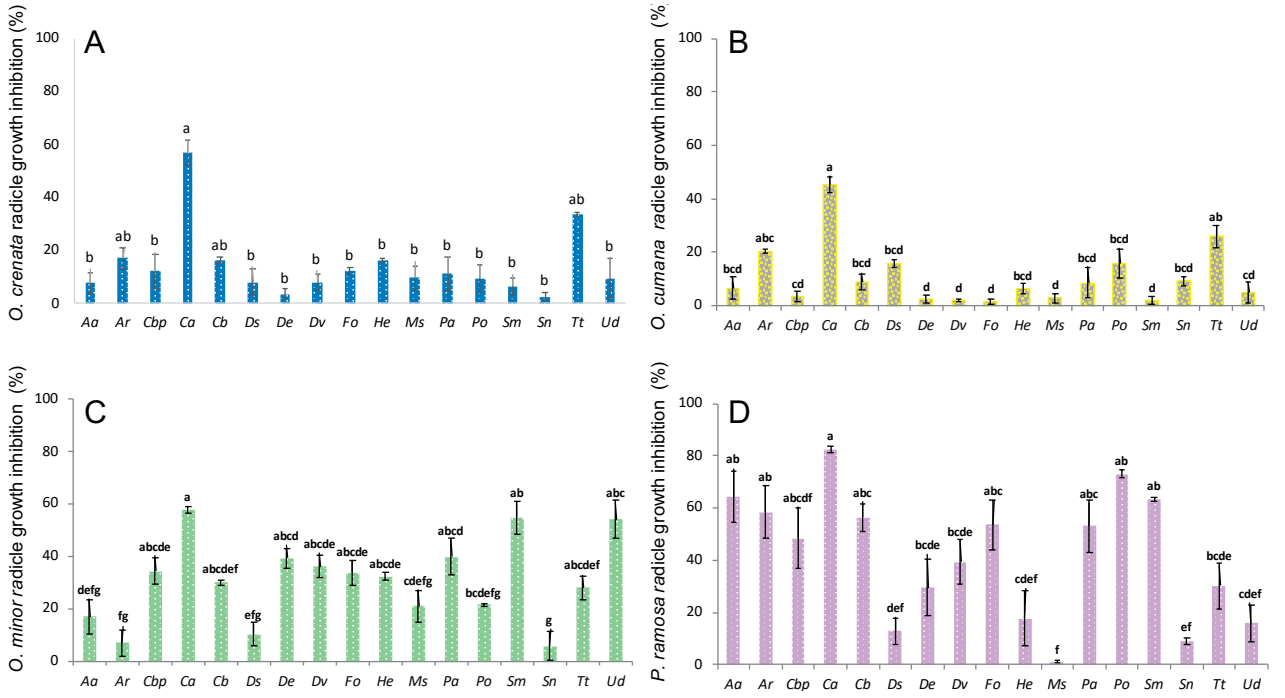

Figure 2. Mean growth inhibition of broomrape radicle growth induced by organic extracts from roots of seventeen weed species, including: *Amaranthus albus* L. (Aa); *Amaranthus retroflexus* L. (Ar); Cbp, *Capsella bursa-pastoris* (L.) Medik.; Ca, *Convolvulus arvensis* L.; Cb, *Conyza bonariensis* L.; Ds, *Datura stramonium* L.; De, *Diplotaxis erucoides* (L.) DC.; Dv, *Diplotaxis virgate* (Cav.) DC.; Fo, *Fumaria officinalis* L., He, *Heliotropium europaeum* L.; Ms, *Malva sylvestris* L.; Pa, *Polygonum aviculare* L.; Po, *Portulaca oleracea* L.; Sm, *Silybum marianum* (L.) Gaertn., *Solanum nigrum* L.; Tt, *Tribulus terrestris* Boiss.; Ud, *Urtica dioica* L.. Extracts were assessed at 100 µg per mL of organic extract (10^{-6}M) on radicles of four broomrape species, including: *Orobanche crenata* Forsk. (A); *Orobanche cumana* Wallr. (B); *Orobanche minor* Sm. (C); and *Phelipanche ramosa* (L.) Pomel (D). Means accompanied by different letters are significantly different according to the LSD test ($P < 0.05$). Error bars represent the standard error of the mean.

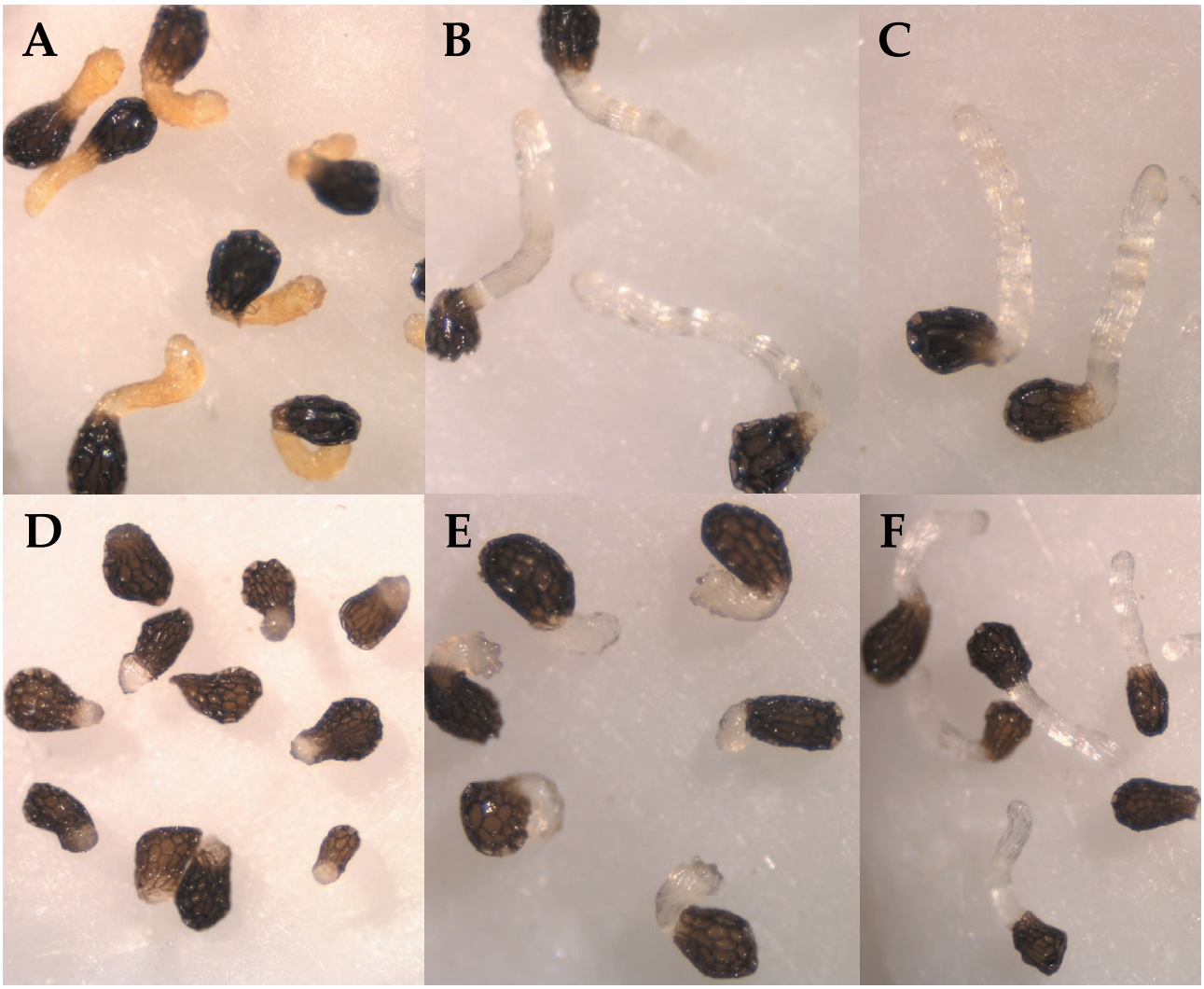

Figure 3. Photographs illustrating effects of CH_2Cl_2 organic extracts from roots of *Convolvulus arvensis* L. (A and D), and *Portulaca oleracea* L. (B and E), both compared with respective experimental controls (C and F) on radicle growth of (A-C) *Orobanche crenata* Forsk. and (D-F) *Phelipanche ramosa* (L.) Pomel.

those from *Datura stramonium* L., *H. europaeum, M. sylvestris, S. nigrum* L. and *Urtica dioica* L. Radicle growth of *O. minor* was also inhibited by most of the weed extracts, except those from *A. retroflexus, D. stramonium*, *M. sylvestris, P. oleracea* and *S. nigrum*. Except for *C. arvensis,* weed extracts had low inhibitory effects on *O. cumana* radicle growth, but low (and statistically significant) inhibitory activity was found for extracts from *A. retroflexus, D. stramonium, P. oleracea* and *T. terrestris*. The growth inhibition induced by extracts from these four weeds in *O. cumana* was less than 20% of the growth of control radicles.

Organic extracts were first analysed using TLC on direct (Figure 4A and B) and reverse phase (Figure 4C) plates. Figure 4A and B indicates that all the root extracts gave a similar mixtures of two metabolites at R_f = 0.53 and 0.63 when the TLC analysis was performed with $CHCl_3$-*iso*-PrOH 9:1 v/v but revealed with two different methods (exposure to UV light at 254 nm, Figure 4A; and by spraying first with 10% H_2SO_4 in MeOH, and then with 5% phosphomolybdic acid in EtOH, Figure 4B). However, other metabolites were present in the organic extracts from *C. arvensis*, *S. nigrum*, *T. terrestris*, *S. marianum*, *P. oleracea*, *F. officinalis*, *C. bursa-pastoris* and *D. virgata*. These results were also confirmed by the chromatographic profiles obtained using reverse phase plates eluted with MeCN-H_2O 6:4 v/v and spots visualized by exposure to UV light (254 nm) (Figure 4C).

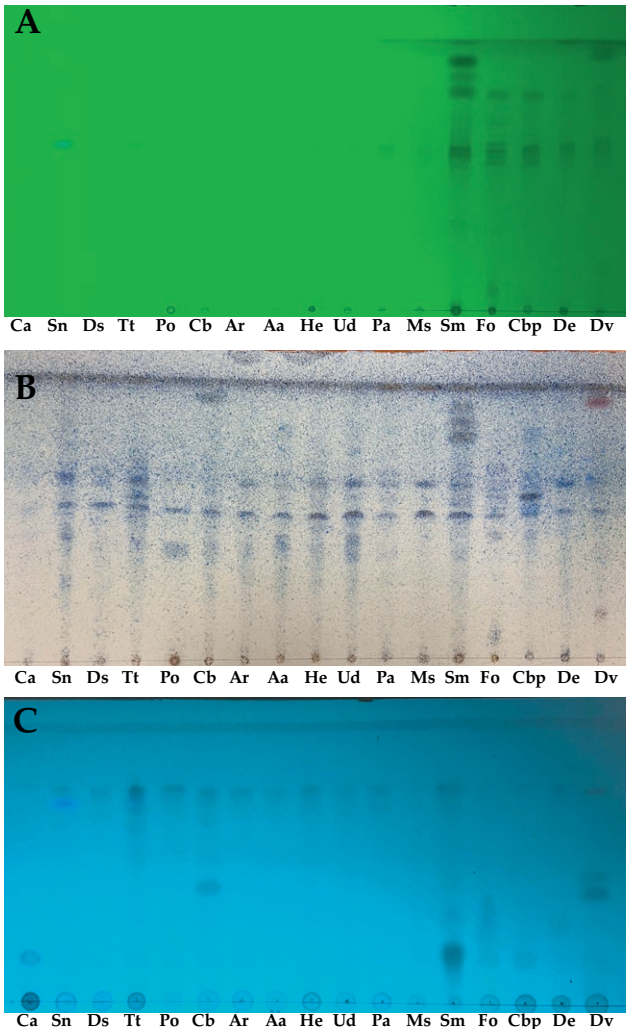

Figure 4. TLC analyses of plant root extracts from: Ca, *Convolvulus arvensis* L.; Sn, *Solanum nigrum* L.; Ds, *Datura stramonium* L.; Tt, *Tribulus terrestris* Boiss.; Po, *Portulaca oleracea* L.; Cb, *Conyza bonariensis* L.; Ar, *Amaranthus retroflexus* L.; Aa, *Amaranthus albus* L.; He, *Heliotropium europaeum* L.; Ud, *Urtica dioica* L.; Pa, *Polygonum aviculare* L.; Ms, *Malva sylvestris* L.; Sm, *Silybum marianum* (L.) Gaertn.; Fo, *Fumaria officinalis* L.; *Capsella bursa-pastoris* (L.) Medik.; De, *D. erucoides* (L.) DC. and Dv, *D. virgate* (Cav.) DC.. A, Chromatograms obtained using silica gel plates eluted with $CHCl_3$-*iso*-PrOH 9:1 v/v and spots visualized by exposure to UV light (254 nm); B, Chromatograms obtained using silica gel plates eluted with $CHCl_3$-*iso*-PrOH 9:1 v/v and visualized by spraying first with 10% H_2SO_4 in MeOH, and then with 5% phosphomolybdic acid in EtOH, followed by heating at 110°C for 10 min; C, Chromatogram obtained using reverse phase plates eluted with MeCN-H_2O 6:4 v/v and spots visualized by exposure to UV light (254 nm).

The organic extracts were also analyzed using HPLC, using the conditions designated a (see above). The optimized HPLC analyses (using the conditions designated b, above) of extracts from the active plants are reported in Figure 5. In particular, the extracts analyzed were those of *C. bonariensis*, which gave high germination inducing activity for *P. ramosa* and *O. minor* but were not active for *O. cumana* or *O. crenata*; *H. europaeum* and *S. nigrum* which gave high seed germination induction for *O. cumana* and *P. ramosa*, but not for *O. minor* or *O. crenata; A. albus* and *A. retroflexus* which gave high levels of germination of *O. cumana* seeds, but low or no activity for seeds of *O. crenata, O. minor* or *P. ramosa* and root extracts of *C. arvensis* which did not induce germination in any of the broomrape species assessed.

Among these active organic extracts, the present study has identified those obtained from *C. arvensis, C. bonariensis*, *P. oleracea,* and *D. euricoides* for future isolation and characterization of bioactive metabolites with herbicidal activity against early stages of broomrape development, particularly focusing on the promising TLC profiles and HPLC analyses. Phytochemical analysis of these weed species components have been reported for some of the plants assessed in the present study. From *C. arvenis*, carbohydrates, coumarins, saponins, flavanoids, lipids, steroids, terpenoids, alkaloids, tannins and lactones have been isolated from *Convolvulus* (Salehi *et al.,* 2020), while homoisoflavonoids, terpenoids, alkaloids, cerebrosides, coumarins, flavonoids and organic acids have been isolated from *P. oleracea* (Yan *et al.,* 2012; Wang *et al.,* 2017). Phenylpropanoids, flavonoids, sesquiterpenes, alkaloids, and phenolic acids have been isolated from *A. retroflexus* (Fiorito *et al.,* 2017), and glycosides and monoterpenes have been isolated from *C. bonariensis* (Kong *et al.,* 2001; Zahoor *et al.,* 2010; Miranda *et al.,* 2015). Flavonoids and their glycosides have been obtained from *D. eurocoides* (Salah *et al.,* 2015; Hussein *et al.,* 2017). Roots extract from these plants could be used combined with other broomrape management methods (e.g. crop resistance to haustorial infection, modification of crop sowing dates, fertilizer applications, biological control agents) as components of strategies for integrated broomrape management. These strategies will reduce the use of synthetic herbicide for eco-friendly weed control practices (Scavo and Mauromicale, 2020).

In conclusion, this paper is the first report of the allelopathic potential of seventeen weeds for management of *Orobanche* and *Phelipanche* species which can be responsible of heavy losses in important crops. Assessments of weed root organic extracts were carried out to characterize antagonist activity as well as corresponding chemical composition. These results are an important starting point for the isolation and characterization of metabolites with allelopathic activity against parasitic weeds. Further investigations will potentially

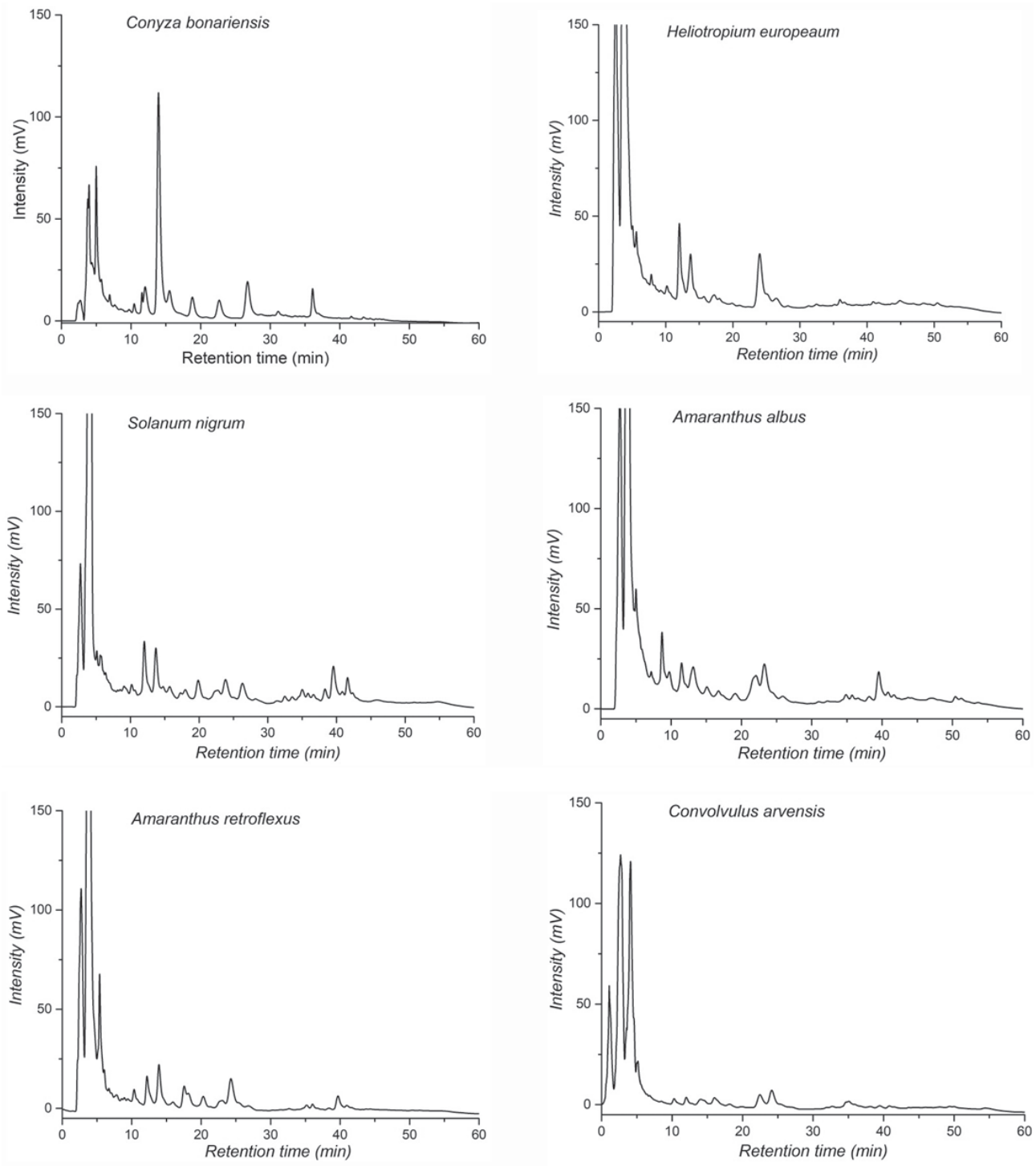

Figure 5. Optimized HPLC analysis of the extracts of the active plants: *Conyza bonariensis* L., *Heliotropium europaeum* L., *Solanum nigrum* L., *Amaranthus albus* L., *Amaranthus retroflexus* L. and *Convolvulus arvensis* L.. The HPLCs were obtained using a 0.5 mL min^{-1} flow rate and the gradient: commencing from 60% MeCN – 40% 0.1% HCOOH for 30 min, and then linearly increasing from 60% to 90% MeCN in 20 min, and remaining at these conditions for 10 min. The phase was then followed by a re-equilibrium to the initial gradient composition for 10 min.

allow development of broomrape biocontrol method based on formulations containing active metabolites.

ACKNOWLEDGEMENTS

This research was funded by the Spanish Ministry of Science and Innovation (RYC-2015-18961 and AGL2017-87693-R) and from a CSIC-ALGOSUR research contract. Antonio Evidente is associated with the Istituto di Chimica Biomolecolare del CNR, Pozzuoli, Italy. Authors wish to thank INPS (Istituto Nazionale Previdenza Sociale) for funding a Ph.D. grant to Gabriele Soriano.

LITERATURE CITED

Aliche E.B., Screpanti C., De Mesmaeker A., Munnik T., Bouwmeester H.J., 2020. Science and application of strigolactones. *New Phytologyst* 227: 1001–1011.

Boutet-Mercey S., Perreau F., Roux A., Clave G., Pillot J.P., … Boyer F.D., 2018. Validated method for strigolactone quantification by ultra high-performance liquid chromatography-electrospray ionisation tandem mass spectrometry using novel deuterium labelled standards. *Phytochemical Analysis* 29: 59–68.

Cimmino A., Fernández-Aparicio M., Andolfi A., Basso S., Rubiales D., Evidente, A., 2014. Effect of fungal and plant metabolites on broomrapes (*Orobanche* and *Phelipanche* spp.) seed germination and radicle growth. *Journal of Agricultural and Food Chemistry* 62: 10485–10492.

Cimmino A., Masi M., Evidente M., Superchi S., Evidente A., 2015. Fungal phytotoxins with potential herbicidal activity: chemical and biological characterization. *Natural Product Reports* 32: 1629–1653.

Cimmino A., Masi M., Rubiales D., Evidente A., Fernández-Aparicio M., 2018. Allelopathy for parasitic plant management. *Natural Product Communications* 13: 289–294.

Dayan F.E., Duke S.O., 2014. Natural compounds as next-generation herbicides. *Plant Physiology* 166: 1090–1105.

Duke S.O., 2012. Why have no new herbicide modes of action appeared in recent years? *Pest Management Science* 68: 505–512.

Eizenberg H., Hershenhorn J., Ephrath J.H., Kanampiu F. 2013. Chemical control. In *Parasitic Orobanchaceae* (Joel D.M., Gressel J., Musselman L.J., Eds.). Springer: Berlin/Heidelberg, Germany, pp. 415–432.

Evidente A., Cimmino A., Fernández-Aparicio M., Andolfi A., Rubiales D., Motta A., 2010. Polyphenols, including the new peapolyphenols A–C, from pea root exudates stimulate *Orobanche foetida* seed germination. *Journal of Agricultural and Food Chemistry* 58: 2902–2907.

Evidente A., Cimmino A., Fernández-Aparicio M., Rubiales D., Andolfi A., Melck D., 2011. Soyasapogenol B and trans-22-dehydrocampesterol from common vetch (*Vicia sativa* L.) root exudates stimulate broomrape seed germination. *Pest Management Science* 67: 1015–1022.

Evidente A., Fernández-Aparicio M., Cimmino A., Rubiales D., Andolfi A., Motta A., 2009. Peagol and peagoldione, two new strigolactone like metabolites isolated from pea root exudates. *Tetrahedron Letters* 50: 6955–6958.

Fernández-Aparicio M., Andolfi A., Evidente A., Pérez-de-Luque A., Rubiales D., 2008. Fenugreek root exudates show species-specific stimulation of *Orobanche* seed germination. *Weed Research* 48: 163–168.

Fernández-Aparicio M., Cimmino A., Evidente A., Rubiales D., 2013. Inhibition of *Orobanche crenata* seed germination and radicle growth by allelochemicals identified in cereals. *Journal of Agricultural and Food Chemistry* 61: 9797–9803.

Fernández-Aparicio M., Delavault P., Timko M., 2020. Management of infection by parasitic weeds: A review. *Plants* 9: 1184.

Fernández-Aparicio M., Flores, F., Rubiales, D., 2009. Recognition of root exudates by seeds of broomrape (*Orobanche* and *Phelipanche*) species. *Ann. Bot.* 103: 423–431.

Fernández-Aparicio M., Kisugi T., Xie X., Rubiales D., Yoneyama K., 2014. Low strigolactone root exudation: A novel mechanism of broomrape (*Orobanche* and *Phelipanche* spp.) resistance available for faba bean breeding. *Journal of Agricultural and Food Chemistry* 62: 7063–7071.

Fernández-Aparicio M., Yoneyama K., Rubiales D., 2011. The role of strigolactones in host specificity of *Orobanche* and *Phelipanche* seed germination. *Seed Science Research* 21: 55–61.

Fernández-Aparicio, M., Flores F., Rubiales D., 2016. The effect of *Orobanche crenata* infection severity in faba bean, field pea and grass pea productivity. *Frontiers in Plant Science* 7: 1049.

Fiorito S., Epifano F., Palmisano R., Genovese S., Taddeo V.A., 2017. A re-investigation of the phytochemical composition of the edible herb *Amaranthus retroflexus* L. *Journal of pharmaceutical and biomedical analysis* 143: 183–187.

Gibot-Leclerc S., Abdennebi-Abdemessed N., Reibel C., Colbach N., 2013. Non-host facilitators, a new category that unexpectedly favours parasitic weeds. *Agronomy for Sustainable Development* 33: 787–793.

Halouzka R., Zeljkovic S.C., Klejdus B., Tarkowski P., 2020. Analytical methods in strigolactone research. *Plant Methods* 16: 76.

Heap I. *The International Survey of Herbicide Resistant Weeds*. www. weedscience.com. Accessed: March 21, 2021.

Huet S., Pouvreau J.-B., Delage E., Delgrange S., Marais C., … Poulin L., 2020. Populations of the parasitic plant *Phelipanche ramosa* influence their seed microbiota. *Frontiers in Plant Science* 11: 1075.

Hussein S.R., Marzouk M.M., Kassem M.E., Abdel Latif R.R., Mohammed R.S., 2017. Chemosystematic significance of flavonoids isolated from *Diplotaxis acris* (Brassicaceae) and related taxa. *Natural Product Research* 31: 347–350.

Ibn H., Tyrwhitt T., 1781. Orpheus Peri Lithôn de Lapidibus, Poema Orpheo a Quibusdam Adscriptum. Payne, White, and Elmsly, London.

International Allelopathy Society (IAS) Constitution and Bylaws 1996. [Online].

Joel D.M., 2013. Functional structure of the mature haustorium. In *Parasitic Orobanchaceae*; (D.M. Joel, J. Gressel, L.J. Musselman ed.) Springer, Berlin/Heidelberg, Germany, 25–60.

Kong L.D., Abliz Z., Zhou C.X., Li L.J., Cheng C.H.K., Tan R.X., 2001. Glycosides and xanthine oxidase inhibitors from *Conyza bonariensis*. *Phytochemistry* 58: 645–651.

Lechat M.M., Pouvreau J.B., Péron,T., Gauthier M., Montiel G., … Delavault P. 2012. PrCYP707A1, an ABA catabolic gene, is a key component of *Phelipanche ramosa* seed germination in response to the strigolactone analogue GR24. *Journal of Experimental Botany* 63: 5311–5322.

Matusova R., Rani K., Verstappen F.W.A., Franssen M.C.R., Beale M.H., Bouwmeester, H.J., 2005. The strigolactone germination stimulants of the plant-parasitic *Striga* and *Orobanche* spp. are derived from the carotenoid pathway. *Plant Physiologist* 139: 920–934.

Miranda C.A.S.F., Carvalho M.L.M., Gomes M.S., Santiago J.A., Santiago W.D.; Teixeira M.L., 2015. Evaluation of the chemical composition and allelopathic potential of essential oils from three species of *Asteraceae* against seed germination and seedling vigor of lettuce *Journal of Advanced Pharmaceutical Technology & Research* 11: 3669-3677.

Parker C., 2009. Observations on the current status of *Orobanche* and *Striga* problems worldwide. *Pest Management Science* 65: 453–459.

Parker C., 2013. The parasitic weeds of the Orobanchaceae. In *Parasitic Orobanchaceae*. Joel D.M., Gressel J., Musselman L.J., Eds.; Springer: Berlin/Heidelberg, Germany; pp. 313–344.

Pimentel D., Zuniga R., Morrison D. 2005. Update on the environmental and economic costs associated with alien-invasive species in the United States. *Ecological Economics* 52: 273–288.

Riopel J.L., Timko M.P., 1995. Haustorial initiation and differentiation. In: *Parasitic Plants*. (M.C. Press, J.D. Graves, ed.) Chapman & Hall, London, UK, 39–79.

Salah N.B., Casabianca H., Jannet H.B., Chenavas S., Sanglar C., Fildier A., Bouzouita N., 2015. Phytochemical and biological investigation of two *Diplotaxis* species growing in Tunisia: *D. virgata* & *D. erucoides*. *Molecules* 20: 18128–18143.

Salehi B., Krochmal-Marczak B., Skiba D., Patra J.K., Das S.K., Das G., Martorell M., 2020. *Convolvulus* plant-A comprehensive review from phytochemical composition to pharmacy. *Phytotherapy Research* 34: 315–328.

Scavo, A., Mauromicale, G., 2020. Integrated Weed Management in Herbaceous Field Crops. *Agronomy* 10(4): 466. https://doi.org/10.3390/agronomy10040466

Vurro M., Boari A., Evidente A., Andolfi A., Zermane N., 2009. Natural metabolites for parasitic weed management. *Pest Management Science* 65: 566–571.

Wang H., Zhang L., Wang Y., 2017. Isolating and identifying organic acids from *Portulaca oleracea* and determining their anti-cyanobacterial activity. *Polish Journal of Environmental Studies* 26: 441–445.

Westwood J.H., Charudattan R., Duke S.O., Fennimore S.A., Marrone P., … Swanton C., Zollinger R., 2018. Weed Management in 2050: Perspectives on the Future of Weed Science. *Weed Science*, 10.1017/wsc.2017.78.

Westwood, J.H., Foy, C.L. 1999. Influence of nitrogen on germination and early development of broomrape (*Orobanche* spp.). *Weed Science* 47: 2–7.

Xie X., 2016. Structural diversity of strigolactones and their distribution in the plant kingdom. *Journal of Pesticide Science* 41: 175–180.

Xie X., Yoneyama K., Yoneyama K., 2010. The strigolactone story. *Annual Review of Phytopathology* 48: 93–117.

Yan J., Sun L.R., Zhou Z.Y., Chen Y.C., Zhang W.M., Dai H.F., Tan J.W., 2012. Homoisoflavonoids from the medicinal plant *Portulaca oleracea*. *Phytochemistry* 80: 37–41.

Yoneyama K., Xie X., Nomura T., Yoneyama K., 2016. Extraction and measurement of strigolactones in sorghum roots. *Bio-protocol* 6: e1763.

Zahoor A., Siddiqui I.N., Khan A., Ahmad V.U., Ahmed A., Hassan Z., Iqbal, S. 2010. Two new glycosides from *Conyza bonariensis*. *Natural Product Communications* 5: 1099–1102.

Zwanenburg B., Mwakaboko A.S., Kannan C., 2016. Suicidal germination for parasitic weed control. *Pest Management Science* 72: 2016–2025.

Phytopathologia Mediterranea
The international journal of the
Mediterranean Phytopathological Union

Firenze University Press
www.fupress.com/pm

Research Papers

Dissemination of esca-related pathogens in German vineyards: do arthropods play roles in vectoring spores?

Elisa Maria KALVELAGE[1,2,*], Ralf Thomas VOEGELE[2], Michael FISCHER[1]

[1] *Julius Kühn-Institute (JKI), Institute for Plant Protection in Fruit Crops and Viticulture, Siebeldingen, Germany*
[2] *Institute of Phytomedicine, University of Hohenheim, Stuttgart, Germany*
*Corresponding author. E-mail: elisa.kalvelage@julius-kuehn.de

Summary. Grapevine Trunk Diseases (GTDs) such as esca challenge viticulture. The main fungal agents of Petri disease or young esca, *Phaeomoniella chlamydospora* (*Pch*), diverse *Phaeoacremonium* species (*Pm* spp.) and *Cadophora luteo-olivacea* (*Clo*), are transmitted to pruning wounds of vines by rain splashes and air currents. Arthropod-mediated dispersal is another possibility for the pathogens to reach pruning wounds. The present study was the first to evaluate possible involvement of arthropods in the dissemination process of esca-related pathogens in German vineyards. Diversity of arthropods on grapevine trunks was determined in 2019 and 2020, using cardboard traps mounted on vine trunks. Captured arthropods were surveyed for the presence of esca-related pathogens on their exoskeletons by using a nested multiplex PCR. In total, 2099 arthropods were examined, of which 35% were positive for *Phaeomoniella chlamydospora* (*Pch*), 21% for *Phaeoacremonium* spp. (*Pm*), and 7% for *Cadophora luteo-olivacea* (*Clo*). Earwigs and spiders were the most prevalent trapped arthropods; *Pch* was detected on 27% of earwigs and 38% of spiders, *Pm* spp. on 17 and 19%, and *Clo* on 3 and 8% of these arthropods. In both years, arthropods carrying the pathogens were already present in April, and therefore within the presumed susceptibility phase of pruned vines. These results indicate involvement of arthropods in the dispersal of esca-related pathogens in German vineyards. Further research, particularly to determine the infection potential of insect-borne fungi, is needed to confirm transmission risk. These results underline the importance of protecting vine pruning wounds to prevent host invasion by GTD pathogens.

Keywords. Grapevine trunk diseases, *Phaeomoniella chlamydospora*, *Phaeoacremonium* spp., *Cadophora luteo-olivacea*, dispersal, pruning wounds.

OPEN ACCESS

Citation: E.M. Kalvelage, R.T. Voegele, M. Fischer (2021) Dissemination of esca-related pathogens in German vineyards: do arthropods play roles in vectoring spores?. *Phytopathologia Mediterranea* 60(3): 467-478. doi: 10.36253/phyto-12948

Accepted: October 10, 2021

Published: December 30, 2021

Data Availability Statement: All relevant data are within the paper and its Supporting Information files.

Competing Interests: The Author(s) declare(s) no conflict of interest.

Editor: Jose R. Urbez Torres, Agriculture and Agri-Food Canada.

INTRODUCTION

Grapevine health is severely affected by Grapevine Trunk Diseases (GTDs). According to symptomatology of leaves, berries and wood, and in relation to a variety of wood-inhabiting fungi, GTDs can be subdivided into different diseases or syndromes (Mugnai *et al.,* 1999; Bertsch *et al.,* 2013; Fontaine *et al.,* 2016; Mondello *et al.,* 2018). All of these cause general deteri-

oration of vine vascular systems eventually reducing the production and longevity of vineyards (Vasquez *et al.,* 2007; Hofstetter *et al.,* 2012; Lecomte *et al.,* 2012).

Esca is one of the most important GTDs, and is a disease complex related to distinct symptoms, pathogens and vine age. This includes the so-called grapevine leaf stripe disease (GLSD, previously known as "young esca"), characterized by "tiger-stripes" on host leaves, which is the most important and widespread GTD (Mugnai *et al.,* 1999; Surico, 2009; Mondello *et al.,* 2018). Others include brown wood streaking, Petri disease (black goo or slow dieback), "vine apoplexy" or "acute esca", and "esca proper" (including white rot, caused by *Fomitiporia mediterranea*; Fischer, 2002). Co-existence of GLSD and "esca proper" is a widespread phenomenon in old vineyards. To complicate matters, all of these diseases may overlap, and also occur with other canker agents such as *Botryosphaeriaceae* and/or *Diatrypaceae* (Rolshausen *et al.,* 2010; Gramaje *et al.,* 2018; Moyo *et al.,* 2018). In addition, these diseases are often cryptic and symptoms may take several years to develop (Surico *et al.,* 2000; Surico *et al.,* 2006; Christen *et al.,* 2007).

Crucial for all early stages of esca are trachaeomycotic fungi, including *Phaeomoniella chlamydospora* (*Pch*) (Crous and Gams, 2000), *Phaeoacremonium* spp. (*Pm* spp.) (Mostert *et al.,* 2006) and, possibly, *Cadophora* spp. (Halleen *et al.*, 2007; Gramaje *et al.,* 2011; Travadon *et al.*, 2014). In German vineyards, besides the frequently occurring *Pch*, diverse *Pm* spp. such as *Pm. fraxinopennsylvanicum*, *Pm. viticola* and, above all, *Pm. minimum* have been isolated from symptomatic grapevines (Fischer and Kassemeyer, 2003; Fischer *et al.,* 2016; Kraus *et al.,* 2019). Among *Cadophora*, *C. luteo-olivacea* (*Clo*) was the most frequent species (Fischer *et al.,* 2016; Haag, 2018; Fischer, 2019; Kraus *et al.,* 2019).

For all vine-growing regions, pruning wounds are considered as major entry points for esca-related pathogens (Larignon and Dubos, 1997; Mugnai *et al.*, 1999; Larignon and Dubos, 2000; van Niekerk *et al.,* 2011). Susceptibility of pruning wounds in California to *Pch* and *Pm. minimum* was found to last for up to 4 months (Eskalen *et al.,* 2007), and in Spain susceptibility to *Pch* was found to last for up to 12 weeks (Elena and Luque, 2016). Sucker wounds caused by vineyard management may also be entry points for the pathogens (Makatini, 2014).

Concerning the inoculum sources, *Pch* was observed abundantly sporulating in cracks of vine bark (Edwards *et al.,* 2001), and fruit bodies of *Togninia minima*, the teleomorph of *Pm. minimum* (Mostert *et al.,* 2003), were found in wood crevices of diseased vine trunks (Rooney-Latham *et al.*, 2005b; Baloyi *et al.,* 2013). Dispersal of all these fungi is by airborne spores in rain splashes or carried by wind (Larignon and Dubos, 2000; Eskalen and Gubler, 2001), and this is also likely for *Clo* (Gramaje *et al.,* 2011). In German vineyards, the presence of airborne *Pch* inoculum has been repeatedly verified by isolation or molecular detection from spore traps (Haag, 2018; Kraus *et al.,* 2020; Molnar *et al.,* 2020).

Arthropods including spiders, ants, and millipedes have been demonstrated as vectors for *Pch, Pm* spp. and other GTD-related pathogens in South Africa (Moyo *et al.,* 2014). The possible significance of arthropods in the transmission of several plant diseases has long been accepted (Leach, 1940). One prominent example for arthropod-mediated dispersal is the association of bark beetles and *Ophiostoma novo-ulmi*, the cause of the Dutch elm disease (Brasier, 1991).

No previous studies have surveyed the possible involvement of arthropods in the dispersal of esca-related pathogens in German vineyards. With a focus on the relationship between pruning measures and epidemiology of esca-related pathogens, the aims of the present study were to determine: i) the occurrence and diversity of arthropods on vine trunks in Germany; and, specifically, ii) the occurrence and identification of *Pch, Pm* spp. and *Clo* on arthropod exoskeletons.

Results from this study provide new information about the epidemiology of esca-related pathogens and may eventually contribute to enhancing measures to reduce the spread of esca, mostly so with regard to an efficient protection of pruning wounds.

MATERIALS AND METHODS

Sampling sites

Arthropod diversity was assessed in 2019 and 2020 in experimental vineyards located at the Julius Kühn-Institute in Siebeldingen, Germany. Two vineyards of different ages, cultivars and management practices were chosen. Vineyard "A" (49°13'00.2"N; 8°02'53.1"E) was planted in 1996, and vineyard "B" (49°13'08.8"N; 8°02'39.6"E) was planted in 2002. Vineyard "A" contained the fungus-resistant (PIWI-) cultivar *Vitis vinifera* cv. 'Phoenix' and was chosen because of the high incidence of GLSD-symptoms and apoplexy observed in previous years (Molnar *et al.,* 2020). Vineyard "B" comprised four different cultivars (PIWI-cultivars 'Calandro' and 'Regent' and the traditional cultivars 'Pinot Noir' and 'Riesling'), and GLSD-symptoms had been observed only rarely on these vines in previous years. Plant protection measures were integrated in vineyard "A" and organic in "B".

Monitoring of arthropods on vine pruning wounds and trunks

A preliminary survey was conducted in April 2019 to monitor arthropods visiting pruning wounds. One camera (Raspberry Pi 3 Model B V1.2, Raspberry Pi Foundation) was installed next to each pruning wound (pruning had been performed in February) on trunks of four different vines in vineyard "A" (Figure 1A). Images were captured every 5 sec for 24 h, and these were subsequently assessed for visiting arthropods. Visual surveys of vines were also carried out at 2 week intervals during the collection of arthropods from cardboard traps.

Assessment of arthropod diversity on vine trunks using cardboard traps

Traps were made from strips of corrugated cardboard (approx. 25 × 60 cm), and these were each wrapped twice around the trunk of each monitored vine (Moyo *et al.,* 2014; Figure 1B). Twelve traps were placed randomly on trunks in vineyards "A" and "B", with three traps used for each of the four cultivars in vineyard "B". During wintertime (November to March), no arthropods were visible in preliminary inspections, so the traps were mounted by early April when temperatures were moderate and arthropods were first observed. Trapping was then continued until the end of October in 2019, and also to the end of November in 2020. Every second week, traps were each emptied into a large plastic box and arthropods were individually transferred with sterile forceps into sterile 2 mL capacity reaction tubes. Due to the high number of European earwigs (*Forficula auricularia* L.), five individuals were pooled into a small glass container and were considered as one sample. A maximum of five such samples was taken per trap. Springtails (collembolans) from the same trap were also pooled into 2 mL capacity reaction tubes using a vacuum cup. Arthropods were morphologically identified using an identification guide for German fauna (Schaefer, 2017) and spiders were identified using a field guide for spiders (Roberts, 1995).

Figure 1. Camera focused on pruning wounds (A), and cardboard trap mounted around a grapevine trunk (B), used to monitor insects on grapevines.

Washing of arthropod exoskeletons and DNA extractions

For detection of esca-related pathogens on arthropod exoskeletons, the protocol of Moyo *et al.* (2014) was followed, with modifications. Arthropods transferred into reaction tubes were freeze-killed at -20°C for 1–2 h. 1.5 ml of sterile distilled water was then added to each tube, and the tubes were vortexed for 60 sec. Washing suspensions containing possible fungal material were transferred into sterile 1.5 mL capacity reaction tubes, and arthropods were stored in 80% ethanol for later identification.

DNA extractions from the washing suspensions were carried out using the protocol of Tillet and Neilan (2000), with modifications. Tubes with washing suspensions were centrifuged at 15,000 rpm for 10 min and the supernatant was discarded. Two 3-mm steel beads, 750 µL XS-buffer and 50 µL cold TE-buffer were then added to the tubes. Samples were then placed in a tissue-lyser (Tissue Lyser 2; Qiagen) for 3 min at 30,000 Hz, and were then incubated for 1 h at 70°C in a thermomixer (ThermoMixer comfort; Eppendorf AG) at 350 rpm. Samples were vortexed for 10 sec and then put on ice for 30 min prior to centrifugation at 14,000 rpm for 10 min. Supernatant (700 µL) from each sample was then transferred into a new 1.5 mL capacity reaction tube and 700 µL of ice cold 80% isopropanol was added. For DNA precipitation, samples were incubated at room temperature for 15 min prior to centrifugation at 10,000 rpm for 10 min. The supernatant from each sample was discarded and the DNA pellet was then washed with 250 µL of ice cold ethanol. After another centrifugation step at 10,000 rpm for 10 min, the ethanol was discarded and the DNA pellet was air dried. The DNA was then resuspended in 30 µL of TE-buffer and left overnight at 4°C.

Detection of esca-related pathogens using nested multiplex PCR

DNA extracted from washing suspensions was subjected to a nested PCR. In primary PCR reactions,

primers ITS5 and ITS4 (White *et al.,* 1990) were used to amplify fungus-specific DNA. In secondary PCRs, *Pch*-specific primers Pch1H: 5'-CCC GAT CTC CAA CCC TTT GTT T-3' and Pch2H: 5'-CGG GCC TAT CTT CTA TGA AAG-3' (Haag, 2018), *Pm* spp.-specific primers Pm5H: 5'-GGA GGG CAC AGA CTC TGT ATT-3' and Pm3H: 5'-GTA AAC TAC TGC GCT CGG AG-3' (Haag, 2018) and *Clo*-specific primers CLO1F: 5'-TAC TAG AGC AAA GGA CAG GCA GC-3' (Navarette *et al.,* 2011) and Clo3H: 5'-GAA CCC CAA TAC CAA GCG AGA G-3' (Haag, 2018) were used. All primers had final concentrations of 0.2 µM. PCR reactions were carried out in a SimpliAmp™ Thermal Cycler (Applied Biosystems). The primary reactions were each carried out with SuperHot Taq DNA Polymerase (Genaxxon BioScience GmbH) in a reaction volume of 25 µL, according to the user manual, and 1 µL of the extracted DNA was used as template. The conditions of the primary reactions were as follows (Haag, 2018): initial denaturation at 95°C for 10 min; 25 cycles 30 sec at 95°C, 30 sec at 57°C and 30 sec at 72°C; final extension for 10 min at 72°C. After the primary PCR, the reaction was diluted 1:50 with "BioScience-Grade" water (Roth) and 1 µL of the dilution was used for the secondary PCR reaction conducted with the KAPA2G Fast Multiplex PCR Kit (Kapa Biosystems). Each reaction was carried out in a total volume of 10 µL and was composed as advised in the user manual. Parameters were (Haag, 2018): initial denaturation at 95°C for 3 min; 10 cycles at 95°C for 15 sec, 30 sec at 69°C and 30 sec at 72°C; 25 cycles at 95°C for 15 sec, 30 sec at 60°C and 30 sec at 72°C; final extension at 72°C for 3 min. PCR products were loaded on a 2% agarose gel and run at 6 V/5 cm for 1.5 h. PCR products were visualized under ultraviolet (UV) light using a QUANTUM ST5 gel documentation system (Vilber Lourmat). A 100 bp ladder (New England Biolabs) marked the molecular size of the PCR-products, which were 433 bp for *Clo*, 381 bp for *Pch* and approx. 330 bp for *Pm* spp.

RESULTS

Monitoring of arthropods on vine pruning wounds and trunks

Monitoring in April 2019 only rarely detected arthropods. In total, six arthropod orders were documented, including spiders, mites, bugs, ants, nocturnal centipedes and woodlice (Figure 2). Visual surveys of vine trunks frequently revealed ants (*Temnothorax; Formicidae: Myrmicinae*, or *Lasius niger* L., *Formicidae*: *Formicinae*) moving up and down the trunks during sunny weather, as well as red velvet mites (*Allothrombium fuliginosum* Hermann, *Acari*: *Trombidiidae*). Spider webs were often observed inside vine crevices, and from the end of May onwards, earwigs were sometimes observed within cracks in the bark.

Arthropod diversity on vine trunks assessed with cardboard traps

In 2019 and 2020, and from all sampling sites, a total of 2099 arthropods, assigned to 22 families, were collected from the cardboard traps. Significant families and the abundance of associated taxa are outlined in Table 1. Of all samples, approx. 30% (640) were earwigs (*Dermaptera*: *Forficulidae*) and 27% (568) were spiders (*Aranea*). Only one earwig species, the European earwig *Forficula auricularia* (L.) (Figure 3A), was found in the traps, and was the prevalent arthropod in vineyard "A". In many cases, more than 40 individuals were found in each cardboard trap. In contrast, spiders were the dominant arthropod order in vineyard "B". As the most

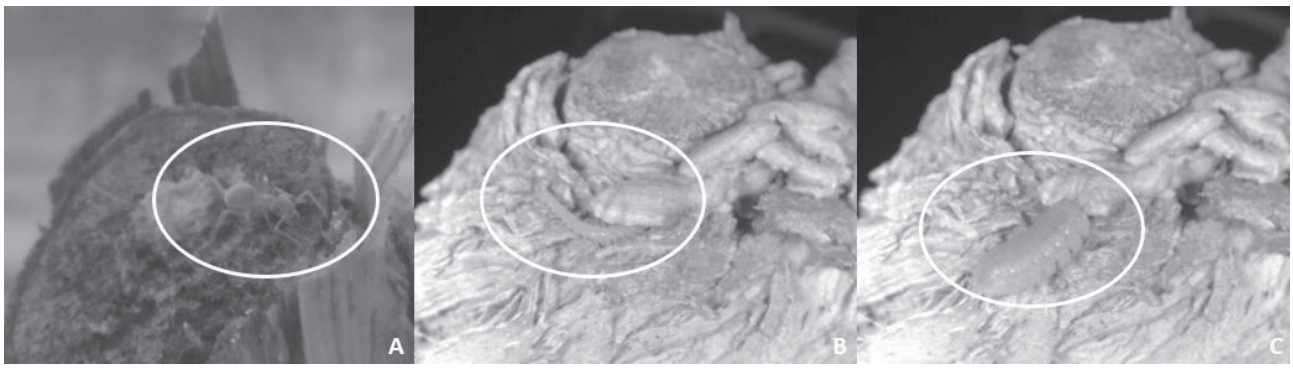

Figure 2. Images of arthropods visiting vine pruning wounds: A, an ant (*Formicidae*: *Formicinae*); B, a centipede (*Chilopoda*: *Lithobiidae*); C, a woodlouse (*Isopoda*: *Armadillidiidae*).

diverse order, trapped spiders were of nine families, with 58% being *Salticidae* (jumping spiders), 10% *Gnaphosidae* (ground spiders), 9% *Linyphiidae* (sheet weavers) and 9% being *Thomisidae* (crab spiders). In total, 329 jumping spiders were trapped, of which 57% were *Marpissa muscosa* (Clerck) (Figure 3B), and 43% were *Synageles venator* (Lucas) (Figure 3C). In vineyard "B", *Raglius alboacuminatus* (Goeze) (*Heteroptera*: *Rhyparochromidae*) (Figure 3D), a dirt-coloured seed bug, was frequently found (165). Only 23 individuals of this species were detected in vineyard "A", giving a total number of 188 (9%) of this species from both vineyards and years. Thus, bugs, mainly *R. alboacuminatus*, were the third most common arthropod order. Woodlice were found irregularly in the traps, with a total number of 107. Cockroaches, ants, springtails, harvestmen, centipedes, mites, millipedes and beetles were all collected in total numbers <100 (for species numbers see Table 1).

Arthropods testing positive for esca-related pathogens

Thirty-five percent of the 2099 arthropod samples tested positive for *Pch*, 21% for *Pm* spp. and 7% for *Clo* (Table 1). For the predominant arthropod, the European earwig (640 samples), 27% carried *Pch*, 17% carried *Pm*. spp. and 3% carried *Clo* on their exoskeletons. However, due to the pooling method applied for this species, these are maximum numbers, because pathogen-free individuals may have occurred side-by-side with positive individuals in a sample. For spiders, as the second most common arthropod order (568 samples), 38% were positive for *Pch*, 19% for *Pm* spp., and 8% were positive for *Clo*. *Pch* was detected most frequently on mites (59%) and centipedes (57%), *Pm* spp. most frequently on millipedes (43%) and centipedes (40%), and *Clo* most frequently on woodlice (31%).

The rates of *Pch*-positive arthropods were very similar for vineyards "A" and "B", at, respectively, 36% and 35%. Above average in vineyard "A" were bugs, woodlice and mites (respectively, 56%, 51% and 67%). In vineyard "B", 42% of ants tested positive for *Pch*. The rate of arthropods carrying *Pm* spp. was greater in vineyard "A" (25%) than in "B" (16%). In vineyard "A", greatest rates for *Pm* spp. were found from spiders (30%), bugs (37%), cockroaches (41%), mites (42%) or beetles (30%), while this was greatest for woodlice (36%) in vineyard "B". The proportions of *Clo*-positive arthropods was very similar in both vineyards, at 6% in vineyard "A" and 7% in vineyard "B". Very high numbers of woodlice (48%) and harvestmen (23%) were found in vineyard "B".

Some arthropods tested positive for more than one esca-related pathogen (Table 2). Of 2099 surveyed arthropods, 12% carried both *Pch* and *Pm* spp., 1% carried *Pch* and *Clo*, 1% carried *Clo* and *Pm* spp., and 2% carried all three pathogens. Nine percent of earwigs, 10% of spiders and 11% of bugs tested positive for both *Pch* and *Pm* spp. For arthropods collected in smaller numbers, the greatest rates of detection for the combination *Pch* and *Pm* spp. were from centipedes (36%), mites (30%) and millipedes (20%).

Figure 3. Most commonly found arthropods in cardboard-traps mounted to grapevine trunks in two vineyards: A, *Forficula auricularia* L. (*Dermaptera*: *Forficulidae*); B, *Marpissa muscosa* Clerck (*Aranea*: *Salticidae*); C, *Synageles venator* Lucas (*Aranea*: *Salticidae*); and D, *Raglius alboacuminatus* Goeze (*Heteroptera*: *Rhyparochromidae*).

Occurrence of positive arthropods during the period of putative pruning wound susceptibility

Figure 4 presents an overview of arthropods that carried at least one of the esca-related pathogens during the sampling periods of April through June in 2019 and 2020. In both years, first occurrence of arthropods was noted at the beginning of April, with increasing numbers over the following months. In April, cumulated over both years and vineyards, spiders were the predominant arthropod order and 35% (30 of 85) tested positive for esca-related pathogens. Ants, as the second most common arthropods, were positive in 41% (12 out of 29) of their captures. The numbers of samples of all other arthropods was <20. In May, spiders were still the most common arthropod order and 52% (35 out of 67) of the captures tested positive for esca pathogens. The first earwigs were found in the same month and 37% (22 of 59) carried esca-related pathogens. Ants and cockroackes had pathogen-positive proportions of 52% (14 of 27) in May. By June, earwigs had replaced spiders as the pre-

Table 1. Overview of arthropods testing positive for the esca-related pathogens *Phaeomoniella chlamydospora* (*Pch*), *Phaeoacremonium* spp. (*Pm* spp.) and *Cadophora luteo-olivacea* (*Clo*). Species identity only given for most frequently detected arthropods in vineyards "A" and "B".

Order (common names)	Vineyard Family/Genus/Species	Vineyard "A"				Vineyard "B"				Total (vineyards "A" and "B")			
		Sum of arthropods	Esca-related pathogens			Sum of arthropods	Esca-related pathogens			Sum of arthropods	Esca-related pathogens		
			Pch	*Pm* spp.	*Clo*		*Pch*	*Pm* spp.	*Clo*		*Pch*	*Pm* spp.	*Clo*
Total	**Various taxa**	**1002**	358 (36)	253 (25)	59 (6)	**1097**	384 (35)	178 (16)	89 (8)	**2099**	742 (35)	431 (21)	148 (7)
Dermaptera (earwigs)	***Forficulidae***												
	Forficula auricularia (L.)	**440**	124 (28)	82 (19)	14 (3)	**200**	47 (24)	27 (14)	6 (3)	**640**	171 (27)	109 (17)	20 (3)
Aranea (spiders)	**Total**	**176**	67 (38)	53 (30)	17 (10)	**392**	149 (38)	53 (14)	26 (7)	**568**	216 (38)	106 (19)	43 (8)
	Salticidae	**63**	22 (35)	24 (38)	8 (13)	**266**	101 (38)	35 (13)	11 (4)	**329**	123 (37)	59 (18)	19 (6)
	Marpissa muscosa (Clerck)	**57**	18 (32)	21 (37)	7 (12)	**129**	51 (40)	20 (16)	9 (7)	**186**	69 (37)	41 (22)	16 (9)
	Synageles venator (Lucas)	**6**	4 (67)	3 (50)	1 (17)	**137**	50 (37)	14 (10)	2 (2)	**143**	54 (38)	17 (12)	3 (2)
Heteroptera (bugs)	**Total**	**27**	15 (56)	10 (37)	1 (4)	**183**	56 (31)	23 (13)	4 (2)	**210**	71 (34)	33 (16)	5 (2)
	Rhyparochromidae												
	Raglius alboacuminatus (Goeze)	**23**	13 (57)	8 (35)	0 (0)	**165**	54 (33)	22 (13)	3 (2)	**188**	67 (36)	30 (16)	3 (2)
Isopoda (woodlice)	Armadillidiidae												
	Armadillidium spp.	**49**	25 (51)	14 (29)	5 (10)	**58**	21 (36)	21 (36)	28 (48)	**107**	46 (43)	35 (33)	33 (31)
Blattoptera (cockroaches)	***Ectobiinae***												
	Ectobius spp.	**46**	17 (37)	19 (41)	6 (13)	**42**	19 (45)	10 (24)	4 (10)	**88**	36 (41)	29 (33)	10 (11)
Formicidae (ants)	**Total**	**43**	14 (33)	5 (12)	1 (2)	**43**	18 (42)	4 (9)	2 (5)	**86**	32 (37)	9 (11)	3 (4)
	Formicinae												
	Lasius niger (L.)	**6**	4 (67)	1 (17)	0 (0)	**39**	15 (38)	3 (8)	2 (5)	**45**	19 (42)	4 (9)	2 (4)
	Myrmicinae												
	Temnothorax spp.	**37**	10 (27)	4 (11)	1 (3)	**4**	3 (75)	1 (25)	0 (0)	**41**	13 (32)	5 (12)	1 (2)
Collembola (springtails)	Isotomidae	**42**	18 (43)	12 (29)	5 (12)	**37**	15 (41)	3 (8)	5 (14)	**79**	33 (42)	15 (19)	10 (13)
Opiliones (harvestmen)	Phalangiidae	**34**	13 (38)	6 (18)	1 (3)	**35**	13 (37)	8 (23)	8 (23)	**69**	26 (38)	14 (20)	9 (13)
Chilopoda (centipedes)	**Total**	**13**	6 (46)	5 (39)	0 (0)	**42**	25 (60)	17 (41)	2 (5)	**55**	31 (56)	22 (40)	2 (3)
	Linotaeniidae	**5**	2 (40)	1 (20)	0 (0)	**1**	0 (0)	0 (0)	0 (0)	**6**	2 (33)	1 (17)	0 (0)
	Lithobiidae												
	Lithobius forficatus (L.)	**8**	4 (50)	4 (50)	0 (0)	**41**	25 (61)	17 (41)	2 (5)	**49**	29 (59)	21 (43)	2 (4)
Diplopoda (millipedes)	***Polyxenidae***												
	Polyxenus lagurus (L.)	**42**	19 (45)	18 (43)	4 (10)	**2**	0 (0)	1 (50)	1 (50)	**44**	19 (43)	19 (43)	5 (11)
Acari (mites)	***Trombidiidae***												
	Allothrombium fuliginosum (Hermann)	**24**	16 (67)	10 (42)	0 (0)	**20**	10 (50)	5 (25)	1 (5)	**44**	26 (59)	15 (34)	1 (2)
Coleoptera (beetles)	various families	**20**	7 (35)	6 (30)	0 (0)	**17**	6 (35)	3 (18)	0 (0)	**37**	13 (35)	9 (24)	0 (0)
Unidentified	various taxa	**46**	17 (37)	13 (28)	5 (11)	**26**	5 (19)	3 (12)	2 (8)	**72**	22 (31)	16 (22)	7 (10)

Total numbers of recovered arthropods in **bold** and numbers of arthropods tested positive (%).

Table 2. Overview of arthropods testing positive for more than one of the esca-related pathogens *Phaeomoniella chlamydospora* (*Pch*), *Phaeoacremonium* spp. (*Pm* spp.) and *Cadophora luteo-olivacea* (*Clo*). Species identity only given for most frequent and representative arthropods.

Order (common names)	Family/Genus/Species	Esca-related pathogens (combinations)				
		Sum of arthropods	*Pch* + *Pm* spp.	*Pch* + *Clo*	*Clo* + *Pm* spp.	*Pch* + *Pm* spp. + *Clo*
Total	Various taxa	**2099**	248 (12)	28 (1)	18 (1)	46 (2)
Dermaptera (earwigs)	***Forficulidae***					
	Forficula auricularia (L.)	**640**	58 (9)	6 (1)	2 (0)	6 (1)
Aranea (spiders)	**Total**	**568**	57 (10)	11 (2)	7 (1)	8 (1)
	Salticidae	**329**	31 (9)	5 (2)	4 (1)	4 (1)
	Marpissa muscosa (Clerck)	**186**	22 (12)	4 (2)	2 (1)	4 (2)
	Synageles venator (Lucas)	**143**	8 (6)	1 (1)	2 (1)	0 (0)
Heteroptera (bugs)	**Total**	**210**	23 (11)	1 (0)	0 (0)	4 (2)
	Rhyparochromidae					
	Raglius alboacuminatus (Goeze)	**188**	22 (12)	0 (0)	0 (0)	3 (2)
Isopoda (woodlice)	**Armadillidiidae**					
	Armadillidium spp.	**107**	16 (15)	1 (1)	3 (3)	10 (9)
Blattoptera (cockroaches)	**Ectobiinae**					
	Ectobius spp.	**88**	17 (19)	1 (1)	1 (1)	2 (2)
Formicidae (ants)	**Total**	**86**	6 (7)	2 (2)	0 (0)	1 (1)
	Formicinae					
	Lasius niger (L.)	**45**	3 (7)	2 (4)	0 (0)	0 (0)
	Myrmicinae					
	Temnothorax spp.	**41**	3 (7)	0 (0)	0 (0)	1 (2)
Collembola (springtails)	***Isotomidae***	**79**	8 (10)	3 (4)	1 (1)	4 (5)
Opiliones (harvestmen)	***Phalangiidae***	**69**	9 (13)	0 (0)	1 (1)	3 (4)
Chilopoda (centipedes)	**Total**	**55**	20 (36)	0 (0)	0 (0)	2 (3)
	Linotaeniidae	**6**	1 (17)	0 (0)	0 (0)	0 (0)
	Lithobiidae	**49**	17 (35)	0 (0)	0 (0)	2 (4)
Diplopoda (millipedes)	**Polyxenidae**					
	Polyxenus lagurus (L.)	**44**	9 (20)	0 (0)	1 (2)	4 (9)
Acari (mites)	***Trombidiidae***					
	Allothrombium fuliginosum (Hermann)	**44**	13 (30)	1 (2)	0 (0)	0 (0)
Coleoptera (beetles)	Various families	**37**	5 (14)	0 (0)	0 (0)	0 (0)
Unidentified	Various taxa	**72**	7 (10)	2 (3)	2 (3)	2 (3)

Total numbers of recovered arthropods in **bold** and numbers of arthropods tested positive (%).

dominant group. They tested positive in 29% (39 of 134) of the cases, while 47% (24 of 51) of spiders carried esca pathogens. Of the cockraches, 77% (23 of 30) were pathogen-positive. The rate of positive ants had decreased to 29% (eight of 28).

DISCUSSION

Moyo *et al.* (2014) in South Africa were the first and, to date, the only authors to demonstrate possible involvement of arthropods in the dissemination of GTD-, more precisely, esca-related pathogens. Arthropod mediated dispersal of these pathogens was previously suggested when *T. minima* (teleomorph of *Pm. minimum*) was detected on mites and termites found on symptomatic grapevines (Eskalen *et al.*, unpublished, in Rooney-Latham *et al.,* 2005a), and when *Pm. rubrigenum* was isolated from bark beetles in Czechia (Kubátová *et al.,* 2004). Accumulation of collembolans and mites in grapevine cracks around sporulating mycelium of *Pch* was repeatedly observed by Edwards *et al.* (2001). As esca-related pathogens were frequently documented on arthropod exoskeletons in the present study of Ger-

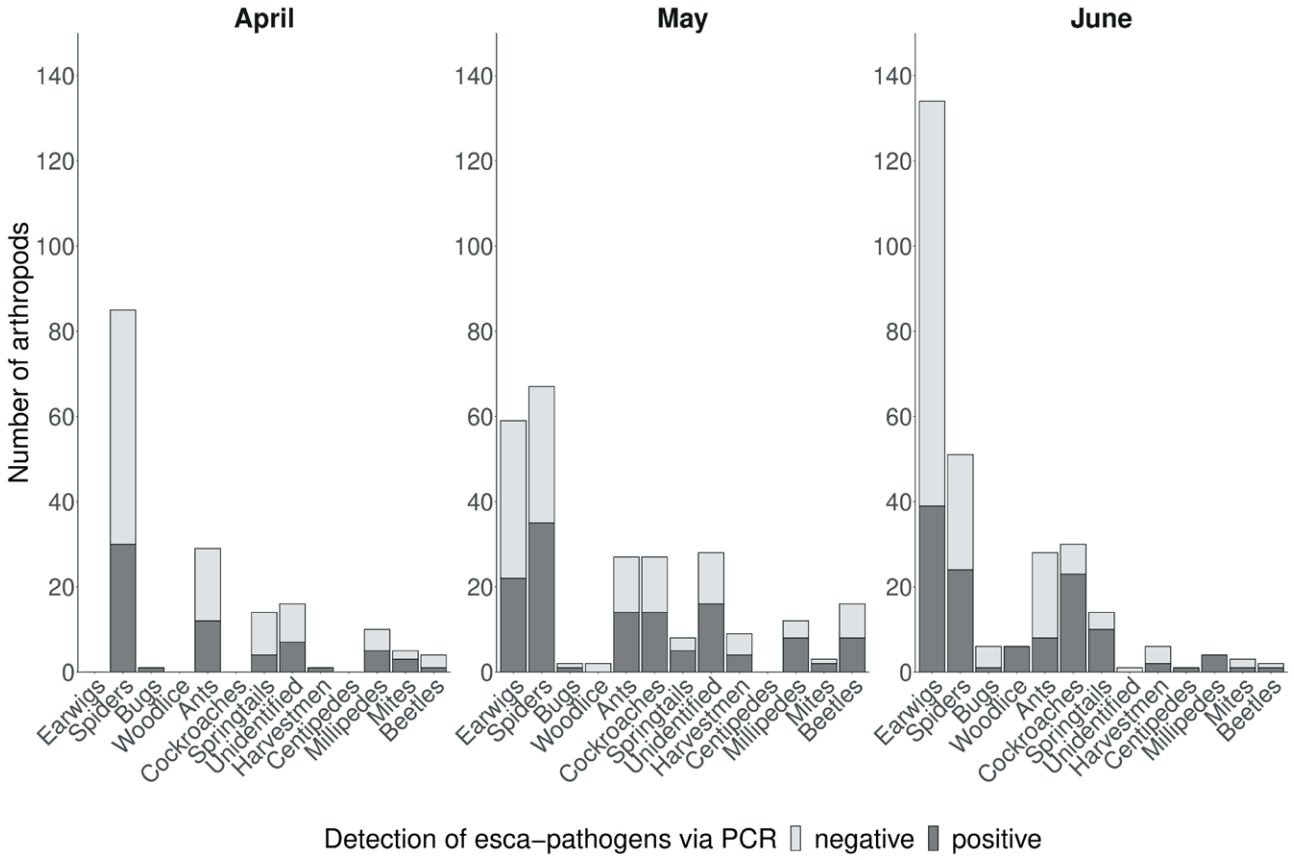

Figure 4. Arthropods testing negative or positive for esca-related pathogens in April, May and June of 2019 and 2020. Arthropods were collected from two different vineyards at 2 week intervals using cardboard traps mounted to grapevine trunks.

man vineyards, this confirms broad geographical indication that arthropods may be vectors for GTD pathogens.

In contrast to the study of Moyo *et al.* (2014) in South Africa, the present study used cardboard traps applied only to grapevine trunks, with no traps directly mounted around pruning wounds, so only arthropods directly collected from trunks were surveyed. Nonetheless, it can be assumed that these arthropods were also active during foraging on pruning wounds. This was confirmed by the camera-mediated monitoring, which showed activity of arthropods on pruning wounds during the putative host susceptibility phase (Figure 2). Particular attraction of arthropods to these wounds, as demonstrated by Moyo *et al.* (2014), was not observed in the present study. While wound sap in German vineyards is usually evident each year for a few weeks from mid March, temperatures during the two survey periods at that time were too low for arthropods to become active.

Moyo *et al.* (2014) in South Africa examined 5,677 arthropods, and 13% of these tested positive for *Pch* and 18% for *Pm* spp. In contrast, the present study of 2,099 arthropods showed greater pathogen-positive proportions of 35% for *Pch* and 21% for *Pm* spp. Possible reasons for this discrepancy could be ages of the studied vineyards, the cultivars, and the overall weather conditions.

A broad range of *Pm* spp. plays roles in GTDs (Mostert *et al.,* 2006; Gramaje *et al.,* 2015; Baloyi *et al.,* 2018). As several of these species, most commonly *Pm. minimum*, occur in German vineyards (Fischer and Kassemeyer, 2003; Fischer *et al.,* 2016; Kraus *et al.,* 2019), a genus-specific primer pair was used to verify their presence on arthropod exoskeletons. Following *Pch* on 35% of the arthropods, *Pm* spp. were detected in 21% of washing suspensions. These results confirm that structures of both *Pch* (Crous and Gams, 2000) and *Pm* spp. (Mostert *et al.,* 2003; Rooney-Latham *et al.,* 2005a; Mostert *et al.,* 2006) are suitable for the adhesion of conidia or mycelium fragments to arthropod exoskeletons. The present study is the first to investigate the roles of arthropods for dissemination of *Clo*. The low frequency of *Clo* on arthropod exoskeletons (7%) cannot be explained, but agrees with previous reports of low *Clo*

isolation rates from previous Germany-based studies (Fischer *et al.,* 2016; Kraus *et al.,* 2019).

In the sampled vineyards, the European earwig *F. auricularia,* was the predominant arthropod followed by different spider species. The increasing numbers of earwigs in German vineyards and beyond, and their putative status as beneficial insects is seen critically (Huth, 2011; Kehrli *et al*., 2012; Mohr, 2012). Our study reveals a possible involvement of earwigs in the dispersal of GTDs, as individuals were found to carry *Pch* (27% of earwigs assayed), *Pm* spp. (17%) and *Clo* (3%). As well, 9% of earwigs tested positive for both *Pch* and *Pm* spp. As the omnivorous earwigs can migrate over considerable distances during foraging, depending on food sources (Lamb, 1975), they are likely to incidentally disperse the pathogens over several vines, also by wandering across pruning wounds. However, the pathogenic relevance may still be low because earwigs were present each year in the surveyed vineyards only from the end of May onwards (see also Huth, 2011). This indicates that earwigs occurred outside the immediate pruning wound susceptibility phase. As the susceptibility of wounds declines with time (Eskalen *et al.,* 2007; Van Niekerk *et al.,* 2011; Elena and Luque, 2016), earwigs are likely to be relevant for late-pruned vines that are potentially susceptible to pathogens until May or June each year.

Besides pruning wounds, three other aspects relate to infection processes and/or disease epidemiology. i) Wounds, caused by vineyard management such as sucker removal, may also be entry points for earwig-mediated pathogen dispersal during the vegetative grapevine phase (Makatini, 2014). ii) Conidia and/or mycelium fragments adhering to the earwig exoskeletons may be spread within and between vines. iii) The faeces of omnivorous earwigs could also be inoculum sources, which is indicated by *Pch* spores maintaining germinability after gut passage of millipedes (Moyo *et al.,* 2014). Whether earwigs feed on esca-related pathogens in the field, and to which amount the resulting faeces may be inoculum sources, remain to be determined.

The majority of spiders found on vine trunks (58%) were *Salticidae* (jumping spiders) with two dominant species, *M. muscosa* and the myrmecomorphic *S. venator* which has been previously identified as a dominant salticid in vineyards (Havlová *et al.,* 2015). In total, 37% of jumping spiders tested positive for *Pch,* 18% were positive for *Pm* spp., and 6% were positive for *Clo,* and 9% of salticids carried both *Pch* and *Pm* spp. on their exoskeletons. Salticids are free-hunting spiders which are very active during warm and sunny weather, and most likely migrate between vines in search of prey (Stresemann, 1992; Roberts, 1995). The small size of the ant-like *S. venator* (3–4 mm) makes it likely that these spiders, during hunting, encounter fungal pathogens sporulating between cracks and crevices in vine bark (Edwards *et al.,* 2001; Baloyi *et al.,* 2013). In the experimental plots of the present study, spiders were already common in April each year, when late-pruned vines are most likely to still be susceptible to GTD pathogens. Salticids tested positive for esca-related pathogens in April (35%), May (52%) and June (47%), which indicates a possible risk for pathogen dissemination. Moreover, 10% of all spiders tested positive for both *Pch* and *Pm* spp.

All other arthropods, i.e. bugs, woodlice, centipedes, millipedes, cockroaches, ants, springtails, harvestmen, mites and beetles, were not as common as earwigs and spiders. Based on these results, these arthropods are likely to only be of low importance as GTD pathogen dispersal agents. However, woodlice frequently tested positive for all three pathogens, with 43% testing positive for *Pch*, 33% for *Pm* spp. and 31% for *Clo*., and 15% of woodlice were also co-positive for *Pch* and *Pm* spp. As woodlice were not commonly found (a total of 107 over the two seasons), their significance as pathogen vectors remains unclear. Also 36% of the centipedes and 20% of the millipedes carried both *Pch* and *Pm* spp. on their exoskeletons. As for woodlice, few centipedes (55 over the two seasons) and millipedes (44) were found in the traps, and these two arthropods were especially rare during the presumed pruning wound susceptibility phase.

Ants, indicated as important vectors of esca pathogens in South Africa (Moyo *et al.,* 2014), were infrequent during the sampling periods of the present study. However, they were more common during the presumed months of vine susceptibility, and 41% of these insects tested positive for the pathogens in April, 52% were positive in May and 29% were positive in June. Ants were repeatedly observed moving up and down the vines, and were also captured visiting pruning wounds by the cameras in April (Figure 2A). Total numbers were less than 30 per month, and, in contrast to the observations of Moyo *et al.* (2014) in South Africa, no particular attraction by these insects to wound sap was detected.

The present study results, during 2019 and 2020, revealed a possible relationship between many different arthropod orders and esca-related pathogens. The predominant earwigs and spiders, representing 57% of the arthropods caught in traps, may disseminate pathogens in German vineyards, while spiders were already numerous in the presumed host pruning wound susceptibility phase. Furthermore, 12% of all surveyed arthropods tested positive for both *Pch* and *Pm* spp., which indicated possible co-existence of the pathogens on individual vines or within the arthropod migration ranges. No par-

ticular attraction of arthropods to the pruning wounds was noted, which may have been due to the lack of sap during the arthropod activity periods.

Under Central European conditions we therefore conclude that arthropods may be incidental vectors of GTD pathogens. These arthropods could spread pathogens between several vines, as the majority of examined arthropods migrate during foraging.

The present study has broadened understanding of the epidemiology of GTDs. However, accurate assessment of the arthropod contributions to pathogen dissemination remains to be achieved. Besides incidentally vectoring pathogen propagules to vine wounds, the spatial dissemination of esca-causing pathogens on and between grapevines is likely to increase inoculum sources.

Future studies should address several related aspects. i) The actual propagule loads and infection potential carried by frequently occurring arthropods should be evaluated, to assess the significance of these as efficient pathogen vectors. ii) The susceptibility phase of wounds at different periods after grapevine pruning should be evaluated in German vineyards, to determine the risks of arthropod-mediated pathogen spread. iii) The role of earwig faeces as inoculum sources in vineyards needs to be elucidated. As precautionary measures to prevent disease-spread through arthropods, the greening management in vineyards should be adequately adjusted; also, the application of appropriate pruning wound protection should possibly be increased. Usage of insecticides is not encouraged here.

ACKNOWLEDGEMENT

The authors thank the team of the Mycology Group at the Julius Kühn-Institute, Siebeldingen, for their support in the laboratory and field.

LITERATURE CITED

Baloyi M.A., Halleen F., Mostert L., Eskalen A., 2013. First report of *Togninia minima* perithecia on esca- and Petri-diseased grapevines in South Africa. *Plant Disease* 97(9): 1247.

Baloyi M.A., Mostert L., Halleen, F., 2018. Pathogenicity of ten *Phaeoacremonium* species associated with esca and Petri disease of grapevine. *Phytopathologia Mediterranea* 57(3): 538–546.

Bertsch C., Ramírez-Suero M., Magnin-Robert M., Larignon P., Chong J., … Fontaine F., 2013. Grapevine trunk diseases: complex and still poorly understood. *Plant Pathology* 62(2): 243–265.

Brasier C.M., 1991. *Ophiostoma novo-ulmi* sp. nov., causative agent of current Dutch elm disease pandemics. *Mycopathologia* 115(3): 151–161.

Christen D., Schönmann S., Jermini M., Strasser R.J., Défago G., 2007. Characterization and early detection of grapevine (*Vitis vinifera*) stress responses to esca disease by *in situ* chlorophyll fluorescence and comparison with drought stress. *Environmental and Experimental Botany* 60(3): 504–514.

Crous P.W., Gams W., 2000. *Phaeomoniella chlamydospora* gen. et comb. nov., a causal organism of Petri grapevine decline and esca. *Phytopathologia Mediterranea* 39(1): 112–118.

Edwards J., Laukart N., Pascoe I.G., 2001. *In situ* sporulation of *Phaeomoniella chlamydospora* in the vineyard. *Phytopathologia Mediterranea* 40(1): 61–66.

Elena G., Luque J., 2016. Seasonal susceptibility of grapevine pruning wounds and cane colonization in Catalonia, Spain following artificial infection with *Diplodia seriata* and *Phaeomoniella chlamydospora*. *Plant Disease* 100(8): 1651–1659.

Eskalen A., Gubler W.D., 2001. Association of spores of *Phaeomoniella chlamydospora*, *Phaeoacremonium inflatipes*, and *Pm. aleophilum* with grapevine cordons in California. *Phytopathologia Mediterranea* 40: S429–S432.

Eskalen A., Feliciano A.J., Gubler W.D., 2007. Susceptibility of grapevine pruning wounds and symptom development in response to infection by *Phaeoacremonium aleophilum* and *Phaeomoniella chlamydospora*. *Plant Disease* 91(9): 1100–1104.

Fischer M., 2002. A new wood-decaying basidiomycete species associated with esca of grapevine: *Fomitiporia mediterranea* (Hymenochaetales). *Mycological Progress* 1(3): 315–324.

Fischer M., 2019. Grapevine trunk diseases in German viticulture. III. Biodiversity and spatial distribution of fungal pathogens in rootstock mother plants and possible relation to leaf symptoms. *Vitis* 58: 141-149.

Fischer M., Kassemeyer H.-H., 2003. Fungi associated with Esca disease of grapevine in Germany. *Vitis* 42(3): 109–116.

Fischer M., Schneider P., Kraus C., Molnar M., Dubois C., d'Aguiar D., Haag N., 2016. Grapevine trunk disease in German viticulture: Occurrence of lesser known fungi and first report of *Phaeoacremonium viticola* and *P. fraxinopennsylvanicum*. *Vitis* 55: 145–156.

Fontaine F., Pinto C., Vallet J., Clément C., Gomes A.C., Spagnolo A., 2016. The effects of grapevine trunk

diseases (GTDs) on vine physiology. *European Journal of Plant Pathology* 144(4): 707–721.

Gramaje D., Mostert L., Armengol J., 2011. Characterization of *Cadophora luteo-olivacea* and *C. melinii* isolates obtained from grapevines and environmental samples from grapevine nurseries in Spain. *Phytopathologia Mediterranea* 50: S112–S126.

Gramaje D., Mostert L., Groenewald J. Z., Crous P.W., 2015. *Phaeoacremonium*: from esca disease to phaeohyphomycosis. *Fungal Biology* 119(9): 759–783.

Gramaje D., Úrbez-Torres J.R., Sosnowski M.R., 2018. Managing Grapevine Trunk Diseases with respect to etiology and epidemiology: Current strategies and future prospects. *Plant Disease* 102(1): 12–39.

Haag N., 2018. Grapevine Trunk Diseases: Epidemiologie und Molekulardiagnose wichtiger Esca-Erreger während der Pflanzguterzeugung. PhD Thesis, University of Hohenheim, Germany, 123 pp.

Halleen F., Mostert L., Crous P.W., 2007. Pathogenicity testing of lesser-known vascular fungi of grapevines. *Australasian Plant Pathology* 36: 277–285.

Havlová L., Hula V., Niedobová J., 2015. Spiders of the vine plants in Southern Moravia. *Acta Universitatis Agriculturae et Silviculturae Mendelianae Brunensis* 63(5): 1471–1476.

Hofstetter V., Buyck B., Croll D., Viret O., Couloux A., Gindro K., 2012. What if esca disease of grapevine were not a fungal disease? *Fungal Diversity* 54(1): 51–67.

Huth C.D., 2011. Untersuchungen zur Lebensweise und zur Populationskontrolle des Gemeinen Ohrwurms *Forficula auricularia* L. (Insecta, Dermaptera) in Rebanlagen. PhD Thesis, University of Mainz, Germany, 329 pp.

Kehrli P., Karp J., Burdet J.-P., Deneulin P., Danthe E., … Linder C., 2012. Impact of processed earwigs and their faeces on the aroma and taste of 'Chasselas' and 'Pinot Noir' wines. *Vitis* 51(2): 87–93.

Kraus C., Voegele R.T., Fischer M., 2019. Temporal development of the culturable, endophytic fungal community in healthy grapevine branches and occurrence of GTD-associated fungi. *Microbial Ecology* 77(4): 866–876.

Kraus C., Damm U., Bien S., Voegele R.T., Fischer M., 2020. New species of *Phaeomoniellales* from a German vineyard and their potential threat to grapevine (*Vitis vinifera*) health. *Fungal Systematics and Evolution* 6: 139–155.

Kubátová A., Kolařík M., Pažoutová S., 2004. *Phaeoacremonium rubrigenum* – Hyphomycete associated with bark beetles found in Czechia. *Folia Microbiologica* 49(2): 99–104.

Lamb R.J., 1975. Effects of dispersion, travel, and environmental heterogeneity on populations of the earwig *Forficula auricularia* L.. *Canadian Journal of Zoology* 53: 1855–1867.

Larignon P., Dubos B., 1997. Fungi associated with esca disease in grapevine. *European Journal of Plant Pathology* 103: 147–157.

Larignon P., Dubos B., 2000. Preliminary studies on the biology of *Phaeoacremonium*. *Phytopathologia Mediterranea* 39(1): 184–189.

Leach J.G., 1940. *Insect transmission of plant diseases*. McGraw-Hill Book Company, Inc. New York and London, 615 pages.

Lecomte P., Darrieutort G., Liminana J.-M., Comont G., Muruamendiaraz A., … Fermaud M., 2012. New insights into esca of grapevine: The development of foliar symptoms and their association with xylem discoloration. *Plant Disease* 96(7): 924–934.

Makatini G.J., 2014. The role of sucker wounds as portals for grapevine trunk pathogen infections. MSc Thesis, University of Stellenbosch, South Africa, 108 pages.

Mohr H.D., 2012. *Farbatlas Krankheiten, Schädlinge und Nützlinge an der Weinrebe*. 2nd edition. Eugen Ulmer KG, Stuttgart, Germany, 335 pages.

Molnar M., Voegele R.T., Fischer M., 2020. Grapevine trunk disease in German viticulture IV. Spreading of spores of the Esca related fungus *Phaeomoniella chlamydospora* and the occurrence of foliar esca-symptoms in German vineyards. *Vitis* 59: 63–69.

Mondello V., Songy A., Battiston E., Pinto C., Coppin C., … Fontaine F., 2018. Grapevine Trunk Diseases: A review of fifteen years of trials for their control with chemicals and biocontrol agents. *Plant Disease* 102(7): 1189–1217.

Mostert L., Crous P.W., Groenewald J.Z., Gams W., Summerbell R.C., 2003. *Togninia* (Calosphaeriales) is confirmed as teleomorph of *Phaeoacremonium* by means of morphology, sexual compatibility and DNA phylogeny. *Mycologia* 95(4): 646–659.

Mostert L., Groenewald J.Z., Summerbell R.C., Gams W., Crous P.W., 2006. Taxonomy and pathology of *Togninia* (Diaporthales) and its *Phaeoacremonium* anamorphs. *Studies in Mycology* 54: 1–113.

Moyo P., Allsopp E., Roets F., Mostert L., Halleen F., 2014. Arthropods vector grapevine trunk disease pathogens. *Phytopathology* 104(10): 1063–1069.

Moyo P., Mostert L., Spies C.F.J., Damm U., Halleen F., 2018. Diversity of *Diatrypaceae* species associated with dieback of grapevines in South Africa, with the description of *Eutypa cremea* sp. nov. *Plant Disease* 102(1): 220–230.

Mugnai L., Graniti A., Surico G., 1999. Esca (black measles) and brown wood-streaking: Two old and elusive diseases of grapevines. *Plant Disease* 83(5): 404–418.

Navarrete F., Abreo E., Martínez S., Bettucci L., Lupo S., 2011. Pathogenicitiy and molecular detection of Uruguayan isolates of *Greeneria uvicola* and *Cadophora luteo-olivacea* associated with grapevine trunk diseases. *Phytopathologia Mediterranea* 50: S166-S175.

Roberts M. J., 1995. *Spiders of Britain & Northern Europe.* Collins field guide, Harper Collins Publishers, London, UK, 383 pages.

Rolshausen P.E., Úrbez-Torres J.R., Rooney-Latham S., Eskalen A., Smith R.J., Gubler W.D., 2010. Evaluation of pruning wound susceptibility and protection against fungi associated with grapevine trunk diseases. *American Journal of Enology and Viticulture* 61(1): 113–119.

Rooney-Latham S., Eskalen A., Gubler W.D., 2005a. Ascospore release of *Togninia minima*, cause of Esca and grapevine decline in California. *Plant Health Progress* 6: 16 (1).

Rooney-Latham S., Eskalen A., Gubler W.D., 2005b. Occurrence of *Togninia minima* perithecia in esca-affected vineyards in California. *Plant Disease* 89(8): 867-871.

Schaefer, M., 2017. Brohmer – Fauna von Deutschland. 24th edition. Quelle & Meyer Verlag GmbH & Co., Wiebelsheim, Germany, 765 pages.

Stresemann E., 1992. *Exkursionsfauna von Deutschland*. Band 1. Wirbellose (ohne Insekten). Volk und Wissen Verlag GmbH Berlin, Germany, 637 pages.

Surico G., Marchi G., Ferrandino F.J., Braccini P., Mugnai L., 2000. Analysis of the spatial spread of esca in some Tuscan vineyards (Italy). *Phytopathologia Mediterranea* 39(1): 211-224.

Surico G., Mugnai L., Marchi G., 2006. Older and more recent observation on esca: a critical overview. *Phytopathologia Mediterranea* 45: S68-S86.

Surico G., 2009. Towards a redefinition of the diseases within the esca complex of grapevine. *Phytopathologia Mediterranea* 48(1): 5–10.

Tillett D., Neilan A., 2000. Xanthogenat nucleic acid isolation from cultured and environmental cyanobacteria. *Journal of Phycology* 36: 251–258.

Travadon R., Lawrence D.P., Rooney-Latham S., Gubler W.D., Wilcox W.F., … Baumgartner K., 2015. *Cadophora* species associated with wood-decay of grapevine in North America. *Fungal Biology* 119(1): 53–66.

Van Niekerk J.M., Halleen F., Fourie P.H., 2011. Temporal susceptibility of grapevine pruning wounds to trunk pathogen infection in South African grapevines. *Phytopathologia Mediterranea* 50: S139-S150.

Vasquez S. J., Gubler W.D., Leavitt G.M., 2007. Economic loss in California's table grape vineyards due to measles. *Phytopathologia Mediterranea* 46: 118.

White T. J., Bruns T., Lee S., Taylor J., 1990. *Amplification and direct sequencing of fungal ribosomal RNA genes for phylogenetics*. In: PCR Protocols: A Guide to Methods and Applications, (Innis M.A., Gelfand D.H., Sninsky J.J. & White T.J, eds.). Academic Press, Inc., San Diego, CA, USA, 315–322.

Phytopathologia Mediterranea
The international journal of the
Mediterranean Phytopathological Union

Firenze University Press
www.fupress.com/pm

Research Papers

Leaf anthracnose and defoliation of blueberry caused by *Colletotrichum helleniense* in Northern Italy

Vladimiro GUARNACCIA[1,2,*], Ilaria MARTINO[1], Luca BRONDINO[3], Angelo GARIBALDI[1], Maria Lodovica GULLINO[1]

[1] *Centre for Innovation in the Agro-Environmental Sector, AGROINNOVA, University of Torino, Largo Braccini 2, 10095 Grugliasco (TO), Italy*
[2] *Department of Agricultural, Forest and Food Sciences (DISAFA), University of Torino, Largo Braccini 2, 10095 Grugliasco (TO), Italy*
[3] *Ortofruit Italia Soc. Agr. Coop. O.P., Via Colombaro dei Rossi 16/bis, 12037 Saluzzo (CN), Italy*
[*]Corresponding author. E-mail: vladimiro.guarnaccia@unito.it

Summary. Highbush blueberry is an increasingly important crop due to its economic value and demonstrated health benefits of blueberries. Leaf spots are considered as minor diseases of blueberry plants, but they adversely affect blueberry productivity, causing reduced photosynthetic activity, flower bud formation and berry production. Surveys of blueberry crops were conducted in Piedmont, Northern Italy, during 2019-2020. Fungi isolated from leaf spots of the blueberry cultivar 'Blue Ribbon' were identified as *Colletotrichum helleniense* through a robust multi-locus phylogeny. Eight genomic loci were considered: *tub*, *gapdh*, *act*, *cal*, *his3*, *chs-1*, *ApMat* and *gs*. Morphological characters of a representative strain were assessed. Pathogenicity was confirmed on four blueberry cultivars, although with different levels of aggressiveness to the cultivars. This study shows the importance of a polyphasic approach to investigate species of *Colletotrichum*, and the relevance of molecular tools for the species-level characterization within the 'Kahawae' clade. This is the first report of *Colletotrichum helleniense* causing leaf anthracnose on *Vaccinium corymbosum*.

Keywords. *Vaccinium corymbosum*, multi-locus typing, berry fruit.

OPEN ACCESS

Citation: V. Guarnaccia, I. Martino, L. Brondino, A. Garibaldi, M.L. Gullino (2021) Leaf anthracnose and defoliation of blueberry caused by *Colletotrichum helleniense* in Northern Italy. *Phytopathologia Mediterranea* 60(3): 479-491. doi: 10.36253/phyto-12377

Accepted: July 28, 2021

Published: December 30, 2021

Data Availability Statement: All relevant data are within the paper and its Supporting Information files.

Competing Interests: The Author(s) declare(s) no conflict of interest.

Editor: Josep Armengol Forti, Polytechnical University of Valencia, Spain.

INTRODUCTION

Highbush blueberry (*Vaccinium corymbosum*, *Ericaceae*) is an increasingly important crop in Italy, with Piedmont, Veneto and Trentino Alto Adige as the major production areas (Brazelton, 2011). During the last decade, new cultivars and modern agricultural practices have been adopted, resulting in consistent improvement in berry production in Italy, with 1.675 tons harvested from 172 ha in 2018 (FAOSTAT 2019). Increasing emphasis on healthy life-styles and the recognition of blueberries as natural functional food have favoured berryfruit consumption and influenced the increased world produc-

tion (Polashock *et al*., 2017; Romo-Muñoz *et al*., 2019). However, this led to increased global movement and trade of plant materials, resulting in the spread of pathogens and emergence of new diseases (Polashock *et al*., 2017; Guarnaccia *et al*., 2020; Liu *et al*., 2020).

Anthracnose is one of the most economically important diseases of blueberry (Retamales and Hancock, 2018), and the most frequent and relevant disease of blueberry fruit is anthracnose caused by *Colletotrichum* spp. However, shoot tip blight and leaf spot caused by the same pathogens are included among the additional symptoms, and could develop during growing seasons. Leaf symptoms could reduce photosynthesis, cause premature defoliation and affect subsequent flower bud formation (Polashock *et al*., 2017). Species of *Colletotrichum* have been reported in association with anthracnose on blueberry leaves in different international regions (Farr and Rossman, 2020). Several *Colletotrichum* spp. are important plant pathogens, affecting a wide range of hosts in different climatic regions (Dean *et al*., 2012). Assessment of morphological features of these fungi has been the common method to classify species within *Colletotrichum*. However, adoption of molecular approaches has allowed profound taxonomic revision of the genus (Weir *et al*., 2012; Cabral *et al*., 2020). Previous studies based on morphological features ascribed the species causing blueberry anthracnose mainly to the *Colletotrichum acutatum* species complex (SC), (*C. acutatum sensu stricto*, *C. fioriniae*, *C. nymphaeae*), *C. gloeosporioides* SC (*C. fructicola*, *C. gloeosporioides sensu stricto*, *C. kahawae*, *C. siamense*), *C. boninense* SC (*C. karstii*) and *C. orchidearum* SC (*C. sichuaninese*) (Hartung *et al*., 1981; Barrau *et al*., 2001; Kim *et al*., 2009; Xu *et al*., 2013; Rios *et al*., 2015; Pszczolkowska *et al*., 2016; Ali *et al*., 2019; Liu *et al*. 2020). Liu *et al*. (2020) reported *Colletotrichum fructicola* as the dominant species affecting blueberry leaves in Sichuan Province, China, followed by *Colletotrichum siamense*, *C. kahawae*, *C. karstii*, *C. nymphaeae* and *C. sichuaninese*. Species of *Colletotrichum gloeosporioides* SC were responsible for blueberry leaf spot in China (Xu *et al*., 2013), Korea (Kim *et al*., 2009), Georgia (Ali *et al*., 2019) and the United States of America (Hartung *et al*., 1981). Species of the *Colletotrichum acutatum* SC were found in association with leaf anthracnose in Australia (Shivas *et al*., 2009; 2016), Canada (Verma *et al*., 2006), China (Xu *et al*., 2013), Japan (Yoshida and Tsukiboshi, 2002; Yoshida *et al*., 2007), Korea (Kim *et al*., 2009), New Zealand (Pennycook, 1989; Gadgil *et al*., 2005), Poland (Pszczółkowska *et al*., 2016), Spain (Barrau *et al*., 2001), The Netherlands (Nirenberg *et al*., 2002) and the United States of America (Guerber *et al*., 2003). Rios *et al*. (2015) reported *Colletotrichum karstii* in association with blueberry leaf spots in Brazil. However, since these species could persist as sources of inoculum in the field, affecting orchards and possibly cross-infecting other nearby crops while switching to a pathogenic lifestyles, specific pathogen identification should be provided (Fuentes-Aragón *et al*., 2020). Currently, molecular data are combined with morphological characters and pathogenicity tests in a polyphasic approach to clearly identify species within the *Colletotrichum* SC (Guarnaccia *et al*., 2019, 2021a; Damm *et al*., 2019).

Leaf anthracnose of blueberry bushes was observed in Piedmont, Northern Italy. The aims of the present study were: i) to characterize fungi isolated from this disease using morphological, molecular and phylogenetic tools, and ii) to test their pathogenicity to fulfil Koch's postulates.

MATERIALS AND METHODS

Field sampling and fungus isolation

Surveys were conducted from March to September 2019 in two blueberry plantations in Cuneo, Piedmont, Northern Italy (Orchard 1: 44°37'39.1"N 7°34'14.1"E; Orchard 2: 44°38'20.3"N 7°31'23.8"E). Anthracnose incidence (DI) was assessed based on the percentage of affected plants. Ten symptomatic leaves were randomly collected from about twenty plants. Portions of symptomatic leaves (5–10 mm) were surface sterilised in 1% sodium hypochlorite for 1 min, rinsed in sterile distilled water (SDW) for 1 min and dried on sterile absorbent paper. Small fragments (2–3 mm) were cut from lesion margins and plated on potato dextrose agar (PDA, Merck) amended with 25 ppm of streptomycin sulphate (PDA-S, Sigma-Aldrich). The plates were incubated at 25 ± 1°C under a 12 h photoperiod. Following 48 to 72 h of incubation, sporulating conidiomata obtained were collected and crushed in drops of sterile water and then spread over the surface of PDA-S plates. After 24 h, germinating spores were individually transferred onto PDA plates. Ten isolates were obtained and two of these were used for molecular characterization (Table 1). Stock cultures are maintained at -80°C at the Agroinnova Centre of Competence, University of Torino, Torino, Italy.

DNA extraction, polymerase chain reaction (PCR) amplification, and sequencing

DNA was extracted from two isolates with an E.Z.N.A.® Fungal DNA Mini Kit (Omega Bio-Tek,

Table 1. Collection details of *Colletotrichum* isolates, and GenBank accession numbers of other *Colletotrichum* isolates, included in this study.

Species	Culture No.[1]	Host	Locality	GenBank No. [2]							
				gapdh	*tub*	*act*	*his3*	*calm*	*Ap/MAT*	*gs*	*chs-1*
C. acutatum	CBS 112996 [T]	*Carica papaya*	Australia	JQ948677	JQ005860	JQ005839	JQ005818	-	-	-	-
C. aenigma	ICMP 18608 [T]	*Persea americana*	Israel	JX010044	JX010389	JX009443	-	JX009683	KM360143	JX010078	JX009774
C. aeschynomenes	ICMP 17673 [T]	*Aeschynomene virginica*	USA	JX009930	JX010392	JX009483	-	JX009721	KM360145	JX010081	JX009799
C. alienum	ICMP 12071 [T]	*Malus domestica*	New Zealand	JX010028	JX010411	JX009572	-	JX009654	KM360144	JX010101	JX009882
C. aotearoa	ICMP 18537; C1282.4	*Coprosma* sp.	New Zealand	JX010005	JX010420	JX009564	-	JX009611	HE655663	JX010113	JX009853
C. asianum	ICMP 18580; CBS 130418	*Coffea arabica*	Thailand	JX010053	JX010406	JX009584	KY856305	JX009727	-	JX010096	JX009867
C. camelliae	LC1364; CGMCC3.14925	*Camellia sinensis*	China	KJ954782	KJ955230	KJ954363	-	KJ954634	KJ954497	KJ954932	-
C. chrysophilum	CMM4268[T]	*Musa* sp.	Brazil	KX094183	KX094285	KX093982	-	KX094063	KX094325	KX094204	KX094083
C. cigarro	CBS 112984; ICMP17932; STE-U4445; JT1096	*Banksia* sp.	Portugal	KC296989	KC297082	KC296923	KC297048	KC296944	-	KC297014	KC296966
	ICMP 18534; C1252.12	*Kunzea ericoides*	New Zealand	JX009904	JX010427	JX009473	-	JX009634	HE655657	JX010116	JX009765
	ICMP 18539 [T]; C1262.12	*Olea europaea*	Australia	JX009966	JX010434	JX009523	-	JX009635	HE655658	JX010132	JX009800
C. clidemiae	ICMP 18658; C1317.1	*Clidemia hirta*	USA (Hawai)	JX009989	JX010438	JX009537	-	JX009645	KC888929	JX010129	JX009877
C. conoides	CGMCC3.17615	*Capsicum annuum*	China	KP890168	KP890174	-	-	KP890150	-	JX010128	KP890156
C. cordylinicola	MFLUCC 090551 [T]; ICMP 18579	*Cordyline fructicosa*	Thailand	JX009975	JX010440	HM470235	-	HM470238	-	JX010122	JX009864
C. fructicola	ICMP 18581; CBS 130416[T]	*Coffea arabica*	Thailand	JX010033	JX010405	FJ907426	-	FJ917508	-	JX010095	JX009866
C. fructivorum	CBS 124.22[T]; ICMP19122	*Vaccinium* sp.	USA	JX009950	JX010433	JX009536	-	JX009744	JX145278	JX010134	JX009902
C. gloeosporioides	ICMP 17821; CBS 112999	*Citrus sinensis*	Italy	JX010056	JX010445	JX009531	KY856316	JX009731	-	JX010085	JX009818
C. grevilleae	CBS 132879 [T]	*Grevillea* sp.	Italy	KC297010	KC297102	KC296941	KC297056	KC296963	-	KC297033	KC296987
C. grossum	CGMCC 3.17614 [T]	*Capsicum annuum*	China	KP890159	KP890171	KP890141	-	KP890147	-	-	KP890153
C. hebeiense	JZB330028	*Vitis vinifera*	China	KF377495	KF288975	KF377532	-	-	KF377562	-	KF289008
C. helleniense	CBS 142418; CPC 26844	*Poncirus trifoliata*	Greece	KY856270	KY856528	KY856019	KY856361	KY856099	-	-	KY856186
	CVG628	*Vaccinium corymbosum* 'Blue Ribbon'	Italy	**MW368901**	**MW368899**	**MW368903**	**MW368913**	**MW368905**	**MW368907**	**MW368911**	**MW368909**
	CVG629	*Vaccinium corymbosum* 'Blue Ribbon'	Italy	**MW368902**	**MW368900**	**MW368904**	**MW368914**	**MW368906**	**MW368908**	**MW368912**	**MW368910**
C. henanense	LC3030, CGMCC 3.17354, LF238[T]	*Citrus sinensis*	China	KJ954810	KJ955257	KM023257	-	KJ954662	KJ954524	KJ954960	-
C. horii	NBRC 7478 [T]; ICMP 10492	*Diospyros kaki*	Japan	GQ329681	JX010450	JX009438	-	JX009604	JQ807840	JX010137	JX009752
C. hystricis	CBS 142411; CPC 28153	*Citrus hystrix*	Italy	KY856274	KY856532	KY856023	KY856365	KY856103	-	-	-
C. jiangxiense	CGMCC 3.17363 [T]; LC3463; LF687	*Camellia sinensis*	China	KJ954902	KJ955348	KJ954471	-	KJ954752	KJ954607	KJ955051	-

(Continued)

Table 1. (Continued).

Species	Culture No.[1]	Host	Locality	GenBank No. [2]							
				gapdh	*tub*	*act*	*his3*	*calm*	*Ap/MAT*	*gs*	*chs-1*
C. kahawae	CBS 982.69; ICMP17915	*Coffea arabica*	Angola	JX010040	JX010435	JX009474	-	JX009638	-	JX010125	JX009829
	ICMP 17816; IMI 301220	*Coffea arabica*	Kenya	JX010012	JX010444	JX009452	-	JX009642	JQ894579	JX010130	JX009813
	IMI 301220; ICMP17811	*Coffea arabica*	Malawi	JX009970	JX010430	JX009555	-	JX009641	-	JX010131	JX009817
	IMI 361501; ICMP17905	*Coffea arabica*	Cameroon	JX010046	JX010431	JX009561	-	JX009644	-	JX010127	JX009816
C. musae	ICMP 17817	*Musa sapientum*	Kenya	JX010015	JX010395	JX009432	-	JX009689	-	JX010084	JX009815
C. nupharicola	CBS 470.96; ICMP 18187	*Nuphar lutea* subsp. *polysepala*	USA	JX009972	JX010398	JX009437	-	JX009663	-	JX010088	JX009835
C. proteae	CBS 132882	*Protea* sp.	South Africa	KC297009	KC297101	KC296940	KC297045	KC296960	-	KC297032	KC296986
C. psidii	CBS 145.29 [T]	*Psidium* sp.	Italy	JX009967	JX010443	JX009515	-	JX009743	-	JX010133	JX009901
C. queenslandicum	ICMP 1778 [T]	*Carica papaya*	Australia	JX009934	JX010414	JX009447	-	JX009691	KC888928	JX010104	JX009899
C. rhexiae	CBS 133134; Coll1026	*Rhexia virginica*	USA	-	JX145179	-	-	-	JX145290	-	-
C. salsolae	ICMP 19051	*Salsola tragus*	Hungary	JX009916	JX010403	JX009562	-	JX009696	KC888925	JX010093	JX009863
C. siamense	ICMP 18578, CBS 130417[T]	*Coffea arabica*	Thailand	JX009924	JX010404	FJ907423	-	JX009714	JQ899289	JX010094	JX009865
C. temperatum	CBS 133122; Coll883; BPI884100	*Vaccinium macrocarpon*	USA	-	JX145211	-	-	-	JX145298	-	-
C. theobromicola	ICMP 18649 [T]	*Theobroma cacao*	Panama	JX010006	JX010447	JX009444	-	JX009591	-	JX010139	JX009869
C. ti	ICMP 4832 [T]	*Coryline* sp.	New Zealand	JX009952	JX010442	JX009520	-	JX009649	KM360146	JX010123	JX009898
C. tropicale	CBS 124949 [T]	*Theobroma cacao*	Panama	JX010007	JX010407	JX009489	-	JX009719	-	JX010097	JX009870
C. viniferum	GZAAS 5.08601 [T]	*Vitis vinifera* 'Shuijing'	China	JN412798	JN412813	JN412795	-	-	-	JN412787	-
C. wuxiense	JS1A32; CGMCC 3.17894; JS1A44	*Camellia sinensis*	China	KU252046	KU252200	-	-	KU251834	KU251722	KU252101	KU251940
C. xanthorrhoeae	BRIP 45094, ICMP 17903, CBS 127831[T]	*Xanthorrhoea preissii*	Australia	JX009927	JX010448	JX009478		JX009653	KC790689	JX010138	JX009823

[1]ATCC: American Type Culture Collection, Virginia, USA; BRIP: Biosecurity Queensland Plant Pathology Herbarium, Queensland, Australia; CBS: Westerdijk Fungal Biodiversity Institute, Utrecht, the Netherlands; CGMCC: China General Microbiological Culture Collection Center, Beijing, China; CMM: Culture Collection of Phytopathogenic Fungi Prof. Maria Menezes, Recife, Pernambuco, Brazil; CVG: Agroinnova, Grugliasco, Torino, Italy; ICMP: International Collection of Microorganisms from Plants, Landcare Research, Auckland, New Zealand; IMI: Culture collection of CABI Europe UK Centre, Egham, UK; LC = working collection of Lei Cai, CAS, China; MFLUCC: Mae Fah Luang University Culture Collection, Chiang Rai, Thailand; NBRC: NBRC Culture Collection, Chiba, Japan. Ex-type and ex-epitype cultures are indicated with [T].

[2] *tub2*: beta-tubulin gene; *gapdh*: glyceraldehyde-3-phosphate dehydrogenase gene; *act*: actin gene; *his3*: histone3; *calm*: calmodulin; *ApMat*: Apn2-Mat1-2 intergenic spacer and partial mating type (*Mat1-2*); *gs*: glutamine synthetase; *chs-1*: chitin synthase 1. Strains recovered and sequences generated in this study are indicated in bold.

Darmstadt, Germany) from 0.1 g of mycelium grown on PDA, following the minikit manufacturer's instructions. Species identification was achieved by DNA sequencing of a combined dataset of eight genomic loci, including beta-tubulin (*tub2*), glyceraldehyde-3-phosphate dehydrogenase (*gapdh*), actin (*act*), calmodulin (*cal*), histone3 (*his3*), chitin synthase 1 (*chs-1*), Apn2-Mat1-2 intergenic spacer and partial mating type (*Mat1-2*) (*ApMat*), and glutamine synthetase (*gs*). The primers used for each locus shown in Table 2. The amplification mixtures of PCR and respective cycling conditions of Guarnaccia *et al.* (2017) were used for the *tub2*, *gapdh*, *act*, *cal*, *his3* and *chs-1* regions. The *gs* partial gene and *Mat1-2/ApMat* region were amplified using the PCR protocols of Liu *et al.* (2015). Five µL of PCR product for each PCR reaction was examined by electrophoresis at 100V on 1% agarose (VWR Life Science AMRESCO® biochemicals) gels stained with GelRed™. PCR products were sequenced in both directions by Eurofins Genomics Service. The generated sequences were analysed and consensus sequences were computed using the program Geneious v. 11.1.5 (Auckland, New Zealand).

Phylogenetic analyses

New sequences obtained in this study were blasted against the NCBI's GenBank nucleotide database to determine the closest relatives for a taxonomic framework of the studied isolates. Alignments of different gene regions, including sequences obtained from this study and sequences downloaded from GenBank, were initially performed with the MAFFT v. 7 online server (http://mafft.cbrc.jp/alignment/server/index.html) (Katoh and Standley 2013), and then manually adjusted in MEGA v. 7 (Kumar *et al.*, 2016). The phylogenies were based on Maximum Parsimony (MP) and Bayesian Inference (BI) for the multi-locus analyses. The MP analyses were performed using Phylogenetic Analysis Using Parsimony (PAUP) v.4.0b10 (Swofford, 2003). Phylogenetic relationships were estimated by heuristic searches with 100 random addition sequences. Tree bisection-reconnection was used, with the branch swapping option set on 'best trees', with all characters weighted equally and alignment gaps treated as fifth state. Tree length (TL), consistency index (CI), retention index (RI) and rescaled consistence index (RC) were calculated for parsimony, and the bootstrap analyses (Hillis and Bull, 1993) were based on 1000 replications. Sequences generated in this study were deposited in GenBank (Table 1). For BI, the best evolutionary model for each partition was determined using MrModeltest v. 2.3 (Nylander, 2004) and incorporated into the analyses. MrBayes v. 3.2.5 (Ronquist *et al.*, 2012) was used to generate phylogenetic trees under optimal criteria per partition. The Markov Chain Monte Carlo (MCMC) analysis used four chains and started from a random tree topology. The heating parameter was set at 0.2 and trees were sampled every 1000 generations. Analyses stopped when the average standard deviation of split frequencies was less than 0.01.

Table 2. Primers used in this study.

Locus	Primer name	Primer sequence 5'->3'	Reference
tub	T1	AACATGCGTGAGATTGTAAGT	Glass and Donaldson, 1995
	Bt2b	ACCCTCAGTGTAGTGACCCTTGGC	O'Donnell and Cigelnik, 1997
gapdh	GDF1	GCCGTCAACGACCCCTTCATTGA	Guerber *et al.* 2003
	GDR1	GGGTGGAGTCGTACTTGAGCATGT	
act	ACT-512F	ATGTGCAAGGCCGGTTTCGC	Carbone and Kohn, 1999
	ACT-783R	TAGGAGTCCTTCTGACCCAT	
cal	CL1	GARTWCAAGGAGGCCTTCTC	O'Donnell *et al.*, 2000
	CL2	TTTTTGCATCATGACCCTTGGC	
his3	CYLH3F	GCAACATCTCGTCCGCTCT	Crous *et al.*, 2004
	CYLH3R	AGCTGGATGTCCTTGGACTG	
chs	CHS-79F	TGGGGCAAGGATGCCTGGAAGAAG	Carbone and Kohn, 1999
	CHS-345R	TGGAAGAACCATCTGTGGGAGTTG	
ApMat	AMF1	TCATTCTACGTATGTGCCCG	Silva *et al.*, 2012
	AMR1	CCAGAAATACACCGAACTTGC	
gs	GSF1	ATGGCCGATACATCTGG	Stephenson *et al.*, 1997
	GSR1	GAACCGTCGAAGTTCCAC	

Isolate morphology

Agar plugs (5 mm diam.) of the strains CVG628 and CVG629 were taken from the edges of actively growing cultures on PDA-S and were transferred onto the centres of Petri dishes (9 cm diam.) containing PDA, then incubated at 25 ± 1°C under 12 h photoperiod for 7 d. Three cultures plates of each strain were investigated. Colony characters and diameters were observed/measured after 7 d. Cultures were examined over time for development of ascomata, conidiomata and setae. The morphological characteristics of the fungi were examined by mounting structures in water, and 30 measurements at 400× magnification were determined for each isolate using a microscope (Nikon Eclipse 55i).

Pathogenicity testing

The pathogenicity of a representative strain CVG629 was tested on detached leaves of each of the four blueberry cultivars 'Blue Ribbon', 'Duke', 'Last Call' and 'Top Shelf'. Thirty leaves of each cultivar were inoculated and 30 leaves were used as controls. Each leaf was disinfested in a 1% sodium hypochlorite solution for 60s followed by three washes of 60s in sterile distilled water and blot dried on sterile absorbent paper before inoculation. The leaves were placed in plastic plates (12.5 × 12.5 × 1.5 cm [length × width × height]) with wet sterile absorbent paper to create a humid chambers. Each leaf was slightly wounded with a sterile needle and then inoculated with 10 µL of a conidium suspension (10^6 conidia mL^{-1}) obtained from a 10d-old culture of the representative isolate grown on PDA. Sterile distilled water was used for the control leaves. The plates were incubated at 25 ± 1°C under 12 h photoperiod for 7 days. The strains CVG628 and CVG629 were also tested *in planta* on attached leaves of the same cultivars. A total of 20 mL of a conidium suspension, obtained as described before, was sprayed on wounded and unwounded leaves. Six plants of each cultivar were used, and three of these were wounded with a sterile needle. A further six plants were similarly treated but spayed with sterile water as experimental controls. The plants were covered with a transparent plastic film to keep high relative humidity, and were transferred to a growth chamber and kept at 25°C with a 12 h photoperiod. The plastic film was removed 3 d post inoculation (dpi). Each trial was repeated once. Data of the replications of the repeated experiments were pooled and analysed together for each trial. Disease severity was evaluated 7 dpi for the trial on detached leaves or 10 dpi for the attached leaves, using a diagrammatic scale for percentage of infected leaf area (Gullino *et al.*, 2017). The scale was: symptomless leaf (0); up to 5% infected leaf area (1); 6 to 10% (2); 11 to 25% (3); 26 to 50% (4); and 51 to 100% (5). Disease severity (DS) was calculated as $DS = \Sigma(\text{no. of leaves} \times X_{0-5})/(\text{no. of leaves})$, where X_{0-5} refers to an approximate class midpoint as follows: $X_0 = 0$; $X_1 = 3\%$; $X_2 = 8\%$; $X_3 = 18\%$; $X_4 = 38\%$; $X_5 = 76\%$. Because no normal distribution was observed, the data were analysed using Kruskal-Wallis non-parametric test (at $P = 0.05$) to determine significant differences among the tested cultivars. The data analyses were conducted using SPSS software 26 (IBM Corporate). The identity of the re-isolated strains was confirmed through sequencing the *gapdh* and *gs* loci, to fulfil Koch's postulates.

RESULTS

Field sampling and fungus isolation

Symptoms identified as those typically caused by *Colletotrichum* spp. were found in two blueberry plantations of the cultivars 'Blue Ribbon' and 'Last Call'. Disease incidence was assessed at 20%, considering the percentage of affected plants. The symptoms observed consisted of brown-to-black, necrotic lesions occurring on mature leaves grown on 1-year-old twigs (Figure 1). Stem defoliation occurred. Based on colony aspect and growth, and conidial morphology characteristics, the fungal strains isolated from symptomatic leaves collected during the surveys were ascribed to *Colletotrichum* spp. and pure fungal cultures were obtained.

Phylogenetic analyses

The combined locus phylogeny of *Colletotrichum* consisted of 46 sequences. A total of 3749 characters (*tub2*: 1–510, *gapdh*: 517–795, *act*: 802–1030, *cal*: 1037–1655, *his3*: 1662–2040, *chs-1*: 2047–2250, *ApMat*: 2257–2927 and *gs*: 2934–3749) were included in the phylogenetic analyses. A maximum of 1000 equally most parsimonious trees were saved, and characteristics of the combined gene partitions used for each phylogenetic analysis are reported in Table 3. Bootstrap support values from the parsimony analysis were plotted on the Bayesian phylogenies (Figure 2). For the Bayesian analyses, MrModel test recommended the models in Table 3. Unique site patterns for each partition and all the parameters of the Bayesian analyses are reported in Table 3. In the generated phylogenetic tree, the strains isolated from *Vaccinium* plants clustered with the ex-type reference strain of *C. helleniense*, within the 'Kaha-

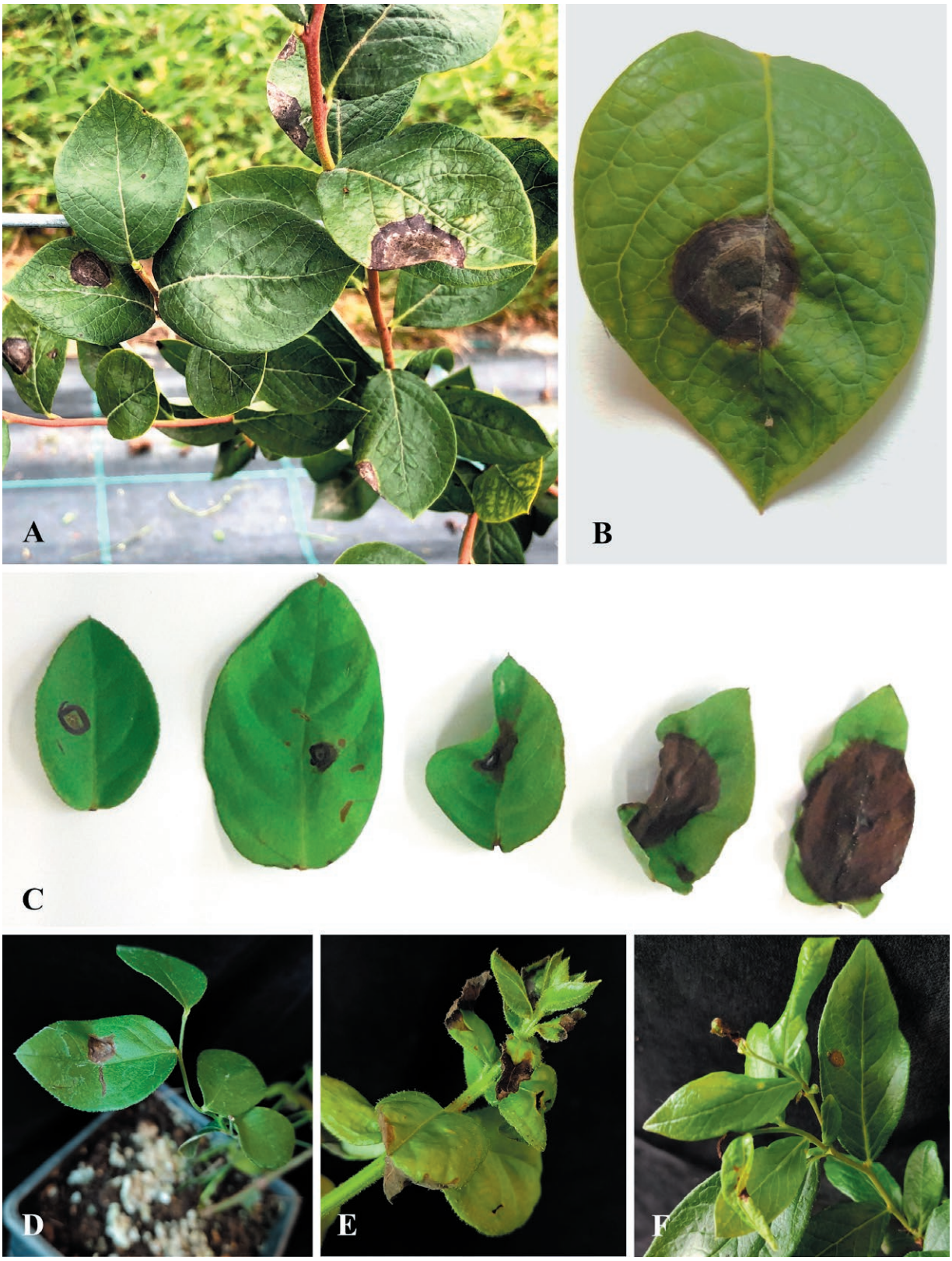

Figure 1. Leaf anthracnose (A and B) of *Vaccinium corymbosum* 'Blue Ribbon' in the field, and leaves of 'Last Call' at different necrotic stages after inoculation (C). Anthracnose developed after inoculations on 'Last Call' wounded (D and F) and unwounded (E) attached leaves.

Table 3. Maximum Parsimony, evolutionary models and Bayesian analysis characteristics of this study.

Parsimony analysis	Total sites	Constant sites	Variable sites	Parsimony informative sites	Tree length	Consistency index	Retention index	Rescaled consistence index	-	-	-
	3707	2066	973	668	2634	0.784	0.865	0.678	-	-	-
Evolutionary model	*tub2*	*gapdh*	*Act*	*cal*	*his3*	*chs-1*	*ApMat*	*gs*	-	-	-
	SYM+G	K80	HKY	SYM+G	HKY+G	K80+G	K80+G	GTR+G	-	-	-
Bayesian analysis	U.S.P.[1] *tub2*	U.S.P. *gapdh*	U.S.P. *act*	U.S.P. *cal*	U.S.P. *his3*	U.S.P. chs-1	U.S.P. *ApMat*	U.S.P. *gs*	Generation ran	Generated trees	Sampled trees
	156	188	97	130	52	42	269	296	8.315.000	8316	6237

[1] U.S.P.: Unique Site Patterns.

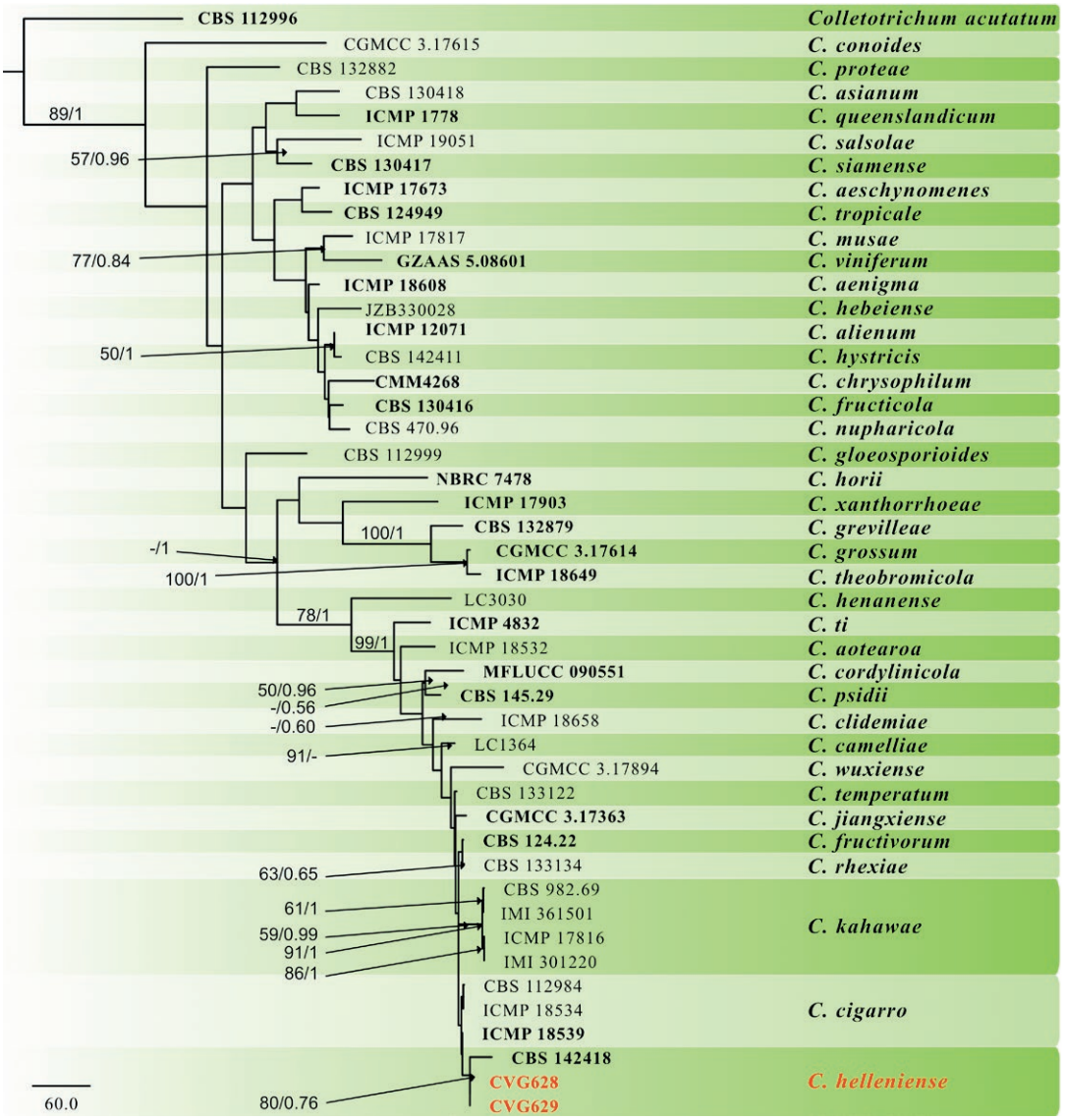

Figure 2. Maximum parsimony (MP) best-tree phylograms obtained from 46 *Colletotrichum gloeosporioides* species complex strains. Numbers on the nodes are MP bootstrap and Bayesian posterior probability values. Isolates obtained from *Vaccinium* in the present study are indicated in red font. Ex-type strains are indicated in bold. The tree was rooted to *Colletotrichum acutatum* (CBS 112996).

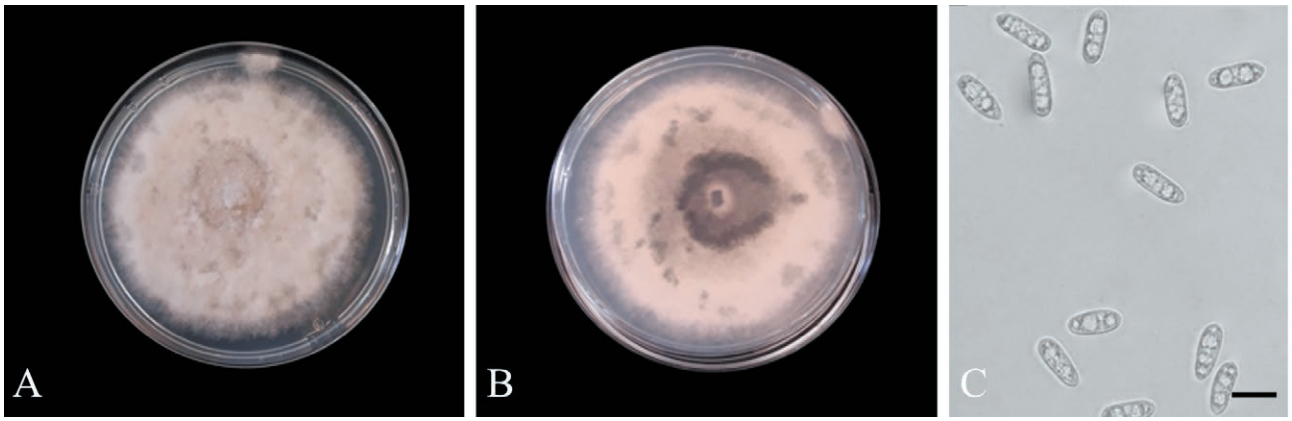

Figure 3. Front (A) and reverse (B) sides of a *Colletotrichum helleniense* colony (CVG629 strain) grown for 7 d on PDA, and conidia (C). Scale bar = 10 µm.

wae' clade and closely related with *C. cigarro*, *C. fructivorum*, *C. jiangxiense*, *C. kahawae*, *C. rhexiae* and *C. temperatum*.

Morphology

Morphological observations, supported by phylogenetic inference, were used to describe the representative strain of *Colletotrichum helleniense* (Figure 3).

Asexual morph on PDA: Conidiomata acervular. Hyphae hyaline, septate and branched. Setae not observed. Conidia hyaline, aseptate, cylindrical with rounded apices and bases, guttulate, mean dimensions 12.2 ± 1.4 × 5.0 ± 0.5 µm for the strain CVG628 and 13.5 ± 1.5 × 4.5 ± 0.5 µm for CVG629. Colonies on PDA with entire margins, grey in the centres and white to pale buff at the margins, entirely covered with floccose to dense, white to grey aerial mycelium, and with black conidiomata. Conidia present in pinkish-salmon-orange masses. Reverse of colonies grey to pale luteous, mean diam. after 7 d = 80 mm for strain CVG628 and 79 mm for CVG629.

Pathogenicity tests

The strains were pathogenic when inoculated on detached leaves, and on wounded and unwounded attached leaves of all the blueberry cultivars tested, although with different levels of aggressiveness (Figures 4 and 5). Symptoms on the leaves consisted of dark brown necrotic spots expanding circularly from the point of inoculation. The pathogenic strains were re-isolated from inoculated leaves, and were identified as described above by blast analysis of the *gapdh* and *gs* loci. This fulfilled Koch's postulates for the two assessed

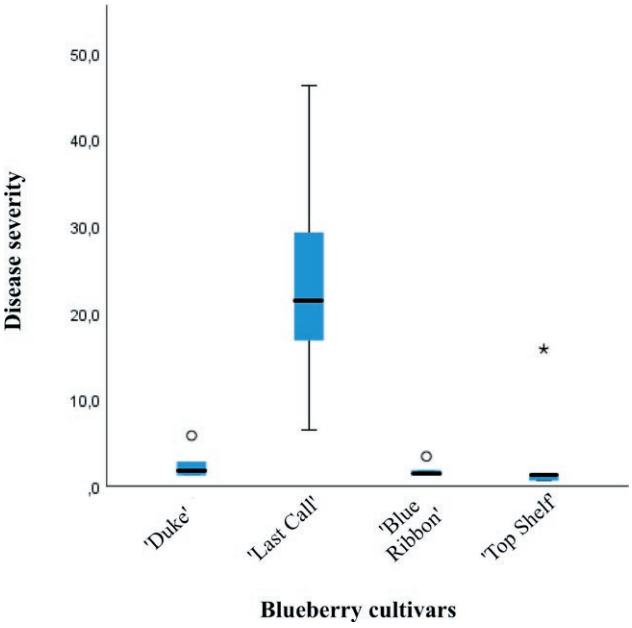

Figure 4. Box plot of results of pathogenicity tests on detached blueberry leaves. Boxes represent the interquartile range, and the horizontal line within each box indicates the average value. The Kruskal-Wallis test was used to compare the mean leaf areas infected after inoculations of four cultivars, and significant differences were accepted at $P < 0.05$.

strains. In test with detached leaves, the pairwise comparison obtained from the Kruskal-Wallis test showed differences ($P < 0.05$) in susceptibility between 'Last Call' and the other three cultivars (Supplementary Table 1). No differences ($P > 0.05$) were observed among 'Blue Ribbon', 'Duke' and 'Top Shelf'. In the test with attached leaves, the pairwise comparison showed differences ($P < 0.05$) only between 'Blue Ribbon' and 'Top Shelf' and

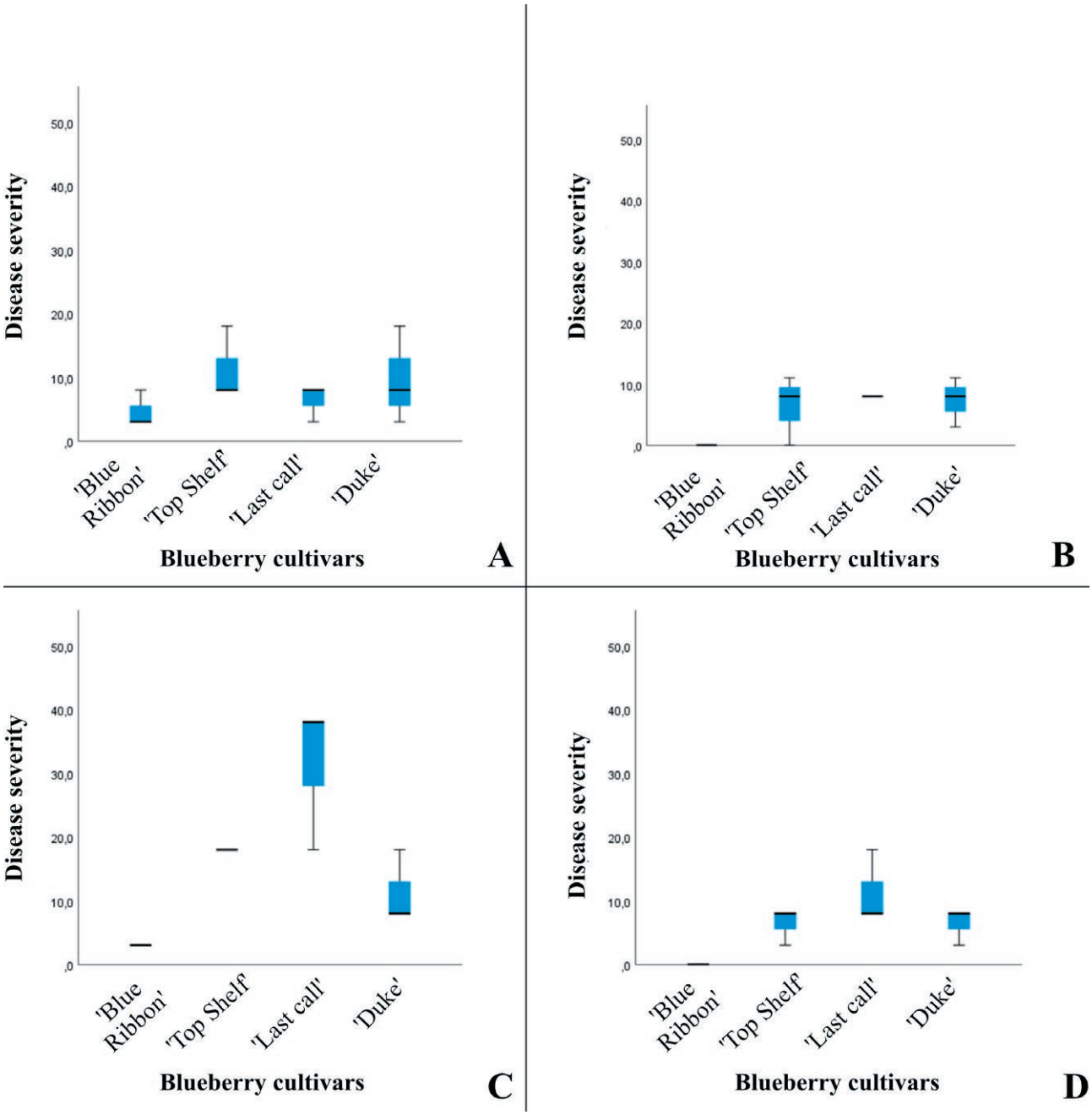

Figure 5. Box plots showing the results of the pathogenicity tests on wounded attached blueberry leaves (A with strain CVG628 and C with CVG629), and on unwounded attached leaves (B with strain CVG628 and D with CVG629). Boxes represent the interquartile range, and the horizontal line within each box indicates the average value. The Kruskal-Wallis test was carried used to compare the mean leaf areas infected after inoculations on four cultivars, and significant differences were accepted at $P < 0.05$.

'Last Call', and between 'Duke' and 'Last Call', and this was only for leaves wounded and inoculated with the strain CVG629 (Supplementary Table 2). The strain CVG628 gave high severity on 'Top Shelf', 'Last Call' and 'Duke' with no difference between wounded and unwounded leaves. The strain CVG629 caused weak symptoms on wounded and unwounded 'Blue Ribbon' leaves, but very severe symptoms on wounded 'Last Call' leaves. No symptoms were observed on control leaves in the detached or attached leaf pathogenicity assays.

DISCUSSION

Different *Colletotrichum* spp. have been reported in association with anthracnose diseases on several fruit crops, where pre- and post-harvest fruit rots are the most common symptoms observed and the most investigated diseases (Dean *et al*., 2012). However, leaf spots also represent a serious threat to fruit production (Benjamin, 2018; Guarnaccia *et al*., 2021b). Necrotic leaf lesions caused by *Colletotrichum* have been reported on blueberry plants, resulting in defoliation and reduced berry yields (Retamales and Hancock, 2018).

The present study is the first investigation of blueberry anthracnose conducted in the major production area of Italy. Since previous *Colletotrichum* studies were based on morphological characterization and ITS region analyses, which were insufficient for species identification (Cai *et al*., 2009), eight different genomic loci have been considered to provide robust multi-locus phylogenies and are useful tools for analyses of target loci for *Colletotrichum* spp. classification. The fungus strains isolated in the present study were identified as *Colletotrichum helleniense*, a species in the *C. kahawae* clade within the *C. gloeosporioides* SC. *Colletotrichum helleniense* has been described by Guarnaccia *et al.* (2017) in association with *Citrus reticulata* fruit lesions and with *Poncirus trifoliata* whither-tip twigs in Greece. The different reported hosts of *C. helleniense* confirms the pathogen's broad host range. This potential cross-infection ability combined with the complex life cycles of *Colletotrichum* spp. increases the difficulties for managing anthracnose diseases (De Silva *et al*., 2017). Cabral *et al.* (2020) provided taxonomic clarification within the 'Kahawae' clade to distinguish *C. kahawae* from *C. cigarro comb. et stat. nov*. Pathological, morphological, cytogenomic and biochemical data were combined with analysis of a nine-locus concatenated dataset including the *ApMat* and *gs* regions. These genomic regions, reported by Cabral *et al.* (2020) as useful to identify *Colletotrichum* spp. within the *C. gloeosporioides* SC, were considered to analyse the isolated *Colletotrichum* spp. investigated in the present study. This is the first report of *Colletotrichum helleniense* on *Vaccinium corymbosum* in Italy, as well as worldwide. However, further studies are required to provide insight on the species members of the 'Kahawae' clade based on genome sequencing, and to ascertain differentiation between *C. cigarro* and *C. helleniense*.

The pathogenicity tests reported here have confirmed the aggressiveness of *C. helleniense,* although the four assessed blueberry cultivars showed different susceptibilities to leaf anthracnose. *Colletotrichum* infections usually start with conidium germination and appressorium production on host tissues. However, direct penetration through stomata or wounds with no appressoria has also been reported, for example, during the infection process of mulberry leaves by *C. gloeosporioides* (De Silva *et al*., 2017). The present study demonstrates the ability of *C. helleniense* to cause anthracnose with and without wounds on attached blueberry leaves. All the cultivars tested were susceptible to the pathogen. However, 'Blue Ribbon' was generally less susceptible, while 'Last Call' developed more severe symptoms, confirming the results obtained from the inoculations on detached leaves. Different climate factors such as hail, rain and freezing, common in the surveyed area of Italy, can induce lesion development on leaves and are abiotic stress factors having potential roles in the disease development. Further studies should be conducted to assess the roles of climate factors and environment conditions on blueberry anthracnose. The pathogenicity results obtained in the present study need to be integrated with further experiments conducted at different temperatures and humidities.

After a first investigation of wood diseases and losses of production caused by several fungal pathogens (Guarnaccia *et al*., 2020), the present study provides new insights on the phytosanitary status of blueberry crops in Northern Italy. Considering the economic relevance of blueberry in this area, further research is required to determine the possible roles of other fungi, the epidemiology of the involved pathogens, and their responses to the currently adopted disease management protocols. This research should aim to establish new effective and sustainable disease management strategies for blueberry crops.

ACKNOWLEDGEMENTS

This study was supported by the Foundation CRT in the project "Avversità del MIRtillo in Piemonte: dove e come combAtteRlE (MIRARE)". The authors thank Dr G. Tabone (AGROINNOVA, University of Torino) for the technical support.

LITERATURE CITED

Ali M.E., Hudson O., Hemphill W.H., Brenneman T.B., Oliver J.E., 2019. First report of resistance to pyraclostrobin, boscalid, and thiophanate–methyl in *Colletotrichum gloeosporioides* from blueberry in Georgia. *Plant Health Progress* 20: 261–262.

Barrau C., De los Santos B., Romero F., 2001. First report of *Colletotrichum acutatum* in blueberry plants in Spain. *Plant Disease* 85: 1285.

Benjamin E., 2018. *Biotecnology for Fruit Crop Improvement*. Scientific e–Resources, 352 pp.

Brazelton C., 2011. World blueberry acreage and production report. *US Highbush Blueberry Council* 1–51.

Cabral A., Azinheira H.G., Talhinhas P., Batista D., Ramos A.P., ... Várzea V., 2020. Pathological, morphological, cytogenomic, biochemical and molecular data support the distinction between *Colletotrichum cigarro comb. et stat. nov*. and *Colletotrichum kahawae*. *Plants* 9: 502.

Cai L., Hyde K.D., Taylor P.W.J., Weir B., Waller J., ... Prihastuti H., 2009. A polyphasic approach for studying *Colletotrichum*. *Fungal Diversity* 39: 183–204.

Carbone I., Kohn L.M., 1999. A method for designing primer sets for speciation studies in filamentous ascomycetes. *Mycologia* 91: 553–556.

Crous P.W., Groenewald J.Z., Risède J.M., Simoneau P., Hywel–Jones N.L., 2004. *Calonectria* species and their *Cylindrocladium* anamorphs: species with sphaeropedunculate vesicles. *Studies in Mycology* 50: 415–430.

Damm U., Sato T., Alizadeh A., Groenewald J.Z., Crous P.W., 2019. The *Colletotrichum dracaenophilum*, *C.* ámagnum and *C.* áorchidearum species complexes. *Studies in Mycology* 92: 1–46.

Dean R., Van Kan J.A., Pretorius Z.A., Hammond-Kosack, K.E., Di Pietro A., ... Foster G.D., 2012. The Top 10 fungal pathogens in molecular plant pathology. *Molecular Plant Pathology* 13: 414–430.

De Silva D.D., Crous P.W., Ades P.K., Hyde K.D., Taylor P.W., 2017. Life styles of *Colletotrichum* species and implications for plant biosecurity. *Fungal Biology Reviews* 31: 155–168.

FAOSTAT, 2019. Food and Agriculture Organization of the United Nations http://www.fao.org/faostat/en/#home. Accessed on November 2020.

Farr D.F., Rossman A.Y., 2020. Fungal Databases U.S. National *Fungus* Collections ARS USDA.

Fuentes-Aragón D., Guarnaccia V., Rebollar-Alviter A., Juárez-Vázquez S.B., Aguirre-Rayo F., Silva-Rojas H.V., 2020. Multilocus identification and thiophanate-methyl sensitivity of *Colletotrichum gloeosporioides* species complex associated with fruit with symptoms and symptomless leaves of mango. *Plant Pathology* 69: 1125–1138.

Gadgil P.D., Dick M.A., Hood I.A., Pennycook S.R., 2005. *Fungi on Trees and Shrubs in New Zealand* (Vol. 4). Fungal Diversity Press.

Glass N.L., Donaldson G.C., 1995. Development of primer sets designed for use with the PCR to amplify conserved genes from filamentous ascomycetes. *Applied and Environmental Microbiology* 61: 1323–1330.

Guarnaccia V., Groenewald J.Z., Polizzi G., Crous P.W., 2017. High species diversity in *Colletotrichum* associated with citrus diseases in Europe. *Persoonia: Molecular Phylogeny and Evolution of Fungi* 39: 32–50.

Guarnaccia V., Gilardi G., Martino I., Garibaldi A., Gullino M.L., 2019. Species diversity in *Colletotrichum* causing anthracnose of aromatic and ornamental Lamiaceae in Italy. *Agronomy* 9: 613.

Guarnaccia V., Martino I., Tabone G., Brondino L., Gullino M.L., 2020. Fungal pathogens associated with stem blight and dieback of blueberry in northern Italy. *Phytopathologia Mediterranea* 59: 229–245.

Guarnaccia V., Martino I., Gilardi G., Garibaldi A., Gullino, M.L., 2021a. *Colletotrichum* spp. causing anthracnose on ornamental plants in Northern Italy. *Journal of Plant Pathology* 103: 127–137.

Guarnaccia V., Peduto Hand F., Garibaldi A., Gullino M.L., 2021b. Bedding plant production and the challenge of fungal diseases. *Plant Disease* in press, DOI:10.1094/PDIS-09-20-1955-FE.

Guerber J.C., Liu B., Correll J.C., Johnston P.R., 2003. Characterization of diversity in *Colletotrichum acutatum* sensu lato by sequence analysis of two gene introns, mtDNA and intron RFLPs, and mating compatibility. *Mycologia* 95: 872–895.

Gullino M.L., Gilardi G., Garibaldi A., 2017. Evaluating severity of leaf spot of lettuce, caused by *Allophoma tropica*, under a climate change scenario. *Phytopathologia Mediterranea*. 56: 235–241.

Hartung J.S., Burton C.L., Ramsdell D.C., 1981. Epidemiological studies of blueberry anthracnose disease caused by *Colletotrichum gloeosporioides*. *Phytopathology* 71: 449–453.

Hillis D.M., Bull J.J., 1993. An empirical test of bootstrapping as a method for assessing confidence in phylogenetic analysis. *Systematic Biology* 42: 182–192.

Katoh K., Standley D.M., 2013. MAFFT Multiple sequence alignment software version 7: improvements in performance and usability. *Molecular Biology and Evolution* 30: 772–780.

Kim W.G., Hong S.K., Choi H.W., Lee Y.K., 2009. Occurrence of anthracnose on highbush blueberry caused by *Colletotrichum* species in Korea. *Mycobiology* 37: 310–312.

Kumar S., Stecher G., Tamura K., 2016. MEGA7: Molecular Evolutionary Genetics Analysis version 7.0 for bigger datasets. *Molecular Biology and Evolution* 33: 1870–1874.

Liu F., Weir B.S., Damm U., Crous P.W., Wang Y., ... Cai L., 2015. Unravelling *Colletotrichum* species associ-

ated with Camellia: employing *ApMat* and *GS* loci to resolve species in the *C. gloeosporioides* complex. *Persoonia: Molecular Phylogeny and Evolution of Fungi* 35: 63.

Liu X., Zheng X., Khaskheli M.I., Sun X., Chang X., Gong G., 2020. Identification of *Colletotrichum* species associated with blueberry anthracnose in Sichuan, China. *Pathogens* 9: 718.

Nirenberg H.I., Feiler U., Hagedorn G., 2002. Description of *Colletotrichum lupini* comb. nov. in modern terms. *Mycologia* 94: 307–320.

Nylander J.A.A., 2004. MrModeltest v. 2. Program distributed by the author. Uppsala Evolutionary Biology Centre Uppsala University.

O'Donnell K., Cigelnik E., 1997. Two divergent intragenomic rDNA ITS2 types within a monophyletic lineage of the fungus Fusarium are nonorthologous. *Molecular Phylogenetics and Evolution* 7: 103–116.

O'Donnell K., Nirenberg H.I., Aoki T., Cigelnik E., 2000. A multigene phylogeny of the *Gibberella fujikuroi* species complex: detection of additional phylogenetically distinct species. *Mycoscience* 41: 61–78.

Pennycook S.R., 1989. *Plant Diseases Recorded in New Zealand. Volumes 1, 2 and 3.* Plant Diseases Division, DSIR.

Polashock J.J., Caruso F.L., Averill A.L., Schilder A.C., 2017. *Compendium of Blueberry Cranberry and Lingonberry Diseases and Pests*, 2nd edn. APS Press St. Paul.

Pszczółkowska A., Okorski A., Paukszo Ł., Jastrzębski, J., 2016. First report of anthracnose disease caused by *Colletotrichum fioriniae* on blueberry in western Poland. *Plant Disease* 100: 2167–2167.

Retamales J.B., Hancock J.F., 2018. *Blueberries*, 2nd edition. CABI, Wallingford, UK.

Rios J.A., Pinho D.B., Moreira W.R., Pereira O.L., Rodrigues F.A., 2015. First report of *Colletotrichum karstii* causing anthracnose on blueberry leaves in Brazil. *Plant Disease* 99: 157–157.

Romo-Muñoz R.R., Dote-Pardo J.D., Garrido-Henríquez H.G., 2019. Blueberry consumption and healthy lifestyles in an emerging market. *Spanish Journal of Agricultural Research* 17: e0111.

Ronquist F., Teslenko M., Van der Mark P., Ayres D.L., Darling A., … Huelsenbeck J.P., 2012. MrBayes 3.2: efficient Bayesian phylogenetic inference and model choice across a large model space. *Systematic Biology* 61: 539–542.

Shivas R.G., Yu Y.P., 2009. A taxonomic re–assessment of *Colletotrichum acutatum*, introducing *C. fioriniae comb. et stat. nov.* and *C. simmondsii* sp. nov. *Fungal Diversity* 39: e122.

Shivas R.G., Tan Y.P., Edwards J., Dinh Q., Maxwell A., ... Coates L.M., 2016. *Colletotrichum* species in Australia. *Australasian Plant Pathology* 45: 447–464.

Silva D.N., Talhinhas P., Várzea V., Cai L., Paulo O.S., Batista D., 2012. Application of the Apn2/MAT locus to improve the systematics of the *Colletotrichum gloeosporioides* complex: an example from coffee (Coffea spp.) hosts. *Mycologia* 10: 396–409.

Stephenson S.A., Green J.R., Manners J.M., Maclean D.J., (1997). Cloning and characterisation of glutamine synthetase from Colletotrichum gloeosporioides and demonstration of elevated expression during pathogenesis on *Stylosanthes guianensis*. *Current Genetics* 31: 447-454.

Swofford D.L., 2003. PAUP*. Phylogenetic analysis using parsimony (*and other methods) v. 4.0b10. Sinauer Associates Sunderland Massachusetts.

Verma N., MacDonald L., Punja Z.K., 2006. Inoculum prevalence, host infection and biological control of *Colletotrichum acutatum*: causal agent of blueberry anthracnose in British Columbia. *Plant Pathology* 55: 442–450.

Weir B.S., Johnston P.R., Damm U., 2012. The *Colletotrichum gloeosporioides* species complex. *Studies in Mycology* 73: 115–180.

Xu C.N., Zhou Z.S., Wu Y.X., Chi F.M., Ji Z.R., Zhang H.J., 2013. First report of stem and leaf anthracnose on blueberry caused by *Colletotrichum gloeosporioides* in China. *Plant disease* 97: 845–845.

Yoshida S., Tsukiboshi T., 2002. Shoot blight and leaf spot of blueberry anthracnose caused by *Colletotrichum acutatum*. *Journal of General Plant Pathology: JGPP* 68: 246.

Yoshida S., Tsukiboshi T., Shinohara H., Koitabashi M., Tsushima S., 2007. Occurrence and development of *Colletotrichum acutatum* on symptomless blueberry bushes. *Plant Pathology* 56: 871–877.

Phytopathologia Mediterranea
The international journal of the
Mediterranean Phytopathological Union

Firenze University Press
www.fupress.com/pm

Review

Viruses of cucurbit crops: current status in the Mediterranean Region

Nabil RADOUANE[1,2], Said EZRARI[1,2], Zineb BELABESS[3], Abdessalem TAHIRI[2,*], Rachid TAHZIMA[4], Sebastien MASSART[4], Haissam JIJAKLI[4], Meryem BENJELLOUN[1], Rachid LAHLALI[2,*]

[1] *Laboratory of Functional Ecology and Engineering Environment, Sidi Mohamed Ben Abdellah University, PO Box 2202, Route d'Imouzzer, Fez, Morocco*
[2] *Department of Plant Protection, Phytopathology Unit, Ecole Nationale d'Agriculture de Meknès, BP S 40, Meknès, Morocco*
[3] *Plant Protection Laboratory. INRA, Centre Régional de la Recherche Agronomique (CRRA), Oujda 60000, Qualipole de Berkane, Berkane 63300, Morocco*
[4] *University of Liège- Integrated and Urban Plant Pathology Laboratory, Gembloux Agro-Biotech (ULg), 5030 Gembloux, Belgium*
*Corresponding authors. E-mail: atahiri@enameknes.ac.ma; rlahlali@enameknes.ac.ma

Summary. Cucurbits are among the most cultivated crops, and the most economically important species are melon (*Cucumis melo* L.), cucumber (*Cucumis sativus* L.), watermelon (*Citrullus lanatus* Thumb.), squash (*Cucurbita pepo* L.), and pumpkin (*Cucurbita* spp.). These crops have become important income sources providing export and local consumption commodities in many Mediterranean countries. Increased area of cucurbits has led to the emergence of several viral diseases, which can have impacts on crop production and threaten agricultural sustainability. An overview of the most damaging cucurbit viruses in the Mediterranean area is provided to improve understanding of the diseases they cause and to emphasize effective disease management strategies. An updating of the geographical distribution of these viruses, the symptoms they cause and their means of transmission is also provided. Disease management methods and measures by farmers and phytosanitary authorities to address the virus outbreaks are outlined, including diagnostics, use of tolerant cultivars, and chemical and biological vector control. Mediterranean region farmers have learned many lessons from the damaging pandemics caused by cucurbit viruses, through the extensive published research, and this review provides a basis for managing future outbreaks of newly emerging virus infections.

Keywords. Alternative disease management strategies, whitefly-borne viruses, aphid-borne viruses, emerging diseases.

OPEN ACCESS

Citation: N. Radouane, S. Ezrari, Z. Belabess, A. Tahiri, R. Tahzima, S. Massart, H. Jijakli, M. Benjelloun, R. Lahlali (2021) Viruses of cucurbit crops: current status in the Mediterranean Region. *Phytopathologia Mediterranea* 60(3): 493-519. doi: 10.36253/phyto-12340

Accepted: August 31, 2021

Published: December 30, 2021

Data Availability Statement: All relevant data are within the paper and its Supporting Information files.

Competing Interests: The Author(s) declare(s) no conflict of interest.

Editor: Nihal Buzkan, Kahramanmaraş Sütçü Imam University, Turkey.

ORCID
NR: 0000-0002-1173-470X
SE: 0000-0003-3227-0948
RT: 0000-0002-0115-8366
RL: 0000-0002-1299-5733

INTRODUCTION

The *Cucurbitaceae* family includes more than 800 plant species in 120 genera (Welbaum, 2015), which are herbaceous plants, annuals or perennials, found in temperate and tropical regions. The most cultivated cucurbit crops in

the Mediterranean region are cucumber (*Cucumis sativus* L.), melon (*Cucumis melo* L.), watermelon (*Citrullus lanatus* Thunb.), pumpkin (*Cucurbita maxima* Duch. and *Cucurbita moschata* Duch.), and zucchini (*Cucurbita pepo* L.) (Robinson *et al*., 1997). Due to the economic importance of these crops, cucurbit-producing countries need to improve the quality and quantity of their production.

Cucurbits are threatened by a large number of pests and pathogens, including viruses. About 28 plant viruses are currently threatening cucurbit crop production in the Mediterranean region (Lecoq and Desbiez, 2012). The emergence of new virus diseases is now common the pathogens evolve and their genetic diversity increases. This is mainly due to the favourable Mediterranean conditions for virus vectors (mainly insects) to settle and reproduce. Ecosystem simplification, expanding trade, and movement are also important factors of virus dispersion, and vectors play important roles in virus evolution through pathogen dispersion in a variety of plants and zones. This leads recombination and genetic variation in the pathogens, and this continuous and evolutionary process has allowed viruses to adapt to their hosts, by integrating their most complex properties (Navas-Castillo *et al*., 2014; Pozzi *et al*., 2020).

Virus diseases have been emerging for decades among cucurbit species, causing economic and food security threats. These diseases are widely described and studied. The appearance of new viral species over time in several families is frequent (Juárez *et al*., 2019). The incidence and geographical distribution of these viruses increase and expand over time. It is worth noting that viral disease symptoms are variable and diverse and the majority of the viruses induce similar symptoms which makes their identification, based only on symptoms, a difficult task.

Cucurbit-producing countries annually report detection of new viruses or virus isolates. Common symptoms caused by cucurbit viruses include leaf mosaic and curling, and plant size reduction, severe wilting, deformation, discolouration, mottling, embossing, yellowing, and necrosis, symptoms which affect the aesthetic value and yields of produced cucurbit fruit (Blancard *et al*., 1994). The main symptoms observed on cucurbit crops grown in Morocco are illustrated in Figure 1.

Understanding the factors leading to virus disease emergence is the first step in their management, and innovative control strategies are now required. The best disease prevention and management strategies rely on knowledge of the viruses and their vectors (including biological properties and epidemiology), the application of prophylactic measures, and recourse to biological and chemical control methods when required.

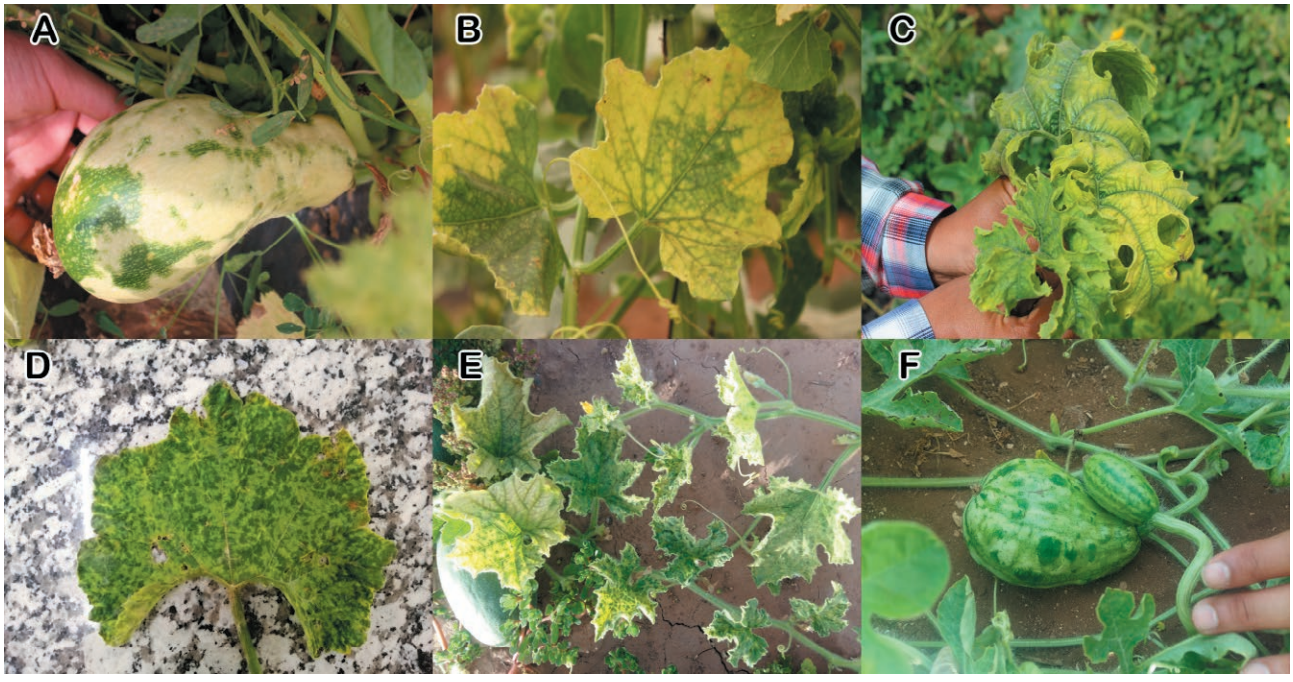

Figure 1. Symptoms of virus infections on several cucurbit crops. A. ToLCNDV affecting zucchini fruit, B. ToLCNDV affecting melon leaves C. ToLCNDV affecting zucchini leaf, D. ToLCNDV affecting squash leaf, E. Viral infection symptoms on melon leaves, and F. Viral infection symptoms on watermelon fruits.

This review emphasizes the current situation of the main virus diseases of cucurbits in the Mediterranean region. The viruses included are the most important since they cause significant losses in this area. Research is reviewed on virus genetic diversity, host ranges, transmission, biological properties, and the symptoms they cause. Genetic diversity and mutation and recombination of these pathogens are perceived as major driving forces in the evolution of viruses. Different detection and diagnostic methods are also summarized, which assist understanding of the virus genetic variability and taxonomy. Common strategies for management of cucurbit viruses are also reviewed, including prophylactic measures, pesticides, tolerant host varieties, and biological control.

Cucurbit crops are infected by a variety of viruses that belong to different families. *Geminiviridae* (especially *Begomovirus*) includes the greatest number of viruses reported to cause significant economic losses to cucurbit production (Lecoq and Desbiez, 2012). Other economically important viruses are in *Potyviridae, Bromoviridae,* and *Luteoviridae*. These include *cucurbit aphid-borne yellow virus* (CABYV), *watermelon mosaic virus* (WMV), *cucumber mosaic virus* (CMV), and *zucchini yellow mosaic virus* (ZYMV), which are reported in most Mediterranean countries and are associated with important economic production losses (Adams *et al*., 2011; Lecoq and Desbiez, 2012). Different types of insects act as vectors for cucurbit viruses, including aphids, leafhoppers, and whiteflies which have been the most reported, and these vectors transmit the majority of virus species that affect cucurbits. Several factors are involved in virus emergence through transmission by insects, including virus genetic variation and long-distance transport for trade of vegetables. These can spread viruses to new geographical regions with potential to infect new hosts (Navas-Castillo *et al*., 2011).

MAJOR VIRUSES THAT AFFECT CUCURBIT CROPS IN THE MEDITERRANEAN REGION

Begomoviruses

Tomato leaf curl New Delhi virus (ToLCNDV)

ToLCNDV (*Geminiviridae*, *Begomovirus*) is a bipartite begomovirus. The DNA strand of this virus encodes AV1 and AV2 genes in sense orientation of DNA-A, and AC1, AC2, AC3 and AC4 in the complementary sense orientation (Zaidi *et al*., 2017). ToLCNDV DNA-B encodes a nuclear shuttle protein NSR (Open reading frame BV1) and a movement protein MP (Open reading frame BC1). For both ToLCNDV components, virus genes are separated with an intergenic region that comprises a conserved sequence between DNA-A and DNA-B. This region is termed the common region (CR) (Zaidi *et al*., 2017).

ToLCNDV is the only bipartite *Begomovirus* with an extensive host range (Briddon *et al*., 2014). After the first report of this virus on tomato crops (*Solanum lycopersicum* L.) in India (Padidam *et al*., 1995), ToLCNDV was found to be associated with several cultivated plants, including cucurbit crops (watermelon, cucumber, melon, and squash) (Ruiz *et al*., 2016; Moriones *et al*., 2017).

When first described, ToLCNDV was limited to Asian countries including Pakistan, Thailand, Indonesia, Bangladesh, and the Indian subcontinent. Recently, the virus has spread to new geographical regions and has extended its host range. ToLCNDV is present in several countries, from the Middle East (Iran) to the Mediterranean Basin (Morocco, Algeria, Tunisia, Italy, and Spain) (Moriones *et al*., 2017; Kheireddine *et al*., 2019) (Figure 2).

ToLCNDV was spreading in the Mediterranean region during the period 2012 to 2017. It was first identified in Spain in 2012 in Murcia and Almeria provinces, causing leaf curl on cucurbit plants. In 2013, similar symptoms were observed on zucchini crops grown in Almeria (López *et al*., 2015). Severe damage was observed in 2015 in Tunisia on zucchini, melon, and cucumber crops. Symptoms consisted of severe yellowing and mosaic and curling of young leaves (Mnari-Hattab *et al*., 2015). These symptoms were observed on zucchini squash in Italy in 2015 (Panno *et al*., 2016). In Morocco, similar symptoms were observed in 2017, on zucchini crops grown in Agadir and Taroudant regions (Radouane *et al*., 2018). The virus was also reported in southern France in September 2020 on zucchini (EPPO, 2020; Desbiez *et al*., 2021). These reports suggest recent ToLCNDV introductions into North Africa and Southern Europe. This could be the result of several factors (e.g international trade, vector migration) which could be enhanced by climatic changes.

ToLCNDV is transmitted by the whitefly *Bemisia tabaci* Gennadius in a circulative and persistent manner (Sáez *et al*., 2016). Several genetically distinct but morphologically indistinguishable *B. tabaci* morphocryptic species were identified as vectors of ToLCNDV. The Middle East-Asia Minor 1 and Asia II 1/5/7 strains were reported to transmit the virus in different South Asian regions. However, different *B. tabaci* morphocryptic species were reported to spread the virus in the Mediterranean area. In Spain, ToLCNDV is transmitted by the Q1 cryptic species in tomato, melon, and zucchini crops (Moriones *et al*., 2017). Many ToLCNDV isolates can be

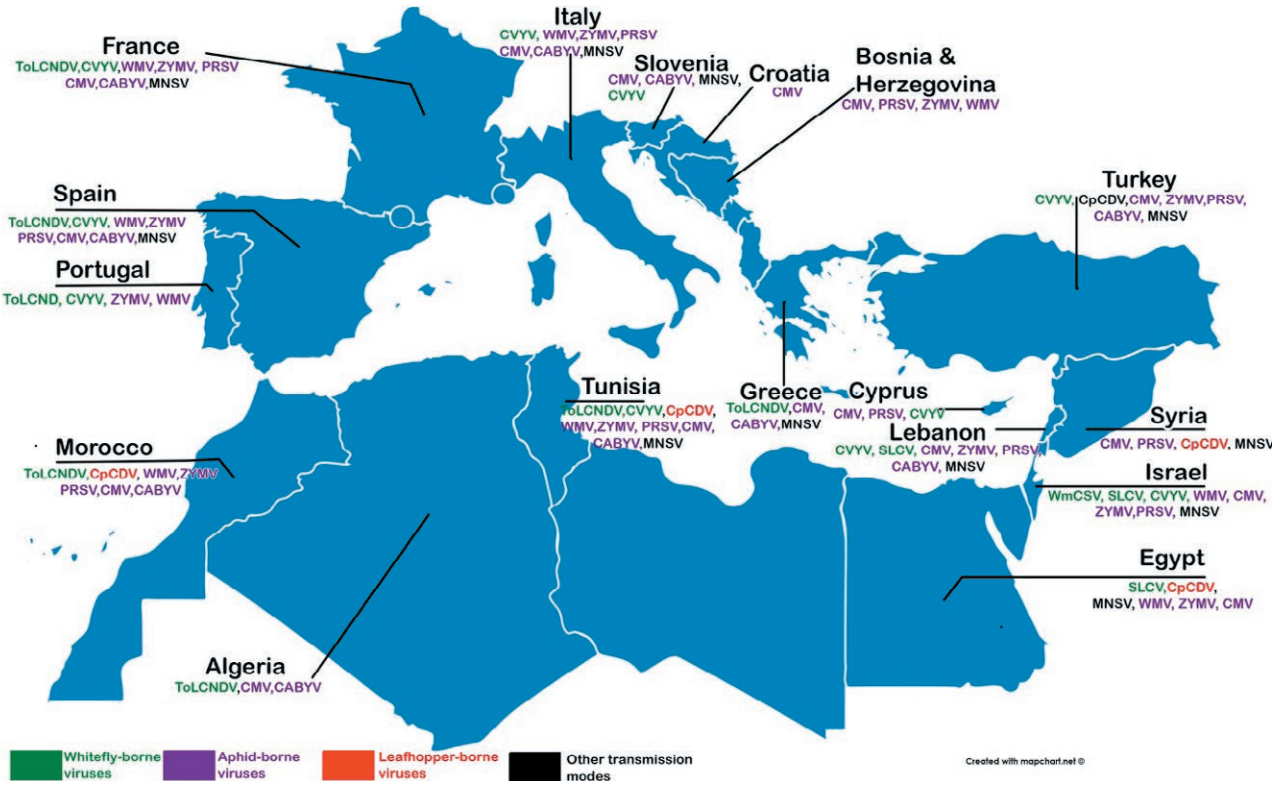

Figure 2. Geographic distribution of viruses affecting cucurbit crops in the Mediterranean region.

mechanically transmitted to several hosts. In Taiwan, ToLCNDV causes leaf curl and mosaic, and was reported to be sap transmitted to *Nicotiana benthamniana* Domin and some cucurbit crops including zucchini and cucumber (López *et al*., 2015).

Squash leaf curl virus (SLCV)

SLCV (*Geminiviridae*, *Begomovirus*) is a bipartite begomovirus. It has geminate particles of 22 x 38 nm (Cohen *et al*., 1983). The SLCV genome encodes genes in the virion (AV1, BV1) and complementary (AC1, AC2, AC3, AC4, BC1) senses (Abrahamian and Abou-Jawdah, 2013). SLCV was first reported in the United States of America (USA), in Texas (Isakeit, 1994). In the Mediterranean area (CABI/EPPO, 2014), SLCV has been recorded Lebanon (Sobh *et al*., 2012), Egypt (Mazyad, 2014), and Israel (Antignus *et al*., 2003). Its geographical distribution was extended to Asia (Jordan and Saudi Arabia), North America (Mexico, Arizona, and California), Central America, and the Caribbean (Guatemala) (CABI/EPPO, 2014) (Figure 2).

SLCV is restricted to cucurbit hosts, including *C. melo, C. sativus*, *C. lanatus, C. pepo, C. maxima,* and *C. moschata*. Cucurbit plants infected by SLCV show severe symptoms, including systemic stunting and leaf curling, and chlorosis and mosaic symptoms are observed on watermelon and squash (CABI, 2019). SLCV is naturally transmitted by *B. tabaci*, in a persistent manner (Cohen *et al*., 1983).

Watermelon chlorotic stunt virus (WmCSV)

WmCSV (*Geminiviridae*, *Begomovirus*) is a bipartite begomovirus. The structure and organization of the WmCSV genome are similar to those of the SLCV (Loebenstein and Lecoq, 2012). Symptoms caused by WmCSV have been observed on almost all cultivated cucurbits, and the virus causes severe damage to watermelon and melon (Abudy *et al*., 2010). WmCSV was first reported in Yemen, in 1986, on watermelon crops (Walkey *et al*., 1990), and was subsequently reported in Uganda, Sudan, Iran, Jordan, Oman, and Palestine (Bedford *et al*., 1994; Kheyr-Pour *et al*., 2000; Abudy *et al*., 2010; Al-Musa *et al*., 2011; Khan *et al*., 2012; Ali-Shtayeh *et al*., 2014). In 2002, the virus was isolated from watermelon fields, in Eilat, on the Red Sea coast. Despite eradication of entire crops where WmCSV was report-

ed, the virus quickly spread to many other regions. The first report of WmCSV in the Mediterranean basin was in Israel and Lebanon in 2010 (Samsatly *et al*., 2012). WmCSV has not been reported in other Mediterranean countries, although WmCSV outbreaks could occur in the Mediterranean region (Abudy *et al*., 2010; Lecoq and Desbiez, 2012) (Figure 2).

WmCSV infects watermelon and melon crops, and has also been recorded on snake cucumber (*C. melo* '*flexuosus*'), *C. moschata,* and wild cucurbits including *Citrullus colocynthis*, and *C. melo* '*agrestis*'. Symptoms include chlorotic mottling, vein yellowing, growth delay of young leaves, and reductions in fruit yield. Typical yellowing of shoot apices occurs on watermelon (Kheyr-Pour *et al*., 2000). WmCSV is transmitted by *B. tabaci* in circulative and persistent mode (Lecoq and Desbiez, 2012).

Potyviruses

Cucumber vein yellowing virus (CVYV)

CVYV (*Potyviridae*, *Ipomovirus*) has a single 9.7 kb filament (Janssen et al., 2005; Lecoq et al., 2000). CVYV was first reported in Israel by Cohen and Nitzany (1960). It has since been reported in the Mediterranean area (Spain, Portugal, Cyprus, and Tunisia) (Louro *et al*., 2004; Cuadrado *et al*., 2007; Yakoubi *et al*., 2007), in the Middle East (Lebanon, Iran, Jordan, and Turkey) (Mansour and Al-Musa, 1993; Bananej *et al*., 2007; Abrahamian *et al*., 2013), in France (Lecoq *et al*., 2007), and in Sudan (Martelli and Gallitelli, 2008).

CVYV infects several cucurbit hosts including *C. melo*, *C. sativus*, *C. pepo,* and C. *lanatus*. The virus was also identified in several weed species including *Sonchus oleraceus*, *S. asper, S. tenerrimus* (*Compositae*), *Convolvulus arvensis* (*Convolvulaceae*), *Ecballium elaterium* (*Cucurbitaceae*), and *Malva parviflora* (*Malvaceae*) (Janssen *et al*., 2002) (Figure 2). CVYV induces severe vein yellowing symptoms. Plant growth is also reduced following CVYV infection, causing crop yield losses (Cohen and Nitzany, 1960). Fruit from CVYV-infected cucumber plants expressed pale green mosaic symptoms. Watermelon plants infected with CVYV develop clearly visible leaf cracks. Infected melon plants have symptoms of thinning, necrosis, and retarded growth, with associated yield reductions. CVYV is a yield-limiting factor for cucurbit production in Spain, in single infections or infections with other viruses (Gil-Salas *et al*., 2012).

CVYV is transmitted by *B. tabaci* (Mansour and Al-Musa, 1993) in a semi-persistent manner, and this vector retains the virus for less than 6 h. Therefore, individuals moving to non-host plants may not remain viruliferous long enough to transmit the virus. *Aphis gossypii* Glover. and *Myzus persicae* Sulzer have not been reported as vectors of CVYV (Martelli and Gallitelli, 2008), and the virus was also reported to be mechanically transmitted.

Watermelon mosaic virus (WMV)

WMV (*Potyviridae*, *Potyvirus*) has flexuous and filiform morphology and particle length 730–780 mp. It is considered as one of the main viruses infecting cucurbit crops in temperate and Mediterranean regions. The virus causes serious diseases in legumes, orchids, and weeds (Desbiez *et al*., 2009; Lecoq and Desbiez, 2012).WMV was first reported in Israel in 1963 (Cohen and Nitzany, 1963). The virus was then reported in the USA (in 1965) (Rajbanshi and Ali, 2016), Yugoslavia (1967), Egypt (1969), Spain, Italy (1973), Tunisia (1975), France (1976), Bosnia and Herzegovina, China (2015), and Morocco (2016) (Radouane *et al*., 2020). WMV is currently considered one of the most widespread and severe cucurbit viruses in the Mediterranean region (Loebenstein and Lecoq, 2012). Foliar symptoms induced by WMV include mosaic, vein banding, deformation, blisters, and size reduction. Fruit from affected plants of some cultivars have severe discolouration and slight deformation. Necrosis of grafted watermelon fruits was caused by newly identified isolates reported from Italy (Crescenzi *et al*., 2001) (Figure 2). WMV can infect 170 plant species under experimental conditions, including watermelon, melon, zucchini, and squash (Wang and Li, 2017).

WMV transmission is has been demonstrated for at least 35 aphid species (in 19 genera), and transmission is in a non-persistent manner. *Aphis craccivora* Kock, *A. gossypii*, and *M. persicae* are considered as the most efficient vectors of WMV (Lecoq and Desbiez, 2008).

Zucchini yellow mosaic virus (ZYMV)

ZYMV (*Potyviridae*, *Potyvirus*) infects cucurbits plants, mainly squash, melon, and cucumber. High variability has been observed within ZYMV field isolates, which influences the expressed symptoms. Some isolates induced severe symptoms including mosaic, necrosis, and wilting, whereas others caused mild symptoms, while some ZYMV-infected plants remain asymptomatic. Trials to assess the resistance of some melon and squash cultivars to ZYMV have been conducted in the Mediterranean region, and these have indicated that 81 squash varieties show resistance to different ZYMV isolates (Pitrat and Lecoq, 1984; Desbiez *et al*., 2003).

ZYMV was first reported in Italy, in 1973 (Desbiez and Lecoq, 1997). In 1979, several melon crops were destroyed by this virus in southwestern France (Desbiez and Lecoq, 1997). Subsequently, ZYMV spread rapidly to other countries, including Lebanon (in 1979), Israel and Spain (1982), Egypt and Turkey (1983) (Desbiez and Lecoq, 1997), India (Verma *et al*., 2007), Argentina (Gracia, 2007), Ivory Coast (Koné *et al*., 2010), Pakistan (Ashfaq *et al*., 2015), Korea (Cho *et al*., 2019), China (Niu *et al*., 2015), and Morocco (Radouane *et al*., 2020) (Figure 2).

ZYMV mainly infects cucurbits (Lecoq and Desbiez, 2008), causing vein thinning, yellow mosaic, plant stunting, leaf deformation, and fruit mottling in melon plants following their infection by ZYMV (Pitrat and Lecoq, 1984; Desbiez and Lecoq, 1997). Squash plants manifest severe symptoms on the leaves. Fruit deformation is also observed, with external mosaic, necrotic cracks, and flesh hardening. Symptoms on cucumber and watermelon include severe mosaic on leaves and fruit deformations.

M. persicae and *A. gossypii* are the most efficient ZYMV vectors. They transmit the virus in a non-persistent mode. Recorded transmission rates for these aphids have been 41% for *M. persicae* and 35% for *A. gossypii* (Simmons *et al*., 2013). ZYMV seed-borne transmission has been demonstrated for: *C. pepo* '*styriaca*' (clamshell pumpkin), *C. pepo* subsp. *Texana* (Simmons *et al*., 2013), and squash (Coutts *et al*., 2011). Plants from infected seeds remain asymptomatic, and this makes diagnosis difficult, especially when standard serological tests are applied, and only Reverse Transcription-Polymerase Chain Reaction (RT-PCR) techniques can detect the virus in these plants (Simmons *et al*., 2013). In some tropical and subtropical regions, where cucurbits are planted throughout each year, ZYMV can easily switch from previous to new crops.

Papaya ring spot virus (PRSV)

The PRSV (*Potyviridae*, *Potyvirus*) genome is 9000 to 10,326 nts, and the virus particles are flexuous filamentous rod, and measuring 760-800 × 12 nm. The particles are encapsidated by a CP of 30 – 36 kD (Gogoi *et al*., 2019). PRSV isolates are classified into two main types; type P and type W. PRSV-P can infect papaya and cucurbit crop species, but PRSV-W infects only cucurbits (Cabrera Mederos *et al*., 2019).

PRSV occurs in many Mediterranean countries, including Cyprus, Lebanon, France, Spain, Syria, Tunisia, Bulgaria, Turkey, Italy, Israel (Papayiannis *et al*., 2005; Köklü and Yilmaz, 2006), and Morocco (Radouane *et al*., 2020). The virus was also reported in India, Brazil, Iran, Sudan, and Bangladesh (Pourrahim *et al*., 2003; Jain *et al*., 2004; Verma *et al*., 2006; Jadão *et al*., 2010) (Figure 2). The PRSV host range is isolate-dependent, and the virus infects many cucurbits, including melon, cucumber, zucchini, bottle gourd, bitter gourd, watermelon, and squash (CABI, 2020).

Aphids transmit PRSV, in non-persistent modes (dos Santos Martins *et al*., 2016), and approx. 21 aphid species have been reported to transmit the virus (Allan, 1980). These include *Acyrthosiphon malvae* (Mosley), *A. craccivora*, *A. fabae* Scopoli, *A. coreopsidis* Thomas, *A. gossypii*, *A. medicaginis* Koch, *A. nerii* Boyer de Fonscolombe, *A. rumicis* Linnaeus, *A. spiraecola* Patch, *Uroleucon sonchi* Linnaeus, *M. persicae*, *Pentalonia nigronervosa* Coquerel, *Rhopalosiphum maidis* (Fitch), *Toxoptera aurantii* (Boyer de Fonscolombe), and *T. citricidus* (Kirkaldy) (Allan, 1980).

Other virus genera

Cucumber mosaic virus (CMV)

CMV (*Bromoviridae*, *Cucumovirus*) was associated with the mosaic diseases of cucurbit crops in the early 20th century (Doolittle, 1916) in the USA. The CMV genome comprises three +ssRNA, with isometric particles containing 180 subunits, and diameter of 29 nm. Symptoms caused by the virus are variable, which makes diagnosis difficult. Use of Double Antibody Sandwich-Enzyme Linked ImmunoSorbent Assay (DAS-ELISA) was reported to ensure easy and quick diagnosis of the virus (Adams *et al*., 2011).

CMV was first reported 1916 in the USA, and the virus has since spread to several countries including those of the Mediterranean region, and is very common on cucurbit crops grown in temperate and Mediterranean areas (Lecoq and Desbiez, 2012) (Figure 2). CMV infects melon and squash, and can also infect weed species which play key roles in inoculum conservation after cucurbit crops have been harvested.

In melon and cucumber, CMV induced typical mosaic leaf symptom accompanied by plant stunting and yield reductions. Mottling and mosaic symptoms may also occur on fruit, and rapid and complete wilting can occur on adult cucumber plants. Symptoms of CMV in squash are more severe, including leaf mosaic, yellow spots, and deformations with plant stunting and decreased fruit yields. Watermelon infection by CMV is rare, but is manifested by appearance of dark necrotic lesions on fruit (Lecoq and Desbiez, 2012).

More than 60 aphid species, including *A. gossypii* and *M. persicae*, can transmit CMV (Kennedy *et al*., 1962). Acquisition of the virus by vectors takes at least

one minute, with the absence of a latency phase, and the vectors retain the virus for 4 h. CMV is not transmitted to vector progeny. CMV is seed transmitted in seed-producing squash varieties, and natural root grafting spread of CMV has been demonstrated in pepper crops (Mauck *et al.*, 2015).

Cucumber aphid-borne yellows virus (CABYV)

CABYV (*Luteoviridae, Polerovirus*) is a phloem-restricted virus, of approx. 5.7 kb, with virions of approx. 25 nm in diam. (Kassem *et al.*, 2007). CABYV was first reported in France, in 1992 (Lecoq, 1992). DAS-ELISA has been the most commonly used test for CABYV diagnoses in the Mediterranean region (Lecoq *et al.*, 1992). This virus has been reported in 15 Mediterranean countries, including Algeria, Turkey, Greece (Lecoq and Desbiez, 2012), Lebanon (Abou-Jawdah *et al.*, 1997), Spain (Juarez *et al.*, 2004), Italy (Tomassoli and Meneghini, 2007), Tunisia (Mnari-Hattab *et al.*, 2009), Morocco (Aarabe *et al.*, 2018), and Slovenia (Mehle *et al.*, 2019). In Spain, CABYV incidence was determined in 924 melon and squash samples collected during 2003 to 2004. The virus was detected in 83% of melon crops and 66% of squash crops. In Tunisia, CABYV incidence was approx. 70% in 330 cucurbit samples collected between 2000 and 2004 (Mnari-Hattab *et al.*, 2009). The virus was has also been reported outside the Mediterranean region, especially in Iran, China, Saudi Arabia, Pakistan, Tanzania, the USA, Czech Republic, Serbia, Korea, and India (Lemaire, 1993; Bananej *et al.*, 2006; Xiang *et al.*, 2008; Svoboda *et al.*, 2011; Vučurović *et al.*, 2011; Al-Saleh *et al.*, 2015; Choi and Choi, 2016; Desbiez *et al.*, 2016; Suveditha *et al.*, 2017; Ahsan *et al.*, 2020) (Figure 2).

CABYV has a wide, mostly cucurbit, host range, but can also infect fodder beet and lettuce (Lecoq *et al.*, 1992). The main cucurbit species infected with this virus are cucumber, melon, squash, watermelon, and pumpkin. Symptoms include yellowing of old leaves that progressively thicken and become brittle, and severity of symptoms depends on host cultivar, varying from limited yellowing of a few old leaves to complete discolouration of whole plants (Lecoq *et al.*, 1992).

CABYV incidence depends on the host growing conditions, and crop yields can be reduced by 50% from cucumber and 15% from melon (Lecoq, 1999).

Fruit quality is not affected by CABYV infections. However, the virus can cause flower abortion, resulting in reductions of numbers of fruit per plant (Lecoq *et al.*, 1992). CABYV is transmitted by *A. gossypii, M. persicae* and *M. euphorbiae* Thomas, with persistent modes (Lecoq *et al.*, 1992; Dogimont *et al.*, 1996).

Chickpea chlorotic dwarf virus (CpCDV)

CpCDV (*Geminiviridae*, *Mastrevirus*) is a circular monopartite virus with a ssDNA genome of approx. 2.5–2.7 kb (Khalid *et al.*, 2017). All mastreviruses infecting chickpea, isolated from Africa, Australia, and Asia with at least 78% nucleotide sequence similarity were considered as one species, CpCDV (Muhire *et al.*, 2013; Marwal *et al.*, 2014).

Symptoms induced by CpCDV are similar to those caused by other mastreviruses. These include host stunting, yellowing, necrosis, and leaf curling (Marwal *et al.*, 2014). CpCDV was first reported in chickpea plants in India (Horn *et al.*, 1993), and has since spread widely. The virus has been reported in Asia (Pakistan, Iran), Africa (Morocco, Tunisia, Egypt, Burkina Faso, Sudan, South Africa, Nigeria, Eritiria), the Middle East (Yemen, Turkey, Syria, Oman), and Australia (Kraberger *et al.*, 2013, 2015; Zaagueri *et al.*, 2017; Kanakala and Kuria, 2019; Radouane *et al.*, 2019) (Figure 2). In addition to chickpea, the virus was reported to infect other hosts, including watermelon, zucchini, and tomato (Kumari *et al.*, 2006). A high rate of infection with CpCDV (100%) has been demonstrated when the virus infects before host flowering.

Studies to identify CpCDV vector(s) have been conducted in different countries. In Pakistan, two aphids (*A. craccivora* and *M. persicae*) and two leafhoppers (*Empoasca devastans* Distant. and *Orosius albicinctus* Distant.) were assessed. Transmission tests showed that only the leafhopper *O. albicinctus* transmitted CpCDV. The presence of CpCDV in the inoculated plants and *O. albicinctus* was confirmed by DAS-ELISA using specific polyclonal antibodies (Horn *et al.*, 1993). Studies in Iran showed that *O. orientalis* efficiently transmitted CpCDV to numerous plant species belonging to *Chenopodiaceae*, *Fabaceae*, and *Solanaceae*. Symptoms reported on plants tested for CpCDV transmission by *O. albicinctus* were similar in tested plants for CpCDV transmission by *O. orientalis* (Farzadfar *et al.*, 2009). A minimum period of 5 min has been reported for CpCDV acquisition by *O. orientalis*, and the latency phase lasts 3 h. The vector can retain CpCDV for 17 d until the vector dies, and efficiency of CpCDV transmission is positively correlated with the number of insect vectors feeding on an infected plant (Hamed, 2007). CpCDV is not mechanically transmitted, but can be transmitted by *Agrobacterium* spp. to the plants in the laboratory (Adams *et al.*, 2011).

Melon necrotic spot virus (MNSV)

MNSV (*Tombusviridae, Carmovirus)* is an isometric phytovirus of 30 nm with a single-stranded RNA

genome. MNSV causes heavy damage in open fields and in cucumber and melon crops under shelter. The virus has spherical morphology, with a positive sense single RNA molecule. Its genome is approximately 4,266 nts (Mackie *et al*., 2020).

MNSV was first reported Japan in 1966 (Kishi, 1966). It has since been reported in Asia, America, Europe (Yakoubi *et al*., 2008), and Mediterranean countries, including Lebanon, Syria, Israel, Turkey, Greece, France, Italy, Spain, and Tunisia (CABI and EPPO, 2010). The virus was also been reported in the Netherlands, USA, Brazil, Panama, Guatemala, and China (Choi *et al*., 2003; Jordá *et al*., 2005; Herrera *et al*., 2006; Yu *et al*., 2016; Moura *et al*., 2018) (Figure 2). MNSV has a narrow host range. It does not infect all *Cucurbitaceae* species, and melon, cucumber, and watermelon are the main MNSV hosts (Gonzalez-Garza *et al*., 1979).

In watermelon, cucumber, and melon, MNSV causes leaf necroses, and streaks on the stems, and also kills infected plants. The virus can cause significant economic losses in melon. Infected fruits have decreased sugar contents and also develop necrotic spots (Kido *et al*., 2008). MNSV is very common in hydroponic crops because the virus is mainly transmitted by the fungus *Olpidium bornovanus* (Sahtiy.) Karling (Riviere *et al*., 1989).

MNSV is generally introduced into new areas by transport of infected plant debris or as virions carried by surface water in irrigation or precipitation. The virus is very stable and can remain viable in the soil for up to several years (Gosalvez *et al*., 2003). This virus is also seed- and soil-transmitted, and can be mechanically transmitted under artificial conditions (Ohshima *et al*., 2000). Seed transmission poses a serious risk for MNSV dissemination (Kubo *et al*., 2005).

FACTORS AFFECTING EMERGENCE OF CUCURBIT VIRUSES

Several definitions of emerging viruses exist. A virus is considered to be emerging when it occupies a new zone or a new niche. Several cucurbit viruses were reported to from cucurbit crops during the last decade, but a majority did not constitute real danger to cucurbit production due to the presence of resistant cultivars. This is the case for ZYMV and WMV (Rojas and Gilbertson, 2008; Lecoq and Katis, 2014). However, recently introduced ToLCNDV, or CpCDV, that have evolved to affect cucurbits crops in the Mediterranean region, are affecting cucurbit production in the region. Lecoq & Katis (2014) showed that the number of viruses that infect cucurbits crops has increased since 2003 from 55 to 70 in 2014, and some of these viruses can cause severe symptoms and major cucurbit yield losses. However, not all the viruses were widespread in the region. Some virus species were limited to some geographical zones, while others were having minor economic importance, or were limited to specific cropping systems. Among the long-established viruses that still cause important agronomic impacts is the aphid transmitted virus CMV; while the whitefly transmitted viruses also becoming major problems in the region (Desbiez, 2020).

Several factors have contributed to emergence of new virus species in the Mediterranean region. These include the rapid expansion of international seeds and plant trades, movement of crop plants away from their domestication centres to be cultivated elsewhere as monocultures, issues from seed production by multinational seed companies, and from free trade. These factors have increased the risks of seed crop infections with seed-borne viruses that can emerge into the local crops and vegetation. Difficulties in management of virus diseases due to climate instability and global warming are also important (Jones, 2021).

Climatic changes have also affected viruses and vectors leading to the emergence of new virus species or new strains of regionally established viruses. Changes in the hormonal and physiological defense systems in plants and changes in virus virulence from DNA/RNA mutations were also affected by the environment. Temperature increases have not affected some viruses. However, observation of CVYV infection was suggested to have increased with high temperatures in cucumber crops, but for vectors, high temperatures increase insect activity, which probably increased virus transmission in open fields (Velasco *et al*., 2020). Movement of pests and pathogens has possibly increased with increasing temperatures, due to "global warming driven pest movement" (Bebber *et al*., 2013).

Table 1 provides an overview of the most known viruses associated with cucurbit crops.

VIRUS EVOLUTION IN CUCURBIT CROPS

Much research indicates that virus multiplication generates new variants (Hull, 2014), with variability resulting from errors during copying processes of virus genomes. These mutations can then be redistributed by recombination (Roossinck, 1997). Since the generation time of viruses is short compared to that for hosts and/or vectors, and because large numbers of virus descendants are produced in each generation, evolution is discernible

Table 1. Taxonomy, virion shape, host range, and origin of detection of viruses inducing diseases on cucurbit crops.

Family	Genus	Virus species	Virion shape	Vector	Cucurbit host species	Geographical origin	First description	First report
Geminiviridae	*Begomovirus*	*Tomato leaf curl New Delhi virus* (ToLCNDV)	Twinned (Geminate)	*Bemisia tabaci*	*Citrullus lanatus* *Cucumis sativus* *Cucumis melo* *Cucurbita pepo*	India	1995	Padidam *et al.*, 1995
		Watermelon chlorotic stunt virus (WmCSV)	Twinned (Geminate)	*Bemisia tabaci*	*Citrullus lanatus* *Cucumis melo* *Cucurbita moschata* *Citrullus colocynthis*	Yemen	1990	Walkey *et al.*, 1990
		Squash leaf curl virus (SLCV)	Twinned (Geminate)	*Bemisia tabaci*	*Cucumis melo* *Cucumis sativus* *Citrullus lanatus* *Cucurbita pepo* *C. maxima* *C. moschata*	Texas	1994	Isakeit, 1994
	Mastrevirus	*Chickpea chlorotic dwarf virus* (CpCDV)	Twinned (Geminate)	*Aphis craccivora* *Myzus persicae* *Empoasca devastans* *Orosius albicinctus*	*Citrullus lanatus* *Cucurbita pepo* *Cucumis sativus*	India	1993	Horn *et al.*, 1993
Potyviridae	*Ipomovirus*	*Cucumber vein yellowing virus* (CVYV)	Flexuous filaments with no envelope	*Bemisia tabaci*	*Cucumis sativus* *Cucumis melo* *Citrullus lanatus* *Cucurbita pepo*	Israel	1960	Cohen and Nitzany, 1960
	Potyvirus	*Watermelon mosaic virus* (WMV)	Flexuous filaments with no envelope	*Aphis craccivora* *Aphis gossypii* *Myzus persicae*	*Citrullus lanatus* *Cucurbita pepo* *Cucumis melo* *Cucurbita moschata*	Israel	1963	Cohen and Nitzany, 1963
		Zucchini yellow mosaic virus (ZYMV)	Flexuous filaments with no envelope	*Aphis gossypii*	*Cucurbita pepo* *Citrullus lanatus* *Cucumis sativus*	Italy	1973	Lisa *et al.*, 1981
		Papaya ring spot virus (PRSV)	Flexuous filaments with no envelope	Aphid species	*Cucumis sativus* *Cucumis melo* *Cucurbita pepo* *Citrullus lanatus* *Cucurbita moschata*	India	1948	Yeh, 1984
Bromoviridae	*Cucumovirus*	*Cucumber mosaic virus* (CMV)	Spherical/ Quasi-spherical	Aphid species	*Cucumis sativus* *Cucumis melo* *Cucurbita pepo* *Citrullus lanatus*	United States	1916	Doolittle, 1916
Luteoviridae	*Polerovirus*	*Cucumber aphid-borne yellows virus* (CABYV)	Hexagonal in outline with no envelope	*Aphis gossypii* *Myzus persicae* *Macrosiphum euphorbia*	*Cucumis sativus* *Cucumis melo* *Cucurbita pepo* *Citrullus lanatus*	France	1992	Lecoq, 1992
Tombusviridae	*Carmovirus*	*Melon necrotic spot virus* (MNSV)	Icosahedral	*Olpidium bornovanus*	*Cucumis melo* *Citrullus lanatus* *Cucumis sativus* *Citrullus vulgaris*	Japan	1966	Kishi, 1966

process (Astier *et al.*, 2001). Mutations are generated by polymerase errors when synthesizing new nucleic acid molecules (García-Arenal *et al.*, 2001; Pita and Roossinck, 2007). These errors result in imperfect copies of genetic material from parents to progeny (Acosta-Leal *et al.*, 2011). These alterations correspond to punctual

errors which generally appear in three forms: substitution, insertion, or deletion of nucleotide bases (Smith and Inglis, 1987). Unlike mutations, the molecular changes caused by recombination are induced by incorporation of one or more nucleotides from another genome or from another genomic region. Recombination is a molecular process by which nucleotide sequences are exchanged. New combinations of genetic material can thus be generated within a genome when the parents are genetically different (Nagy and Simon, 1997; Vuillaume *et al*., 2011). Recombination probably makes important contributions to evolution and epidemiology of viruses infecting plants and animals (Burke, 1997; Padidam *et al*., 1999; Froissart *et al*., 2005; He *et al*., 2009). Pseudorecombination ("reassortment"), is different from recombination. It is a process whereby entire components of multipartite viruses (with genome divided into at least two segments) are exchanged between variants, strains, or species (Martin *et al*., 2011). By extrapolation, pseudo-recombination can also include virus/satellite associations (Briddon *et al*., 2001). Satellites are small circular ssDNAs with sizes of approx. 1.3 kb. These are associated with some (but not all) Eastern Hemisphere monopartite begomoviruses. Satellites are divided into two types; beta- and alpha-satellites (Briddon *et al*., 2001). The points discussed above show that mutation, recombination, and pseudo-recombination together generate significant genomic diversity, which can potentially lead to the emergence of viruses with new phenotypic characters.

The mutation frequency analysis by Juárez *et al*., (2019) for ToLCNDV virus strains from different geographical locations in Spain showed average mutation frequency rates (mutations/nucleotide) of 6.5×10^{-3} to 5.7×10^{-3} for both DNA components. This could explain the genetic diversity of ToLCNDV populations and indicate that wild plants could be the key driving ToLCNDV evolution.

Changes in vector transmission of some cucurbit viruses has been reported through recombination. This was the case for CABYV, an RNA virus, for which (Costa *et al*., 2020) reported that the recombinant CABYV isolate was transmitted by the whitefly *B. tabaci* MEAM1, rather than *A. gossipii*. Furthermore, a DNA mastrevirus infecting dicotyledonous plants was able to recombine. The first report of mixed infection by a mastrevirus and a begomovirus was in 2012 in *Xanthium strumarium* L. A recombination event was also reported between CpCDV and *Cotton leaf curl Burewala virus* (CLCuBuV) under experimental conditions the exchange of the CP of CpCDV by that of CLCuBuV resulted in the CpCDV-CLCUBuV recombinant which was whitefly transmitted, whereas CpCDV was transmissible by leafhopper species (Khalid *et al*., 2017).

For DNA viruses in mixed infections, DNA-A and DNA-B components of ToLCNDV interact with a variety of virus and betasatellite diseases (Shah Nawaz-Ul-Rehman and Fauquet, 2009; Zaidi *et al*., 2017). ToLCNDV can interact with betasatellites associated with other begomoviruses, thus expanding its host range. However, the mechanisms of these interactions remain unknown (Zaidi *et al*., 2017). A pseudorecombination event has been detected between two distinct begomoviruses under natural conditions, between the severe ToLCNDV strain and the Varanasi strain of *Tomato leaf curl Gujarat virus* (ToLCGV) which causes severe leaf curl of tomato in India (Chakraborty *et al*., 2008). In Spain, genetic analysis showed that the new strain of ToLCNDV spreading in that country resulted from recombination events (Fortes *et al*., 2016). The effect of the pseudo-recombination event between ToLCNDV and ToLCGV on viral pathogenesis was first demonstrated experimentally, and the recombinant virus was associated with severe pathogenicity. A similar effect was also observed in a recombinant between ToLCNDV and isolates of the begomovirus *Tomato leaf curl Palampur virus* (ToLCPMV) (Moriones *et al*., 2017).

ToLCNDV infects tomato, which is the main host crop for numerous *Tomato yellow leaf curl disease* (TYLCD)-associated viruses. The possible occurrence of mixed infections by ToLCNDV and TYLCD-associated begomoviruses either in tomato or cucurbits constitutes a serious threat for these crops, because begomoviruses are prone to recombination (Fortes *et al*., 2016). The recombination event has also been shown to be frequent within SLCV isolates under natural conditions, and occurs in DNA-A and DNA-B components. Most SLCV recombinants infect hosts other than cucurbits, indicating that recombination plays a major role in virus host ranges (Hassan, 2019). In Indonesia, ToLCNDV was reported to be recombinant with the *Squash leaf curl China virus* (SLCCNV) under natural conditions. Phylogenic analysis based on the AV1 gene has shown that ToLCNDV has clustered with SLCCNV (Wilisiani *et al*., 2019).

Pseudo-recombination has been produced in the laboratory, between closely related begomoviruses such as *Tomato golden mosaic virus* (TGMV), *Bean golden mosaic virus* (BGMV), and SLCV, by reassortment of their genome components (Chakraborty *et al*., 2008). The begomoviruses WmCSV and ToLCPMV have also been shown to possibly pseudo-recombine under experimental conditions (Esmaeili *et al*., 2015). The replication protein of DNA-A of one virus bound to the DNA-B of the other to induce systemic symptoms.

The RNA virus CABYV was shown to result from a recombination event between ancestors of CABYV and

MABYV in Taiwan (Knierim *et al*., 2010). This virus was reported to be transmitted by whiteflies in Brazil, rather than by aphids. Since whiteflies are the most frequent vectors of plant viruses, and because of the dominant crop production in Brazil, the virus was named recombinant CABYV-M1. This virus had new properties; it was spread throughout Brazil, and it was not able to infect several cucurbits (*C. lanatus, C. sativus* and *L. sativa*) which were known hosts of the common type CABYV. The recombinant CABYV was able to overcome the resistance of *C. melo* 'TGR 1551' that was reported to be resistant to common CABYV. Therefore, the virus was reclassified as *Cucurbit Whitefly Borne Yellow virus* (Costa *et al*., 2019, 2020). Recombinations between subgroups of CMV has been widely reported under natural conditions. The different strains of CMV were classified into three main subgroups (IA, IB, and II) (Bonnet *et al*., 2005; Ouedraogo *et al*., 2019), notably in Spain with the prevalence of recombination events in RNA3. However, phylogenic analysis of Polish CMV isolates belonging to subgroups IA and II have revealed the prevalence of subgroup II, with detection of a new recombinant with the IA-MP/II-CP pattern (Hasiów-Jaroszewska *et al*., 2017). CMV showed recombination between two strains (A and B), which followed the exchange of 3A and CP in RNA3 and the formation of hybrid 1a and 2a in RNA1 and 2 (Sztuba-Solińska *et al*., 2011). Inoculations with two CMV isolates and *Tomato aspermy virus* (TAV) showed establishment of a recombination event across RNA3 in co-infected plants under experimental conditions. Precise homologous recombination had occurred at several RNA3 sites (Morroni *et al*., 2013). In Tunisia, many isolates of CMV have shown pseudo-recombination, mostly IB-IA-IA and IB-IA-IB in pepper crops. Fifty-five of 57 isolates were able to break host resistance when tested against polygenic resistance to CMV movement in pepper, which indicates that resistance was not a good strategy for control of CMV in Tunisia (Ben Tamarzizt *et al*., 2013). The reported recombination events in ZYMV and WMV were limited to the same species. Most recombination events reported in ZYMV were limited to P1, CI, HC-Pro, P3, CP, and NIb regions under natural conditions. Those described in WMV were in the N-terminal part of the CP and CI coding regions (Desbiez *et al*., 2011; Maina *et al*., 2019).

METHODS FOR DETECTING CUCURBIT VIRUSES

Serological techniques: Enzyme-linked Immunosorbent Assays (ELISA)

ELISA (Enzyme Linked Immunoabsorbent Assay) has become widely accepted as an immunodetection method. These assays provide high sensitivity, ease of use, rapidity, and the ability to quantify pathogen biomass in plant tissues and other matrices (Miller and Martin, 1988). The technique consists of the detection of viruses via their capsid proteins or of proteins coded by each virus that remain specific. The principle of this technique is based on the antibody-antigen pair, which is an immune defense where the virus plays the role of antigen. The most widely used serological technique involves Enzyme-linked Immunosorbent Assays (ELISA).

ELISA methods, including double antibody sandwich (DAS) ELISA, direct tissue blot immunoassay (DTBIA), and tissue-print (TP) ELISA, are the most commonly used, and several modifications have been made to the technique, including antigen-coated plate enzyme-linked immunosorbent assays (ACP-ELISA) (Mehetre *et al*., 2021).

In a polystyrene plate, the wells are first coated with an anti-CP antibody. Excess antibody is then washed away leaving the antigen-anti-CP antibody complex. A second antibody conjugated antibody-CP is then applied, obtaining the antigen-antibody conjugate complex. Each antigen is thus surrounded by two antibodies, one at the base and one at the apex. Following this coupling, an enzyme reacts with an added substrate that stains the solution yellow, and the optical density of the solution is then visualized by a spectrophotometer (Miller and Martin, 1988) (Table 2).

This technique is commonly used in many diagnoses and analyses, and especially for virus detection, and the sensitive and specific technique rapidly produces results. It is also very practical, and sensitivity increases depending on the type used. However, direct and indirect types have two main disadvantages; direct types can give a false positive results and indirect types have problems of immobilization and non-specific reactions (Aydin, 2015).

Nucleic acid-based methods

Polymerase chain reaction (PCR) and reverse transcription-PCR

PCR is a technique for *in vitro* amplification and visualization of fragments of specific genomes. Four main elements must be available, including DNA, DNA polymerase, $MgCl_2$, and primers which are the initiators of amplification (replication). Primers are comprised of approx. 10 to 30 bases. Their position in the viral genome delimits the size of the fragment to be amplified (Table 3). The PCR takes place in three phases: denaturation, hybridization, and elongation. At the level of

Table 2. Serological tests, based on ELISA and its modified methods, used for detection of cucurbit-associated viruses.

Virus name	Host plants	ELISA based methods	References
Tomato leaf curl New Delhi virus (ToLCNDV)	Luffa Tomato	Double antibody sandwich enzyme-linked immunosorbent assay (DAS-ELISA) Triple antibody sandwich enzyme-linked immunosorbent assay (TAS-ELISA)	Mantilla Paredes, 2018; Zubair *et al.*, 2020
Chickpea chlorotic dwarf virus (CpCDV)	Chickpea	DAS-ELISA Dot-blot ELISA Direct antigen-coating DAC-ELISA	Kumari *et al.*, 2006
Watermelon chlorotic stunt virus (WmCSV) *Squash leaf curl virus* (SLCV)	Watermelon Squash	DAS-ELISA	Ahmad *et al.*, 2018
Watermelon mosaic virus (WMV)	Melon	DAS-ELISA	López-Berenguer *et al.*, 2021
Cucurbit aphid-borne yellows virus (CABYV)	Zucchini Watermelon	DAS-ELISA	Radouane *et al.*, 2020
Zucchini yellow mosaic virus (ZYMV)	Squash Melon Watermelon	DAS-ELISA	Tripathi *et al.*, 2021
Melon necrotic spot virus (MNSV)	melon Cucumber Zucchini	TAS-ELISA DAS-ELISA	Miras *et al.*, 2020; Torre *et al.*, 2020
Cucumber vein yellowing virus **(CVYV)**	Cucumber Melon	DAS-ELISA	Desbiez *et al.*, 2019
Papaya ringspot virus (PRSV)	Papaya Melon Watermelon	DAS-ELISA DAC-ELISA	Hartati *et al.*, 2020; Kumar *et al.*, 2021
Cucumber mosaic virus (CMV)	Squash	Plate-trapped antigen ELISA PTA-ELISA	Nascimento *et al.*, 2017

reverse transcription (RT), there is synthesis of a complementary DNA (cDNA) from one RNA strand by the action of a reverse transcriptase enzyme (DNA polymerase, RNA-dependent). This technique is mainly used for the identification and detection of RNA viruses, transforming their genomes into cDNA which is the basic material for completion of PCR tests.

Several PCR tests have been used to detect phytoviruses, such as the use of specific primers (dual priming oligonucleotide; DPO) (Table 4). The primers give high levels of specificity and sensitivity. The difference between conventional primers and DPO primers is structural; primers consist of two separate primer segments bridged by polydeoxyinosine linkers with a low melting temperatures (Kwon *et al.*, 2014).

Loop-mediated isothermal amplification (LAMP)

The loop-mediated isothermal amplification (LAMP) method is a rapid technique for DNA amplification using specific primers, and DNA polymerases with strand displacement activity (Kuan *et al.*, 2010). The technique is highly sensitive and cost-effective, which could be used in daily routine tests, and especially *in situ* testing of crop pathogens (Waliullah *et al.*, 2020).

The LAMP method is an auto-cycling strand displacement DNA synthesis using four to six primers, which bind with high specificity to the targets, and the amplified products can then be visualized using gel electrophoresis, or by intercalating dyes such as SYBR Green I, or using a real-time quantitative measurements. LAMP is an important technology for use in laboratory or field conditions. LAMP has also addressed the limitations of qPCR and PCR, that require specific equipment and reagents that are often not available in poorly resourced laboratories or in the field (Waliullah *et al.*, 2020).

LAMP has been widely used to detected important DNA viruses, such as SLCV (Kuan et al., 2010), and for RNA viruses including *Cucurbit chlorotic yellows virus* (*Closteroviridae*; *Crinivirus*; CCYV) (Okuda *et al.*, 2015), CMV (Bhat *et al.*, 2013) and *Cucumber green mottle mosaic virus* (*Virgaviridae* ; *Tobamovirus* ; CGMMV) (Li *et al.*, 2013). Bhat *et al.*, (2013) compared the detection sensitivity of CMV on black pepper using RT-LAMP, RT-PCR and qRT-PCR. They showed that detection sensitivity of CMV with RT-LAMP was 100 times

Table 3. Primers used for the detection of viruses.

Virus	Primer name	Sequence (5'-3')	Amplicon size (bp)	Annealing temperature	Source
ToLCNDV	A1-F A1-R	ACCAACAGGCCGATGAACA TTCCCACTATCTTCCTGTGCA	750	55°C	Radouane *et al.*, 2018
	To-B1F To-B1R	GAAACACAAGAGGGCTCGGA GCTCCACTATCAAAGGGC GT	677	55°C	Sáez *et al.*, 2016
WmCSV	WmA150F WmA 1350R	GTCAGTATGTGGGATCCATTGC GCAAATACGATTCAACCACAACC	1201	57°C	Ali-Shtayeh *et al.*, 2014
	WmB672F WmB2000R	CGCCGTTGCCTGGAGGATGTTCAC GCAGCACAGGCTGCCTTCACCTTC	1329	65°C	Ali-Shtayeh *et al.*, 2014
SLCV	SqA2F SqA1R	TATCTCCCATCTTGGCAAGG AGCTGTATCTTGGGCAACAGA	601	55°C	Sobh *et al.*, 2012
CpCDV	CpCDV-SEQ2 CpCDV-Tu-1145-R	CGACACATAAGGTTCAGGTTG AGGCAACCCTTGGGAGTCA	544	55°C	Radouane *et al.*, 2019
CVYV	CV- CV+	GCGCCGCAAGTGCAAATAAAT AGCTAGCGCGTATGGGGTGAC	450	55°C	EPPO, 2007
WMV	WMV-5 WMV-3	GGCTTCTGAG CAAAGATG CCCAYCAACTG TYGGAAG	408	55°C	Desbiez *et al.*, 2007
ZYMV	GK ZYMV F1 GK ZYMV R2	ATAGCTGAGACAGCACT CGGCAGCRAAACGATAACCT	1004	57°C	Nagendran *et al.*, 2017
PRSV	GK PRSV F GK PRSV R	GCAATGATAGARTCATGGGG AAGCGGTGGCGCAGCCACACT	1267	61°C	Nagendran *et al.*, 2017
CMV	GK CMV F GK CMV R	GAGTTCTTCCGCGTCCCGCT AAACCTAGGAGATGGTTTCA	1218	54 °C	Nagendran *et al.*, 2017
CABYV	CE9 CE10	GAATACGGTCGCGGCTAGAAATC CTATTTCGGGTTCTGGACCTGGC	600	58°C	Wilson *et al.*, 2012
MNSV	VP 51-2 VP 51-1	TGGATCCGGTAGTAGGAATG TTTACCCACAGTGAAGCTTCG	405	47 °C	Navarro *et al.*, 2006

Table 4. DPO primer list.

Virus	Primer name	Sequence (5'-3')	Amplicon size (bp)	Annealing temperature	Source
WMV	WMV F WMV R	GGTAATTTTGTTTGGGGCGAACIIIIIAAGCATTC GCGTGATCAACTAAAATGCGTGGIIIIICAGCATTCC	623	63	Kwon *et al.*, 2014
PRSV	PRSV F PRSV R	CGGAAATGATGTGTCAACTAGCACIIIIICTGGAGAGA ATGCTTCTGCCGCGTTACIIIIITGAGCCATAATTTG	458	63	Kwon *et al.*, 2014
ZYMV	ZYMV F ZYMV R	GTTACAGGCTCCGGCTCAIIIIIGAAAACAGTAG TCCATTAATGTCGGGTGAAGTGCCIIIIICAATGCACC	345	63	Kwon *et al.*, 2014

greater than that with conventional RT-PCR and 10 time more sensitive than SYBER green-based qRT-PCR.

High-throughput sequencing tools in viral diagnosis

Since 2002, more than 800 metagenomic studies of viruses have been published with the development of high-throughput screening (HTS) (Breitbart *et al.*, 2002). This metagenomic revolution is expanding epidemiological knowledge of health-related infections, in particular by redeploying geographical sampling areas and taking increased account of wild areas. The number of species sequenced by this approach greatly increases the amount of available genetic information. Phylogenetic reconstructions that are inferred from this information can reliably infer epidemiological links between isolates at spatial and temporal scales, and allow elucidation of inter-host transmission chains.

HTS provides a key step in metagenomics that encompasses sequencing technologies. It allows the

sequencing of multiple strands of DNA in parallel, resulting in greater throughput than conventional sequencing allows. As NSGs have become cheaper and more accessible, they have been used to address a growing range of biological problems, including issues related to food safety and quality (Bernardo *et al*., 2013).

HTS has provided an efficient tool for virus detection and identification in plants, which gives accurate and sensitive diagnoses of virus infections. Rodríguez-Negrete *et al*., (2019) have employed the technique to determine the viral diversity in seven states in Northern-Pacific Mexico, to characterize the begomovirus naturally existing in non-cultivated plant hosts. Their study used HTS analyses to give subsequent *de novo* assembly of important DNA signatures related to geminiviruses (80 to 100%). This showed that DNA signatures belonged to 52 geminivuruses infecting crop hosts 35 geminiviruses infecting noncultivated plants, identified in different plant species. Their study demonstrated that HTS analyses can increase knowledge of virus diversity, and assist identification and detection of novel emerging known and unknown viruses without requirement for disease etiological information (Karavina *et al*., 2020).

In Poland, Minicka *et al*., (2020) used the HTS technique for detection and identification of viruses occurring in mixed and single infections, allowing identification of 13 species, from 20 tested samples of different plant species, and identification of two new emerging viruses in Poland, *Clover yellow mosaic virus* (*Alphaflexiviridae*; *Potexvirus*; ClYMV) and *Melandrium yellow fleck virus* (*Bromoviridae*; *Bromovirus* ; MYFV), as well as a new strain of CABYV that belong to two different groups. These authors also concluded that HTS rapidly provided information about the viruses that were not detected in the region.

In France, the use of HTS analyses for the study of virus evolution has revealed the presence of undescribed variants, such as WMV and CMV on solanaceous crops, and complex virus populations within individual plants. However, spatial genetic variation of CABYV was related to landscape structure, while introduction and recurrence of WMV were mainly due to the human exchange of plant materials, giving a complex spatial pattern of genetic variation (Desbiez *et al*., 2020).

Drawbacks have been reported for HTS technology. These include the need to annotate contigs/singletons via *de novo* assembly, which could affect sequences by creation of chimeras deriving from different genomes, and the differentiation of sequences that need confirmation through cloning and sanger sequencing. However, the metagenomics analyses could greatly assist identification of genetic variability in virus populations, and facilitate study of genome evolution, to determine environmental factors that influence the generation of novel from established species (Rodríguez-Negrete *et al*., 2019).

STRATEGIES FOR CONTROL OF CUCURBIT VIRUSES

Prophylaxis

Vertical transmission

In Spain, crop protection is based on prevention through the use of healthy seed. The use of virus-free seeds is an important strategy for preventing introduction of virus into production sites. This is also the case for the use of nets, mainly in greenhouse crops, elimination of crop residues, and use of crop rotation (Janssen *et al*., 2003).

Hydrochloric acid treatment and drying for the disinfection of melon seeds remains the most effective way to obtain healthy seeds and limit the spread of MNSV (Dumas de Vaulx, 1970). In addition, hydrogen peroxide, hot water, and sodium hypochlorite are also used as seed treatments.

Horizontal transmission

Prophylactic measures also aim to prevent or limit the contact of virus vectors with cultivated plants. These include efficient weed removal near crops and avoiding overlapping crops in the same area to reduce sources of viruses.

Establishment of integrated pest management is essential for the management of cucurbitaceous pathogens. Weed control is also crucial because these plants ca n be reservoirs for vectors and viruses. Recourse to genetic resistance is also applied to control cucurbit viruses (Wintermantel *et al*., 2017).

For aphid vectors, the use of plastic mulches limits the spread of viruses because the plastic is aphid-repellent. However, these mulches confer limited protection; the more the plants cover the mulch surfaces, the lower is the effectiveness of the mulches. There are also rows of woven or perforated plastic that prevent winged aphids from reaching plants, but these must be removed during pollination, which allows aphids to feed on plants (Lecoq, 1992). For example, plastic mulching delayed the spread of CABYV for 2 weeks (Lecoq, 1999).

Rotations of different crops, mainly using non-host plants belonging to families other than *Cucurbitaceae*, can limit the spread of the viruses.

Breeding for resistance

Resistance to the virus

Breeding for resistance to plant viruses is among the most effective strategy for management of diseases caused by these pathogens. In melon, MNSV was controlled by the use of resistant cultivars. The dominant TGR 1551 gene in melon offered genetic resistance against *Cucurbit yellow stunting disorder virus* (*Closteroviridae*; *Crinivirus*; CYSDV). In addition, oligo-genic resistance allowed CMV control in melon. Collection of CMV isolates between 1974 and 1978 revealed the presence of the "Song" pathotype that overcame this resistance (Sugiyama, 2013). However, resistance to CMV in melon was reported to be recessive and in most cases oligogenic, but, in the subgroup II strains of CMV which are monogenic, the resistance depends on only one gene, *cmv1*, which prevents movement of the virus and systemic infection (Pascual *et al*., 2019).

Romay et *al*. (2019) studied the resistance to two unrelated begomoviruses, ToLCNDV and *Melon chlorotic mosaic virus* (MeCMV), to evaluate host genetic variation that could target these two viruses, and that could provide resistance breeding material and information on resistance factors for use in melon breeding programmes. They found that melon families were resistant to both viruses, suggesting that the genes involved in resistance were common. They also proposed that the resistance was controlled by the genes *bgm*-1, *Bgsm*-2 in ToLCNDV and MeCMV.

Resistance to ZYMV in melon was reported to be linked to three loci, and that it was dominant and monogenic, and also oligogenic. The three loci are mainly *Zym*-1, *Zym*-2, and *Zym*-3 and all are essential for the resistance (Danin-Poleg *et al*., 1997; Martín-Hernández and Picó, 2020).

Resistance to vectors

For aphids, melon has two cases of resistance to viruses: either the resistance to viruses, or to vectors conferred by the *VAT* gene. This is the case for *A. gossypii*. In the field, resistance to the CABYV conferred by the *cab1* and *cab2* genes ensures high efficacy (Boissot *et al*., 2016). However, Martín-Hernández and Picó (2020) reported that this virus could also be controlled by one dominant gene, which leads to accumulation of the virus in the inoculated host tissues, but not in systemic tissues, which was suggested to be the cause of the impairment of virus movement in the host vascular system.

Resistant cultivars

Several commercial cultivars have been genetically modified by the introduction of the *VAT* gene that confers resistance to *A. gossypii*, the vector of CABYV, WMV, and ZYMV. However, effectiveness of this gene is limited because these viruses are transmitted by many species of aphids other than *A. gossypii* (Boissot *et al*., 2016). For ZYMV, the use of genetic host resistance is extensive. The cucumber "*Zym*" gene confers long-lasting resistance, but this gene confers only partial resistance in melon, and this resistance can be overcome by the virus. Squash had *Zym* resistance to ZYMV, and the gene was incorporated into zucchini. This gave tolerance to the virus with expression of mild symptoms and reduced virus multiplication within host plants. However, a mutation in the P3 protein of the virus allowed overcoming of the host tolerance. Although the tolerance was easily overcome, the relative fitness of the tolerance-breaking variant was reduced compared to wild-type virus on zucchini cultivars(Desbiez *et al*., 2003). Cucumber, squash, and melon showed resistance to PRSV (Lecoq and Desbiez, 2012). In cucumber and squash/zucchini, cucumber has different levels of CMV resistance (Lecoq and Desbiez, 2012). Several efforts have been made to find resistance to WMV. Some commercial cucumber and zucchini cultivars are tolerant to WMV, but their efficiency toward the virus remains limited. CP is the only gene that has shown better resistance to WMV and ZYMV. Freedom II, a transgenic squash that contains CP genes of both of these viruses, was released in 1995 in the USA. This was the first virus transgenic crop to be commercially cultivated, and was reported efficient in the field conditions against WMV. However, other hybrids including resistance to CMV in the USA, but these could not be used in the Mediterranean region to the restrictions of genetically modified (GMO) crops in the region (Loebenstein and Lecoq, 2012).

Biological control

Biological control is one of the most commonly used vector management strategies but not for eradicating diseases.

Amblyseius swirskii Athias Henriot (Arachnida: *Phytoseiidae*) has been the subject of a recent study for control of *B. tabaci* populations and reducing the spread of ToLCNDV in a range of crops including cucumber and pepper (Rodríguez *et al*., 2019).

The mite *A. swirskii* has limited adult *B. tabaci* by feeding on eggs and larvae. On zucchini, pre-installation of the predator on plants was assessed. Significant

negative impacts of the mite on the number of emerging whiteflies adults were detected, due to colonization of the eggs by the phytoseiid predator. Control of the vector minimized plant infection by ToLCNDV (Tellez *et al*., 2017).

Management of virus diseases associated with cucumber and transmitted by *A. gossypii* has been studied in Egypt (Eid *et al*., 2018). A biological control trial released the parasitic aphid *Aphidius colemani* Viereck and larvae of the predatory ladybird *Coccinella septempunctata* L. Control of *A. gossypii* was carried out in two greenhouses, one using biological control and the other using conventional chemical treatments. The experiment was conducted in 2015 and 2016, to validate the results under different meteorological conditions. For summer cucumber, this study indicated that effective control was achieved with more than ten *C. septempunctata* and more than four *A. colemani* per m^2. Although costs of the biological controls were are high and aphid populations were not less compared to the chemicals, the cucumbers quality and yields were satisfactory.

Biological control was not evaluated as a strategy to slow the spread or reduce severity of vectors, but dissemination of nonpersistent viruses by vectors was gradually prevented. For example, aphids emit alarm pheromones that trigger and increased vector movements when they are attacked by their enemies, and this increases virus dissemination. Control of nonpersistent viruses is still not well established. Studies have concluded that the use of biological control could prevent secondary virus spread, and reduction of vector numbers could stop the spread of viruses to nearby crops (Hooks and Fereres, 2006).

For severe virus infections, biological vector control does not provide effective disease management solutions because complete vector control is required.

Chemical control

Several chemical methods, using detergents, insecticides, essential oils, and combinations of these substances, have been used for management of vector pests and the diseases they transmit. Control using these materials are not always satisfactory. These treatments aim to prevent secondary damage caused by the insect vectors, including reduction of virus transmission and deposition of honeydew (Johnstone and Rapley, 1981; Gibson and Rice, 1986).

Greenhouse and field trials were carried out in the USA in 2016 assessing management of CYSDV by controlling *B. tabaci* (Castle *et al*., 2017). Eight foliar and systemic insecticides were assessed, including the active ingredients acetamiprid, dinotefuran, pyrifluquinazon, thiamethoxam, cyantraniliprole, imidacloprid, or flupyradifurone, either as foliar or soil treatments. Virus transmission rates were reduced by less than 10% by some of the active ingredients. Foliar treatments gave good results compared to those applied to the soil, and the insecticides had the same effects in the greenhouse and in the field. Of the seven active ingredients, foliar applications of flupyradifurone, acetamiprid or dinotefuran gave the best management of the virus, by decreasing the populations of *B. tabaci*.

Limiting spread of viruses is mostly achieved by controlling vectors. Flupyradifurone is has very rapid activity against the tobacco whitefly vector of more than a hundred viruses. The trials of Castle *et al.* (2017) aimed to manage *Tomato yellow leaf curl virus* (*Geminiviridae*; *Begomovirus*; TYLCV) associated with tomato, but the results are still valid for other vegetable crops affected by *B. tabaci*. Foliar treatments of thiamethoxam or flupyradifurone reduced virus transmission by 85% because of the anti-feeding activity of the active ingredients (Roditakis *et al*., 2017). Given the potential environmental danger linked to thiamethoxam, it should not be used at the full bloom crop development stage to limit the risk of bee poisoning (Chahbar *et al*., 2011). Similarly, flupyradifurone could have similar harmful effects on bees and birds (European Food Safety Authority, 2015). However, these treatments remain ineffective because of the small proportion of whiteflies required to cause symptoms of viruses associated with *Tomato yellow leaf curl* (TYLCD-viruses), and because of development of resistant *B. tabaci* populations. Increasingly strict regulatory restrictions on the use of pesticides cause producers to seek alternative solutions using biological control and prophylactic systems in integrated protection systems in greenhouse crops.

Current strategies, aim to eliminate and exclude vector through the use of insecticides to reduce aphid and whitefly populations. If the frequency of treatments is high, the insecticides have not been effective. This is the case for CABYV, following the pesticide resistance developed by the vector, and also for *B. tabaci* which has become very resistant to chemical treatments at all stages of development (Willrich Siebert *et al*., 2012).

Management of *O. bornovanus* was based on the application of a surfactant that affected zoospores of the fungus or seed treatments this study suggested a prolonged seed treatment of 144 h at 70°C (Tomlinson and Thomas, 1986). This was effective removed MNSV and increased seed germination rates (Herrera-Vásquez *et al*., 2009).

Nonpersistent transmission of viruses presents a significant challenge for vector control because the

time between acquisition and transmission is very short (a few seconds) compared to viruses transmitted by semipersistent and persistent modes (Castle *et al*., 2017).

The use of mixtures of insecticides with different modes of action reduces the likelihood of the emergence of pesticide resistant insect strains. Combinations of insecticides/insecticides, insecticides/synergists or insecticides/repellents make it possible to produce a synergistic effects capable of increasing the duration of effectiveness of the active substances, of reducing the effective doses. These strategies may also give insecticidal action on insects with single active ingredient resistance(Baldet *et al*., 2014).

CONCLUSIONS

In natural conditions, there are more than 90 viruses that have been recorded infecting cucurbit crops, and the major problems are caused by ten viruses (Desbiez, 2020). This diversity of pathogens probably due to the genetic and ecological diversity of cucurbit hosts in the Mediterranean region. Cucurbits are cultivated in a variety of agroecosystems which provide variably favourable conditions for these viruses and/or their vectors.

Successful management strategies for virus diseases relies on multi-dimensional understanding of virus biologies, including epidemiology, evolution, environmental effects, and virus/plant and virus/vector interactions. Knowledge of these biological factors will facilitate future management of these diseases (Romay *et al*., 2014).

Methods for controlling these diseases and pathogen vectors are not completely effective, and cucurbit producers require innovative control methods that are economical and easy to implement.

Sustainable approaches to improve cucurbit crop productivity through phytosanitary quality must combine complementary approaches that involve the plant hosts and the natural and anthropic environmental factors (Romay *et al*., 2014).

Research on plant virus interactions and development of control methods is required to achieve sustainable cucurbit production. New molecular approaches, such as high-throughput sequencing metagenomic analyses, need to be applied in plant science, to understand disease resistance mechanisms, epidemiology, and virus transmission and interactions. Understanding in these aspects assist rapid diagnoses for sustainable plant management strategies by cucurbit producers in the Mediterranean region.

ACKNOWLEDGMENTS

Preparation of this review was supported by the Phytopathology Unit, Department of Plant Protection and Environment of the National School of Agriculture (ENA- Meknès), Morocco.

LITERATURE CITED

Aarabe A., Chebli B., Afechtal M., 2018. First report of *cucurbit aphid-borne yellows virus* from Morocco. *Australasian Plant Disease Notes* 13: 7–8. DOI: 10.1007/s13314-018-0312-7.

Abou-Jawdah Y., Sobh H., Fayyad A., Lecoq H., 1997. First report of *cucurbit aphid-borne yellows luteovirus* in Lebanon. *Plant Disease* 81:1331. DOI: 10.1094/PDIS.1997.81.11.1331D

Abrahamian P.E., Abou-Jawdah Y., 2013. Detection and quantitation of the new world *Squash leaf curl virus* by TaqMan real-time PCR. *Journal of Virological Methods* 191: 76–81. DOI: 10.1016/j.jviromet.2013.04.001.

Abrahamian P.E., Sobh H., Seblani R., Samsatly J., Jawhari M., Abou-Jawdah Y., 2013. First report of *Cucumber vein yellowing virus* on Cucumber in Lebanon. *Plant Disease* 97: 1516. DOI: 10.1094/PDIS-05-13-0471-PDN.

Abudy A., Sufrin-Ringwald T., Dayan-Glick C., Guenoune-Gelbart D., Livneh O., … Lapidot M., 2010. *Watermelon chlorotic stunt* and *Squash leaf curl* begomoviruses – New threats to cucurbit crops in the Middle East. *Israel Journal of Plant Sciences* 58: 33–42. DOI: 10.1560/IJPS.58.1.33.

Acosta-Leal R., Duffy S., Xiong Z., Hammond R.W., Elena S.F., 2011. Advances in plant virus evolution: translating evolutionary insights into better disease management. *Phytopathology* 101: 1136–1148. DOI: 10.1094/PHYTO-01-11-0017.

Adams M., Christian P., Ghabrial S., Knowles N., 2011. *Virus Taxonomy: Classification And Nomenclature Of Viruses: Ninth Report of the International Committee on Taxonomy of Viruses*. Elsevier Academic Press, London.

Ahmad M.H., Shakeel M.T., Al-Shahwan I.M., Al-Saleh M.A., Amer M.A., 2018. Insights into the incidence of w*atermelon chlorotic stunt virus* causing yellowing disease of watermelon in western and southwestern regions of Saudi Arabia. *Plant Pathology Journal* 34: 426–434. DOI: 10.5423/PPJ.OA.04.2018.0059.

Ahsan M., Ashfaq M., Mukhtar T., Abbasi N.A., Asad Z., 2020. First report of *cucurbit aphid borne yellows*

virus (CABYV) infecting melon in Pakistan. *Journal of Plant Pathology* 102: 563–564. DOI: 10.1007/s42161-019-00450-z.

Al-Musa A., Anfoka G., Al-Abdulat A., Misbeh S., Haj Ahmed F., Otri I., 2011. *Watermelon chlorotic stunt virus* (WmCSV): A serious disease threatening watermelon production in Jordan. *Virus Genes* 43: 79–89. DOI: 10.1007/s11262-011-0594-8.

Al-Saleh M.A., Al-Shahwan I.M., Amer M.A., Shakeel M.T., Kamran A., … Katis N.I., 2015. First report of *Cucurbit aphid-borne yellows virus* in cucurbit crops in Saudi Arabia. *Plant Disease* 99: 894. DOI: 10.1094/PDIS-11-14-1102-PDN.

Ali-Shtayeh M.S., Jamous R.M., Mallah O.B., Abu-Zeitoun S.Y., 2014. Molecular Characterization of *Watermelon Chlorotic Stunt Virus* (WmCSV) from Palestine. *Viruses* 6: 2444–2462. DOI: 10.3390/v6062444.

Allan F.L., 1980. Transmission and properties of viruses isolated from Carica papaya in Nigeria. *Journal of Horticultural Science*, Informa UK Limited 55: 191–197. DOI: 10.1080/00221589.1980.11514922.

Antignus Y., Lachman O.., Pearlsman M.., Omer S.., Yunis H.., … Koren A., 2003. *Squash leaf curl geminivirus* - a new illegal immigrant from the Western Hemisphere and a threat to cucurbit crops in Israel. Abstracts of presentations made at the 24th Congress of the Israeli Phytopathological Society. *Phytoparasitica* 31: 410–425. DOI: 10.1007/BF02979813.

Ashfaq M., Saeed U., Mukhtar T., ul Haq M.I., 2015. First Report of *Zucchini yellow mosaic virus* in Ridge Gourd in Pakistan. *Plant Disease* 99: 1870. DOI: 10.1094/PDIS-05-15-0553-PDN.

Astier S., Albouy J., Maury Y., Lecoq H., 2001. *Principes de Virologie Végétale: Génome, Pouvoir Pathogène, Ecologie des Virus*. Editions Quae. 488 pp.

Aydin S., 2015. A short history, principles, and types of ELISA, and our laboratory experience with peptide/protein analyses using ELISA. *Peptides* 72: 4–15. DOI: 10.1016/j.peptides.2015.04.012.

Kennedy J. S., Day M. F., Eastop V. F. , 1962. *A Conspectus of Aphids as Vectors of Plant Viruses,* by. Commonwealth Institute of Entomology, 114 pp. The Eastern Press Ltd., London and Reading, paperbound.

Baldet T., Chandre F., Darriet F., David J.-P., Dusfour I., … Lagadic L., 2014. *Utilisation des Insecticides et Gestion de la Resistance*. Centre National d'Expertise sur les Vecteurs, 70 pp.

Bananej K., Desbiez C., Girard M., Wipf-Scheibel C., Vahdat I., … Lecoq H., 2007. First Report of *Cucumber vein yellowing virus* on Cucumber, Melon, and Watermelon in Iran. *Plant Disease* 90: 1113–1113. DOI: 10.1094/PD-90-1113C.

Bananej K., Desbiez C., Wipf-Scheibel C., Vahdat I., Kheyr-Pour A., … Lecoq H., 2006. First report of *Cucurbit aphid-borne yellows virus* in Iran causing yellows on four cucurbit crops. *Plant Disease* 90: 526. DOI: 10.1094/PD-90-0526A.

Bebber D.P., Ramotowski M.A.T., Gurr S.J., 2013. Crop pests and pathogens move polewards in a warming world. *Nature Climate Change* 3: 985–988. DOI: 10.1038/nclimate1990.

Bedford I.D., Briddon R.W., Brown J.K., Rosell R.C., Markham P.G., 1994. Geminivirus transmission and biological characterisation of *Bemisia tabaci* (Gennadius) biotypes from different geographic regions. *Annals of Applied Biology* 125: 311–325. DOI: 10.1111/j.1744-7348.1994.tb04972.x.

Ben Tamarzizt H., Montarry J., Girardot G., Fakhfakh H., Tepfer M., Jacquemond M., 2013. *Cucumber mosaic virus* populations in Tunisian pepper crops are mainly composed of virus reassortants with resistance-breaking properties. *Plant Pathology* 62: 1415–1428. DOI: 10.1111/ppa.12032.

Bernardo P., Albina E., Eloit M., Roumagnac P., 2013. Métagénomique virale et pathologie. *Médecine/sciences* 29: 501–508. DOI: 10.1051/medsci/2013295013.

Bhat A.I., Siljo A., Deeshma K.P., 2013. Rapid detection of *Piper yellow mottle virus* and *Cucumber mosaic virus* infecting black pepper (*Piper nigrum*) by loop-mediated isothermal amplification (LAMP). *Journal of Virological Methods* 193: 190–196. DOI: 10.1016/j.jviromet.2013.06.012.

Blancard D., Lecoq H., Pitrat M., 1994. *A Colour Atlas of Cucurbit Diseases: Observation, Identification and Control.* Manson Publishing Ltd, 299 pp.

Boissot N., Schoeny A., Vanlerberghe-Masutti F., 2016. Vat, an amazing gene conferring resistance to aphids and viruses they carry: From molecular structure to field effects. *Frontiers in Plant Science* 7:1420.

Bonnet J., Fraile A., Sacristán S., Malpica J.M., García-Arenal F., 2005. Role of recombination in the evolution of natural populations of *Cucumber mosaic virus*, a tripartite RNA plant virus. *Virology* 332: 359–368. DOI: 10.1016/j.virol.2004.11.017.

Breitbart M., Salamon P., Andresen B., Mahaffy J.M., Segall A.M., … Rohwer F., 2002. Genomic analysis of uncultured marine viral communities. *Proceedings of the National Academy of Sciences* 99: 14250–14255. DOI: 10.1073/pnas.202488399.

Briddon R.W., Akbar F., Iqbal Z., Amrao L., Amin I., … Mansoor S., 2014. Effects of genetic changes to the begomovirus/betasatellite complex causing cotton leaf curl disease in South Asia post-resistance breaking. *Virus Research* 186: 114–119. DOI: 10.1016/j.virusres.2013.12.008.

Briddon R.W., Mansoor S., Bedford I.D., Pinner M.S., Saunders K., … Markham P.G., 2001. Identification of dna components required for induction of cotton leaf curl disease. *Virology* 285: 234–243. DOI: 10.1006/VIRO.2001.0949.

Burke D.S., 1997. Recombination in HIV: An important viral evolutionary strategy. *Emerging Infectious Diseases* 3: 253–259. DOI: 10.3201/eid0303.970301.

CABI/EPPO, 2014. *Squash leaf curl virus. [Distribution map]. Distribution Maps of Plant Diseases*, CABI; Wallingford; UK, Map 996 (Edition 2).

CABI, 2019. *Squash leaf curl virus* (leaf curl of squash). Available at: https://www.cabi.org/isc/datasheet/15038. Accessed April 27, 2020.

CABI, 2020. *Papaya Ringspot Virus*. Available at: https://www.cabi.org/isc/datasheet/45962.

CABI, EPPO, 2010. *Melon necrotic spot virus*. [Distribution map]. *Plant Dis.s No 1089, CABI Wallingford UK*.

Cabrera Mederos D., Giolitti F., Torres C., Portal O., 2019. Distribution and phylodynamics of *Papaya ringspot virus* on *Carica papaya* in Cuba. *Plant Pathology* 68: 239–250. DOI: 10.1111/ppa.12942.

Castle S.J.J., Palumbo J.P.P., Merten P., 2017. Field evaluation of *Cucurbit yellow stunting disorder virus* transmission by *Bemisia tabaci*. *Virus Research* 241: 220–227. DOI: 10.1016/j.virusres.2017.03.017.

Chahbar N., Belzunces P., Doumandji S., 2011. Effect of insecticide use in plant protection : thiamethoxam on the bee saharan *Apis mellifera sahariensis*. *Algerian Journal of Arid Environment* 1: 11-21.

Chakraborty S., Vanitharani R., Chattopadhyay B., Fauquet C.M., 2008. Supervirulent pseudorecombination and asymmetric synergism between genomic components of two distinct species of begomovirus associated with severe tomato leaf curl disease in India. *Journal of General Virology* 89: 818–828. DOI: 10.1099/vir.0.82873-0.

Cho I.-S., Chung B.-N., Kwon S.-J., Yoon J.-Y., Choi G.-S., … Lim H.-S., 2019. First report of *Zucchini yellow mosaic virus* in muskmelon (*Cucumis melo*) in Korea. *Journal of Plant Pathology* 101: 771. DOI: 10.1007/s42161-018-00239-6.

Choi G.S., Kim J.S.J.H., Kim J.S.J.H., 2003. Characterization of *Melon necrotic spot virus* isolated from muskmelon. *Plant Pathology Journal* 19: 123–127. DOI: 10.5423/PPJ.2003.19.2.123.

Choi S.K., Choi G.S., 2016. First report of *Cucurbit aphid-borne yellows virus* in *Cucumis melo* in Korea. *Plant Disease* 100: 234. DOI: 10.1094/PDIS-06-15-0627-PDN.

Cohen S., Duffus J.E., Larsen R.C., Liu H.Y., Flock R.A., 1983. Purification, Serology, and Vector Relationships of *Squash Leaf Curl Virus*, a Whitefly-Transmitted Geminivirus. *Phytopathology* 73:1669-1673.

Cohen S., Nitzany F.E., 1960. A whitefly transmitted virus of Cucurbits in Israel. *Phytopathologia Mediterranea*, Firenze University Press 1: 44–46.

Cohen S., Nitzany F.E., 1963. Identity of viruses affecting cucurbits in Israel. *Phytopathology*, Worcester, Mass. 53.

Costa T.M., Blawid R., Aranda M.A., Freitas D.M.S., Andrade G.P., … Nagata T., 2019. *Cucurbit aphid-borne yellows virus* from melon plants in Brazil is an interspecific recombinant. *Archives of Virology* 164: 249–254. DOI: 10.1007/s00705-018-4024-2.

Costa T.M., Inoue-Nagata A.K., Vidal A.H., Ribeiro S. da G., Nagata T., 2020. The recombinant isolate of *Cucurbit aphid-borne yellows virus* from Brazil is a polerovirus transmitted by whiteflies. *Plant Pathology* 69: 1042-1050. DOI: 10.1111/ppa.13186.

Coutts B.A., Kehoe M.A., Webster C.G., Wylie S.J., Jones R.A.C., 2011. *Zucchini yellow mosaic virus*: Biological properties, detection procedures and comparison of coat protein gene sequences. *Archives of Virology* 156: 2119–2131. DOI: 10.1007/s00705-011-1102-0.

Crescenzi A., Fanigliulo A., Comes S., Masenga V., Pacella R., Piazzolla P., 2001. Necrosis of watermelon caused by *Watermelon mosaic virus*. *Journal of Plant Pathology* 83: 227. DOI: 10.2307/41998070.

Cuadrado I.M., Janssen D., Velasco L., Ruiz L., Segundo E., 2007. First Report of *Cucumber vein yellowing virus* in Spain. *Plant Disease* 85: 336–336. DOI: 10.1094/PDIS.2001.85.3.336A.

Danin-Poleg Y., Paris H.S., Cohen S., Rabinowitch H.D., Karchi Z., 1997. Oligogenic inheritance of resistance to *Zucchini yellow mosaic virus* in melons. *Euphytica* 93: 331–337. DOI: 10.1023/A:1002944432083.

Desbiez C., 2020. The never-ending story of cucurbits and viruses. *Acta Horticulturae* 1294: 173–191. DOI: 10.17660/ACTAHORTIC.2020.1294.23.

Desbiez C., Caciagli P., Wipf-Scheibel C., Millot P., Ruiz L., … Lecoq H., 2019. Evidence for long-term prevalence of *Cucumber vein yellowing virus* in Sudan and genetic variation of the virus in Sudan and the Mediterranean Basin. *Plant Pathology* 68: 1268–1275. DOI: 10.1111/ppa.13055.

Desbiez C., Costa C., Wipf-Scheibel C., Girard M., Lecoq H., 2007. Serological and molecular variability of *Watermelon mosaic virus* (genus Potyvirus). *Archives of Virology* 152: 775–781. DOI: 10.1007/s00705-006-0899-4.

Desbiez C., Gal-On A., Girard M., Wipf-Scheibel C., Lecoq H., 2003. Increase in *Zucchini yellow mosaic virus* symptom severity in tolerant zucchini cultivars is related to a point mutation in p3 protein and is associated with a loss of relative fitness on susceptible

plants. *Phytopathology* 93: 1478–1484. DOI: 10.1094/PHYTO.2003.93.12.1478.

Desbiez C., Gentit P., Cousseau-Suhard P., Renaudin I., Verdin E., 2021. First report of *Tomato leaf curl New Delhi virus* infecting courgette in France. *New Disease Reports* 43: e12006. DOI: 10.1002/ndr2.12006.

Desbiez C., Joannon B., Wipf-Scheibel C., Chandeysson C., Lecoq H., 2009. Emergence of new strains of *Watermelon mosaic virus* in South-eastern France: Evidence for limited spread but rapid local population shift. *Virus Research* 141: 201–208.

Desbiez C., Joannon B., Wipf-Scheibel C., Chandeysson C., Lecoq H., 2011. Recombination in natural populations of *Watermelon mosaic virus*: new agronomic threat or damp squib? *Journal of General Virology* 92: 1939–1948. DOI: 10.1099/vir.0.031401-0.

Desbiez C., Lecoq H., 1997. *Zucchini yellow mosaic virus*. *Plant Pathology*, Blackwell Publishing Ltd 46: 809–829. DOI: 10.1046/j.1365-3059.1997.d01-87.x.

Desbiez C., Millot P., Wipf-Scheibel C., Blancard D., Chesneau T., Lecoq H., 2016. First report of *Pepo aphid-borne yellows virus* in cucurbits in Tanzania and Mayotte. *New Disease Reports* 33: 20. DOI: 10.5197/j.2044-0588.2016.033.020.

Desbiez C., Wipf-Scheibel C., Millot P., Berthier K., Girardot G., … Verdin E., 2020. Distribution and evolution of the major viruses infecting cucurbitaceous and solanaceous crops in the French Mediterranean area. *Virus Research* 286: 198042. DOI: 10.1016/j.virusres.2020.198042.

Dogimont C., Slama S., Martin J., Lecoq H., Pitrat M., 1996. Sources of resistance to *Cucurbit aphid-borne yellows luteovirus* in a melon germ plasm collection. *Plant Disease* 180: 1379–1382.

Doolittle S., 1916. *A New Infectious Mosaic Disease of Cucumber*. *Phytopathology* 6: 145–147.

dos Santos Martins D., Aires Ventura J., de assia AL Paula R.C., Jos Fornazier M., Rezende J.A., … Sousa-Silva C.R., 2016. Aphid vectors of *Papaya ringspot virus* and their weed hosts in orchards in the major papaya producing and exporting region of Brazil. *Crop Protection* 90: 191–196. DOI: 10.1016/j.cropro.2016.08.030.

Dumas de Vaulx R., 1970. *Étude de la Transmission du Virus de la Criblure*. 46-50 in *Rapport d'activité 1969–1970 Station D'Amélioration des Plantes Maraichères*, INRA Montfavet, France 46–50.

Eid A.E., El-Heneidy A.H., Hafez A.A., Shalaby F.F., Adly D., 2018. On the control of the cotton aphid, *Aphis gossypii* Glov. (Hemiptera: *Aphididae*), on cucumber in greenhouses. *Egyptian Journal of Biological Pest Control* 28: 64. DOI: 10.1186/s41938-018-0065-9.

EPPO, 2007. PM 7/81 (1): *Cucumber vein yellowing virus* (Ipomovirus). *EPPO Bulletin* 37: 554–559. DOI: 10.1111/j.1365-2338.2005.00846.x.

EPPO, 2020. *Tomato leaf curl New Delhi virus* (TOLCND) [World distribution]| EPPO Global Database. Available at: https://gd.eppo.int/taxon/TOLCND/distribution. Accessed April 18, 2021.

Esmaeili M., Heydarnejad J., Massumi H., Varsani A., 2015. Analysis of *Watermelon chlorotic stunt virus* and *Tomato leaf curl Palampur virus* mixed and pseudo-recombination infections. *Virus Genes* 51: 408–416. DOI: 10.1007/s11262-015-1250-5.

European Food Safety Authority, 2015. Conclusion on the peer review of the pesticide risk assessment of the active substance flupyradifurone. *EFSA Journal* 13: 1–106. DOI: 10.2903/j.efsa.2015.4020.

Farzadfar S., Pourrahim R., Golnaraghi A.R., Ahoonmanesh A., 2009. PCR detection and partial molecular characterization of *Chickpea chlorotic dwarf virus* in naturally infected sugar beet plants in Iran. *Journal of Plant Pathology* 90: 247–251. DOI: 10.4454/jpp.v90i2.659.

Fortes I.M., Sánchez-Campos S., Fiallo-Olivé E., Díaz-Pendón J.A., Navas-Castillo J., Moriones E., 2016. A novel strain of *Tomato leaf curl New Delhi virus* has spread to the Mediterranean basin. *Viruses* 8: 307. DOI: 10.3390/v8110307.

Froissart R., Roze D., Uzest M., Galibert L., Blanc S., Michalakis Y., 2005. Recombination Every Day: Abundant Recombination in a Virus during a Single Multi-Cellular Host Infection. *PLoS Biology* 3: e89. DOI: 10.1371/journal.pbio.0030089.

García-Arenal F., Fraile A., Malpica J.M., 2001. Variability and genetic structure of plant virus populations. *Annual Review of Phytopathology* 39: 157–186.

Gibson R.W., Rice A.D., 1986. The combined use of mineral oils and pyrethroids to control plant viruses transmitted non- and semi-persistently by *Myzus persicae*. *Annals of Applied Biology* 109: 465–472. DOI: 10.1111/j.1744-7348.1986.tb03203.x.

Gil-Salas F.M., Peters J., Boonham N., Cuadrado I.M., Janssen D., 2012. Co-infection with *Cucumber vein yellowing virus* and *Cucurbit yellow stunting disorder virus* leading to synergism in cucumber. *Plant Pathology* 61: 468–478. DOI: 10.1111/j.1365-3059.2011.02545.x.

Gogoi S.H., Nath P.D., Thakuria N., Gogoi S., Das B., … Raj K., 2019. Molecular Detection and Characterization of *Papaya Ring Spot Virus* (PRSV) Disease in Jorhat District of Assam, India. *International Journal of Current Microbiology and Applied Sciences* 8: 1564–1571. DOI: 10.20546/ijcmas.2019.802.183.

Gonzalez-Garza R., Gumpf D.J., Kishaba A.N., Bohn G.W., 1979. Identification, seed transmission, and host range pathogenicity of a California isolate of melon necrotic spot virus. *Phytopathology* 69: 340–345.

Gosalvez B., Navarro J.. A., Lorca A., Botella F., Sánchez-Pina M.. A., Pallas V., 2003. Detection of *Melon necrotic spot virus* in water samples and melon plants by molecular methods. *Journal of Virological Methods* 113: 87–93. DOI: 10.1016/S0166-0934(03)00224-6.

Gracia O., 2007. First Report of *Zucchini yellow mosaic virus* in Argentina. *Plant Disease* 84: 371–371. DOI: 10.1094/PDIS.2000.84.3.371B.

Hamed A.A., 2007. *Epidemiology and Management of Chickpea chlorotic dwarf virus (cpcdv) in chickpea (Cicer arierinum) in River Nile State-Sudan*. M.Sc Thesis, University of Gezira, Sudan, 102 pp.

Hartati L., Bakti D., Tantawi A.R., Lisnawita, 2020. Detection of virus causes *Papaya ringspot virus* - with the DAS-Elisa (Double Antibody Sandwich-Enzyme-Linked Immunosorbent Assay) method at different levels in North Sumatra. *IOP Conference Series: Earth and Environmental Science* 454: 012182. DOI: 10.1088/1755-1315/454/1/012182.

Hasiów-Jaroszewska B., Chrzanowski M., Budzyńska D., Rymelska N., Borodynko-Filas N., 2017. Genetic diversity, distant phylogenetic relationships and the occurrence of recombination events among *Cucumber mosaic virus* isolates from zucchini in Poland. *Archives of Virology* 162: 1751–1756. DOI: 10.1007/s00705-017-3285-5.

Hassan M., 2019. Rolling circle amplification-based detection and recombination analysis of Squash leaf curl virus in Egypt. *Middle East Journal of Applied Sciences* 9: 155–166.

He C.Q., Xie Z.X., Han G.Z., Dong J.B., Wang D., … Li G.R., 2009. Homologous recombination as an evolutionary force in the Avian influenza A virus. *Molecular Biology and Evolution* 26: 177–187. DOI: 10.1093/molbev/msn238.

Herrera-Vásquez J.A., Córdoba-Sellés M.C., Cebrián M.C., Alfaro-Fernández A., Jordá C., 2009. Seed transmission of *Melon necrotic spot virus* and efficacy of seed-disinfection treatments. *Plant Pathology* 58: 436–442. DOI: 10.1111/j.1365-3059.2008.01985.x.

Herrera J.A., Cebrián M.C., Jordá C., 2006. First Report of *Melon necrotic spot virus* in Panama . *Plant Disease* 90: 1261–1261. DOI: 10.1094/pd-90-1261a.

Hooks C.R.R., Fereres A., 2006. Protecting crops from non-persistently aphid-transmitted viruses: A review on the use of barrier plants as a management tool. *Virus Research* 120: 1–16.

Horn N.M., Reddy S. V., Roberts I.M., Reddy D.V.R., 1993. *Chickpea chlorotic dwarf virus*, a new leafhopper-transmitted geminivirus of chickpea in India. *Annals of Applied Biology* 122: 467–479. DOI: 10.1111/j.1744-7348.1993.tb04050.x.

Hull R., 2014. *Plant Virology*. (R. Hull, ed.), Elsevier, 1120 pp.

Isakeit T., 1994. First Report of *Squash leaf curl virus* on Watermelon in Texas. *Plant Disease* 78: 10. DOI: 10.1094/pd-78-1010d.

Jadão A.S., Buriola J.E., Rezende J.A.M., 2010. First Report of *Papaya ringspot virus* –Type W and *Zucchini yellow mosaic virus* Infecting *Trichosanthes cucumerina* in Brazil. *Plant Disease* 94: 789–789. DOI: 10.1094/PDIS-94-6-0789B.

Jain R.K., Nasiruddin K.M., Sharma J., Pant R.P., Varma A., 2004. First Report of Occurrence of *Papaya ring spot virus* Infecting Papaya in Bangladesh . *Plant Disease* 88: 221–221. DOI: 10.1094/pdis.2004.88.2.221c.

Janssen D., Martín G., Velasco L., Gómez P., Segundo E., … Cuadrado I.M., 2005. Absence of a coding region for the helper component-proteinase in the genome of *Cucumber vein yellowing virus*, a whitefly-transmitted member of the *Potyviridae*. *Archives of Virology* 150: 1439–1447. DOI: 10.1007/s00705-005-0515-z.

Janssen D., Ruiz L., Cano M., Belmonte A., Martin G., … Cuadrado I.M., 2003. Physical and genetic control of *Bemisia tabaci*-transmitted *Cucurbit yellow stunting disorder virus* and *Cucumber vein yellowing virus* in cucumber. *IOBC wprs Bulletin* 26: 101–106.

Janssen D., Ruiz L., Velasco L., Segundo E., Cuadrado I.M., 2002. Non-cucurbitaceous weed species shown to be natural hosts of *Cucumber vein yellowing virus* in south-eastern Spain. *Plant Pathology* 51: 797–797. DOI: 10.1046/j.1365-3059.2002.00767.x.

Johnstone G.R., Rapley P.E.L., 1981. Control of subterranean *Clover red leaf virus* in broad bean crops with aphicides. *Annals of Applied Biology* 99: 135–141. DOI: 10.1111/j.1744-7348.1981.tb05140.x.

Jones R.A.C., 2021. Global plant virus disease pandemics and epidemics. *Plants* 10: 233. DOI: 10.3390/plants10020233.

Jordá C., Font M.I., Martínez-Culebra P., Tello J., 2005. Viral etiology of diseases detected in melon in guatemala. *Plant Disease* 89: 338–338. DOI: 10.1094/pd-89-0338a.

Juárez M., Rabádan M.P., Martínez L.D., Tayahi M., Grande-Pérez A., Gómez P., 2019. Natural hosts and genetic diversity of the emerging *Tomato leaf curl New Delhi virus* in Spain. *Frontiers in Microbiology* 10: 140. DOI: 10.3389/fmicb.2019.00140.

Juarez M., Truniger V., Aranda M.A., 2004. First Report of *Cucurbit aphid-borne yellows virus* in Spain . *Plant Disease* 88: 907–907. DOI: 10.1094/pdis.2004.88.8.907a.

Kanakala S., Kuria P., 2019. *Chickpea chlorotic dwarf virus*: An emerging monopartite dicot infecting mastrevirus. *Viruses* 11: 1–15. DOI: 10.3390/v11010005.

Karavina C., Ibaba J.D., Gubba A., 2020. High-throughput sequencing of virus-infected *Cucurbita pepo* samples revealed the presence of *Zucchini shoestring virus* in Zimbabwe. *BMC Research Notes* 13: 53. DOI: 10.1186/s13104-020-4927-3.

Kassem M.A., Sempere R.N., Juárez M., Aranda M.A., Truniger V., 2007. *Cucurbit aphid-borne yellows virus* is prevalent in field-grown cucurbit crops of southeastern Spain. *Plant Disease* 91: 232–238. DOI: 10.1094/PDIS-91-3-0232.

Khalid S., Zia-ur-Rehman M., Ali S.A., Hameed U., Khan F., … Haider M.S., 2017. Construction of an infectious chimeric geminivirus by molecular cloning based on coinfection and recombination. *International Journal of Agriculture and Biology* 19: 629–634. DOI: 10.17957/IJAB/15.0310.

Khan A.J., Akhtar S., Briddon R.W., Ammara U., Al-Matrooshi A.M., Mansoor S., 2012. Complete nucleotide sequence of *Watermelon chlorotic stunt virus* originating from Oman. *Viruses* 4: 1169–1181. DOI: 10.3390/v4071169.

Kheireddine A., Sifres A., Sáez C., Picó B., López C., 2019. First Report of *Tomato leaf curl new delhi virus* Infecting Cucurbit Plants in Algeria. *Plant Disease* 103: 3291-3291. PDIS-05-19-1118. DOI: 10.1094/pdis-05-19-1118-pdn.

Kheyr-Pour A., Bananej K., Dafalla G.A., Caciagli P., Noris E., … Gronenborn B., 2000. *Watermelon chlorotic stunt virus* from the Sudan and Iran: Sequence comparisons and identification of a whitefly-transmission determinant. *Phytopathology* 90: 629–635. DOI: 10.1094/PHYTO.2000.90.6.629.

Kido K., Tanaka C., Mochizuki T., Kubota K., Ohki T., … Tsuda S., 2008. High temperatures activate local viral multiplication and cell-to-cell movement of *Melon necrotic spot virus* but restrict expression of systemic symptoms. *Phytopathology* 98: 181–186.

Kishi K., 1966. Necrotic spot of melon, a new virus disease. *Japanese Journal of Phytopathology* 32: 138–144.

Knierim D., Deng T.C., Tsai W.S., Green S.K., Kenyon L., 2010. Molecular identification of three distinct Polerovirus species and a recombinant *Cucurbit aphid-borne yellows virus* strain infecting cucurbit crops in Taiwan. *Plant Pathology* 59: 991–1002. DOI: 10.1111/j.1365-3059.2010.02327.x.

Köklü G., Yilmaz Ö., 2006. Occurrence of cucurbit viruses on field-grown melon and watermelon in the Thrace region of Turkey. *Phytoprotection* 87: 123–130. DOI: 10.7202/015854ar.

Koné D., Aké S., Abo K., Soro S., N'Guessan C.A., … Lecoq H., 2010. First Report of *Zucchini yellow mosaic virus* in Cucurbits in Ivory Coast . *Plant Disease* 94: 1378–1378. DOI: 10.1094/pdis-06-10-0416.

Kraberger S., Harkins G.W., Kumari S.G., Thomas J.E., Schwinghamer M.W., … Varsani A., 2013. Evidence that dicot-infecting mastreviruses are particularly prone to inter-species recombination and have likely been circulating in Australia for longer than in Africa and the Middle East. *Virology* 444: 282–291. DOI: 10.1016/J.VIROL.2013.06.024.

Kraberger S., Kumari S.G., Hamed A.A., Gronenborn B., Thomas J.E., … Varsani A., 2015. Molecular diversity of *Chickpea chlorotic dwarf virus* in Sudan: High rates of intra-species recombination - a driving force in the emergence of new strains. *Infection, Genetics and Evolution* 29: 203–215. DOI: 10.1016/j.meegid.2014.11.024.

Kuan C.P., Wu M.T., Lu Y.L., Huang H.C., 2010. Rapid detection of *Squash leaf curl virus* by loop-mediated isothermal amplification. *Journal of Virological Methods* 169: 61–65. DOI: 10.1016/j.jviromet.2010.06.017.

Kubo C., Nakazono-Nagaoka E., Hagiwara K., Kajihara H., Takeuchi S., … Omura T., 2005. New severe strains of *Melon necrotic spot virus*: symptomatology and sequencing. *Plant Pathology* 54: 615–620. DOI: 10.1111/j.1365-3059.2005.01253.x.

Kumar A., Vallabhbhai Patel S., Kumar Professor P., Siwach J., Sharma V., … Kumar P., 2021. Occurrence of *Papaya ringspot virus* (PRSV) infection in India. *Journal of Pharmacognosy and Phytochemistry* 10: 110-113.

Kumari S.G., Makkouk K.M., Attar N., 2006. An improved antiserum for sensitive serologic detection of *Chickpea chlorotic dwarf virus*. *Journal of Phytopathology* 154: 129–133. DOI: 10.1111/j.1439-0434.2006.01068.x.

Kwon J.Y., Hong J.S., Kim M.J., Choi S.H., Min B.E., … Ryu K.H., 2014. Simultaneous multiplex PCR detection of seven cucurbit-infecting viruses. *Journal of Virological Methods* 206: 133–139. DOI: 10.1016/j.jviromet.2014.06.009.

Lecoq H., 1992. *Les Virus des Cultures de Melon et de Courgette de Plein Champ. II. PHM Revue Horticole*, 15–25 pp.

Lecoq H., 1999. *Epidemiology of Cucurbit Aphid-Borne Yellows Virus. The Luteoviridae*, CABI Publishing, Wallingford, UK, 243–248 pp.

Lecoq H., Bourdin D., Wipf-Scheibel C., Bon M., Llot H., … Herbach E., 1992. A new yellowing disease of cucurbits caused by a luteovirus, *Cucurbit aphid-borne yellows virus*. *Plant Pathology* 41: 749–761. DOI: 10.1111/j.1365-3059.1992.tb02559.x.

Lecoq H., Desbiez C., 2008. *Watermelon mosaic virus* and *Zucchini yellow mosaic virus*. *Encyclopedia of Virology* 433–440. DOI: 10.1016/B978-012374410-4.00740-8.

Lecoq H., Desbiez C., 2012. Viruses of Cucurbit Crops in the Mediterranean Region. An Ever-Changing Picture. *Advances in Virus Research* 84: 67–126.

Lecoq H., Desbiez C., Dele B., Cohen S., Mansour A., 2000. Cytological and molecular evidence that the whitefly-transmitted *Cucumber vein yellowing virus* is a tentative member of the family Potyviridae. *Journal of General Virology* 81:2289–2293.

Lecoq H., Dufour O., Wipf-Scheibel C., Girard M., Cotillon A.C., Desbiez C., 2007. First Report of *Cucumber vein yellowing virus* in Melon in France . *Plant Disease* 91: 909–909. DOI: 10.1094/pdis-91-7-0909c.

Lecoq H., Katis N., 2014. *Control of Cucurbit Viruses. Advances in Virus Research* 90: 255–296.

Lemaire O.J., 1993. First report of *Cucurbit aphid-borne yellows* luteovirus in the united states. *Plant Disease* 77: 1169B. DOI: 10.1094/pd-77-1169b.

Li J. yu, Wei Q. wei, Liu Y., Tan X. qiu, Zhang W. na, … Tao X. rong, 2013. One-step reverse transcription loop-mediated isothermal amplification for the rapid detection of *Cucumber green mottle mosaic virus*. *Journal of Virological Methods* 193: 583–588. DOI: 10.1016/j.jviromet.2013.07.059.

Lisa V., Boccardo G., D'Agostino G., Dellavalle G., d'Aquilio M., 1981. Characterization of a potyvirus that causes zucchini yellow mosaic. *Phytopathology* 71: 667–672. DOI: 10.1094/Phyto-71-667.

Loebenstein G. (Gad), Lecoq H., 2012. *Viruses and Virus Diseases of the Vegetables in the Mediterranean Basin*. Academic Press: San Diego, California, United States of America, 570 pp.

López-Berenguer C., Donaire L., González-Ibeas D., Gómez-Aix C., Truniger V., … Aranda M.A., 2021. Virus-Infected Melon Plants Emit Volatiles that Induce Gene Deregulation in Neighboring Healthy Plants. *Phytopathology* 111*:* 862-869. DOI: 10.1094/PHYTO-07-20-0301-R.

López C., Ferriol M., Picó M.B., 2015. Mechanical transmission of T*omato leaf curl New Delhi virus* to cucurbit germplasm: selection of tolerance sources in *Cucumis melo*. *Euphytica* 204: 679–691. DOI: 10.1007/s10681-015-1371-x.

Louro D., Quinot A., Neto E., Fernandes J.E., Marian D., … Vaira A.M., 2004. Occurrence of *Cucumber vein yellowing virus* in cucurbitaceous species in southern Portugal. *Plant Pathology* 53: 241-241. DOI: 10.1111/j.0032-0862.2004.00996.x.

Mackie J., Higgins E., Chambers G.A., Tesoriero L., Aldaoud R., … Constable F.E., 2020. Genome Analysis of *Melon necrotic spot virus* Incursions and Seed Interceptions in Australia. *Plant Disease* 104: 1969-1978. DOI: 10.1094/pdis-04-19-0846-re.

Maina S., Barbetti M.J., Edwards O.R., Minemba D., Areke M.W., Jones R.A.C., 2019. *Zucchini yellow mosaic virus* genomic sequences from papua new guinea: Lack of genetic connectivity with northern australian or east timorese genomes, and new recombination findings. *Plant Disease* 103: 1326–1336. DOI: 10.1094/PDIS-09-18-1666-RE.

Mansour A., Al-Musa A., 1993. *Cucumber vein yellowing virus*; Host Range and Virus Vector Relationships. *Journal of Phytopathology* 137: 73–78. DOI: 10.1111/j.1439-0434.1993.tb01327.x.

Mantilla Paredes B.A., 2018. *Búsqueda de Fuentes de Resistencia al Virus Del Rizado Amarillo Del Tomate Nueva Delhi (Tomato Leaf Curl New Delhi Virus, TOLCNDV) en Tomate*. M.Sc Thesis, Universitat Politècnica de València, Spain, 105 pp.

Martelli G.P., Gallitelli D., 2008. Emerging and Reemerging Virus Diseases of Plants. *Encyclopedia of Virology* 86–92. DOI: 10.1016/B978-012374410-4.00705-6.

Martín-Hernández A.M., Picó B., 2020. Natural Resistances to Viruses in Cucurbits. *Agronomy* 11: 23. DOI: 10.3390/agronomy11010023.

Martin D.P., Biagini P., Lefeuvre P., Golden M., Roumagnac P., Varsani A., 2011. Recombination in Eukaryotic Single Stranded DNA Viruses. *Viruses* 3: 1699–1738. DOI: 10.3390/V3091699.

Marwal A., Sahu A.K., Gaur R.K., 2014. *Transmission and Host Interaction of Geminivirus In Weeds. Plant Virus-Host Interaction: Molecular Approaches and Viral Evolution,* Chapter 7. Academic Press, Elsevier, 143–161 pp.

Mauck K.E., De Moraes C.M., Mescher M.C., 2015. Infection of host plants by *Cucumber mosaic virus* increases the susceptibility of *Myzus persicae* aphids to the parasitoid *Aphidius colemani*. *Scientific Reports* 5: 1-9. DOI: 10.1038/srep10963.

Mazyad H.M., 2014. Molecular and biological characterization of *Squash leaf curl virus* (SLCV) affecting common beans in Egypt. *Egyptian Journal of Virology* 11: 14–27.

Mehetre G.T., Leo V.V., Singh G., Sorokan A., Maksimov I., … Singh B.P., 2021. Current Developments and Challenges in Plant Viral Diagnostics: A Systematic Review. *Viruses* 13: 412. DOI: 10.3390/V13030412.

Mehle N., Kutnjak D., Jakoš N., Seljak G., Pecman A., … Ravnikar M., 2019. First report of *Cucurbit aphid-borne yellows virus* in *Cucurbita pepo* and *Cucurbita maxima* in Slovenia. *Plant Disease* 104: 599. DOI: 10.1094/PDIS-07-19-1524-PDN.

Miller S.A., Martin R.R., 1988. Molecular Diagnosis of Plant Disease*. *Annual Review of Phytopathology* 26: 409–432. DOI: 10.1146/annurev.py.26.090188.002205.

Minicka J., Zarzyńska-Nowak A., Budzyńska D., Borodynko-Filas N., Hasiów-Jaroszewska B., 2020. High-Throughput Sequencing Facilitates Discovery of New Plant Viruses in Poland. *Plants* 9: 820. DOI: 10.3390/plants9070820.

Miras M., Torre C., Gómez-Aix C., Hernando Y., Aranda M.A., 2020. Development of monoclonal antibodies against *Melon necrotic spot virus* and their use for virus detection. *Journal of Virological Methods* 278: 113837. DOI: 10.1016/J.JVIROMET.2020.113837.

Mnari-Hattab M., Gauthier N., Zouba A., 2009. Biological and molecular characterization of the *Cucurbit aphid-borne yellows virus* affecting cucurbits in tunisia. *Plant Disease* 93: 1065–1072. DOI: 10.1094/PDIS-93-10-1065.

Mnari-Hattab M., Zammouri S., Belkadhi M.S., Bellon Doña D., ben Nahia E., Hajlaoui M.R., 2015. First report of *Tomato leaf curl new delhi virus* infecting cucurbits in Tunisia. *New Disease Reports* 31: 21. DOI: 10.5197/j.2044-0588.2015.031.021.

Moriones E., Praveen S., Chakraborty S., 2017. *Tomato leaf curl new delhi virus*: An emerging virus complex threatening vegetable and fiber crops. *Viruses* 9: 264. DOI: 10.3390/v9100264.

Morroni M., Jacquemond M., Tepfer M., 2013. Deep Sequencing of Recombinant Virus Populations in Transgenic and Nontransgenic Plants Infected with *Cucumber mosaic virus*. *Molecular Plant-Microbe Interactions* 26: 801–811. DOI: 10.1094/MPMI-02-13-0057-R.

Moura M.C.F., Holanda I.S.A., Sales Júnior R., Queiroz A.P.O., Araújo E.O.A., … Negreiros A.M.P., 2018. First report of *Melon necrotic spot virus* in melon plantations in Brazil. *Plant Disease* 102: 1048-1048.

Muhire B., Martin D.P., Brown J.K., Navas-Castillo J., Moriones E., … Varsani A., 2013. A genome-wide pairwise-identity-based proposal for the classification of viruses in the genus Mastrevirus (family *Geminiviridae*). *Archives of Virology* 158: 1411–1424. DOI: 10.1007/s00705-012-1601-7.

Nagendran K., Mohankumar S., Aravintharaj R., Balaji C.G., Manoranjitham S.K., … Karthikeyan G., 2017. The occurrence and distribution of major viruses infecting cucurbits in Tamil Nadu state, India. *Crop Protection* 99: 10–16. DOI: 10.1016/j.cropro.2017.05.006.

Nagy P.D., Simon A.E., 1997. New insights into the mechanisms of RNA recombination. *Virology* 235: 1–9. DOI: 10.1006/viro.1997.8681.

Nascimento A.K.Q., Lima J.A.A., Barbosa G. da S., 2017. A Simple Kit of Plate-Trapped Antigen Enzyme-Linked Immunosorbent Assay for Identification of Plant Viruses. *Revista Ciência Agronômica*, Universidade Federal do Ceará 48: 216–220. DOI: 10.5935/1806-6690.20170025.

Navarro J.A., Genovés A., Climent J., Saurí A., Martínez-Gil L., … Pallás V., 2006. RNA-binding properties and membrane insertion of *Melon necrotic spot virus* (MNSV) double gene block movement proteins. *Virology* 356: 57–67. DOI: 10.1016/j.virol.2006.07.040.

Navas-Castillo J., Fiallo-Olivé E., Sánchez-Campos S., 2011. Emerging Virus Diseases Transmitted by Whiteflies. *Annual Review of Phytopathology* 49: 219–248. DOI: 10.1146/annurev-phyto-072910-095235.

Navas-Castillo J., López-Moya J.J., Aranda M.A., 2014. Whitefly-transmitted RNA viruses that affect intensive vegetable production. *Annals of Applied Biology* 165: 155–171. DOI: 10.1111/aab.12147.

Niu E.B., Chen L.J., Niu Y.B., 2015. First report of *Zucchini yellow mosaic virus* in Chrysanthemum. *Plant Disease* 99: 1289-1289.

Ohshima K., Ando T., Motomura N., Matsuo K., Sako N., 2000. Comparative study on genomes of two Japanese *Melon necrotic spot virus* isolates. *Acta Virologica* 44: 309–314.

Okuda M., Okuda S., Iwai H., 2015. Detection of *Cucurbit chlorotic yellows virus* from bemisia tabaci captured on sticky traps using reverse transcription loop-mediated isothermal amplification (RT-LAMP) and simple template preparation. *Journal of Virological Methods* 221: 9–14. DOI: 10.1016/j.jviromet.2015.04.014.

Ouedraogo R.S., Pita J.S., Somda I.P., Traore O., Roossinck M.J., 2019. Impact of cultivated hosts on the recombination of *Cucumber mosaic virus*. *Journal of Virology* 93: 1–9. DOI: 10.1128/JVI.01770-18.

Padidam M., Beachy R.N., Fauquet C.M., 1995. Tomato leaf curl geminivirus from India has a bipartite genome and coat protein is not essential for infectivity. *Journal of General Virology* 76: 25–35. DOI: 10.1099/0022-1317-76-1-25.

Padidam M., Sawyer S., Fauquet C.M., 1999. Possible emergence of new geminiviruses by frequent recombination. *Virology* 265: 218–225. DOI: 10.1006/viro.1999.0056.

Panno S., Iacono G., Davino M., Marchione S., Zappardo V., … Davino S., 2016. First report of *Tomato leaf curl new delhi virus* affecting zucchini squash in an important horticultural area of southern Italy. *New Disease Reports* 33: 6. DOI: 10.5197/j.2044-0588.2016.033.006.

Papayiannis L.C., Ioannou N., Boubourakas I.N., Dovas C.I., Katis N.I., Falk B.W., 2005. Incidence of viruses infecting cucurbits in Cyprus. *Journal of Phytopathology* 153: 530–535. DOI: 10.1111/j.1439-0434.2005.01015.x.

Pascual L., Yan J., Pujol M., Monforte A.J., Picó B., Martín-Hernández A.M., 2019. CmVPS41 is a general gatekeeper for resistance to *Cucumber mosaic virus* phloem entry in melon. *Frontiers in Plant Science* 10: 1219. DOI: 10.3389/fpls.2019.01219.

Pita J.S., Roossinck M.J., 2007. *Virus Populations, Mutation Rates and Frequencies*. In: *Plant Virus Evolution*, Springer Berlin Heidelberg, 109–121.

Pitrat M., Lecoq H., 1984. Inheritance of *Zucchini yellow mosaic virus* resistance in *Cucumis melo* L. *Euphytica* 33: 57–61. DOI: 10.1007/BF00022750.

Pourrahim R., Farzadfar S., Golnaraghi A.R., Shahraeen N., 2003. First Report of *Papaya ringspot virus* on Papaya in Iran . *Plant Disease* 87: 1148–1148. DOI: 10.1094/pdis.2003.87.9.1148b.

Pozzi E.A., Bruno C., Luciani C.E., Celli M.G., Conci V.C., Perotto M.C., 2020. Relative incidence of cucurbit viruses and relationship with bio-meteorological variables. *Australasian Plant Pathology* 49: 167–174. DOI: 10.1007/s13313-020-00687-8.

Radouane N., Ermadi S., Ezrari S., Al Figuigui J., Benjelloune M., … Lahlali R., 2020. Occurrence and distribution of viruses infecting Zucchini and Watermelon in Morocco. *Archives of Phytopathology and Plant Protection* 54: 375-387. DOI: 10.1080/03235408.2020.1833280.

Radouane N., Ezrari S., Accotto G.P., Benjelloun M., Lahlali R., … Vaira A.M., 2019. First report of *chickpea chlorotic dwarf virus* in watermelon (*Citrullus lanatus*) in Morocco. *New Disease Reports* 39: 4404. DOI: 10.5197/j.2044-0588.2019.039.002.

Radouane N., Tahiri A., El Ghadraoui L., Al Figuigui J., Lahlali R., 2018. First report of *Tomato leaf curl new delhi* virus in Morocco. *New Disease Reports* 37: 2. DOI: 10.5197/j.2044-0588.2018.037.002.

Rajbanshi N., Ali A., 2016. First Complete Genome Sequence of a *Watermelon mosaic virus* Isolated from Watermelon in the United States. *Genome Announcements* 4: e00299-16. DOI: 10.1128/genomeA.00299-16.

Riviere C.J., Pot J., Tremaine J.H., Rochon D.M., 1989. Coat protein of *melon necrotic spot carmovirus* is more similar to those of tombusviruses than those of carmoviruses. *Journal of General Virology* 70: 3033–3042. DOI: 10.1099/0022-1317-70-11-3033.

Robinson R.W., Robinson R.W., Decker-Walters D.S., 1997. *Cucurbits*. Crop production science in horticulture. Cab International, New York, United states of America, 226 pp.

Roditakis A., Steinbach E.;, Moritz D.;, Journal A., 2017. Ryanodine receptor point mutations confer diamide insecticide resistance in tomato leafminer, Tuta absoluta (Lepidoptera: *Gelechiidae*). *Insect Biochemistry and Molecular Biology* 80: 11-20.

Rodríguez-Negrete E.A., Morales-Aguilar J.J., Domínguez-Duran G., Torres-Devora G., Camacho-Beltrán E., … Méndez-Lozano J., 2019. High-Throughput Sequencing Reveals Differential Begomovirus Species Diversity in Non-Cultivated Plants in Northern-Pacific Mexico. *Viruses* 11: 594. DOI: 10.3390/v11070594.

Rodríguez E., Téllez M.M., Janssen D., 2019. Whitefly control strategies against *Tomato leaf curl new delhi virus* in greenhouse zucchini. *International Journal of Environmental Research and Public Health* 16: 2673. DOI: 10.3390/ijerph16152673.

Rojas M.R., Gilbertson R.L., 2008. *Emerging Plant Viruses: a Diversity of Mechanisms and Opportunities.* In: *Plant Virus Evolution*, Berlin, Heidelberg, Springer Berlin Heidelberg, 27–51.

Romay G., Lecoq H., Geraud-Pouey F., Chirinos D.T., Desbiez C., 2014. Current status of cucurbit viruses in Venezuela and characterization of Venezuelan isolates of *Zucchini yellow mosaic virus*. *Plant Pathology* 63: 78–87. DOI: 10.1111/ppa.12072.

Romay G., Pitrat M., Lecoq H., Wipf-Scheibel C., Millot P., … Desbiez C., 2019. Resistance against *Melon chlorotic mosaic virus* and *Tomato leaf curl new delhi virus* in Melon. *Plant Disease* 103: 2913–2919. DOI: 10.1094/PDIS-02-19-0298-RE.

Roossinck M.J., 1997. Mechanisms of plant virus evolution. *Annual Review of Phytopathology* 35: 191–209.

Ruiz L., Simon A., Velasco L., Janssen D., 2016. Biological characterization of *Tomato leaf curl New Delhi virus* from Spain. *Plant Pathology* 66: 376–382. DOI: 10.1111/ppa.12587.

Sáez C., Martínez C., Ferriol M., Manzano S., Velasco L., … Picó B., 2016. Resistance to *Tomato leaf curl New Delhi virus* in *Cucurbita* spp. *Annals of Applied Biology* 169: 91–105.

Samsatly J., Sobh H., Jawhari M., Najjar C., Haidar A., Abou-Jawdah Y., 2012. First report of *Watermelon chlorotic stunt virus* in cucurbits in Lebanon. *Plant Disease* 96: 1703-1703.

Shah Nawaz-Ul-Rehman M., Fauquet C.M., 2009. Evolution of geminiviruses and their satellites. *FEBS letters* 583: 1825-1832. DOI: 10.1016/j.febslet.2009.05.045.

Simmons H.E.E., Dunham J.P.P., Zinn K.E.E., Munkvold G.P.P., Holmes E.C.C., Stephenson A.G.G., 2013. *Zucchini yellow mosaic virus* (ZYMV, Potyvirus): Vertical transmission, seed infection and cryptic infections. *Virus Research* 176: 259–264. DOI: 10.1016/j.virusres.2013.06.016.

Smith D.B., Inglis S.C., 1987. The mutation rate and variability of eukaryotic viruses: an analytical review. *Journal of General Virology* 68: 2729–2740. DOI: 10.1099/0022-1317-68-11-2729.

Sobh H., Samsatly J., Jawhari M., Najjar C., Haidar A., Abou-Jawdah Y., 2012. First Report of *Squash leaf curl virus* in Cucurbits in Lebanon. *Plant Disease* 96: 1231–1231. DOI: 10.1094/PDIS-04-12-0365-PDN.

Sugiyama M., 2013. The present status of breeding and germplasm collection for resistance to viral diseases of cucurbits in Japan. *Journal of the Japanese Society for Horticultural Science* 82: 193–202.

Suveditha S., Bharathi L.K., Krishna Reddy M., 2017. First report of *Cucurbit aphid-borne yellows virus* infecting bitter gourd (*Momordica charantia*) and teasel gourd (*Momordica subangulata* subsp. *renigera*) in India. *New Disease Reports* 36: 7. DOI: 10.5197/j.2044-0588.2017.036.007.

Svoboda J., Leisova-Svobodova L., Lecoq H., 2011. First report of *Cucurbit aphid-borne yellows virus* in squash in the Czech Republic. *Plant Disease* 95 : 220-220.

Sztuba-Solińska J., Urbanowicz A., Figlerowicz M., Bujarski J.J., 2011. RNA-RNA Recombination in Plant Virus Replication and Evolution. *Annual Review of Phytopathology* 49: 415–443. DOI: 10.1146/annurev-phyto-072910-095351.

Tellez M. del M., Simon A., Rodriguez E., Janssen D., 2017. Control of *Tomato leaf curl New Delhi virus* in zucchini using the predatory mite *Amblyseius swirskii*. *Biological Control* 114: 106–113. DOI: 10.1016/j.biocontrol.2017.08.008.

Tomassoli L., Meneghini M., 2007. First report of *Cucurbit aphid-borne yellows virus* in Italy. *Plant Pathology* 56: 720–720. DOI: 10.1111/j.1365-3059.2007.01583.x.

Tomlinson J.A., Thomas B.J., 1986. Studies on *melon necrotic spot virus* disease of cucumber and on the control of the fungus vector (*Olpidium radicale*). *Annals of Applied Biology* 108: 71–80. DOI: 10.1111/j.1744-7348.1986.tb01967.x.

Torre C., Agüero J., Gómez-Aix C., Aranda M.A., 2020. Comparison of DAS-ELISA and qRT-PCR for the detection of cucurbit viruses in seeds. *Annals of Applied Biology* 176: 158–169. DOI: 10.1111/AAB.12543.

Tripathi S., Verma A., Kushwah S.S., Verma R., 2021. First report of occurrence of *Zucchini yellow mosaic virus* in *Luffa aegyptiaca* in India. *Journal of Plant Pathology* 103: 1017–1017. DOI: 10.1007/S42161-021-00836-Y.

Velasco L., Ruiz L., Galipienso L., Rubio L., Janssen D., 2020. A Historical Account of Viruses in Intensive Horticultural Crops in the Spanish Mediterranean Arc: New Challenges for a Sustainable Agriculture. *Agronomy* 10: 860. DOI: 10.3390/agronomy10060860.

Verma R., Ahlawat Y.S., Tomer S.P.S., Prakash S., Pant R.P., 2007. First Report of *Zucchini yellow mosaic virus* in Bottlegourd (*Lagenaria siceraria*) in India. *Plant Disease* 88: 426. DOI: 10.1094/PDIS.2004.88.4.426C.

Verma R., Baranwal V.K., Prakash S., Tomer S.P.S., Pant R.P., Ahlawat Y.S., 2006. First Report of *Papaya ringspot virus* W in Sponge Gourd from India. *Plant Disease* 90: 974–974. DOI: 10.1094/pd-90-0974b.

Vučurović A., Bulajić A., Stanković I., Ristić D., Berenji J., … Krstić B., 2011. First Report of the Occurrence of *Cucurbit aphid-borne yellows virus* on Oilseed Pumpkin in Serbia . *Plant Disease* 95: 1035–1035. DOI: 10.1094/pdis-02-11-0147.

Vuillaume F., Thébaud G., Urbino C., Forfert N., Granier M., … Peterschmitt M., 2011. Distribution of the phenotypic effects of random homologous recombination between two virus species. *PLoS pathogens* 7: e1002028. DOI: 10.1371/journal.ppat.1002028.

Waliullah S., Ling K.-S., Cieniewicz E.J., Oliver J.E., Ji P., Ali M.E., 2020. Development of Loop-Mediated Isothermal Amplification Assay for Rapid Detection of *Cucurbit leaf crumple virus*. *International Journal of Molecular Sciences* 21: 1756. DOI: 10.3390/ijms21051756.

Walkey D.G.A., Alhubaishi A.A., Webb M.J.W., 1990. Plant virus diseases in the yemen arab republic. *Tropical Pest Management* 36: 195–206. DOI: 10.1080/09670879009371471.

Wang D., Li G., 2017. Host Reaction of *Watermelon mosaic virus* Isolates Infecting Melon from Different Geographical Origins in Xinjiang of China. *Horticultural Plant Journal* 3: 23–28. DOI: 10.1016/j.hpj.2017.01.010.

Welbaum G.E., 2015. *Vegetable Production and Practices*. CAB International Publisher, 189-204.

Wilisiani F., Mashiko T., Wang W.Q., Suzuki T., Hartono S., … Natsuaki T., 2019. New recombinant of *Tomato leaf curl New Delhi virus* infecting melon in Indonesia. *Journal of General Plant Pathology* 85: 306–310. DOI: 10.1007/s10327-019-00849-7.

Willrich Siebert M., Thomas J.D., Nolting S.P., Rogers Leonard B., Gore J., … Siebert J., 2012. Field evaluations of sulfoxaflor, a novel insecticide, against tarnished plant bug (hemiptera: *miridae*) in cotton. *The Journal of Cotton Science* 16: 129–143 pp.

Wilson C.R., Lambert S.J., Dann A.L., Cross P., Hay F.S., 2012. Occurrence of viruses within Tasmanian vegetable crops and identification of a novel Polerovirus infecting pea. *Australasian Plant Pathology* 41: 311–319. DOI: 10.1007/s13313-011-0114-2.

Wintermantel W.M., Gilbertson R.L., Natwick E.T., McCreight J.D., 2017. Emergence and epidemiology of *Cucurbit yellow stunting disorder virus* in the American Desert Southwest, and development of host plant resistance in melon. *Virus Research* 241: 213–219. DOI: 10.1016/j.virusres.2017.06.004.

Xiang H.Y., Shang Q.X., Han C.G., Li D.W., Yu J.L., 2008. First report on the occurrence of *Cucurbit aphid-borne yellows virus* on nine cucurbitaceous species in China. *Plant Pathology* 57: 390–390. DOI: 10.1111/j.1365-3059.2007.01664.x.

Yakoubi S., Desbiez C., Fakhfakh H., Wipf-Scheibel C., Marrakchi M., Lecoq H., 2007. Occurrence of *Cucurbit yellow stunting disorder virus* and *Cucumber vein yellowing virus* in Tunisia. *Journal of Plant Pathology* 89: 417–420. DOI: 10.4454/jpp.v89i3.775.

Yakoubi S., Desbiez C., Fakhfakh H., Wipf-Scheibel C., Marrakchi M., Lecoq H., 2008. First report of *Melon necrotic spot virus* on melon in Tunisia. *Plant Pathology* 57: 386..

Yeh S.-D., 1984. Comparative Studies on Host Range and Serology of *Papaya ringspot virus* and *Watermelon mosaic virus* 1. *Phytopathology* 74: 1081-1085. DOI: 10.1094/phyto-74-1081.

Yu C., Wang D., Zhang X., Shi K., Li X., Yuan X., 2016. First report of *Melon necrotic spot virus* in watermelon in China. *Plant Disease* 100: 1511. DOI: 10.1094/PDIS-01-16-0056-PDN.

Zaagueri T., Mnari-Hattab M., Zammouri S., Hajlaoui M.R., Accotto G.P., Vaira A.M., 2017. First report of *Chickpea chlorotic dwarf virus* in watermelon (*Citrullus lanatus*) in Tunisia. *Plant Disease* 101: 392. DOI: 10.1094/PDIS-07-16-1028-PDN.

Zaidi S.S.E.A., Martin D.P., Amin I., Farooq M., Mansoor S., 2017. *Tomato leaf curl New Delhi virus*: a widespread bipartite begomovirus in the territory of monopartite begomoviruses. *Molecular Plant Pathology* 18: 901–911. DOI: 10.1111/mpp.12481.

Zubair M., Khan R.A.A., Ali A., Ullah N., Ahmad S., … Akhtar K.P., 2020. First Report of *Tomato leaf curl New Delhi virus* in *Physalis minima* in Pakistan. *Plant Disease* 104: 1878. DOI: 10.1094/PDIS-12-19-2607-PDN.

Phytopathologia Mediterranea
The international journal of the
Mediterranean Phytopathological Union

Firenze University Press
www.fupress.com/pm

Research Papers

The distribution of *Phytophthora cinnamomi* in the Americas is related to its main host (*Persea americana*), but with high potential for expansion

Joaquín Guillermo RAMÍREZ-GIL[1,*], Juan Gonzalo MORALES-OSORIO[2], A. Townsend PETERSON[3]

[1] *Departamento de Agronomía, Facultad de Ciencias Agrarias, Universidad Nacional de Colombia, sede Bogotá, Colombia*
[2] *Departamento de Ciencias Agronómicas, Facultad de Ciencias Agrarias, Universidad Nacional de Colombia, sede Medellín, Colombia*
[3] *Biodiversity Institute, University of Kansas, Lawrence, KS, 66045 USA*
* Corresponding author. E-mail: jgramireg@unal.edu.co

Summary. *Phytophthora cinnamomi* is among the most destructive plant pathogens that affect many host plants in different ecosystems. Economically important hosts of this pathogen include avocado (*Persea americana*), and this oomycete may cause large-scale destructive epidemics. This study analyzed the potential geographic distribution of *P. cinnamomi* (pathogen) and avocado (host), and distribution of the pathogen in relation to multiple hosts in the Americas. Niche overlap between hosts and pathogen were also evaluated, using a multistep process of ecological niche modelling and the MaxEnt algorithm. Niche similarity among pathogen populations in different hosts and related niche similarity were also examined. As a complement, a tool was designed to visualize the risk of this pathogen in avocado. Results showed that the pathogen was randomly distributed in the avocado niche environmental space, but the niche of the pathogenwas narrower than that of its principal host. The niche of the pathogen was largely a function of the host niches. Areas with potential to grow avocado could present low risk of *P. cinnamomi*, but given the invasiveness of this pathogen, they may be affected in the future.

Keywords. Ecological Niche Model, environment, niche overlap, plant epidemiology, risk maps.

OPEN ACCESS

Citation: J.G. Ramírez-Gil, J.G. Morales-Osorio, A.T. Peterson (2021) The distribution of *Phytophthora cinnamomi* in the Americas is related to its main host (*Persea americana*), but with high potential for expansion. *Phytopathologia Mediterranea* 60(3): 521-534. doi: 10.36253/phyto-12327

Accepted: October 29, 2021

Published: December 30, 2021

Data Availability Statement: All relevant data are within the paper and its Supporting Information files.

Competing Interests: The Author(s) declare(s) no conflict of interest.

Editor: Matteo Garbelotto, University of California, Berkeley CA, USA.

INTRODUCTION

Phytophthora cinnamomi Rands is one of the most important and devastating plant pathogens (Zentmyer, 1980; Bohlen, 2006; Burgess *et al*., 2017; Hardham and Blackman, 2018). This oomycete is known to infect >3000 host plant species, causing disease in orchard and forestry species. It has the potential to occupy a broad geographic distribution, due to its genetic plasticity under different environmental conditions (Zentmyer, 1980; Burgess *et al*., 2017; Hardham and Blackman, 2018; Ramírez-Gil and Peterson, 2019). This pathogen causes root rot of avocado (*Persea americana* Mill), which is

the most serious disease of avocado in the most countries where this crop is grown (Zentmyer, 1980; 1984; Ramírez-Gil *et al*., 2017; Hardham and Blackman, 2018).

Phytophthora cinnamomi is reported from tropical and subtropical zones and from many different ecosystems, where it may cause severe diseases on crops and wild plants (Pratt and Heather, 1973; Weste and Marks, 1974; Zentmyer, 1997; Duque-Lazo *et al*., 2016; Burgess *et al*., 2017; Hardham and Blackman, 2018; Ramírez-Gil and Peterson, 2019). Zentmyer (1997) reported that *P. cinnamomi* had not been recovered from any native trees growing at undisturbed sites in America, suggesting that it is not a native pathogen of these plants. This is supported by this pathogen having scattered distribution, and by the high susceptibility of America's native flora (Weste and Marks, 1974). The scattered distribution is likely to be the result of different introduction histories of the pathogen. *Phytophthora cinnamomi* could have been introduced into America by human-mediated movement, probably from Southeast Asia (Zentmyer, 1988, 1997; Socorro-Serrano *et al*., 2019) .

Avocado is one of the most economically important hosts of *P. cinnamomi* (Zentmyer, 1980; Ramírez-Gil *et al*., 2017; Hardham and Blackman, 2018). The centre of origin of *P. americana* is tropical America (GalindoTovar *et al*., 2008). This fruit tree is the most important cultivated species in *Lauraceae* (Schaffer *et al*., 2013), and includes three botanical races: Mexican (*P. americana* var. *drymifolia*), Guatemalan (*P. americana* var. *guatemalensis*), and West Indian (*P. americana* var. *americana*) (GalindoTovar *et al*., 2008). Hybridization among races has generated great phenotypic variability, and avocados are now grown under diverse environmental conditions, including semiarid Mediterranean, subtropical, and tropical climates (Papadakis, 1966; Knight and Campbell, 1999; Chen *et al*., 2009; Bost *et al*., 2013).

Ecological niche models (ENMs) relate known occurrence of species to environmental variation, to determine the ecological requirements of species. Based on those requirements the potential geographic distribution of such species can be estimated (Peterson *et al*., 2011). ENMs may have diverse practical applications in agriculture, including prediction of geographic distribution of economic crops and their pest and diseases, modelling of productivity, assessment of the potential for biological invasions by insects, weeds and pathogens, and forecast climate change impacts (Meyer *et al*., 2010; Burgess *et al*., 2017; Narouei-Khandan *et al*., 2017; Ramírez-Gil *et al*., 2018; Johnson *et al*., 2019; Ramírez-Gil and Peterson, 2019). Another application of ENMs is assessment of niche similarity among different species to establish whether those niches are different or have diverged (Maher *et al*., 2010; Qiao *et al*., 2017).

ENMs have been used to determine the potential distribution of *P. cinnamomi* in natural ecosystems (Duque-Lazo *et al*., 2016; Burgess *et al*., 2017; Hernández-Lambraño *et al*., 2018; Sena *et al*., 2019), and at a regional level in avocado crops (Ramírez-Gil and Peterson, 2019). However, no study evaluating naturally distributed and cultivated *P. cinnamomi* hosts has been reported across the Americas. The present paper reports the application of ENM approaches to provide understanding of how the potential geographical distribution of native and commercially cultivated avocado genotypes and *P. cinnamomi*, varies across the Americas. Ecological niches of *P. cinnamomi* in different plant hosts were also estimated and compared.

MATERIAL AND METHODS

Occurrence and environmental data

Records (15,560) associated with commercial avocado varieties in production fields (cultivars including: Hass, Fuerte, Reed, Zutano, Gottdried, Semil, Ettinger, Bacon, Hall, Lula, Collinred, Edranol, Lorena, Trapp, Booth, Choquette, and Trinidad), and native avocado genotypes related to the three races in natural ecosystems (*P. americana* var. *drymifolia*, *P. americana* var. *guatemalensis*, and *P. americana* var. *americana*). The records were obtained from Argentina, Brazil, Chile, Peru, Ecuador, Colombia, Panamá, Costa Rica, Cuba, Dominican Republic, El Salvador, Haiti, Honduras, Puerto Rico, Trinidad and Tobago, Guatemala, Mexico and the United States of America (USA; California and Florida). Data were obtained from different ecological conditions in a wide range of altitude (0 to 3200 m above sea level). Details about the origins of data and how they were obtained are described in Supplementary Information 1. Each data point was corroborated by visual inspection in Google Earth (accessed 3 March 2017), eliminating 2,503 sites that clearly did not correspond to avocado fields, or that were duplicated. Effects of spatial autocorrelation in data occurrence were reduced using 4.5 km distance filtering in the SDMtoolbox implemented in ArcGis (ESRI ™) (Brown, 2014), leaving a final set of 1,286 occurrence records for further analyses (Figure 1 A). The criterion for selecting this distance was determined based on the spatial resolution of the predictive variables (i.e., bioclimatic variables; see following paragraphs).

Occurrence data for *P. cinnamomi* on different hosts were obtained from published reports, databases, websites including the Global Biodiversity Information

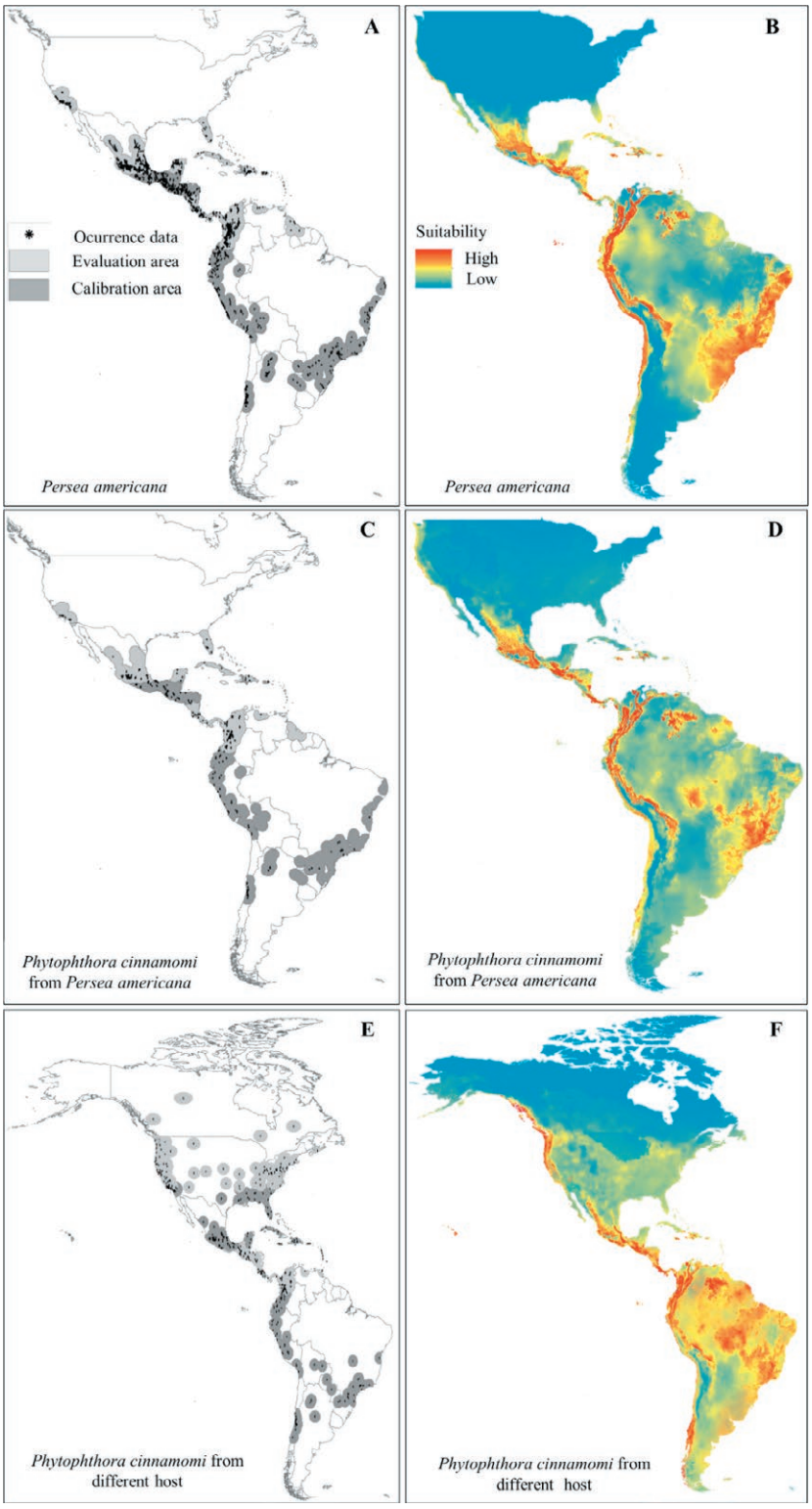

Figure 1. Potential distributions of *Persea americana* and *Phytophthora cinnamomi* under present environmental conditions in North and South America. Model calibration and evaluation areas (dark and light grey), and presence (black dots) data, documenting occurrences *Persea americana*, *Phytophthora cinnamomi* from *Persea americana*, and *P. cinnamomi* from hosts different to avocado (A, C, and E). Potential distribution of *P. americana*, *P. cinnamomi* from *P. americana*, and *P. cinnamomi* from all hosts (B, D, and F) under current environmental conditions in America. The map is the median of the logistic suitable index across the 10 replica models reported in Table 1.

Facility (GBIF; www.gbif.org), Invasive Species Compendium (https://www.cabi.org/isc/datasheet/40957), Center for Invasive Species and Ecosystems Health (https://www.invasive.org/species.cfm), Forest Phytophthoras of the World (http://forestphytophthoras.org/species/cinnamomi/disease), Plantwise Knowledge Bank (https://www.plantwise.org/knowledgebank/#.), and individual researchers (see Supplementary Information 1 for a list of sources for each country). A total of 206 records were collected from avocado, from across Latin America and the USA , and 194 additional records collected from other hosts distributed across the Americas, including four records from Canada (Figure 1, C and E). The criteria described above were applied to each of presence (i, corroborating that the coordinates were associated with the reported region, ii, removing duplicates, and iii, reducing spatial autocorrelation (4.5 km distance filtering)). The final data consisted of 205 records from avocado and 192 from other hosts (Figure 1, C and E).

All presences of *P. cinnamomi* from avocado, from different hosts; and from *P. americana* were randomly divided into four groups, each with equal numbers according to latitude (Figure 1, A, C and E), where 50% was used for calibration and the other 50% for evaluation of the models.

As environmental predictors, the bioclimatic variables available from the WorldClim climate data archive (Hijmans *et al.*, 2005) were initially used. The variables bio 8 (Mean Temperature of Wettest Quarter), 9 (Mean Temperature of Driest Quarter), 18 (Precipitation of Warmest Quarter), and 19 (Precipitation of Coldest Quarter) were eliminated *a priori*, due to known spatial artifacts in these data layers (Escobar *et al.*, 2014). All analyses were conducted at a spatial resolution of 2.5' (approx. 4 km^2), as a balance between obtaining sufficient spatial detail and avoiding excessive computational load and storage demands. Climate data sets were masked to temperate and tropical America, excluding Canada, Alaska, and small Caribbean islands, for avocado and *P. cinnamomi*-infected avocado data. In addition, the predictive analysis was extended to all America including data of *P. cinnamomi* from hosts different to avocado.

Ecological niche modelling

Three ecological niche models (ENMs) were developed. The first was for avocados (including commercial varieties and native genotypes associated with the three botanical races). The second model was for *P. cinnamomi* that was reported infecting avocado (Supplementary Information 1). The third model was for *P. cinnamomi* infecting hosts different from avocado in the Americas (Supplementary Information 1). ENMs were based on the maximum entropy algorithm implemented in Maxent version 3.3.3k (Phillips *et al.*, 2006).

Three steps were used for the development of ENMs with the best predictive ability. The first was definition of a calibration area as the area accessible to the species of study over a relevant period (termed M) (Barve *et al.*, 2011; Saupe *et al.*, 2012). M was selected as all land areas within 100 km^2 for avocado presence, within 150 km^2 for *P. cinnamomi* from avocados, and within 200 km^2 for *P. cinnamomi* from different hosts to avocado. This was based on potential areas of influence of *P. cinnamomi* and its hosts (Figure 1, A, C, and E). For the second step, the best set of environmental predictors for our models was selected using jackknife routines in Maxent software. The third step used model selection approaches to optimize parameter settings in Maxent, based on Akaike Information Criterion (AIC_c) values calculated using ENMTools version 1.3 (Warren *et al.*, 2010), from models calibrated with 50% of input points (all calibration points that corresponded to 50% of all presences), ten cross-validated replicates, and raw model outputs. Combinations were evaluated of the regularization multiplier (β) (0.25, 0.5, 1, 1.5, 2, 4, 6, 8 and 10), response types (L, LQ, LQP, LQPT, and LQPTH; where L = linear, Q = quadratic, P = product, T = threshold, and H = hinge), and the six sets of environmental variables (the climatic variables 5, 7, 9, 11, 13, and 15) using jackknife routines as described above. In total 270 models were evaluated.

To assess the robustness and predictive ability of the obtained models, three groups were selected based on the AIC_c values for each of the target taxa (Figure 1), that showed the least, medium and greatest AIC_c values, but with different parameter settings and environmental data layers (for details, the summary of the total models evaluated in Table 1). For each of the ENMs, four sub-regions were created with approximately equal numbers of occurrences, by dividing the region according to latitude. The sub-regions were: 1 (south of Colombia, Ecuador, Peru, Bolivia; Brazil, Paraguay, Uruguay, Argentina, and Chile); 2 (north of Colombia, south of Central America and the Caribbean islands); 3 (north of Central America, south of Mexico, and north the Caribbean islands; and 4 (north of Mexico, California, Florida; USA, and part of Canada) (Figure 1, A, C, and E). Maxent was then used with ten cross-validated replicates and logistic output format. For this stage of analysis, sub-regions 1 and 3 were used for calibration, and sub-regions 2 and 4 were used for evaluations (Figure 1, A, C, and E).

Model quality was evaluated based on complexity, using AIC_c values (above), and the significance of

predictions based on partial receiver operating characteristic (partialROC) approaches (Peterson *et al.*, 2008). Functions used are available in Niche Toolbox (http://shiny.conabio.gob.mx:3838/nichetoolb2/). An acceptable omission rate of E = 5%, and bootstrap analysis with 1000 iterations were used, with random subsamples of 50% of each dataset tested for each of the generated models. The probability associated with the test was determined by direct count of replicates in which the partial ROC statistics was ≤1. Performance was evaluated with the omission rate (OR) calculated via thresholding models of the calibration sub-regions, based on the greatest model output value that was associated with ≤5% omission of calibration data. Once this threshold was imposed on the other sub-regions, OR was calculated based on the evaluation data.

The best models from the three data groups (avocado, *P. cinnamomi* from avocado), and *P. cinnamomi* from different hosts to avocado, were chosen considering, firstly, significance (partial ROC), then performance (OR < 6.2%), and lastly, the minimum complexity (lowest values of AICc), in that order (Table 1). Next, only models within 2 units of the minimum AICc values were retained. These models were then projected across temperate and tropical America, excluding Canada, Alaska, and small Caribbean islands, for avocado and avocado infected with *P. cinnamomi*, but all America was included for *P. cinnamomi* from different hosts to avocado, using Maxent with no clamping or extrapolation, and with ten bootstrap replicates and logistic outputs.

Niche similarity

To assess whether *P. cinnamomi* has an ecological niche distinct from that of its avocado host, a resampling exercise was carried out from the presences of avocado (native and commercial genotypes) in the Americas associated with the occurrence of this species under different environmental conditions (edaphic properties, climatic, topographic, or biophysical variables), contrasting anthropic conditions (agronomic management practices, culture), and genetic variability. One hundred random combinations were drawn of avocado occurrence points to mimic 204 infected points (described above) that were available, using our code in R (R Development Core Team, 2021). For each point, values were extracted that were associated with the environmental variables coinciding in the selection of the ENMs of avocado and *P. cinnamomi* described above (bio 1, 5, 10, and 12. Table 1), and frequency histograms were made of means among these null replicates. The actual mean and standard deviation values observed for known occurrences of *P. cinnamomic* were then compared. This test was designed to assess whether the pathogen (*P. cinnamomi*) had a niche distinct to that of its economic host of study (avocado).

NicheA was used for the visualization of niche overlap based on minimum volume ellipsoids for the species in three PCA dimensions (Qiao *et al.*, 2016), considering the climatic variables that the three models had in common (bio 1, 5, 10, and 12. Table 1). Subsequently, this analysis was complemented with the Jaccard index (I_J), as a numerical metric of environmental overlap between the two species studied (Jaccard, 1912; Qiao *et al.*, 2017).

Risk visualization of Phytophthora cinnamomi in avocado in the Americas

To determine the risk of *P. cinnamomi* in avocado (cultivated varieties and native races) in the Americas, the outputs of the ENMs from avocado, *P. cinnamomi* from avocado, and *P. cinnamomi* from other hosts were used to determine three areas. These were: (i) areas with avocado with current distribution of *P. cinnamomi*, obtained as the interception of current distribution of avocado and *P. cinnamomi* from avocado (current risk, represented in yellow); (ii) areas with current and potential avocado that could become infected by *P. cinnamomi* in the future, obtained as the current and potential distribution of avocado, which are not related to the *P. cinnamomi* distribution from avocado, but which can be potentially affected with *P. cinnamomi* potential distribution associated with other hosts (potential risk, represented in red); and (iii) areas with avocado that are not suitable to *P. cinnamomi* based on all ENMs from *P. cinnamomi* (low risk, represented in green). The visualization map of the risk of *P. cinnamomi* was made. the three model transfers were reclassified to binary (0 and 1) with a threshold determined on calibration areas as described above, applied to the median value of the ten replicates. Later, we summed these grids to produce a layer with values from 0 to 3 (values with 0 = no host; values with 1 = low risk; values with 2 = potential risk; values with 3 = current risk). The current, potential and low risk in these results were visualized using a grid combination approach (Ramírez-Gil *et al.*, 2019).

RESULTS

Model selection

The three parameters that were explored in selection of the model (features, β regularization multiplier,

and the combination of environmental variables) generated a set of candidate models for further assessment. The best models were selected using these parameters, considering as criteria a prediction capacity greater than random ($P < 0.001$), models with the lower complexity (lower AIC value), and good performance based on low omission rate values (Table 1). As a result, the models with better behaviour for *Persea americana*, *P. cinnamomi* from avocado and *P. cinnamomi* from different hosts to avocado were related to the features responses of the MaxEnt algorithm of quadratic (LQ), quadratic (LQ), and product (LQP) type, with a set of combination of 6, 6, and 7 bioclimatic variables, and β regularization multiplier of 2, 1.5 and 4, respectively. In general, models with high numbers of predictive variables (≥ 9), low or high β regularization multiplier (≤1 and >4) and threshold (LQPT) and hinge (LQPTH) features, showed lower metrics that are desirable for a better model (significance, performance, and complexity) (Table 1)

Geographic distributions

The projection of ENMs for avocados (commercial varieties and native genotypes) indicated that this species shows a wide distribution across the Americas. High-suitability areas were associated with the Valleys of California in the USA, a wide region from central and southern Mexico, parts of Central America distributed in Guatemala, Honduras, El Salvador, Nicaragua, Costa Rica and Panama, small areas in the Caribbean Islands including Southern Cuba, Jamaica, Dominican Republic, Haiti, Puerto Rico, and the Guianas, the highlands of Colombia, Ecuador, Peru, Bolivia, and Venezuela, the Caribbean and Pacific coasts of Colombia and Venezuela, the coastal valleys of Peru and Chile, the Amazonian portion located in the south of Venezuela and the north of Brazil and the southeastern and northeastern coasts of Brazil (Figure 1 B). These results suggested new areas that can be used for planting (potential crops) or by natural expansion (potential areas with natives races). These areas are localized in the South (Brazil, Argentina, Chile, Bolivia, Paraguay, and Uruguay), and North (Mexico and USA) (Figure 1 B). The

Table 1. Description of selected models and corresponding parameters based on the Maxent algorithm.

Target taxa	AIC_c[1] classification	Features[2]	β (regularization multiplier)	Bioclimatic variables	AIC to calibration models[1]	Projected parameters		
						pROC[3]	OR[4]	AICc[1]
Avocado	High	LQPTH	4	1, 3, 4, 5, 6, 10, 12, 14, 15, 16 and 17	1203,431	0.001	5.3	948,609
	High	LQPT	6	1, 3, 4, 5, 6, 10, 12, 15, and 16	1125,101	0.001	6.8	821,319
	Medium	LQPT	4	1, 3, 4, 5, 6, 10, 12, and 15	836,108	0.001	7.3	763,815
	Medium	LQP	2	1, 4, 5, 6, 10, 12, and 16	828,436	0.001	6.8	656,414
	Low	LQP	1.5	1, 4, 6, 10, 12, and 12	718.607	0.001	6.3	648,602
	Low[a]	LQ	2	1, 4, 5, 6, 10, and 12	708,500	0.001	5.8	508,135
P. cinnamomi from avocado	High	LQPTH	4	1, 4, 5, 7, 10, 12, 13, 14, 15, and 16	2301,351	0.001	5.0	1022,452
	High	LQPTH	2	1, 4, 5, 7, 10, 12, 13, 14, and 16	2009,913	0.001	5.3	1211,489
	Medium	LQPT	4	1, 4, 5, 7, 10, 12, 13, and 16	1758,933	0.001	6.8	843,611
	Medium	LQPT	6	1, 4, 5, 7, 10, 12, 13, and 16	1686,231	0.001	5.9	742,981
	Low	LQ	2	1, 4, 5, 10, 12, 13, and 16	1181.607	0.001	5.2	535,142
	Low[b]	LQ	1.5	1, 5, 10, 12, 13, and 16	1011.117	0.001	4.8	505,171
P. cinnamomi from different hosts	High	LQPTH	6	Bio 1, 4, 5, 7, 10, 12, 13, 14, 15, 16 and 17	1985,419	0.001	3.8	928,318
	High	LQPTH	6	Bio 1, 4, 5, 7, 10, 12, 13, 14, 15, and 16	1871,123	0.001	4.2	895,223
	Medium	LQPT	4	Bio 1, 4, 5, 7, 10, 12, 13, 14, and 16	1421,413	0.001	6.4	712,156
	Medium	LQP	2	Bio 1, 4, 5, 7, 10, 12, 13, and 16	1385,142	0.001	6.8	623,412
	Low	LQ	1	Bio 1, 5, 7, 10, 12, 13, and 14	816.101	0.001	6.7	518,201
	Low[c]	LQP	4.0	Bio 1, 5, 7, 12, 13, and 16	745.221	0.001	6.2	507,013

[1] AICc: Akaike information criterion.
[2]Quadratic (LQ), product (LQP), threshold (LQPT), and hinge (LQPTH).
[3] Significance (*P* value).
[4] Omission rate (%).
[a,b and c] Model selected for analyses of, respectively, potential distributions of avocado, *P. cinnamomi* from avocado and *P. cinnamomi* from different hosts.

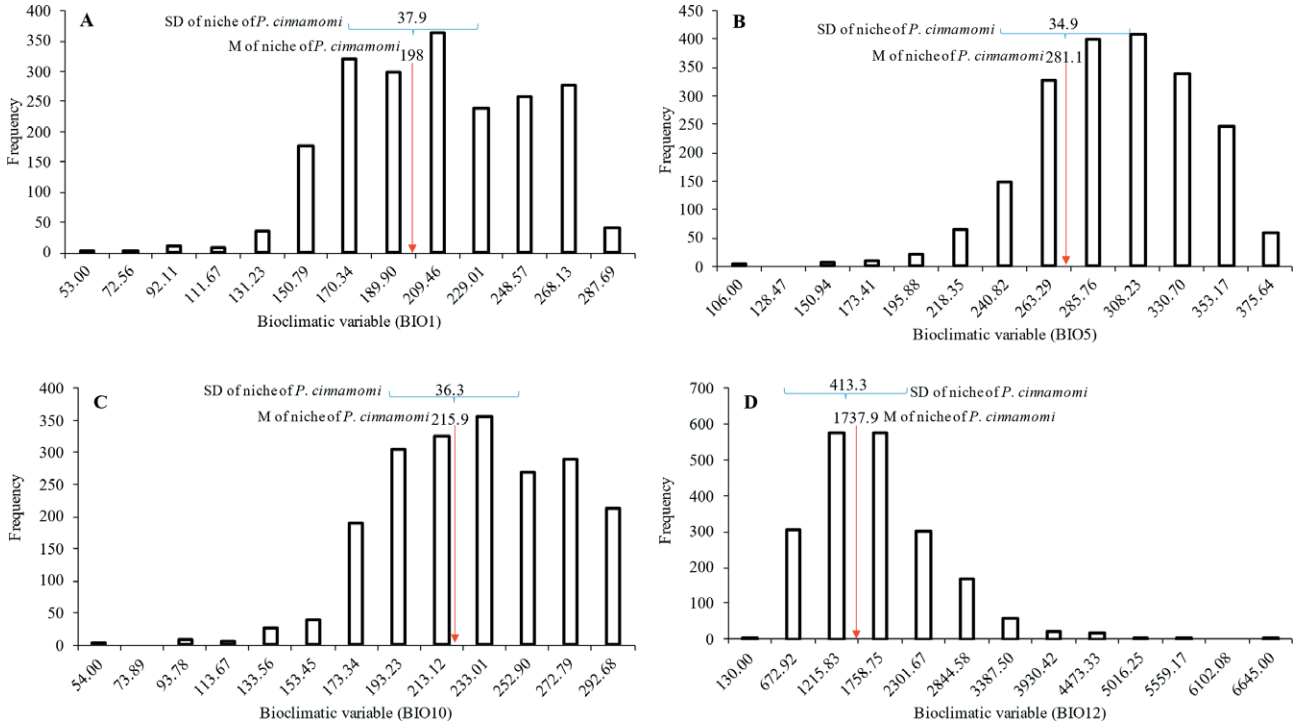

Figure 2. Relationship between coincident bioclimatic variables of the ecological niche models of *Persea americana* and *Phytophthora cinnamomi* from *Persea Americana*. A: BIO 1: Annual Mean Temperature. B: BIO 5: Maximum Temperature of Warmest Month. C: BIO 10: Mean Temperature of Warmest Quarter. D: BIO 12: Annual Precipitation. The values on the blue lines represent the standard deviations (SD), and the red down arrows represent the median (M) of the variables obtained for the niche of *Phytophthora cinnamomi* obtained records from *Persea americana*. Black bars represent the frequency values of the variables for the niche of *P. americana* under Americas. All variable values were obtained from 100 random combinations of occurrence (*Phytophthora cinnamomi* and *Persea americana*) and extracted from the niche of *Phytophthora cinnamomi* and *Persea americana* under Americas distributions.

potential distribution of *P. cinnamomi* isolated from avocado was very similar to that of avocados, although with a smaller overall area. In this model, *P. cinnamomi* suitability was more restricted in the central zone and southeastern and northeastern coasts of Brazil, with lower suitability in the coastal valleys of Peru and Chile. Suitable areas were also reduced in the Caribbean islands. A suitable region was also identified in the centre of Brazil (eastern Mato Grosso) (Figure 1 D).

The ENM for *P. cinnamomi* from hosts other than avocado showed a broader distribution than the other two models (Figure 1 F). The range included areas across much of the Americas and low suitability only in Canada and Alaska. The Amazonian region showed the greatest suitability values, together with the Pacific region of Colombia and Ecuador, the Andean regions from Colombia to Peru, and parts of Chile, Central America, and the Caribbean. Similarly, median suitable zones were noted in parts of Mexico, and the USA. The regions with the lowest suitability for the infection of *P. cinnamomi* were desert regions and some temperate areas (Figure 1 F).

Niche overlap

The initial analysis to compare niches of avocado and *P. cinnamomi* isolated from avocado showed that the mean of occurrences of *P. cinnamomi* was close to that of the null distribution, suggesting that *P. cinnamomi* is randomly distributed within the avocado niche (Figure 2). The Jaccard index indicated an environmental overlap of 0.68 between *P. americana* and *P. cinnamomi*, whereas for *P. americana* and *P. cinnamomi* associated with hosts other than avocado the overlap was of 0.75, and for *P. cinnamomi* isolated from avocado and *P. cinnamomi* isolated from hosts different to avocado the overlap index was 0.58 (Figure 3).

Comparison between niches based on a model of minimum-volume ellipsoids of *P. americana* and *P. cinnamomi* isolated from avocado showed that the latter was narrower than the former. When the three niches were compared, the niche of *P. cinnamomi* generated from different hosts including avocado (in Table 1) was the widest of all (Figure 3).

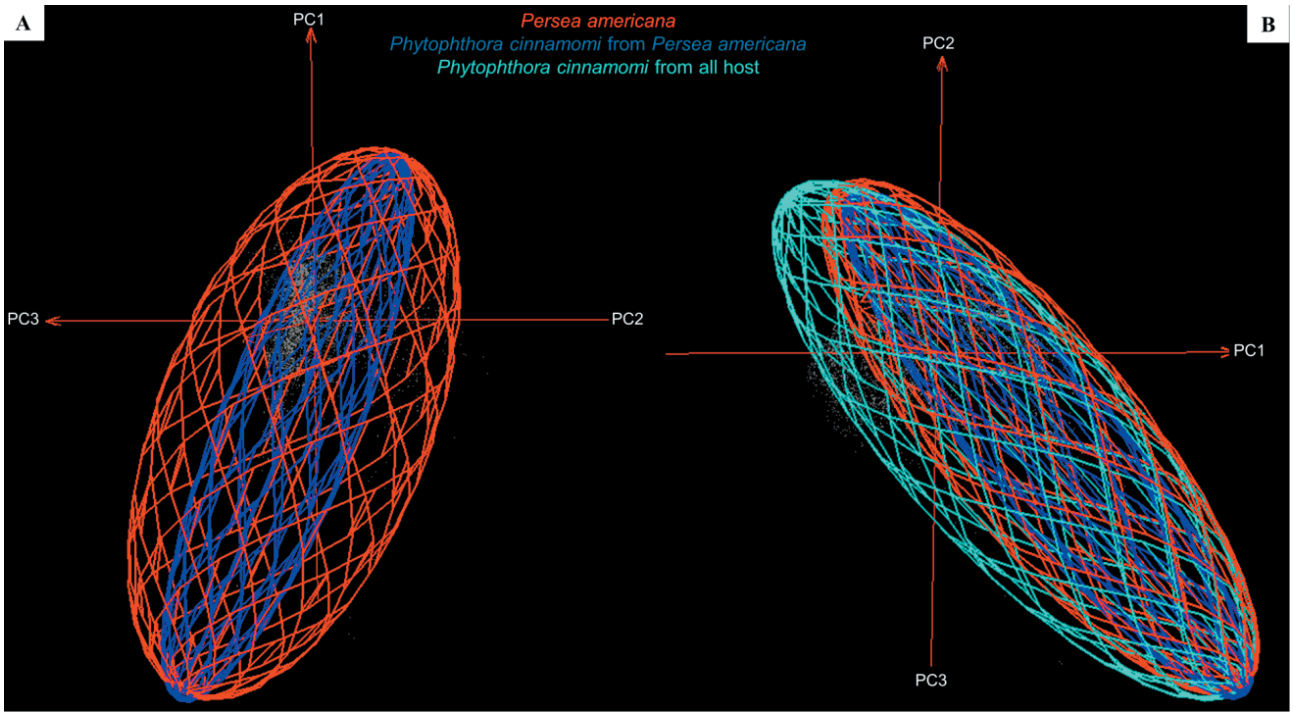

Figure 3. Environmental space of *Persea americana*, *Phytophthora cinnamomi* from *P. americana* (A), and *P. cinnamomi* from different hosts (B), modeled in NicheA. Ecological niche models based on a model of minimum-volume ellipsoids and visualization in three dimensions associated with principal component of bio-variables (Table 1). PC: principal components.

Risk visualization of Phytophthora cinnamomi *in avocado in the Americas*

Three zones with differential risk associated with *P. cinnamomi* were generated in cultivated and native avocados in the Americas (Figure 4). The low risk zone (green), was areas in which there are reports of the presence of *P. cinnamomi* and its main host (avocado), but where conditions for establishment of the pathogen are low, without being null. These areas could have potential for the development of this host without strong pressure from its main pathogen (Figure 4). The current risk zone (yellow), was for places where the conditions for the development of the host and the pathogen are ideal (niche overlap). In these areas root rot occurs continuously with different levels of intensity, which are highly dependent on climatic variations and the stability of the ecosystem (Figure 4). The potential risk zone (red), are areas where the environmental conditions for development of the host are suitable (potential distribution), but which presents current distribution of the pathogen, associated with other hosts. These zones would be restrictive for avocado, given high probability of being infected by the pathogen that causes its most limiting disease (Figure 4).

Figure 4. Risk visualization of *Phytophthora cinnamomi* on avocado (cultivated and native races) in the Americas.

DISCUSSION

Model selection

In recent years the use of ENMs has increased due to their multiple applications (Cobos *et al.*, 2019). These include determination of ecological niches and exploration of potential species distributions (Peterson *et al.*, 2011). Different strategies were used in the present research with the objective to carry out adequate prediction of the ENM and use of the algorithms for its calculation: (i) to clean and reduce the spatial autocorrelation of data occurrence (Varela *et al.*, 2014); (ii) to define an appropriate M, which is based on knowledge of the species to be modelled (Barve *et al.*, 2011; Saupe *et al.*, 2012); (iii) to reduce the dimension of environmental variables, eliminating those with lower prediction capacity (Varela *et al.*, 2014); and (iv) to carry out a strict selection process of criteria for the algorithms used (Warren and Seifert, 2011; Radosavljevic and Anderson, 2014; Ramírez-Gil *et al.*, 2018; Cobos *et al.*, 2019; Ramírez-Gil and Peterson, 2019). Rigour applied in this study gave a robust and reliable framework for the analysis performed, as shown by the sound results obtained.

Geographic distribution and overlapping of niches of Persia americana*,* Phytophthora cinnamomi *isolated from avocado, and* P. cinnamomi *isolated from hosts other than avocado*

The potential distributions generated for *P. americana* achieved a good approximation to the actual geographical distribution of this species. This fruit tree is found in a wide area in the Americas, including Latin America from Mexico to Chile which is an important diversification centre of this species (GalindoTovar *et al.*, 2008; Chen *et al.*, 2009; Bost *et al.*, 2013; Schaffer *et al.*, 2013). This wide range may be due to the existence of three races, which hybridized generating multiple genotypes adapted to different ecological and environmental conditions. The West Indian race is predominantly adapted to low lands (below 1000 m altitude), with high temperatures and high humidities. The Guatemalan race is present mainly at intermediate altitudes (1000-2000 m altitude). The Mexican race grows greater altitudes (>2000 m) in the tropical highlands and sub-tropical climates, which are characterized by relatively low temperatures (Bost *et al.*, 2013; Schaffer *et al.*, 2013).

In addition to the avocado natural races and genotypes, many commercial varieties have been developed, possibly increasing the geographical distribution of this species. This has allowed successful cultivation of avocado in a number of regions different from the centre of host origin, including the dry regions of Chile, Peru, Spain, Israel, South Africa and California in the USA, where agronomic practices such as irrigation have been incorporated into the production systems. Avocado use by native Americans was well known before introduction to other continents. Avocado propagation was probably carried out using seeds produced from plant sexual reproduction, which would have resulted in genetic diversity and adaptation of many genotypes (Chen *et al.*, 2009). Therefore, before being cultivated as monocultures, avocado dispersion by humans was probably from a genetically diverse background. This assumption may explain the wide avocado presence and adaptability observed in the present results.

This study indicated that the Americas include many new areas that support avocado crops under anthropic practices (potential crops) or by natural expansion (potential areas of natives races). The present model outputs should be interpreted with some caution, because some of the areas identified as suitable for avocado are unlikely to be profitable and viable (Ramírez-Gil *et al.*, 2019). In addition, commercial varieties may have implicitly incorporated agronomic components (e.g., irrigation systems, drainage, use of fertilizers, planting techniques). Many areas can also be natural reserve zones, deserts, or other regions where agriculture cannot be implemented (Ramírez-Gil *et al.*, 2019). These factors may introduce bias for the analysis of distributions found in the present study. Therefore, caution should be taken when making conclusions from the data obtained.

The potential geographical distribution of *P. cinnamomi* was strongly influenced by host presence, because niche amplitude varied according to the host number considered for its ENM development. The niche of *P. cinnamomi* generated from *P. americana* was only randomly distributed inside the niche of this host, whereas its amplitude increased when other host presences different to avocado where included in the analyses. Evidence suggests that *P. cinnamomi* was probably introduced to America from Asia (Zentmyer, 1988, 1997; Socorro Serrano *et al.*, 2019). Reproduction of *P. cinnamomi* is mainly asexual generating different clonal lineages as primary sources of human-mediated movement between regions (Pagliaccia *et al.*, 2013; Socorro Serrano *et al.*, 2019). Unlike other regions such as Australia, the *P. cinnamomi* host range in America is mostly unknown, but is mainly wild species (Shearer *et al.*, 2004; Hardham and Blackman, 2018). In most regions of America, research has been focused on commercial crops such as avocado, rather than on natural ecosystems such as the Amazon or Pacific rainforest of Colombia and Ecuador,

which the present research has indicated are regions with high suitability for *P. cinnamomi*.

Many factors determine pathogen dispersion once introduced in a region. *Phytophthora cinnamomi* has a complex (and controversial) lifestyle, varying from saprophytic to hemibiotroph pathogenic, depending on edaphoclimatic conditions and host availability (Hardham and Blackman, 2018). With exception of made for some regions such as California (USA) and Mexico, the population genetic structure of this important pathogen is unknown in hosts other than commercial crops in most regions of America (Pagliaccia *et al*., 2013; Socorro Serrano *et al*., 2019). The saprophytic lifestyle of *P. cinnamomi* has been widely reported (Duvenhage and Kotze, 1991). However, this behaviour has been questioned with results that suggest that *P. cinnamomi* does not behave as a saprophyte, at least under non-sterile soil conditions (McCarren, 2006). If true, this supports the present results, and the hypothesis that the distribution of *P. cinnamomi* follows host distribution but is random with respect to metrics defining the avocado ecological niche, mostly because its current distribution at the long and medium ranges (i.e. the range resolved by the present modelling) is the result of human-mediated introductions rather than natural spread of the pathogen.

A single factor can not explain the current distribution for *P. cinnamomi* in America. Once introduced in a new environment, a microorganism largely depends on the interactions between genetics and environment (Garbelotto, 2008; Burgess *et al*., 2017). The Americas extensive ecosystem variability, suggesting high adaptability in *P. cinnamomi*. The present results do not allow precise determination of the contribution of each independent factor to current distribution of the pathogen. However, and despite a lack of sound basic biological information on this oomycete, it is tempting to speculate that its current distribution in the Americas has resulted from high adaptability to different environments, following host availability. It has been observed, for example, in Colombia in tropical conditions as a pathogen of hosts growing from 0 to ≈3000 m above sea level, in different ecosystems and edaphoclimatic conditions, from dry tropical dry forests to very humid or pluvial forests (Figure 1).

Despite being suitable for *P. cinnamomi,* there were areas where the pathogen has not been recorded. This may be explained by lack of research particularly on wild plant species, the presence of pathogen suppressive soils in some places, host resistance or host absence, and especially lack of human-mediated introduction pathways. In contrast, *P. cinnamomi* was identified in dry or semi-arid regions which are not suitable for its development. However, these records were mainly on commercial cultivated hosts, where agronomic practices (e.g. irrigation) provide suitable conditions for *P. cinnamomi* development. These conditions could generate bias in determination of distribution areas using the ENMs approach, associated with dependence of presences on the frequency of environmental conditions that occur across geographical space (Broennimann *et al*., 2012).

Phytophthora cinnamomi has a very broad host range (Hardham and Blackman, 2018). Since this pathogen causes severe losses in several crop types, more knowledge is required about host recognition, pathogenicity determinants and environmental factors that favour disease development under different edaphoclimatic and biological conditions where disease has been reported (Hardham and Blackman 2018). Genome sequencing has demonstrated many genes encoding effector proteins, which may help to explain the wide adaptability to different hosts observed for *P. cinnamomi* (Garbelotto, 2008; Hardham and Blackman, 2018).

This may indicate why the niche of *P. cinnamomi* has increased amplitude when host occurrences other than avocado were included in the analyses. From previous and the present results, it is apparent that *P. cinnamomi* strains have a large niche independently of the host of origin, suggesting that this is a pathogen that does not show strong host preference. In addition, Serrano and Garbelotto (2020) showed that *P. cinnamomi* can infect and cause diseases on hosts other than those from which it was isolated, confirming the broad host range of the pathogen. However, they also presented evidence of host specialization (i.e., some isolates were more aggressive on the hosts they were isolated from) and increased virulence of pathogen genotypes that had no history of coexistence with natural host populations. This may have resulted from lack of co-evolution, or could be the outcome of using highly virulent isolates. Further research is required to determine which of these explanations is correct.

Despite the fact that *P. cinnamomi* distribution was strongly influenced by host presence, other factors may determine distribution of the pathogen and extent of damage it causes (Burgess *et al*., 2017). Humid regions were more favourable for *P. cinnamomi*, such as the Amazon, the Colombian and Ecuadorian Pacific, regions X and XI in Chile, wide areas in Central America and Mexico, and the Pacific coast of the USA. In contrast, presence of *P. cinnamomi* was affected in low precipitation regions such as the coastal valleys of Chile and Peru. High precipitation increases soil humidity inducing episodes of hypoxia or anoxia, which, in turn, intensifies pathogen aggressiveness. This increases *P. americana* susceptibility in the soil, affecting root functionality

(Stolzy *et al.*, 1967; Sterne *et al.*, 1977; Gisi *et al.*, 1980; Zentmyer, 1984; Sanclemente *et al.*, 2013; Ramírez-Gil *et al.*, 2017; Ramírez-Gil and Morales-Osorio, 2018). Alteration of natural ecosystems may increase aggressiveness of *P. cinnamomi* and, therefore, increase the possibility of root rot epidemics (Zentmyer, 1988, 1997). Most avocado crops are based on clonal genotypes susceptible to *P. cinnamomi*, including 'Hass', which is the main cultivar grown for fruit export. This narrow genetic background may facilitate *P. cinnamomi* dispersion worldwide. Crop production in general is an ecosystem alteration that may induce severe root rot epidemics.

When *P. cinnamomi* is established in an ecosystem, the factors that most determine its distribution are associated with the presence of susceptible hosts (Pratt and Heather, 1973; Duque-Lazo *et al.*, 2016; Ramírez-Gil and Peterson, 2019; Sena *et al.*, 2019). Additionally, other factors such as humidity, temperature, soil water movement, and nutrient availability are associated with its aggressiveness, and are known as disease conductive variables (Corcobado *et al.*, 2013; Ramírez-Gil and Morales-Osorio, 2018). There are other parameters not included in the present research that may be related to the distribution and establishment of *P. cinnamomi* ecosystems or agroecosystems. These include degrees of host susceptibility, anthropic management practices, dispersal mechanisms, conductive factors, and degrees of ecosystem alteration. As is known for other plant diseases caused by *Phytophthora* species, the present findings confirm that management of diseases caused by *P. cinnamomi* in wild or crop lands may be difficult, because there are several variables that are not well understood which determine host infection. These include basic knowledge required for development of appropriate disease management strategies.

Several questions should be addressed to provide increased understanding of the biology and epidemiology of *P. cinnamomi* in the Americas. These include:

- Is there host specificity within individuals in *P. cinnamomi* populations?
- Which are the main determinants of host infection that may help explain the wide host range of this pathogen?
- Are phylogenetically related plant species infected by specific genetic variants or closely related groups of *P. cinnamomi* individuals?
- Why are *P. cinnamomi* populations pathogenic under highly variable edaphoclimatic and biological conditions?
- What is the genetic variability and population structure of *P. cinnamomi* populations in different hosts from the Americas?
- What role, if any, may different hosts play in pathogen survival and crop epidemics?
- Do the present analyses suggest that more available, still not exploited niches for *P. cinnamomi*?

As the area planted with avocado in Colombia is rapidly increasing, it is important to know the susceptibility of genotypes and places where there are increased probabilities of disease development, to avoid large losses in crop establishment and maintenance, and to protect natural ecosystems from the potentially severe disease caused by *P. cinnamomi*. Further research is needed to provide answer to these questions, providing knowledge that is required for establishment of effective disease management programmes.

Risk visualization of Phytophthora cinnamomi *in avocado in the Americas*

A tool to visualize the risk of *P. cinnamomi* in the Americas has been generated for its main avocado host. The risks from this pathogen are closely associated with the presence of this host. Likewise, it has been found that under certain restricted environmental requirements for the pathogen the intensity of root rot could be reduced. The models possibly under- or over-estimate the risks of *P. cinnamomi* in the many areas of the Americas, associated sampling and presence bias (Broennimann *et al.*, 2012). This is especially when this pathogen has a very broad host range (Hardham and Blackman, 2018), which has been little sampled on these two continents. Additionally, some areas classified as potential risk (south and north of the Americas), may indicate areas with unsuitable conditions for avocado. However, under climate change scenarios, these areas will present suitable conditions for the development of this host (Ramírez-Gil *et al.*, 2019).

CONCLUSIONS

Niche distribution of *P. cinnamomi* is greatly influenced by host niches. *Phytophthora cinnamomi* represented a high risk in planted and native areas with the presence of susceptible hosts throughout the Americas. This study also advances understanding of the potential distribution of the invasive pathogen *P. cinnamomi* across of the Americas.

ACKNOWLEDGMENTS

The authors thank Universidad Nacional de Colombia (Medellín campus), Colciencias, and the programme

Sapiensa for providing funding for the first author, for a PhD fellowship and travel expenses. The University of Kansas funded MEC's research. Several avocado researchers are also thanked for their valuable information and support during this research; including Raúl Ferreyra Espada, Germán Sepulveda-Chavera, Ximena Alejandra Besoain, and Sylvana Soto in Chile; Euder Javier Juarez in Peru; and Salvador Ochoa Ascencio in México.

DATA AVAILABILITY STATEMENT

The data and R code that support the findings of this study are available from the corresponding author upon reasonable request.

LITERATURE CITED

Barve, N., Barve, V., Jiménez-Valverde, A., Lira-Noriega, A., Maher, S.P., … Villalobos, F., 2011. The crucial role of the accessible area in ecological niche modeling and species distribution modeling. *Ecological Modelling* 222: 1810–1819. DOI: 10.1016/j.ecolmodel.2011.02.011.

Bohlen, P.J., 2006. Biological invasions: Linking the aboveground and belowground consequences. *Applied Soil Ecology* 32: 1–5. DOI: 10.1016/j.apsoil.2005.10.001.

Bost, J.B., Smith, N.J., Crane, J.H., 2013. History, distribution and uses. In: *The avocado: botany, production and uses*, Wallingford, UK, CABI Publ, 10–30.

Broennimann, O., Fitzpatrick, M.C., Pearman, P.B., Petitpierre, B., Pellissier, L., … Guisan, A., 2012. Measuring ecological niche overlap from occurrence and spatial environmental data. *Global Ecology and Biogeography* 21: 481–497. DOI: https://doi.org/10.1111/j.1466-8238.2011.00698.x.

Brown, J.L., 2014. SDMtoolbox: a python-based GIS toolkit for landscape genetic, biogeographic and species distribution model analyses. *Methods in Ecology and Evolution* 5: 694–700. DOI: 10.1111/2041-210X.12200.

Burgess, T.I., Scott, J.K., Mcdougall, K.L., Stukely, M.J.C., Crane, C., … Hardy, G.E.St.J., 2017. Current and projected global distribution of *Phytophthora cinnamomi*, one of the world's worst plant pathogens. *Global Change Biology* 23: 1661–1674. DOI: 10.1111/gcb.13492.

Chen, H., Morrell, P.L., Ashworth, V.E.T.M., de la Cruz M., Clegg, M.T., 2009. Tracing the geographic origins of major avocado cultivars. *Journal of Heredity* 100: 56–65. DOI: 10.1093/jhered/esn068.

Cobos, M.E., Peterson, A.T., Osorio-Olvera, L., Jiménez-García, D., 2019. An exhaustive analysis of heuristic methods for variable selection in ecological niche modeling and species distribution modeling. *Ecological Informatics* 53: 100983. DOI: 10.1016/j.ecoinf.2019.100983.

Corcobado, T., Solla, A., Madeira, M.A., Moreno, G., 2013. Combined effects of soil properties and *Phytophthora cinnamomi* infection on *Quercus ilex* decline. *Plant and Soil* 373: 403–413. DOI: 10.1007/s11104-013-1804-z.

Duque-Lazo, J., van Gils, H., Groen, T.A., Navarro-Cerrillo, R.M., 2016. Transferability of species distribution models: The case of *Phytophthora cinnamomi* in Southwest Spain and Southwest Australia. *Ecological Modelling* 320: 62–70. DOI: 10.1016/j.ecolmodel.2015.09.019.

Duvenhage, J., Kotze, J., 1991. The influence of calcium on saprophytic growth and pathogenicity of *Phythophthora cinnamomi* and on resistance avocado to root rot. *South African Avocado Growers' Association Yearbook* 14: 13–14.

Escobar, L.E., Lira-Noriega, A., Medina-Vogel, G., Townsend Peterson, A., 2014. Potential for spread of the white-nose fungus (*Pseudogymnoascus destructans*) in the Americas: use of Maxent and NicheA to assure strict model transference. *Geospatial Health* 9: 221–229. DOI: 10.4081/gh.2014.19.

Galindo-Tovar, M.E., Ogata-Aguilar, N., Alzate-Fernández, A.M., 2008. Some aspects of avocado (*Persea americana* Mill.) diversity and domestication in Mesoamerica. *Genetic Resources and Crop Evolution* 55: 441–450. DOI: DOI 10.1007/s10722-007-9250-5.

Garbelotto, M., 2008. Molecular analysis to study invasions by forest pathogens: examples from Mediterranean ecosystems. *Phytopathologia Mediterranea* 47: 188–203.

Gisi, U., Zentmyer, G.A., Klure, L.J., 1980. Production of sporangia by *Phytophthora cinnamomi* and *P. palmivora* in soils at different matric potentials. *Phytopathology* 70: 301–306.

Hardham, A.R., Blackman, L.M., 2018. *Phytophthora cinnamomi*. *Molecular Plant Pathology* 19: 260–285. DOI: 10.1111/mpp.12568.

Hernández-Lambraño, R.E., González-Moreno, P., Sánchez-Agudo, J.Á., 2018. Environmental factors associated with the spatial distribution of invasive plant pathogens in the Iberian Peninsula: The case of *Phytophthora cinnamomi* Rands. *Forest Ecology and Management* 419–420: 101–109. DOI: 10.1016/j.foreco.2018.03.026.

Hijmans, R.J., Cameron, S.E., Parra, J.L., Jones, P.G., Jarvis, A., 2005. Very high resolution interpolated climate surfaces for global land areas. *International Journal of Climatology* 25: 1965–1978. DOI: 10.1002/joc.1276.

Jaccard, P., 1912. The Distribution of the flora in the Alpine zone. *New Phytologist* 11: 37–50. DOI: 10.1111/j.1469-8137.1912.tb05611.x.

Johnson, E.E., Escobar, L.E., Zambrana-Torrelio, C., 2019. An ecological framework for modeling the geography of disease transmission. *Trends in Ecology & Evolution* 34: 655–668. DOI: 10.1016/j.tree.2019.03.004.

Knight, R.J., Campbell, C.W., 1999. Ecological adaptation and the evolution of modern avocado cultivars. *Revista Chapingo Serie Horticultura* 5: 49–54.

Maher, S.P., Ellis, C., Gage, K.L., Enscore, R.E., Peterson, A.T., 2010. Range-wide determinants of plague distribution in North America. *The American Journal of Tropical Medicine and Hygiene* 83: 736–742. DOI: 10.4269/ajtmh.2010.10-0042.

McCarren, K., 2006. *Saprophytic ability and the contribution of chlamydospores and oospores to the survival of Phytophthora cinnamomi. McCarren, Kathryn <https://researchrepository.murdoch.edu.au/view/author/McCarren, Kathryn.html> (2006) Saprophytic ability and the contribution of chlamydospores and oospores to the survival of Phytophthora cinnamomi. PhD thesis, Murdoch University.*, phd, Murdoch University, Perth, Western Australia, 211 pp.

Meyer, M.D., Robertson, M.P., Mansell, M.W., Ekesi, S., Tsuruta, K., … Peterson, A.T., 2010. Ecological niche and potential geographic distribution of the invasive fruit fly *Bactrocera invadens* (Diptera, Tephritidae). *Bulletin of Entomological Research*, Cambridge University Press 100: 35–48. DOI: 10.1017/S0007485309006713.

Narouei-Khandan, H.A., Harmon, C.L., Harmon, P., Olmstead, J., Zelenev, V.V., … Bruggen, A.H.C. van, 2017. Potential global and regional geographic distribution of *Phomopsis vaccinii* on *Vaccinium* species projected by two species distribution models. *European Journal of Plant Pathology* 148: 919–930. DOI: 10.1007/s10658-017-1146-4.

Pagliaccia, D., Pond, E., McKee, B., Douhan, G.W., 2013. Population genetic structure of *Phytophthora cinnamomi* associated with avocado in California and the discovery of a potentially recent introduction of a new clonal lineage. *Phytopathology* 103: 91–97. DOI: 10.1094/PHYTO-01-12-0016-R.

Papadakis, J., 1966. *Climates of the World and Their Agricultural Potentialities.* Buenos Aires, Argentina, 174 pp.

Peterson, A.T., Papeş, M., Soberón, J., 2008. Rethinking receiver operating characteristic analysis applications in ecological niche modeling. *Ecological Modelling* 213: 63–72. DOI: 10.1016/j.ecolmodel.2007.11.008.

Peterson, A.T., Soberón, J., Anderson, R., Pearson, R., Martínez-Meyer, E., … Araújo, M., 2011. *Ecological Niches and Geographic Distributions*. Princeton University Press, 330 pp.

Phillips, S.J., Anderson, R.P., Schapire, R.E., 2006. Maximum entropy modeling of species geographic distributions. *Ecological Modelling* 190: 231–259. DOI: 10.1016/j.ecolmodel.2005.03.026.

Pratt, B., Heather, W., 1973. The origin and distribution o f *Phytophthora cinnamomi* Rands in Australian native plant communities and the significance og its association with particular plants species. *Autralian Journal of Biological Science* 26: 559–573.

Qiao, H., Peterson, A.T., Campbell, L.P., Soberón, J., Ji, L., Escobar, L.E., 2016. NicheA: creating virtual species and ecological niches in multivariate environmental scenarios. *Ecography* 39: 805–813. DOI: 10.1111/ecog.01961.

Qiao, H., Escobar, L.E., Peterson, A.T., 2017. Accessible areas in ecological niche comparisons of invasive species: Recognized but still overlooked. *Scientific Reports* 7: 1213. DOI: 10.1038/s41598-017-01313-2.

R Development Core Team, 2021. R: The R Project for Statistical Computing. *R Foundation for Statistical Computing, Vienna, Austria*. Available at: https://www.r-project.org/. Accessed January 1, 2021.

Radosavljevic, A., Anderson, R.P., 2014. Making better Maxent models of species distributions: complexity, overfitting and evaluation. *Journal of Biogeography* 41: 629–643. DOI: 10.1111/jbi.12227.

Ramírez-Gil, J.G., Gilchrist Ramelli, E., Morales Osorio, J.G., 2017. Economic impact of the avocado (cv. Hass) wilt disease complex in Antioquia, Colombia, crops under different technological management levels. *Crop Protection* 101: 103–115. DOI: 10.1016/j.cropro.2017.07.023.

Ramírez-Gil, J.G., Morales-Osorio, J.G., 2018. Microbial dynamics in the soil and presence of the avocado wilt complex in plots cultivated with avocado cv. Hass under ENSO phenomena (El Niño – La Niña). *Scientia Horticulturae* 240: 273–280. DOI: 10.1016/j.scienta.2018.06.047.

Ramírez-Gil, J.G., Morales, J.G., Peterson, A.T., 2018. Potential geography and productivity of "Hass" avocado crops in Colombia estimated by ecological niche modeling. *Scientia Horticulturae* 237: 287–295. DOI: 10.1016/j.scienta.2018.04.021.

Ramírez-Gil, J.G., Peterson, A.T., 2019. Current and potential distributions of most important diseases affecting Hass avocado in Antioquia Colombia. *Jour-*

nal of Plant Protection Research 59: 214–228. DOI: 10.24425/jppr.2019.129288.

Ramírez-Gil, J.G., Cobos, M.E., Jiménez-García, D., Morales-Osorio, J.G., Peterson, A.T., 2019. Current and potential future distributions of Hass avocados in the face of climate change across the Americas. *Crop and Pasture Science* 70: 694–708. DOI: 10.1071/CP19094.

Sanclemente, M.A., Schaffer, B., Gil, P.M., Davies, F.S., Crane, J.H., 2013. Leaf removal before flooding influences recovery of avocado (*Persea americana* Mill.) trees from flooding stress. *Scientia Horticulturae* 150: 154–163. DOI: 10.1016/j.scienta.2012.11.002.

Saupe, E.E., Barve, V., Myers, C.E., Soberón, J., Barve, N., … Lira-Noriega, A., 2012. Variation in niche and distribution model performance: The need for a priori assessment of key causal factors. *Ecological Modelling* 237: 11–22. DOI: 10.1016/j.ecolmodel.2012.04.001.

Schaffer, B., Wolstenholme, B.N., Whiley, A.W. (eds), 2013. *The Avocado: Botany, Production and Uses*. Cambridge, MA, CABI, 584 pp.

Sena, K.L., Yang, J., Kohlbrand, A.J., Dreaden, T.J., Barton, C.D., 2019. Landscape variables influence *Phytophthora cinnamomi* distribution within a forested Kentucky watershed. *Forest Ecology and Management* 436: 39–44. DOI: 10.1016/j.foreco.2019.01.008.

Serrano, M.S., Garbelotto, M., 2020. Differential response of four Californian native plants to worldwide *Phytophthora cinnamomi* genotypes: implications for the modeling of disease spread in California. *European Journal of Plant Pathology* 156: 851–866. DOI: 10.1007/s10658-020-01936-8.

Shearer, B.L., Crane, C.E., Cochrane, A., 2004. Quantification of the susceptibility of the native flora of the South-West Botanical Province, Western Australia, to *Phytophthora cinnamomi*. *Australian Journal of Botany*, CSIRO PUBLISHING 52: 435–443. DOI: 10.1071/bt03131.

Socorro-Serrano, M., Osmundson, T., Almaraz-Sánchez, A., Croucher, P.J.P., Swiecki, T., … Garbelotto, M., 2019. A Microsatellite Analysis Used to Identify Global Pathways of Movement of *Phytophthora cinnamomi* and the Likely Sources of Wildland Infestations in California and Mexico. *Phytopathology®*, Scientific Societies 109: 1577–1593. DOI: 10.1094/PHYTO-03-19-0102-R.

Sterne, R.E., Zentmyer, G.A., Kaufmann, M.R., 1977. Effect of matric and osmotic potential of soil on Phytophthora root disease of *Persea indica*. *Phytopathology*.

Stolzy, L., Zentmyer, G., Klotz, L., Labanauskas, C., 1967. Oxygen diffusion, water, and *Phytophthora cinnamomi* in root decay and nutrition of avocados. *American Society for Horticultural science* 90: 67–76.

Varela, S., Anderson, R.P., García-Valdés, R., Fernández-González, F., 2014. Environmental filters reduce the effects of sampling bias and improve predictions of ecological niche models. *Ecography* 37: 1084–1091. DOI: 10.1111/j.1600-0587.2013.00441.x.

Warren, D.L., Glor, R.E., Turelli, M., 2010. ENMTools: a toolbox for comparative studies of environmental niche models. *Ecography* 33: 607–611. DOI: 10.1111/j.1600-0587.2009.06142.x.

Warren, D.L., Seifert, S.N., 2011. Ecological niche modeling in Maxent: the importance of model complexity and the performance of model selection criteria. *Ecological Applications: A Publication of the Ecological Society of America* 21: 335–342.

Weste, G., Marks, G.C., 1974. The distribution of *Phytophthora cinnamomi* in Victoria. *Transactions of the British Mycological Society* 63: 559-IN26. DOI: 10.1016/S0007-1536(74)80105-1.

Zentmyer, G., 1980. Phytophthora cinnamomi *and diseases it causes*. *Monograph n° 10*. St. Paul, MN, The American Phytopathological Society, 96 pp.

Zentmyer, G., 1984. Avocado diseases. *Tropical Pest Management* 30: 677–682.

Zentmyer, G.A., 1988. Origin and distribution of four species of *Phytophthora*. *Transactions of the British Mycological Society* 91: 367–378. DOI: 10.1016/S0007-1536(88)80111-6.

Zentmyer, G.A., 1997. Origin of *Phytophthora cinnamomi*: Evidence that it is not an indigenous fungus in the Americas. *Phytopathology* 67: 1373–1377.

Phytopathologia Mediterranea
The international journal of the
Mediterranean Phytopathological Union

Firenze University Press
www.fupress.com/pm

Research Papers

In vitro evaluation of grapevine endophytes, epiphytes and sap micro-organisms for potential use to control grapevine trunk disease pathogens

Robert BLUNDELL, Molly ARREGUIN, Akif ESKALEN*

Department of Plant Pathology, University of California Davis, One Shields Avenue, Davis, CA, 95616-8751, USA
*Corresponding author. E-mail: aeskalen@ucdavis.edu

OPEN ACCESS

Citation: R. Blundell, M. Arreguin, A. Eskalen (2021) *In vitro* evaluation of grapevine endophytes, epiphytes and sap micro-organisms for potential use to control grapevine trunk disease pathogens. *Phytopathologia Mediterranea* 60(3): 535-548. doi: 10.36253/phyto-12500

Accepted: September 30, 2021

Published: December 30, 2021

Data Availability Statement: All relevant data are within the paper and its Supporting Information files.

Competing Interests: The Author(s) declare(s) no conflict of interest.

Editor: Lizel Mostert, Faculty of AgriSciences, Stellenbosch, South Africa.

Summary. Grapevine trunk diseases (GTDs) threaten the economic sustainability of viticulture, causing reductions of yield and quality of grapes. Biological control is a promising sustainable alternative to cultural and chemical methods to mitigate the effects of pathogens causing GTDs, including Botryosphaeria dieback, Eutypa dieback and Esca. This study aimed to identify naturally occurring potential biological control agents from grapevine sap, cane and pith tissues, and evaluate their *in vitro* antagonistic activity against selected fungal GTD pathogens. Bacterial and fungal isolates were preliminarily screened in dual culture assays to determine their antifungal activity against *Neofusicoccum parvum* and *Eutypa lata*. Among the fungal isolates, *Trichoderma* spp. inhibited mycelium growth of *E. lata* by up to 64% and of *N. parvum* by up to 73%, with overgrowth and growth cessation being the likely antagonistic mechanisms. Among the bacterial isolates, *Bacillus* spp. inhibited mycelium growth of *E. lata* by up to 20% and of *N. parvum* by up to 40%. Selected antagonistic isolates of *Trichoderma, Bacillus* and *Aureobasidium* spp. were subjected to further dual culture antifungal analyses against *Diplodia seriata* and *Diaporthe ampelina,* with *Trichoderma* isolates consistently causing the greatest inhibition. Volatile organic compound antifungal analyses showed that these *Trichoderma* isolates inhibited mycelium growth of *N. parvum* (20% inhibition), *E. lata* (61% inhibition) and *Dia. ampelina* (71% inhibition). Multilocus sequence analyses revealed that the *Trichoderma* isolates were most closely related to *Trichoderma asperellum* and *Trichoderma hamatum*. This study had identified grapevine sap as a novel source of potential biological control agents for control of GTDs. Further testing will be necessary to fully characterize modes of antagonism of these microorganisms, and assess their efficacy for pruning wound protection *in planta*.

Keywords. Biological control**,** endophytes, microbial antagonism, antifungal.

INTRODUCTION

Fungal diseases are major biotic threats to future economic sustainability of table and wine grape production. Grapevine trunk diseases (GTDs) are prevalent in most viticulture regions causing significant yield and quality

reductions, and increasing crop management costs for cultural and chemical disease management (Siebert *et al.,* 2001; Gubler *et al.,* 2005; Úrbez-Torres *et al.,* 2006; Bertsch *et al.,* 2013; Kaplan *et al.,* 2016). GTDs lead to premature decline and dieback of grapevines and are caused by complexes of several taxonomically unrelated Ascomycetes. Botryosphaeria dieback, also known as Black Dead Arm or 'Bot Canker', is one of the most severe GTDs and is currently associated with 26 botryosphaeriaceous taxa including *Botryosphaeria, Diplodia, Dothriorella, Lapsiodiplodia, Neofusicoccum, Neoscytalidium, Phaeobotryosphaeria,* and *Spencermartinsia* (Úrbez-Torres. 2011; Pitt *et al.,* 2013; Rolshausen *et al.,* 2013; Pitt *et al.,* 2015; Yang *et al.,* 2017). Another severe GTD is Eutypa dieback, caused by 24 species of Diatrypaceae, with the most virulent and common being *Eutypa lata* (Trouillas *et al.,* 2010; Pitt *et al.,* 2013; Luque *et al.,* 2014; Rolshausen *et al.,* 2014). Esca and Phomopsis dieback also comprise the GTD complex, and are of worldwide economic importance (Munkvold *et al.,* 1994). GTDs can occur simultaneously, though severity may differ among regions (Mugnai *et al.,* 1999; Pascoe and Cottral, 2000; Halleen *et al*., 2003; Gubler *et al.,* 2005). Characteristic symptoms of Botryosphaeria and Eutypa dieback are development of wedge-shaped cankers in infected grapevine trunks and cordons. From the infection sites, which are often pruning wounds, the fungi will grow downwards occupying vascular elements and adjacent cells. When affected vineyards are no longer economically sustainable, growers face no alternative other than replanting (Gramaje *et al.,* 2018). GTDs can also be found in dormant wood cuttings and young grafted plants, and thus spread to grapevines during plant propagation processes (Waite and Morton, 2007; Aroca *et al.,* 2010; Gramaje and Armengol, 2011; Billones-Baaijens *et al*., 2013).

Management of GTDs is difficult and influenced by the specific disease and/or pathogens involved, but a variety of preventative methods have been studied and implemented. These include cultural practices such as double pruning and application of fungicides (Bertsch *et al.,* 2013). However, these methods have highly variable efficacy, may not be environmentally sustainable, and can be costly (Zanzotto and Morroni, 2016). A promising approach is the use of biological control agents (BCAs) to control pathogens causing GTDs. This utilizes naturally occurring micro-organisms to suppress pests and pathogens (Heimpel and Mills, 2017; Martinez-Diz *et al.,* 2020). Grapevines can be colonized by many micro-organisms that can reside intercellularly or intracellularly as endophytes (West *et al.,* 2010; Gilbert *et al.,* 2014), or they can colonize surfaces of grapevine organs, especially leaves, as epiphytes (Hardoim *et al.,* 2015; Bruisson *et al.,* 2019). Endophytes have been shown to be valuable potential BCAs, as they have been associated with most plant species, and most are non-pathogenic bacteria or fungi that asymptomatically colonize their hosts (Strobel and Daisy. 2003).

Since about 2000, more than 40 BCAs have been isolated, identified and tested against the pathogens responsible for the GTD complex, and while the majority of cultured endophytes do not exhibit inhibitory activity, some *Trichoderma* spp. and *Bacillus* spp. have been highly efficient in protecting pruning wounds against various GTD pathogens *in vitro*, and in greenhouse and field trials (Schmidt *et al.,* 2001; Di Marco *et al.,* 2002; 2004; John *et al.,* 2008; Halleen *et al.,* 2010; Kotze *et al.,* 2011; Rezgui *et al.,* 2016; Mondello *et al.,* 2018; Martinez-Diz *et al.,* 2020) Several successful efforts have also been made to commercialize these organisms as BCAs (Otoguro and Suzuki, 2018). *Trichoderma* spp. can stimulate plant growth and suppress pathogens by direct competition for nutrients and space, exhibit mycoparasitism and antibiosis, and/or induce systemic resistance (John *et al.,* 2005; Harman, 2006; Mukherjee *et al.,* 2013). *Bacillus* spp. can antagonize GTDs through antibiotic production, competition for nutrients, and/or activation of host defense responses (Choudhary and Johri 2009; Cawoy *et al.,* 2011).

There have been no published reports of evaluation of grapevine sap inhabiting microbes for their antifungal activity against GTD pathogens. The majority of antagonistic endophyte studies in relation to GTDs have sourced microbes from grapevine bark or roots. The present study aimed to exploit this knowledge gap by isolating microbes from grapevine sap, both immediately after making fresh pruning cuts and 7 d later, and evaluating their *in vitro* antagonistic activity against several pathogens responsible for GTDs. Isolations of potential antagonists were also made from grapevine pith and cane tissues.

MATERIALS AND METHODS

Isolation of potential biocontrol organisms from grapevine

All microbial sampling was performed at the Plant Pathology Fieldhouse Facility, University of California, Davis in Yolo County (38°31'24.1"N, 121°45'43.3"W) from (*Vitis vinifera*, Cultivar Chenin Blanc – 10-yrs-old) in March 2019 prior to any standard pruning. A total of ten randomly selected apparently 'healthy' vines were used in this study, with samples taken from four randomly pruned spurs per vine. For collection of sap

exudate, the cut points of 1-year-old lignified spurs were sprayed with 70% ethanol for surface sterilization to avoid contamination, and once dry, a horizontal pruning cut was made in each spur with sterile pruning shears. A 100 µL sample of sap exudate was immediately collected from the bleeding wound with a pipette and stored on ice. A 20 µL aliquot of sap exudate from each spur was later spread by a sterile glass rod onto each of petri plates containing either potato dextrose agar amended with 100 mg L^{-1} tetracycline (PDA-T) or nutrient agar (NA). Growing fungal or bacterial cultures were subcultured for *in vitro* screening and molecular identifications. Epiphytic microbes were sampled by scraping dry sap from the pruning surfaces 7 d after the initial cut from the same grapevine canes, and the samples were plated as described above. After incubation at 25°C for approx. 7 d, sub-cultures of all growing microbes were made to fresh PDA-T or NA.

Grapevine endophytes were also isolated in September 2019 from the same vineyard, from untreated canes used in a pruning wound protection trial. The canes were each split longitudinally, and isolations were made from the exposed wood and pith tissues. A total of ten canes were used and three pieces of tissue and three pieces of pith were collected from each cane. These tissue pieces were then plated on PDA-T and NA plates. The plates were incubated at 25°C for approx. 7 d before subcultures were made of growing isolates.

Extractions of genomic DNA

Genomic DNA was extracted from fungi by scraping mycelium from each 1-week-old isolate subculture, and adding this to a 2 mL capacity tube containing 300 mL of Nuclei Lysis Solution and 1 mm diam. glass beads (bioSpec Products). Mycelium was homogenized for 40 s at 6 m s^{-1} in a FastPrep-24™ 5G bead beating grinder and lysis system (MP Biomedicals). Genomic DNA was extracted using a DNA extraction kit (Wizard Genomic DNA Purification Kit; Promega Corporation). Genomic DNA was extracted from each 1-week-old bacterial sub culture by collecting a loop of bacteria with a sterile pipette tip and inoculating a 0.2 mL capacity PCR tube containing 15 mL of Molecular Grade Water culturing for 15 min at 95°C in a thermal cycler.

PCR amplification and sequencing of fungal ITS, TEF-1a and b1-tubulin genes

The internal transcribed spacer (ITS) region of the ribosomal RNA *(rRNA)* gene was amplified using the primers, ITS1 and ITS4 (White *et al.,* 1990). The translation elongation factor 1 alpha gene (TEF-1a) was amplified using the primers, EF1-728F and EF1-968R (Carbone and Kohn, 1999). The beta tubulin gene *(Bt)* was amplified using the primers, Bt2a and Bt2b (Glass and Donaldson, 1995).

PCR amplification and sequencing of Bacterial 16S rRNA, puH and rpoB genes

The 16S rRNA gene was amplified using the primers 16S U1 and 16S U2 (Lu *et al.,* 2000). The purine biosynthesis gene was amplified using the primers, purH-70f and purH-1013r (Rooney *et al.,* 2009). The RNA polymerase subunit B (*rpoB*) gene was amplified using the primers, rpoB-229f and rpoB-3354Rr (Rooney *et al.,* 2009).

PCR assays

PCR assays were each carried out in a final volume of 25 mL, in a reaction mixture containing 0 mM Tris-HCl (pH 8.8), 50 mM KCl, 3 mM MgCl2, 0.2 mM of each dNTP, 1.0 mM of each primer and 1 unit of Go Taq polymerase (Promega Corporation). Primers and excess nucleotides were removed from the amplified DNA using a PCR clean-up kit (EXO SAP; New England BioLabs), and DNA was quantified using a QuantiFluor dsDNA System (Promega Corporation). Purified PCR samples were sent to Quintarabio, Hayward for Sanger Sequencing. Sequence chromatograms were analyzed, and the sequences were assembled using Sequencher version 5.4.6. Alignment was performed with Clustal W. Phylogenetic analysis was carried out with Mega X using the maximum composite likelihood model for estimating genetic differences. A phylogenetic tree was obtained using the neighbour-joining method with 1000 bootstrap replicates.

Dual culture assays

All fungal and bacterial isolates were tested in *in vitro* dual culture assays against the GTD pathogens *N. parvum* and *E. lata*. Fresh subcultures were made from each isolate and incubated at 25°C for 1 week on PDA-T plates for fungal isolates and PDA plates for bacterial isolates for the assay. A 5 mm diam. plug from each isolate culture was then placed 1 cm from the edge of a 100 × 15 mm plate, and a 5 mm diam. plug of 1-week-old *N. parvum* or *E. lata* agar culture was placed 1 cm from the opposite edge of the plate. Plates with only the patho-

gens were used as experimental controls. *Neofusicoccum parvum* assays were incubated at 25°C for 4 d before the percentage of pathogen inhibition was recorded. The *E. lata* assays were incubated at 25°C for 14 d before being recorded. The percentage of inhibition of pathogen mycelium growth was calculated using the formula of Idris *et al.* (2007): % inhibition = [(C-T)/C] × 100), where C is the colony radius (mm) of the pathogen when plated by itself and T is the radius of the pathogen when plated with an isolate. There were a total of ten replicates per isolate in these assays. Representative isolates from each genus exhibiting potential biological control activity against *N. parvum* or *E. lata* were subsequently tested against the GTD pathogens *Diplodia seriata* and *Diaporthe ampelina* using the same assay protocol.

Assays for production of volatile compounds

Production of antifungal volatile organic compounds (VOCs) was assessed using the two-sealed-base-plates method described by Gotor-Vila *et al.* (2017), with modifications. Petri dishes (100 × 15 mm) were each half filled with PDA-T or PDA, and a 5 mm diam. mycelium plug of each 1-week-old isolate were placed in the centre of each base plate. A 5 mm diam. mycelium plug of a pathogen was placed in the centre of another base plate and the two base plates were immediately sealed together using parafilm. Plates with only the pathogen served as experimental controls. *Neofusicoccum parvum* and *D. seriata* assays were incubated at 25°C for 4 d before percentage of pathogen inhibition was recorded, and *E. lata* and *Dia. ampelina* assays were incubated at 25°C for 14 d. The percentage inhibition of pathogen mycelium growth was calculated using the formula of Idris *et al.* (2007) (above). Ten replicates were used for each isolate tested.

Statistical analyses

Data obtained from the dual culture assays were analyzed using one-way ANOVA, and means were separated using the *post hoc* Dunnett's test at $P = 0.05$.

RESULTS

Isolation and ITS/16s sequencing of potential biocontrol organisms

Eleven fungal isolates and two bacterial isolates were cultured on growth media from sampled grapevine tissues (Table 1). The majority of isolates were obtained from either cane tissue or sap collected immediately after pruning cuts were made. Only two isolates were obtained from sap 7 d after pruning, and one isolate was obtained from grapevine pith. PCR amplification of the ITS gene, sequencing and BLAST analyses showed that nine of the fungal isolates were *Aureobasidium* and two were *Trichoderma* (Table 1). PCR amplification of the 16S rRNA, sequencing and BLAST analyses showed that the two bacterial isolates were *Bacillus* genus (Table 1).

Table 1. Sources of isolated microorganisms and their ITS/16S identification

Isolate	Source	**Genus**
UCD 8193	Grapevine cane tissue	*Aureobasidium* (ITS)
UCD 8248	Grapevine cane tissue	*Aureobasidium* (ITS)
UCD 8302	Grapevine sap, collected immediately	*Aureobasidium* (ITS)
UCD 8176	Grapevine cane tissue	*Aureobasidium* (ITS)
UCD 8174	Grapevine sap, collected immediately	*Aureobasidium* (ITS)
UCD 8196	Grapevine sap, collected immediately	*Aureobasidium* (ITS)
UCD 8170	Grapevine sap, collected immediately	*Aureobasidium* (ITS)
UCD 8344	Grapevine cane tissue	*Aureobasidium* (ITS)
UCD 8189	Grapevine sap, collected immediately	*Aureobasidium* (ITS)
UCD 8745	Grapevine sap, collected after 7 days	*Bacillus* (16S)
UCD 8347	Grapevine cane pith tissue	*Bacillus* (16S)
UCD 8368	Grapevine cane tissue	*Trichoderma* (ITS)
UCD 8717	Grapevine sap, collected after 7 days	*Trichoderma* (ITS)

Preliminary screening, dual culture assays with Neofusicoccum parvum *and* Eutypa lata

The *in vitro* antagonistic potential of all subcultured bacterial and fungal isolates (Table 1) was initially evaluated against the GTDs pathogens *N. parvum* and *E. lata* using dual culture assays. While the majority of isolates did not inhibit mycelium growth of *N. parvum*, two *Bacillus* spp. isolates (UCD 8745 and UCD 8347) and two *Trichoderma* isolates (UCD 8368 and UCD 8717) inhibited growth of this pathogen, by 35% to 64% ($P \leq 0.05$; Figure 1A) compared to the *N. parvum* control. When the isolates were tested for antagonistic potential

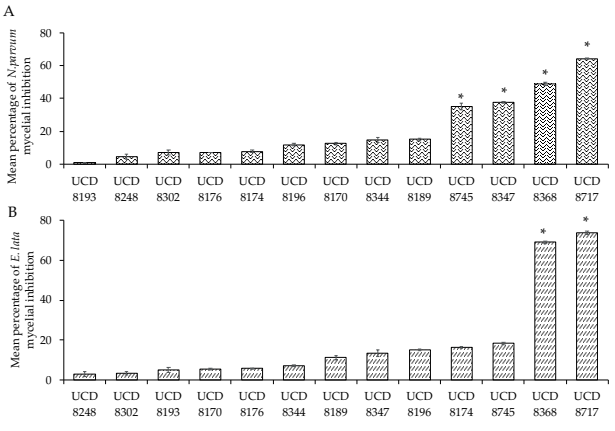

Figure 1. Preliminary *in vitro* dual culture evaluation of isolated microorganisms' ability to inhibit radial mycelium growth of the grapevine trunk disease pathogens (A) *Neofusicoccum parvum* and (B) *Eutypa lata.* Values are means (± standard errors) of ten replicates. * indicates differences compared with experimental controls (Dunnett's test; $P \leq 0.05$).

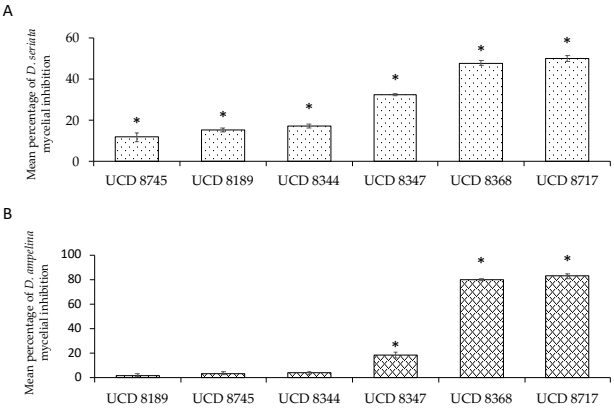

Figure 2. *In vitro* dual culture evaluation of selected microorganisms' ability to inhibit radial mycelial growth of the grapevine trunk disease pathogens (A) *Diplodia seriata* and (B) *Diaporthe ampelina.* Asterisk (*) indicates significant inhibition in comparison with a control (Dunnett's test $P \leq 0.05$).

against *E. lata*, only the *Trichoderma* isolates UCD 8368 and UCD 8717 radial mycelium growth, with both isolated reducing growth by more than 65% ($P \leq 0.05$; Figure. 1B).

Dual culture assays with Diplodia seriata *and* Diaporthe ampelina

The *Trichoderma* isolates UCD 8368 and UCD 8717 and *Bacillus* isolates UCD 8745 and UCD 8347 were further assessed in dual culture assays, as were the *Aureobasidium* isolates, UCD 8189 and UCD 8344, to evaluate these genera for suppression of *D. seriata* and *Dia. ampelina*. All isolates inhibited growth of *D. seriata* by 15% to 50% ($P \leq 0.05$; Figure 2A). Both *Trichoderma* isolates gave the greatest growth inhibition at approx. 50% compared to the controls. There was variation between the *Bacillus* isolates, with UCD 8347 causing approx. 32% inhibition and UCD 8745 causing approx. 11% inhibition. The *Aureobasidium* isolates UCD 8189 and UCD 8344 were similar in their antagonistic activity, causing, respectively, approx. 15% and 17% inhibition. When the isolates were tested against *Dia. ampelina*, the *Trichoderma* isolates UCD 8368 and UCD 8717 caused the greatest inhibition, in excess of 80%. The *Bacillus* isolate UCD 8347 also reduced mycelium radial growth of *Dia. ampelina*, though to a much lesser extent ($P \leq 0.05$; Figures 2B and 3)

Assays for volatile organic compounds

When the isolates were screened against *N. parvum* for antagonistic activity through production of antifungal volatile organic compounds (VOCs), only *Bacillus* isolate UCD 8347 (approx. 10% inhibition) and *Trichoderma* isolate UCD 8368 (approx. 20% inhibition) reduced growth of the pathogen ($P \leq 0.05$; Figure 4A). When the isolates were tested against *E. lata*, all but the *Aureobasidium* isolates reduced radial growth. The *Trichoderma* isolates UCD 8368 and UCD 8717 exhibited the greatest VOC effects, both causing at least 50% growth inhibition, while the *Bacillus* isolates UCD 8745 and UCD 8347 caused, respectively, approx. 37% and 39% inhibition ($P \leq 0.05$; Figure 4B). None of the isolates exhibited any VOC mediated inhibition of *D. seriata* (Figure 7C). However, against *Dia. ampelina*, all isolates gave VOC mediated inhibition, with UCD 8717 causing approx. 70% inhibition. *Trichoderma* isolate, UCD 8368 caused approx. 40% inhibition, while the *Bacillus* isolates UCD 8745 and UCD 8347 and the *Aureobasidium* isolates UCD 8189 and UCD 8344 all caused approx. 20% inhibition ($P \leq 0.05$; Figures 4D and 5).

Multilocus phylogenetic analyses of antagonistic isolates

Multilocus phylogenetic analysis of the *ITS* and *b1-tubulin* genes showed that isolates UCD 8344 and UCD 8189 were most closely related to *Aureobasidium pullulans* (Figure 6). Analysis of the *purH* and *rpoB* genes showed that isolates UCD 8347 and UCD 8745 were most closely related to *Bacillus velezensis* (Figure 7). Analysis of the *ITS* and *TEF-1a* genes showed that

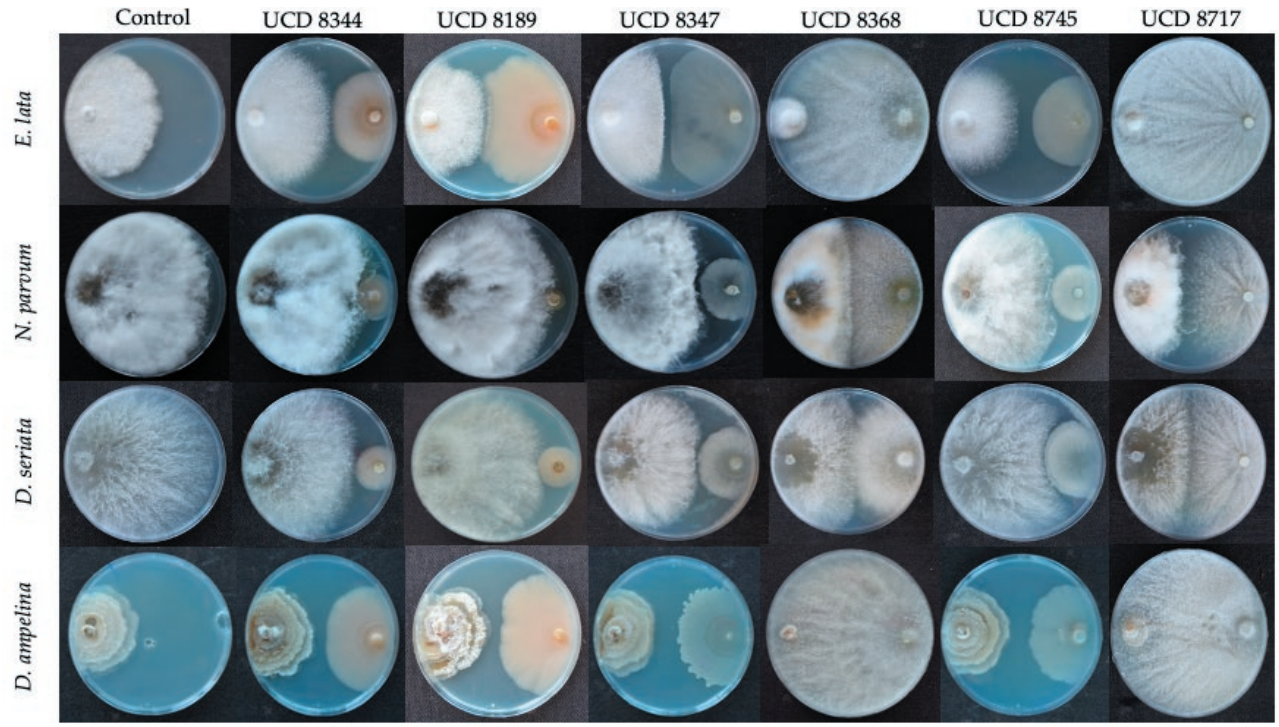

Figure 3. Representative visual summary of *in vitro* dual culture evaluation of selected isolates ability to inhibit radial mycelial growth of selected grapevine trunk disease pathogens.

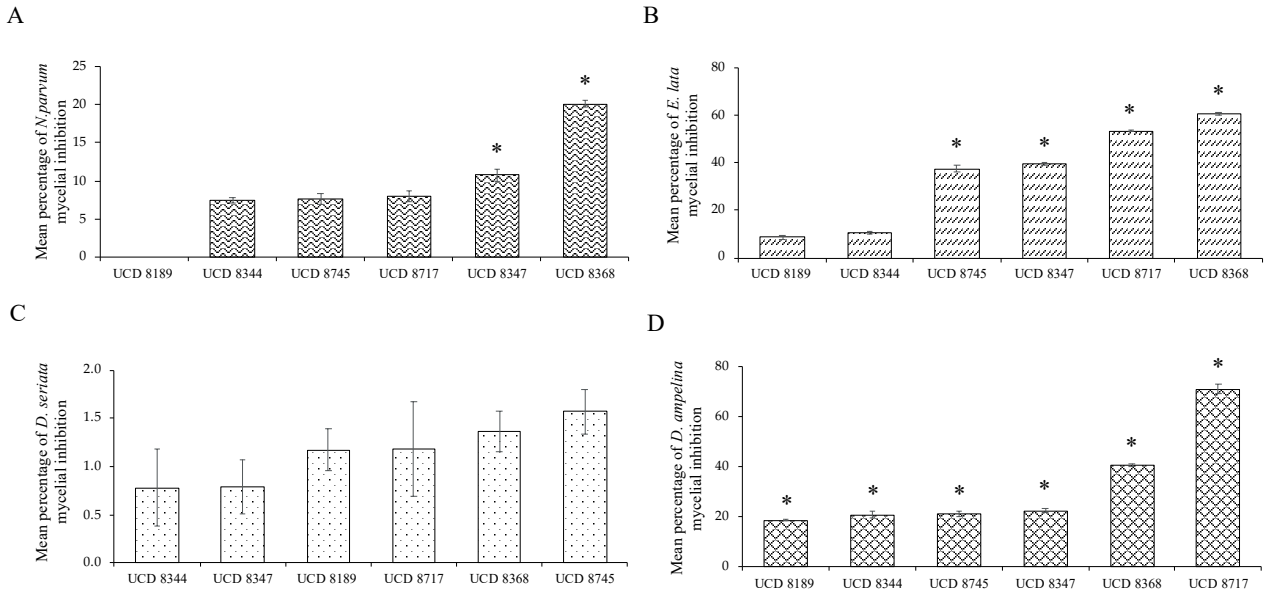

Figure 4. Mean proportions (%) of inhibition of radial mycelium growth of the grapevine trunk disease pathogens (A) *Neofusicoccum parvum,* (B) *Eutypa lata*, (C) *Diplodia seriata* and (D) *Diaporthe ampelina* in assays for volatile organic compound using the sealed-base-plates method with modifications. Values are means (± standard errors) of ten replicates. * indicates inhibition in comparison with controls (Dunnett's test; $P \leq 0.05$).

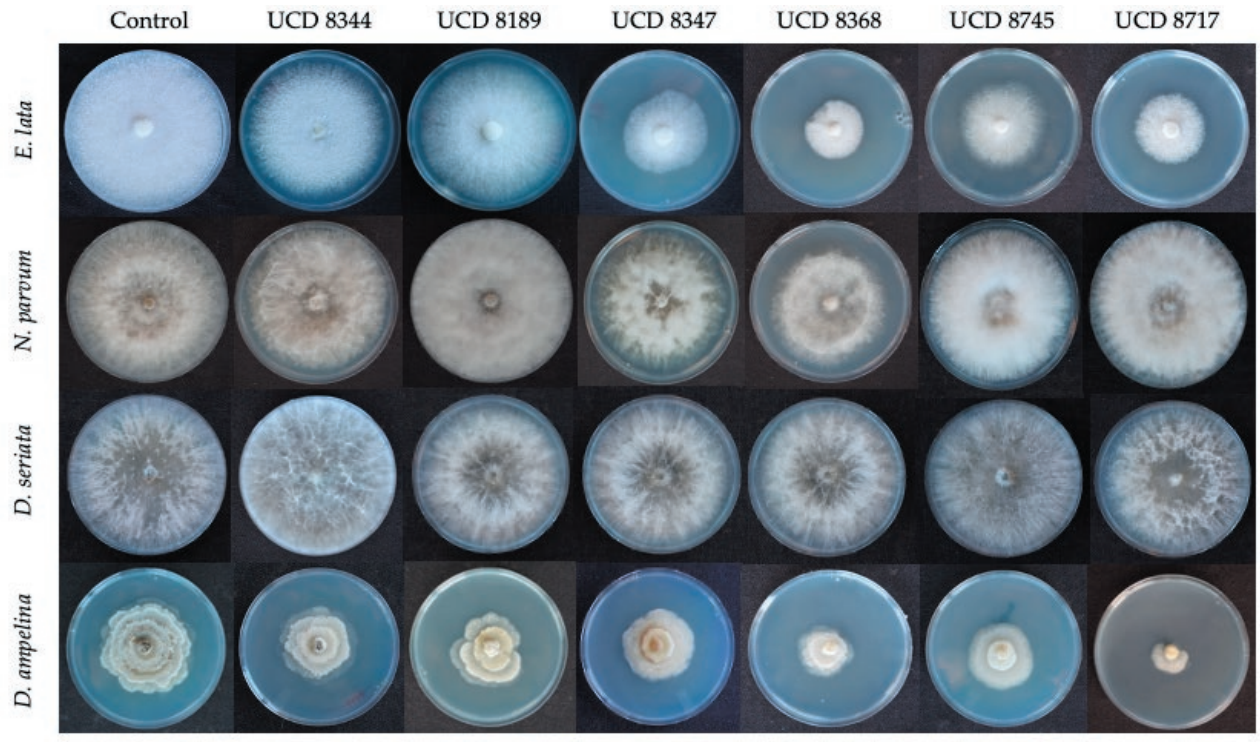

Figure 5. Representative summary of *in vitro* volatile evaluation of abilities of selected microorganisms (columns of culture) to inhibit radial mycelium growth of four grapevine trunk disease pathogens (rows of cultures).

isolates UCD 8368 was most closely related to *Trichoderma asperellum*, and UCD 8717 to *Trichoderma hamatum* (Figure 8).

DISCUSSION

Grapevine pruning wound protection has historically been mediated using synthetic chemicals which have dominated the crop protection industry since the 1980s. However, sustainability of crop production requires a shift towards low pesticide strategies, so there is increasing interest in novel solutions to prevent and control GTDs (Mondello *et al*., 2018). Biological control agents including *Trichoderma* spp. and *Bacillus* spp. have been shown *in vitro* to have potential for pruning wound protection against infections from GTDs (Schmidt *et al.,* 2001; Di Marco *et al.,* 2002; 2004; John *et al*., 2008; Halleen *et al.,* 2010; Kotze *et al.,* 2011; Rezgui *et al.,* 2016). However, microbial inhabitants of nutrient rich grapevine sap have not been previously evaluated for BCA ability against GTDs, so along with microbes isolated from grapevine pith and cane tissues, the present study evaluated microbes for *in vitro* activity against the GTD pathogens *N. parvum*, *E. lata*, *D. seriata* and *Dia. ampelina.*

In vitro dual culture assays are the primary means to detect antagonistic activity of microorganisms (Di Marco *et al.,* 2002; Haidar *et al.,* 2016). Both *Trichoderma* isolates UCD 8368 and UCD 8717 in this study exhibited mycelium growth inhibition against all the tested pathogens in dual culture assays, exhibiting at least 75% inhibition against the slow growing pathogens, *E. lata* and *Dia. ampelina* (Figures 1B and 2B). Isolate UCD 8368, which is closely related to *T. harzianum* (Figure 8) was also shown to similarly reduce *in vitro* growth of *E. lata* (Úrbez-Torres e*t al.,* 2020). Whilst *Trichoderma* spp. possess various antifungal mechanisms, this mycelium inhibition was likely attributed to overgrowth (Kotze e*t al.,* 2011), as the assessed isolates grew more rapidly and surrounded the pathogens in dual cultures (Figure 3). These results are similar to those from other studies, where *Trichoderma* spp. have been subjected to dual culture assays against *N. parvum, D. seriata* and *E. lata* (Mutawila e*t al.,* 2015; Silva-Valderrama e*t al.,* 2020; Úrbez-Torres et *al., 2*020). For example, *Trichoderma i*solates from Southern Italy inhibited N. *parvum r*adial growth by up to 74% (Úrbez-Torres et *al.,* 2020). It is hypothesized that this observed overgrowth by *Trichoderma* spp. *t*ranslates to competition for space and nutrients in

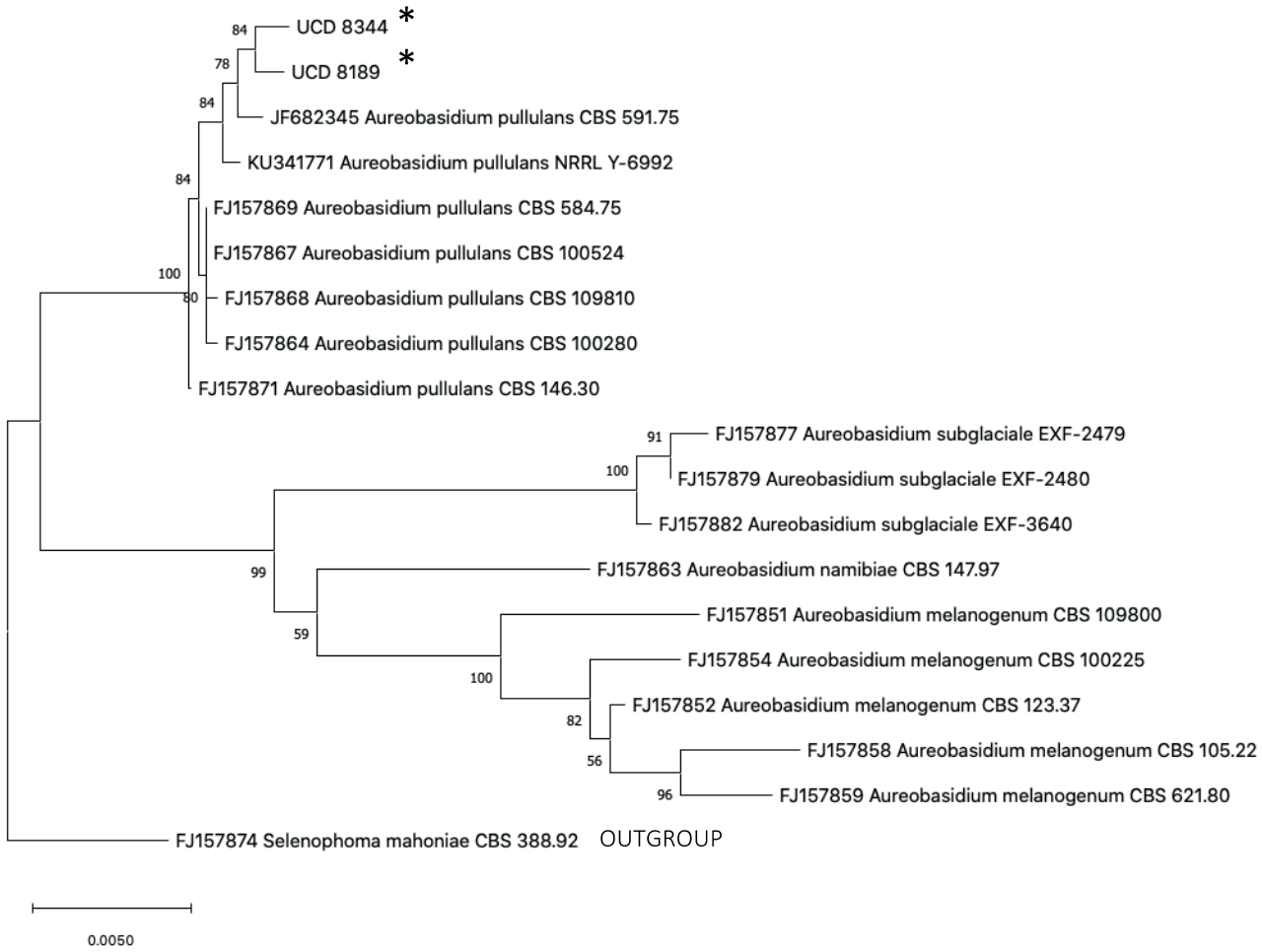

Figure 6. Maximum parsimony phylogenetic tree for isolates UCD 8344 and UCD 8189 based on a multigene data set of internal transcribed spacer rDNA (ITS) and b1-tubulin. Bootstrap support for the maximum-likelihood analysis is given at each node (1000 replicates). * indicates isolates evaluated in the present study. *Selenopoma mahoniae* FJ150872 was used as an outgroup.

grapevine pruning wounds as a mechanism to protect against GTDs (Úrbez-Torres et a*l., 202*0).

In the volatile assay, isolates UCD 8368 and UCD 8717 were still able to inhibit *E. lata* and *Dia. ampelina* (Figure 4B and D), which was probably due to the ability of *Trichoderma* spp. to produce volatile and non-volatile substances which have been shown to inhibit a range of fungi (Chambers and Scott, 1995; John *et al.,* 2004; Kexiang *et al*., 2002; Kucuk and Kivanc, 2004). John *et al.* (2004) showed that volatile compounds synthesized by *T. harzianum* AG1, AG2, and AG3 were inhibited growth of *E. lata*, and growth was completely inhibited by non-volatile compounds. In the present study, isolates UCD-8368 and UCD 8717 elicited a coconut odour which has previously been characterized as 6-n-pentyl-2H- pyran-2-one (Claydon *et al*., 1987), and reported to inhibit fungi including *Rhizoctonia solani*. The inhibition of *N. parvum* and *D. seriata* mycelium growth by isolates UCD 8368 and UCD 8717 in dual culture assays can likely be attributed to growth cessation, when microorganism and pathogens grow until they came in contact with one another and growth of both organisms ceases (Kotze *et al.,* 2011) (Figures 1A, 2A and 3). This mechanism as the primary method of inhibition was also indicated by the volatile assays because there was no inhibition of *N. parvum* and *D. seriata* by isolates UCD 8368 and UCD 8717 (Figures 4A, 4C and 5). The mycoparasitic reactions such as hyphal coiling, adhesion and penetration (Dos Reis Almeida *et al.,* 2007) have been shown to coincide with physical contact interactions; overgrowth and ceased growth. With isolate UCD 8717 being isolated from grapevine sap, this is the first report of a grapevine sap inhabiting microbe showing promising BCA *in vitro* activity against GTDs. Deyett and Rolshausen (2019)

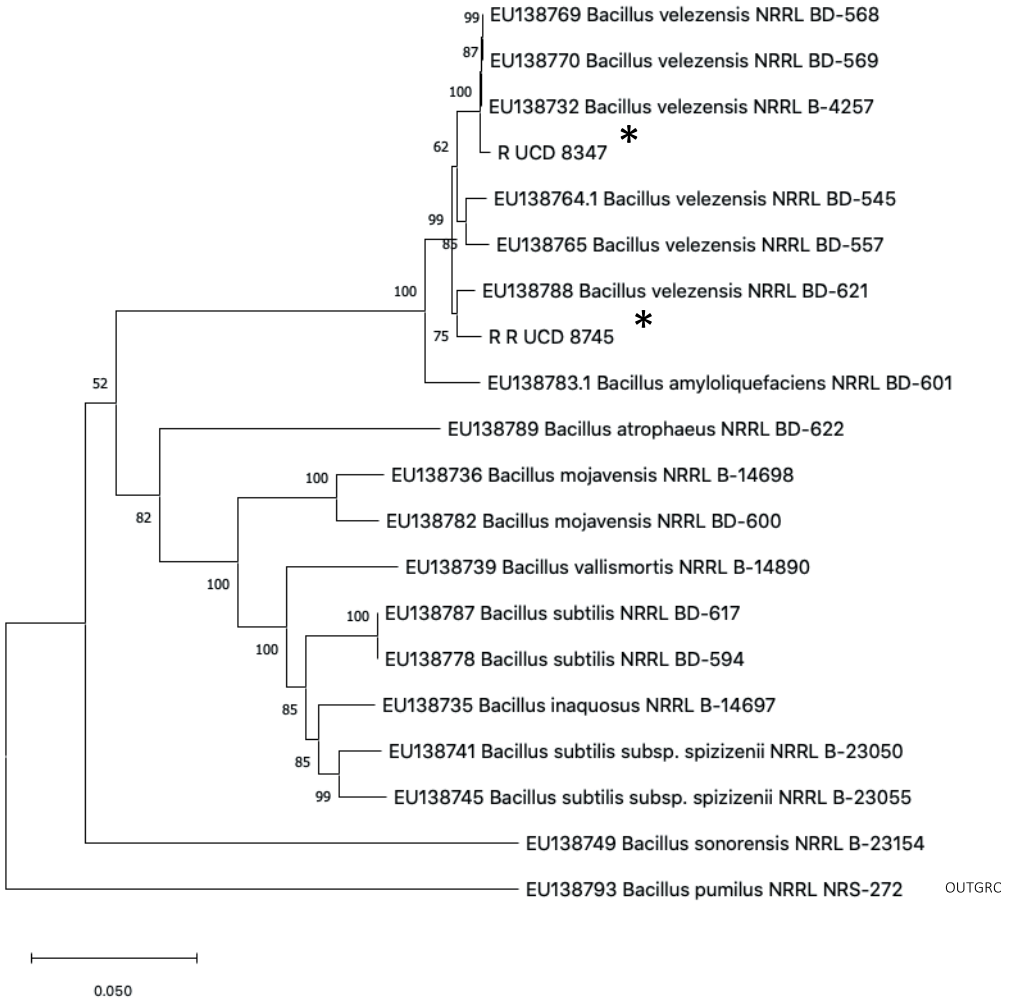

Figure 7. Maximum parsimony phylogenetic tree for isolates of UCD 8347 and UCD 8745 based on a multigene data set of purine biosynthesis (*purH*) and RNA polymerase subunit B (*rpoB*). Bootstrap support for the maximum-likelihood analysis is given at each node (1000 replicates). * indicates isolates evaluated in this study. *Bacillus pumilus* EU138793 was used as an outgroup.

utilized a culture-independent amplicon metagenomic approach to characterize the major bacterial and fungal taxa that comprise grapevine xylem sap microbial communities. They showed that the core microbiome consisted of seven bacterial and five fungal taxa. Grapevine sap is a rich source of glucose, fructose and amino acids, especially in spring, when these nutrients are remobilized to the vegetative parts of grapevines following winter dormancy, providing conducive environments to harbour beneficial microbes (Deyett and Rolshausen, 2019).

The bacterial isolates (*Bacillus* spp.) UCD 8347 and UCD 8745 exhibited varying antifungal ability and mechanisms in this study, depending on the GTD fungal pathogen. In the dual culture assays between UCD 8347 and *E. lata*, zones of inhibition were observed (Figure 3). Inhibition zones are most likely indicative of antibiotic production (Kotze, 2004) as a mechanism of mycoparasitism. Ferreira *et al*., (1991) identified at least two *Bacillus* isolates that produced antibiotic substances responsible for the inhibition of mycelium growth and ascospore germination. Kotze (2011) dual incubated (*in vitro*) *E. lata* with the same isolate and showed that the pathogen displayed little mycelium growth and clear inhibition zones between the cultures. Malformation of the hyphae, specifically swelling, was observed. Kotze (2011) showed that a *Bacillus subtilis* isolate gave clear zones of inhibition against *Phomopsis viticola.* In an assay for volatiles, isolate UCD 8347 inhibited *E. lata*, indicating that the antibiotic substance may have been volatile. Isolate UCD 8347 also gave small zones of inhibition against *N. parvum* in the dual culture assays (Figure 3), and slightly inhibited (by 10%) growth of *N. parvum*.in the assay for

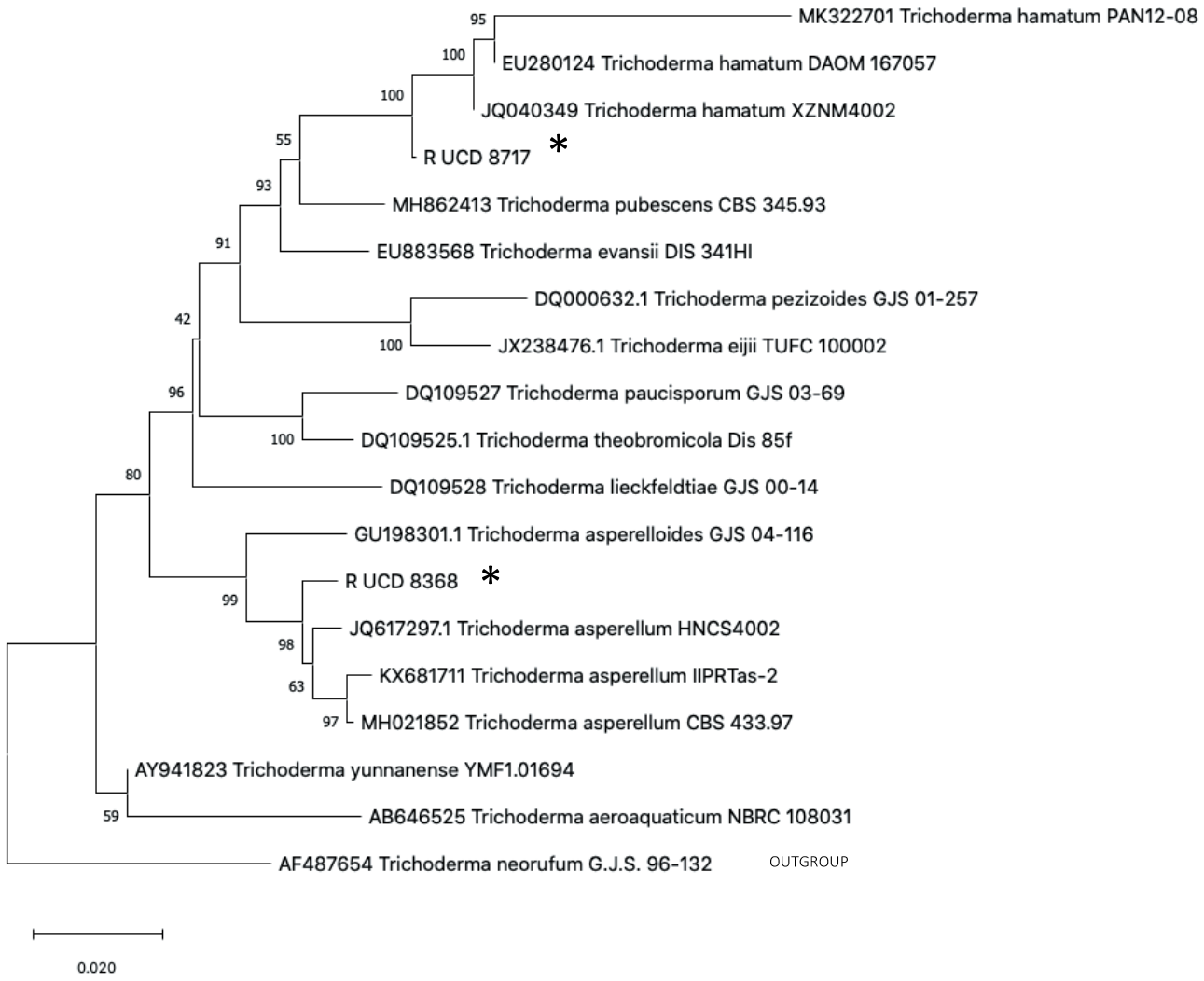

Figure 8. Maximum parsimony phylogenetic tree for isolates UCD 8368 and UCD 8717 based on a multigene alignment of the *Trichoderma* Hamatum/Asperellum clade using internal transcribed spacer rDNA (ITS), and translation elongation factor 1-alpha (TEF1). Bootstrap support for the maximum-likelihood analysis is given at each node (1000 replicates). * indicates subcultures evaluated in this study. *Trichoderma neorufum* AF487654 was used as an outgroup.

volatiles, indicating the antibiotic substance may be a volatile product (Figure 4A). Isolate UCD 8347 also gave inhibition of *D. seriata* and *Dia. ampelina* in the dual culture assay (Figure 2A and B), and of *Dia. ampelina* in the volatile assays (Figure 4D) but the mechanism of inhibition was unclear. Isolate UCD 8745 gave similar results to isolate UCD 8347, although with less inhibition in some assays, and the mechanism of inhibition is not as clear. Subsequent studies should investigate the VOC profiles of these isolates.

Studies of grapevine microbiomes have shown that *A. pullulans* is commonly distributed in grapevines, both in below and above ground structures (Sabate *et al.,* 2002; Martini *et al.,* 2009; Grube *et al.,* 2011; Barata *et al.,* 2012; Pinto *et al.,* 2014), so *A. pullulans* has promise as a potential BCA. In the present study, the *Aureobasidium* isolates UCD 8344 and UCD 8189 showed no antagonistic ability against *N. parvum*, *E. lata* or *Dia. ampelina* in dual culture assays, but these isolates inhibited mycelium growth of *D. seriata* in dual cultures (Figure 2A). This was probably due to ceased growth as these two isolates did not inhibit *D. seriata* in the VOC assays (Figure 4C). Similar results were obtained by Pinto *et al.* (2018), where *A. pullulans* strain Fito_F278 reduced mycelium growth of *D. seriata* F98.1 in a dual culture assay, and was postulated cause ceased growth of the pathogen.

Although different types of microorganisms were tested in the present study, only *Trichoderma* spp. have

been shown to be the most suitable agents for biological control of GTDs. This probably stems from the synergistic actions of different *Trichoderma* spp. biocontrol mechanisms, their ecological characteristics (saprotrophic, endophytic), and their positive effects induced on their host plants. Grapevines accommodate large pools of resident microorganisms embedded in complex micro-ecosystems (Pinto and Gomes, 2016), so further attempts should be made to identify novel strains of *Trichoderma* and other microorganisms to promote advances in GTD management.

With the need to make agricultural practices as sustainable as possible, novel solutions for GTD management are required, so that high quality grapes are produced that comply with the high standards of food safety. While *in vitro* BCA efficacy does not always translate to efficacy *in planta*, these microbes are the most promising, sustainable option for grapevine growers, because of restrictions and concerns with using chemical fungicides for disease control. The present study has identified potential BCAs with potential for simultaneous control of economically important pathogens responsible for GTDs, and has indicated that further studies to characterize BCA modes of antagonism and evaluate their efficacy in field trials. These potential BCAs may provide long lasting protection of grapevines against GTDs because they share the same host as the important GTD pathogens.

ACKNOWLEDGEMENTS

This research received funding from the American Vineyard Foundation.

LITERATURE CITED

Aroca A., Gramaje D., Armengol J., Jose G.-J., Rapaso R., 2010. Evaluation of the grapevine nursery propagation process as a source of *Phaeoacremonium* spp. and *Phaeomoniella chlamydospora* and occurrence of trunk disease pathogens in rootstock mother vines in Spain. *European Journal of Plant Pathology* 126: 165–174.

Barata A., Malfeito-Ferreira M., Loureiro V., 2012. The microbial ecology of wine grape berries. *International Journal of Food Microbiology* 153: 243–259.

Bertsch C., Ramirez-Suero M., Magnin-Robert M., Larignon P., Chong J., Fontaine F., 2013. Grapevine trunk diseases: complex and still poorly understood. *Plant Pathology* 62: 243–265.

Billones-Baaijens R., Jones E. E., Ridgway H. J., Jaspers M. V., 2013. Virulence Affected by Assay Parameters during Grapevine Pathogenicity Studies with Botryosphaeriaceae Nursery Isolates. *Plant Pathology* 62: 1214–25.

Bruisson, S., Zufferey, M., L'haridon, F., Trutmann, E., Anand, A., Weisskopf, L., 2019. Endophytes and Epiphytes From the Grapevine Leaf Microbiome as Potential Biocontrol Agents Against Phytopathogens. *Frontiers in Microbiology* 10: 1-17.

Carbone I., Kohn L. M., 1999. A method for designing primer sets for speciation studies in filamentous ascomycetes. *Mycologia* 91: 553–556.

Cawoy H., Bettiol W., Fickers P., Ongena M., 2011. Bacillus-based biological control of plant diseases, pesticides in the modern world. In: *Pesticides in the Modern World-Pesticides Use and Management* (Stoytcheva, M, ed.), Intech: 273-283.

Chambers, S., Scott E., 1995. In vitro antagonism of *Phytophthora cinnamomi* and *P. citricola* by *Trichoderma* species and *Gliocladium virens*. *Journal of Phytopathology* 143: 471–477.

Choudray D. K., Johri B. N., 2009. Interactions of *Bacillus* spp. and plants – With special reference to induced systemic resistance (ISR). *Microbiological Research* 164: 593–513.

Claydon, N., Allan, M.; Hanson, J. R., Avent, A. G., 1987. Antifungal alkyl pyrones of *Trichoderma harzianum*. *Transactions of the British Mycological Society* 88: 503–513.

Deyett, E., Rolshausen, P. E., Temporal Dynamics of the Sap Microbiome of Grapevine Under High Pierce's Disease Pressure. 2019. *Frontiers in Plant Science* 10: 1-15.

Di Marco, S., Osti, F., Roberti, R., Calzarano, F., Cesari, A., 2002. Attivita` di specie di *Trichoderma* nei confronti *di Phaeomoniella chlamydospora*, patogeno associato al mal delll'esca della vite. *Atti Giornate Fitopatologiche* 419–424.

Di Marco, S., Osti, F., Cesari, A., 2004. Experiments on the control of esca by *Trichoderma*. *Phytopathologia Mediterranea* 43: 108–115.

dos Reis Almeida, F. B., Cerqueira, F. M., Do Nascimento Silva, R., Ulhoa, C. J., Lima, A. L., 2007. Mycoparasitism studies of *Trichoderma harzianum* strains against *Rhizoctonia solani*: evaluation of coiling and hydrolytic enzyme production. *Biotechnology Letters* 29(8): 1189-93.

Ferreira, J. H. S., Matthee, F. N., Thomas, A. C., 1991. Biological Control of Eutypa lata on Grapevine by an Antagonistic Strain of *Bacillus subtilis*. *Ecology and Epidemiology* 81: 283–287.

Gilbert, J. A., Van der Lelie, D., Zarraonaindia, I., 2014. Microbial terroir for wine grapes. *PNAS* 111: 5–6.

Glass, N. L., Donaldson, G. C., 1995. Development of Primer Sets Designed for Use with the PCR To Amplify Conserved Genes from Filamentous Ascomycetes. *Applied and Environmental Microbiology* 61: 1323–1330.

Gotor-Vila, A., Teixado, N., Di Francesco, A., Usall, J., Ugolini, L., Torres, R., Mari, M., 2017. Antifungal effect of volatile organic compounds produced by *Bacillus amyloliquefaciens* CPA-8 against fruit pathogen decays of cherry. *Food Microbiology* 64: 219–225.

Gramaje, D., Armengol, J., 2011. Fungal Trunk Pathogens in the Grapevine Propagation Process: Potential Inoculum Sources, Detection, Identification, and Management Strategies. *Plant Disease* 95: 1040–1055.

Gramaje, D., Úrbez-Torres, J. R., Sosnowski, M. R., 2018. Managing Grapevine Trunk Diseases With Respect to Etiology and Epidemiology: Current Strategies and Future Prospects. *Plant Disease* 102: 12–39.

Grube, M., Schmid, F., Berg, G., 2011 Black fungi and associated bacterial communities in the phyllosphere of grapevine. *Fungal Biology* 115: 978–986.

Gubler, W. D., Rolshausen, P. E., Trouillas, F. P., Úrbez-Torres, J. R., Voegel, T., 2005. Grapevine trunk diseases in California. *Practical Winery and Vineyard*.

Haidar, R., Deschamps, A., Roudet, J., Calvo-Garrido, C., Bruez, E., Rey, P., Fermaud, M., 2016. Multi-organ screening of efficient bacterial control agents against two major pathogens of grapevine. *Biological Control* 92: 55–65.

Halleen, F.; Crous, P.; Petrini, O. 2003. Fungi associated with healthy grapevine cuttings in nurseries, with special reference to pathogens involved in the decline of young vines. *Australasian Plant Pathology* 32: 47–52.

Halleen, F., Fourie, P. H., Lombard, P. J., 2010. Protection of grapevine pruning wounds against Eutypa lata by biological and chemical methods. *South African Journal for Enology and Viticulture* 31: 125–132.

Hardoim, P. R., Can Overbeek, L. S., Berg, G., Pirttila, A. M., Compant, S., Sessitsch, A., 2015. The hidden world within plants: ecological and evolutionary considerations for defining functioning of microbial endophytes. *Microbiology and Molecular. Biology Reviews* 79: 293–320.

Harman, G. E., 2006. Overview of Mechanisms and Uses of *Trichoderma* spp. *Phytopathology* 96: 190–194.

Heimpel, G. E., Mills, N., 2017. Biological Control - Ecology and Applications. *Cambridge University Press,* Cambridge, UK, 1 pp.

Idris, H. A., Labuschagne, N., Korsten, L., 2007. Screening rhizobacteria for biological control of Fusarium root and crown rot of sorghum in Ethiopia. *Biological Control* 40: 97–106.

John, S., Scott, E., Wicks, T. J., Hunt, J., 2004 Interactions between *Eutypa lata* and *Trichoderma harzianum*. *Phytopathologia Mediterranea* 43: 95–104.

John, S., Wicks, T. J., Hunt, J., Lorimer, M., Oakey, H., Scott, E. S., 2005. Protection of grapevine pruning wounds from infection by *Eutypa lata* using *Trichoderma harzianum* and *Fusarium lateritium*. *Australasian Plant Pathology* 34: 569.

John, S., Wicks, T. J., Hunt, J. S., Scott, E. S., 2008. Colonisation of grapevine wood by Trichoderma harzianum and Eutypa lata. *Australian Journal of Grape and Wine Research* 14: 18–24.

Kaplan, J., Travadon., R., Cooper, M., Hilis, V., Lubell, M., Baumgartner, K., 2016. Identifying economic hurdles to early adoption of preventative practices: The case of trunk diseases in California winegrape vineyards. *Wine Economics and Policy* 5: 127–141.

Kexiang, G., Xiaoguang, L., Yonghong, L., Tianbo, Z., Shuliang, W., 2002. Potential of *Trichoderma harzianum* and *T. atroviride* to control *Botryosphaeria berengeriana* f. sp. piricola, the cause of apple ring rot. *Journal of Phytopathology* 150: 271–276.

Kotze, C., Van Niekerk, J., Mostert, L., Halleen, F., Fourie, P., 2011. Evaluation of biocontrol agents for grapevine pruning wound protection against trunk pathogen infection. *Phytopathologia Mediterranea* 50: 247–263.

Kucuk, C., Kivanc, M., 2004. *In Vitro* Antifungal Activity of Strains of *Trichoderma harzianum*. *Turkish Journal of Biology* 28: 111–115.

Lu, J. J., Perng, C. L., Lee, S. Y., Wan, C. C., 2000. Use of PCR with Universal Primers and Restriction Endonuclease Digestions for Detection and Identification of Common Bacterial Pathogens in Cerebrospinal Fluid. *Journal of Clinical Microbiology* 38: 2076–2080.

Luque, J., Elena, G., Garcia-Figueres, F., Reyes, J., Barrios, G., Legorburu, F.J., 2014. Natural infections of pruning wounds by fungal trunk pathogens in mature grapevines in Catalonia (Northeast Spain). *Australian Journal of Grape and Wine Research* 20: 134–143.

Martinez-Diz, M. D. P., Diaz-Losada, E., Andres-Sodupe, M., Bujanda, R., Maldonadao-Gonzalez, M. M., Gramaje, D., 2020. Field evaluation of biocontrol agents against black-foot and Petri diseases of grapevine. *Pest Management. Science.*

Martini, M., Musetti, R., Grisan, R., Polizzotto, R., Borselli, S., Pavan, F., Osler, R., 2009. DNA-dependent detection of the grapevine fungal endophytes *Aureobasidium pullulans* and *Epicoccum nigrum*. *Plant Disease* 93: 993–998.

Mondello, V., Songy, A., Battison, E., Pinto, C., Coppin, C., Fontaine, F., 2018. Grapevine Trunk Diseases: A Review of Fifteen Years of Trials for Their Control with Chemicals and Biocontrol Agents. *Plant Disease* 102: 1189–1217.

Mugnai, L., Graniti, A., Surico, G., 1999. Esca (black measles) and brown wood-streaking: two old and elusive diseases of grapevines. *Plant Disease* 83: 404–418.

Mukherjee, P. K., Horwitz, B. A., Herrera-Estrella, A., Schmoll, M., Kenerley, C. M., 2013. *Trichoderma* Research in the Genome Era. *Annual. Review of Phytopathology* 51: 105–129.

Munkvold, G., Duthie, J., Marois, J., 1994. Reductions in yield and vegetative growth of grapevines due to Euytpa dieback. *Phytopathology* 84: 186–192.

Mutawila, C., Halleen, F., Mostert, L., 2015. Development of benzimidazole resistant *Trichoderma* strains for the integration of chemical and biocontrol methods of grapevine pruning wound protection. *BioControl* 60: 387–399.

Otoguro, M., Suzuki, S., 2018. Status and future of disease protection and grape berry quality alteration by micro-organisms in viticulture. *Letters in Applied Microbiology* 67: 106–112.

Pascoe, I., Cottral, E., 2000. Developments in grapevine trunk diseases research in Australia. *Phytopathologia Mediterranea* 39: 68–75.

Pinto, C., Pinho, D., Sousa, S., Pinheiro, M., Egas, C., Gomes, A. C., 2014. Unravelling the diversity of grapevine microbiome. *PLoS One* 9(1).

Pinto, C., Gomes, A. C., 2016. Vitis vinifera microbiome: from basic research to technological development. *BioControl* 61: 243–256.

Pinto, C., Custodio, V., Nunes, M., Songy, A., Rabenoelina, F., Fontaine, F., 2018. Understand the Potential Role of *Aureobasidium pullulans*, a Resident Microorganism From Grapevine, to Prevent the Infection Caused by *Diplodia seriata*. *Frontiers in Microbiology* 9: 1-15.

Pitt, W. M., Huang, R., Steel, C. C., Savocchia, S., 2013. Pathogenicity and epidemiology of *Botryosphaeriaceae* species isolated from grapevines in Australia. *Australasian Plant Pathology* 42: 573-582.

Pitt, W. M., Úrbez-Torres, J. R., Trouillas, F. P., 2015. *Dothiorella* and *Spencermartinsia*, new species and records from grapevines in Australia. *Australasian Plant Pathology* 44: 43–56.

Rezgui, A., Ghnava-Chakroun, A., Vallance, J., Bruez, E. and Hajlaoui, M. R. 2016. Endophytic bacteria with antagonistic traits inhibit the wood tissues of grapevines from Tunisian vineyards. *Biological Control* 99: 28-37.

Rolshausen, P. E., Akgul, D. S., Perez, R., Eskalen, A., Gispert, C., 2013. First report of wood canker caused by *Neoscytalidium dimidiatum* on grapevine in California. *Plant Disease* 97: 1511.

Rolshausen, P. E., Baumgartner, K., Travadaon, R., Fujiyoshi, P., Pouzoulet, J., Wilcox, W. F., 2014. Identification of *Eutypa* spp. Causing Eutypa dieback of grapevine in eastern North America. *Plant Disease* 98: 483-491.

Rooney, A. P., Price, N. P. J., Erhardt, C., Swezey, J. L., Bannan, J. D., 2009. Phylogeny and molecular taxonomy of the *Bacillus subtilis* species complex and description of *Bacillus subtilis* subsp. inaquosorum subsp. nov. *International Journal of Systematic and Evolutionary Microbiology* 59: 2429–2435.

Sabate, J., Cano, J., Esteve-Zarzoso, B., Guillamón, J. M., 2002. Isolation and identification of yeasts associated with vineyard and winery by RFLP analysis of ribosomal genes and mitochondrial DNA. *Microbiological Research* 157: 267–274.

Schmidt, C. S., Lorenz, D., Wolf, G. A., 2001. Biological control of the grapevine dieback fungus *Eutypa lata* I: Screening of bacterial antagonists. *Journal of Phytopathology* 149: 427–435.

Siebert, J. B, 2001. Eutypa: the economic toll in vineyards. *Wines and Vines* 82: 50–56.

Silva-Valderrama, I., Toapanta, D., de los Angeles Miccono, M., Lolas, M., Diaz, G. A., Cantu, D., Castrro, A., 2021. Biocontrol potential of grapevine endophytic and rhyzophtic fungi against trunk pathogens. *Frontiers in Microbiology* 11.

Strobel, G., Daisy, B., 2003. Bioprospecting for Microbial Endophytes and Their Natural Products. *Microbiology and Molecular Biology Reviews* 67: 491–502.

Trouillas, F. P., Úrbez-Torres, J. R., Gubler, W. D., 2010. Diversity of diatrypaceous fungi associated with grapevine canker diseases in California. *Mycologia* 102: 319–336.

Úrbez-Torres, J. R., 2011. The status of Botryosphaeriaceae species infecting grapevines. *Phytopathologia Mediterranea* 50: 5–45.

Úrbez-Torres, J. R., Leavitt, T. M., Voegel, T. M., Gubler, W. D., 2006. Identification and distribution of *Botryosphaeria* spp. associated with grapevine cankers in California. *Plant Disease.* 90: 1490–1503.

Úrbez-Torres J. R., Tomaselli E., Pollard-Flamand J., Boule J., Gerin D., Pollastro S., 2020. Characterization of *Trichoderma i*solates from southern Italy, and their potential biocontrol activity against grapevine trunk disease fungi. *Phytopathologia Mediterranea* 59(3): 425-439.

Waite, H., Morton, L., 2007. Hot Water Treatment, Trunk Diseases and Other Critical Factors in the Produc-

tion of High-Quality Grapevine Planting Material. *Phytopathologia Mediterranea* 46: 5–17.

West, E. R., Cother, E. J., Steel, C. C., Ash, G. J., 2010. The characterization and diversity of bacterial endophytes of grapevine. *Canadian Journal of Microbiology* 56: 209–216.

White, T. J., Bruns, T., Lee, S. W., Taylor, J. W., 1990. Amplification and Direct Sequencing of Fungal Ribosomal RNA Genes for Phylogenetics. In: *PCR Protocols: A Guide to Methods and Applications*. (M.A. Innis, D.H. Gelfand, J.J. Sninsky, T.J. White, ed.), Academic Press, Cambridge, MA, USA, 317.

Yang, T., Groenewald, Z., Cheewangkoon, R., Jami, F., Abdollahzadeh, J., Crous, P.W., 2017. Families, genera, and species of Botryosphaeriales. *Fungal Biology* 121: 322–346.

Zanzotto, A., Morroni, M., 2016. Major Biocontrol Studies and Measures Against Fungal and Oomycete Pathogens and Grapevines. In: *Biocontrol of Major Grapevine Diseases: Leading Research*. (S. Compant, F. Mathieu, ed.), CAB International, Wallingford, UK 1-34.

Phytopathologia Mediterranea
The international journal of the
Mediterranean Phytopathological Union

Firenze University Press
www.fupress.com/pm

Research Papers

Structure analysis of the ribosomal intergenic spacer region of *Phaeoacremonium italicum* as a study model

Meriem LAIDANI[1,2], Maria Luisa RAIMONDO[1,*], Anna Maria D'ONGHIA[2], Antonia CARLUCCI[1,*]

[1] *Department of Agriculture, Food, Natural resources and Engineering (DAFNE), University of Foggia, 71122 Foggia, Italy*
[2] *Mediterranean Agronomic Institute of Bari, 70010 Valenzano (BA), Italy*
*Corresponding authors. E-mail: marialuisa.raimondo@unifg.it; antonia.carlucci@unifg.it

Summary. Increasing recognition of novel *Phaeoacremonium* species, and their recent taxonomic reassignment through phylogeny based on the β-tubulin and actin genes, have highlighted the presence of paraphyly, intraspecific variation, and incongruence of some *Phaeoacremonium* species. This study investigated the intergenic spacer rDNA regions of a representative collection of 31 *Phaeoacremonium italicum* strains, and compared their structures with those of the closest related species, *Phaeoacremonium alvesii* and *Phaeoacremonium rubrigenum*. These intergenic spacer sequences had five categories of repeat elements that were organised into distinct patterns. Morphological analyses of the *P. italicum* strains provided a more detailed description of *P. italicum*. The phylogenetic tree constructed using the intergenic spacer sequences compared with that obtained by combined analysis of β-tubulin and actin sequences indicated that the intergenic spacer rDNA region distinguished intraspecific and interspecific variations. Further molecular studies are required to determine whether intergenic spacer sequences can improve precision in defining *Phaeoacremonium* phylogeny, and prevent misidentification and the introduction of vague species boundaries for the genus.

Keywords. IGS, intraspecific variation, interspecific variation, *Phaeoacremonium* species.

OPEN ACCESS

Citation: M. Laidani, M.L. Raimondo, A.M. D'Onghia, A. Carlucci (2021) Structure analysis of the ribosomal intergenic spacer region of *Phaeoacremonium italicum* as a study model. *Phytopathologia Mediterranea* 60(3): 549-570. doi: 10.36253/phyto-13159

Accepted: November 18, 2021

Published: December 30, 2021

Data Availability Statement: All relevant data are within the paper and its Supporting Information files.

Competing Interests: The Author(s) declare(s) no conflict of interest.

Editor: Alan J.L. Phillips, University of Lisbon, Portugal.

INTRODUCTION

The genus *Phaeoacremonium* (*Togniniales*, *Togniniaceae*) was originally described in 1996, containing only six species (Crous *et al.,* 1996). Ten years later, Mostert *et al.* (2006) described *Togninia* as the sexual morph of *Phaeoacremonium*, and defined 22 *Phaeoacremonium* and ten *Togninia* species. Gramaje *et al.* (2015) included *Togninia* in *Phaeoacremonium* genus, according to the change to single nomenclature for fungi (Hawksworth *et al.,* 2011). The number of described *Phaeoacremonium* species has continued to

increase to the present 63 (Ariyawansa *et al.,* 2015; Crous *et al.,* 2016; Da Silva *et al.,* 2017; Spies *et al.,* 2018), which also includes the report of *P. thailandense* from freshwater in Thailand (Calabon *et al.,* 2021).

Phaeoacremonium has a wide host range and worldwide distribution. The host range includes woody plants, insect larvae, freshwater and humans, and species have been reported from South, Central and North America, Asia, Europe, the Middle East, the Far East, Oceania and Africa (Gramaje *et al.,* 2015; Spies *et al.,* 2018). Many reports have associated *Phaeoacremonium* species with vascular wood diseases of several plants (Damm *et al.,* 2008; Nigro *et al.,* 2013; Raimondo *et al.,* 2014; Carlucci *et al.,* 2015; Olmo *et al.,* 2015; Spies *et al.,* 2018), where the grapevine trunk diseases, such as Esca and Petri diseases, are considered to be the most destructive and severe. To date, 36 *Phaeoacremonium* species have been isolated abundantly from necrotic wood of grapevines showing Esca and Petri diseases in vineyards, of which 22 species were in Europe and Mediterranean countries (Essakhi *et al.,* 2008; Raimondo *et al.,* 2014; Gramaje *et al.,* 2015; Jayawardena *et al.,* 2018; Spies *et al.,* 2018). *Phaeoacremonium* species have also been isolated from different woody hosts, including olive and other fruit trees that show wilt, decline, dieback and cankers. In particular, 13 *Phaeoacremonium* species have been associated with olive trees, and 34 with fruit trees, of which ten were on olive and 18 were on fruit trees in Europe and Mediterranean countries (Crous and Gams, 2000; Mostert *et al.,* 2006; Nigro *et al.,* 2013; Carlucci *et al.,* 2015; Gramaje *et al.,* 2015; Soltaninejad *et al.,* 2017; Spies *et al.,* 2018; Sohrabi *et al.,* 2020).

The recent taxonomic reassignment and the increasing recognition of novel *Phaeoacremonium* species associated with various woody host plants has highlighted the intraspecific genetic variation and paraphyly within several species-level clades, and also incongruence or lack of resolution for some *Phaeoacremonium* species using β-tubulin and actin sequences (Gramaje *et al.,* 2015; Spies *et al.,* 2018). For example, in the *Phaeoacremonium italicum/ Phaeoacremonium alvesii* group, the phylogenetic position of some strains (e.g., CBS 113590) was incongruent among the combined and individual phylogenies. Spies *et al.* (2018) also reported that the morphological differences described for these closely related species did not correspond to the intraspecific genetic variation observed, and for this reason, morphology cannot be useful to clarify species identity of strains that have unresolved phylogenetic identities.

To improve the resolution of some *Phaeoacremonium* clades, further phylogenetic markers need to be investigated. To date, few studies have attempted to use other genes as putative markers for molecular identification of *Phaeoacremonium* species. Mostert *et al.* (2005) sequenced the calmodulin gene of 19 *Phaeoacremonium* strains that belonged to 11 species to provide greater clarity on the status of the taxa closely related to *Phaeoacremonium rubrigenum*, although the calmodulin gene did not distinguish between *P. alvesii* and *P. rubrigenum* (the closest species), as the sequences were identical. Together with the internal transcribed spacer (ITS) and the β-tubulin and actin genes, Úrbez-Torres *et al.* (2014) sequenced elongation factor (EF)1-α from 56 strains that belonged to 31 *Phaeoacremonium* species, and performed multilocus analyses. The tree obtained by inclusion of the EF1-α DNA marker improved the molecular characterisation and increased the phylogenetic resolution within *Phaeoacremonium*.

Several studies have reported that the nuclear ribosomal DNA (rDNA) intergenic spacer (rDNA IGS) region could be suitable to define evolutionary dynamics of divergent species and populations, to detect genetic variability, and to develop diagnostic markers and carry out phylogenetic analyses (Sugita *et al.,* 2002; Dissanayake *et al.,* 2009; Sampietro *et al.,* 2010; Mirete *et al.,* 2013). The IGS rDNA region has been used to confirm interspecific differentiation and intraspecific discrimination among vegetative compatibility groups of *Verticillium dahliae* (Papaioannou *et al.,* 2013), and to investigate relationships in other fungi at interspecific and intraspecific levels, including for *Metarhizium anisopliae* (Pipe *et al.,* 1995), *Microdochium nivale* (Mahuku *et al.,* 1998), *Hebeloma cylindrosporium* (Guidot *et al.,* 1999), *Cryptococcus neoformans* (Diaz *et al.,* 2005) and *Phomopsis helianthi* (Pecchia *et al.,* 2004).

The present study aimed to investigate the structure of the IGS rDNA regions of a representative collection of *P. italicum* strains as a study model, and to compare them with strains of the closely related species *P. alvesii* and *P. rubrigenum*, to emphasise intraspecific and interspecific genetic variations. For these purposes, the entire IGS regions of 31 *P. italicum*, two *P. alvesii* and two *P. rubrigenum* strains were amplified and sequenced to define the IGS structures. To determine whether morphological features corresponded with putative intraspecific and interspecific genetic variation expressed by the IGS rDNA region, a detailed microscopy study of *P. italicum* strains was also carried out. To verify that IGS rDNA could be used to discriminate the *Phaeoacremonium* species, it was also amplified and sequenced in another 12 *Phaeoacremonium* species. These data were used to obtain a phylogenetic tree and to compare this with that obtained by the markers presently used for molecular identification of *Phaeoacremonium* species.

MATERIALS AND METHODS

Fungal isolates

This study included a total of 57 isolates of *Phaeoacremonium* that were obtained from different hosts and localities, with 49 isolates from the collection of the Department of Agriculture, Food, Natural resources and Engineering (DAFNE), University of Foggia (Italy), one isolate from Instituto de Ciencias de la Vid y del Vino (ICVV) (Spain), and seven isolates from Westerdijk Fungal Biodiversity Institute (CBS, Utrecht, The Netherlands). Two isolates of *Pleurostoma richardsiae* from DAFNE were included in this study as outgroups (Table 1).

DNA extraction, PCR and sequencing

Genomic DNA was extracted from fresh mycelia for each isolate, using the methods of Carlucci *et al.* (2013). Partial sequences of the β-tubulin and actin genes of each of the strains were amplified according to the protocols and conditions described by Raimondo *et al.* (2014). The IGS rDNA region flanking 28S and 18S of each of the strains was amplified using the universal primers LR12R (5'-GAACGCCTCTAAGTCAGAATCC-3'; anchored in the 3' of the LSU gene) and invSR1R (5'-ACTGGCAGAATCAACCAGGTA -3'; anchored in the 5' of SSU of the RNA gene) (Durkin *et al.,* 2015).

The PCR reactions were each performed in a thermal cycler (C-1000 Touch; BioRad) in a final volume of 25 µL. The reaction mixture contained 1× PCR buffer, 3 mM $MgCl_2$, 200 µM deoxynucleotide triphosphates, 0.2 µM of each primer, 1.25 U *Taq* polymerase, and 30 ng template DNA. The *Taq* polymerase (LA Taq long-PCR), nucleotides, $MgCl_2$ and buffer were supplied by TaKaRa Bio Europe. The PCR protocol and conditions were optimised for *P. italicum*, which included 95°C denaturation for 10 min, followed by 25 cycles of denaturation at 95°C for 1 min, annealing at 55°C for 1 min, and extension at 72°C for 2.5 min; with a final extension step at 72°C for 10 min. The same PCR conditions were used for all of the *Phaeoacremonium* species, except for *P. parasiticum* and *P. croatiense*, for which the annealing temperatures were 58°C for *P. parasiticum* and 62°C for *P. croatiense*. For amplifications of the two *P. richardsiae* strains were used PCR conditions of 30 cycles, with annealing temperature of 58°C.

The sequencing was performed in both directions for all of the fungal isolates by Eurofins Genomics. As the complete fragments of the IGS regions were large, the design of additional internal primers was needed (Table 2). The sequence of each locus was assembled and manually corrected (BioEdit version 7.0.9; http://www.mbio.ncsu.edu/BioEdit). The taxonomic identification of the Italian *Phaeoacremonium* strains through BLAST searches was carried out considering threshold similarity values of 98 to 100%, and as comparisons of the β-tubulin and actin sequences with the reference strains as the ex-types. All of the novel DNA sequences generated in this study were deposited to GenBank (Table 1).

Structure analysis of the intergenic spacer region of P. italicum

The IGS sequences obtained from each of the strains were aligned using the online multiple alignment programme MAFFT v.7 (http://mafft.cbrc.jp/alignment/server/) (Katoh and Frith, 2012; Katoh and Standley, 2013), with the iterative refinement method E-INS-I, as recommended for <200 sequences with multiple conserved domains and long gaps. The alignment was checked visually and adjusted manually where necessary. As the sequences were very large, to determine the distribution of polymorphisms among the *P. italicum* strains and those that belonged to the closest species (i.e., *P. alvesii*, *P. rubrigenum*), the GeneQuest program of the Lasergene 6 software package was used (DNAstar). The pairwise identities of the IGS sequences were evaluated using MegAlign version 15 (DNAstar, Madison, WI, USA).

Morphology

The growth rates of the *P. italicum* isolates were determined over 8 d and 16 d on malt extract agar (MEA; 50 g malt extract agar (Oxoid), 1 L water), potato dextrose agar (PDA; 39 g potato dextrose agar (Oxoid), 1 L water), and oatmeal agar (OA; 30 g oats, 8 g agar (Oxoid), 1 L water), with incubations at 23±2°C. The cardinal temperatures for growth of each isolate were determined on MEA, with incubations in the dark at temperatures from 5°C to 40°C, at 5°C intervals, and including 37°C. Colony morphologies were determined on MEA, PDA and OA after 21 d at 23±2°C, and colony colours were determined using the colour charts of Rayner (1970).

Micromorphological characterisation of each isolate was performed according to Raimondo *et al.* (2014). The dimensions and morphologies of the conidiophore structures, and the sizes, phialide types and shapes, presence of bundles, and conidium shapes and sizes were measured from 100% lactic acid mounts as 30 measurements (×100 magnification), using a measurement module

Table 1. Hosts, origins and sources of *Phaeoacremonium* spp. isolates used in this study.

Species	Isolate code	Host	Origin	Source	Sub-group	GenBank		
						β-tubulin	Actin	IGS
P. alvesii	CBS 113590	*Dodonaea viscosa*	Australia	CBS	#7	AY579304	AY579237	MZ468465
	CBS 408.78	*Homo sapiens*	USA	CBS	-	AY579303	AY579236	MZ468464
	CBS 729.97	*Homo sapiens*	USA	CBS	-	AY579302	AY579235	MZ468463
P. amygdalinum	Pm10	*Prunus dulcis*	Foggia (FG), Apulia, Italy	DAFNE	-	MW714562	MW716265	MZ468466
P. croatiense	Pm120	*Vitis vinifera*	Campomarino (CB), Molise, Italy	DAFNE	-	MZ442499	MZ442548	MZ468467
P. fraxinopennsylvanicum	Pm182	*Vitis vinifera*	Torremaggiore (FG), Apulia, Italy	DAFNE	-	MZ442501	MZ442542	MZ468468
P. griseorubrum	CBS 111657^{T}	*Homo sapiens*	Maryland, Texas, USA	CBS	-	AY579294	AY579227	MZ468516
P. hispanicum	CBS 123910	*Vitis vinifera*	Valencia, Spain	ICVV	-	FJ517164	FJ517156	MZ468519
P. iranianum	Pm121	*Vitis vinifera*	Campomarino (CB), Italy	DAFNE	-	MZ442494	MZ442543	MZ468469
	Pm122	*Vitis vinifera*	Campomarino (CB), Italy	DAFNE	-	MZ442495	MZ442544	MZ468470
P. italicum	Pm1	*Olea europaea*	Canosa di Puglia (BT), Apulia, Italy	DAFNE	#1	KJ534074	KJ534046	MZ468517
	Pm2	*Olea europaea*	Canosa di Puglia (BT), Apulia, Italy	DAFNE	#1	MZ442459	MZ442506	MZ468471
	CBS 137763^{T} Pm19	*Vitis vinifera*	San Severo (FG), Apulia, Italy	DAFNE	#1	MZ442458	MZ442507	MZ468472
	CBS 137764 Pm20	*Vitis vinifera*	Cerignola (FG), Apulia, Italy	DAFNE	#1	KJ534075	KJ534047	MZ468518
	Pm32	*Vitis vinifera*	Torremaggiore (FG), Apulia, Italy	DAFNE	#1	KJ534080	KJ534052	MZ468473
	Pm33	*Vitis vinifera*	Cerignola (FG), Apulia, Italy	DAFNE	#1	KJ534081	KJ534053	MZ468474
	Pm38	*Olea europaea*	Canosa di Puglia (BT), Apulia, Italy	DAFNE	#1	MZ442460	MZ442508	MZ468475
	Pm54	*Olea europaea*	Cerignola (FG), Apulia, Italy	DAFNE	#1	MZ442461	MZ442509	MZ468476
	Pm103	*Olea europaea*	San Giovanni Rotondo, (FG), Apulia, Italy	DAFNE	#1	MZ442462	MZ442510	MZ468477
	Pm35M	*Olea europaea*	San Giovanni Rotondo, (FG), Apulia, Italy	DAFNE	#2	MZ442463	MZ442511	MZ468478
	Pm31M	*Prunus dulcis*	San Giovanni Rotondo, (FG), Apulia, Italy	DAFNE	#2	MZ442464	MZ442512	MZ468479
	Pm290M	*Prunus dulcis*	San Giovanni Rotondo, (FG), Apulia, Italy	DAFNE	#2	MZ442465	MZ442513	MZ468480
	Pm340M	*Olea europaea*	San Giovanni Rotondo, (FG), Apulia, Italy	DAFNE	#2	MZ442466	MZ442514	MZ468481
	Pm50M	*Olea europaea*	San Giovanni Rotondo, (FG), Apulia, Italy	DAFNE	#3	MZ442467	MZ442515	MZ468482
	Pm58	*Vitis vinifera*	San Severo (FG), Apulia, Italy	DAFNE	#3	MZ442468	MZ442516	MZ468483
	Pm259	*Olea europaea*	Mattinata (FG), Apulia, Italy	DAFNE	#3	MZ442469	MZ442517	MZ468484
	Pm503	*Prunus dulcis*	Foggia (FG), Apulia, Italy	DAFNE	#3	MZ442470	MZ442518	MZ468485
	Pm45	*Olea europaea*	Carpino (FG), Apulia, Italy	DAFNE	#4	MZ442474	MZ442519	MZ468486
	Pm60	*Olea europaea*	Canosa di Puglia (BT), Apulia, Italy	DAFNE	#4	MZ442475	MZ442520	MZ468487
	Pm105	*Prunus dulcis*	Cerignola (FG), Apulia, Italy	DAFNE	#4	MZ442476	MZ442521	MZ468488
	Pm199	*Vitis vinifera*	Torremaggiore (FG), Apulia, Italy	DAFNE	#4	MZ442477	MZ442522	MZ468489
	Pm303	*Vitis vinifera*	Cerignola (FG), Apulia, Italy	DAFNE	#4	MZ442478	MZ442523	MZ468490
	Pm17	*Olea europaea*	Monte Sant'Angelo (FG), Apulia, Italy	DAFNE	#5	MZ442479	MZ442524	MZ468491
	Pm15	*Olea europaea*	Monte Sant'Angelo (FG), Apulia, Italy	DAFNE	#5	MZ442480	MZ442525	MZ468492
	Pm22	*Olea europaea*	Monte Sant'Angelo (FG), Apulia, Italy	DAFNE	#5	MZ442481	MZ442526	MZ468493

(Continued)

Table 1. (Continued).

Species	Isolate code	Host	Origin	Source	Sub-group	GenBank		
						β-tubulin	Actin	IGS
	Pm180	*Vitis vinifera*	Torremaggiore (FG), Apulia, Italy	DAFNE	#5	MZ442482	MZ442527	MZ468494
	Pm196	*Vitis vinifera*	Stornarella (FG), Apulia, Italy	DAFNE	#5	MZ442483	MZ442528	MZ468495
	Pm210	*Vitis vinifera*	Cerignola (FG), Apulia, Italy	DAFNE	#5	MZ442484	MZ442529	MZ468496
	Pm235	*Olea europaea*	Cerignola (FG), Apulia, Italy	DAFNE	#5	MZ442485	MZ442530	MZ468497
	Pm250	*Prunus dulcis*	Foggia (FG), Apulia, Italy	DAFNE	#5	MZ442486	MZ442531	MZ468498
	Pm59	*Olea europaea*	Canosa di Puglia (BT), Apulia, Italy	DAFNE	#6	MZ442487	MZ442532	MZ468499
	Pm61	*Olea europaea*	Canosa di Puglia (BT), Apulia, Italy	DAFNE	#6	MZ442488	MZ442533	MZ468500
	Pm231	*Vitis vinifera*	Stornara (FG), Apulia, Italy	DAFNE	#6	MZ442489	MZ442534	MZ468501
	Pm297	*Vitis vinifera*	Canosa di Puglia (BT), Apulia, Italy	DAFNE	#6	MZ442490	MZ442535	MZ468502
P. minimum	Pm35	*Olea europaea*	Carpino (FG), Apulia, Italy	DAFNE	-	MZ442473	MZ442538	MZ468503
	Pm39	*Olea europaea*	Torremaggiore (FG), Apulia, Italy	DAFNE	-	MZ442472	MZ442537	MZ468504
	Pm41	*Olea europaea*	Vieste (FG), Apulia, Italy	DAFNE	-	MZ442471	MZ442536	MZ468505
P. oleae	Pm14	*Olea europaea*	Carpino (FG), Apulia, Italy	DAFNE	-	MW714563	MW714561	MZ468506
	Pm46	*Olea europaea*	Carpino (FG), Apulia, Italy	DAFNE	-	MZ442500	MZ442546	MZ468507
P. parasiticum	Pm88	*Olea europaea*	Stornara (FG), Apulia, Italy	DAFNE	-	KM201220	KM201190	MZ468508
	Pm388	*Vitis vinifera*	Torremaggiore (FG), Apulia, Italy	DAFNE	-	MZ442498	MZ442547	MZ468509
P. rubrigenum	CBS 498.94 [T]	*Homo sapiens*	USA	CBS	-	MZ442502	AY579238	MZ468510
	CBS 112046	*Homo sapiens*	USA	CBS	-	MZ442503	AY579239	MZ468511
P. scolyti	CBS 113597[T]	*Vitis vinifera*	Wellington, Western Cape Province, S. Africa	CBS	-	AF246800	AY579224	MZ468462
	Pm5	*Olea europaea*	Foggia (FG), Apulia, Italy	DAFNE	-	MZ442491	MZ442539	MZ468459
	Pm24A	*Vitis vinifera*	Foggia (FG), Apulia, Italy	DAFNE	-	MZ442492	MZ442541	MZ468460
	Pm 155	*Olea europaea*	Foggia (FG), Apulia, Italy	DAFNE	-	MZ442493	MZ442540	MZ468461
P. sicilianum	Pm65	*Olea europaea*	Cerignola (FG), Apulia, Italy	DAFNE	-	KM201209	KM201202	MZ468512
	Pm362	*Vitis vinifera*	Cerignola (FG), Apulia, Italy	DAFNE	-	MZ442496	MZ442549	MZ468513
P. viticola	Pm34	*Olea europaea*	Torremaggiore (FG), Apulia, Italy	DAFNE	-	MZ318696	MZ318697	MZ468514
	Pm43	*Vitis vinifera*	Cerignola (FG), Apulia, Italy	DAFNE	-	MZ442497	MZ442545	MZ468515
Pleurostoma richardsiae	Pl4	*Olea europaea*	Canosa di Puglia (BT), Apulia, Italy	DAFNE	-	MZ442504	MZ468457	MZ468520
	Pl29	*Olea europaea*	Torremaggiore (FG), Apulia, Italy	DAFNE	-	MZ442505	MZ468458	MZ468521

[T], ex-type culture; CBS, Centraalbureau voor Schimmelcultures, Utrecht, The Netherlands; DAFNE, Department of Agriculture, Food, Natural Resources and Engineering, University of Foggia, Italy; ICVV, Instituto de Ciencias de la Vid y del Vino, Logroño, Spain. Bold text, strains analysed as representative of the sub-groups defined.

Table 2. Internal sequencing primers designed to obtain the complete sequences of the intergenic spacer rDNAs.

Primer name	Sequence (5'->3')	Direction
Amygd_INT_F	5'-GCAACCTGCTCTCGACT-3'	Forward
Amygd_INT_R	5'-GACCCTAAGGTGCCACCTAT-3'	Reverse
Croa_INT_ F	5'-GTAGCTGCTCTCGACTTT-3'	Forward
Fraxy_INT_F	5'-GCAACCTGCTCTCGACTT-3'	Forward
Gris_INT_R	5'-GCCTTCCTTAGGTAGGCT-3'	Forward
Hispan_INT_F	5'-GCTCTCGACCTTCTTCCA-3'	Forward
Hispan_INT_R	5'-GCTAGACCTACGCACTGA-3'	Reverse
Iran_INT _F	5'-GCAACCTGCTCTCGACTT-3'	Forward
Iran_INT_R	5'-GCACCTTAGGGTCTAACG-3'	Reverse
Ital_INT_R[a]	5'-ATATAATGTCGCAGGGTC-3'	Reverse
Minim_ INT_R1	5'-GCCTCTTAGGTATCATAC-3'	Reverse
Minim_INT_R2	5'-GGCTATATCCTTATCCTACC-3'	Reverse
Oleae_INT_R	5'-GCCTCTTAGGTATCCTACCT-3'	Reverse
Paras_INT_F	5'-TAGTCGGATCTATAGTTAG-3'	Forward
Scol_INT_F	5'-TGATATCCTTCGCGCTGG-3"	Forward
Vitic_INT_R	5'-GGTCTAGCAATCTGCCAGC-3"	Forward
Pleuro_INT_F	5'-TTTCACTTACCCTACACC-3'	Forward
Pleuro_INT_F	5'-CTGTGATACGATGCCGGA-3'	Forward

[a] The same internal primer was used also for *Phaeoacremonium alvesii* and *P. rubrigenum*.

(Application Suite; Leica Microsystem GmbH). The phialide types and shapes were determined according to Mostert *et al.* (2006). Photomicrographs were recorded with a digital camera (DFC320; Leica) on a DMR microscope (Leica) fitted with Nomarski differential interference contrast optics. The 5th and 95th percentiles were calculated for all of the measurements.

Phylogenetic analyses

The sequences of the β-tubulin and actin genes were aligned using MAFFT v.7 (http://mafft.cbrc.jp/alignment/server/) (Katoh and Standley, 2013), with the default parameters. The alignment was checked visually and improved manually where necessary. Model Finder Plus (Kalyaanamoorthy *et al.,* 2017) implemented in the IQTREE software (Nguyen *et al.,* 2015) was used to select the best-fit DNA substitution models using Bayesian information criteria. The sequences were concatenated in one dataset to perform multilocus analyses. A partitioned model with two segments was created, each with a different model of evolution estimated previously by Model Finder Plus (Kalyaanamoorthy *et al.,* 2017). Phylogenetic analyses were carried out based on maximum likelihood and maximum parsimony. Before performing the phylogenetic analyses, the presence of different phylogenetic hypotheses in a partitioned dataset was assessed by a partition homogeneity test (i.e., an incongruence length difference test) using PAUP version 4.0b10 (Swofford, 2003). In this test, 100 datasets were artificially created by random sampling among all of the observed sites of genotypes, and then swapping sites among the loci, to obtain a *P* value. If the *P* value was >0.01, there was no incongruence among the loci, and so combination of the data improves or does not reduce the phylogenetic accuracy (Cunningham, 1997). Maximum likelihood analysis was performed using the IQTREE software (Nguyen *et al.,* 2015), with 1000 ultrafast bootstrap replicates. The ultrafast bootstrap approximation (Minh *et al*., 2013) assesses branch supports from 10 to 40 times faster than the RAxML rapid bootstrap, and obtains less biased support values (Minh *et al.,* 2013; Hoang *et al*., 2018). Unlike the non-parametric bootstrap, which considers bootstrap values ≥50% as statistically significant, the ultrafast bootstrap considers ≥80% as statistically significant. The maximum parsimony analysis was performed using PAUP version 4.0b10 (Swofford, 2003), with the heuristic search option, 10,000 random taxa additions, and tree bisection and reconstruction as the branch swapping algorithm. Branches of zero length were collapsed and all of the multiple, equally parsimonious trees were saved. The gaps were treated as missing data. Bootstrap support values were calculated from 1000 heuristic search replicates and 1000 random taxon additions. The tree lengths (*TL*), consistency index (*CI*), retention index (*RI*), homoplasy index (*HI*) and rescaled consistency index (*RC*) were calculated, and the resulting trees were visualised with TreeView version 1.6.6 (Page, 1996). The final tree was selected among the suboptimal trees from each run by comparison of the likelihood and bootstrap scores.

The aligned dataset of the IGS sequences was subjected to maximum likelihood and maximum parsimony analyses, as described above. Before performing the maximum likelihood analysis, the IGS dataset was first analysed with Model Finder Plus (Kalyaanamoorthy *et al.,* 2017), as described above. Two strains of *P. richardsiae* (Pl3, Pl29) were used as outgroups in all of the phylogenetic analyses.

RESULTS

PCR amplification and sequencing

The β-tubulin and actin genes were amplified for all of the 61 isolates and produced the expected fragments of 700 bp and 300 bp, respectively. The BLAST search and the comparison of the β-tubulin and actin sequenc-

es with the reference strains as ex-type allowed the 49 Italian strains to be attributed to 11 *Phaeoacremonium* spp., as follows: *P. amygdalinum*, *P. croatiense*, *P. fraxinopennsylvanicum* (one strain each), *P. iranianum* (two strains), *P. italicum* (30), *P. minimum* (three), *P. oleae* (two), *P. parasiticum* (two), *P. scolyti* (three), *P. sicilianum* (two) and *P. viticola* (two strains) (Table 1). The β-tubulin and actin sequences of the remaining *Phaeoacremonium* strains (seven from CBS, one from Spain) were compared with their sequences already deposited in BLAST to confirm the taxonomic identities. Therefore, the newly generated β-tubulin and actin sequences of the above-mentioned strains were not re-submitted to GenBank, except for the β-tubulin sequences of *P. rubrigenum* strains, as those present in GenBank were incomplete (Table 1).

The consensus IGS sequences obtained from 57 different strains of *Phaeoacremonium* spp. and for two *P. richardsiae* strains showed different nucleotide lengths, which ranged from 2088 bp to 2427 bp. The IGS sequence lengths among the *P. italicum* strains were also variable, and ranged from 2264 bp to 2300 bp. Analysis of the complete IGS sequences showed that the 5S rDNA gene was not found, and thus the IGS consists of a single uninterrupted region between the end of the large subunit (LSU) region and the beginning of the next small subunit (SSU) region.

Structural analysis of the intergenic spacer region of Phaeoacremonium italicum

The alignment obtained from all of the 59 strains (i.e., including the outgroup taxa) consisted of 3451 characters, including gaps. Based on the differences observed among the aligned *P. italicum* sequences, seven different sub-groups were identified, and are indicated as sub-groups #1, #2, #3, #4, #5, #6 and #7, where, respectively, the representative strains used to analyse the structures of the IGS regions were defined as CBS 137763 (ex-type), Pm31M, Pm50M, Pm45, Pm17, Pm59 and CBS 113590 (Table 1). Three structural regions were defined: one central polymorphic region (PR, positions 231-2807) that is flanked by two conserved regions (CR1, positions 1-230; CR2, positions 2808-3451) (Figure 1a). CR1 is adjacent to the 28S rDNA region, and it is a conserved sequence that ranges from 99% to 100% for pairwise identities. CR2 is adjacent to the 18S rRNA region, and is also highly conserved (99.6%-100% for pairwise identities). The polymorphisms in these two conserved regions consisted of single base substitutions (i.e., transitions and/or transversions) and small (1 or 2 bp) insertions and deletions (indels).

In contrast, PR is less conserved, with pairwise identities of 84.1%, which has resulted from variable indels and point mutations. Detailed analysis of the IGS structures of the representative *P. italicum* strains of the seven sub-groups revealed the presence of five short repeat elements that are organised in five different patterns, which are here indicated as elements A, B, C, P and R (Figure 2a, b). Element A consists of a pair of perfect repeats of 12 bp; element B consists of an imperfect direct repeat of 15 bp; element C consists of a perfect consecutive repeat of 12 bp; element P consists of a single palindromic sequence of 14 bp located before the first copy of element C; and element R is the most commonly encountered and consists of an imperfect direct repeat of 15 bp (Figure 1b and c). Based on the distributions of the short repeat elements, the central PR can be subdivided into two sub-regions, as PR-a (positions 231-1643) and PR-b (positions 1644-2807) (Figure 1b and c). Sub-region PR-a shares a common structural organisation of three short repeat elements (A, B, R) in all of the isolates.

Each of the *P. italicum* strains that belong to the first six of the sub-groups (i.e., #1 to #6) show the same structural organisation of PR-a, and contain: one perfect repeat copy of element A; nine copies of imperfect repeats of element R (R1–R9); one truncated imperfect repeat indicated here as Rt1; and one imperfect repeat of element B, indicated here as B1 (Figure 1b). Instead, PR-b starts with the element P and shows characteristic differences across the IGS. The main feature of this sub-region consists of a variable number of copies of perfect consecutive repeats of element C (2–10), and of elements R (8–9). For elements R, three (R4, R5, R8) were also contained in the PR-a region, and the other three (indicated as R10, R11 and R12) were newly encountered. In addition, two truncated imperfect repeats (Rt2 and R8t) were identified. The *P. italicum* strains of sub-groups #1, #2 and #3 show eight R elements located in the same positions, while those of sub-groups #4 and #5 show nine R elements (Figure 1b). The *P. italicum* strain of sub-group #6 shows seven R elements and lacks elements R5 and R12 (Figure 1b). Two imperfect repeats of element B, indicated here as B2 and B3, were found for PR-b, and one perfect repeat copy of element A, was found for CR2 (Figure 1b). The strain CBS 113590, representative of sub-group #7, renamed as *P. italicum sensu lato* by Spies *et al.* (2018), showed some differences inside the IGS structure. In particular, for this strain, PR-a includes the same elements of PR-a of *P. italicum* (sub-groups #1 to #6), except for the absence of element R8 (position 1088), and for its modified (*) element R, here indicated as R12* (position 1130). The PR-b has a single copy of element C, and nine elements R in the same positions as sub-groups #4 and #5 (Figure 1b).

In addition, structure analysis was carried out for the closest species to *P. italicum*, as *P. alvesii* and *P. rubrigenum*. The same repeated elements seen for the *P. italicum* sub-groups were also present in *P. alvesii* and *P. rubrigenum*, although the positioning and composition of some of these elements were different (Figure 2b, c). In particular, *P. alvesii* strain CBS 408.78 shows the same IGS structure as *P. italicum sensu lato* (CBS 113590; sub-group #7) (Figure 1c).

For the *P. alvesii* strain CBS 729.97, its PR-a has one perfect repeat copy of element A, one copy of element B1, and nine copies (R1, R2, Rt1, R3, R4, R5, R6, R7, R9) of element R. For its PR-b, there is one copy of modified element P (P*), one copy of element C, and nine copies (R10, R5*, R8, R5, R4, Rt2, R11, R12, R8) of element R, of which R5* is modified. The CR2 is the same as for *P. italicum*, except for the modified element B3 (B3*) (Figures 1c and 2b).

For the *P. rubrigenum* strain CBS 498.94 (ex-type), PR-a shows one perfect repeat copy of element A, one copy of modified element B1 (B1*), and seven copies (R1, R2*, Rt1*, R3*, R8, R12, R9) of imperfect repeats of ele-

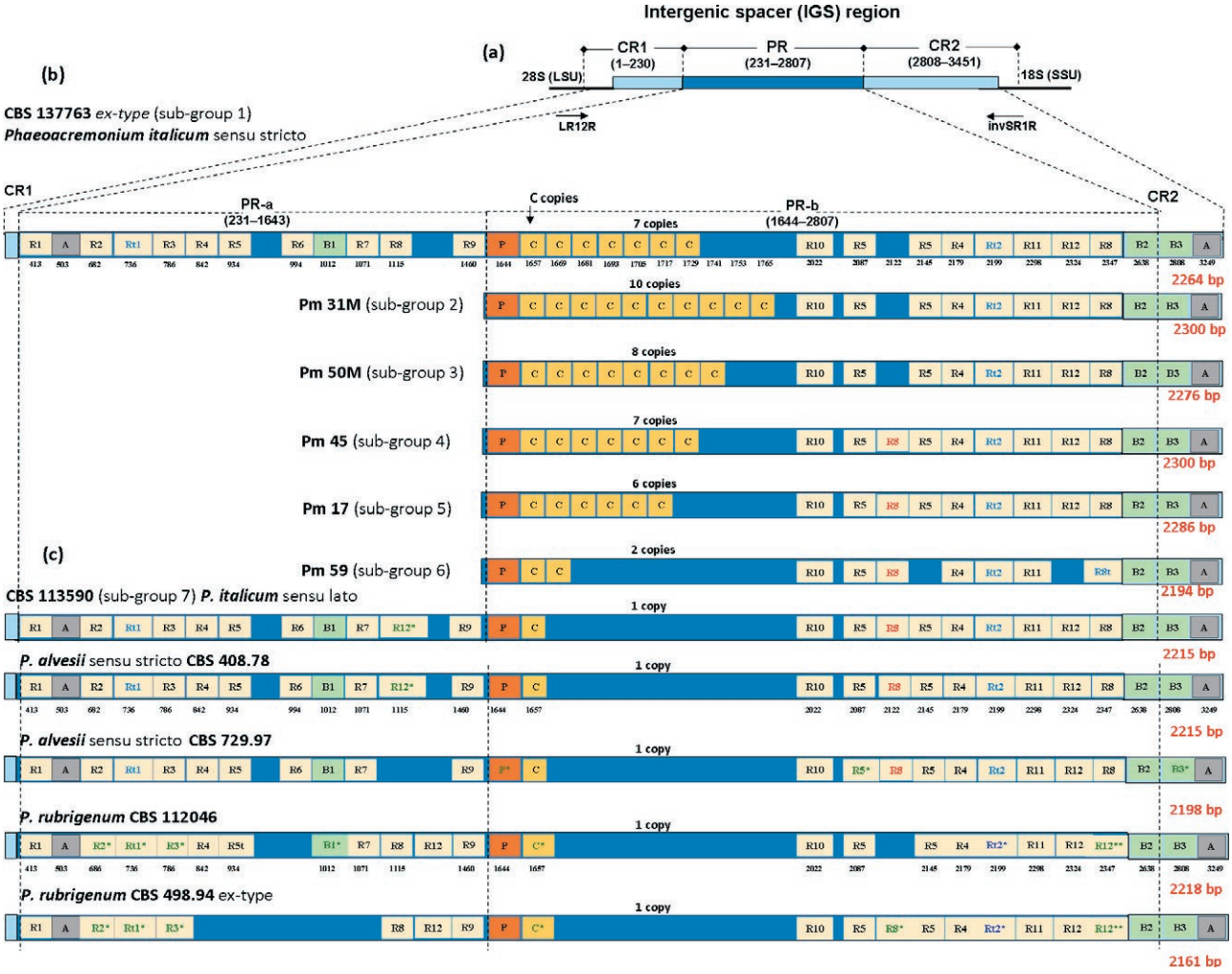

Figure 1. Structures of the IGS rDNA regions in *Phaeoacremonium italicum*, *P. alvesii* and *P. rubrigenum*. **(a)** Organisation of the IGS rDNA sequences into sub-regions CR1 (conserved region), PR (polymorphic region) and CR2 (conserved region), with corresponding nucleotide positions in parentheses. Arrows indicate annealing positions of PCR universal primers LR12R and invSR1R, within the extremities of the 28S and 18S rRNA genes. **(b)** Structural organisation of repeat elements A, B, C, P and R in the IGS region of *P. italicum* sub-groups #1 to #6. Numbers below indicate nucleotide bp of start positions of each element. **(c)** Structural organisation of repeat elements in the IGS region of *P. italicum* sub-group #7, *P. alvesii* and *P. rubrigenum* strains. Numbers below indicate nucleotide bp of start positions of each element. **(b** and **c)** Areas CR1 and CR2 are not shown because they have the same structural organisation in all of the isolates. Sub-region PR-b shares a structural organisation of five short repeat elements (A, B, C, P, R) in all of the isolates that are differently located on the basis of each sub-group defined.

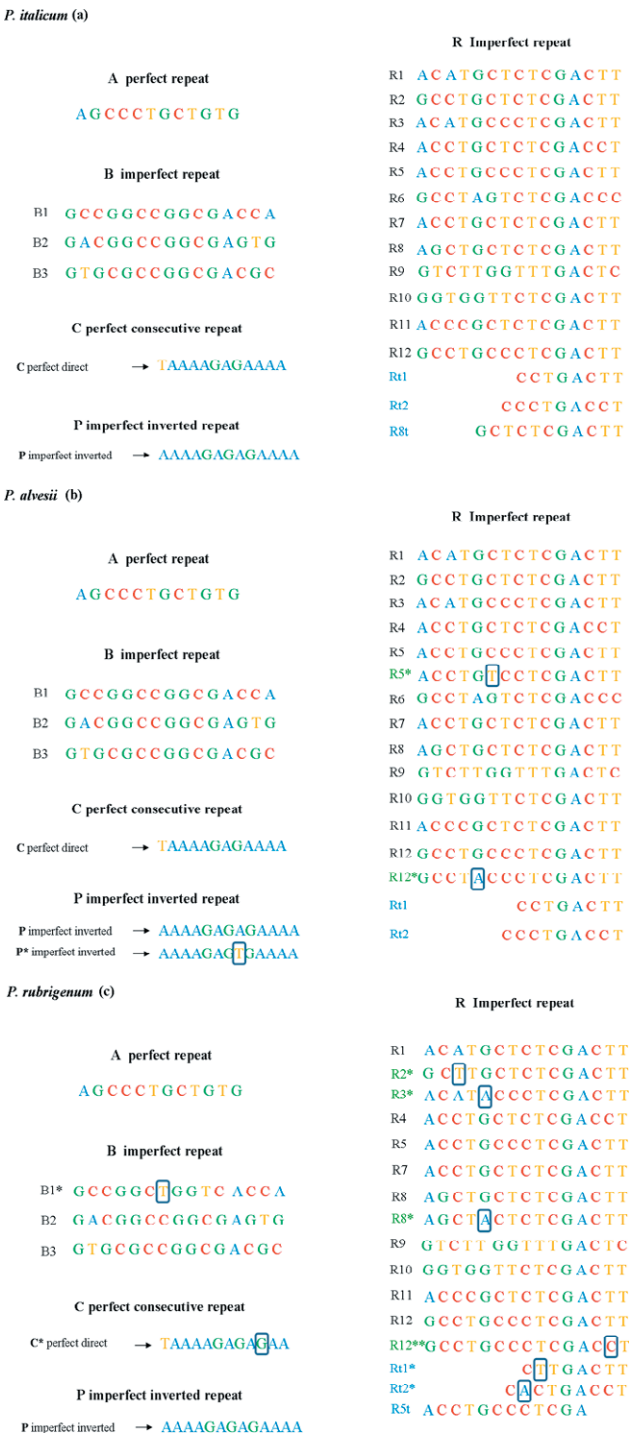

Figure 2. DNA short repeat elements A, B, C, P and R and their variants observed in the *Phaeoacremonium italicum*, *P. alvesii* and *P. rubrigenum* strains. Boxes indicate all polymorphic bases in elements B and R modified (R*).

ment R, of which three (R2*, Rt1*, R3*) were modified. Its PR-b shows one copy of element P, one copy of modified element C (C*), and nine copies (R10, R5, R8*, R5, R4, Rt2*, R11, R12, R12**) of imperfect repeats of element R, of which three (R8*, Rt2*, R12**) were modified (Figures 1c and 2c). For the *P. rubrigenum* strain CBS 112046, PR-a has one perfect repeat copy of element A and ten copies (R1, R2*, Rt1*, R3*, R4, R5t, R7, R8, R12, R9) of imperfect repeats of element R, of which three (R2*, Rt1*, R3*) were modified. PR-b has one copy of modified element C (C*) and eight copies (R10, R5, R5, R4, Rt2*, R11, R12, R12**) of imperfect repeats of element R, of which two (Rt2*, R12**) were modified. For *P. rubrigenum* strain CBS 112046, CR2 is the same as for *P. italicum* (Figures 1c and 2c).

Morphology

The morphological features of the representative isolates of each sub-group of *P. italicum* in culture are outlined in Table 3. The strains that belonged to sub-groups #1 to #6 (respectively, CBS 137763, Pm31, Pm50M, Pm45, Pm17, Pm59) have similar morphologies and culture features. The mycelia consisted of branched and septate hyphae that occurred singly or in bundles, and rarely had tuberculate hyphae, with sub-hyaline to pale brown, verruculose to smooth warts. Unbranched conidiophores were frequently observed, occasionally narrower at the bases, erect, with up to nine septate (generally three or four septate) and each ending in a single terminal phialide, which often had one or two lateral phialides of type II next to the terminal phialide. Percurrent rejuvenation was frequently observed (Figure 3).

Branched conidiophores with different levels of branching were also observed. Phialides were integrated into the terminal or lateral conidiophores, and were monophialidic, and rarely polyphialidic. Phialides arising directly from the mycelia were mainly monophialidic, often polyphialidic; type I phialides were cylindrical, frequently widened at the bases; type II phialides were predominant, one-septate, elongate-ampulliform and attenuated at the bases to navicular, tapering towards the apices; type III phialides were one-septate, mainly cylindrical, often subulate or navicular. Hyphal coils were observed. Conidia were hyaline and mostly oblong-ellipsoidal to reniform or allantoid, biguttulate, and occasionally ovoid (Figure 3). No perithecium formation was observed under laboratory conditions. The colonies reached a radius of 25-33 mm after 16 d at 23±2 °C. Minimum temperature for growth was 15°C, with optimum of 25 to 30 °C, and maximum of 35°C. The strains belonging to sub-groups #4, #5 and #6 reached a colony radius of 5 mm at 37°C.

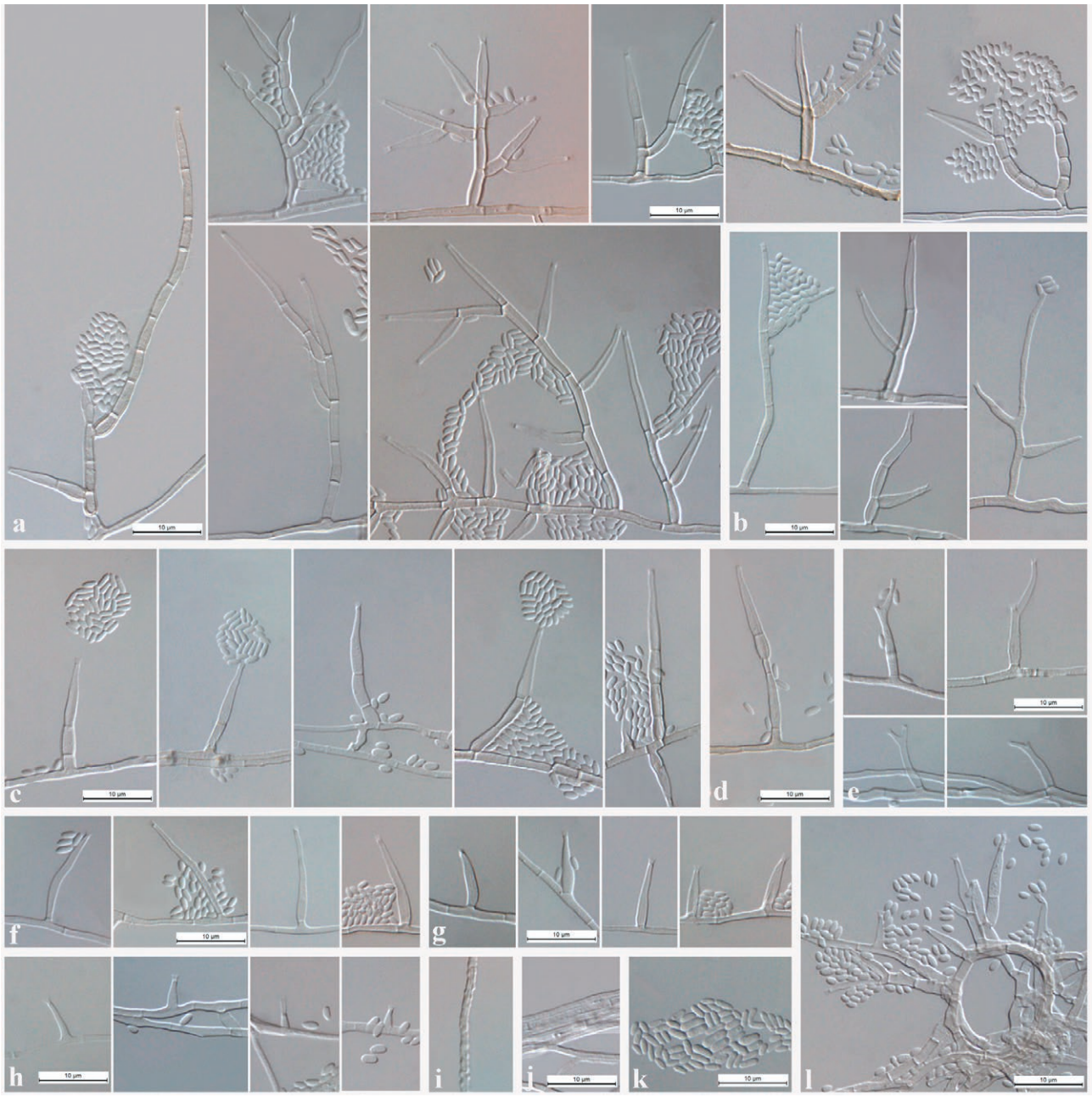

Figure 3. Representative light micrographs (Nomarski differential interference contrast) of *Phaeoacremonium italicum*. (**a**) Branched conidiophores; (**b**) unbranched conidiophores with lateral phialides; (**c**) unbranched septate conidiophores; (**d**) conidiophores showing percurrent rejuvenation; (**e**) polyphialides; (**f**) Type III phialides; (**g**) Type II phialides; (**h**) Type I phialides; (**i**) mycelia, showing prominent exudate droplets observed as warts; (**j**) mycelia occurring in bundles; (**k**) conidia; (**l**) hyphal coils.

The morphology and colour of the colonies were variable among the isolates that belonged to the six sub-groups (Table 3; Figure 4). Yellow pigment was observed on OA for strains that belonged to sub-groups #4 and #5 (Figure 4).

Strain CBS 113590, in sub-group #7 had mycelium with branched septate hyphae occurring singly or in bundles; hyphae were tuberculate with sub-hyaline to pale brown, verruculose to smooth warts. Unbranched conidiophores predominated, and were generally one- or two-septate (up to four-) septate and each ending in a single terminal phialide, often bearing one lateral phialide (mainly of type II) next to the terminal phialide; percurrent rejuvenation was rarely observed (Figure 5).

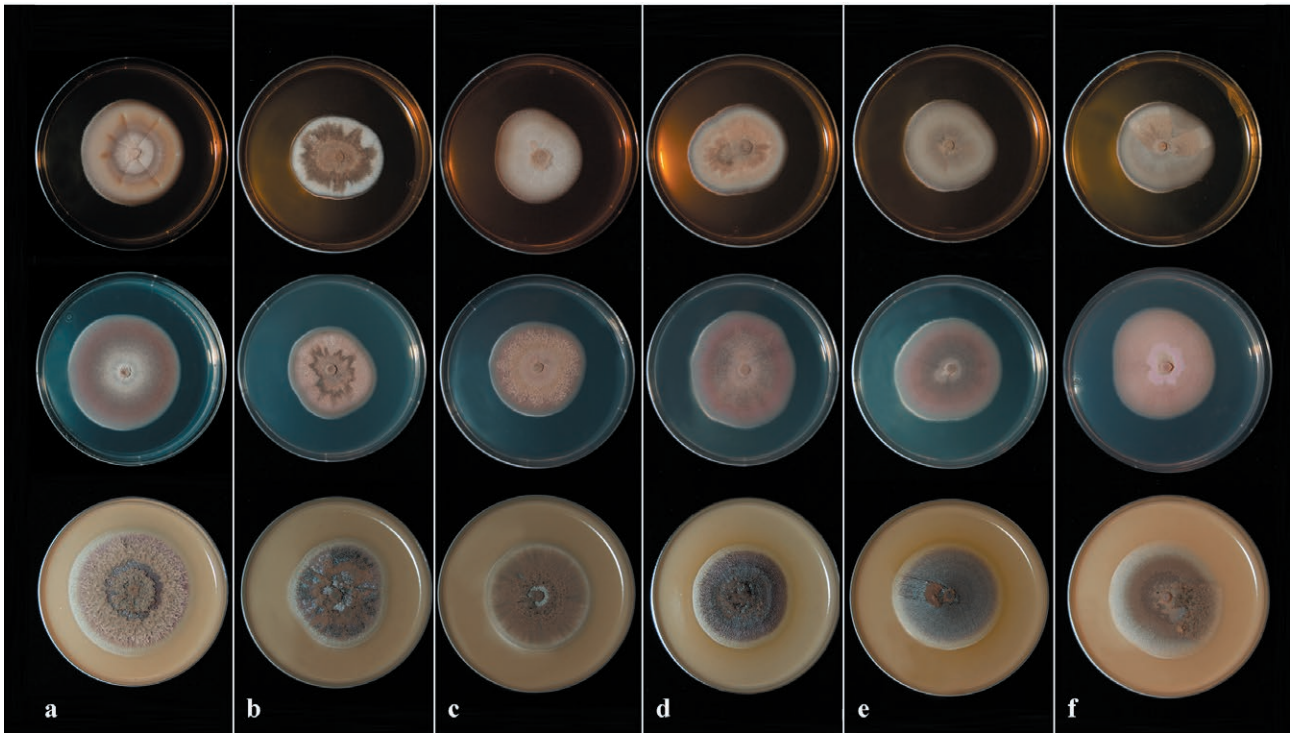

Figure 4. Representative culture morphologies for *Phaeoacremonium italicum*. The cultures were grown at 25°C on malt extract agar (top row), potato dextrose agar (middle) and oatmeal agar (bottom row) for 21 d. (**a**) CBS 137763 strain, representing sub-group #1; (**b**) Pm31 strain, sub-group #2; (**c**) Pm50M strain, sub-group #3; (**d**) Pm45 strain, sub-group #4; (**e**) Pm17 strain, sub-group #5; (**f**) Pm59 strain, sub-group #6.

Branched conidiophores were less frequently observed, with few levels of ramification. Phialides were integrated into the conidiophores terminally and laterally, and arose directly from the mycelia. These phialides were mainly monophialidic but occasionally polyphialidic. Type I phialides were cylindrical, occasionally widened at the base. Type II phialides were one-septate, subcylindrical to navicular, tapering towards the apex. Type III phialides predominated, and were one-septate, mainly navicular to subcylindrical, and occasionally subulate. Hyphal coils were observed. Conidia were hyaline and mostly oblong ellipsoidal to obovoid, frequently biguttulate, and occasionally reniform to allantoid (Figure 5). No perithecium formation was observed under laboratory conditions. The colonies reached a radius of 38–43 mm after 16 d at 23±2°C. The minimum temperature for growth was 15°C, with optimum growth at 30°C, and the maximum temperature for growth was of 37°C. Yellow pigment was produced in OA cultures (Figure 5).

Phylogenetic analyses

Model Finder Plus was used to detect the best-fit DNA substitution models for the β-tubulin and actin genes and for the IGS datasets. The optimum models were: for the β-tubulin gene, the Kimura 2-parameter with invariable site and discrete gamma distribution (K2P+I+G4) (lnL = -3979.7536), and for the actin gene, the Kimura 2-parameter with invariable sites (K2P+I) (lnL = -1726.3321). The calculated parameters for the β-tubulin gene were: assumed nucleotide frequencies, A = 0.250, G = 0.250, T = 0.250 and C = 0.250; substitution rate matrix with A→C substitution = 1.000, A→G = 3.908, A→T = 1.000, C→G = 1.000, C→T = 3.908, and G→T = 1.000; proportion of invariable sites (I) = 0.342, and gamma distribution (G4) with shape parameter = 1.994. The calculated parameters for the actin gene were: assumed nucleotide frequencies, A = 0.250, G = 0.250, T = 0.250 and C = 0.250; substitution rate matrix with A→C substitution = 1.000, A→G = 4.257, A→T = 1.000, C→G = 1.000, C→T = 4.257 and G→T = 1.000; proportion of invariable sites (I) = 0.442.

The optimum model selected for the IGS fragment was the Transversion model with empirical base frequencies and gamma distribution (TVM+F+G4) (lnL = -22064.046). The calculated parameters were: assumed nucleotide frequencies, A = 0.186, G = 0.288, T = 0.234, and C = 0.292; substitution rate matrix with A→C substi-

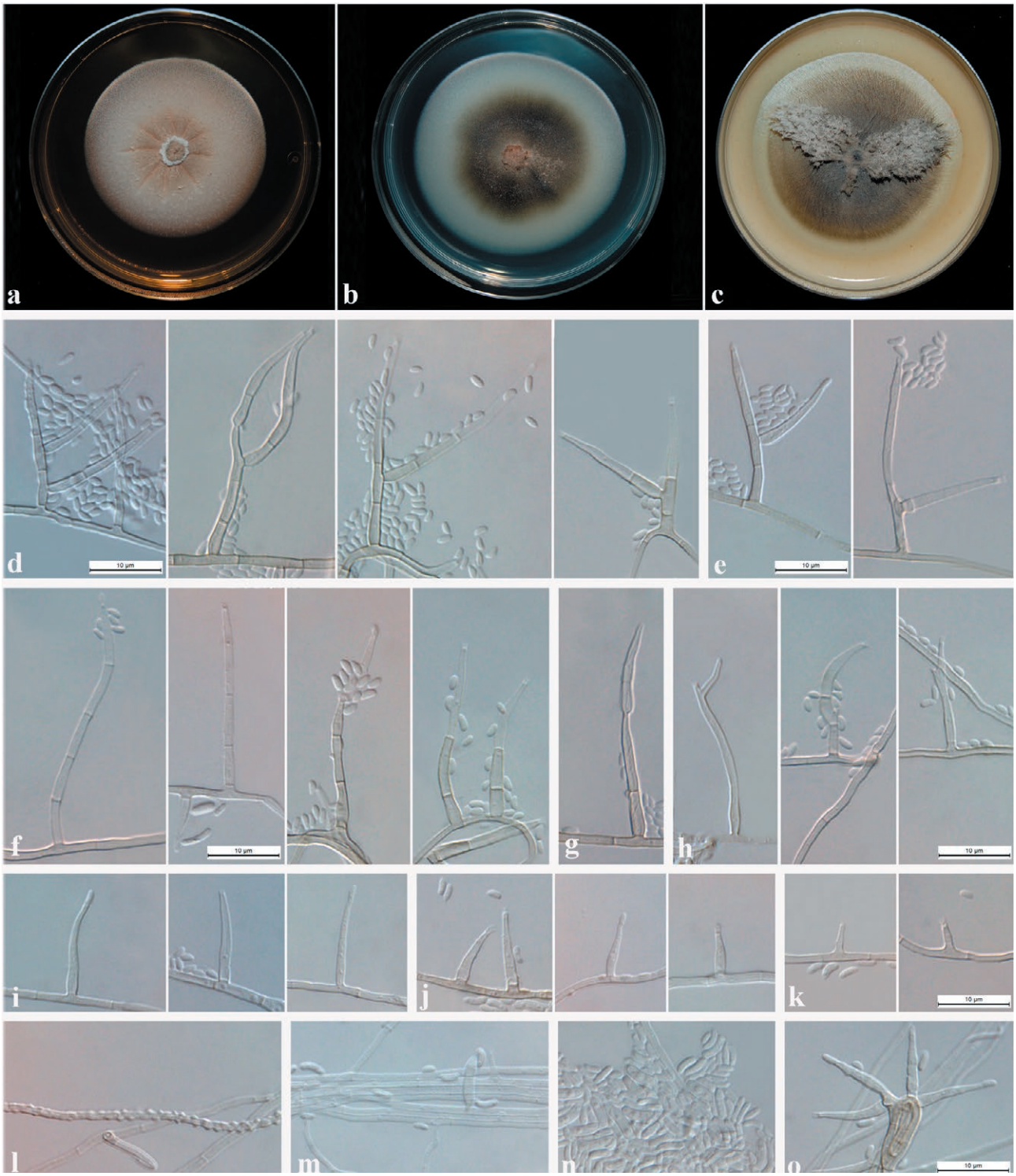

Figure 5. Representative light micrographs (Nomarski differential interference contrast) of *Phaeoacremonium alvesii* CBS 113590 as the representative strain of sub-group #7. Twenty-one-day-old colonies grown on malt extract agar (**a**), potato dextrose agar (**b**) and oatmeal agar (**c**) at 23±2°C; (**d**) branched conidiophores; (**e**) unbranched conidiophores with lateral phialides; (**f**) unbranched septate conidiophores; (**g**) conidiophores with percurrent rejuvenation; (**h**) polyphialides; (**i**) Type III phialides; (**j**) Type II phialides; (**k**) Type I phialides; (**l**) hyphae with prominent exudate droplets observed as warts; (**m**) hyphae occurring in bundles; (**n**) conidia; (**o**) hyphal coils.

Table 3. Morphological features of *Phaeoacremonium italicum* sub-groups in culture.

Feature	Sub-group						
	#1	#2	#3	#4	#5	#6	#7
Representative isolate	CBS 137763	Pm31	Pm50M	Pm45	Pm17	Pm59	CBS 113590
Bundles	Yes	Yes	Yes	Yes	Yes	Yes	Yes
Warts	Yes	Yes	Not observed	Not observed	Yes	Not observed	Yes
Conidiophores: unbranched (μm)							
Length	(12.3–)19.7–24.8(–47.8)	(11.8–)16.1–21.3(–38.4)	(10.0–)14.9–18.8(–35.4)	(11.1–)14.5–17.8(–28.9)	(8.6–)14.5–21.16(–43.8)	(9.14–)15.05–18.7(–26.6)	(15.1–)21.3–23.9(–43.2)
Width	(1.0–)1.5–1.8(–2.4)	(0.38–)1.24–1.43(–1.8)	(1.0–)1.2–1.3(–1.6)	(0.8–)1.2–1.4(–1.7)	(1.0–)1.3–1.5(–1.8)	(0.8–)1.2–1.3(–1.5)	(1.2–)1.6–1.7(–2.2)
Mean	22.3×1.7	18.7 × 1.3	16.93×1.29	16.2×1.3	17.8×1.4	16.9×1.2	22.6×1.7
Number of septa	Up to 7 septate; commonly 2-3	Up to 7 septate; commonly 3-4	Up to 6 septate; commonly 3-4	Up to 5 septate; commonly 3-4	Up to 9 septate; commonly 4-5	Up to 5 septate; commonly 3-4	Up to 3 septate; commonly 2
Conidiophores: branched (μm)						Less frequent	
Length	(21.3–)32.3–40.2(–58.2)	(16.1–)25.9–32.1(–47.3)	(14.6–)25.2–32.3(–48.2)	(17.5–)24.1–30.7(–47.8)	(11.7–)20.5–27.5(–47.8)	(18.7–)32.2–40.7(–65.2)	(18.0–)25.0–31.7(–40.3)
Width	(1.2–)1.4–1.5(–1.8)	(1.0–)1.3–1.49(–1.9)	(0.9–)1.2–1.4(–1.6)	(0.84–)1.2–1.4(–1.7)	(0.9–)1.2–1.3(–1.7)	(0.8–)1.2–1.4(–2.1)	(0.9–)1.5–1.8(–2.2)
Mean	36.3×1.5	29.0×1.4	28.7×1.3	25.2×1.3	24.0×1.2	36.4×1.3	28.3×1.7
Phialide type I (μm)							
Length	(2.1–)5.3–7.3(–11.3)	(1.7–)3.8–4.9(–7.9)	(2.1–)4.1–5.1(–7.2)	(1.1–)2.7–3.7(–5.8)	(1.7–)3.3–4.3(–6.5)	(1.5–)3.7–4.6(–7.6)	(2.9–)4.2–6.7(–11.0)
Width	(0.6–)1.2–1.4(–1.8)	(0.5–)0.9–1.1(–1.5)	(0.7–)0.9–1.0(–1.3)	(0.3–)0.8–1.1(–1.7)	(0.7–)0.9–1.1(–1.5)	(0.5–)0.9–1.0(–1.5)	(0.7–)1.0–1.2(–1.7)
Mean	6.3×1.3	4.8×1.0	4.6×0.9	3.2×0.9	3.8×1.0	4.2×1.0	6.5×1.1
Shape	Cylindrical	Cylindrical, sometimes widened at the base	Cylindrical sometimes widened at the base	Cylindrical and slightly widened at the base	Cylindrical	Cylindrical and sometimes widened at the base	Cylindrical, sometimes widened at the base
Phialide type II (μm)							
Length	(5.2–)8.8–10.2(–14.9)	(6.0–)7.9–9.0(–11.1)	(5.9–)7.9–9.1(–13.7)	(5.1–)6.4–7.6(–11.4)	(5.0–)6.4–7.3(–9.4)	(5.3–)7.4–8.5(–10.5)	(9.1–)12.5–13.2(–14.1)
Width	(0.9–)1.2–1.4(–1.85)	(0.3–)1.3–1.4(–1.8)	(0.8–)1.2–1.3(–1.6)	(0.2–)1.3–1.6(–2.1)	(0.7–)1.2–1.4(–1.8)	(1.0–)1.3–1.4(–1.7)	(1.1–)1.5–1.6(–2.1)
Mean	9.5×1.4	8.5×1.4	8.5×1.2	7.0×1.4	6.9×1.3	7.9×1.3	12.1×1.5
Shape	Elongate-ampulliform to navicular (predominant)	Elongate-ampulliform to navicular (predominant)	Elongate-ampulliform to navicular (predominant)	Elongate-ampulliform to navicular (predominant)	Navicular to elongate-ampulliform (predominant)	Elongate-ampulliform to navicular (predominant)	Subcylindrical to navicular
Phialide type III (μm)							
Length	(10.7–)12.7–14.2(–20.6)	(10.1–)10.8–12.1(–13.7)	(10.7–)11.6–12.5(–14.1)	(10.1–)10.8–12.4(–14.4)	(10.0–)10.9–12.8(–14.7)	(10.1–)10.9–11.9(–13.4)	(12.0–)14.2–16.1(–19.9)
Width	(0.9–)1.3–1.5(-1.8)	(0.9–)1.0–1.2(-1.5)	(0.9–)1.1–1.2(-1.4)	(0.6–)0.9–1.3(-1.6)	(0.7–)1.0–1.3(-1.6)	(1.1–)1.1–1.2(-1.4)	(0.8–)1.5–1.6(-2.4)
Mean	13.5×1.4	11.4×1.1	12.1×1.6	11.6×1.1	11.9×1.2	11.5×1.2	15.9×1.5

(Continued)

Table 3. (Continued).

Feature	Sub-group						
	#1	#2	#3	#4	#5	#6	#7
Shape	Cylindrical to subulate	Cylindrical to subulate	Subulate to cylindrical	Cylindrical to navicular, rarely subulate	Cylindrical to subulate	Cylindrical to navicular	Navicular to subcylindrical, sometimes subulate (predominant)
Polyphialides	Yes	Few	Yes	Few	Yes	Yes	Yes
Rejuvenation	Yes	Yes	Yes	Yes	Yes	Yes	Yes
Coils	Few	Few	Yes	Yes	Yes	Yes	Few
Conidia (mm)							
Length	(2.1–)2.5–2.7(–3.2)	(1.5–)2.1–2.6(–4.32)	(2.1–)2.5–2.8(–3.5)	(1.3–)2.5–2.9(–4.4)	(1.5–)1.9–2.1(–2.9)	(1.4–)2.4–2.8(–4.4)	(2.4–)3.2–3.5(–4.6)
Width	(0.6–)1.0–1.1(–1.4)	(0.6–)0.9–1.1(–1.5)	(0.7–)0.9–0.9(–1.2)	(0.7–)0.94–1.1(–1.6)	(0.6–)0.8–0.8(–1.0)	(0.7–)0.9–0.9(–1.5)	(0.8–)1.1–1.2(–1.9)
Mean	2.6×1.1	2.4×1.1	2.7×0.9	2.7×1.0	1.9×0.8	2.6×0.9	3.4×1.1
Shape	Oblong-ellipsoidal to reniform or allantoid, occasionally ovoid	Oblong-ellipsoidal to allantoid, guttulate	Oblong-ellipsoidal and guttulate, occasionally reniform	Oblong-ellipsoidal to allantoid, guttulate	Oblong-ellipsoidal to allantoid, guttulate	Oblong-ellipsoidal and guttulate, occasionally reniform to allantoid	Obovoid or oblong ellipsoidal, occasionally reniform to allantoid
Yellow pigment	No	No	No	Yes	Yes	No	Yes
Colony colour							
On MEA*	Light Greyish Olive (21'''b) to Fawn (13''') to Tilleul Buff (17'''f)	Vinaceous-Buff (17'''d) to White at margin and Army Brown (13'''i) to Fawn (13''') at the centre	Cream-Buff (19"d) on the entire colony	Vinaceous Buff (17'''d) at margin to Fawn (13''') with irregular sectors Amber Brown (13k) at the centre	Vinaceous-Buff (17'''d) to Fawn (13''') in the centre	Vinaceous-Buff (17'''d) to Fawn (13''') in the centre with irregular sectors of aerial mycelium Vinaceous-Buff (17'''d) to Fawn(13''')	Cameo Brown (7"k) to Vinaceous-Buff (17'''d) to Fawn (13''') in the centre
On PDA*	Vinaceous-Buff (17'''d) to Purplish Vinaceous (1'''b) to Tilleul buff (17'''f)	Vinaceous-Buff (17'''d) at margin with Hazel ring (11'k) to Brownish Vinaceous (5'''b) with irregular ring Army Brown(13'''i) becoming Fawn (13''') at the centre	Vinaceous-Buff (17'''d) at margin to Brownish Vinaceous (5'''b) to Fawn (13''') to Light Grayish Vinaceous (9"d) at the centre	Vinaceous Buff (17'''d) at margin to Pale Brownish Vinaceous (5'''f) becoming Dark Livid Brown (1'''k) toward the centre and Pale Vinaceous-Fawn (13'''f) at the centre	Vinaceous-Buff (17'''d) at margin to Pale Brownish Vinaceous (5'''f) becoming Deep Brownish Vinaceous (5''') to Fawn (13''') in the centre	Vinaceous-Buff (17'''d) at margin (19'd) to Onion-skin Pink (11"b) with irregular ring Mauve (63'b) and Hazel (11'k) at the centre	Cream Buff (19"d) to Hazel (11'k) to Isabella colour (19"i) to Yellowish Olive (23"k) to Fawn (13''')

(Continued)

Table 3. (Continued).

Feature	Sub-group						
	#1	#2	#3	#4	#5	#6	#7
On OA*	Olive (21'm) to Cream-Buff (19'd) above and reverse with Avellaneous (17"b) in the centre	Vinaceous-Buff (17"d) to Vinaceous Purple (65") with aerial mycelium Brownish-Vinaceous (5"b) at the centre	Vinaceous-Buff (17"d) becoming Army Brown (13"i) to Bone Brown (13"m) towards the centre	Vinaceous Buff (17"d) at the margin with Vinaceous Purple (65") with rare aerial mycelium Brownish-Vinaceous (5"b) at the centre	Vinaceous Buff (17"d) at the margin with Vinaceous Purple (65") with rare aerial mycelium Brownish-Vinaceous (5"b) at the centre	Vinaceous-Buff (17"d) at margin to Army Brown (13"i) with irregular sectors of aerial mycelium Vinaceous-Buff (17"d) to Army Brown (13"i) at the centre	Vinaceous-Buff (17"d) at margin to Hazel (11'k) to Sepia (17"m) with irregular sectors of aerial mycelium Vinaceous-Buff (17"d)
Growth temperatures on MEA* (°C)							
Minimum	17	15	15	15	15	15	15
Optimum	25	25	30	30	30	25	30
Maximum	35	35	35	35	35	35	37
Radial growth (mm; 16 d, 23±2°C)	20-25	28-32	28-33	28-32	28-33	27-33	39-43

* MEA, malt extract agar: PDA, potato dextrose agar; OA, oatmeal agar.

tution = 1.014, A→G = 4.371, A→T = 2.087, C→G = 1.273, C→T = 4.371 and G→T = 1.000; rates for variable sites were assumed to follow a gamma distribution (G4) with shape parameter = 0.513.

The partition homogeneity test for the β-tubulin and actin sequences of *Phaeoacremonium* spp. produced a *P*-value of 0.61, which indicated that the dataset was congruent and the two genes could be combined. The combined β-tubulin and actin dataset consisted of 59 taxa, which included the outgroup taxon *P. richardsiae*, and contained 864 characters (β-tubulin, 594; actin, 270; including alignment gaps), of which 416 were constant (β-tubulin, 282; actin, 134), while 27 were variable and parsimony uninformative. Maximum likelihood analysis of the remaining 421 parsimony informative characters (β-tubulin, 296; actin, 125) produced a consensus tree with a Log-likelihood (lnL) = -5742.620763. Maximum parsimony analysis resulted in one most-parsimonious tree (*TL* = 1071; *CI* = 0.675; *RI* = 0.889; *RC* = 0.600; *HI* = 0.325) with similar topology to the maximum likelihood shown in Figure 6 (TreeBASE S28462). The phylogenetic tree obtained by combined analysis of the β-tubulin and actin genes clustered the *Phaeoacremonium* strains into 15 distinct clades, confirming the BLAST identification.

The *P. italicum* strains that belonged to sub-groups #1 to #6 clustered in a single clade that showed intraspecific genetic variation, with bootstrap values ranging from 80 to 98%. Strain CBS 113590 that belonged to sub-group #7 clustered in a sister clade of *P. italicum* (as already reported by Spies *et al.* (2018), with bootstrap support of 80% for maximum parsimony and 98% for maximum likelihood (Figure 6).

The IGS dataset alignment consisted of 59 taxa that included the outgroup taxon *P. richardsiae* and contained 3451 characters (including alignment gaps), of which 1547 were constant, while 202 were variable and parsimony uninformative. Maximum likelihood analysis of the remaining 1702 parsimony informative characters produced a consensus tree with lnL = -20723.212183. Maximum parsimony analysis resulted in 100 most-parsimonious trees (*TL* = 4170; *CI* = 0.720; *RI* = 0.884; *RC* = 0.637; *HI* = 0.280) with similar topology to maximum likelihood, one of which is shown in Figure 7 (TreeBASE S28463). In the comparison of the tree from the phylogenetic analysis of IGS sequences with the phylogenetic tree obtained in the combined analysis of the β-tubulin and actin sequences, the species segregation and tree topology were similar. Although the topology of the trees is not identical, each species was always well separated, and the clusters and segregation of the species were identical to the β-tubulin and actin phylogenetic tree, except for strain CBS 113590 that belonged to

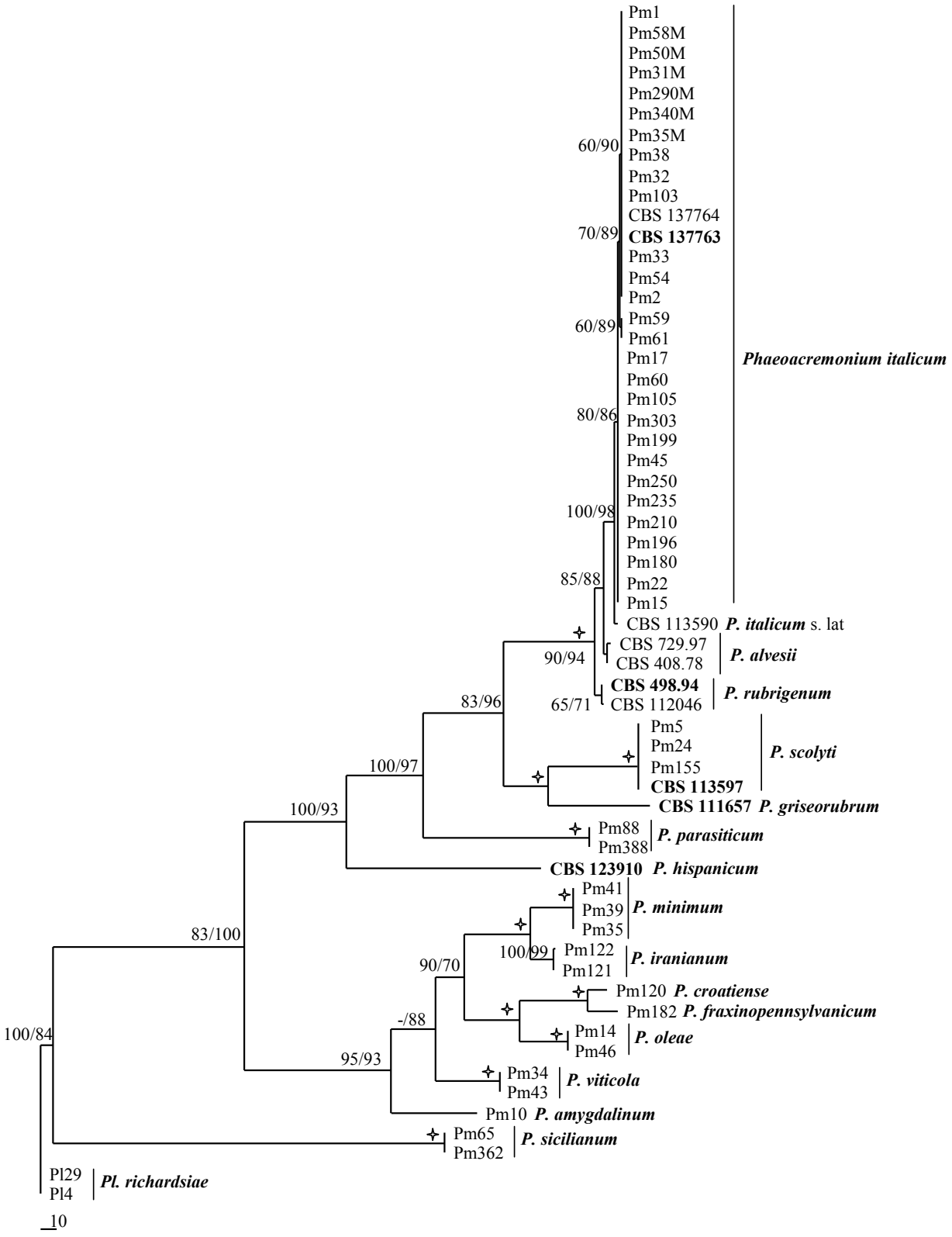

Figure 6. The most parsimonious tree obtained from multiple alignment of the β-tubulin and actin genes, with bootstrap values (1000 replicates) from maximum parsimony/maximum likelihood shown at the internodes. Bootstrap values of 100% are indicated with star symbols, and ex-type sequences are highlighted in bold. *Pleurostoma richardsiae* was included as an outgroup.

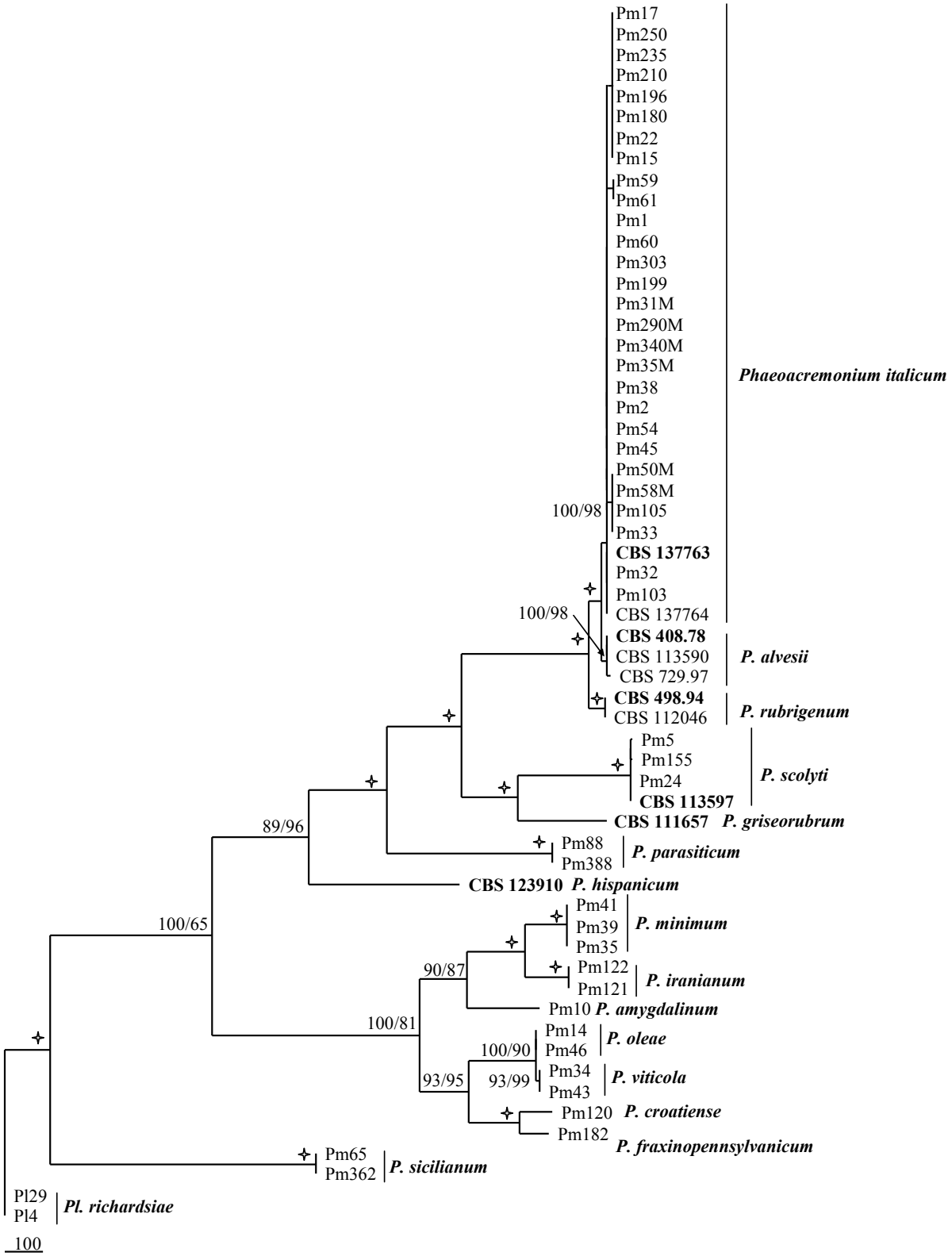

Figure 7. One of the 100 most-parsimonious trees obtained from alignment of the IGS sequences from *Phaeoacremonium* spp., with bootstrap values from 1000 replicates from maximum parsimony/maximum likelihood shown at the internodes. Bootstrap values of 100% are indicated with star symbols, and ex-type sequences are highlighted in bold. *Pleurostoma richardsiae* was included as an outgroup.

P. italicum (sub-group #7) (Figures 6 and 7). In the IGS tree, this strain clustered in the clade of *P. alvesii*, with the strains CBS 408.78 and CBS 729.97.

DISCUSSION

In the present analysis of the IGS regions of a population of *P. italicum* strains collected from different hosts and localities, the entire IGS rDNA regions were successfully amplified using standard primers anchored in the conserved 28S and 18S rDNA gene-coding regions. The same standard primers were used to amplify the closest species to *P. italicum*, as *P. alvesii* and *P. rubrigenum*, and also for 12 other *Phaeoacremonium* species.

As the analyses of the complete IGS rDNA sequences of *Phaeoacremonium* spp. revealed the absence of 5S rDNA, in agreement with Drouin and de Sà (1995), we considered that this region was not linked to the rRNA major transcription unit, but was distributed throughout the genomes, as has been reported for several other filamentous fungi (Lockington *et al.,* 1982; Selker *et al.,* 1986; Garber *et al.,* 1988; Walker *et al.,* 2011). Walker *et al.* (2011) attributed the variable gene linkages for 5S in the Eukaryotes to result from stochastic gains and losses of variant repeat units, where functional 5S rRNA had been transposed by the mechanisms that were responsible for the concerted evolution of tandemly repeated multigene families.

Variations were also seen in sequence lengths for the *P. italicum* strains. It is well known that the IGS region is highly variable, as it contains several repeat elements, indels, variable regions with nucleotide substitutions (Albee *et al.,* 1996; James *et al.,* 2001), and sequences called 'repeat motifs' that are essential for initiation of transcription, RNA processing, transcription termination and replication processes of ribosomal DNA (Van't Hof and Lamm, 1991; Fernandez *et al.,* 2000). In the present study, analysis of the distributions of the polymorphisms through the sequences highlighted the presence of five short repeat elements throughout the IGS rDNA region of the *P. italicum* strains, named here as elements A, B, C, P and R. Elements A, B and P and their locations were common to all of the *P. italicum* strains, while the other two elements, C and R showed different number of copies, compositions and distributions among the strains. The presence of these repeated elements and their distributions allowed identification of one polymorphic region (PR) that was flanked by two conserved regions (CR1; CR2). The presence of indels through the IGS sequences was restricted to only the PR. The nucleotide substitutions consisted of insertions and deletions, and transitions and transversions, with these conversely seen only in the CR1 and CR2 regions. A similar organisation was also reported by Pantou *et al.* (2003) for *Metarhizium anisopliae*, Papaioannou *et al.* (2013) for *Verticillium dahliae*, and Durkin *et al.* (2015) for *Colletotrichum lentis*. Papaioannou *et al.* (2013) reported that this organisation putatively reflected the different functions of these sub-regions, and suggested that the highly conserved sub-regions had functions related to rRNA production and processing. The polymorphic sub-region, PR, may be responsible for the promotion of unequal crossing-over events and the maintenance of homogeneity between rDNA complexes (Mirete *et al.,* 2013).

The analysis of these sequences showed that element C was a 'repeat motif', and the intraspecific variation observed among the *P. italicum* strains was mainly due to the number of copies of element C repeated in the IGS rDNA sequences, as well as to the absence of some elements R in the polymorphic region. Diaz *et al.* (2005) reported that repeat motifs in the transcribed region or upstream of the transcription start can act as promoter enhancers and regulators of transcription of rRNA. These could have originated from processes involved in duplication and amplification of short sequences, and from slippage of replication mechanisms. Many such repeat motifs have been described as highly conserved in different Eukaryote species (Diaz *et al.,* 2005). For example, the repeat motif of CAAAAA has been described as a conserved motif in the promoter region of different crucifers, such as *Brassica* spp. (Bhatia *et al.,* 1996), *Raphanus* spp. (Delcasso *et al.,* 1988) and *Arabidopsis* (Gruendler *et al.,* 1991). Other common repeat motifs, such as the TATA motif, are probably involved in assembly of the pre-initiation complex and selection of transcription sites (Melanè *et al.,* 1998). These have been reported as common elements in fungi, including *Schizophyllum commune* (James *et al.,* 2001), *Laccaria bicolor* (Martin *et al.,* 1999) and *Neurospora* spp. (Selker *et al.,* 1986). The high degree of sequence similarities seen for CR1 and CR2 among the *P. italicum* strains can be used in conjunction with the characteristic repeat motifs of the fungus, for the design of species or group-specific primers for intraspecific group detection (Diaz *et al.*, 2005; Papaioannou *et al.,* 2013).

Based on the presence of repeated elements, on the number of copies of some of these elements, and on their composition, the *P. italicum* strains were grouped into seven different sub-groups (#1 to #7). Comparisons of the results of the polymorphic region PR sequences of all of the *P. italicum* strains analysed in this study showed that these were structurally similar across all

of the sub-groups, although some differences were seen among the different *P. italicum* sub-groups. In particular, sub-groups #1 to #6 all shared the same initial layout of R elements in the first part of the polymorphic regions (PR-a), while they varied mainly in the numbers of copies of element C and for the absence of elements R5, R8 and R12 in the second part of polymorphic region (PR-b). Sub-group #7 contained strain CBS 113590, identified as *P. alvesii* by White *et al.* (2011) and Moyo *et al.* (2014), and more recently classified as *P. italicum sensu lato* by Spies *et al.* (2018); here it showed differences in the disposition and composition of the repeated elements.

Comparing the IGS structures of the sub-groups of *P. italicum* with the closest species of *P. alvesii* and *P. rubrigenum*, it was possible to confirm the same kinds of repeated elements, although they were differently organised and sometimes modified. The IGS structure of *P. alvesii* strain CBS 408.78 was identical to that of strain CBS 113590 of sub-group #7. Micromorphological analyses of the representative isolates of each of the *P. italicum* sub-groups showed similarities among sub-groups #1 to #6, and differences for sub-group #7. In comparison with the strains of sub-groups #1 to #6, CBS 113590 had longer and less septate unbranched conidiophores, rarely branched conidiophores, phialides predominantly of type III, ovoid conidia, more rapid growth rate, and maximum cardinal temperature for growth of 37°C. These features resemble those described by Moster *et al.* (2006) for *P. alvesii*. Based on the observations carried out on the strains of *P. italicum* sub-groups #1 to #6, the present study provides an upgrade of the morphological descriptions reported by Raimondo *et al.* (2014). For instance, compared to the original descriptions: the temperature minimum for growth (15°C) and growth optimum (25-30°C) were slightly different; and the morphological traits, such as branched conidiophores, were frequently, rather than occasionally, encountered. The frequent presence of polyphialides was another trait encountered. Based on the detailed examination carried out on this collection of *P. italicum* and *P. alvesii* strains in the present study, yellow pigment production was not to be a reliable feature for distinguishing these two species according to Spies *et al.* (2018). The strains that belonged to *P. italicum* sub-groups #4 and #5, as well as CBS 113590 of sub-group #7 and *P. alvesii* (CBS 408.78, CBS 729.97), produced yellow pigment on OA. Therefore, the presence of abundant branched conidiophores, the high numbers of septa of the unbranched conidiophores, the predominance of type II phialides, the smaller sizes of type II and III phialides, the colour of the cultures on different media, and the minimum and maximum cardinal temperatures for growth, differentiate *P. italicum* from *P. alvesii*. Comparisons of the phylogenetic trees obtained for the combined analysis of β-tubulin and actin sequences with the phylogenetic analysis of the IGS sequences showed identical clustering and segregation of the *Phaeoacremonium* spp., except for strain CBS 113590. The combined analysis of the β-tubulin and actin sequences segregated this strain into a sister clade of *P. italicum,* while the IGS phylogenetic tree clustered it with *P. alvesii.*

The IGS rDNA region has been successfully used to study relationships in other fungi at intraspecific levels, including for *Fusarium oxysporum* (Appel and Gordon, 1996), *Metarhizium anisopliae* (Pipe *et al.,* 1995), *Microdochium nivale* (Mahuku *et al.,* 1998), *Hebeloma cylindrosporium* (Guidot *et al.,* 1999), *Cryptococcus neoformans* (Diaz *et al.,* 2005), *Phomopsis helianthi* (Pecchia *et al.,* 2004), and *Verticillium albo-atrum* (Mahuku and Platt, 2002). The IGS region is one of the most rapidly evolving regions and provides large datasets that are considered to be phylogenetically useful, and these have provided large numbers of informative characters to delineate the relationships within and between species (Hillis and Dixon, 1991).

Based on micromorphological and molecular data, we conclude that the strain CBS 113590 belongs to *P. alvesii* and not to *P. italicum sensu lato*. Further molecular studies on phylogenetic signals and presence of barcoding gap, and multilocus analyses (β-tubulin, actin, and IGS sequences) using a large number of *Phaeoacremonium* strains will be carried out to determine whether the IGS rDNA region is a suitable marker for phylogenetic resolution of *Phaeoacremonium* species, to be used alone or in combination with β-tubulin and actin markers, to avoid misidentifications and introduction of vague species boundaries.

ACKNOWLEDGEMENTS

Dr David Gramaje of Instituto de Ciencias de la Vid y del Vino (ICVV), Logroño, Spain kindly provided one of the fungus strains used in this study.

LITERATURE CITED

Albee S.R., Mueller G.M., Kropp B.R., 1996. Polymorphisms in the large intergenic spacer of the nuclear ribosomal repeat identify *Laccaria proxima* strains. *Mycologia* 88: 970–976.

Appel D.J., Gordon T.R., 1996. Relationships among pathogenic and nonpathogenic isolates of *Fusarium*

oxysporum based on the partial sequence of the intergenic spacer region of the ribosomal DNA. *Molecular Plant-Microbe Interactions* 9: 125–138.

Ariyawansa H.A., Hyde K.D., Jayasiri S.C., … Chen X.H., 2015. Fungal diversity notes 111–252: taxonomic and phylogenetic contributions to fungal taxa. *Fungal Diversity* 75: 27–274.

Bhatia S., Negi M.S., Lakshmikumaran M., 1996. Structural analysis of the rDNA intergenic spacer of *Brassica nigra*: evolutionary divergence of the spacers of the three diploid *Brassica* species. *Journal of Molecular Evolution* 43: 460–468.

Calabon M.S., Jones E.B.G., Boonmee S., Doilom M., Lumyong S., Hyde K.D., 2021. Five novel freshwater ascomycetes indicate high undiscovered diversity in lotic habitats in Thailand. *Journal of Fungi* 7: 117–143.

Carlucci A., Lops F., Cibelli F., Raimondo M.L., 2015. *Phaeoacremonium* species associated with olive wilt and decline in southern Italy. *European Journal of Plant Pathology* 141: 717–729.

Carlucci A., Raimondo M.L., Cibelli F., Phillips A.J.L., Lops F., 2013. *Pleurostomophora richardsiae, Neofusicoccum parvum* and *Phaeoacremonium aleophilum* associated with a decline of olives in southern Italy. *Phytopathologia Mediterranea* 52: 517–527.

Crous P.W., Gams W., 2000. *Phaeomoniella chlamydospora* gen. et comb. nov., a causal organism of Petri grapevine decline and esca. *Phytopathologia Mediterranea* 39: 112–118.

Crous P.W., Gams W., Wingfield M.J., Van Wyk P.S., 1996. *Phaeoacremonium* gen. nov. associated with wilt and decline diseases of woody hosts and human infections. *Mycologia* 88: 786–796.

Crous P.W., Wingfield M.J., Burgess T.I., ... Groenewald J.Z., 2016. Fungal planet description sheets: 469–557. *Persoonia* 37: 340–341.

Cunningham C.W., 1997. Can three incongruence tests predict when data should be combined? *Molecular Biology Evolution* 14: 733–740.

Da Silva M.A., Correia K.C., Barbosa M.A.G., Camara M.P.S., Gramaje D., Michereff S.J., 2017. Characterization of *Phaeoacremonium* isolates associated with Petri disease of table grapes in northeastern Brazil, with description of *Phaeoacremonium nordesticola* sp. nov. *European Journal of Plant Pathology* 149: 695–709.

Damm U., Mostert L., Crous P.W., Fourie P.H., 2008. Novel *Phaeoacremonium* species associated with necrotic wood of *Prunus* trees. *Persoonia* 20: 87–102.

Delcasso-Tremousaygue D., Grellet F., Panabieres F., Ananiev E.D., Delseney M., 1988. Structural and transcriptional characterization of the external spacer of a ribosomal RNA nuclear gene from a higher plant. *European Journal of Biochemistry* 172: 767–776.

Diaz M.R., Boekhout T., Kiesling T., Fell J.W., 2005. Comparative analysis of the intergenic spacer regions and population structure of the species complex of the pathogenic yeast *Cryptococcus neoformans*. *FEMS Yeast Research* 5: 1129–1140.

Dissanayake M.L.M.C., Kashima R., Tanaka S., Ito S.I., 2009. Genetic diversity and pathogenicity of *Fusarium oxysporum* isolated from wilted Welsh onion in Japan. *Journal of General Plant Pathology* 75: 125–130.

Drouin G., de Sà M.M., 1995. The concerted evolution of 5S ribosomal genes linked to the repeat units of other multigene families. *Molecular Biology and Evolution* 12: 481–493.

Durkin J., Bissett J., Pahlavani M., Mooney B., Buchwaldt L., 2015. IGS minisatellites useful for race differentiation in *Colletotrichum lentis* and a likely site of small RNA synthesis affecting pathogenicity. *PLoS One* 10: e0137398.

Essakhi S., Mugnai L., Crous P.W., Groenewald J.Z., Surico G., 2008. Molecular and phenotypic characterisation of novel *Phaeoacremonium* species isolated from esca diseased grapevines. *Persoonia* 21: 119–134.

Fernandez M., Polanco C., Ruiz M.L., Perez de la Vega M., 2000. A comparative study of the structure of the rDNA intergenic spacer of *Lens culinaris* Medik. and other legume species. *Genome* 43: 597–602.

Garber R.C., Turgeon B.G., Selker E.U., Yoder O.C., 1988. Organization of ribosomal RNA genes in the fungus *Cochliobolus heterostrophus*. *Current Genetics* 14: 573–582.

Gramaje D., Mostert L., Groenewald J.Z., Crous P.W., 2015. *Phaeoacremonium*: from esca disease to phaeohyphomycosis. *Fungal Biology* 119: 759–783.

Gruendler P., Unfried I., Pointne R., Schweizer C., 1991. Nucleotide sequence of the 25S-18S ribosomal gene spacer from *Arabidopsis thaliana*. *Nucleic Acids Research* 17: 6395–6396.

Guidot A., Lumini E., Debaud J.C., Marmeisse R., 1999. The nuclear ribosomal DNA intergenic spacer as a target sequence to study intraspecific diversity of the ectomycorrhizal basidiomycete *Hebeloma cylindrosporum* directly on *Pinus* root systems. *Applied Environmental Microbiology* 65: 903–909.

Hawksworth D.L., Crous P.W., Redhead S.A., Scott A., Reynolds Don R., … Frisvad J.C., 2011. Fungal nomenclature 2. The Amsterdam declaration on fungal nomenclature. *Mycotaxon* 116: 491–500.

Hillis D.M., Dixon M.T., 1991. Ribosomal DNA: molecular evolution and phylogenetic inference. *The Quarterly Review of Biology* 66: 411–453.

Hoang D.T., Chernomor O., von Haeseler A., Minh B.Q., Vinh L.S., 2018. UFBoot2: Improving the Ultrafast Bootstrap Approximation. *Molecular Biology Evolution* 5: 518–522.

James T.Y., Moncalvo J.M., Li S., Vilgalys R., 2001. Polymorphism at the ribosomal DNA spacers and its relation to breeding structure of the widespread mushroom *Schizophyllum commune*. *Genetics* 157: 149–161.

Jayawardena R.S., Purahong W., Zhang W., Wubet T., Li X.H., Yan J., 2018. Biodiversity of fungi on *Vitis vinifera* L. revealed by traditional and high-resolution culture-independent approaches. *Fungal Diversity* 90: 1–84.

Kalyaanamoorthy S., Minh B.Q., Wong T.K.F., von Haeseler A., Jermiin L.S., 2017. ModelFinder: fast model selection for accurate phylogenetic estimates. *Nature Methods* 14: 587–589.

Katoh F., Frith M.C., 2012. Adding unaligned sequences into an existing alignment using MAFFT and LAST. *Bioinformatics* 28: 3144–3146.

Katoh K., Standley D.M., 2013. MAFFT multiple sequence alignment software version 7: Improvements in performance and usability. *Molecular Biology Evolution* 30: 772–780.

Lockington R.A., Taylor G.C., Winther M., Scazzocchio C., Davies R.W., 1982. A physical map of the ribosomal DNA repeat unit of *Aspergillus nidulans*. *Gene* 20: 135–137.

Mahuku G.S., Hsiang T., Yang L., 1998. Genetic diversity of *Microdochium nivale* isolates from turfgrass. *Mycological Research* 102: 559–567.

Mahuku G.S., Platt HW., 2002. Molecular evidence that *Verticillium albo-atrum* Grp 2 isolates are distinct from *V. albo-atrum* Grp 1 and *V. tricorpus*. *Molecular Plant Pathology* 3: 71–79.

Martin F., Selosse M.A., Le Tacon F., 1999. The nuclear rDNA intergenic spacer of the ectomycorrhizal basidiomycete *Laccaria bicolor*: structural analysis and allelic polymorphism. *Microbiology* 145: 1605–1611.

Melané A., Vivier M.A., Pretorius I.S., 1998. Identification of a functional TATA element in the STA2 glucoamylase gene promoter from *Saccharomyces cerevisiae*. *Current Genetics* 33: 10–15.

Minh B.Q., Nguyen M.A.T., von Haeseler A., 2013. Ultrafast approximation for phylogenetic bootstrap. *Molecular Biology and Evolution* 30: 1188–1195.

Mirete S., Patiño B., Jurado M., Vázquez C., González-Jaén M.T., 2013. Structural variation and dynamics of the nuclear ribosomal intergenic spacer region in key members of the *Gibberella fujikuroi* species complex. *Genome* 56: 205–213.

Mostert L., Groenewald J.Z., Summerbell R.C., Gams W., Crous P.W., 2006. Taxonomy and pathology of *Togninia* (Diaporthales) and its *Phaeoacremonium* anamorphs. *Studies in Mycology* 54: 1–113.

Mostert L., Groenewald J.Z., Summerbell R.C., Robert V., Sutton D.A., Padhye A.A., Crous P.W., 2005. Species of *Phaeoacremonium* associated with infections in humans and environmental reservoirs in infected woody plants. *Journal of Clinical Microbiology* 43: 1752–1767.

Moyo P., Allsopp E., Roets F., Mostert L., Halleen F., 2014. Arthropods vector grapevine trunk disease pathogens. *Phytopathology* 104: 1063–1069.

Nguyen L.T., Schmidt H.A., von Haeseler A., Minh B.Q., 2015. IQ-TREE: A fast and effective stochastic algorithm for estimating maximum likelihood phylogenies. *Molecular Biology and Evolution* 32: 268–274.

Nigro F., Boscia D., Antelmi I., Ippolito A., 2013. Fungal species associated with a severe decline of olive in southern Italy. *Journal of Plant Pathology* 95: 668.

Olmo D., Armengol J., León M., Gramaje D., 2015. Pathogenicity testing of lesser-known fungal trunk pathogens associated with wood decay of almond trees. *European Journal of Plant Pathology* 143: 607–611.

Page R.D., 1996. TreeView: an application to display phylogenetic trees on personal computers. *Computer Application in Bioscience* 12: 357–358.

Pantou M.P., Mavridou A., Typas M.A., 2003. IGS sequence variation, group-I introns and the complete nuclear ribosomal DNA of the entomopathogenic fungus *Metarhizium*: excellent tools for isolate detection and phylogenetic analysis. *Fungal Genetics and Biology* 38: 159–174.

Papaioannou I.A., Dimopoulou C.D., Typas M.A., 2013. Structural and phylogenetic analysis of the rDNA intergenic spacer region of *Verticillium dahliae*. *FEMS Microbiological Letters* 347: 23–32.

Pecchia S., Mercatelli E., Vannacci G., 2004. Intraspecific diversity within *Diaporthe helianthi*: evidence from rDNA intergenic spacer (IGS) sequence analysis. *Mycopathologia* 157: 317–326.

Pipe N.D., Chandler D., Bainbridge B.W., Heale J.B., 1995. Restriction length polymorphisms in the ribosomal RNA gene complex of isolates of the entomopathogenic fungus *Metarhizium anisopliae*. *Mycological Research* 99: 485–491.

Raimondo M.L., Lops F., Carlucci A., 2014. *Phaeoacremonium italicum* sp. nov., associated with esca of grapevine in southern Italy. *Mycologia* 106: 1119–1126.

Rayner R.W., 1970. *A mycological colour chart.* Commonwealth Mycological Institute, Kew, Surrey, UK.

Sampietro D.A., Marín P., Iglesias J., Presello D.A., Vattuone M.A., …González-Jaén M.T., 2010. A molecular based strategy for rapid diagnosis of toxigenic *Fusarium* species associated to cereal grains from Argentina. *Fungal Biology* 114: 74–81.

Selker E.U., Morzycka-Wroblewska E., Stevens J.N., Metzenberg R.L., 1986. An upstream signal is required for *in-vitro* transcription of *Neurospora* 5S RNA genes. *Molecular Genetics and Genomics* 205: 189–192.

Sohrabi M., Mohammadi H., Leon M., Armengol J., Banihashemi Z., 2020. Fungal pathogens associated with branch and trunk cankers of nut crops in Iran. *European Journal of Plant Pathology* 157: 327–351.

Soltaninejad N., Mohammadi H., Massumi H., 2017. Isolation, identification and pathogenicity of Botryosphaeriaceae and *Phaeoacremonium* species associated with decline of *Prunus* species in Iran. *Journal of Plant Pathology* 99: 571–581.

Spies C.F.J., Moyo P., Halleen F., Mostert L., 2018. *Phaeoacremonium* species diversity on woody hosts in the Western Cape Province of South Africa. *Persoonia* 40: 26–62.

Sugita T., Nakajima M., Ikeda R., Matsushima T., Takako S., 2002. Sequence analysis of the ribosomal DNA intergenic spacer 1 regions of *Trichosporon* species. *Journal of Clinical Microbiology* 40: 1826–1830.

Swofford D.L., PAUP*. 2003. *Phylogenetic Analysis Using Parsimony, Version 4.* Sinauer Associates, Sunderland, UK.

Úrbez-Torres J.R., Haag P., Bowen P., O'Gorman D.T., 2014. Grapevine trunk diseases in British Columbia: incidence and characterization of the fungal pathogens associated with Esca and Petri disease of grapevine. *Plant Disease* 98: 469–482.

Van't Hof J., Lamm S.S., 1991. Single stranded replication intermediates of ribosomal DNA replicons of pea. *The EMBO Journal* 10: 1949–1953.

Walker A.S., Bouguennec A., Confais J., Morgant G., Leroux P., 2011. Evidence of host-range expansion from new powdery mildew (*Blumeria graminis*) infections of triticale (× Triticosecale) in France. *Plant Pathology* 60: 207–220.

White C.L., Halleen F., Fischer M., Mostert L., 2011. Characterisation of the fungi associated with esca diseased grapevines in South Africa. *Phytopathologia Mediterranea* 50: 204–223.

We warmly thank for their kind cooperation the following referees who have reviewed papers during this year in order to publish this Volume (Phytopathologia Mediterranea 60, 2021):

Abdollahzadeh Jafar, Kurdistan, Sanandaj, Iran
Aglietti Chiara, Firenze, Italy
Agustí-Brisach Carlos, Cordoba, Spain
Alves Artur, Aveiro, Portugal
Andersen Mark, Auckland, New Zealand
Armengol Forti Josep, Valencia, Spain
Avilés Manuel, Sevilla, Spain
Beccari Giovanni, Perugia, Italy
Belz Regina, Stoccarda, Germany
Bénédicte Lebas, Liege, Belgium
Bezerra Jadson, Goiás, Brazil
Bianco Piero, Milano, Italy
Cağlayan Kadriye, Antakya, Turkey
Calzarano Francesco, Teramo,Italy
Campos Maria Doroteia, Evora, Portugal
Cappelletti Eleonora, Bologna, Italy
Cerboneschi Matteo, Florence,Italy
Chatterton Syama, Lethbridge, Canada
Chatzidimopoulos Michael, Volos, Greece
Chooi Karmun, Auckland, New Zealand
Choueiri Elia, Beirut, Lebanon
Cobos Rebeca, Leon, France
Cohen Daniel, Auckland, New Zealand
Cola Gabriele, Milano, Italy
Couthino teresa, Pretoria, South African
D'Onghia Anna Maria, Valenzano, Bari, Italy
Del Frari Giovanni, Lisbon, Portugal
Egel Daniel,Vincennes,Indiana, USA
Eichmeier Ales, Brünn (Brno), Repubblica Ceca
Eskalen Akif, Davis, CA, USA
Faggioli Francesco, Rome, Italy
Fedele Giorgia, Piacenza, Italy
Fontaine Florence, Reims, France
Fontdevila Pareta, Gembloux, Belgium
Fuchs Marc, New York, USA
Gambino Giorgio, Torino, Italy
Gambley Cherie, Stanthorpe Queensland, Australia
Ghelardini Luisa, Florence, Italy
Gonthier Paolo, Torino, Italy
González-Biosca Elena, València , Spain
Gonzalez-Dominguez Elisa, Piacenza, Italy
Gramaje David, Logroño, Spain
Guarnaccia Vladimiro, Torino, Italy
Hausladen Hans, Freising, Germany
Hirsch Judith, Avignon, France
Loos Renaud, Angers, Francia
Isakeit Thomas, College Station, Texas (USA)
Jany Jean-Luc,Brest, France
Jayawardena Ruvishika, Chiang Rai, Thailand
Karaoglanidis Georgios, Thessaloniki, Greece
Kassemeyer Hanns-Heinz, Freiburg, Germany
Kavroulakis Nektarios, Chania, Greece
Kerlan Marie Claire, Leu Reu, France
Knierim Dennis, Braunschweig, Germany
Koruda keiko, Kobe, Japan
Kumari Shweta,Uttar Pradesh, Indian
Llorente Isidre, Girona
Loconsole Giuliana, Bari, Italy
Loiseau Marianne, Angers, France
Lombard Lorenzo, Utrecht, Netherlands
Luigi Marta, Rome, Italy
Magnin-Robert Maryline, Calais, France
Marhadour Sylvie, Paris, France
Markakis Emmanouil, Chania, Crete, Greece.
Masiello Mario, Bari, Italy
Mauromicale Giovanni, Catania, italy
McTaggart Alistair, Queensland, Australian
Meca giuseppe, Valencia, Spain
Mesterhazy Akos, Szeged, Hungary
Michailides Themis, Californian, USA
Migliorini Duccio, Firenze, Italy
Mondello Vincenzo, Reims, France
Munir Shahzad, Kunming, China
Murillo Jesus, Navarra, Spain
Natsuaki Tomohide, Tokyo, Japan
Nemes Katalin, Budapest, Hungary
Nyamesorto Bernard, Montana, USA
Ochoa-Corona Francisco, Oklahoma, USA
Parkinson Louisa, Brisbane, Queensland, Australie
Patriarca Andrea, Buenos Aires, Argentina
Peres Natalia A., Florida, USA
Picot Adeline, Plouzané, France
Prodi Antonio, Bologna, Italy
Prospero Simone, Birmensdorf, Switzerland
Ramirez Maria, Rio Cuarto, Argentine
Rivière Céline, Lille, France
Rizzo Domenico, Tuscany, Italy
Romanazzi Gianfranco, Ancona, Italy
Saldarelli Pasquale, Torino, Italy
Santini Alberto, Florence, Italy
Santosa Adyatma Irawan, Diskapi, Ankara
Santosa Adyatma Irawan, Diskapi, Ankara
Schmitt Annegret, Dresden, Germania
Serrano Maria, Berkeley, USA
Shiskoff Nina, Maryland, USA
Silva Isidora, Santiago, Chile
Skoric Dijana, Zagreb, Croatia
Smilanick Joseph, California, USA

Finito di stampare da
Logo s.r.l. – Borgoricco (PD) – Italia

Mediterranean Phytopathological Union

Founded by Antonio Ciccarone

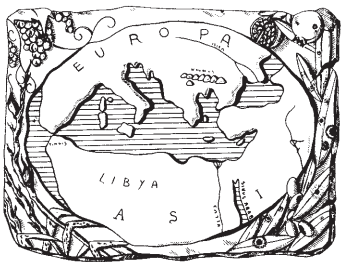

The Mediterranean Phytopathological Union (MPU) is a non-profit society open to organizations and individuals involved in plant pathology with a specific interest in the aspects related to the Mediterranean area considered as an ecological region. The MPU was created with the aim of stimulating contacts among plant pathologists and facilitating the spread of information, news and scientific material on plant diseases occurring in the area. MPU also intends to facilitate and promote studies and research on diseases of Mediterranean crops and their control.
The MPU is affiliated to the International Society for Plant Pathology.

MPU Governing Board

Affiliated Societies

Arab Society for Plant Protection (ASPP), http://www.asplantprotection.org/
French Society for Phytopathology (FSP), http://www.sfp-asso.org/
Hellenic Phytopathological Society (HPS), http://efe.aua.gr/
Israeli Phytopathological Society (IPS), http://www.phytopathology.org.il/
Italian Phytopathological Society (SIPAV), http://www.sipav.org/
Portuguese Phytopathological Society (PPS), http://www.spfitopatologia.org/
Spanish Society for Plant Pathology (SEF), http://www.sef.es/sef/

2021 MPU Membership Dues

Institutional MPU Membership: : € 200.00 (college and university departments, libraries and other facilities or organizations). Beside the open-access on-line version of *Phytopathologia Mediterranea*, the print version can be received with a € 50 contribution to mail charges (total € 250,00 to receive the print version). Researchers belonging to an Institution which is a member of the Union are entitled to publish with a reduced page contribution, as the Individual Regular members.
Individual Regular MPU Membership*: € 50.00 (free access to the open-access on-line version of Phytopathologia Mediterranea and can get the print version with a contribution to mail charges of € 50 (total € 100,00 to receive the print version).

*Students can join the MPU as a Student member on the recommendation of a Regular member. Student MPU members are entitled to a 50% reduction of the membership dues (proof of student status must be provided).

Payment information and online membership renewal and subscription at www.mpunion.com

For subscriptions and other information visit the MPU web site:
www.mpunion.com
or contact us at: Phone +39 39 055 2755861/862 – E-mail: phymed@unifi.it

Phytopathologia Mediterranea

Volume 60, December, 2021

Contents

Direttore responsabile: Giuseppe Surico • Autorizzazione del Tribunale di Firenze n. 4923 del 5-1-2000 • *Printed by* Logo S.r.l. - Padova, February 2022
€ 70,00